

THE  
ELECTRONICS  
OF  
LABORATORY  
AND  
PROCESS  
INSTRUMENTS

V. S. GRIFFITHS  
and  
W. H. LEE

THE  
ELECTRONICS  
OF  
LABORATORY  
AND  
PROCESS  
INSTRUMENTS



V. S. GRIFFITHS

Ph.D., F.R.I.C.

and

W. H. LEE

Ph.D., F.R.I.C.

CHATTO  
and  
WINDUS

THE first part of this book reviews the behaviour of resistances, and of inductances under direct and alternating voltages, and emphasizes the practical importance of resonance. The principles of thermionic emission are considered, and various types of valves and photo-cells described. The authors deal in a general way with the application of these valves and of such ancillary devices as metal rectifiers and vibrators, under the headings rectification, amplification and oscillation. The 'soft' tube and its applications are also discussed, and a brief outline of semi-conductor devices is included.

The second part of the book deals with particular pieces of apparatus, e.g. pH meters, conductivity bridges, dielectric constant bridges, spectrophotometers, etc. It also contains reference to industrial applications and the elements of control theory.

This book is not intended for the electronics engineer, physicist or designer but for the scientist, engineer or technologist who, with a background of general physics, wishes to gain a working knowledge of the operation of some electronic instruments in general use in chemical and control laboratories. Such acquaintance with the principles behind the apparatus should enable the operator to make the best use of his instrument, to realise its limitations, and to be in a position either to modify or to suggest modifications to the manufacturer.

Dr. Griffiths and Dr. Lee are on the staff of the Battersea College of Technology, London.



**THE ELECTRONICS OF LABORATORY AND  
PROCESS INSTRUMENTS**





# The Electronics of Laboratory and Process Instruments

*By*

V. S. GRIFFITHS

Ph.D., F.R.I.C.

*and*

W. H. LEE

Ph.D., F.R.I.C.

1962

CHATTO AND WINDUS  
LONDON

Published by  
Chatto & Windus Ltd  
42 William IV Street  
London W.C.2

★

Clarke, Irwin & Co. Ltd  
Toronto

© V. S. Griffiths and W. H. Lee 1962

Printed in Great Britain by  
Spottiswoode, Ballantyne & Co. Ltd  
London and Colchester

# Contents

<i>List of symbols</i>	<i>page ix</i>
<i>Preface</i>	<i>xv</i>
<b>CHAPTER</b>	
<b>I Components and their characteristics</b>	
Introduction. Resistance, inductance and capacitance in direct current circuits	1
<i>Problems</i>	19
<b>II Alternating current</b>	
Introduction. Measurement of alternating currents and voltages. Resistance, capacitance and inductance in alternating current circuits. Power in alternating current circuits. The power-factor of capacitors. Comparison of powers: the decibel scale	20
<i>Problems</i>	51
<b>III Tuned circuits</b>	
Tuned circuits. $Q$ -factor. The universal resonance curve. Acceptor and rejector circuits. Coupled circuits. The transformer. The auto-transformer. Maximum power transfer. Impedence matching	53
<i>Problems</i>	73
<b>IV Thermionic emission</b>	
Thermionic emission. The diode. The triode. Limitation of the triode. The tetrode. The beam tetrode. The pentode. Multi-grid valves. Composite valves. 'Soft' tubes. Cold cathode tubes. Valve bases	74
<i>Problems</i>	99
<b>V Applications of thermionic valves (I)</b>	
Rectification of alternating voltages. Metal rectifiers. Stabilised power supplies. Hard valve stabilisation. Detection	101
<i>Problems</i>	121
<b>VI Applications of thermionic valves (II)</b>	
Amplification: general principles. Power amplification. Push-pull amplification. Coupled amplifiers. Negative feedback. The cathode follower. The classification of valve amplifiers. D.C. amplifiers	123
<i>Problems</i>	152

# CONTENTS

CHAPTER	<i>page</i>
<b>VII Applications of thermionic valves (III)</b>	
Introduction—practical valve oscillators. Automatic grid bias for oscillators. Dynatron oscillator. The <i>R-C</i> oscillator. Crystal frequency-control. Low-frequency oscillators. The multivibrator. Other relaxation oscillators	153
<i>Problems</i>	172
<b>VIII Miscellaneous electronic tubes</b>	
Photo-cells. Photomultiplier tubes. The dekatron tube. The ribbon beam tube. The Geiger-Müller tube. The proportional counter tube. The cathode ray oscilloscope. 'Tuning' indicator ('Magic-Eye' tube)	173
<i>Problems</i>	201
<b>IX Semiconductors and transistors</b>	
Introduction. Symbols and nomenclature. Theory of semiconductors. The junction diode. The junction transistor. The manufacture of transistors. Basic types of connections. Some transistor circuits. Transistor characteristics	202
<i>Problems</i>	226
<b>X The measurement of electrical conductance of solutions</b>	
Introduction. Bridge circuits. The fixed-resistance potential drop method. A direct current instrument. The transformer bridge. High-frequency conductivity	227
<i>Problems</i>	253
<b>XI Section I. The measurement of electromotive force and electrode potential</b>	
Electrode potentials. Hydrogen ion concentration and the pH scale. Potentiometric measurement. The glass electrode. Measurement of e.m.f.s produced in high resistance electrode systems. Direct reading instrument	254
<b>Section II. Dielectric constants and capacitance measurement</b>	
Capacity bridge method. Experimental methods of measurement. Solid dielectrics	271
<i>Problems</i>	284
<b>XII Polarography</b>	
Principles. Instruments. Residual or charging currents. Differential and derivative polarography. A.C. polarography. Cathode ray polarographs	285
<i>Problems</i>	310



## CONTENTS

CHAPTER	<i>page</i>
<b>XIII Radioactivity measurement</b>	
Introduction. Ionisation instruments. Other methods of measurement. Electronic equipment. Quenching probe. Rate-meter. Pulse amplifiers. Pulse analyser or 'kicksorter'. Scalers	312
<i>Problems</i>	337
<b>XIV Photometers and spectrophotometers</b>	
Introduction. Photoelectric colorimeters or absorptiometers. Spectrophotometers: visible, ultra-violet and infra-red. Monochromators. Detectors. Amplifiers. The complete instrument. Non-dispersive infra-red gas-analyser	338
<i>Problems</i>	363
<i>Index</i>	365



## List of Symbols Used

$\text{\AA}$	Ångström unit ( $10^{-8}$ cm)
$a$	area
A.F.	audio-frequency
$C$	capacity; concentration
$C_g$	equivalent capacitance of grid circuit
$C_{g,a}$	grid-anode capacity
$C_{g,c}$	grid-cathode capacity
$C_i$	input capacity
$C_s$	associated (stray) capacity
C.R.O.	cathode ray oscilloscope
$\cos \phi$	power factor
c/s	cycles per second
$D$	dielectric constant
$D_f$	second harmonic distortion factor
$D_{fn}$	second harmonic distortion factor, with negative feedback
$d$	distance apart
db	decibels
d.c.	direct current
d.m.e.	dropping mercury electrode
$E$	alternating voltage; extinction coefficient or optical density
$\bar{E}$	average value of $E$
$E_g$	amplitude of grid voltage
$\bar{E}_\lambda$	average voltage, full-wave rectification
$\bar{E}_{\lambda/2}$	average voltage, half-wave rectification
$\bar{E}_m$	amplitude of alternating voltage
$\bar{E}_m$	amplitude of second harmonic component of voltage
$E_n$	noise-component amplitude
$E_{nf}$	noise-component amplitude, with negative feedback
$E_{r.m.s.}$	root mean square voltage
$E_T$	turnover voltage
E.H.T.	extra high-tension voltage
$e$	instantaneous voltage
$e_b$	electron flow from base

# LIST OF SYMBOLS USED

$e_g$	instantaneous grid voltage
$e_{s.i.}$	induced e.m.f.
$\bar{e^2}$	average value of $e^2$
exp	exponential
$F$	Faraday ( $9.65 \times 10^4$ coulombs)
F	farad (capacity)
$f$	frequency
$f_c$	carrier frequency
$f_m$	modulation frequency
$f_0$	resonant frequency
$g_1, g_2, g_3$	control, screen and suppressor grids
$g_m$	mutual conductance
$I$	current; intensity of transmitted light
$I_a$	steady anode current
$\bar{I}_\lambda$	average current, full-wave rectification
$\bar{I}_{\lambda/2}$	average current, half-wave rectification
$I_{max}$	maximum current
$I_0$	intensity of incident light
$I_{r.m.s}$	root mean square current
$i$	instantaneous current
$i_a$	instantaneous anode current
$i_c$	collector-to-base current (emitter short-circuited)
$i_{co}$	collector-to-base current (emitter open-circuited)
$i_e$	total emitter current
$i_f$	forward current
$i_g$	instantaneous grid current
$i_L$	load current
$i_r$	reverse current
$i_t$	total current
I.F.	intermediate frequency
k	kilo- ( $10^3$ )
$k$	coupling factor; Boltzmann's constant
$k_c$	critical coupling factor
$L$	inductance
$l$	length (cm); path length
L.F.	low frequency
$M$	mutual inductance; stage gain of amplifier
m	milli- ( $10^{-3}$ )
mil	$\frac{1}{1000}$ inch
N	Avogadro's number



# LIST OF SYMBOLS USED

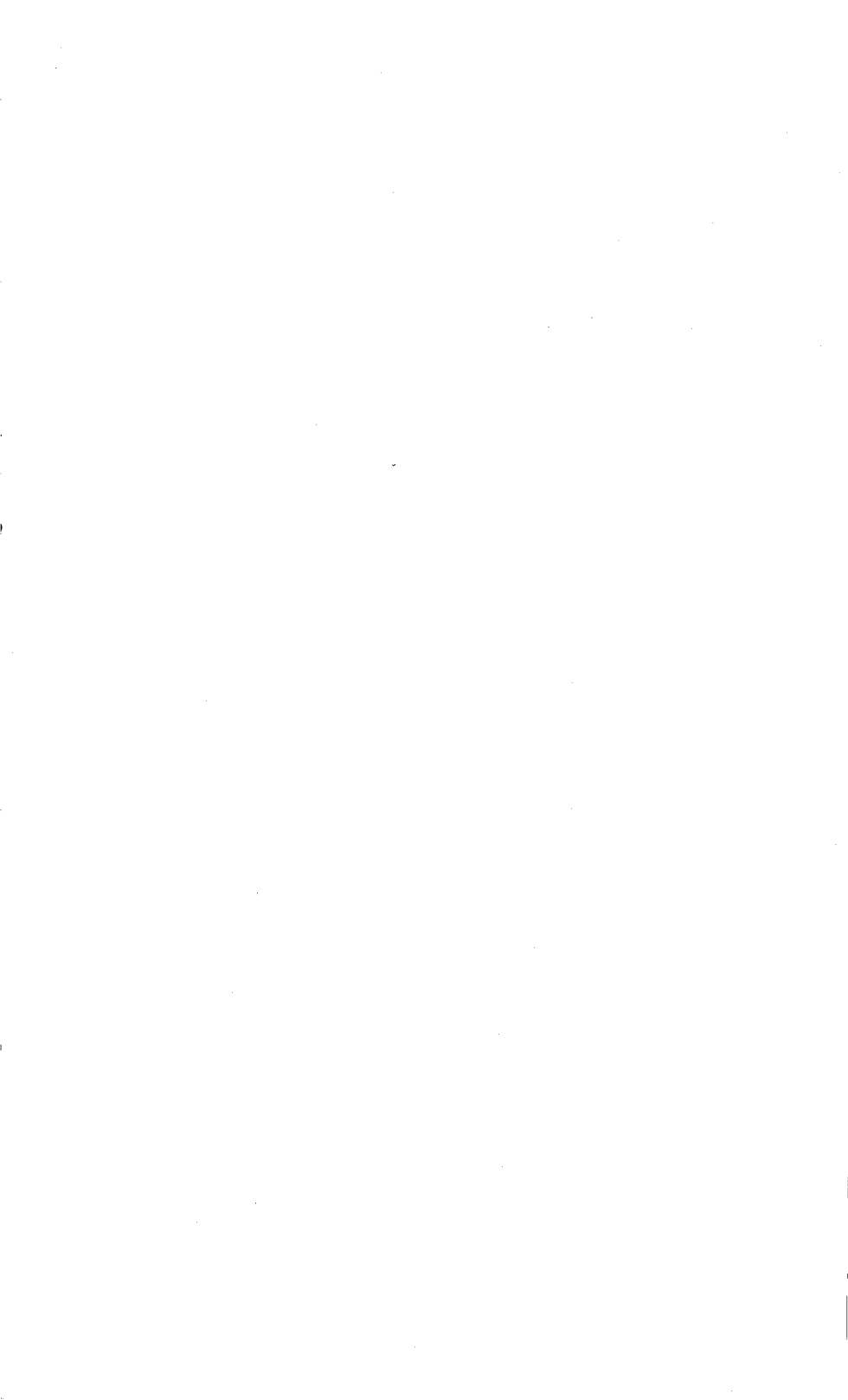
$N$	true number of counts per minute
$N_0$	number of counts observed per minute
$N_p$	number of pulses per second
$n_T$	number of atoms present at time $T$
N.H.E.	normal hydrogen electrode
N.T.P.	normal temperature and pressure
$^0$	superscript denoting values at resonance, e.g. $X_L^0$
o/p	output
$P_A$	anode power
$P_L$	power developed in a load $L$
$p$	instantaneous power; subscript, primary parameters, e.g. $R_p$
$\bar{p}$	average power
pF	pico-farad ( $10^{-12}$ F)
p.d.	potential difference
pH	hydrogen ion concentration exponent
$Q$	charge; magnification
$Q'$	wattless power
$q_i$	instantaneous charge
$R$	resistance
$R_b$	battery internal resistance
$R_d$	dynamic impedance
$R_g$	grid resistance
$R_L$	load resistance
$r_a$	anode resistance
R.F.	radio frequency
R.F.C.	radio-frequency choke
r.m.s.	root mean square
$S$	apparent power
$s$	subscript, secondary parameters, e.g. $R_s$
$T$	period of harmonic motion; sweep-time; turns-ratio of transformer; absolute temperature
$T_p$	paralysis time
$T_q$	quench time
$T_{1/2}$	half-life
$t$	time; temperature, °C.
$V$	direct voltage
$V_a$	steady anode voltage
$V_b$	battery voltage; burning voltage of neon tube
$V_c$	amplitude of carrier voltage

# LIST OF SYMBOLS USED

$V_f$	filament voltage
$V_g$	grid voltage
$V_{g.c.o.}$	cut-off grid voltage
$V_m$	amplitude of modulation voltage
$V_{1/2}$	half-wave potential
$V_+$	anode voltage for applied grid voltage $+E_g$
$V_-$	anode voltage for applied grid voltage $-E_g$
$V_{ign}$	ignition voltage of neon tube
$W$	watts
$W_0$	Maximum anode dissipation, watts
$W'$	number of turns on transformer winding
$X$	reactance
$X_L$	inductive reactance
$X_C$	capacitive reactance
$Y$	admittance
$Z$	impedance
$Z_g$	internal impedance of a generator
$Z_L$	load impedance
$\alpha$	radioactive decay constant
$\alpha_{c.b.}$	amplification factor for collector-to-base current
$\alpha_{c.e.}$	amplification factor for collector-to-emitter current
$\beta$	feedback coefficient
$\delta$	small change in
$\epsilon$	molar extinction coefficient
$\theta$	angle of rotation
$\kappa$	permittivity; specific conductance
$\lambda$	wavelength
$\Lambda$	equivalent conductance
$\mu$	amplification factor; micron ( $10^{-4}$ mm.)
$\mu-$	micro- ( $10^{-6}$ )
$\mu\mu-$	micro micro- ( $10^{-12}$ )
$\rho$	resistivity
$\Sigma$	sum of
$\tau$	time constant
$\phi$	phase-angle; flux
$\omega$	pulsatance, $2\pi f$
$\omega_c$	carrier pulsatance, $2\pi f_c$
$\omega_m$	modulation pulsatance, $2\pi f_m$
$\omega_0$	resonant dulsatance, $2\pi f_0$
$\Omega$	ohm

# LIST OF SYMBOLS USED

$\sim$	subtract the smaller from the great
$\approx$	approximately equal to
$\equiv$	symbol for earth connection
$<$	is less than
$>$	is greater than
$\propto$	is proportional to
$\odot$	generator of a.c.
$\oplus$	alternative symbols for gas-filled tubes





## Preface

For a number of years we have given at this college a course of lectures to our research students in physical chemistry, and to others interested, on elementary electronics. We considered that, knowing something of the design and construction of the many items of electronic equipment now available, they would be better able to choose that most suitable for their purpose, and to use it more intelligently within its inherent limitations. The more efficient use of apparatus has, we believe, justified the instruction.

With the advent of technological courses, lectures and laboratory work in this subject have been included in the syllabus. For example, students reading for the Diploma of Technology in Applied Chemistry study basic physics during their first year; in the second year, theoretical instruction follows broadly the lines of the present book, together with relevant practical work in the electronics, spectroscopic and radio-activity measurement laboratories. The student working with spectrophotometers, polarographs, and similar equipment, in the later stages of his course, is thus able to gain the maximum information from the manufacturer's handbooks and data sheets relating to those instruments.

In addition, we believe that the student who has worked through the following chapters will be able to construct, cheaply and quickly, small circuits involving the use of thermionic valves or of transistors as rectifiers, amplifiers, or oscillators. He will be able to carry out elementary fault-finding on equipment, to decide whether local repair is feasible, and—most important—whether re-calibration of the instrument will be necessary. Briefly, he will know enough to change a valve or electrolytic capacitor, and to leave a tuned circuit or attenuator alone.

The number of items of electronic equipment at the service of chemists, chemical engineers, metallurgists and physicists, in these days of rapid development in new techniques, grows ever greater. We shall feel gratified if through this book the worker becomes familiar with rather more of their function than is disclosed by the 'Operating Instructions'.

*Battersea College of Technology,  
December, 1960*

V. S. G.  
W. H. L.



## CHAPTER I

# Components and Their Characteristics

### Introduction

The properties of electronic circuits and devices may be expressed in terms of certain variables, the circuit parameters—just as the properties of a gas mixture may be stated in terms of temperature, pressure and composition. The circuit parameters are those we meet with in elementary physics, i.e. resistance, inductance and capacitance. But electronic components are usually much smaller than those of the physics laboratory, and they are directly soldered into the circuit, instead of being connected by wires and terminals. There are good reasons for these differences. Extreme accuracy and stability are not generally demanded of the individual components; and, because much higher frequencies are dealt with, there are great advantages in keeping physical size, and length of connecting leads, as small as possible. In fact, the tendency is for the physical as distinct from the electrical size of components to be reduced as much as possible, particularly where the electrical power handled is small; recent developments, such as the miniature valve, transistors and printed circuits, have taken this process much further.

We shall begin by considering the circuit parameters, and, in this chapter, their behaviour under direct current (d.c.) conditions.

### Resistance

Some of the resistance of a circuit is deliberately introduced by manufactured resistors; the remainder is introduced by the imperfection of the other components. We must of course consider both in analysing the behaviour of the circuit.

The form of a resistor depends mainly upon its power rating, or its 'dissipation' in watts,  $W$ , and it can be shown that

$$W = RI^2 = E^2/R = EI$$

where  $I$  is in amperes,  $E$  in volts and  $R$  in ohms ( $\Omega$ ). Carbon resistors are used for low-power circuits, in which the power

## LABORATORY AND PROCESS INSTRUMENTS

dissipated by the resistor is below 5 W; above this, wire-wound resistors, barretters or line cords are used.

The physical size of a carbon resistor depends upon its power rating, and not at all upon the resistance value, which may be as high as, or higher than  $10^7 \Omega$  (10 M $\Omega$ ). Resistors consist of cylinders of a graphite-resin composition, either varnished, or with a ceramic covering. Connection is made by brass caps at the ends, or by a few turns of wire, taken round the ends of the resistor.

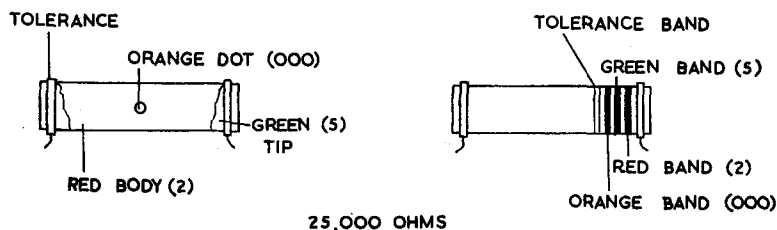


Fig. 1.1. The colour code for resistors

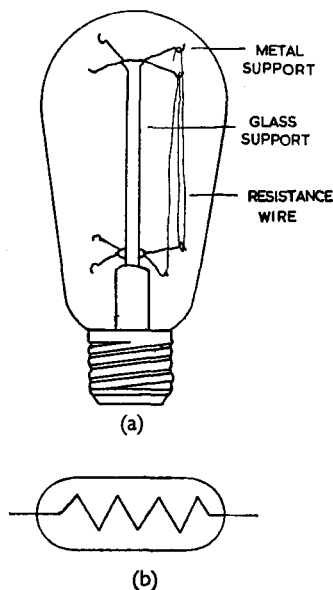
Colour	Body or 1st band	Tip or 2nd band	Dot or 3rd band	Tolerance band
Black	0	0	—	—
Brown	1	1	0	—
Red	2	2	00	—
Orange	3	3	000	—
Yellow	4	4	0000	—
Green	5	5	00000	—
Blue	6	6	000000	—
Purple	7	7	—	—
Grey	8	8	—	—
White	9	9	—	—
Gold	—	—	—	5%
Silver	—	—	—	10%
None	—	—	—	20%

The resistance value is generally indicated by a code of colours, as follows: brown = 1, red 2, orange 3, yellow 4, green 5, blue 6, violet 7, grey 8, white 9, black 0. The body-colour is read first, then the colour of the tip; the 'spot' colour gives the number of noughts to be added. Thus, a yellow body with a violet tip and orange spot indicates 4, 7 and 000, i.e. 47,000  $\Omega$ , or 47 k $\Omega$ . Sometimes, the resistance is indicated by a series of coloured bands at one end. The same code applies, and the bands are read from the outside, towards the centre (see Fig. 1.1).

## COMPONENTS AND THEIR CHARACTERISTICS

Carbon resistors may vary by as much as  $\pm 20\%$  about the nominal resistance value; selected resistors, within  $10\%$  of the rated value are marked with a silver spot or band, and those of closer tolerance,  $\pm 5\%$ , by a gold spot or band. Special quality high-stability resistors are denoted by a pink band.

*Wire-wound resistors* are generally coated with a vitreous, non-conducting layer; in some forms, metal bands at the ends clip into a holder mounted on the chassis, so that they may be easily



(a) Barretter (b) Symbol

Fig. 1.2. The barretter

replaced. Such resistors may have tappings at various points along their length. They should be mounted well clear of other components, since they usually get quite hot in operation.

Barretters are lengths of resistance wire sealed inside a glass envelope, containing hydrogen gas at low pressure (Fig. 1.2). They have the property of increasing resistance with increasing applied voltage in a linear manner, within limits; so that such a resistance passes an approximately constant current despite

## LABORATORY AND PROCESS INSTRUMENTS

changes of supply voltage. A typical current-voltage curve for a barretter is shown in (Fig. 1.3).

A *line-cord* is a length of resistance wire, woven in asbestos fibres, and made up into a cable resembling 15 amp 'flex'. Line cords are rated in ohms per foot, and the maximum safe current for the wire is also stated. They may dissipate considerable quantities of heat; for example, to supply 100 V at 0.2 amps, for the filaments of a valve amplifier, from the 240 V mains supply requires a resistance of  $700\ \Omega$ , and this dissipates 28 W, or nearly 7 calories per second.

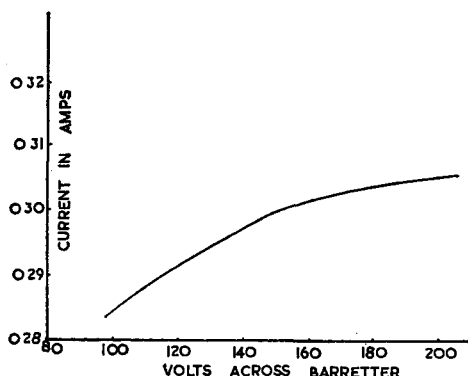


Fig. 1.3. Voltage-current relationship for the barretter

All resistors, unless specially designed, change their values with change of temperature. Wire-wound resistors, line cords, and metal filament lamps show a positive temperature coefficient of resistance, i.e. the resistance increases with increasing temperature; carbon resistors, and carbon filament lamps, show a negative coefficient. Thus experiments to verify Ohm's law should be carried out under isothermal conditions. In Fig. 1.4 are shown some of the current-voltage relationships found in practice; these are not all due to temperature change. Curve *a* represents the ideal Ohm's law relationship; curve *b* that of a barretter; curve *c* shows the output of a voltage-stabiliser circuit, in which the voltage is maintained approximately constant for a considerable variation in current supplied. Curve *d* shows an example of

## COMPONENTS AND THEIR CHARACTERISTICS

negative resistance; this is not the behaviour of a resistor, but shows, for example, the relationship of one pair of currents and voltages in the tetrode valve (see p. 85).

Fig. 1.5 shows the current-voltage relationship (the 'characteristic curve') of a tungsten-filament lamp. Between 20 V and 200 V, the resistance changes from 133–533  $\Omega$ . Carbon-filament lamps show a similar variation, but in the reverse sense. Hence, if a lamp is to be used as a ballast resistor, i.e. at other than its

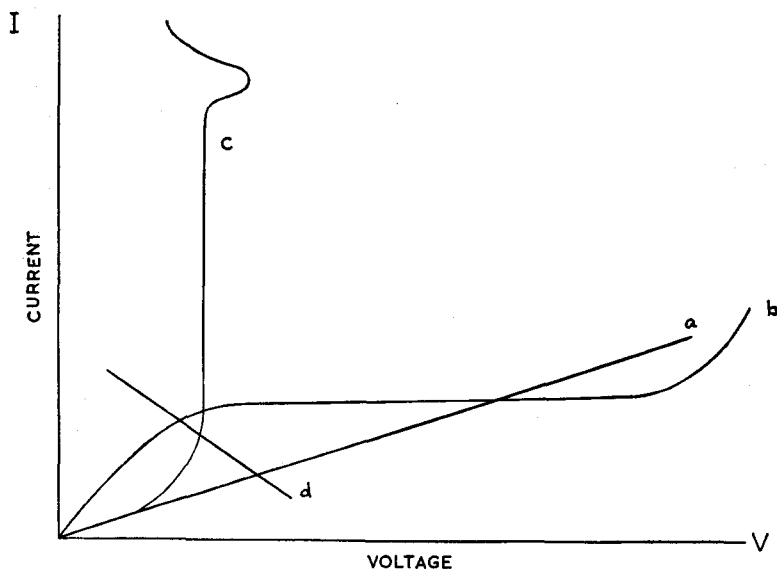


Fig. 1.4. Some voltage-current relationships

nominal voltage, we cannot deduce its resistance from the watts rating, and must measure it under the working conditions.

Some resistors are specially sensitive towards changes of temperature; they are called *thermistors*, and are used in the measurement or control of temperature. If the resistance of a length of nichrome wire is 100  $\Omega$  at 0°C, this increases to 100.4  $\Omega$  at 10°C; it is a small change compared with that of a typical thermistor, having a resistance of 2000  $\Omega$  at 0°C and of 1000  $\Omega$  at 10°C. All thermistors have a very large *negative* temperature coefficient of resistance. They consist of a bead of semiconductor material (p. 204), fused to a pair of leads, which may be enclosed

## LABORATORY AND PROCESS INSTRUMENTS

in a gas-filled, or evacuated, glass envelope. Their power rating is very low, so that they are usually employed in bridge circuits, the off-balance current operating a temperature recorder or controller. Thermistors are rated according to their maximum power dissipation and their most useful temperature range.

Whenever possible, carbon resistors are used in electronic circuits, because they are physically small, cheap, robust and introduce only small non-resistive parameters into the circuit. On the other hand, they cannot dissipate large amounts of power,

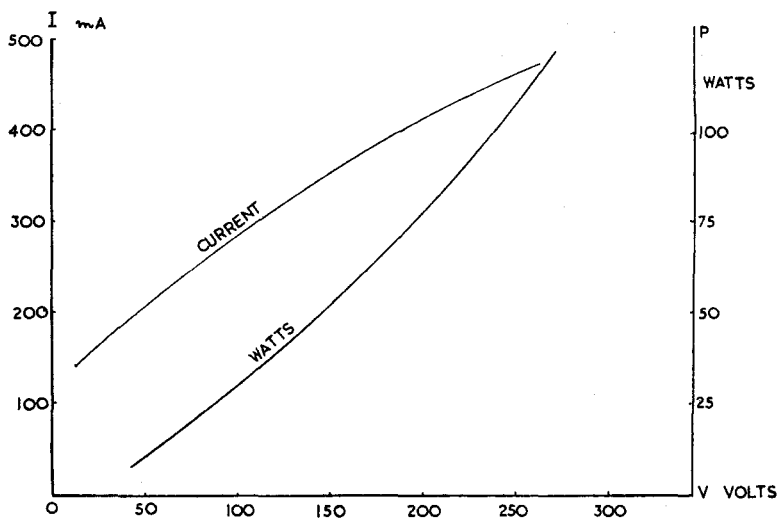


Fig. 1.5. Characteristic curve of the tungsten filament lamp

and are constructed to a comparatively wide tolerance—though obviously any required value could be obtained by selection. A more serious objection is that, by oscillation of the carbon granules at 'thermal' frequencies (i.e. oscillations produced by heating) spurious frequencies may be introduced into the circuit, giving rise to 'noise'.

Variable resistors and potentiometers may consist of a metal arm moving over a carbon track coated on an insulator; the power rating is very low, and such resistors are particularly prone to generate 'noise'. For higher power rating, and for more precise values, wire-wound potentiometers are chosen.



## COMPONENTS AND THEIR CHARACTERISTICS

Two new types of resistors have recently been introduced. 'Fiberloy'† resistors consist of a precious metal film deposited on a glass fibre; this is wound on a ceramic former, and protected by an epoxy-resin coating. The following values are available:

2.7 kΩ to 700 kΩ, 1 W rating, tolerance 10%

5.4 kΩ to 2 MΩ, 2.5 W rating, tolerance 10%

Closer tolerance resistors are available within more restricted ranges, e.g. 0.5% for 100 kΩ to 700 kΩ, 1 W rating, and 200 kΩ to 1.4 MΩ, 2.5 W rating. The stability is much greater than for carbon resistors, and the size is comparable.

'Metlohm'† metal film resistors are made by firing a noble-metal alloy film on to the surface of a glass sheet. Silver connectors are fired on to the track, and a protective coating is applied. The 'noise' generated by these resistors is extremely small; they may be operated at temperatures up to 180°C, and inductive and capacitive reactances are practically negligible. 'Metlohm' resistors are available in the range 15 Ω to 250 kΩ, rated at 0.25 W.

### Inductance

Electronic inductors are coils of wire, wound on hollow (usually cylindrical) formers, and having inertia towards change of current flowing through them. Such a coil generates an opposition e.m.f. given by  $E = -L \cdot di/dt$ , where  $di/dt$  is the rate of change of the current flowing through the coil. This equation defines  $L$ , the self-inductance of the coil; a coil generating 1 V when  $di/dt$  is 1 amp per second has unit self-inductance of 1 Henry (H). When a steady voltage is applied to a circuit including inductance  $L$ , current builds up exponentially; the current  $i_t$  at time  $t$  after switching on is:

$$i_t = E/R \cdot [1 - \exp(-Rt/L)]$$

The final steady current is thus  $E/R$ ,  $E$  being the applied voltage, and  $R$  the ohmic resistance of the circuit. On switching off, the decay of current is also exponential, and  $i_t = E/R \cdot [\exp(-Rt/L)]$ .

† Both 'Fiberloy' and 'Metlohm' resistors are manufactured by Messrs. Painton & Co. Ltd., Kingsthorpe, Northampton. Moulded Metal Film Resistors are manufactured by The International Resistance Co., Philadelphia, Pa.

## LABORATORY AND PROCESS INSTRUMENTS

After a period of time  $(L/R)$  seconds,  $i$  has risen from zero to  $0.632 E/R$ , or has fallen from  $E/R$  to  $0.368 E/R$ ; this period is referred to as the *time constant*  $\tau$  of the circuit of which the inductor is a part (see Fig. 1.6). Thus, a coil of inductance 5 H, and resistance 100  $\Omega$ , forms a circuit of time constant 50 milliseconds; this time constant would be increased if there was an additional resistance in the circuit.

Small inductors, of 0.1 micro-henrys (or  $\mu\text{H}$ ) to 100 milli-henrys (or mH), have air cores; they are used in circuits tuned to

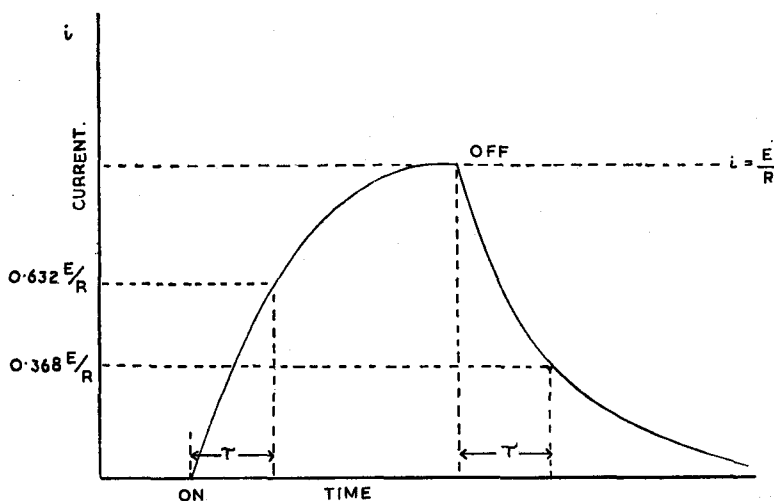


Fig. 1.6. Variation of current with time-series  $L$ - $R$  circuit, supply voltage  $E$  volts

resonate at high frequencies. Large inductors, up to 100 henrys or more, are wound on soft-iron formers, or employ one of the new ferromagnetic materials as core; they are used in filter circuits for low-frequency voltages. Such inductances are used in d.c. power-supply units working from an alternating voltage source.

Coils may be wound to a particular inductance, according to dimensions, permeability of core and number of turns. Ideally, the inductance  $L$  in henrys is given by:  $L = \mu 4\pi N^2 al \cdot 10^{-9}$ ,  $\mu$  being the permeability of the core,  $N$  the total number of turns,  $a$  the cross-sectional area, and  $l$  the length of the coil. However,

## COMPONENTS AND THEIR CHARACTERISTICS

the permeability depends upon the current passed through the coil; a short coil (one for which the ratio of length to diameter is less than 10) has a considerably smaller inductance than that predicted by the above equation, due to the depolarisation by its ends. A table of correction factors (Nagaoka's constant), and of the variation of inductance with current, is given in such works of reference† as Terman or Langford-Smith. These works also include details of multi-layer coils, which are much smaller for a given inductance than single-layer coils, and of toroidal coils (the shape of a ring doughnut). Co-axial cable, or 'feeder', introduces inductance (and capacitance) into the circuit, proportional to its length. Such cable is illustrated in Fig. 1.7.

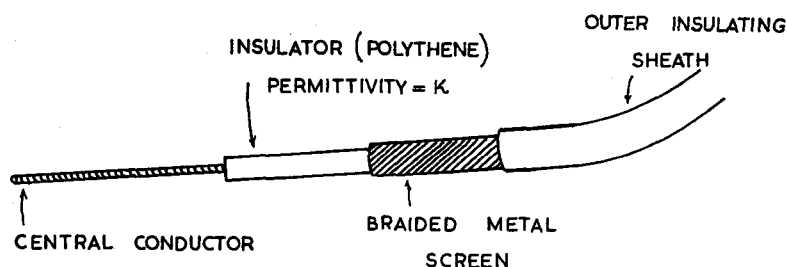


Fig. 1.7. Coaxial feeder. Capacitance =  $0.2416\kappa/\log r_1/r_2$  pF per cm; inductance =  $0.00461 \log r_2/r_1$   $\mu$ H per cm

Coils designed to limit currents of a particular range of frequencies are called 'chokes', and are rated according to inductance, current capacity (not necessarily that of the wire—the 'saturation-current' of the core‡) and resistance. Typical values are: for low-frequency chokes, from 3 H, 250 mA and 50  $\Omega$  to 40 H, 70 mA and 1200  $\Omega$ ; for high-frequency chokes, 14 mH, 10  $\Omega$  (iron-dust cored) (see Fig. 1.8).

It is obvious that a coil must introduce resistance into a circuit; less obviously, it must also introduce capacitance, referred to as the 'self-capacitance' of the coil. Thus a high-frequency coil may, due to its self-capacitance, constitute a resonant circuit (p. 39).

† For references, see p. 19.

‡ For 'saturation current', see p. 132.

## LABORATORY AND PROCESS INSTRUMENTS

For a combination of  $n$  inductors in series, without mutual coupling, the resultant inductance  $L_R = \sum_n L$ ; for combination in parallel  $1/L_R = \sum_n (1/L)$ . Where two coils  $L_1$  and  $L_2$  are in close proximity, particularly if they are wound on a common core as in the transformer, mutual coupling exists between them. The mutual inductance  $M$  is given by the equation  $M = k\sqrt{(L_1 L_2)}$ , where  $k$  is the *coupling factor*. Coupling modifies the resultant inductance of coils in series to:

$$L_R = L_1 + L_2 + \dots \pm 2M$$

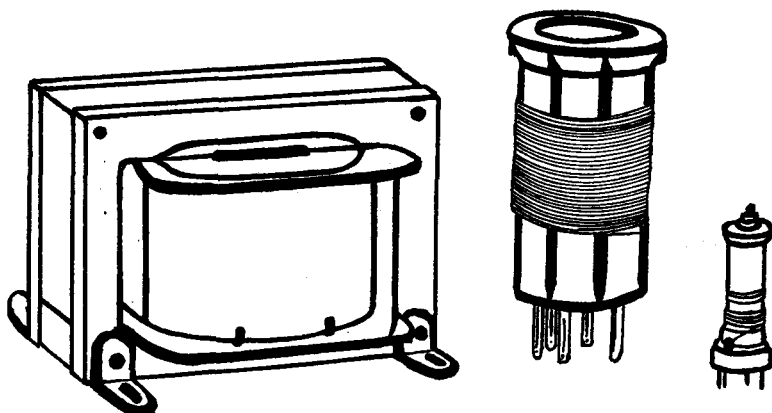


Fig. 1.8. Some typical inductors. Values left to right: 20 H, 73.5  $\mu$ H, 0.18  $\mu$ H

and of coils in parallel:

$$L_R = \frac{L_1 L_2 - M^2}{L_1 + L_2 \pm 2M}$$

according as the fields of the coils assist or oppose, which in turn depends on the relative direction of winding. Where coupling is unwanted it may be reduced practically to zero by screening the coils with earthed metal 'cans'.

### Capacitance

Capacitance is introduced into a circuit by an electrical 'condenser' or *capacitor*; the range of capacitors used in electronic circuits extends from about 1 micro-microfarad ( $1\mu\mu$ F, or 1

## COMPONENTS AND THEIR CHARACTERISTICS

pico-farad, 1 pF) to 1000  $\mu$ farads,  $\mu$ F. The capacitance may be of fixed value, or may be continuously variable. The capacity of a pair of plates of area  $A$  and distance  $d$  apart, separated by a medium of permittivity  $\kappa$  is given by:

$$C = \frac{\kappa A}{4\pi d} \times 1.1 \times 10^{-12} \text{ F}$$

where  $A$  is in  $\text{cm}^2$ , and  $d$  in cm. Hence, the larger the capacity, the larger the physical size of the capacitor; the size is also determined by the voltage at which the charge is stored.

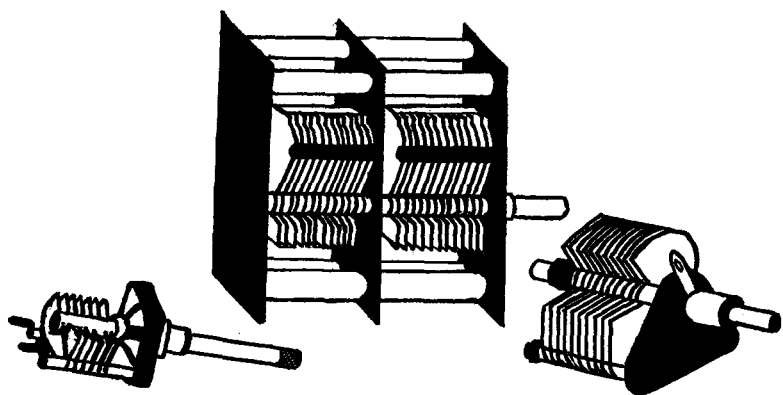


Fig. 1.9. Variable capacitors. Left to right: 50 pF trimmer, two-gang, 2 x 500 pF tuning capacitor, 150 pF variable capacitor

The medium between the plates is called the *dielectric*, and a useful classification of capacitors is in terms of the dielectric between the plates. Common dielectrics are air, mica, ceramics, paper and oil; an oxide film is used in the 'electrolytic' capacitors.

(i) *Air* ( $\kappa = 1$ ). These are mostly small variable capacitors. The plates may be shaped so that capacitance and angle of rotation are related, e.g. by a linear, or a logarithmic law (Fig. 1.9).

(ii) *Mica* ( $\kappa = 6$  approx.). These are usually small-capacity fixed or variable capacitors. The high dielectric strength, and ability to maintain the charge for a long period, i.e. the so-called 'low loss', together with the low temperature-coefficient, render them suitable for high voltages, and as secondary standards. 'Silver mica' capacitors, in which are stacked thin (1-mil) mica

## LABORATORY AND PROCESS INSTRUMENTS

sheets, sprayed with finely divided silver, are the most accurate of the mass-produced varieties. The silver layer is very thin, so that these capacitors are less suitable than paper or electrolytics, where large ripple currents are met with.

(iii) *Ceramics*. The dielectric constant for ceramics is variable, depending on the material, temperature, amplitude and frequency of the applied voltage. The dielectric strength is high, and suitable ceramics are available for very high frequencies.

(iv) *Paper* ( $\kappa = 2.5$  approx. for waxed paper). The dielectric strength of paper is high, so that very thin sheets may be used. For example, two strips of metal foil, each of dimensions 20 ft  $\times$  3.0 in.  $\times$  0.0005 in., separated by a waxed-paper strip 20 ft  $\times$  3.5 in.  $\times$  0.0005 in., form a capacitor of  $2\mu\text{F}$  capacity, and able to withstand a p.d. of 500 V. The strips may be folded into a very small bundle.

(v) *Oil* ( $\kappa$  less than 10). Generally, oil-filled capacitors are intended for high-voltage operation (10 kV or more), with capacitance 0.01 to 1.0  $\mu\text{F}$ ; they are used, for example, in the power supplies of cathode ray tube circuits, and in 'flash-tube' circuits used in photography.

(vi) *Oxide-film dielectric*. In practice the film is of aluminium oxide,  $\text{Al}_2\text{O}_3$ , formed on a very pure aluminium anode by the electrolysis of a suitable solution, e.g. ammonium borate. This film is very thin, and although it may appear that it would puncture easily this is not serious because a small amount of electrolysis then occurs, leading to 'healing' of the film. These capacitors are called 'electrolytics'; they are usually polarised—i.e. they must be correctly orientated in the circuit, as regards polarity, like a d.c. meter. However, some electrolytics contain two formed anodes, in which case polarity need not be observed. There are three main types of 'electrolytics':

*Wet type*. These have a rigid anode. The cathode is the outside 'can', containing the electrolyte, and a rubber gas-vent is fitted.

*Semi-dry type*. Two aluminium foil strips are separated by a gauze 'spacer', impregnated with boric acid-glycerol. The foils are the electrodes, often isolated from the can.

*Dry type*. As for the semi-dry, but incorporating a solid electrolyte, e.g. boric acid and gum in alcohol.

Electrolytic capacitors have rather high leakage currents; however, they can be made very compact; a (32+32)  $\mu\text{F}$  (i.e.

## COMPONENTS AND THEIR CHARACTERISTICS

two separate sections each of  $32 \mu\text{F}$ ), rated at 500 V, may be contained in a 1 in. diameter cylinder, 2 in. in length. The actual anode surface area is about  $500 \text{ in}^2$ .

In a new type of electrolytic capacitor an oxide-film dielectric is formed on a tantalum anode, sulphuric acid being the electrolyte. Such capacitors operate satisfactorily at very low temperatures, and their size is considerably reduced from that of standard electrolytic capacitors. The size reduction makes them particularly suitable for use in portable equipment employing transistors; the voltage rating is at present limited to about 100 V, but high-voltage operation is not required in this application.

After a period of storage, electrolytic capacitors may need re-forming, by connecting them for a time to a d.c. source, well below the rated maximum voltage, and with due regard to polarity.

The polarity of electrolytic capacitors is usually indicated in a circuit diagram. Thus, in Fig. 5.17, the 'rectangular' plate of  $C_4$  is the positive, a single line representing the negative plate. Sometimes, polarities are assigned by '+' and '-' signs.

A range of ceramic materials incorporating barium titanate is now available, having very high dielectric strength (i.e. resistance to break down under charged conditions), and with permittivities as high as 4000; most alumina ceramics have dielectric constants of 2-3. These materials are suitable for capacitor dielectrics, since they are not polarised, do not deteriorate on storage, and may be used at ambient temperatures up to  $100^\circ\text{C}$ . The resulting capacitors are very compact.

Two capacitors in series have a resultant capacitance  $C_R$  less than either:  $C_R = C_1 C_2 / (C_1 + C_2)$ . However, the voltage rating is higher than that of either capacitor alone. The capacitances of capacitors in parallel are additive:  $C_R = C_1 + C_2$ . The voltage rating of the combination, however, is the lower of the ratings of the separate components.

There is a colour code for capacitors, but it is not so universally employed as for resistors. Three 'dots' of colour are read in the direction of an engraved arrow; the first dot gives the first figure, the second the number of zeros (giving the capacity in  $\mu\mu\text{F}$ ), and the third the voltage rating. The same code applies as for resistors.

### Capacitance in a D.C. Circuit

When a capacitor is connected to a source of direct current, such as a battery, current initially flows in the circuit. This current dies away with time exponentially; similarly, the charge on the capacitor, and the voltage across it (which opposes the voltage of the battery) increase exponentially to their final values. The law of build-up of charge is:

$$q_t = CE \cdot [1 - \exp(-t/CR)]$$

where  $C$  is the capacitance,  $E$  the battery voltage and  $R$  the resistance of the circuit. The last term includes the resistance of the wire and the internal resistance of the battery, as well as any added resistance: thus, it is never zero. If  $C$  is in farads and  $E$  in volts, the charge built up  $t$  seconds after switching on,  $q_t$ , is given in coulombs. Similarly, the voltage across the condenser after time  $t$  will be given by

$$e_t = E \cdot [1 - \exp(-t/CR)]$$

The factor  $(CR)$  is the time-constant  $\tau$  of the circuit; with  $C$  in farads and  $R$  in ohms,  $\tau$  has the units of seconds. Just as in the case of inductance, after a time  $\tau$  the rising parameter (in this case charge or voltage) has attained 0.632 of its ultimate value.

If the charged capacitor is allowed to discharge through a total resistance  $R$ , the charge and voltage fall exponentially, so that, for example,  $e_t = E \cdot \exp(-t/CR)$ . These relationships are shown in Fig. 1.10. Some values of  $\tau$  are as follows:

$C$	$R$	$\tau$
50 $\mu\text{F}$	10 $\text{k}\Omega$	0.5 $\mu\text{second}$
50 $\mu\text{F}$	1 $\text{M}\Omega$	50 $\mu\text{seconds}$
8 $\mu\text{F}$	10 $\text{k}\Omega$	80 $\text{m-seconds}$
8 $\mu\text{F}$	1 $\text{M}\Omega$	8 $\text{seconds}$

Many timing circuits, such as those which control the horizontal movement of the spot of light on a cathode ray tube screen, make use of this ability to vary the charging time of a capacitor by varying the resistance in series with it.

A capacitor of capacitance  $C$  farads, charged to a potential  $V$  volts, stores a charge  $Q$ , equal to  $(CV)$  coulombs, and energy  $(\frac{1}{2}CV^2)$ , or  $(\frac{1}{2}Q^2/C)$ , joules. For example, a 100  $\mu\text{F}$  capacitor at



## COMPONENTS AND THEIR CHARACTERISTICS

5 kV stores a charge of 0.5 coulomb and 1250 joules energy. This is the equivalent of about 300 calories, and may be used to produce energetic radiation such as is used in flash-photolysis experiments.

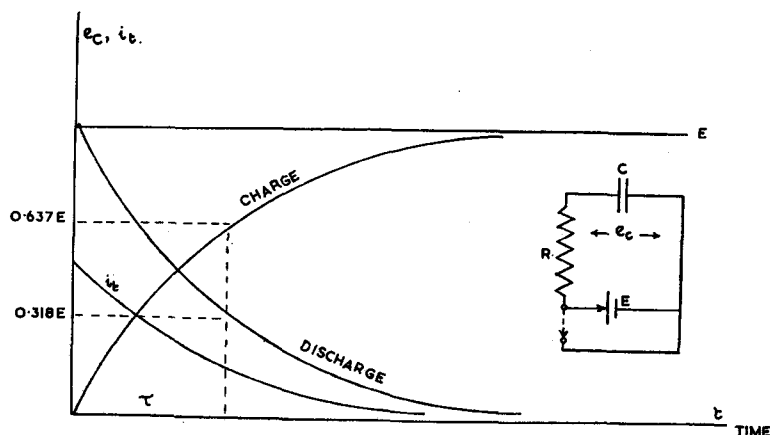


Fig. 1.10. Charge and discharge of capacitor  $C$  through resistor  $R$ . Supply voltage  $E$  volts

## Inductance, Capacitance and Resistance in Series in D.C. Circuits

Suppose we set up the circuit of Fig. 1.11 and put the switch to position 1. Then the variation with time of the charge stored in the capacitor is as shown in this figure.

If the resistance is large, so that  $R^2 > 4L/C$ , the broken curve is followed, and  $q_i$  rises to its final value rather as in the case of a simple  $C$ - $R$  circuit. But if the resistance is small, so that  $R^2 < 4L/C$ , the full curve is followed, showing that the charge oscillates about its ultimate value, becoming steady only after a comparatively long period of time. The oscillations resemble those set up in a vibrating string; their amplitude decreases with time, but their period remains constant. They are in fact damped oscillations of decrement  $e^{-Rt/2L}$ , and period  $T = 2\pi / \sqrt{(1/LC - R^2/4L^2)}$  seconds. The inverse of  $T$  is the frequency,  $f$ , i.e.  $f = 1/2\pi \cdot \sqrt{(1/LC - R^2/4L^2)}$  cycles per second (c/s). If  $R \ll 4L^2$ ,  $f \approx 1/2\pi \cdot \sqrt{(1/LC)}$  per second. Thus, if  $L = 10$  mH and  $C = 0.1$   $\mu$ F,  $f = 5$  kilocycles per second (kc/s).

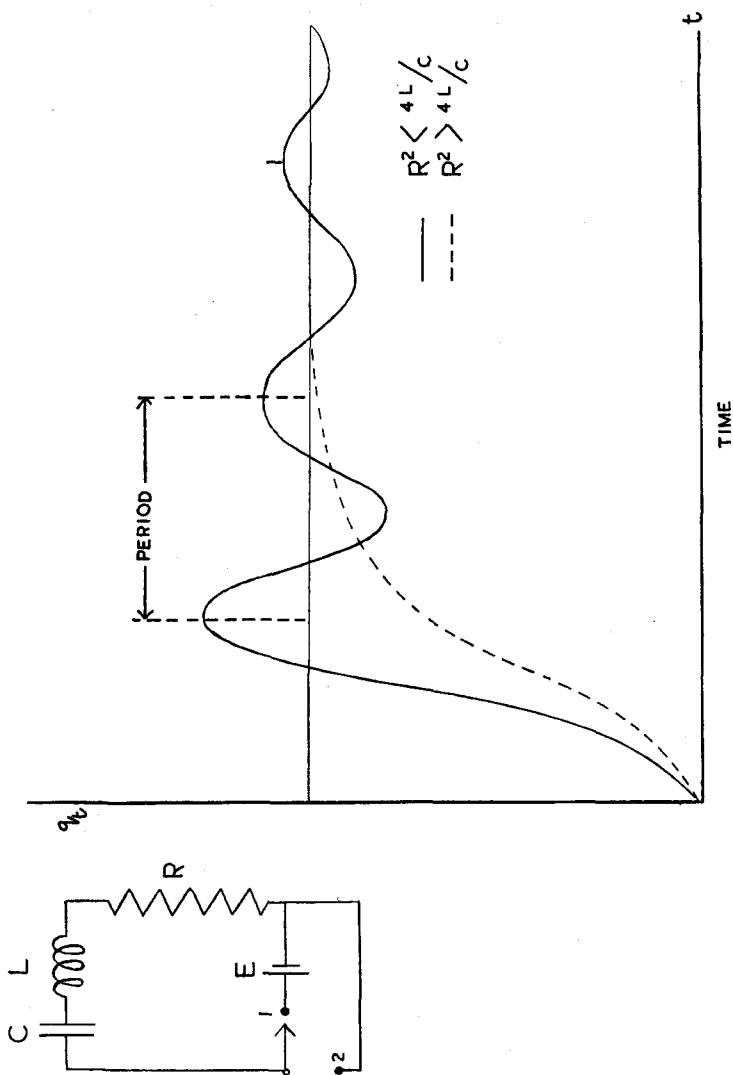


Fig. 1.11. Charge-time relationship for the  $L$ - $C$ - $R$  series circuit. Oscillatory, and damped, charging of a capacitor

## COMPONENTS AND THEIR CHARACTERISTICS

If after the capacitor has become charged the switch is moved to position 2, the decay of charge or capacitor voltage follows one or other of the curves of Fig. 1.12. Again, the broken curve, showing a steady decay towards zero, corresponds to  $R^2 > 4L/C$ , and the full curve, showing oscillatory decay, to  $R^2 < 4L/C$ .

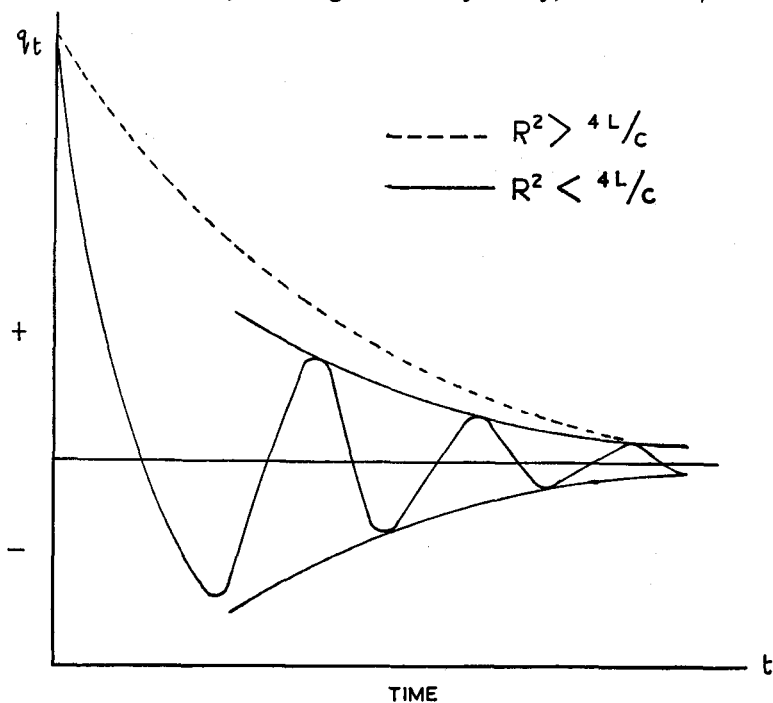


Fig. 1.12. Discharge-time relationship for the  $L$ - $C$ - $R$  series circuit. Oscillatory and damped, discharge of a capacitor

If  $R$  were zero, the oscillations would be undamped, and constant amplitude maintained. This is never the case; but, as we shall see later, the thermionic valve oscillator is able to make up for the loss, and produce constant-amplitude oscillations. A limiting case arises when  $R^2 = 4L/C$ ; in the previous example this corresponds to  $R = 630 \Omega$ . This is the critical condition for oscillation, and the circuit is said to be *critically damped*.

The reason for oscillatory charge or discharge lies in the periodic interchange of energy between the capacitor and the inductor. The initial current flow sets up a field round the coil,

## LABORATORY AND PROCESS INSTRUMENTS

which in collapsing adds to the strain in the capacitor dielectric, and the charge rises above the maximum which the battery can maintain. As this excess charge dies away the reversed current again builds up a field, and the process is repeated, but with diminished amplitude, due to energy lost through heating the resistance. For a complete mathematical analysis of the problem see the references at the end of this chapter.

### NOTES

A useful construction for determining the resultant of two resistors or inductors in parallel, or of two capacitors in series, is shown in Fig. 1.13.

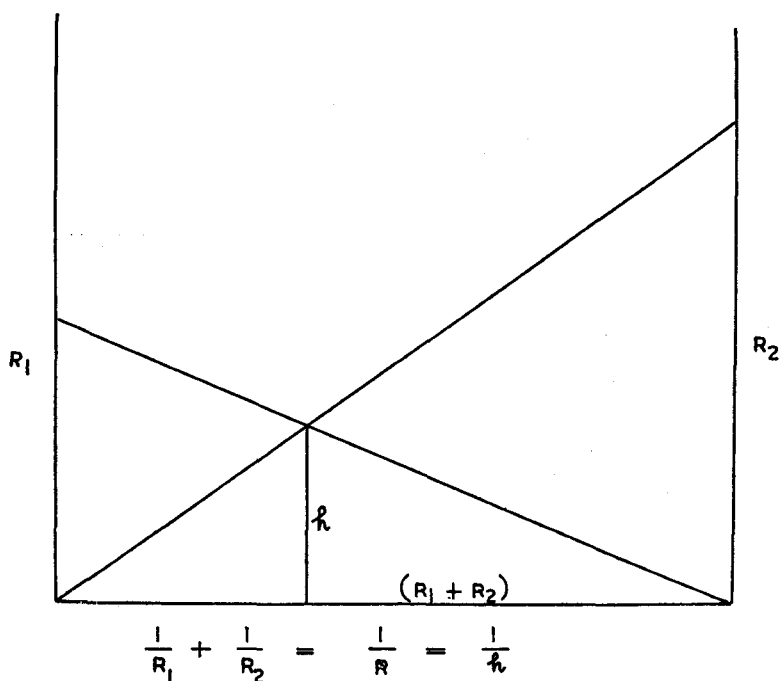


Fig. 1.13. Resultant of two resistors or inductors in parallel, or of two capacitors in series

The left-hand ordinate is  $R_1$  (or  $L_1$  or  $C_1$ ); the right-hand ordinate is  $R_2$  (or  $L_2$  or  $C_2$ ); and the abscissa is  $R_1 + R_2$  (or  $L_1 + L_2$ , or  $C_1 + C_2$ ). The diagonals from  $R_1$  and  $R_2$  intersect at a

## COMPONENTS AND THEIR CHARACTERISTICS

point whose height above the abscissa is  $h$ ; then  $h$  is the reciprocal of the resultant,  $R_1 R_2 / (R_1 + R_2)$ , etc., i.e.  $1/R_1 + 1/R_2 = 1/h$ . The construction is the same as that for the determination of the focal length of a lens, from object and image distance measurements.

### References

- GEORGIEV, A. M. (1945). *The Electrolytic Capacitor*. Murray Hill.  
LANGFORD SMITH, F. (Ed.) (1953). *Radio Designer's Handbook*, 4th edition. Iliffe.  
SCROGGIE, M. G. (1954). *Radio Laboratory Handbook*, 6th edition. Iliffe.  
SMITH, C. E. (1942). *Communication Circuit Fundamentals*. McGraw Hill.  
STARLING, S. G., and WOODALL, A. J. (1956). *Electricity and Magnetism for Degree Students*. Arnold.  
TERMAN, F. E. (1944). *Radio Engineer's Handbook*. McGraw Hill.

### Problems

1. A moving-coil meter of full-scale deflection  $100 \mu\text{amp}$  and internal resistance  $500 \Omega$  is to be used to measure (a)  $10 \text{ amp d.c.}$ ; (b)  $100 \text{ V d.c.}$

Calculate the resistance required, together with their power-ratings.

Answer. (a)  $0.005 \Omega$ ,  $0.5 \text{ W}$ . (b)  $1 \text{ M}\Omega$ ,  $0.01 \text{ W}$ .

2. A thermostat tank holds  $200 \text{ l.}$  of water. Find the wattage of a suitable heater required to raise the temperature from  $18^\circ\text{C}$  to  $25^\circ\text{C}$  in  $1 \text{ hour}$ .

Answer.  $1.6 \text{ kW}$ .

3. Calculate the inductance of a single-layer coil of wire of  $100$  turns, length  $10 \text{ cm}$  and mean radius  $5 \text{ cm}$ . What voltage is induced in the coil by a current changing at the rate of  $0.1 \text{ amp/second}$ ? (Nagaoka's constant for this coil:  $0.688$ .)

Answer.  $L = 678 \mu\text{H}$ ;  $e_{\text{S.I.}} = 67.8 \mu\text{V}$ .

4. Two capacitors of  $3 \mu\text{F}$  and  $5 \mu\text{F}$  are connected in series. Determine their joint capacitance, and the voltage and charge of each if the circuit includes a  $50 \text{ V}$  battery.

Answer.  $C = 1.875 \mu\text{F}$ ; charge  $= 93.75 \mu\text{coulombs}$ .  $V_1 = 31.25 \text{ V}$ ,  $V_2 = 18.75 \text{ V}$ .

5. Calculate the natural frequency of an  $L$ - $C$ - $R$  series circuit, having  $L = 1 \text{ mH}$ ,  $C = 1000 \mu\mu\text{f}$ ,  $R = 1000 \Omega$ . What extra resistance is required for critically damping this circuit?

Answer.  $f = 137 \text{ kc/s}$ ; extra resistance  $= 1000 \Omega$ .

6. Give an account of the electrical characteristics of the following components, and explain one use of each in an electronic circuit: electrolytic condenser, thermistor, line-cord, piezo-electric crystal.

## CHAPTER II

# Alternating Current

### Introduction

The electricity supply from a generating station, whether for industrial or domestic use, is almost always alternating current. The voltage and current change direction at regular intervals; two such changes restore the original direction and constitute a *cycle*. The number of cycles occurring per second is called the *frequency* of the supply. Alternating voltages are supplied by dynamos fitted with slip rings in place of the commutators of direct current (d.c.) machines. The supply mains in this and many Western European countries has a frequency of 50 c/s; in the U.S.A. the frequency is 60 c/s. The heating effect of an electric current is independent of the direction of current flow, since it is proportional to  $i^2$ ; however, the reading of a moving coil ammeter, or the product of an electrolysis, depends upon the polarity of the source. Again, as we shall see, a thermionic valve requires unidirectional supply voltages to be applied to anode and screen. Thus, for some purposes, we must change the alternating supply into a unidirectional one ('direct current', or d.c.) before using it, a process of conversion known as *rectification*. This is a disadvantage of alternating current, but it is enormously outweighed by the advantage of being able to raise or lower the voltage by a very simple device—the transformer (p. 65).

The generating station is able to produce its power at a convenient voltage, say 2000 V; this is sent across country at a much higher pressure, perhaps 220 kV, which may then be reduced, in stages, to the 1100 V of some electric railway systems, or the 240 V or so of our domestic supply. The advantage lies in the relationship:  $\text{power} = \text{current} \times \text{voltage}$ , so that the cross-country transmission involves only relatively small currents, with correspondingly small voltage drop and loss of power through the resistance of many miles of electric cable. Again, it is quite easy to convert the 240 V 'mains' alternating supply into 250 V d.c.

## ALTERNATING CURRENT

for a valve anode, or into the 6.3 V a.c. to heat its filament; the supply to a cathode ray tube, or to an ozoniser, requires a much higher voltage, but this also is readily obtainable. Most scientific instruments are designed to plug-in directly to the a.c. mains, and provide their own direct voltages, as necessary (p. 101).

The variation of voltage with time is sinusoidal; that is to say, the generator voltage at any instant is given by an expression of the form:  $e_t = E_m \cdot \sin 2\pi ft$ , where  $f$  is the frequency of the supply,  $e_t$  is the voltage at time  $t$  and  $E_m$  is the maximum value that the voltage attains at any point during the cycle—the voltage *amplitude*. From this equation,  $e_t = E_m$  when  $2\pi ft = 90^\circ$ , so that we are evidently counting time  $t$  from an instant of zero voltage. The term  $(2\pi f)$ , the *pulsatance*, is usually denoted by  $\omega$  so that  $\omega t$  represents the angular displacement of the voltage vector in radians, assuming that this was zero at time  $t = 0$ . If in fact the vector had an angular displacement  $\phi$  initially, we could show this by writing  $e_t = E_m \cdot \sin(\omega t + \phi)$ , and  $\phi$  is called the *phase* of this voltage. Unless otherwise stated, such phase-angles will be expressed in *radians*. In this case,  $e_t$  attains its maximum value,  $E_m$ , when  $\omega t = (\pi/2 - \phi)$ . It should be noted that at three points in the cycle the voltage is zero, and that on average, it is just as often negative as positive throughout a complete cycle. This is why a moving-coil meter would not respond to an alternating voltage even of a frequency of 50 c/s.

Theoretically, we can regard such alternating voltages as the low-frequency end of the electromagnetic spectrum, extending from such frequencies, via regions variously designated 'radio', 'heat', 'light', into the X-rays. All these phenomena are propagated with a constant velocity, because they are all alike in origin; this velocity, sometimes called the velocity of light, has the value  $3 \times 10^{10}$  cm per second, *in vacuo*. Now for any wave motion, we have the relationship: velocity of propagation = frequency  $\times$  wavelength. Consequently the wavelength,  $\lambda$ , in centimetres, is given by  $\lambda = 3 \times 10^{10}/f$ , where  $f$  is the frequency in cycles per second. The frequency, and therefore the wavelength, extend over a very wide range throughout the electromagnetic spectrum; this is illustrated in Fig. 2.1, where logarithmic scales are employed.

In electronics, including communications and the relatively new field of micro-wave instruments, we are interested in a small

## LABORATORY AND PROCESS INSTRUMENTS

part of the complete spectrum; nevertheless, we cover a comparatively wide range of wavelengths. The wavelength of the London Home Service transmitter is 330 metres, that of the B.B.C. V.H.F. is about 3.3 metres, whilst radar during the 1939-45 War used 10 cm and 3 cm wavelengths. Modern micro-wave spectroscopy starts in this region, and has now reached millimetre wavelengths. The 'electronic' spectrum may be sub-divided roughly as follows:

Audio or low frequencies (A.F. or L.F.)	30 c/s to 15 kc/s
Intermediate frequencies (I.F.)	110 kc/s to 465 kc/s
Radio frequencies (R.F.)	500 kc/s to 30 mc/s.

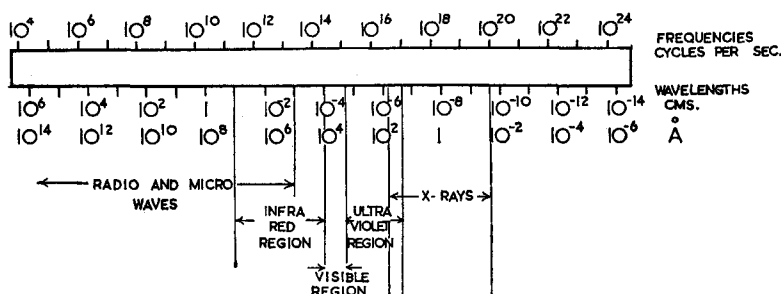


Fig. 2.1. The electromagnetic spectrum

Audio frequencies are mainly used in the determination of electrolyte conductances, and in bridge measurements involving reactances.

Intermediate frequencies are employed for the major part of the amplification in radio receivers of the superheterodyne type.

Radio frequencies are employed in some bridge measurements, in certain 'electrodeless' conductance comparisons, and in nuclear magnetic resonance measurements.

Very much higher frequencies up to 30,000 Mc/s are used in paramagnetic resonance measurements, and in micro-wave spectroscopy. They involve quite different principles of generation, transmission and measurement from those frequencies already mentioned, and we cannot consider here the new techniques involved.



## ALTERNATING CURRENT

### The Measurement of Alternating Currents and Voltages

The average value over one complete cycle of a sinusoidal voltage, which may be represented:

$$e = E_m \sin \omega t$$

(where  $e$  is the instantaneous value of the voltage; the subscript  $t$  has been discarded) is evidently zero, so that any instrument which responds to this average value, such as a moving-coil voltmeter connected to 50 c/s supply will fail to register. The inertia of the electron beam of a cathode ray oscilloscope is very low, so that the 'spot' is able to trace out the waveform—here again, however, its average displacement over one cycle is zero.

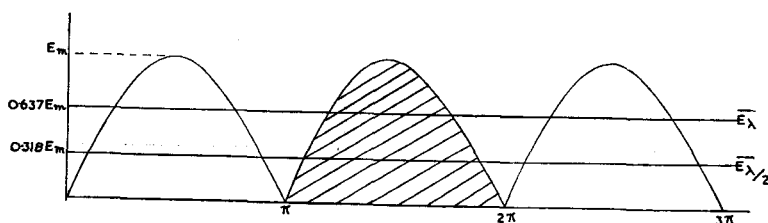


Fig. 2.2. Full-wave and half-wave rectification of a sinusoidal voltage,  
 $e = E_m \sin \omega t$

A full-wave rectifier (or  $\lambda$ -rectifier) (p. 104) makes the voltage pulses unidirectional, so that there is now an average voltage,  $\bar{E}$  to which the meter may respond. This average voltage is given by:

$$\begin{aligned} \bar{E} &= \frac{E_m}{t} \int_0^t \sin \omega t \cdot dt = \frac{E_m}{\pi/\omega} \cdot \int_0^{\pi/\omega} \sin \omega t \cdot dt \\ &= \frac{E_m}{\pi} \cdot [-\cos \omega t]_0^{\pi/\omega} \end{aligned}$$

or  $0.637E_m$ , which value we denote by  $\bar{E}_\lambda$ . A moving-coil milliammeter responds to this value, if supplied via a full-wave rectifier. It should be noted that the integration is taken over one half-cycle, since this is exactly duplicated by the succeeding half-cycle (Fig. 2.2).

## LABORATORY AND PROCESS INSTRUMENTS

If the meter is supplied via a half-wave rectifier (a  $\lambda/2$  rectifier) the *original* - ve half-cycle (shown shaded in Fig. 2.2) is removed; the remaining voltage must now be averaged over a complete cycle, and hence:

$$\begin{aligned}\overline{E_{\lambda/2}} &= \frac{E_m}{2\pi/\omega} \cdot \int_0^{\pi/\omega} \sin \omega t \cdot dt \\ &= E_m/\pi \quad \text{or} \quad 0.318E_m\end{aligned}$$

Although, therefore, the supply voltage is the same, the meter reading has dropped to one-half its previous value.

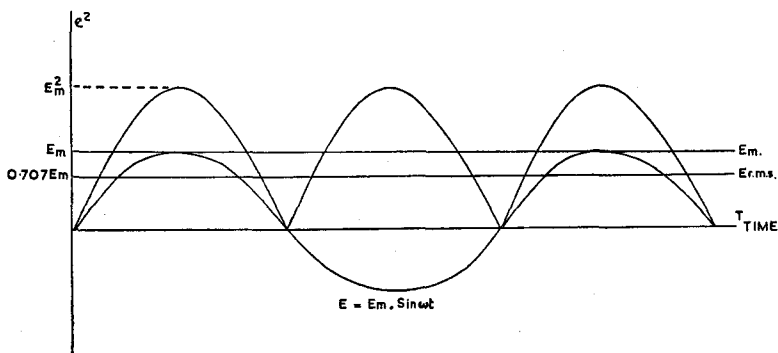


Fig. 2.3. Root-mean-square value of a sinusoidal voltage of amplitude  $E_m$

For many practical purposes, we are interested in the average of the voltage irrespective of its sign, i.e. in  $\sqrt{\overline{E^2}}$ . Now

$$\begin{aligned}\overline{E^2} &= \frac{E_m^2}{\pi/\omega} \cdot \int_0^{\pi/\omega} \sin^2 \omega t \cdot dt \\ &= E_m^2 \cdot \frac{\omega}{2\pi} \cdot \int_0^{\pi/\omega} (1 - \cos 2\omega t) \cdot dt \\ &= \frac{E_m^2 \omega}{2\pi} \cdot [t]_0^{\pi/\omega} = \frac{E_m^2}{2}\end{aligned}$$

Hence  $\sqrt{\overline{E^2}} = \frac{E_m}{\sqrt{2}} \quad \text{or} \quad 0.707E_m$

These voltages are shown in Fig. 2.3.  $\sqrt{\overline{E^2}}$  is a very important quantity, known as the *Root Mean Square* (r.m.s.) voltage of the

## ALTERNATING CURRENT

supply; the r.m.s. values of current and voltage are represented by capital letters without subscript, thus:  $I$ ,  $E$ .

A direct voltage  $V$  applied across a conductor of resistance  $R$  would dissipate power at the rate of  $V^2/R$  watts; a sinusoidal alternating voltage will dissipate power *at the same rate* if its r.m.s. value is also  $V$ , i.e. if  $E_m = V/0.707 = 1.404 V$ . Because of its importance, it is the r.m.s. value which most measuring instruments record, although, as we have seen, a moving-coil meter with a rectifier 'sees' either  $0.637E_m$ , or  $0.319E_m$ . This is a simple matter, because there is a linear relationship between these voltages:

$$E = 0.707E_m; \overline{E_\lambda} = 0.637E_m$$

$$E = E_\lambda \times \frac{0.707}{0.637} = 1.110\overline{E_\lambda}$$

Exactly the same considerations apply to a sinusoidal alternating current flowing in a circuit. Consider a voltage represented by  $e = 50 \sin 100\pi t$  (i.e. a voltage of amplitude 50 V and of frequency 50 c/s, so that  $\omega$  is  $100\pi$ ) applied to a resistance of 100  $\Omega$ . Here,  $f = 50$  c/s,  $E_m = 50$  V. Tabulating the results:

$E_m$	$\overline{E_\lambda}$	$\overline{E_{\lambda/2}}$	$E$ (r.m.s.)	
50	31.85	15.93	35.35	(volts)
$I_m$	$\overline{I_\lambda}$	$\overline{I_{\lambda/2}}$	$I$ (r.m.s.)	
0.5	0.319	0.159	0.354	(amp)

and power dissipated,  $P = 12.50$  W.

Frequently, alternating and direct currents flow in the same circuit—for example, in the anode load of a thermionic valve. If the total instantaneous current  $i = I_1 + I_m \sin \omega t$ , where  $I_1$  is the direct component,

$$i^2 = I_1^2 + I_m^2 \sin^2 \omega t + 2I_1 I_m \sin \omega t$$

Since the first term is constant, the second has been shown to have the average value  $I_m/2$ , and the product term has an average value of zero over one cycle, the mean current during one cycle is:

$$\sqrt{\overline{i^2}} = \sqrt{(I_1^2 + I_m^2/2)}$$

# LABORATORY AND PROCESS INSTRUMENTS

i.e.  $I$  (r.m.s. value)  $= \sqrt{(I_1^2 + I_m^2/2)}$ . For example, if a 12 V accumulator is included with the previous voltage generator and resistor, as shown in Fig. 2.4, we have:

$$I_1 = 12/100 = 0.12 \text{ amp}$$

$$I_m = 50/100 = 0.5 \text{ amp}$$

$$I = \sqrt{\left((0.12)^2 + \frac{0.5^2}{2}\right)} = 0.373 \text{ amp}$$

It is generally the r.m.s. value which is quoted for an alternating voltage or current. '230 V, 50 c/s' thus represents a voltage of peak value  $230 \times 1.404 = 285 \text{ V}$ , and the insulation must be able

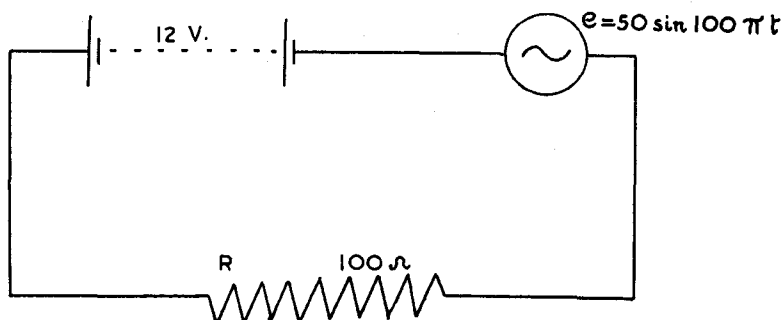


Fig. 2.4. D.C. and a.c. generators in series, in a resistive circuit

to withstand this peak voltage; the instantaneous voltage is given by:  $e = 285 \sin 100\pi t$ .

The relationships between r.m.s. and peak values of voltage, and  $\overline{E}_\lambda$  and  $\overline{E}_{\lambda/2}$  depend upon the waveform. If, for example, we apply the previous analysis to a 'square' waveform (Fig. 2.5), the following results are obtained:  $\sqrt{e^2} = E$  (r.m.s.)  $= E_m$  and  $\overline{E}_\lambda = E_m$ ,  $\overline{E}_{\lambda/2} = E_m/2$ .

The ratio  $E/\overline{E}_\lambda$ , or of  $I/\overline{I}_\lambda$ , is called the *form factor* of the supply voltage. For sinusoidal  $e$  and  $i$  it has the value 1.110; for square waves it is unity. The so-called constant voltage transformer (p. 107) supplied from a sinusoidal generator, produces across the secondary winding a voltage which is not sinusoidal, but 'flat-topped'. A moving coil meter with rectifier may, because of its form factor, register 6% too high a voltage.

## ALTERNATING CURRENT

The hot-wire ammeter is deflected as a result of the heating effect of the current, and so responds to  $I(\text{r.m.s.})^2$ . The moving-iron meter also responds to  $I^2$ , so that both of these are non-linear instruments with respect to current.

Radio-frequency currents are usually measured by a thermocouple meter. The thermocouple elements are spot-welded to a fine-gauge heater wire, and the thermal e.m.f. recorded by a d.c. milliammeter. The combination is again non-linear. The heater wire is easily burnt out by overload, and such instruments must be treated with great care.†

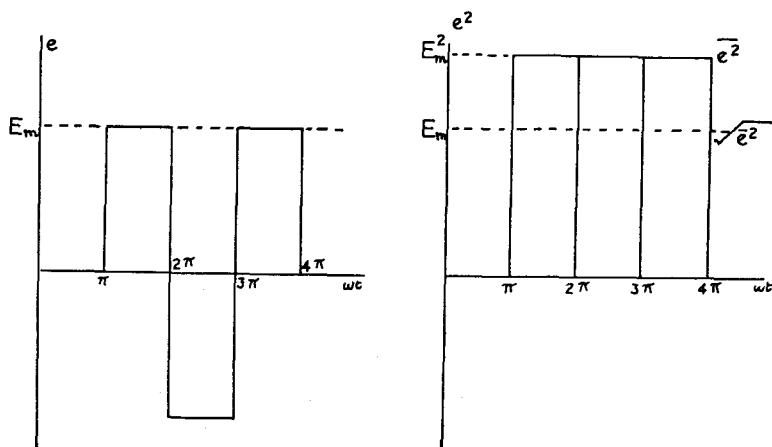


Fig. 2.5. Square-wave voltage, amplitude  $E_m$ :  $e$ ,  $e^2$  and  $\overline{e^2}$

### Resistance, Capacitance and Inductance in Alternating Current Circuits

(i) *Resistance*. Provided that the frequency is not too high, a resistor behaves similarly towards both direct and alternating currents. The power dissipated in it is  $RI^2$ ,  $I$  being the direct current or the r.m.s. value of the alternating current.

If the applied voltage is

$$e = E_m \sin \omega t$$

the resultant current is

$$i = I_m \sin \omega t$$

† See first reference, p. 51, at end of this chapter, concerning meters.

# LABORATORY AND PROCESS INSTRUMENTS

where  $E_m = RI_m$ , and the current and voltage are therefore *in phase* (Fig. 2.6).

When the frequency is very high however, a rapidly alternating field is set up inside the conductor, which repels the 'mobile' electrons towards the outer layers. The effective cross-sectional area of the conductor is therefore reduced, and its resistance is increased. The increase in resistance of a conductor with increase in frequency of the voltage applied to it, is called the *skin effect*;

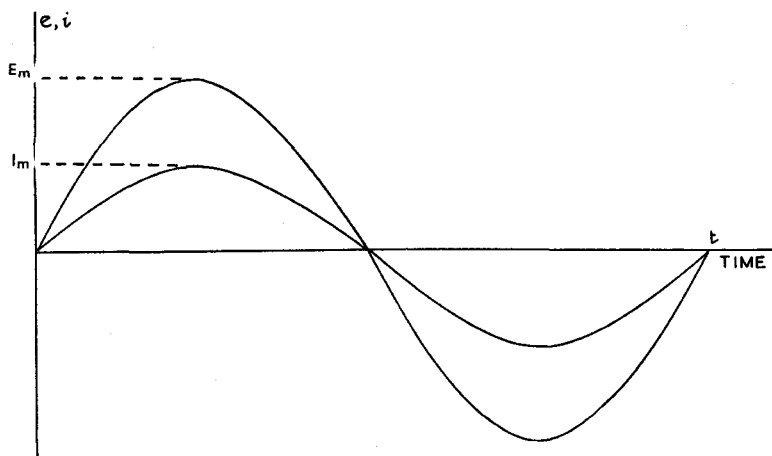


Fig. 2.6. Alternating voltage and current relationships in a resistive circuit

it becomes appreciable above about 100 kc/s. As an example, 56.5 cm of copper wire of gauge 35 has a resistance of 1  $\Omega$  towards direct current. The resistance increases with frequency as follows:

$f$ (c/s)	$R$	Percentage increase
$10^4$	1.000	—
$10^5$	1.003	0.3
$10^6$	1.317	31.7
$10^7$	32.7	3270

The increase is seen to be  $\propto f^2$ . It is much greater for a conductor of small cross-sectional area, such as the wire considered, than for a carbon resistor of perhaps 0.3 cm radius. Even carbon

## ALTERNATING CURRENT

resistors, however, show an increase in resistance above the nominal value at high frequencies.

(ii) *Inductance*. Suppose a current, represented by

$$i = I_m \sin \omega t$$

flows through an inductor of  $L$  henrys which has negligible resistance. An e.m.f. is induced,  $e_{s.i.}$ , of value:

$$\begin{aligned} e_{s.i.} &= -L \cdot di/dt = -\omega L \cdot I_m \cos \omega t \\ &= \omega L I_m \sin(\omega t - \pi/2) \end{aligned}$$

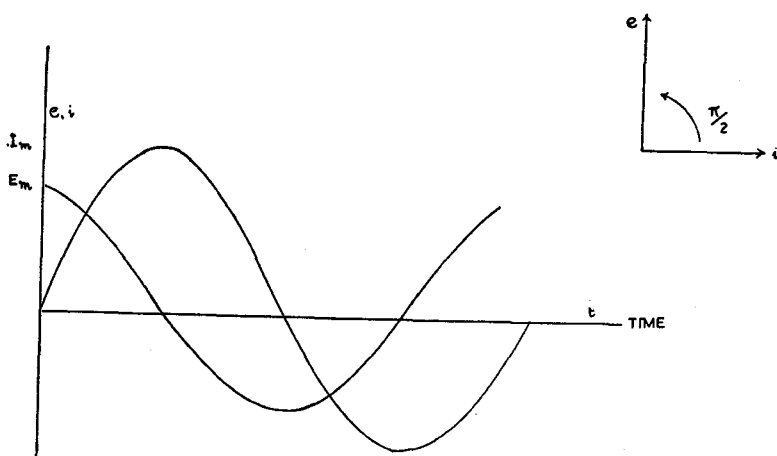


Fig. 2.7. Alternating voltage and current relationships in a purely inductive circuit. Vector diagram

The induced e.m.f. thus *lags* behind the current by  $\pi/2$ . Now the current  $i$  is maintained by the applied e.m.f.  $e$ , which just balances the 'back-e.m.f.'  $e_{s.i.}$ . Since

$$e_{s.i.} = -\omega L I_m \cos \omega t$$

$$e = \omega L I_m \cos \omega t$$

$$= \omega L I_m \sin(\omega t + \pi/2)$$

and the applied voltage *leads* the resultant current by  $\pi/2$ . In this case current and voltage are out of phase by  $\pi/2$ , as shown in Fig. 2.7.

## LABORATORY AND PROCESS INSTRUMENTS

The amplitude of the current is  $I_m$ ; that of the voltage is  $\omega LI_m$ , i.e.  $E_m = \omega LI_m$ ; we could express the voltage-current relationship in this circuit in the alternative form:

$$e = E_m \sin \omega t$$

$$i = \frac{E_m}{\omega L} \sin(\omega t - \pi/2)$$

We may compare the term:  $E_m/(\omega L)$ , with that for the current in a resistive circuit:  $E_m/R$ . Evidently,  $\omega L$  behaves rather similarly to  $R$  in determining the current which results from the application of a given voltage; it is called the *reactance* (symbol  $X_L$ ) of the

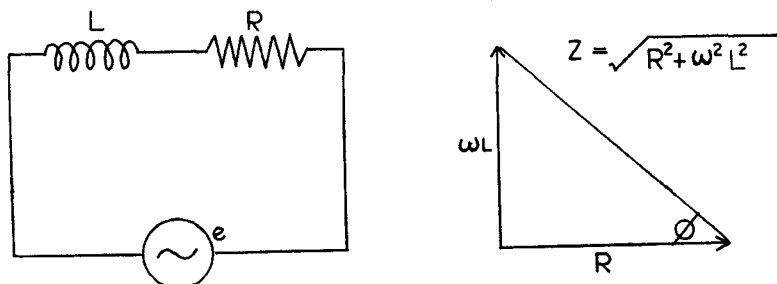


Fig. 2.8. The  $L$ - $R$  series circuit, with sinusoidal supply voltage,  $e = E_m \sin \omega t$ . Impedance diagram

coil, and its value varies directly with frequency.  $X_L$  is measured in *ohms*; for example, a 0.1 H coil has a reactance of 31.5  $\Omega$  at 50 c/s, which increases to 630  $\Omega$  at 1000 c/s. Unlike resistance, however, the reactance does not give rise to heating, and consequently to power loss. Energy is stored in the magnetic field of the coil, and returned to the generator when this field collapses; and  $i = \frac{E_m}{\omega L} \sin \omega t$ , is called a *wattless* current. The question of power in reactive circuits in general will be dealt with later (p. 45).

An actual inductor will have a resistance, so that it may be represented by a series  $L$ - $R$  combination. Now in a purely resistive circuit,  $e$  and  $i$  are in phase, whilst in a purely inductive circuit,  $e$  leads  $i$  by  $\pi/2$ , i.e. voltage and current are in *phase*



## ALTERNATING CURRENT

*quadrature*. We might expect, then, that in a circuit containing both resistance and inductance,  $e$  will lead  $i$ , but by a phase-angle  $\phi$  between  $0^\circ$  and  $90^\circ$  ( $\pi/2$  radians). If

$$e = E_m \sin \omega t, \quad i = I_m \sin(\omega t - \phi).$$

The applied e.m.f.  $e$  overcomes the e.m.f. of self-inductance of the coil, and also produces a voltage across the resistance, i.e.

$$e = e_R - e_{S.I.}$$

$$E_m \sin \omega t = RI_m \sin(\omega t - \phi) + \omega LI_m \cos(\omega t - \phi)$$

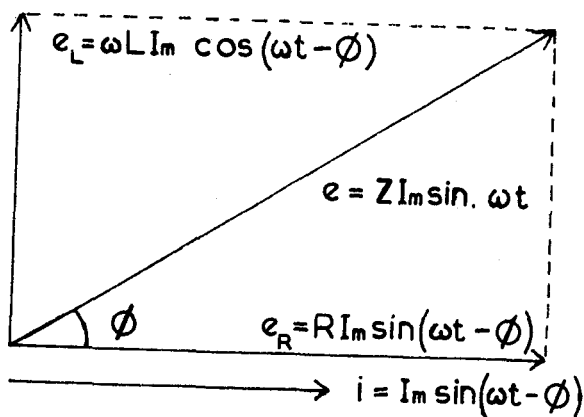


Fig. 2.9. Voltage and current diagram, series  $L$ - $R$  circuit

This is the equation of the  $L$ - $R$  series circuit shown in Fig. 2.8. To evaluate  $\phi$ , we put ( $t = 0$ ); then

$$0 = -RI_m \sin \phi + \omega LI_m \cos \phi, \quad \text{so that } \phi = \tan^{-1} \omega L/R$$

To evaluate  $I_m$ , put ( $t = \phi/\omega$ ), so that ( $\omega t - \phi$ ) = 0; then

$$E_m \sin \phi = \omega LI_m$$

Now

$$\sin \phi = \omega L / \sqrt{R^2 + \omega^2 L^2}$$

hence

$$I_m = E_m / \sqrt{R^2 + \omega^2 L^2}$$

The analogue of reactance for this circuit is a composite term, the vector sum of resistance  $R$  and reactance  $\omega L$ , called the

# LABORATORY AND PROCESS INSTRUMENTS

*impedance* (symbol  $Z$ ), also measured in ohms. A complete expression for the current flowing in the circuit is:

$$i = \frac{E_m}{Z} \cdot \sin(\omega t - \phi)$$

where

$$Z = \sqrt{(R^2 + \omega^2 L^2)}$$

and

$$\phi = \tan^{-1} \omega L / R$$

the angle by which the current lags behind the voltage (Fig. 2.8).

## Example

In the circuit illustrated in Fig. 2.8, if  $L = 0.1$  H,  $R = 493 \Omega$  and  $e = 10 \sin(2000\pi t)$ :

$$\begin{aligned} Z &= \sqrt{[(493)^2 + (2000\pi \times 0.1)^2]} \quad (\text{i.e. } f = 1000 \text{ c/s}) \\ &= \sqrt{[(493)^2 + (630)^2]} \\ &= 800 \Omega \end{aligned}$$

$$\phi = \tan^{-1} \frac{(2000\pi \times 0.1)}{493} \simeq 0.9 \text{ radian, or } 51.9^\circ$$

$$I_m = \frac{E_m}{Z} = \frac{10}{800} = 12.5 \text{ mA}$$

Power dissipated in the resistance,  $P$  watts,

$$\begin{aligned} &= R \times (\text{r.m.s. current})^2 \\ &= R \times (I_m \times 0.707)^2 \\ &= 493 \times \frac{(12.5 \times 0.707)^2}{(1000)} \end{aligned}$$

i.e.  $P = 38.5 \text{ mW}$ .

(iii) *Capacitance*. If a voltage  $e = E_m \sin \omega t$  is applied to a capacitor of capacitance  $C$  farads, and of zero resistance, the current

$$\begin{aligned} i &= dq/dt = C \cdot de/dt \\ &= C \cdot \omega E_m \cos \omega t \\ &= \omega C \cdot E_m \sin(\omega t + \pi/2) \end{aligned}$$

## ALTERNATING CURRENT

So that here the current *leads* the applied voltage by  $\pi/2$ . At time ( $t = 0$ ),  $i = I_m = \omega C E_m$ , and thus the reactance  $X_c$  of this circuit is  $1/(\omega C) \Omega$ , since  $E_m/(1/\omega C) = I_m$ .

As in the case of inductive reactance there is no power loss; the current is limited by the opposing e.m.f. of the charge stored in the capacitor. The capacitive reactance is inversely proportional to frequency; thus, a condenser of capacitance  $0.1 \mu\text{F}$  has a reactance of  $30 \text{ k}\Omega$  at 50 c/s, but of only  $1500 \Omega$  at 1000 c/s. If there is a resistance in series with the capacitance, the current again leads the voltage, but by an angle less than  $\pi/2$ . This circuit is illustrated in Fig. 2.10.

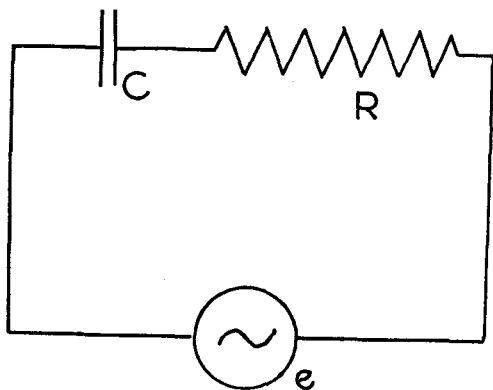


Fig. 2.10. The C-R series circuit, with sinusoidal supply voltage,  $e = E_m \sin \omega t$

If the supply voltage  $e = E_m \sin \omega t$ , and the current leads the voltage by the phase-angle  $\phi$ ,

$$i = I_m \sin(\omega t + \phi)$$

and

$$e = \overline{e_R + e_C}$$

where *vectorial* addition is implied by the bar signs. Hence:

$$\begin{aligned} E_m \sin \omega t &= R I_m \sin(\omega t + \phi) + I_m \sin(\omega t + \phi)/\omega C \\ &= R I_m \sin(\omega t + \phi) - I_m \cos(\omega t + \phi)/\omega C \end{aligned}$$

at  $t = 0$ , the equation becomes:

$$0 = R I_m \sin \phi - I_m \cos \phi / \omega C$$

so that  $\phi = \tan^{-1} 1/\omega C R$ .

## LABORATORY AND PROCESS INSTRUMENTS

At  $t = -\phi/\omega$ , the equation reduces to:

$$-E_m \sin \phi = -I_m/\omega C$$

so that  $I_m = \omega C \cdot E_m \sin \phi$ . Substituting for  $\sin \phi$ :

$$I_m = E_m/\sqrt{(R^2 + 1/\omega^2 C^2)}$$

The instantaneous value of the current  $i$  is given by:

$$i = E_m \sin(\omega t + \phi)/Z.$$

where  $Z = \sqrt{(R^2 + 1/\omega^2 C^2)}$  and  $\phi = \tan^{-1} 1/\omega CR$  (Fig. 2.11).

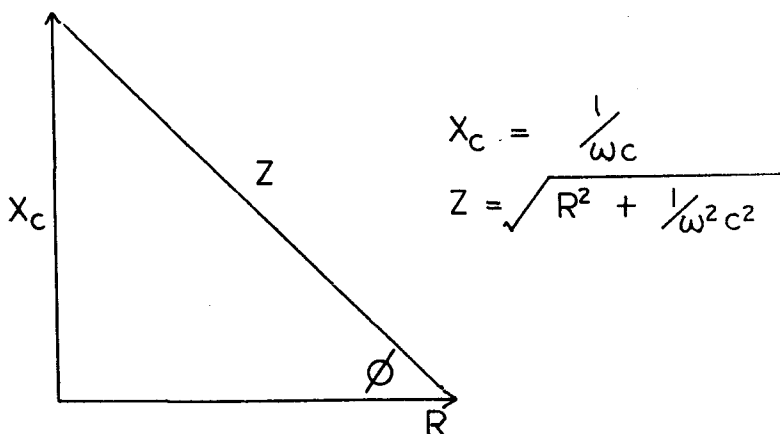


Fig. 2.11. Vector diagram of reactance and impedance in  $C$ - $R$  series circuit

### Example

If in Fig. 2.10,  $C = 0.1 \mu\text{F}$ ,  $R = 2000 \Omega$  and  $e = 10 \sin(2000\pi \cdot t)$ ,

$$\begin{aligned} Z &= \sqrt{[(2000)^2 + (10^7/2000\pi)^2]} \\ &= 2550 \Omega \end{aligned}$$

The current leads the voltage by  $\tan^{-1} 10/4\pi = 0.67$  radian, or  $38^\circ 23'$ . The peak current is  $I_m = E_m/Z = 10/2550$ , or  $3.92 \text{ mA}$ . The power dissipated in resistor  $R$

$$\begin{aligned} &= R \times (\text{r.m.s. current})^2 \\ &= 2000 \times (0.707 I_m)^2 \\ &= 2000 \times (0.707 \times 3.92/1000)^2 \\ &= 15.4 \text{ mW} \end{aligned}$$

## ALTERNATING CURRENT

(iv) *The R-L-C series circuit.* In the circuit of Fig. 2.12(a), suppose an applied voltage  $e = E_m \sin \omega t$  causes a current  $i = I_m \sin(\omega t - \phi)$  to flow, where  $\phi$  may be -ve ( $i$  leading  $e$ ) or +ve ( $i$  lagging behind  $e$ ). The sign of  $\phi$  will depend upon the frequency of the applied voltage, as compared with the resonant frequency (p. 37).

Now  $e = e_R + (e_L \sim e_C)$ , the sign ' $\sim$ ' signifying that the lesser voltage is to be subtracted from the greater. Then:

$$E_m \sin \omega t = RI_m \sin(\omega t - \phi) + \omega LI_m \cos(\omega t - \phi) - \frac{I_m}{\omega C} \cos(\omega t - \phi)$$

At time  $t = 0$ :

$$0 = -RI_m \sin \phi + \left( \omega LI_m - \frac{I_m}{\omega C} \right) \cos \phi$$

and 
$$\phi = \tan^{-1} \frac{[\omega L - (1/\omega C)]}{R}$$

At  $t = \phi/\omega$ :

$$E_m \sin \phi = \left( \omega L - \frac{1}{\omega C} \right) \cdot I_m$$

and 
$$I_m = \frac{E_m}{[\omega L - (1/\omega C)]} \times \frac{[\omega L - (1/\omega C)]}{\sqrt{\{R^2 + [\omega L - (1/\omega C)]^2\}}}$$

So that the impedance  $Z$  of this circuit is given by:

$$Z = \sqrt{\{R^2 + [\omega L - (1/\omega C)]^2\}}$$

The vector diagram is shown in Fig. 2.12(b). The current  $i$  may therefore be expressed:

$$i = \frac{E_m}{Z} \cdot \sin(\omega t - \phi)$$

where 
$$Z = \sqrt{\{R^2 + [\omega L - (1/\omega C)]^2\}}$$

and 
$$\phi = \tan^{-1} \frac{[\omega L - (1/\omega C)]}{R}$$

If  $\omega L$  is greater than  $1/\omega C$ ,  $\phi$  is positive, and  $i$  lags behind  $e$ —the circuit behaves like the  $L$ - $R$  circuits previously considered. If  $\omega L$  is less than  $1/\omega C$ ,  $\phi$  is negative,  $i$  leads  $e$ ; the circuit behaves similarly to the  $C$ - $R$  circuits previously considered.

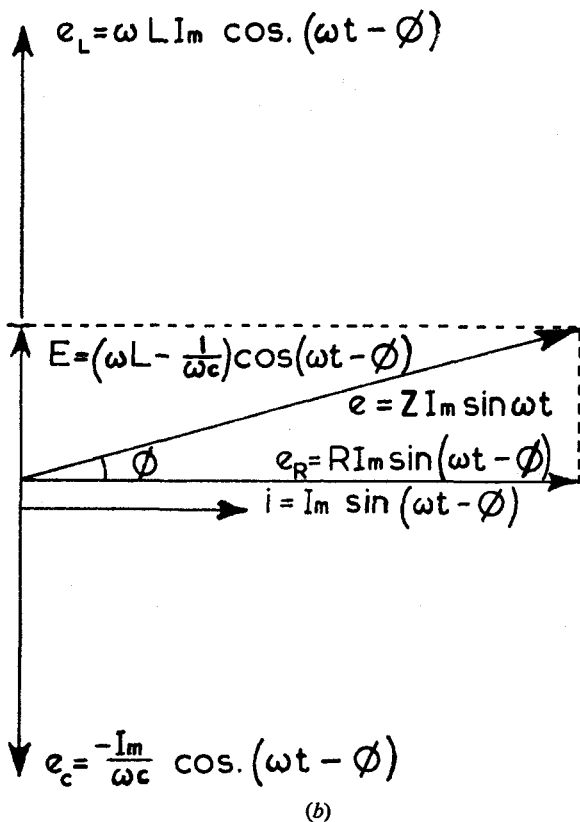
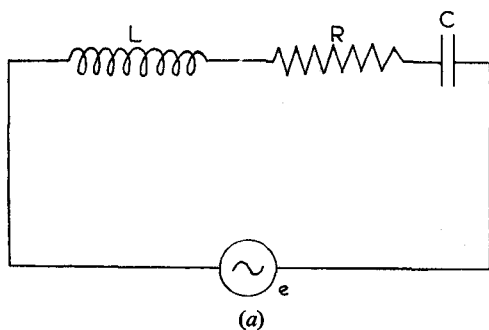


Fig. 2.12. (a) The  $L$ - $C$ - $R$  series circuit, with sinusoidal supply voltage,  $e = E_m \sin \omega t$ . (b) Vector diagram

## ALTERNATING CURRENT

A very important special case arises when  $\omega L = 1/\omega C$ .  $\phi$  is now zero, so that  $i$  and  $e$  are *in phase*. Also,  $Z = R$ , and  $I_m = E_m/R$ , the reactances cancelling; the circuit thus behaves as though only resistance  $R$  were present.

The condition  $\omega L = 1/\omega C$  defines an  $\omega$ , which we denote by  $\omega_0$ , such that  $\omega_0 = \sqrt{1/LC}$ , or a frequency  $f_0$ , defined by  $f_0 = \left(\frac{1}{2\pi}\right)\sqrt{1/LC}$ , where  $f_0 = \omega_0/2\pi$ . This particular frequency is

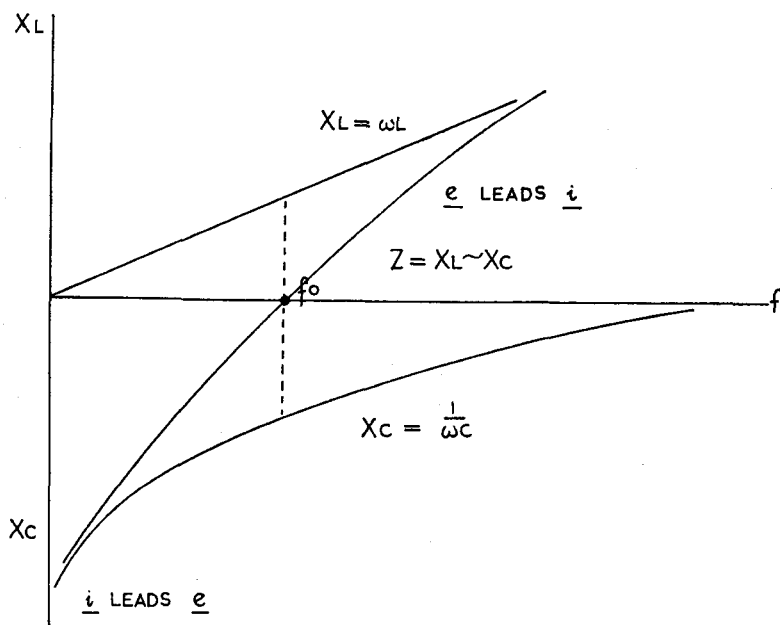


Fig. 2.13. Reactance and impedance of the  $L$ - $C$ - $R$  series circuit, as functions of frequency

called the *resonant frequency* of the circuit, and we say that the circuit *resonates* (or is in a state of *resonance*) at this frequency.

At frequencies less than  $f_0$ ,  $1/\omega C$  is greater than  $\omega L$ , and most of the applied voltage lies across the capacitor  $C$ ; at frequencies greater than  $f_0$ ,  $\omega L$  is greater than  $1/\omega C$ , and the voltage is predominantly across the inductor  $L$ . The impedance-frequency relationship is illustrated in Fig. 2.13.

The current flowing in a *series*  $L$ - $C$ - $R$  circuit attains a maximum value, and the impedance of the circuit a minimum value,

## LABORATORY AND PROCESS INSTRUMENTS

at the resonant frequency  $f_0$ . In general, the impedance at resonance is denoted by  $Z_0$ ; for the series circuit,  $Z_0$  is evidently equal to the resistance  $R$  of the circuit.

### Example

Referring to the circuit of Fig. 2.12(a), if  $L = 0.01$  H,  $C = 0.01$   $\mu$ F and  $R = 100$   $\Omega$ :

$$\text{resonant frequency } f_0 = 1/2\pi \cdot \sqrt{1/LC} = 15.92 \text{ kc/s}$$

If the supply voltage is given by  $e = 10 \sin \omega t$ :

for  $\omega = 2\pi \cdot 15,920t$ , i.e.  $f = f_0$ , the peak current at resonance,  
 $I_m^0 = E_m/R = 100$  mA.

for  $\omega = 2\pi \cdot 12,000t$ ,  $f = 12$  kc/s i.e. below  $f_0$ ,  $\omega L = 752$   $\Omega$ ,  
 $1/\omega C = 1330$   $\Omega$  and impedance  $Z = \sqrt{R^2 + (X_C - X_L)^2} = 586$   $\Omega$ .

The peak current  $I_m = E_m/Z = 17.1$  mA, and  $i$  leads  $e$  by  $\tan^{-1} 5.8$ , i.e. by  $80^\circ 14'$ .

for  $\omega = 2\pi \cdot 20,000t$ ,  $f = 20$  kc/s i.e. above  $f_0$ ,  $\omega L = 1257$   $\Omega$  and  
 $1/\omega C = 796$   $\Omega$ .

The impedance  $Z$  is now 480  $\Omega$ ; for  $\omega = 2\pi \cdot 20,000t$ , the peak current  $I_m = 21.2$  mA;  $e$  now leads  $i$  by  $\tan^{-1} 4.7$ , i.e. by  $77^\circ$ .

(v) *Parallel circuits.* These are more difficult to deal with; for a complete treatment, see reference, p. 51. In outline the problem may be treated as follows:

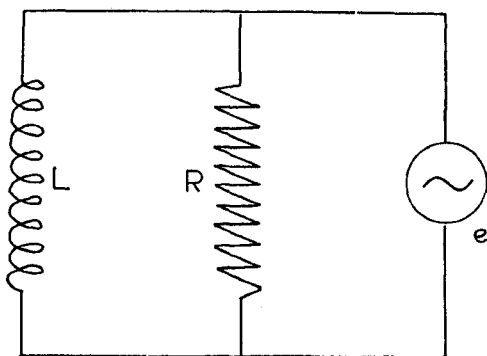


Fig. 2.14. The  $L$ - $R$  parallel circuit, with sinusoidal supply voltage,  
 $e = E_m \sin \omega t$

In the case of the  $L$ - $R$  parallel circuit (Fig. 2.14):

$$1/Z^2 = 1/R^2 + 1/\omega^2 L^2$$



## ALTERNATING CURRENT

and  $i = \overline{i_L + i_R} = E_m/R \cdot \sin \omega t + E_m/\omega L \cdot \sin(\omega t - \pi/2)$

where  $i$  is the vector sum of  $i_L$  and  $i_R$ , the subscripts showing through which component a particular current flows.

$$I_m = E_m/Z = E_m \cdot \sqrt{(R^2 + \omega^2 L^2)}/R\omega L$$

Similar considerations apply to the  $C$ - $R$  parallel circuit.

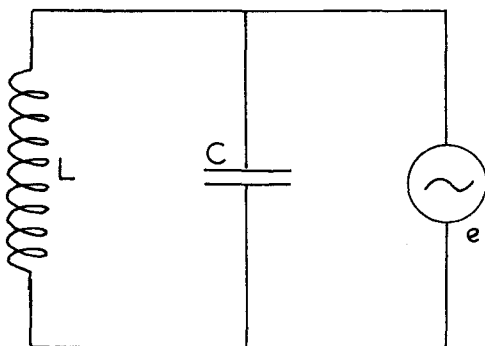


Fig. 2.15. The  $L$ - $C$  parallel circuit, with supply voltage  $e = E_m \sin \omega t$

We consider next the  $L$ - $C$  (resistanceless) case (Fig. 2.15):

$$i_L = E_m/\omega L \cdot \sin(\omega t - \pi/2)$$

$$i_c = E_m \omega C \cdot \sin(\omega t + \pi/2)$$

the subscripts having their previous meanings. Hence the resultant current through the generator  $i$  is given by:

$$i = E_m(1/\omega L \sim \omega C) \sin(\omega t + \phi)$$

where, for  $\omega L < 1/\omega C$ ,

$$\phi = -\pi/2 \text{ for } (i_L > i_c)$$

and, for  $\omega L > 1/\omega C$ ,

$$\phi = +\pi/2 \text{ for } (i_L < i_c)$$

The circuit impedance  $Z = E_m/I_m = 1/(1/\omega L \sim \omega C)$ . We can again consider ( $\omega L = 1/\omega C$ ) as defining the condition of *resonance*

# LABORATORY AND PROCESS INSTRUMENTS

and the resonant frequency  $f_0$  for the circuit;  $f_0 = 1/2\pi\sqrt{1/LC}$  as before. At this frequency  $(1/\omega L - \omega C)$  is zero, and hence  $Z_0$  is infinite; no resultant current flows in this circuit at resonance. The impedance relationships are shown in Fig. 2.16.

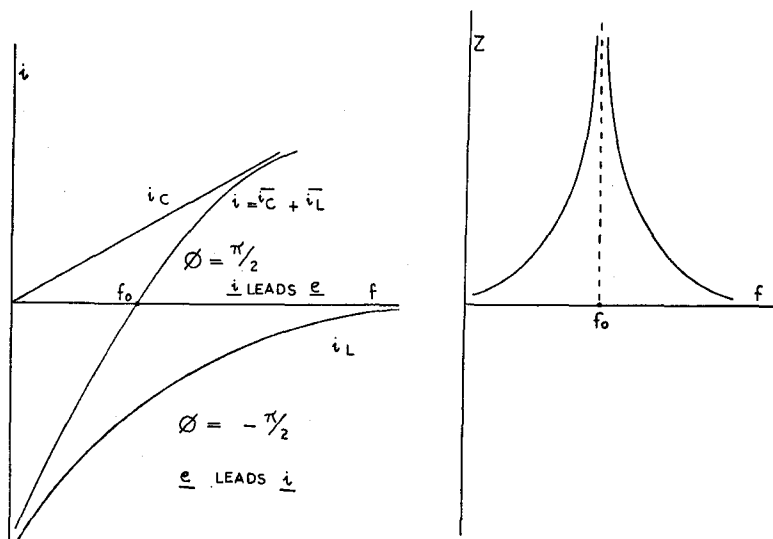


Fig. 2.16. Components of current and impedance of the  $L$ - $C$  parallel circuit

## Example

If  $C = 0.01 \mu\text{F}$  and  $L = 0.01 \text{ H}$ , the resonant frequency is  $15.92 \text{ kc/s}$ , as for the series circuit.

At  $f = 12 \text{ kc/s}$ :  $\omega L = 240\pi$ ,  $= 754 \Omega$ ;  $1/\omega C = 10^5/24\pi$ ,  $= 1326 \Omega$ .

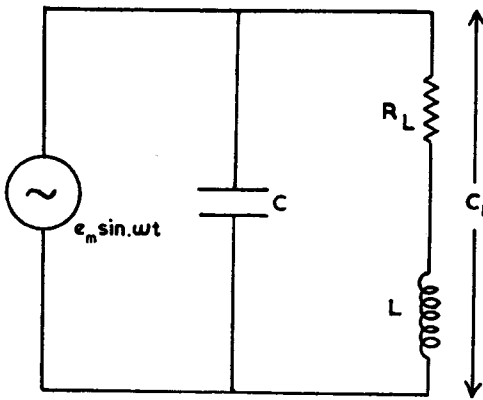
For an applied e.m.f. of peak voltage  $= 10 \text{ V}$ ,  $i_L = 13.3 \text{ mA}$ ,  $i_C = 7.5 \text{ mA}$  and  $i = i_L - i_C = 5.8 \text{ mA}$ , lagging behind  $e$  by  $\pi/2$ .

At  $f = 14 \text{ kc/s}$ :  $\omega L = 280\pi$ ,  $= 880 \Omega$ ;  $1/\omega C = 10^5/28\pi$ ,  $= 1136 \Omega$ , and  $i = 2.6 \text{ mA}$ , lagging behind  $e$  by  $\pi/2$ .

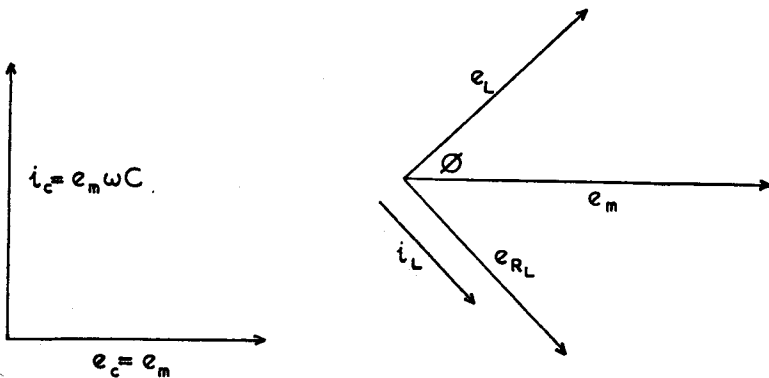
At  $f = 18 \text{ kc/s}$ :  $\omega L = 360\pi$ ,  $= 1131 \Omega$ ;  $1/\omega C = 10^5/36\pi$ ,  $= 884 \Omega$ , and  $i = 2.6 \text{ mA}$ , leading  $e$  by  $\pi/2$ .

## ALTERNATING CURRENT

However, an inductor  $L$  always contains resistance,  $R_L$ , so that the practical circuit is as shown in Fig. 2.17.



(a)



(b)

Fig. 2.17. (a) The  $L$ - $C$  parallel circuit, with resistance in the inductive arm.

(b) Vector diagram

We now have:

$$i_L = \frac{E_m}{\sqrt{(R_L^2 + \omega^2 L^2)}} \cdot \sin(\omega t - \phi)$$

where  $\phi = \tan^{-1} \omega L / R_L$  and  $i_C = E_m \omega C \cdot \sin(\omega t + \pi/2)$ . The resultant current through the generator  $i$  is the vector sum of  $i_L$  and  $i_C$ ; and

$$I_m = \sqrt{[(I_L \sin \phi + I_C)^2 + I_L^2 \cos^2 \phi]}$$

## LABORATORY AND PROCESS INSTRUMENTS

In the general case, as shown in the circuit of Fig. 2.18, both the inductive and capacitive arms contain resistance; the component  $R_c$  may be an added circuit component, or may represent 'leakage' of the capacitor  $C$ , as explained on p. 49.

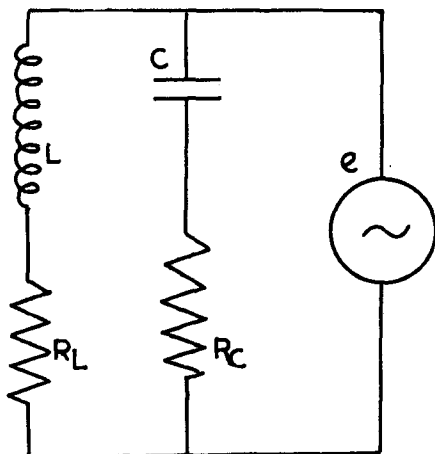


Fig. 2.18. The  $L$ - $C$  parallel circuit, with resistance in both arms

The vector diagram for this circuit is shown in Fig. 2.19. For an applied e.m.f.  $e = E_m \sin \omega t$ :

$$i_L = \frac{E_m}{\sqrt{(R_L^2 + \omega^2 L^2)}} \cdot \sin(\omega t - \phi_L) = i_L \cdot \cos \phi_L + i_L \cdot \sin \phi_L$$

$$i_C = \frac{E_m}{\sqrt{(R_C^2 + 1/\omega^2 C^2)}} \cdot \sin(\omega t + \phi_C) = i_C \cdot \cos \phi_C + i_C \cdot \sin \phi_C$$

The resultant current  $i$  is the vector sum of  $i_L$  and  $i_C$ .

In the general case under discussion we define resonance by the condition that  $i$  is in phase with  $e$ ; this is no longer equivalent to ( $\omega L = 1/\omega C$ ). The out-of-phase components of the current must therefore cancel, i.e.

$$i_C \cdot \sin \phi_C = i_L \cdot \sin \phi_L.$$

And

$$\sin \phi_C = \frac{1/\omega C}{\sqrt{(R_C^2 + 1/\omega^2 C^2)}}$$

$$\sin \phi_L = \frac{\omega L}{\sqrt{(R_L^2 + \omega^2 L^2)}}$$

# ALTERNATING CURRENT

so that the condition for resonance is:

$$\frac{E_m}{\sqrt{(R_C^2 + 1/\omega^2 C^2)}} \cdot \frac{1/\omega C}{\sqrt{(R_C^2 + 1/\omega^2 C^2)}} = \frac{E_m}{\sqrt{(R_L^2 + \omega^2 L^2)}} \cdot \frac{\omega L}{\sqrt{(R_L^2 + \omega^2 L^2)}}$$

from which we derive

$$\omega_0^2 = \frac{L - R_L^2 C}{L^2 C - LC^2 R_C^2}; \quad f_0 \simeq 1/2\pi \cdot \sqrt{\left( \frac{L - CR_L^2}{L^2 C - LC^2 R_C^2} \right)}$$

If, as is usual,  $R_C$  is comparatively small,

$$f_0 \simeq 1/2\pi \cdot \sqrt{(1/LC - R_L^2/L^2)}$$

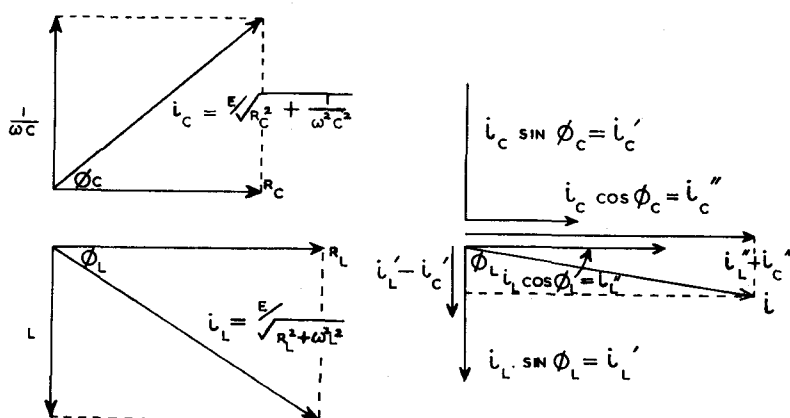


Fig. 2.19. The  $L$ - $C$  parallel circuit-vector diagram. General case of resistance in both arms

this assumption is in fact a return to the circuit of Fig. 2.17. Thus, the resonant frequency of a parallel  $L$ - $C$ - $R$  combination is less than that of the same components in series, by the term  $(R_L^2/L^2)$ . If  $R_L$  and  $R_C$  are both small, we have the ideal case of purely reactive components (Fig. 2.14); the resonant frequency is now  $f_0 = 1/2\pi \cdot \sqrt{(1/LC)}$ .

Returning to the practical case of Fig. 2.18,  $i$  and  $e$  are in phase at resonance, but the impedance at resonance,  $Z_0$ , is no longer infinite; since the out-of-phase components cancel, the current at resonance,  $i_0$ , is given by:

$$i_0 = (i_C \cdot \cos \phi + i_L \cdot \cos \phi) \cdot \sin \omega_0 t$$

# LABORATORY AND PROCESS INSTRUMENTS

The amplitude of this current is  $I_m^0$ :

$$\begin{aligned} I_m^0 &= \frac{E_m}{\sqrt{(R_C^2 + 1/\omega_0^2 C^2)}} \cdot \frac{R_C}{\sqrt{(R_C^2 + 1/\omega_0^2 C^2)}} \\ &\quad + \frac{E_m}{\sqrt{(R_L^2 + \omega_0^2 L^2)}} \cdot \frac{R_L}{\sqrt{(R_L^2 + \omega_0^2 L^2)}} \\ &= E_m \cdot \left( \frac{R_C}{R_C^2 + 1/\omega_0^2 C^2} + \frac{R_L}{R_L^2 + \omega_0^2 L^2} \right) \end{aligned}$$

Hence  $Z_0$ , which  $= E_m/I_m^0$

$$= \left( \frac{R_C}{R_C^2 + 1/\omega_0^2 C^2} + \frac{R_L}{R_L^2 + \omega_0^2 L^2} \right)^{-1}$$

which is the general expression for the resonant impedance  $Z_0$ . If as before  $R_C$  is small, so that  $\omega_0^2 C^2 R_C^2 \ll 1$ , and if in addition the reactance of the coil is much greater than its resistance, so that  $\omega_0 L \gg R_L$ , we have

$$Z_0 \approx (\omega_0^2 C^2 R_C + R_L/\omega_0^2 L^2)^{-1}$$

$$\text{and } \omega_0^2 = 1/LC - R_L^2/L^2$$

$$\text{i.e. } Z_0 = [R_C \cdot C/L - R_L^2 R_C C^2/L^2 + R_L/(L/C - R_L^2)]^{-1}$$

$$\approx \frac{L/C}{R_C + R_L} = L/CR_L$$

This approximate value of  $Z_0$  is sometimes called the *dynamic impedance* of the circuit and is represented by  $R_D$ ; for  $R_C \approx 0$ ,  $R_L = R$  and  $R_D = L/CR$ .

## Example

For the circuit of Fig. 2.17, if  $L = 0.01$  H,  $C = 0.01$   $\mu$ F,  $R = 200$   $\Omega$ , the resonant frequency

$$f_0 = 1/2\pi \sqrt{(1/LC - R_L^2/L^2)} = 15.58 \text{ kc/s.}$$

If  $R_L$  is decreased,  $f_0$  increases slightly; when  $R$  is zero,  $f_0 = 15.92$  kc/s. The dynamic impedance  $Z_0 = L/CR = 5000$   $\Omega$  at  $R = 200$   $\Omega$ , increasing rapidly as  $R$  decreases to zero. If  $E_m = 10$  V, then with

## ALTERNATING CURRENT

$R = 200 \, \Omega$ , the peak current at resonance  $I_m^0 = 10/5000 = 2.0 \, \text{mA}$ . This current is made up of two components,  $I_C^0$  in the capacitive arm and  $I_L^0$  in the inductive arm, which are given by:

$$I_C^0 = 10/(1/\omega C) = 9.79 \, \text{mA}$$

leading the applied voltage by  $\pi/2$ .

$$I_L^0 = 10/\sqrt{R^2 + \omega^2 L^2} = 10.01 \, \text{mA}$$

lagging behind the supply voltage by the phase-angle  $\phi_L$ , where  $\phi_L = \tan^{-1} \omega L/R = 78^\circ 24'$ . And the resultant current is

$$I_L^0 \cos \phi_L = 2.02 \, \text{mA}$$

compared with the value  $2.0 \, \text{mA}$  derived from the approximate value  $Z_0 = L/CR$ .

### Power in Alternating Current Circuits

In a direct-current (d.c.) circuit, the product of current and voltage is *power*, available for doing work, and denoted by the symbol  $P$ ; if the current is in amperes and the voltage in volts,  $P$  is in *watts*. Under alternating conditions, the product of r.m.s. values of current and voltage gives the *apparent* power,  $S$ , measured in volt-amperes; this is the maximum power which could be drawn from the circuit if the current and voltage were *in phase*. We can show this as follows:

If voltage  $e$  and current  $i$  are in phase, and  $e = E_m \cdot \cos \omega t$ , so that  $ei = E_m I_m \cdot \cos^2 \omega t = \frac{1}{2} E_m I_m \cdot (1 + \cos 2\omega t)$ , the mean power per cycle,

$$\begin{aligned} \bar{p} &= \frac{E_m I_m}{2\pi/\omega} \cdot \int_0^{2\pi/\omega} \frac{1}{2} (1 + \cos 2\omega t) \cdot dt \\ &= E_m I_m \cdot \frac{\omega}{4\pi} \cdot [t]_0^{2\pi/\omega} = \frac{E_m I_m}{2} \\ &= E \cdot I \end{aligned}$$

where  $E$  and  $I$  are the r.m.s. values. The term  $(\cos 2\omega t)$  in the expression for  $\bar{p}$  shows that the power frequency is twice that of the voltage and current.

Frequently, however, as we have seen,  $e$  and  $i$  are not in phase;

## LABORATORY AND PROCESS INSTRUMENTS

e.g. if  $e = E_m \cos \omega t$ ,  $i = I_m \cdot \cos(\omega t - \phi)$ , the voltage leads the current by a phase angle  $\phi$ , and hence:

$$\begin{aligned}\bar{p} &= \frac{E_m I_m}{2\pi/\omega} \int_0^{2\pi/\omega} \cos \omega t \cdot \cos(\omega t - \phi) \cdot dt \\ &= \frac{E_m I_m \cdot \omega}{2\pi} \cdot \int_0^{2\pi/\omega} [\tfrac{1}{2} \cos(2\omega t - \phi) + \tfrac{1}{2} \cos \phi] \cdot dt \\ &= \frac{E_m I_m}{2} \cdot \cos \phi \text{ watts}\end{aligned}$$

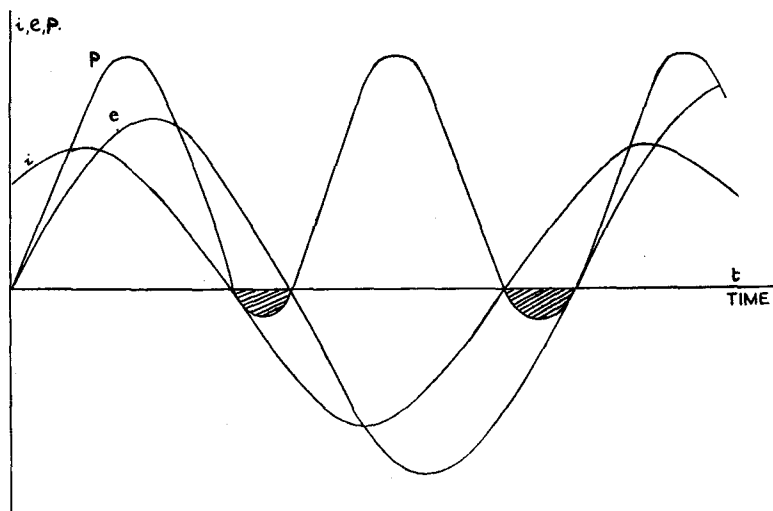


Fig. 2.20. Power relationship in the reactive circuit

The result would obviously be the same if  $\phi$  were an angle of lead, so that, in general, a phase difference between current and voltage reduces the available power by the factor  $(\cos \phi)$ , called the *power factor*. As  $\phi$  increases,  $\bar{p}$  decreases, becoming zero for  $\phi = \pi/2$ , i.e. when current and voltage are in phase quadrature. It is the nature of the load to which the supply is connected—i.e. the ratio of reactance to resistance—which determines  $\phi$ , so that we speak of the power factor ‘of a particular load’; maximum power is developed in the load only if it is effectively resistive.

In Fig. 2.20, curves are drawn for

$$e = E_m \sin \omega t, i = I_m \sin(\omega t + \pi/4) \text{ and } p = ei$$



## ALTERNATING CURRENT

The shaded area under the  $p$ -curve represents negative power, i.e. power stored in the inductor field or in the capacitor. The useful power is thus represented by the *difference* in area of the shaded and unshaded areas under the  $p$ -curve, which is

$$\left(\frac{E_m I_m}{2} \cdot \cos \phi\right) \text{ watts}$$

and the shaded area represents stored, or 'wattless', power, symbol  $Q'$ . The product  $(E_m I_m)/2$  is the *apparent* power  $S$ , in volt-amp;  $(E_m I_m \cos \phi)/2$  is the *true* power,  $P$ , in watts.

A *wattmeter* measures the useful power expended in a given load or in a component of a circuit, and this instrument is illustrated in Fig. 2.21. The 'fixed' coil CC carries the current passing through the load, and the 'moving' coil VV in shunt with the load, passes a current proportional to the voltage across the load. The torque developed between the two coils is proportional to the product of current through, and voltage across, the load, i.e. to  $E \cdot I \cdot \cos \phi$ , where  $E$  and  $I$  are the r.m.s. values.

### Example

In the series circuit of Fig. 2.12, if  $L = 0.01$  H,  $C = 0.01 \mu\text{F}$  and  $R = 100 \Omega$ , the resonant frequency  $f_0 = 15.92$  kc/s. At  $f = 17$  kc/s

$$Z = \sqrt{[R^2 + (\omega L - 1/\omega C)^2]} = 166 \Omega$$

If the supply voltage  $e = 50 \sin (34,000\pi t)$

$$I_m = E_m/Z = 0.302 \text{ amp}$$

$$\text{Apparent power } S = \frac{E_m I_m}{2} = 7.55 \text{ volt-amp}$$

$$\text{True power } P = \frac{R \cdot I_m^2}{2} = 4.56 \text{ W}$$

$$\text{Wattless power } Q' = (S - P) = 2.99 \text{ volt-amp}$$

$$\text{Power factor } \cos \phi = R/Z = 0.604$$

And  $S \cos \phi = 4.56 \text{ W} = P$ , as before.

At this frequency, the circuit behaves inductively; the power factor could be 'corrected' (brought nearer to unity) by the introduction of more  $X_c$  into the circuit. If  $C$  were reduced to  $0.0091 \mu\text{F}$ ,  $Z$  at 17 kc/s =  $107 \Omega$  and  $\cos \phi = 0.935$ ;  $S = 11.7$  volt-amp,  $P = 10.9 \text{ W}$ .

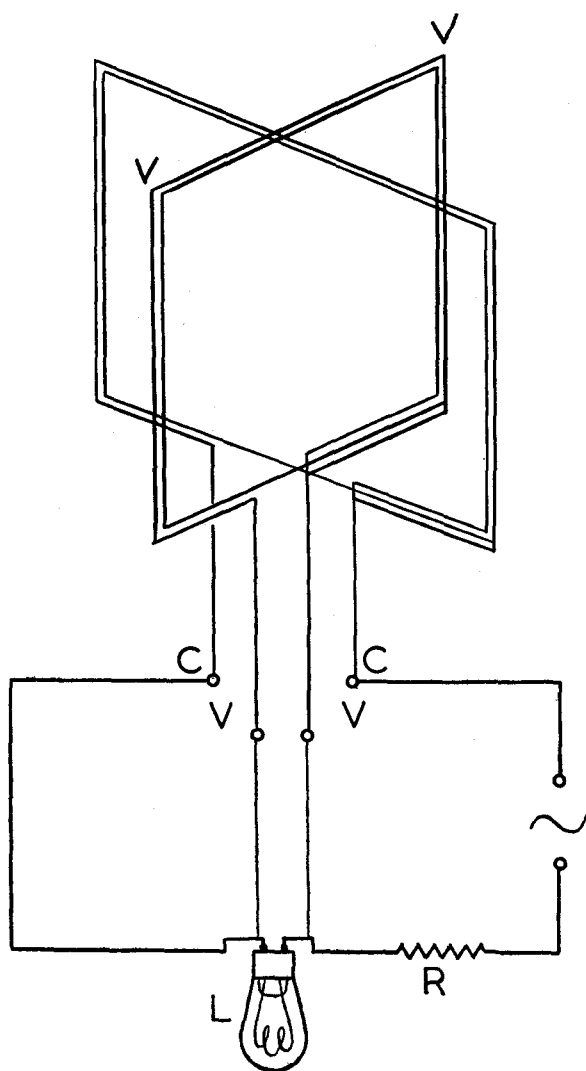


Fig. 2.21. The wattmeter in circuit. Measurement of power dissipated in lamp

# The Power Factor of Capacitors

If a capacitor has a high-resistance leakage path between the plates it cannot be adequately represented by the symbol of Fig. 2.22(a), but must be replaced by the parallel circuit of Fig. 2.22(b), where  $R_p$ ,  $C_p$  are components of the combination which represents the behaviour of the 'leaky' capacitor. If the impedance of this circuit is  $Z_p$ :

$$1/Z_p = \sqrt{[(\omega C_p)^2 + (1/R_p)^2]} = 1/R_p \sqrt{(1 + \omega^2 C_p^2 R_p^2)}$$

and the current through  $C_p$  leads that through  $R_p$  by the phase-angle  $\phi_p$ , where  $\phi_p = \tan^{-1} \omega C_p R_p$ . The subscripts 'p' here denote the parallel circuit.

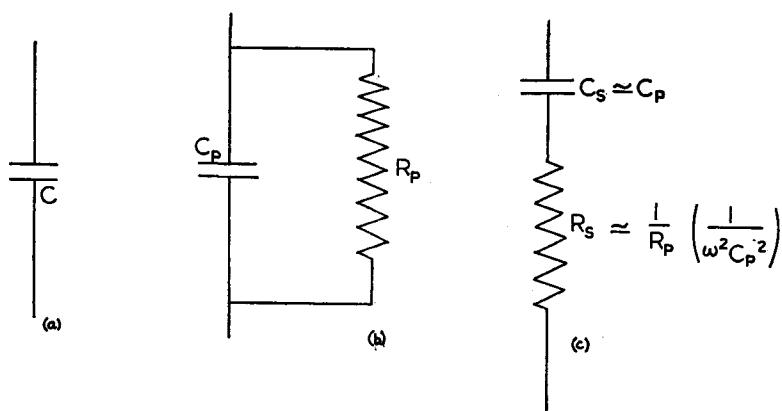


Fig. 2.22. Equivalent series and parallel C-R combinations

Now such a combination may be replaced by a series circuit having the same behaviour, but involving new components  $C_s$  and  $R_s$  (Fig. 2.22(c)). We now have:

$$Z_s = \sqrt{(R_s^2 + 1/\omega^2 C_s^2)}$$

$$\phi_s = \tan^{-1} 1/\omega C_s R_s$$

where 's' denotes the series combination. For the two circuits to be equivalent, at frequency  $\omega/2\pi$ :

$$R_s^2 + 1/\omega^2 C_s^2 = R_p^2/(1 + \omega^2 C_p^2 R_p^2)$$

i.e.  $Z_s = Z_p$  and

$$1/\omega C_s R_s = \omega C_p R_p$$

i.e.  $\phi_s = \phi_p$ . Hence,

$$R_s = R_p \left( \frac{1}{1 + \omega^2 C_p^2 R_p^2} \right)$$

and

$$C_s = C_p \left( 1 + \frac{1}{\omega^2 C_p^2 R_p^2} \right)$$

If the 'leak' resistance  $R_p$  is very high,  $R_p \gg 1/\omega C_p$ , and we have:

$$R_s \simeq \frac{1}{R_p} \left( \frac{1}{\omega^2 C_p^2} \right)$$

$$C_s \simeq C_p$$

### Example

The series circuit of Fig. 2.22(c) is equivalent to the parallel circuit of Fig. 2.22(b), in which a  $0.01 \mu\text{F}$  capacitor has a leakage resistance of  $100 \text{ k}\Omega$  at  $10 \text{ kc/s}$ , if  $C_s$ , the series capacitor, is also  $0.01 \mu\text{F}$ , but  $R_s$ , the series resistor, is  $25 \Omega$ . The current leads the voltage by the phase-angle  $\phi$ , where  $\phi = \tan^{-1} 1/\omega C R_s = 89^\circ 6'$ .

If the peak value of the supply voltage is  $50 \text{ V}$ , and this is applied across the circuit, the peak current

$$I_m = E_m \cdot \omega C = 50 \times 2\pi/10^4 = 31.4 \text{ mA}$$

The power dissipated in  $R_s$  is:

$$= \frac{E_m I_m}{2} \cdot \cos \phi = 50 \times 31.4/2 \times 0.0157$$

$$= 12.3 \text{ mW}$$

### Comparison of Powers: the Decibel Scale

If we measure the power dissipated in a load  $R_L$  on two different occasions, we can express the *change* in power over the time interval between the measurements by the ratio  $P_2/P_1$ , i.e. the ratio of final power to initial power. It is more convenient for most purposes to express the ratio on a logarithmic scale, rather like the 'pH' scale which is used to express hydrogen ion concentration.

If  $P_2/P_1 = 10^x$ , then the ratio of  $P_2:P_1$  is said to be  $x$  *bels*, or  $10x$  *decibels* (abbreviated to *db*). Thus:

$$\log_{10} P_2/P_1 = x \text{ bels}; 10 \log_{10} P_2/P_1 = (10x) \text{ decibels (db)}$$

## ALTERNATING CURRENT

For example, if  $P_1 = 10 \text{ mW}$  and  $P_2 = 500 \text{ mW}$ , we could refer to a *gain* of  $(10 \log 500/10)$ , or 17 db, over the period of time between measurements. If  $P_1 = 500 \text{ mW}$ ,  $P_2 = 10 \text{ mW}$ , we could refer to a *loss* of 17 db, or a *gain* of  $-17 \text{ db}$ , over the period.

A high-gain amplifier, developing 50 mW of output power from an input of  $5 \mu\text{W}$ , has an overall gain of  $(10 \log 10^4)$ , or 40 db. Power is proportional to (voltage)<sup>2</sup>, so that

$$P_2/P_1 = \frac{E_2^2/R_2}{E_1^2/R_1}$$

If  $R_1 = R_2$ ,  $P_2/P_1 = E_2^2/E_1^2$  and

$$10 \log P_2/P_1 = 10 \log (E_2/E_1)^2 = \text{change in db}$$

Hence the voltage gain in db =  $20 \log E_2/E_1$ . For example, using the previous notation, if  $E_1 = 10 \text{ mV}$ ,  $E_2 = 500 \text{ mV}$  the *gain* =  $(20 \log 500/10) = 34 \text{ db}$  if both voltage measurements are taken across the same load resistance.

If  $R_1$  and  $R_2$  are not equal the resistance change must be taken into account. Suppose the input voltage of an amplifier is 5 mV across  $600 \Omega$  and the output is 2.5 V across  $50 \Omega$ , then

$$P_2/P_1 = \frac{2.5^2/50}{0.005^2/600} = 3 \times 10^6$$

and the amplifier gain is  $10 \log (3 \times 10^6)$ , or 65 db. Considering the voltage, of course, there is a gain of 500.

### References

- RENTON, R. N. (1950). *Telecommunications Principles*. Pitman.  
 SLATER, J. C. (1954). *Microwave Electronics*. D. van Nostrand.  
 SMITH, C. E. (1942). *Communications Circuit Fundamentals*. McGraw Hill.  
 YARWOOD, J. (1950). *Electronics*. Chapman and Hall.

### Problems

1. Calculate (a) the frequency of a micro-wave oscillator of wavelength 3 cm; (b) the wavelength of the V.H.F. broadcast at 93.5 Mc/s.

*Answer.* (a)  $f = 10^4 \text{ Mc/s}$ ; (b)  $\lambda = 320 \text{ cm}$ .

2. Draw an impedance triangle for an  $L$ - $R$  series circuit which passes 200 mA r.m.s., and dissipates 12 W, on a 50 c/s 100 V r.m.s. mains supply.

# LABORATORY AND PROCESS INSTRUMENTS

( $R = 300 \Omega$ ;  $\omega L = 400 \Omega$ ;  $\phi = 53^\circ 8'$ .)

3. A resonant circuit consists of  $L = 1 \text{ mH}$ , having  $R = 20 \Omega$ , in series with a variable capacitor. An e.m.f. of  $1 \text{ V}$  at  $100 \text{ kc/s}$  is induced in the coil; what must be the value of the capacitor to produce resonance with this e.m.f. and what will then be the p.d. across this capacitor?

*Answer.*  $C = 2500 \mu\text{F}$ ;  $V = 31.4 \text{ V}$ .

4. An inductor of  $0.01 \text{ H}$  is connected in series with a capacitor of  $0.01 \mu\text{F}$  and a resistor of  $100 \Omega$ . Calculate the magnitude and type of the impedance at  $10 \text{ kc/s}$  and at  $20 \text{ kc/s}$ ; the resonant frequency; and the power developed at resonance in the resistor, from a voltage source of amplitude  $10 \text{ V}$ .

*Answer.* At  $10 \text{ kc/s}$   $X_{\text{capacitive}} = 954 \Omega$ ; at  $20 \text{ kc/s}$   $X_{\text{inductive}} = 485 \Omega$ ;  $f_0 = 15.9 \text{ kc/s}$ ;  $W = 0.5 \text{ W}$ .

5. A current of  $0.5 \text{ amp}$  is taken from  $250 \text{ V } 50 \text{ c/s}$  mains by an inductor; the power factor is  $0.6$ . Calculate the total current and power factor when a  $4 \mu\text{F}$  capacitor is connected in parallel with the coil.

*Answer.*  $0.312 \text{ amp}$ ;  $\cos \phi = 0.96$ .

6. Find the power factor, true power and apparent power, for a circuit consisting of a  $2 \text{ mH}$  inductor in series with a  $0.001 \mu\text{F}$  capacitor and a  $100 \Omega$  resistor subjected to a voltage  $e = 50 \sin 10^6 t$ .

*Answer.*  $\cos \phi = 0.1$ ;  $W = 125 \text{ mW}$ ; apparent power =  $1250 \text{ mW}$ .

## CHAPTER III

# Tuned Circuits

### Tuned Circuits

The resonant frequencies of series and parallel circuits may be varied by variation of either the capacitance or the inductance in the circuit.

Variable capacitors are generally air-spaced; the degree of rotation is often indicated on an engraved dial. If the 'law' of the capacitor is  $C = k\vartheta^2 + C_0$ , where  $\vartheta$  is the angle of rotation

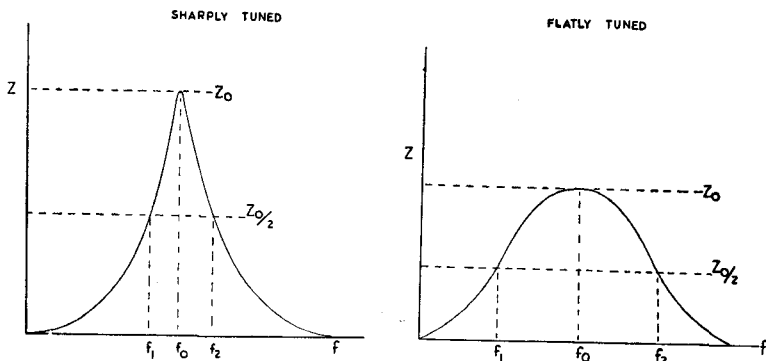


Fig. 3.1. Selectivity curves of tuned circuits

from the minimum (fully-closed) position, the dial may be directly calibrated in frequency (since this is approximately proportional to  $1/\sqrt{C}$ ).

Fine adjustment of frequency is usually made by varying the position of a high-permeability core, or 'slug', within the coil; the adjustment must be made with a non-metallic screwdriver.

The change in the impedance  $Z$  for a small change in frequency about the resonant frequency  $f_0$ , i.e.  $(dZ/df)_0$ , is a measure of the sharpness of tuning, or *selectivity*, of the resonant circuit. Circuits of very different selectivity produce the response curves of Fig. 3.1.

### Q-factor

The ratio (reactance)/(resistance) for a component ( $= X/R$ ), or of (impedance)/(resistance) for a circuit ( $= Z/R$ ) is called the *magnification-factor*, or the *Q-factor*, of that component or circuit. Thus, the  $Q$  of an inductor  $Q_L = \omega L/R$ ;  $Q$  for a capacitor  $Q_C = 1/\omega CR$ .

At resonance the circuit would develop a voltage  $E_L^0$  across the inductor, where  $E_L^0 = X_L^0 \cdot I^0 = \omega^0 L \cdot E_m/R = Q_L^0 E_m$  (the superscript  $^0$  refers to the values of the parameters at resonance). Similarly, a voltage  $E_C^0$  is developed across the capacitor:

$$E_C^0 = (1/\omega_0 C) \cdot E_m/R = Q_C^0 E_m$$

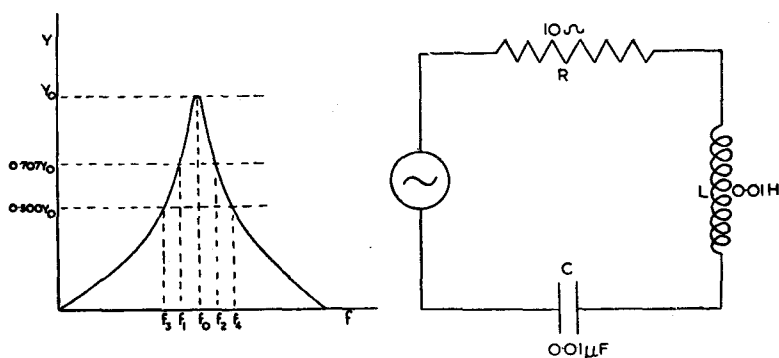


Fig. 3.2. Admittance-frequency curve of series resonant circuit

Since  $\omega_0 = \sqrt{1/LC}$ ,  $Q^0 = (L/R)\sqrt{1/LC}$ . Hence

$$Q^0 = (1/CR)\sqrt{LC} = (1/R)\sqrt{L/C}$$

which defines the  $Q$ -factor of the *circuit* at resonance. The magnified voltages across  $L$  and  $C$  are given by the product of the  $Q$ -factor for each component and the supply voltage. At resonance,  $Q_L^0 = Q_C^0 = Q^0$  for the circuit.

#### Example

For a series circuit with  $L = 0.01$  H,  $C = 0.01$   $\mu$ F,  $R = 10$   $\Omega$  (Fig. 3.2),  $Q^0 = 1/10 \cdot \sqrt{(10^{-2}/10^{-8})} = 100$ . A supply e.m.f. of 1 V peak value at the resonant frequency (15.92 kc/s) develops 100 V across both  $L$  and  $C$ , these voltages being in phase opposition. As  $R$  increases,  $Q^0$  decreases:  $Q \propto 1/R$ .



## TUNED CIRCUITS

In this example the peak current at resonance  $I_m^0$  is 100 mA. Suppose that, at two frequencies  $f_1$  and  $f_2$ ,  $I_m = I_m^0/\sqrt{2}$ , i.e.  $0.707 I_m^0$ , where  $f_1$  and  $f_2$  lie on either side of the resonant frequency  $f_0$ . We may then write:

$$I_1 \text{ (i.e. } I_m \text{ at } f = f_1, f_1 < f_0) = E_m/\sqrt{[R^2 + (1/\omega_1 C - \omega_1 L)^2]}$$

and

$$I_2 \text{ (i.e. } I_m \text{ at } f = f_2, f_2 > f_0) = E_m/\sqrt{[R^2 + (\omega_2 L - 1/\omega_2 C)^2]}$$

$$\text{And } I_1 = I_2 = I_m^0/\sqrt{2} = E_m/[\sqrt{(2) \cdot R}]$$

Hence  $R^2 + (1/\omega_1 C - \omega_1 L)^2 = 2R^2$ , which may be solved for  $\omega_1$ :

$$\omega_1 = \frac{CR + \sqrt{(C^2 R^2 + 4LC)}}{2LC}$$

similarly,

$$\omega_2 = \frac{-CR + \sqrt{(C^2 R^2 + 4LC)}}{2LC}$$

and

$$(\omega_2 - \omega_1) = R/L$$

$$\omega_0/(\omega_2 - \omega_1) = \frac{1}{\sqrt{LC}} \cdot \frac{L}{R} = \frac{1}{R} \cdot \sqrt{L/C} = Q^0$$

for the circuit.

Returning to the circuit of the previous example, since  $Q^0 = 100$  and  $f_0 = 15.92 \text{ kc/s}$ ,

$$(\omega_2 - \omega_1) = \omega_0/Q^0 = 1 \text{ kc/s}$$

$$\therefore (f_2 - f_1) = 1/2\pi \text{ kc/s} = 0.16 \text{ kc/s}$$

$$\text{And } f_1 = f_0 - 0.08 = 15.84 \text{ kc/s}$$

$$f_2 = f_0 + 0.08 = 16.00 \text{ kc/s}$$

If we plot the *admittance* of this circuit  $Y$  ( $Y = 1/Z$ ) against frequency, we obtain the 'response-curve' of Fig. 3.2 with a maximum admittance  $Y_0$  at  $f = f_0$ . The frequency interval  $(f_2 - f_1)$  is called the *bandwidth* at  $0.707 Y_0$ ; since

$$Q^0 = \omega_0/(\omega_2 - \omega_1) = f_0/(f_2 - f_1)$$

this bandwidth is given by  $f_0/Q^0$ . Alternatively, the  $Q$ -factor of a series circuit at resonance may be found by measuring the resonant frequency and the bandwidth at  $0.707 Y_0$ .

# LABORATORY AND PROCESS INSTRUMENTS

If, at frequencies  $f_3$  and  $f_4$ ,  $Y_3 = Y_4 = Y_0/2$ , we may easily show that  $(f_4 - f_3) = \sqrt{3} \cdot R/2\pi L$ . Similarly, at frequencies  $f_5$  and  $f_6$ , where  $(f_6 - f_5) = 2(f_2 - f_1) = 2 \cdot R/2\pi L$ , the admittance

$$Y_{5,6} = Y_0/\sqrt{5}$$

These frequencies are listed in Table 3.1 for the circuit of Fig. 3.2. Since

$$Q^0 = \frac{\omega_0}{(\omega_2 - \omega_1)} = \frac{f_0}{(f_2 - f_1)}$$

a high value of  $Q^0$  corresponds to a small difference  $(f_2 - f_1)$ , and hence to a sharply tuned, or highly selective, circuit.

TABLE 3.1

( $Q^0 = 100$ )

Frequency	kc/s	$Y$ ( $\Omega^{-1}$ )	$P$ (db)
$f_0$	15.92	0.10	0 (= $P_0$ )
$f_1$	15.84	0.071	-3
$f_2$	16.00	0.071	-3
$f_3$	15.78	0.05	-6
$f_4$	16.06	0.05	-6
$f_5$	15.76	0.045	-7
$f_6$	16.08	0.045	-7

As  $Y$  decreases, so  $I_m (= E_m Y)$  decreases. Now the power  $P$  is  $\propto I^2$ , so that at  $f_1$  and  $f_2$ ,  $P = P_0/2$ , and at  $f_3$  and  $f_4$ ,  $P = P_0/4$ . Since the power ratio in decibels (p. 50) is  $10 \log P_\beta/P_\alpha$ , where  $P_\beta$  and  $P_\alpha$  are the powers compared, we may express the power reduction in the circuit as the frequency varies from  $f_0$  in decibels, as in the last column of this table.

The bandwidth of this tuned circuit is 0.28 kc/s at -6 db, so that all frequencies within  $\pm 0.14$  kc/s of  $f_0$  are accepted with a maximum attenuation of 6 db. If  $R$  increases,  $Q^0$  decreases; for  $R = 100 \Omega$ ,  $Q^0 = 10$ . The selectivity of the circuit is thus very much reduced, and the bandwidth at -6 db has increased to 2.7 kc/s.

For a parallel resonant circuit  $Z_0 = L/CR$  and  $Q^0 = \omega_0 L/R$ , so that  $Z_0 = Q^0/\omega_0 C = Q^0 \cdot X_C$ , where  $X_C$  is the capacitive

## TUNED CIRCUITS

reactance (p. 33). Also,  $Q^0 = (1/R) \cdot \sqrt{L/C}$ , so that  $Z_0 = R \cdot Q^0$ . In this case the variation of impedance  $Z$  with frequency follows closely that of admittance  $Y$  in the series case; in particular, a similar bandwidth/db relationship holds.

### The Universal Resonance Curve

A convenient means of comparing the response of a tuned circuit at resonance with the response at some other frequency is provided by the *universal resonance curve*. Consider a *series* resonant circuit; at any frequency, the impedance  $Z$  is given by:

$$Z = \sqrt{R^2 + (\omega L - 1/\omega C)^2} = R\sqrt{1 + (\omega L/R - 1/\omega CR)^2}$$

And

$$Q^0 = \omega_0 L/R = 1/\omega_0 CR$$

so that

$$\begin{aligned} Z &= R\sqrt{1 + (\omega Q^0/\omega_0 - \omega_0 Q^0/\omega)^2} \\ &= R\sqrt{1 + (fQ^0/f_0 - f_0 Q^0/f)^2} \end{aligned}$$

We represent the quantity  $(f_0 \sim f)/f_0$  by the symbol  $\delta$ ; then  $f/f_0 = 1 - \delta$  and  $f_0/f \approx 1 + \delta$ . Hence

$$\begin{aligned} Z &= R\sqrt{1 + [(1 + \delta)Q^0 - (1 - \delta)Q^0]^2} \\ &= R\sqrt{1 + (2Q^0\delta)^2} \quad \text{or} \quad Z/R = I_m^0/I_m = \sqrt{1 + (2Q^0\delta)^2} \end{aligned}$$

For a *parallel* resonant circuit  $Z/R = I_m/I_m^0$ , so that in this case

$$I_m/I_m^0 = \sqrt{1 + (2Q^0\delta)^2}$$

This function is plotted in Fig. 3.3, for  $Q^0 = 100$ , with  $\delta$  as the independent variable.

### Examples

(1). For a series circuit of  $Q^0 = 100$ , what is the attenuation at  $f = f_0 \pm 50$  kc/s, if  $f_0 = 465$  kc/s?

Here  $\delta = 50/465 = 0.108$ . From the figure,  $I_m^0/I_m = 1.675$  or  $I_m = 0.575I_m^0$ .

(2). What is the bandwidth of a parallel circuit at  $Z = 66\%$  of  $Z_0$ , if  $Q^0 = 100$  and  $f_0 = 10$  Mc/s?

## LABORATORY AND PROCESS INSTRUMENTS

At  $Z_0/Z = 1/0.66 = 1.50$ , the graph gives  $\delta = 0.088$ :

$$\frac{10-f_1}{10} = 0.088 \quad \text{and} \quad 10-f_1 = 0.88$$

so that  $f_2-f_1 = 1.76$  Mc/s, the required bandwidth.

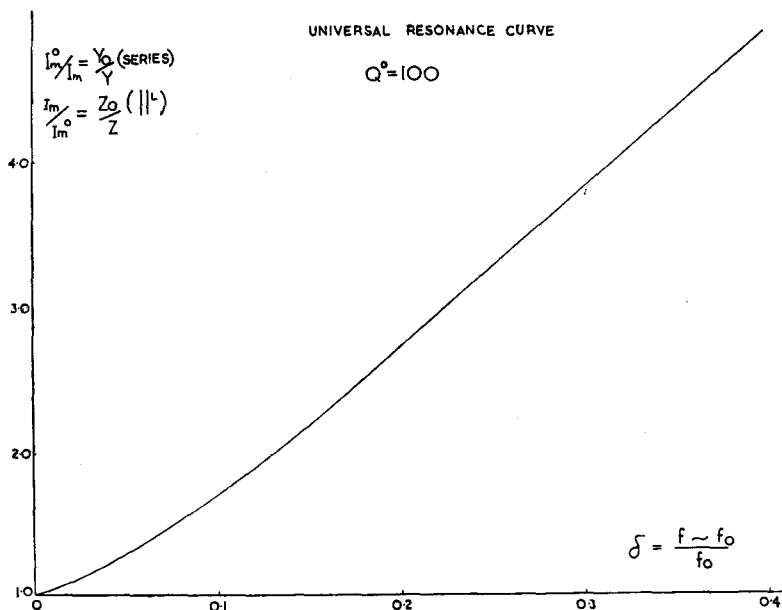


Fig. 3.3. Universal resonance curve

### Acceptor and Rejector Circuits

It is not necessary that the resonant circuit should contain a generator; an e.m.f. may be induced in it by mutual coupling through a transformer to the generator circuit. If the frequency were sufficiently high, the e.m.f. might be induced directly by electromagnetic radiation—as in the aerial circuit of a radio receiver. The voltage-current relationships previously derived will still apply, according as the circuit is a series-, or a parallel-resonant circuit. Such tuned circuits are common in electronic equipment.

For example, an unwanted signal at a pick-up probe could be eliminated by connecting a *series* resonant circuit ('acceptor' circuit), tuned to the frequency of the unwanted signal, from the

## TUNED CIRCUITS

probe to earth. Alternatively, the capacitance of a capacitor is often measured by incorporating it, together with a known inductor to form a *parallel* resonant circuit (the 'rejector' circuit). Applying a voltage source of variable frequency to the circuit, that frequency at which maximum voltage is developed across the circuit ( $Z$  is a maximum  $= Z_0$ ) is the resonant frequency and its measurement enables the capacitance to be evaluated. This procedure is often used to determine the dielectric constant of the medium between the capacitor plates (p. 271).

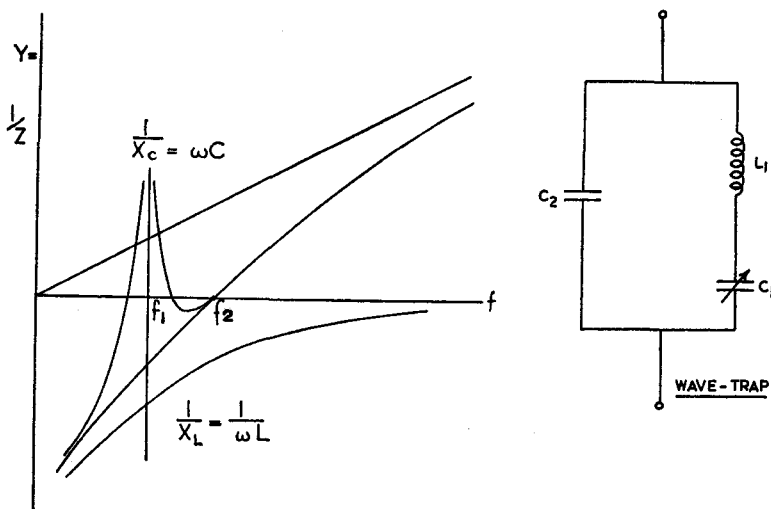


Fig. 3.4. The wave-trap and its response curve

The characteristics of both acceptor and rejector circuits are combined in the *wave-trap* shown in Fig. 3.4. The variable capacitor  $C_1$  is adjusted so that  $L_1 C_1$  form a series resonant circuit at frequency  $f_1$ ;  $C_2$  is then adjusted so that the complete circuit is parallel-resonant ('antiresonant') at frequency  $f_2$ . Thus:

at  $\omega_1^2 = 1/L_1 C_1$ ,  $Z_1 = 0$ , so that if  $\omega_1 = 1/\sqrt{(L_1 C_1)}$  no voltage is developed across the circuit.

at  $\omega_2^2 = (C_1 + C_2)/(L_1 C_1 C_2)$ ,  $Z_2 \rightarrow \infty$ , and for

$$\omega_2 = 1/\sqrt{[(L_1 C_1 C_2)/(C_1 + C_2)]}$$

maximum voltage is developed across the circuit.

### Coupled Circuits

Suppose that the generator, for example a valve oscillator (Chapter VII), produces e.m.f.s of several frequencies, only one of which is required. We could 'filter-out' the other components by applying the complete e.m.f. to a rejector circuit tuned to the desired frequency; maximum impedance will then be presented to this particular frequency. However, a single circuit, unless of very high  $Q^0$  would probably be insufficiently selective to remove all the unwanted components.

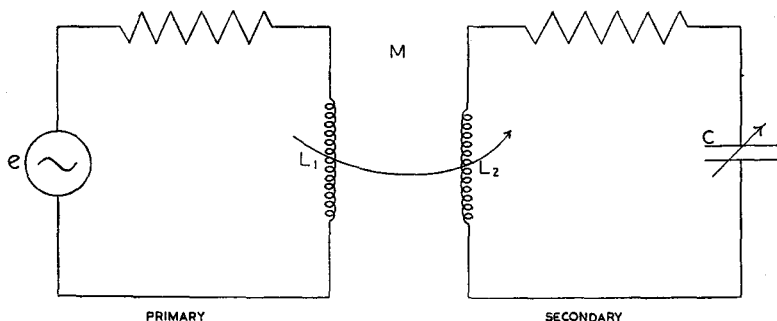


Fig. 3.5. Mutually-coupled circuits

Alternatively, we may wish to accept a band of frequencies, symmetrically disposed about a mean. A single tuned circuit would not differentiate sufficiently between two frequencies, one lying just within the band and the other just outside it.

In both cases it is advantageous to couple mutually the resonant circuit and the generator circuit, using some form of transformer. This is shown in Fig. 3.5.

The transfer of energy between the primary and secondary windings depends upon the *coupling factor*  $k$  defined by:

$$k = \frac{\text{Mutual reactance}}{\sqrt{(\text{Product of all such reactances in the circuits})}}$$

In this case, the 'mutual reactance' is the mutual *inductance*  $M$ ,

$$\therefore k = \frac{M}{\sqrt{(L_1 L_2)}}$$

## TUNED CIRCUITS

If the secondary circuit is tuned to resonate at a frequency  $f_0$ , the behaviour of the complete circuit is governed by the tightness of coupling between primary and secondary—i.e. by the coupling factor  $k$ .

If  $k$  is very small (less than 0.001), the circuits are described as 'loosely coupled'. Little energy is transferred to the secondary circuit, and the complete circuit resonates at  $f_0$ —but with much greater selectivity than if the generator were in the output circuit.

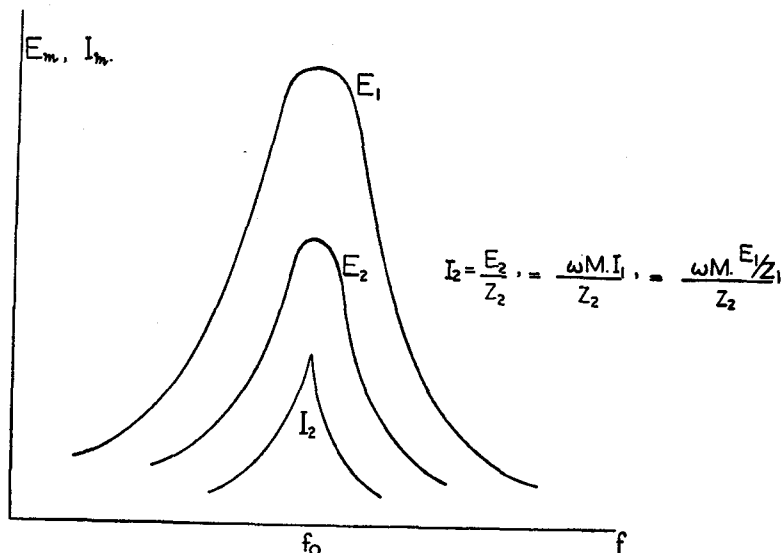


Fig. 3.6. Response curves of loosely-coupled circuits

This is because the induced e.m.f.  $E_2$ , and the secondary impedance  $Z_2$ , are both functions of frequency (for a series circuit,  $Z_2$  is inversely proportional to the frequency), so that the admittance of the circuit  $Y$ , defined by  $Y = I_2/E_2$ , is more sharply dependent upon frequency than is  $Z_2$ . The 'response-curve' is as shown in Fig. 3.6.

If both primary and secondary circuits are tuned to the same frequency  $f_0$ , and the coupling is *tight* ( $k$  greater than 0.05), the *complete* circuit resonates at *two* frequencies,  $f_1$  and  $f_2$ , defined by  $f_1 = f_0 / \sqrt{1+k}$ ,  $f_2 = f_0 / \sqrt{1-k}$ .

# LABORATORY AND PROCESS INSTRUMENTS

The effect of the secondary circuit upon the primary is to increase its impedance by the factor

$$\omega^2 M^2 / Z_2 = \frac{\omega^2 k^2 L_1 L_2}{Z_2}$$

so that the primary impedance is given by:

$$Z_p = Z_1 + \frac{\omega^2 M^2}{Z_2}$$

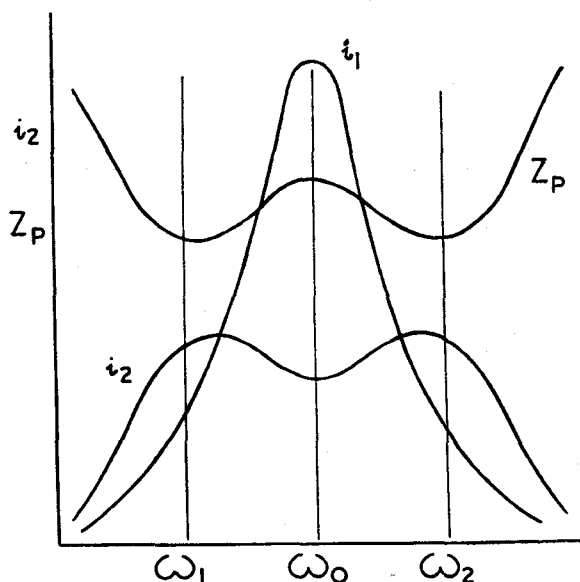


Fig. 3.7. Response curve of tightly-coupled circuit—double-humped curve

This reduces to  $Z_p = Z_1$  under loose-coupling conditions ( $k$  very small). As resonance is approached  $Z_1$  decreases and  $(\omega^2 M^2)/Z_2$  increases; the minimum value of  $Z_p$  is reached when

$$Z_1 = \frac{\omega^2 M^2}{Z_2}$$

This condition defines the frequencies  $f_1 (= f_0 / \sqrt{1+k})$  and  $f_2 (= f_0 / \sqrt{1-k})$ , which are the twin 'humps' of the overall resonance curve. At these frequencies, maximum current flows in the primary circuit, and maximum e.m.f. is induced in the secondary circuit.



## TUNED CIRCUITS

The ratio  $Z_p^0$ , (i.e.  $Z_p$  at  $\omega = \omega_0$ ) to  $Z_p^1$ , (i.e.  $Z_p$  at  $\omega = \omega_1$ ) may be shown to be:

$$\frac{Z_p^0}{Z_p^1} = \frac{R_1 + \omega_0^2 M^2 R_2}{R_1 + \omega_1^2 M^2 R_2} \cdot \frac{R_2^2 + X_2^2}{R_2^2}$$

$X_2$  being the secondary reactance at  $\omega_1$ . From  $\omega_1$  to  $\omega_2$ ,  $Z_p$  first increases to  $Z_p^0$ , then decreases:  $Z_p$  (at  $\omega = \omega_1$ ) =  $Z_p$  (at  $\omega = \omega_2$ ).  $Z_p$  increases rapidly as  $\omega$  changes from  $\omega_1 \rightarrow 0$ , and from  $\omega_2 \rightarrow \infty$ , as seen in Fig. 3.7.

*Example (Fig. 3.8(a))*

If  $L_1 = L_2 = 100 \mu\text{H}$ ,  $M = 10 \mu\text{H}$ ,  $R_1$  (generator internal resistance) =  $50 \Omega$ ,

$$C_1 = C_2 = 100 \text{ pF} \quad \text{and} \quad R_2 = 100 \Omega$$

the coupling factor

$$k = M/\sqrt{(L_1 L_2)} = 10/\sqrt{10^4} = 0.1$$

so that the coupling is 'tight'.

$$f_0 = 1/2\pi \cdot \sqrt{(1/LC)} = 1.59 \text{ Mc/s}$$

$$f_1 = f_0/\sqrt{(1+k)} = 1.59 \times 10^6/\sqrt{1.10} = 1.51 \text{ Mc/s}$$

$$f_2 = f_0/\sqrt{(1-k)} = 1.59 \times 10^6/\sqrt{0.90} = 1.68 \text{ Mc/s}$$

The *bandwidth* is thus 170 kc/s.

In the *previous* example,  $Z_p^0/Z_p^1 = 1.11$ . For the two maxima at  $\omega_1$  and  $\omega_2$  to coalesce,  $k = \sqrt{(R_1 R_2/\omega_0^2 L_1 L_2)}$ ; this value of  $k$  is the *critical coupling factor*  $k_c$ , and defines the condition of *critical coupling*. In the present example

$$k_c = \sqrt{\left(\frac{50 \times 100}{4\pi^2(1.59 \times 10^6)^2 \cdot 10^{-8}}\right)} = 0.071$$

hence for this circuit to become critically coupled we would have to reduce the mutual coupling  $M$  from  $10 \mu\text{H}$ , so that

$$M'/\sqrt{(L_1 L_2)} = 0.071$$

The new value  $M'$  is thus  $7.1 \mu\text{H}$ . The response curve for the critically coupled circuit is shown in Fig. 3.8(b).

For a tightly coupled circuit the ratio  $I_2'(f=f_1 \text{ or } f_2)/I_2^0(f=f_0)$  may be shown to be  $(k^2 + k_c^2)/2k \cdot k_c$ , where  $k$  is the coupling factor and  $k_c$  the *critical coupling factor* for the circuit. In this example,  $I_2'/I_2^0 = 1.06$ .

# LABORATORY AND PROCESS INSTRUMENTS

Maximum *transfer of energy* from the primary circuit to the secondary circuit is obtained under the conditions of *critical coupling* at frequency  $f_0$ . Maximum *selectivity* is attained by *loose coupling*, but the energy transfer is small. A comparatively flat response between certain frequency limits ( $f_1$  and  $f_2$ )—the *band-pass* characteristic—results from tight coupling.

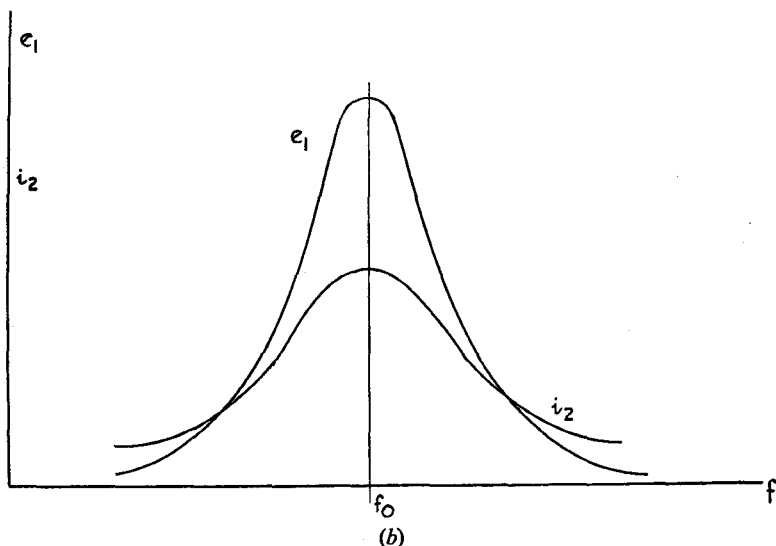
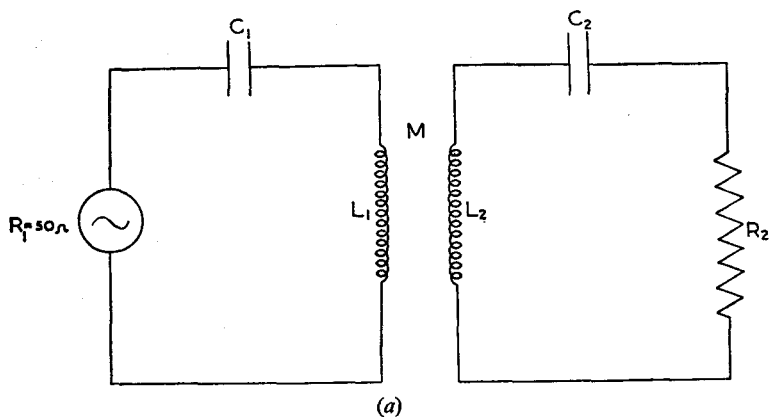


Fig. 3.8. (a) Coupled circuit, with generator resistance included. (b) Response curve—critical coupling

## The Transformer

An important advantage of alternating voltages has already been mentioned, namely, the ease of conversion of one voltage to another by means of a *transformer*.

In one type of transformer frequently used two similar coils are wound upon iron cores built up of lightly oxidised laminations, the magnetic circuit being completed by iron 'yokes' across the ends of the coils. The coils are connected in series. Three typical transformers are shown in Fig. 3.9.

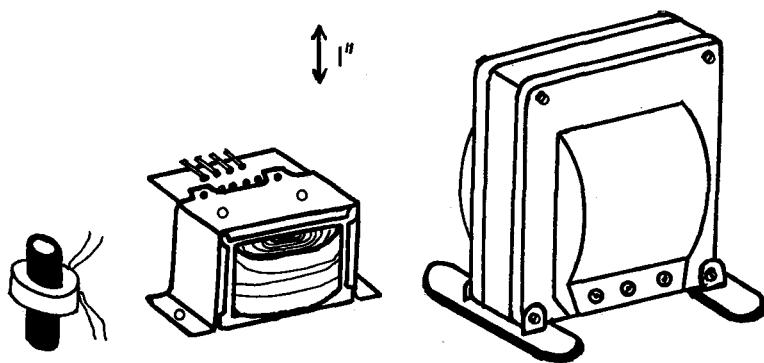


Fig. 3.9. Typical transformers. Left to right: tuned intermediate-frequency; mains transformer; audio-frequency output transformer

We adopt the symbols  $n_p$ ,  $R_p$ ,  $L_p$  for the number of turns, resistance and inductance of the primary winding, respectively; similarly  $n_s$ ,  $R_s$  and  $L_s$  refer to the secondary coil. If in Fig. 3.10(a) an e.m.f.  $e = E_m \cos \omega t$  is applied to the primary winding with the secondary left open-circuited, a primary current  $i_p$  flows, given by:

$$i_p = E_m \cos(\omega t - \phi) / \sqrt{(R_p^2 + \omega^2 L_p^2)}$$

if  $\omega L_p \gg R_p$ ,  $i_p \approx E_m \cos(\omega t - \pi/2) / \omega L_p$ .

The applied e.m.f. is exactly balanced by an e.m.f. of self-induction in the primary,  $e_p$ , given by:

$$e_p = -L_p \cdot di_p/dt = -L_p \cdot d/dt \left( \frac{E_m}{\omega L_p} \cdot \cos(\omega t - \pi/2) \right) = -E_m \cdot \cos \omega t$$

# LABORATORY AND PROCESS INSTRUMENTS

Thus,  $e_p$  leads  $i_p$  by  $\pi/2$ , and leads  $e$  by  $\pi$ . The flux  $\phi$  due to the primary current cuts the secondary winding, and an e.m.f.  $e_s$  is induced in this winding. If every turn of the secondary is linked by the primary flux

$$e_p/e_s = \frac{n_p \cdot d\phi/dt}{n_s \cdot d\phi/dt}$$

so that  $e_s = e_p \cdot n_s/n_p = e_p \cdot T$ , where  $T$  is the *turns ratio* of the transformer,  $n_s/n_p$ .

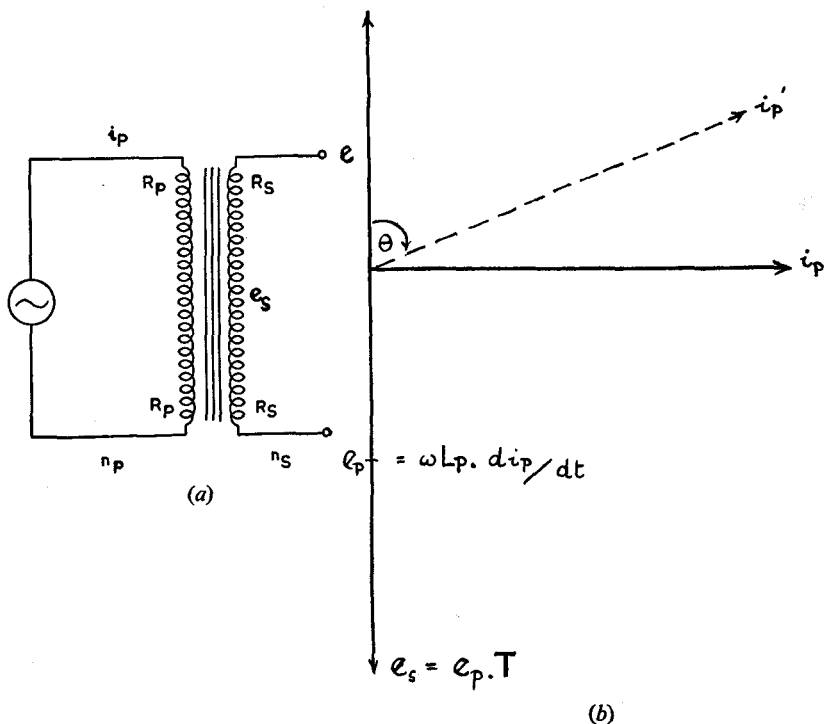


Fig. 3.10. (a) The transformer. Circuit parameters on 'no load'. (b) Transformer vector diagram on 'no load'

The secondary e.m.f.  $e_s$ , like  $e_p$ , is in phase quadrature with the primary current  $i_p$ , so that the induced e.m.f.s  $e_p$  and  $e_s$  are *in phase*, as shown in Fig. 3.10(b). In this diagram  $e_s$  is greater than  $e_p$ , which would be the case for a *step-up* transformer ( $T > 1$ ). The converse would be true of a *step-down* transformer.

## TUNED CIRCUITS

If the primary resistance  $R_p$  is not negligible compared with  $\omega L_p$ ,  $i_p$  leads  $e$  by an angle  $\vartheta$ , less than  $\pi/2$ ;  $\vartheta = \tan^{-1} \cdot \omega L_p / R_p$ . The primary current is represented by the vector  $i'_p$ , in Fig. 3.10(b); there is evidently a large component of this current,  $i'_p \sin \vartheta$ , in quadrature with  $e$ , and this is the magnetising current. A small component  $i'_p \cos \vartheta$ , in phase with  $e$ , represents the 'loss' current, and the product  $e \cdot i'_p \cos \vartheta$  is the power loss in the resistance of the primary winding.

If a load  $Z_L$  is connected across the secondary winding a secondary current  $i_s$  flows, setting up an e.m.f. in opposition to  $e_s$ , which was produced by  $i_p$ . Effectively, the primary inductance is decreased, and  $i_p$  must increase to restore equilibrium between  $e$  and  $e_p$ . An extra current, the *primary load current*  $i_L$ , therefore flows in the primary when a load is connected to the secondary, and the equilibrium condition requires  $n_p i_L = n_s i_s$ , or  $i_L = i_s \cdot T$ . For a step-up transformer ( $T > 1$ )  $i_L > i_s$ ; and, if  $i_s$  is itself large,  $i_L$  may be very much greater than  $i_p$ , the primary current with open-circuited secondary. If we call the total primary current  $I_p$ :

$$I_p = i_p + i_L \simeq i_L$$

Hence  $I_p = T \cdot i_s = (e_s / e_p) i_s$ , so that  $e_p \cdot I_p = e_s \cdot i_s$ , and the input and output powers are equal, i.e. the transformer is 100% efficient. This is only true, however, if the primary resistance  $R_p$  may be neglected.

If the secondary load  $Z_L$  were purely resistive (i.e.  $Z_L = R_L$ ), the secondary current  $i_s$  would be in phase with  $e_s$ , and of magnitude  $e_s / R_L$ , as shown in Fig. 3.11. We have just seen that if the primary resistance  $R_p$  is taken into account,  $i'_p$  leads  $e$ , the supply voltage, by  $\vartheta$ , and  $e_p$  leads  $e$  by  $\pi$ ;  $i_s$  is in phase with  $e_p$ , and  $i_L$  (of magnitude  $T \cdot i_s$ ) is in phase opposition.  $I_p$ , the resultant of  $i_L$  and  $i'_p$ , is the total primary current, and leads  $e$  by an angle  $\phi$ , where

$$\tan \phi = \frac{i'_p \sin \vartheta}{i_L + i'_p \cos \vartheta}$$

For a given primary resistance, or 'loss' (i.e.  $\vartheta$  constant),  $\phi$  decreases as  $i_L$  increases; when  $i_L \gg i'_p$ ,  $i_p$  and  $e$  are in phase. Thus, in a fully-loaded transformer with resistive load, current and voltage are *in phase*, in both primary and secondary windings; the secondary components lead the primary, however, by  $\pi$ .

## LABORATORY AND PROCESS INSTRUMENTS

In general, the secondary load  $Z_L$  will be complex, containing reactance as well as resistance; secondary current and voltage are now no longer in phase. If  $Z_L$  is inductive,  $i_s$  lags behind  $e_s$ .

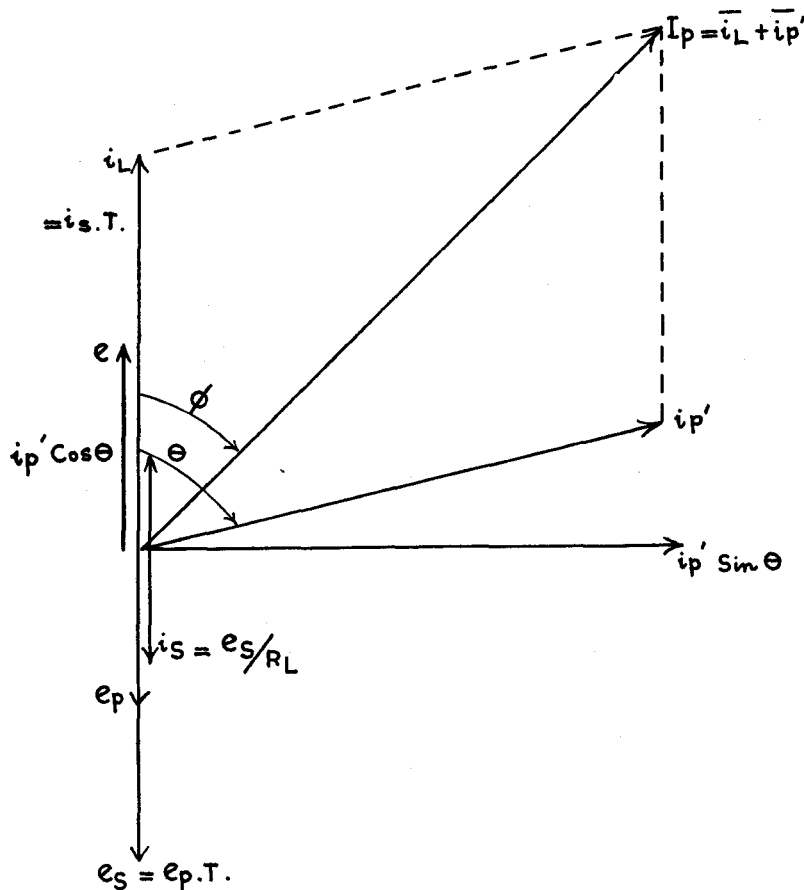


**Fig. 3.11. Transformer vector diagram—resistive load**

by an angle  $\phi_2$ , where  $\phi_2 = \tan^{-1} \omega L' / R'$ ,  $L'$  and  $R'$  being the components of  $Z_L$ . The vector diagram for this case is shown in Fig. 3.12.

## TUNED CIRCUITS

$I_p$  leads  $e$  by an angle  $\phi_p > \phi_2$ . As  $i_s$  increases,  $i_L$  increases, and  $\phi_p$  approaches  $\phi_2$ , so that on full load the secondary current again leads the total primary current by  $\pi$ . Secondary current and voltage, however, are no longer in phase.

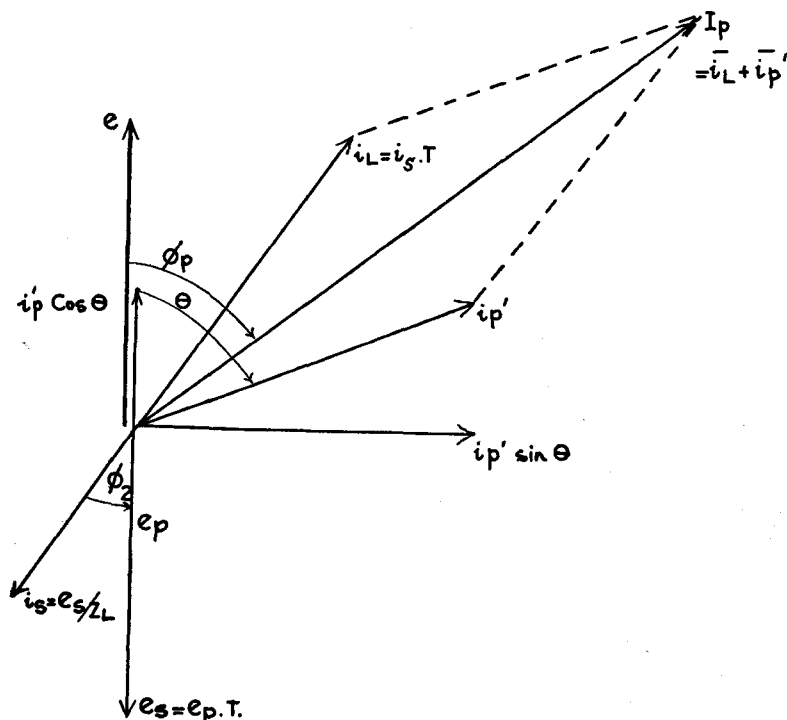


Fig. 3.12. Transformer vector diagram—reactive load

## The Auto-transformer

Transformers which consist of a single winding, across part of which the supply voltage is connected, the secondary voltage being selected by an arm which rotates round the coil, are called auto-transformers. In the circuit of Fig. 3.13, the turns-ratio of the transformer is given by:

$$\frac{(\text{number of turns in coil } BC)}{(\text{number of turns in coil } AB)}$$

## LABORATORY AND PROCESS INSTRUMENTS

Evidently if the rotating arm moves to *D* we have a step-up transformer. Auto-transformers are relatively simple in construction, and may easily be made continuously variable; however, the load is not isolated from the mains supply voltage, and great care must be taken to ensure that the point *B* is the *neutral* of the supply.

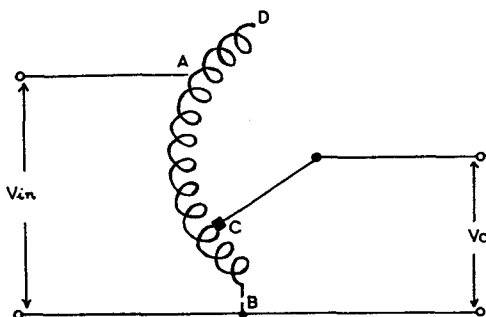


Fig. 3.13. The auto-transformer

The range of auto-transformers known as 'Variac'† transformers provide output voltages continuously variable between 0–270 V (for 230 V input), or 0–135 V (for 115 V input), at power ratings from 60 VA to 7 kVA. Spring-loaded carbon brushes on the moving arm make contact with the coil. (For constant voltage transformers, see p. 107.)

### Maximum Power Transfer

Consider a generator, which might be a valve oscillator, or an electrical machine, connected in series with an impedance  $Z_g$  consisting of its internal resistance and associated circuit, and with a load of impedance  $Z_L$  (Fig. 3.14). It is important to know the relationship between  $Z_g$  and  $Z_L$  for maximum power to be developed in the load.

We consider first the simpler case of a battery, having an e.m.f.  $E$  and internal resistance  $R_b$ , connected to a load  $R_L$ . The current is then  $E/(R_b + R_L)$ , and the power developed in  $R_L$  is:

$$P_L = R_L \cdot \frac{E^2}{(R_b + R_L)^2}$$

† Manufactured by General Radio Co., Cambridge, Mass., U.S.A., and by Zenith Electric Co. Ltd., London.



## TUNED CIRCUITS

For  $P_L$  to be a maximum,  $dP_L/dR_L = 0$ , i.e.

$$(R_b + R_L)^2 \cdot E^2 - 2(R_b + R_L) \cdot R_L E^2 = 0$$

$R_b + R_L = 2R_L$ , or  $R_L = R_b$ . Thus, maximum power is developed in the load when its resistance is equal to the internal resistance of the battery.

For the more general case of reactive circuits (Fig. 3.14),

$$I = E / \sqrt{[(R_g + R_L)^2 + (X_g + X_L)^2]}$$

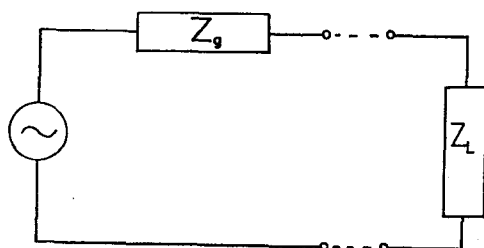


Fig. 3.14. Generator internal impedance

and  $P_L = E^2 \cdot R_L / \sqrt{[(R_g + R_L)^2 + (X_g + X_L)^2]}$ . The power  $P_L$  is a maximum for  $X_g = -X_L$ , and  $R_g = R_L$ ; this is the case when  $Z_g$  and  $Z_L$  are equal in magnitude but of opposite sign, i.e. are *conjugate impedances*.

### Impedance Matching

In the previous section, we found the condition for maximum power to be obtained in a load directly connected to a generator. Usually, however, we cannot vary  $Z_L$ , and must connect it indirectly to the generator if it differs considerably from  $Z_g$ . Consider the general case shown in Fig. 3.15, in which load and generator are connected by a transformer.

$Z_g$  is the impedance of the generator, and  $Z_L$  is the load impedance.  $L_p$  and  $Z_p$  are the inductance and impedance respectively of the primary winding, and  $L_s$ ,  $Z_s$  the corresponding terms for the secondary. If  $M$  is the mutual inductance of the windings, the supply e.m.f.  $e$  is given by:

$$e^2 = (Z_g + Z_p)^2 i_p^2 + \omega^2 M^2 i_s^2$$

where  $i_p$  and  $i_s$  are the primary and secondary currents. We have also:

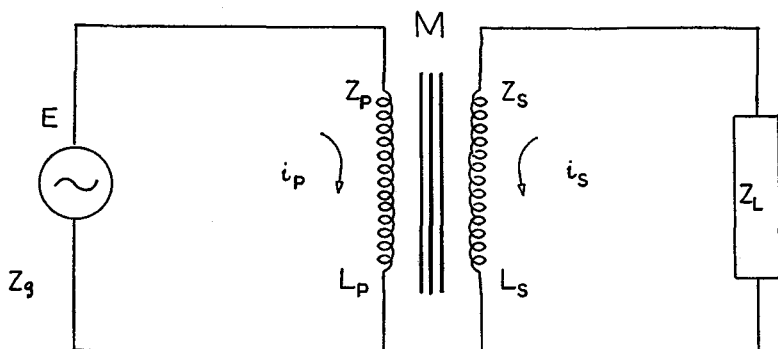
$$(Z_s + Z_L)^2 i_s^2 = -\omega^2 M^2 i_p^2$$

Eliminating  $i_s$ , by vectorial addition we have:

$$e = \left( Z_g + Z_p + \frac{\omega^2 M^2}{Z_s + Z_L} \right) \cdot i_p$$

If the primary and secondary resistances are small, so that

$$Z_p = \omega L_p, Z_s = \omega L_s, e = \left( Z_g + \omega L_p - \frac{\omega^2 M^2}{Z_L + \omega L_s} \right) \cdot i_p$$



$Z_g$  = Generator impedance  
 $Z_L$  = Load impedance  
 $Z_p, Z_s$  = Primary and secondary winding impedances  
 $L_p, L_s$  = Primary and secondary inductances

Fig. 3.15. Matching of generator and load impedances

If we assume  $\omega L_p, \omega L_s$  to be  $\gg Z_L$  and  $\omega M$ , and also that  $M^2 = L_p L_s$  (i.e. the coupling factor  $k = 1$ ):

$$e = (Z_g + Z_L L_p / L_s) \cdot i_p$$

Now  $L_p \propto n_p^2$ , and  $L_s \propto n_s^2$ , and

$$e = (Z_g + Z_L n_p^2 / n_s^2) \cdot i_p = (Z_g + Z_L / T^2) \cdot i_s T$$

where  $T$  is the turns ratio of the transformer. Hence

$$i_s = e / T (Z_g + Z_L / T^2)^2$$

The power developed in the load  $Z_L$  is  $P_L = i_s^2 Z_L$ , i.e.

$$P_L = Z_L \cdot e^2 / T^2 (Z_g + Z_L / T^2)^2$$

## TUNED CIRCUITS

For maximum power in the load we equate  $dP_L/dZ_L$  to zero, in the usual way, obtaining the condition

$$(Z_g + Z_L/T^2) \cdot e^2/T^2 = Z_L(e^2/T^2)[2(Z_g + Z_L/T^2)/T^2]$$

i.e.  $Z_L = T^2 \cdot Z_g$ .

Thus, for maximum power to be developed in  $Z_L$ , this load should be matched to the generator impedance  $Z_g$  by coupling the circuits together through a transformer of turns-ratio  $T = \sqrt{Z_L/Z_g}$ . To 'match' a high-impedance load to a low-impedance generator requires a step-up transformer—and vice versa.

### Example

In the output stage of an audio-frequency amplifier, the  $15\ \Omega$  coil of a loudspeaker could be matched to the  $5000\ \Omega$  anode load impedance of a typical output valve by a transformer of  $T = \sqrt{(15/5000)}$ , i.e. a step-down transformer of ratio 1:18.

## References

- RENTON, R. N. (1950). *Telecommunications Principles*. Pitman.  
 STARR, A. T. (1954). *Electronics*. Pitman.  
 WELLER, B. F. (1951). *Radio Technology*. Chapman and Hall.

## Problems

1. Two similar circuits consisting of  $L = 150\ \mu\text{H}$ ,  $R = 100\ \Omega$  and  $C = 0.001\ \mu\text{F}$ , are inductively coupled, the coupling factor being 0.2. An e.m.f. of 10 V r.m.s. at 500 kc/s is applied in series with one circuit; calculate the current in each circuit.

*Answer.* Primary current = 85 mA; secondary current = 43 mA.

2. A parallel resonant circuit has  $Q_0 = 150$ ,  $f_0 = 490\ \text{kc/s}$ . Calculate the voltage attenuation at  $f = f_0 \pm 25\ \text{kc/s}$ . What is the bandwidth at 6 db down?

*Answer.* Attenuation = 3 db; bandwidth = 127 kc/s.

3. The inductances of two coupled coils  $L_1 L_2$  are 2 mH and 20 mH, respectively, and the coupling coefficient is 0.5. If their resistances are negligible, calculate the open-circuit voltage across  $L_2$  when 1 V is applied across  $L_1$ .

*Answer.* 1.582 V.

4. Find the ratio of a transformer suitable for matching the  $10\ \Omega$  input coil of a pen recorder to a valve anode of effective resistance  $2000\ \Omega$ .

*Answer.* Ratio 14.1:1.

## CHAPTER IV

### Thermionic Emission

#### Thermionic Emission

When a thin wire of a metal such as tungsten is raised to a high temperature, electrons are detached from the outer atoms of the metal, and form a cloud in the vicinity of the wire. Equilibrium

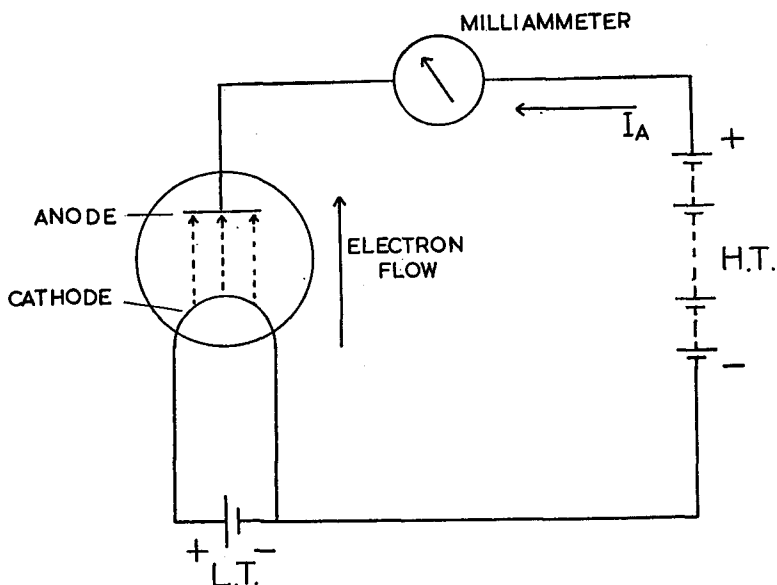


Fig. 4.1. Thermionic emission—the diode valve

will be established when the rate of this 'evaporation' is equal to the rate of return of electrons from the cloud to the wire; the absorption of electrons by gas molecules such as the nitrogen and oxygen molecules of the air is practically eliminated by enclosing the wire in a highly evacuated glass, or silica, envelope.

This phenomenon is called *thermionic emission*. To make use of it, we introduce a positively charged electrode (the anode, or

## THERMIONIC EMISSION

'plate') into the envelope, so that electrons are attracted away from the cloud (or space charge) and an electron-current flows across from the heated wire to the anode. This device, shown in circuit with its supply batteries in Fig. 4.1, is called a *diode*. A general name for similar components is 'valve' (p. 76). The thin tungsten wire, or *filament*, is electrically heated by the low tension (L.T.) battery to about  $2400^{\circ}\text{C}$ . Anode current  $I_a$  flows through the high tension (H.T.) battery, the circuit being completed by the electron stream in the diode.

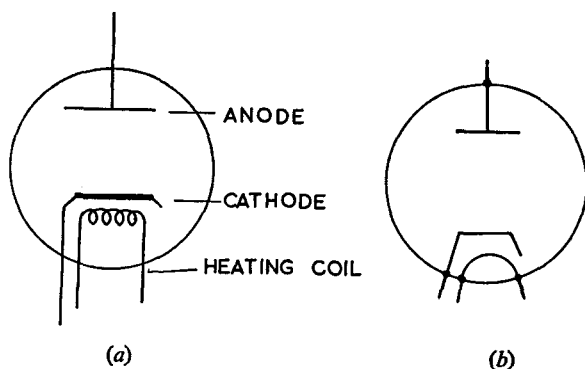


Fig. 4.2. Indirectly heated valve: (a) schematic diagram; (b) commonly used symbol

The efficiency of such a device is low;  $I_a$  is about 2 mA per watt expended in heating the filament. This may be improved by coating the wire with a mixture of alkaline earth oxides, or by using the wire merely to heat a nickel cylinder (the cathode) coated with similar emissive material, and electrically insulated from the heating filament. The efficiency is raised to about 40 mA/W, at a lower temperature of about  $1900^{\circ}\text{C}$ . Diodes and other tubes of the emissive-filament type are said to be *directly* heated; those of the emissive cathode type, *indirectly* heated. They are illustrated in Figs. 4.1 and 4.2.

The filaments of directly heated valves must be heated by direct current, because variations of filament voltage would be impressed upon the anode current. With indirectly heated valves alternating current may be used to heat the cathode, which

attains a mean temperature; the electron current is thus much more constant.

Directly heated diodes are still used where large anode currents are involved, but in general instrumental use indirectly heated valves are invariably used.

Anodes of small valves are usually of steel, corrugated for strength, and to improve their radiation of heat; larger valves have molybdenum or tantalum anodes. Considerable heat is generated when the electrons are brought to rest, and the valve must be able to dissipate this without distortion of its electrodes.

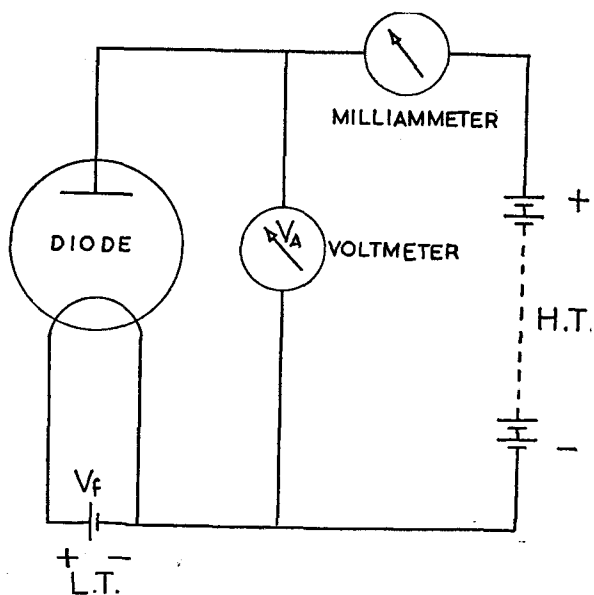
The diode allows anode current  $I_a$  to flow if the anode is positive with respect to the cathode or filament; if this polarity is reversed, no current flows. For this reason, thermionic devices of this kind have become known in England as 'valves', whether they are in fact operating as unidirectional devices or not. In America the term 'tube' is used (German *rohre*, French *lampe*).

### The Diode

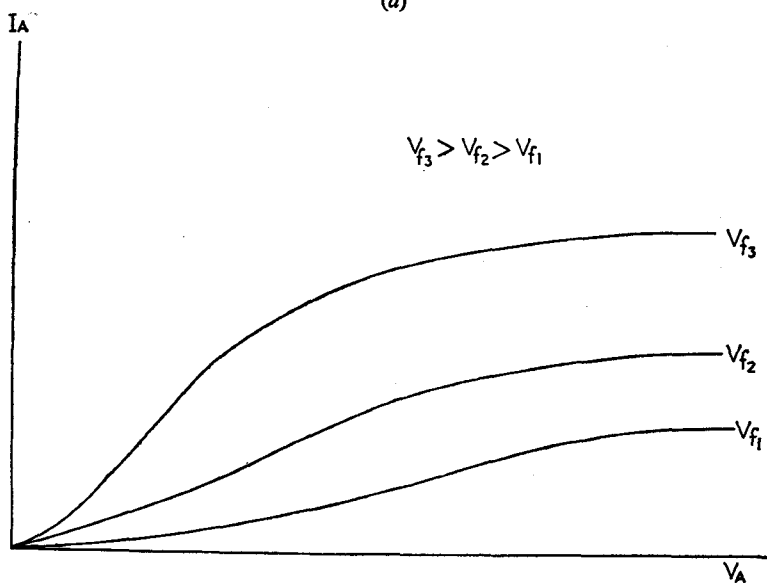
If the circuit of Fig. 4.3(a) is set up we can investigate the variation in anode current  $I_a$  with change of anode voltage  $V_a$  at a number of values of filament voltage  $V_f$ . We obtain a series of  $I_a/V_a$  curves, as shown in Fig. 4.3(b); at each value of the filament voltage  $V_f$ , increase of  $V_a$  leads to the attainment of a maximum anode current, when electrons are withdrawn from the space charge at the same rate as they are supplied from the cathode. This maximum value is the *saturation current*; it increases as  $V_f$  increases.

In practice however the anode current is *never* varied by alteration of  $V_f$ ; this is fixed at the manufacturer's specification, so that the cathode is heated to optimum temperature. Under these conditions  $I_a$  follows a 'three-halves' law; for example, for concentric-cylinder anode and cathode,  $I_a = k/r(V_a^{3/2})$ , where  $r$  is the radius of the anode cylinder, assumed large in comparison with that of the cathode, and  $k$  is a constant.

The diode is mainly used for the conversion of alternating into direct current. In the circuit of Fig. 4.4 current flows through the valve only when the anode is at a positive potential with respect to the cathode; no current flows when the reverse condition applies. However, charge will be stored in the capacitor  $C$ , and may be drawn upon during the 'non-conductive' half-cycle to even out the flow of current through the load (see Figs. 5.1 and 5.2).



(a)



(b)

Fig. 4.3. Diode characteristics: (a) circuit; (b) characteristic curves

## LABORATORY AND PROCESS INSTRUMENTS

Diodes vary in size from the large tubes capable of supplying 1–10 amp, to ‘detector’ diodes dealing with a few micro-amp. For a further consideration of diode rectification, see p. 101.

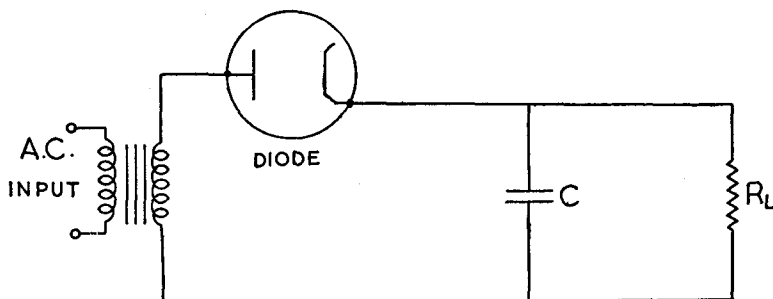


Fig. 4.4. Diode half-wave rectifier circuit

### The Triode

The usefulness of the diode is enormously enhanced if a third electrode is introduced—thus converting it into a triode. This extra electrode is a wire mesh, usually of molybdenum, placed near to the cathode, called the *control grid* and designated  $g_1$ . The grid has a much stronger control over the anode current than has the anode, because it is nearer to the cathode. In Fig. 4.5(a) the anode current is shown as a function of anode voltage at various grid voltages; in Fig. 4.5(b) anode current is shown as a function of grid voltage at various anode voltages. It will be noticed that, in the latter diagram, both positive and negative values of grid voltage are considered; in practice, however, the grid is never maintained at a positive voltage, for reasons which we shall consider later.

The (anode current)–(anode voltage) curves are similar to those of the diode, except that the anode voltage required for saturation current may be increased by making the grid more negative.

The (anode current)–(grid voltage) curves are called the *mutual characteristics* of the triode; over a considerable range of (negative) grid voltage they are almost linear, so that  $I_a$  is proportional to  $V_g$ . At any given anode voltage there is a limiting grid voltage which just reduces the anode current to zero; this is the *cut-off*



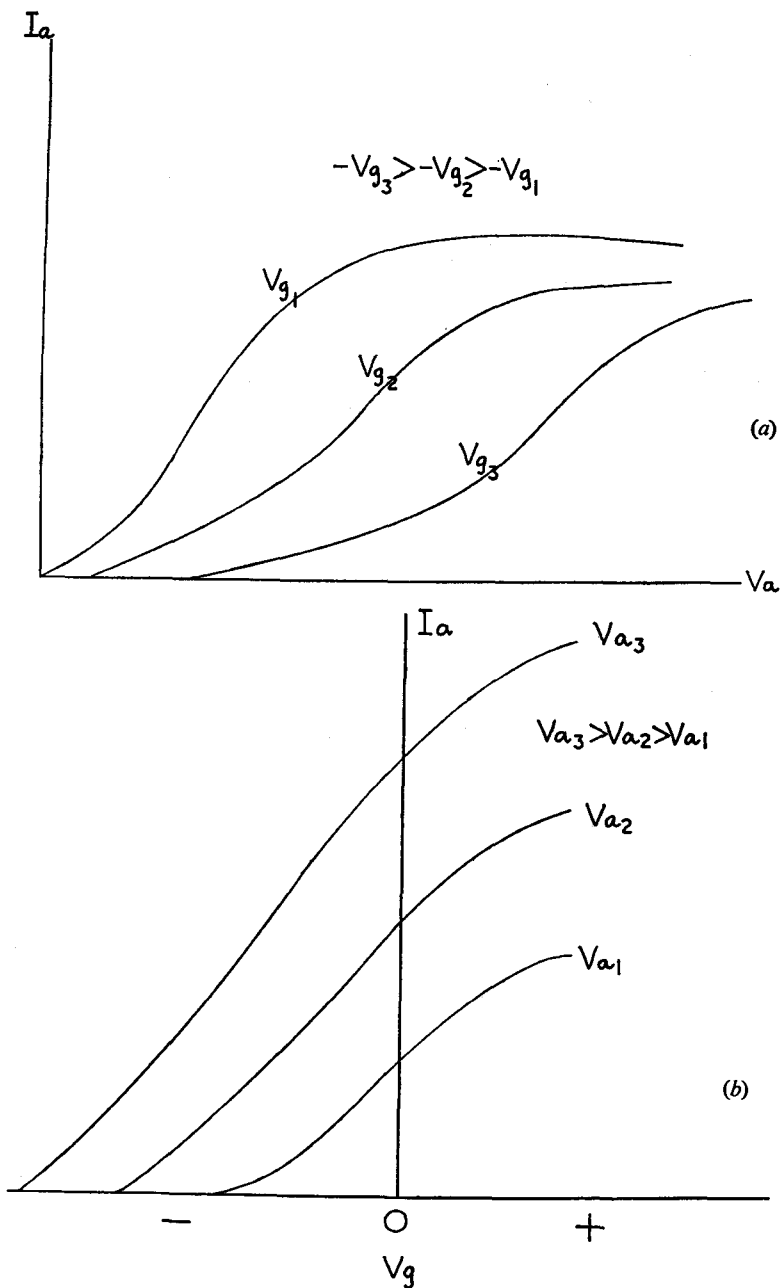


Fig. 4.5. Triode characteristics: (a) anode current/anode voltage; (b) anode current/grid voltage

# LABORATORY AND PROCESS INSTRUMENTS

voltage  $V_{g_{c.o.}}$ . The mutual characteristics are curved in the vicinity of  $V_{g_{c.o.}}$ , and also in regions of positive grid voltage; in practice, however, we arrange the steady grid voltage (the *grid bias*) so that only the linear portion is utilised. In particular, we avoid allowing the grid voltage to become positive, for it would then attract electrons, causing a flow of 'grid current'; this damps the input circuit (p. 155), and may damage the valve by overheating and distorting the grid.

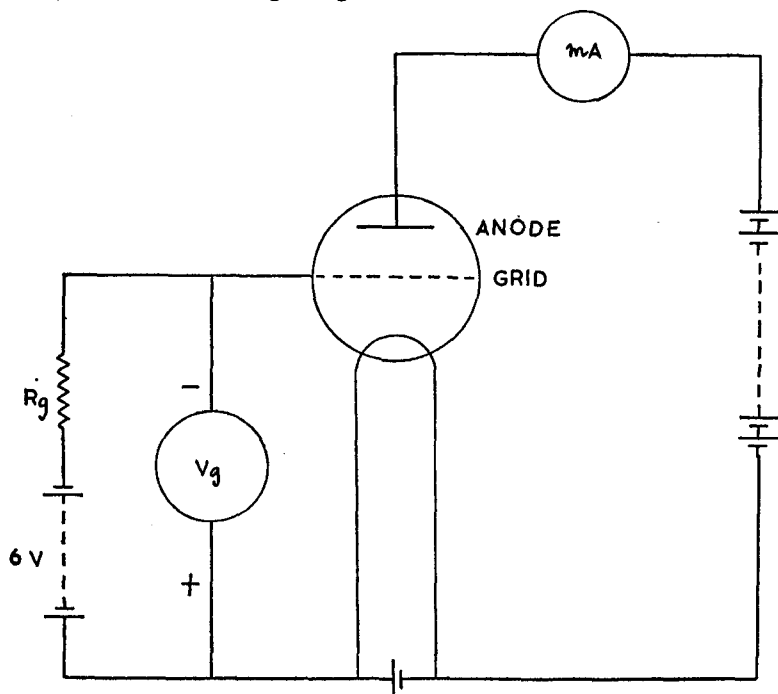


Fig. 4.6. (a) Grid bias for directly heated triode.

The slope of the (anode current)–(anode voltage) curve is  $(\partial I_A / \partial V_A)_{V_g}$ , the subscript indicating that this is appropriate to a given value of grid voltage  $V_g$ . The inverse of the mean slope  $(\partial V_A / \partial I_A)_{V_g}$  is called the *anode resistance*, and given the symbol  $r_a$ ; it is measured in ohms. The slope of the (anode current)–(grid voltage) curve is  $(\partial I_A / \partial V_g)_{V_a}$ , called the *mutual conductance*, symbol  $g_m$ ; it is measured in mA/V. The product  $(r_a \cdot g_m)$ , where  $r_a$  is in *kilohms* and  $g_m$  in mA/V, is dimensionless; it indicates the

## THERMIONIC EMISSION

relative control of grid and anode over the anode current and is called the *amplification factor*,  $\mu$ , of the valve.

These three parameters of a valve,  $r_a$ ,  $g_m$ , and  $\mu$ , are called the *valve characteristics*, and are quoted by the manufacturer as an aid in designing a suitable circuit, and choosing suitable operating conditions for that valve.

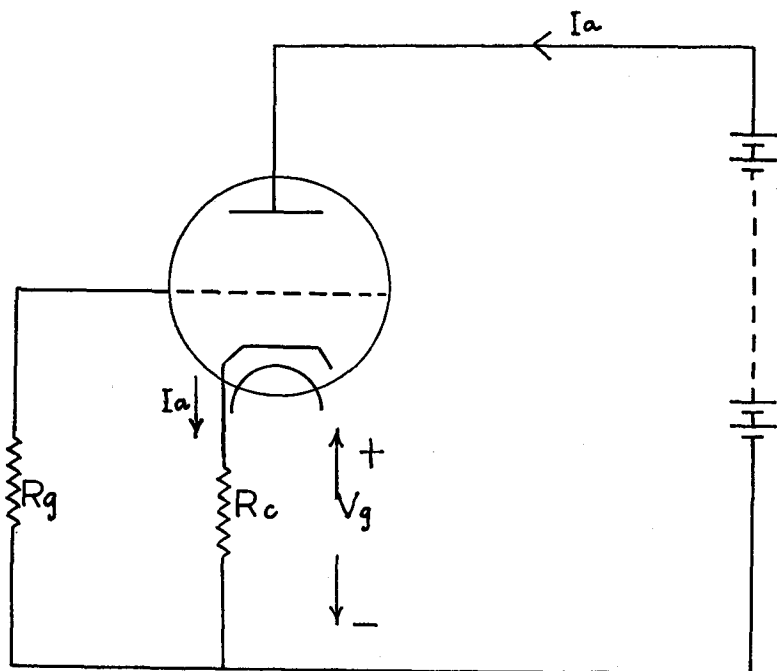


Fig. 4.6. (b) Cathode bias for indirectly heated triode

Triodes are designed for two main purposes: *voltage* amplification and *current* amplification. The characteristics of typical examples of these two types are listed below:

	<i>Mullard ECC35†</i> voltage amplifier	<i>Mullard PM202</i> current amplifier	
$I_a$ (mean anode current)	2.3	14	(mA)
$r_a$ (mean)	34	2.0	(k $\Omega$ )
$g_m$ (mean)	2.0	3.5	(mA/V)
$\mu$ (mean)	68	14	

† Half of the double triode.

Triodes, like diodes and other valves, may be directly or indirectly heated. The heater and anode voltages may be derived from batteries or from a power-supply unit (p. 104). The steady voltage applied to the grid—the grid bias voltage—may be obtained from a small dry battery, or, in the case of indirectly heated valves, may be developed across a resistor in the cathode circuit. Thus in Fig. 4.6(b) the potential of the grid with respect to the cathode will be  $-V_g$ , as in Fig. 4.6(a), if  $I_a R_c = V_g$ . Cathode bias resistors usually have values between 200 and 2000  $\Omega$ , and are ‘decoupled’ (p. 141) by an electrolytic capacitor of high capacity. The resistor  $R_g$  is called the *grid leak*; it provides a return path to H.T. –ve for those stray electrons which collide with the grid, so that a negative charge does not accumulate. To prevent damping of the input impedance  $R_g$  is large, usually between 250 k $\Omega$  and 3 M $\Omega$ .

### Limitations of the Triode

The triode finds many applications as an amplifier (p. 123), oscillator (p. 153) and detector (p. 114). Its use is limited, however, by the inter-electrode capacity between anode and grid ( $C_{g,a}$ ) of capacitance 1.5–5 pF. There are of course other inter-electrode capacities, such as that between grid and cathode ( $C_{g,c}$ ), but it is  $C_{g,a}$  which has the greatest effect—sometimes called the Miller effect.

The grid and anode circuits of a triode valve are interconnected (‘coupled’) by  $C_{g,a}$ , so that energy may be fed back from the anode into the grid; if this feedback voltage is *in phase* with the grid voltage, amplification increases progressively and very rapidly, and the valve generates ‘oscillations’ (p. 154). This is particularly the case at radio frequencies, where  $C_{g,a}$  forms a comparatively easy path; for this reason, we cannot in general use a triode as a high-frequency amplifier unless the effect of  $C_{g,a}$  is overcome.

There are two ways in which this may be accomplished, the first being known as ‘neutralising’. In Fig. 4.7 the anode is connected to an inductor  $L$  centre-tapped to the H.T. +ve, the other end of which returns to the grid via the small variable capacitor  $C_n$ —the *neutralising* capacitor. Since H.T.+ and the cathode are at the same a.c. potential, the voltages at the ends

### THERMIONIC EMISSION

of  $L$  are in antiphase, and the voltages fed back via  $C_n$  and  $C_{g,a}$  tend to cancel out;  $C_n$  may be adjusted for exact cancellation. The circuit may be re-drawn in a.c. Wheatstone bridge form, as

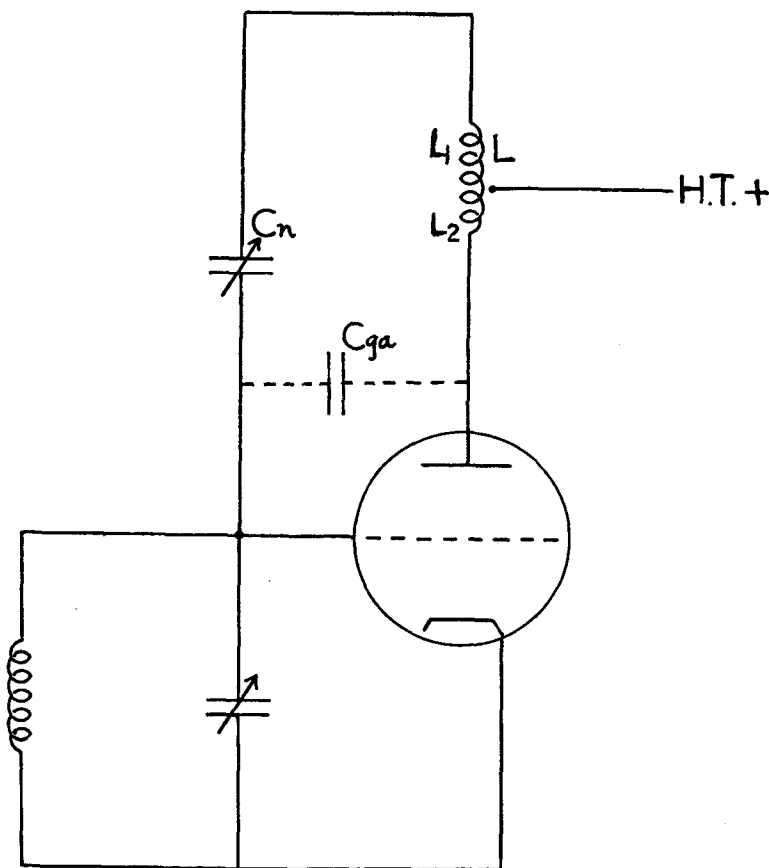


Fig. 4.7. Neutralisation of  $C_{g,a}$  of triode valve

shown in Fig. 4.8. Neutralisation is achieved when, so far as this circuit is concerned, point  $G$  is at earth potential, i.e. when  $C_n/C_{g,a} = L_1/L_2$ , where  $L_1$  and  $L_2$  are the inductances of the two sections of the anode coil.

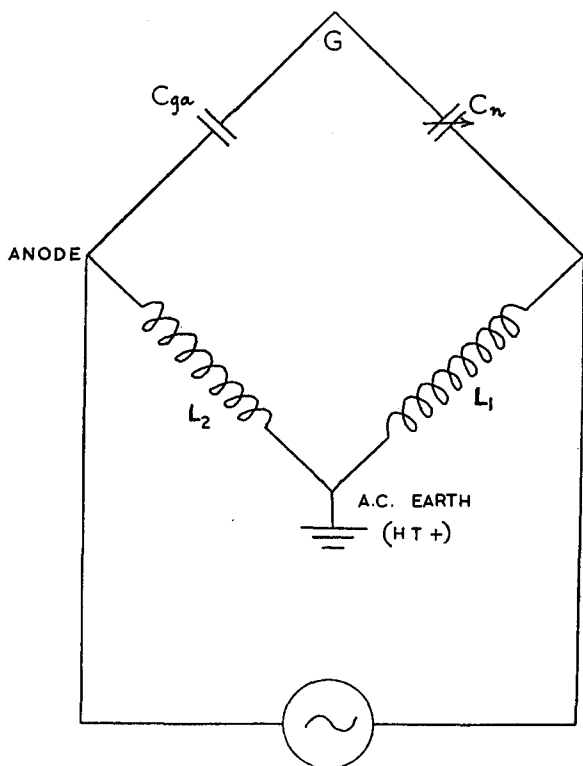


Fig. 4.8. Equivalent bridge circuit of Fig. 4.7

### The Tetrode

A second method of overcoming the Miller effect is to reduce  $C_{g,a}$  inside the valve, by introducing a second grid between the control grid and the anode. This second, or 'screen' grid, is connected to a source of high d.c. potential, so as not to reduce the anode current; but it is maintained practically at earth potential as regards alternating voltages, by a relatively large capacitor to earth. An earthed screen has thus been effectively introduced within  $C_{g,a}$ , so that no voltage may be fed directly from grid to anode. This is shown, together with the line diagram of a tetrode valve, in Fig. 4.9.  $C_{g,a}$  is reduced to 0.01 pF, or even less, in the tetrode.

## THERMIONIC EMISSION

The screen grid is referred to by the symbol  $g_2$ , and the (d.c.) potential of this grid is written  $V_{g_2}$ . The mutual characteristic  $g_m$  must now be defined as  $(\partial I_a / \partial V_{g_2})_{V_a, V_{g_1}}$ , i.e. the values of anode and screen voltage must be specified. The value of  $g_m$  is not very different from that of a triode; the (anode current)–(anode voltage) curve, however, as shown in Fig. 4.10(b)†, shows a marked difference from the corresponding curve for a triode.

Suppose  $V_{g_2}$  remains constant, whilst the anode voltage  $V_a$  is increased from zero. At first the anode current  $I_a$  increases, and the screen-grid current  $I_{g_2}$  decreases. Over the range of anode voltage ( $V_a = A$ ) to ( $V_a = B$ ), however, increase in  $V_a$  decreases  $I_a$

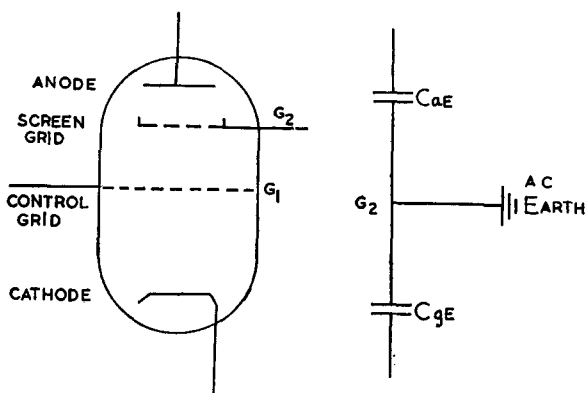


Fig. 4.9. Tetrode valve and inter-electrode capacities

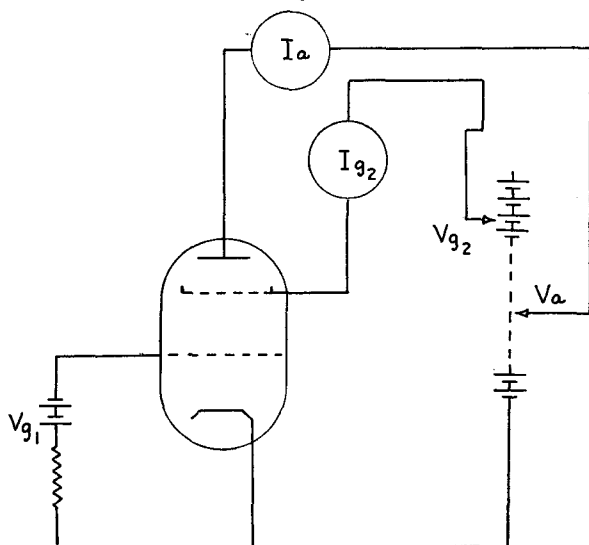
and increases  $I_{g_2}$ ; evidently over this region  $(\partial V_a / \partial I_a)$  is negative, corresponding to a negative anode resistance. Beyond ( $V_a = B$ ),  $I_a$  increases with increase in  $V_a$ , until saturation current is reached, and  $I_{g_2}$  decreases correspondingly.

The behaviour over the range  $A$ – $B$  is due to the phenomenon of *secondary emission*. If the anode voltage is sufficiently great, the electrons, accelerated by this voltage, arrive at the anode with enough energy to cause other electrons to be emitted from the anode material; these are called *secondary electrons*. As  $V_a$  is increased, the number of secondary electrons increases also; and at some point (corresponding to  $V_a = A$  in Fig. 4.10(b)) it exceeds the number of 'primary' electrons arriving from the cathode.

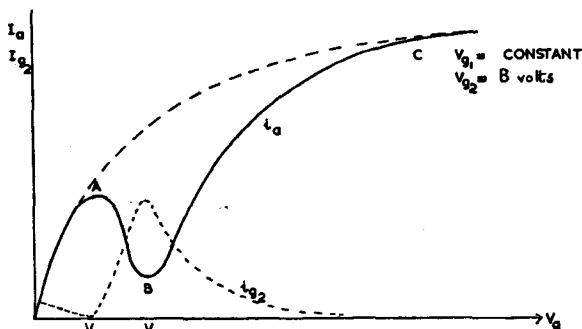
† Obtained by measurements on the circuit of Fig. 4.10(a).

# LABORATORY AND PROCESS INSTRUMENTS

Now this value of anode voltage is *less* than  $V_{g_2}$ , so that once they are ejected from the anode the secondary electrons are accelerated towards the screen grid; effectively,  $I_a$  falls and  $I_{g_2}$ ,



(a)



(b)

Fig. 4.10. Tetrode characteristics: (a) circuit; (b) anode and screen currents as functions of anode voltage

rises. The process continues until  $V_a = V_{g_2}$  (about the point *B* on the diagram); secondary electrons now return to the anode, and fewer primary electrons 'stick to' the screen, so that  $I_a$  rises and  $I_{g_2}$  falls.



## THERMIONIC EMISSION

The region  $A-B$ , over which  $r_a$  is negative, is made use of in the dynatron oscillator (p. 160), but for amplification purposes only the region beyond  $B$  is employed.

Apart from reducing  $C_{g,a}$  the screen grid, by interposing a positive potential between cathode and anode, reduces the control of the latter over the anode current. Since  $r_a = (\partial V_a / \partial I_a)$ , and  $\mu = g_m \cdot r_a$ , both  $r_a$  and  $\mu$  will be greater for the tetrode valve than for the triode, average values might be  $r_a$ , 100 k $\Omega$  to 2 M $\Omega$ ;  $\mu = 200-1000$ .

### The Beam Tetrode

The 'kink' in the  $I_a/V_a$  curve of the tetrode limits its working range as an amplifier. One way of smoothing the curve out is by very careful alignment of screen and control-grid wires, so that

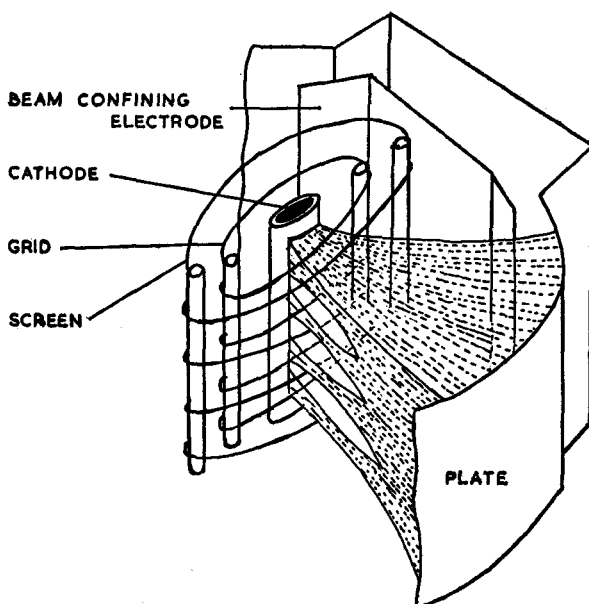


Fig. 4.11. Beam tetrode—electron beam

electrons are 'beamed' to the anode through the screen grid mesh; and by beam-forming plates, at anode potential, which return the electrons produced by secondary emission to the anode.

## LABORATORY AND PROCESS INSTRUMENTS

Such valves are known as *beam tetrodes*, and are much used as audio-power output valves, e.g. the Brimar 807 having:

$$r_a = 39 \text{ K}\Omega, g_m = 5.7 \text{ mA/V}, W_o = 11.7 \text{ W at } V_a = 500 \text{ V}, \\ V_{g_2} = 200 \text{ V}, i_a = 50 \text{ mA}.$$

These characteristics are similar to those of an output pentode valve (see next section). The beam tetrode action is illustrated in Fig. 4.11.

### The Pentode

Another way of removing the tetrode 'kink' is to prevent electrons produced by secondary emission from being attracted to the screen by placing a low-potential grid between the screen

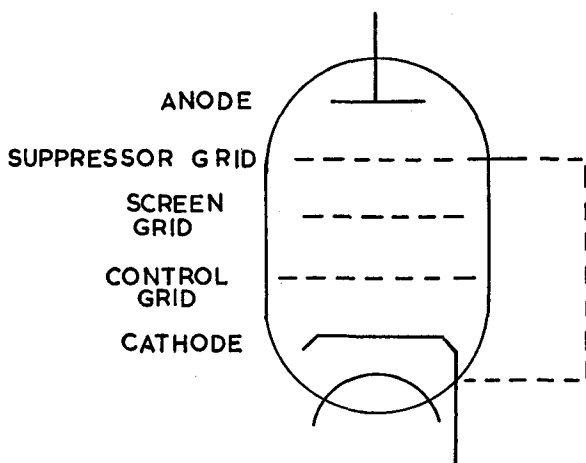


Fig. 4.12. Pentode valve—disposition of electrodes

and the anode. This third grid is called the *suppressor* grid, and given the symbol  $g_3$ . The voltage on this grid  $V_{g_3}$  is usually the same as the cathode voltage, which may be ensured by connecting  $g_3$  internally to the cathode; sometimes, however,  $g_3$  is brought out to a separate pin on the valve base (p. 96), which may then be earthed, or connected to a small negative bias voltage. Secondary electrons now return to the anode even when  $V_a$  is less than  $V_{g_2}$ ; the original purpose of the screen grid  $g_2$ , which was to reduce  $C_{g,a}$ , is not affected. The pentode valve is illustrated in Fig. 4.12.

## THERMIONIC EMISSION

Pentodes, like triodes, are of two main types, designed for voltage amplification and current amplification. The characteristics of two typical valves are listed below:

	Mullard EF36 <i>R.F. voltage amplifier</i>	Mullard EL37 <i>current amplifier (output pentode)</i>	
$I_a$	2.0	100	(mA/V)
$r_a$	2500	2.5	(k $\Omega$ )
$g_m$	1.8	11	(mA/V)
$\mu$	4500	27.5	

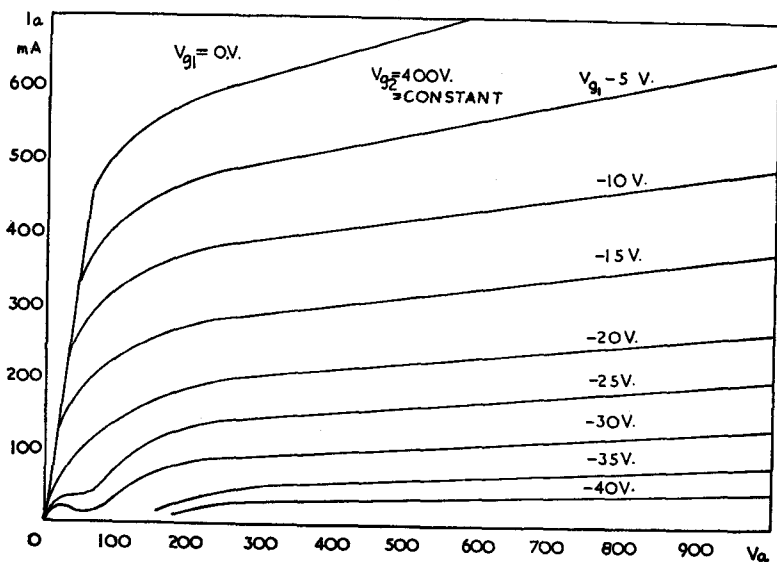


Fig. 4.13. Pentode valve—anode current/anode voltage curves

The variation of anode current with anode voltage, for varying grid voltages, is shown in Fig. 4.13. Above about  $V_a = 150$  V, the anode current is almost constant despite changes in  $V_a$ , and for this reason the pentode valve is sometimes referred to as a constant current device.

The curves of anode current against grid voltage (the mutual characteristics) so far considered have been linear over most of the range between  $V_g = V_{g_{c.o.}}$  and  $V_g = 0$ . Hence over this range  $g_m$  is constant. In certain voltage-amplifying valves, however,

# LABORATORY AND PROCESS INSTRUMENTS

the  $I_a/V_g$  characteristic is made non-linear, so that  $g_m$  varies from one bias voltage to another. Thus, the  $\mu$  of the valve ( $= g_m \cdot r_a$ ) may be varied by altering the steady negative grid voltage, or *working point* (p. 125); such valves are designated *variable- $\mu$* , and a typical variable- $\mu$  mutual characteristic curve is shown in Fig. 4.14. These valves are generally used in circuits employing some form of automatic gain-control. Suppose that part of the

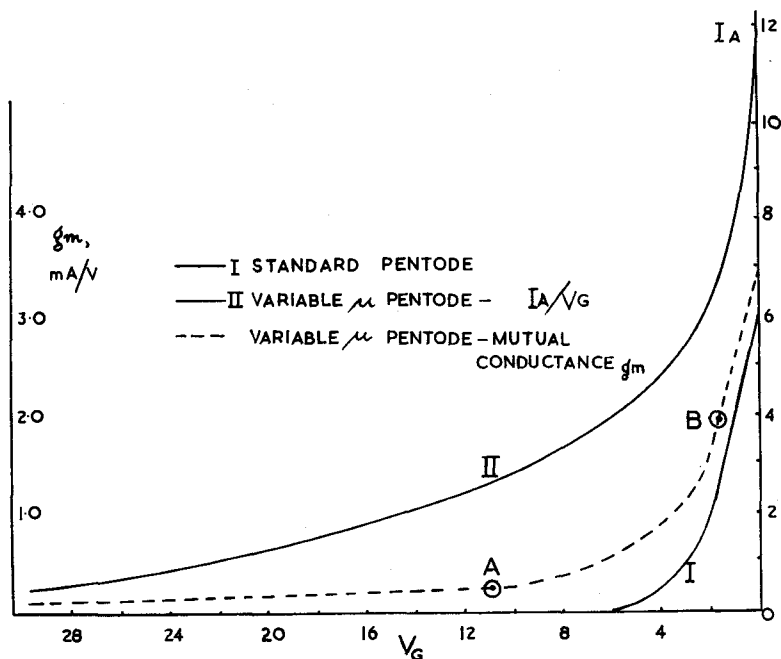


Fig. 4.14. The variable-valve; mutual conductance/grid voltage

amplified signal voltage is rectified and used as the negative grid bias voltage, the point *A* might be fixed by a negative voltage derived from the amplified signal. The slope of the tangent to the curve at *A* gives  $g_m$  under these conditions. If now the amplitude of the signal voltage is for some reason reduced, the negative bias developed from it will also be reduced, so that, for example, we may have a change of working point from *A* to *B*. At this point,  $g_m$  is greater than at *A*, so that the amplification of the weaker signal is automatically increased. If the signal voltage

## THERMIONIC EMISSION

increases, the negative bias is increased, and a smaller value of  $g_m$  is obtained. Thus, the output tends to remain constant, irrespective of the input voltage.

### Multi-grid Valves

Hexode and heptode valves contain further grids, as the names suggest; they are chiefly used as 'mixers' (see below). Consider the electrode arrangement of the valve shown in Fig. 4.15(a).

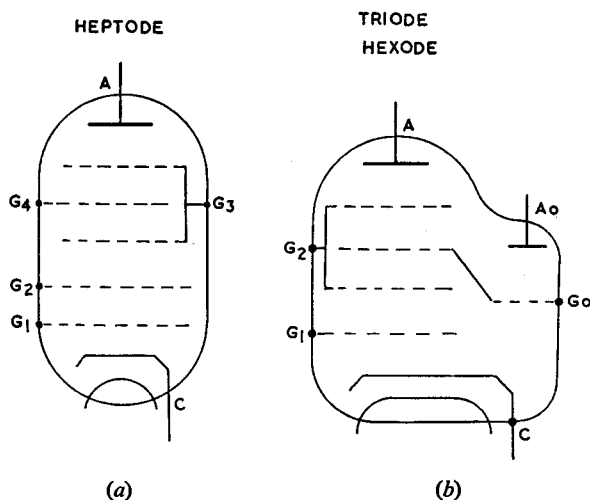


Fig. 4.15. (a) Heptode valve—enumeration of grids:  $G_1$ , oscillator grid;  $G_2$ , oscillator anode;  $G_3$ , screen;  $G_4$ , signal grid. (b) Triode hexode valve:  $G_1$ , signal grid;  $G_2$ , screen grid;  $G_0$ , oscillator grid;  $A_0$ , oscillator anode

The electron stream passes through two control grids,  $g_1$  and  $g_4$ , separated by the screen grid  $g_3$ ; the anode current is therefore modified by voltages on either or both of these control grids.† If the voltages on the control grids are  $v_{g_1}$  and  $v_{g_4}$ , where

$$v_{g_1} = V_1 \sin \omega_1 t$$

and  $v_{g_4} = V_4 \sin \omega_4 t$ , the anode current is a product function of both these voltages, containing the component

$$g_m \cdot V_1 V_4 \sin \omega_1 t \cdot \sin \omega_4 t$$

† In Fig. 4.15(b) the oscillator grid  $g_0$  corresponds to the second control grid  $g_4$  of Fig. 4.15(a).

this may be written in the alternative form:

$$g_m \left[ \frac{1}{2} V_1 V_4 \cos(\omega_1 - \omega_4) t - \frac{1}{2} V_1 V_4 \cos(\omega_1 + \omega_4) t \right]$$

Hence sum and difference frequency components appear in the anode current, and could be separated by suitable tuned circuits. This is the basis of *mixing*, or *frequency changing*; if the anode circuit is tuned to the frequency  $(\omega_1 - \omega_4)/2\pi$ , the component of

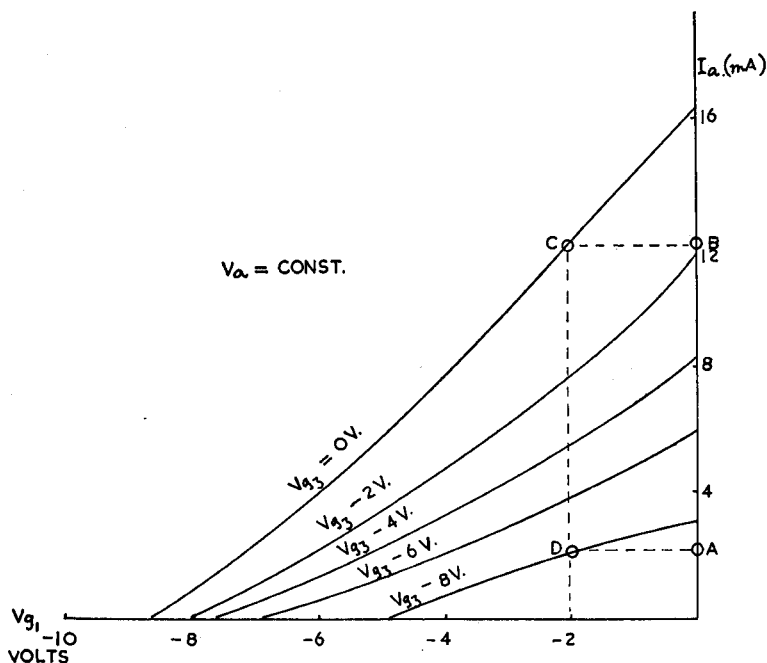


Fig. 4.16. Mixer valve—conversion conductance

this frequency will be magnified by the  $Q$  of the circuit, and the remaining components effectively eliminated. This principle is used in the superheterodyne radio receiver, where most of the amplification takes place at the difference frequency  $(\omega_s - \omega_L)/2\pi$ ,  $\omega_s/2\pi$  being the incoming signal frequency, and  $\omega_L/2\pi$  the frequency of a signal generated by an oscillator within the receiver (the 'local oscillator'). It is also made use of in the *beat-frequency oscillator*, which generates voltages in the audio-frequency range. The voltage derived from a fixed-frequency oscillator (e.g. 1000

## THERMIONIC EMISSION

kc/s) is mixed with the output of a second oscillator, whose frequency may be varied (e.g. between 900 and 1000 kc/s). The difference-frequency voltage is selected by a tuned circuit, so that the output frequency is variable also (in this case it may be varied continuously between 100 kc/s and zero).

An important parameter of a mixer valve is the Conversion Conductance. In Fig. 4.16, the mutual characteristics of the hexode section are drawn, with constant anode voltage  $V_a$ , but with varying oscillator-grid voltage  $V_g$ . If the signal grid bias  $V_{g1}$  is  $-2$  V, and  $V_g$  swings between zero and  $-8$  V, the anode current  $i_a$  varies between the points *A* and *B*. The mutual conductance of the hexode  $g_m$  is defined by  $(\partial i_a / \partial V_{g1})$  at anode voltage  $V_a$  and at the maximum positive value of  $V_g$ , i.e.  $V_g = 0$ ; hence  $g_m$  is given by the slope of the mutual characteristic at the point *C*. At the extreme negative value of  $V_g$  (point *D*) the slope is much less, so that the mean slope within the range *A-B* is approximately  $g_m/2$ . The mean slope determines the Conversion Conductance  $g'_m$ , which is  $(\partial i'_a / \partial V_{g1})$  at anode voltage  $V_a$ , and with  $V_g$  the oscillator voltage;  $i'_a$  is the component of anode current at the difference frequency  $(\omega_S - \omega_L/2\pi)$ . Optimum conversion occurs at  $g'_m = g_m/2$ , the conditions which apply here.

### Composite Valves

For full-wave rectification (p. 104) it is convenient to enclose two diodes, with or without separate cathodes, in one envelope, to form the *double diode* valve. In small diodes used for signal-voltage rectification an amplifying triode is often included, forming a diode (or double diode) triode; the diodes rectify the signal and the triode then amplifies it (p. 123).

Double triodes, and triode pentodes, are mainly used at audio-frequencies, since they have fairly large inter-electrode capacities. In the triode hexode, the triode section operates as an oscillator (p. 153) and provides a voltage to be 'mixed' with the incoming signal in the hexode section, rather as in the beat-frequency oscillator already described. The triode grid is internally connected to grid  $g_3$  of the hexode.

### 'Soft' Tubes

The valves so far described are evacuated to a pressure of about  $10^{-3}$  mm of mercury (a 'hard' vacuum, which is obtained by

## LABORATORY AND PROCESS INSTRUMENTS

pumping out the air and removing the last traces of it, after sealing the tube, by firing a small magnesium coil—technically known as a 'getter'—inside it). In two important classes of tubes, however, the envelope is subsequently filled with an inert gas, e.g. neon or argon, to a pressure somewhat greater than atmospheric. These tubes are divisible into gas-filled *diodes*, used as voltage stabilisers and reference tubes and gas-filled *triodes* and *tetrodes*, known as *thyatron*s; both are referred to as 'soft' tubes.

In thyatron, a filament heats up the cathode, and electrons are accelerated towards a positively charged anode, as in 'hard' tubes; voltage stabilisers† are 'cold-cathode' tubes. In

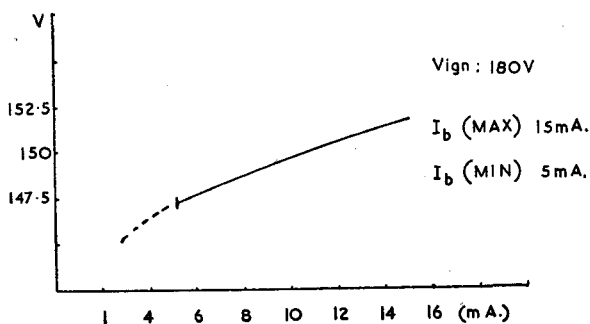


Fig. 4.17. Voltage stabiliser tube—characteristic curve

their passage to the anode, however, the electrons collide with gas atoms or molecules, and cause some of these to ionise; most of the current is conducted (from anode to cathode) by the positive ions formed. The anode voltage at which conduction occurs, and which determines the velocity acquired by the primary electrons, is fixed by the dimensions of the tube, its geometry and the nature and pressure of the gas. Gas-filled tubes are available to conduct, or 'strike', at voltages within the range 75–150 V. The operating, or 'burning', voltage is usually 15–30 V below the striking voltage. The characteristic curve for a 'soft' diode is shown in Fig. 4.17.

Between  $I_{\min}$  and  $I_{\max}$ , the voltage rises only by about 5 V, or 4%; the current may increase by a factor of 8–12 over this range. This property accounts for the use of 'soft' diodes as voltage stabilisers and as voltage reference tubes (see p. 108).

† Also called voltage regulating tubes.



## THERMIONIC EMISSION

Thyratrons are gas-filled triodes and tetrodes. If the grid is maintained at a large negative voltage, the anode voltage may be raised considerably above the normal striking voltage without the tube conducting. Reduction of the grid bias may now cause the tube to fire. The thyratron characteristic is shown in Fig. 4.18.

If, with the anode voltage held at  $V_a$ ,  $V_g$  is increased from  $V_{g1}$  (i.e. the negative bias is *decreased*) the tube fires at  $V_{g1}$ . Return to  $V_{g1}$ , or even beyond, will not reduce the current  $I_a$  through the tube; once the tube fires, the grid loses control, and only reduction of  $V_a$  below the critical value  $V_{ac}$  can extinguish it. The

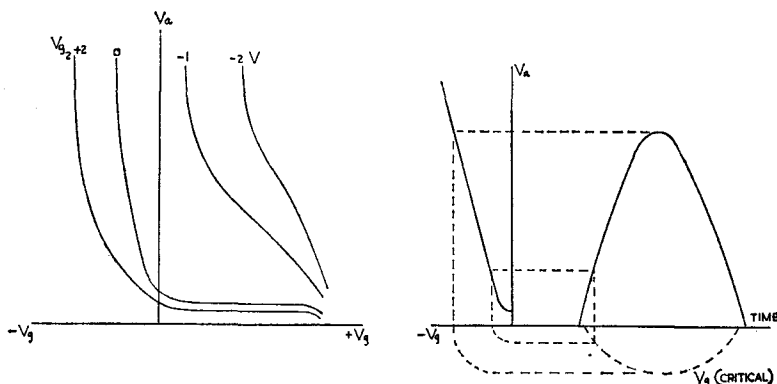


Fig. 4.18. Thyratron characteristics

thyatron may be regarded as a switch—turned ‘on’ by the grid voltage  $V_g$ , and ‘off’ by the anode voltage  $V_a$ . For applications of the thyatron, see p. 171.

Small, neon-filled discharge tubes are often used as ‘on-off’ indicators in mains equipment. They strike at about 180 V and burn at 150 V, with a current consumption of 0.5 mA. On 240 V mains, therefore, they operate with a 120 k $\Omega$  resistor in series. Their consumption is about 0.1 W as compared with the average torch bulb, or ‘pea-lamp’, which, consuming 0.3 amp at 4.5 V, dissipates 1.35 W.

However, where a pea-lamp is used in electronic apparatus, it must be replaced when necessary by one of similar watts rating. This is obviously necessary if the bulb is connected in series with, e.g. a chain of valve filaments; but equally, if it is fed in parallel with other components from a small transformer, it may, by its

## LABORATORY AND PROCESS INSTRUMENTS

added current, reduce the voltage applied to these components. For example, on one occasion it was found that the failure of two such lamps, in parallel across part of a valve-filament circuit, raised the voltage applied to the heaters from 6.3 to 7.5 V.

### Cold Cathode Tubes

In these tubes the cathode is not heated, and electrons are drawn from it by the close proximity of the anode. A positive voltage applied to a subsidiary electrode—the *trigger*—may initiate conduction. Such devices are called 'trigger-tubes', for example the Mullard Z803U shown in a typical circuit in Fig. 4.19.

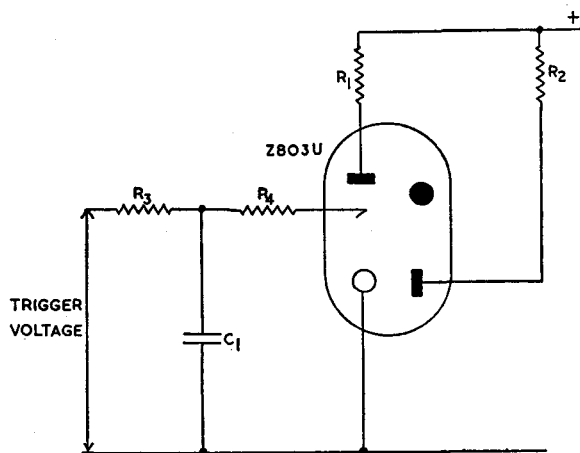


Fig. 4.19. Trigger tube—basic circuit

In this tube, a fourth electrode is provided so that a priming current of about  $10\ \mu\text{A}$ , derived from the H.T. supply, may be passed. This stabilises the operation of the tube. With an anode voltage of 200 V the application of a positive pulse of about 130 V peak to the trigger causes conduction, and the tube passes about 10 mA until the anode circuit is broken.

### Valve Bases

Originally all valves had pins at one end, which plugged into a corresponding valve base; there were from four to eight pins, numbered *clockwise* looking on to the pins—or at the *underside*

# THERMIONIC EMISSION

of the valve base. A typical arrangement for a pentode valve with eight pins is shown in Fig. 4.20. The valve plugs into a valve base with eight holes (an octal base); as the valve pins are arranged symmetrically, there is a locating spigot on the valve, and a corresponding central 'keyway' in the valve-base so that the orientation is fixed. Some valves which plug into octal bases have only six or seven pins, and even if the valve has eight pins they

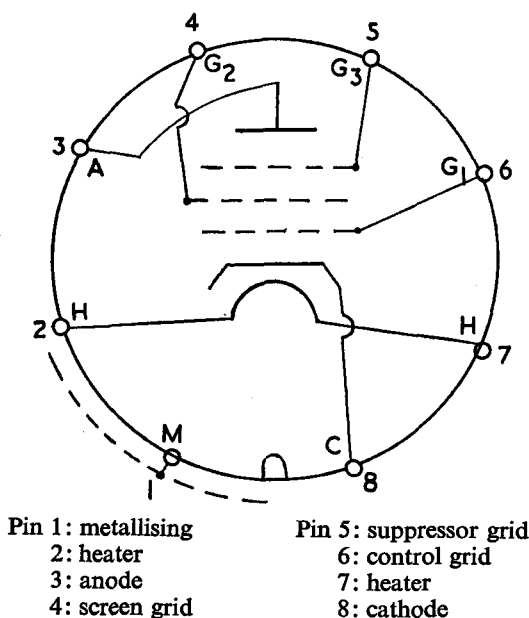


Fig. 4.20. Schematic diagram of pentode valve with octal base

may not all be connected internally. In some older valves, one or more connections were provided at the end opposite from the pins, to which anode and/or grid were connected. The electrode locations of such a valve might, for example, read (see footnote, p.98):

1	2	3	4	5	6	7	8	$T/C$
$M$	$h$	$a$	-	$d_1$	-	$h$	$d_2$	$g_1$

This valve is a double-diode triode, pins 4 and 6 not being used, and having a top-cap control grid connection.

## LABORATORY AND PROCESS INSTRUMENTS

Until recently the pins were connected to the various electrodes by wires sealed in a glass sandwich—the 'pinch'—and this was a source of considerable inter-electrode capacity. Although medium-power diodes, and some large low-frequency amplifying valves, are still of this type, modern valves differ considerably.

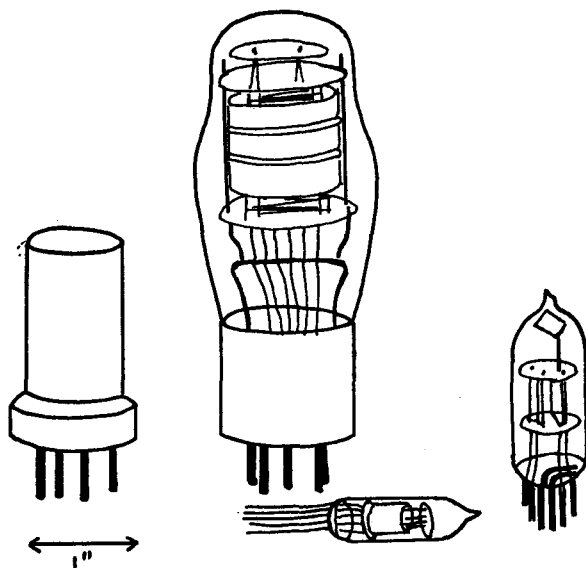


Fig. 4.21. Comparison of some electronic valves

In the first place they are much smaller, whilst retaining the same heat dissipation. Secondly, the electrode wires are themselves brought out through the base, without a pinch; there are no separate pins, or top-caps. The connections to a modern triode hexode are as follows†:

1	2	3	4	5	6	7	8	9
<i>M</i>	<i>h</i>	<i>a</i> (H)	<i>g</i> <sub>2</sub>	<i>g</i> <sub>3</sub>	<i>a</i> (T)	<i>h</i>	<i>c</i>	<i>g</i> <sub>1</sub> (H)
			<i>g</i> <sub>4</sub>	<i>g</i> (T)				

(H = hexode section; T = triode section)

† The symbols used are: *M*, metallising; *h*, heater; *a*, anode; *g*<sub>1-4</sub> grids; *d*, diode; *c*, cathode.

## THERMIONIC EMISSION

There is a comparatively large gap between pins 1 and 9, which enables the valve to be correctly located in its base, and fixes the starting point for the enumeration of the pins.

Some very small (sub-miniature) valves have no base, leads from the electrodes being brought through the glass envelope, so that they may be directly soldered into the circuit. Examples of these various types are shown in Fig. 4.21.

There are several fairly comprehensive lists of British and American low-power valves, including all the types mentioned in this chapter. The important valve parameters, and typical operating conditions of current, voltage, load and power, as well as the base connections, are listed.

### References

- A Guide to the Application of Voltage Reference and Stabiliser Tubes.* Mullard technical publication MVT8066 (1955).
- ALDOUS, W. H. and APPLETON, SIR EDWARD (1952). *Thermionic Vacuum Tubes and their Applications.* Methuen.
- EASTMAN, A. V. (1949). *Fundamentals of Vacuum Tubes.* McGraw Hill.
- SPANGENBERG, K. R. (1948). *Thermionic Vacuum Tubes.* McGraw Hill.
- Thyratrons for Industrial Control.* Mullard technical publication TP318 (1957).
- WALKER, R. C. (1950). *Industrial Applications of Gas-filled Triodes (Thyratrons).* Chapman and Hall.
- 'Wireless World'—*Radio Valve Data Handbook.* Iliffe (1956).

### Problems

1. An indirectly heated valve has an anode load of  $25,000\ \Omega$  and a cathode resistor of  $600\ \Omega$ . The grid is returned to the low-potential end of the cathode resistor. If the voltage drop across the anode load is 75 V, calculate (a) the anode current; (b) the effective grid bias voltage of the valve.

*Answer.*  $I_A = 3\ \text{mA}$ ;  $V_g = -1.8\ \text{V}$ .

2. From the following data, calculate the anode resistance ( $r_a$ ) mutual conductance ( $g_m$ ) and amplification factor ( $\mu$ ) of the valve.

$V_g$	$I_a$	$V_a$	$V_g$	$I_a$	$V_a$
0	0.5 mA	20 V	-0.5 V	0.5 mA	50 V
1		40	1		90
2		95	2		150
3		142	3		190
4		180	4		230

# LABORATORY AND PROCESS INSTRUMENTS

$V_g$	$I_a$	$V_a$	$V_g$	$I_a$	$V_a$
-1 V	0.5 mA	100 V	-2 V	0.5 mA	195 V
	1	140		1	235
	2	198		2	245
	3	240			

Answer.  $r_a = 50 \text{ k}\Omega$ ;  $g_m = 2 \text{ mA/V}$ ;  $\mu = 100$ .

3. The following data give the anode current ( $i_a$  m-amp)/anode voltage ( $V_a$  V) values for a *tetrode* valve, at three values of grid voltage ( $V_g$  V), and at constant screen voltage +80 V. Plot the  $i_a/V_g$  curves, and comment upon the results.

$V_g$	$V_a$	$i_a$	$V_g$	$V_a$	$i_a$	$V_g$	$V_a$	$i_a$
0	20	3.25	-1.0	20	1.6	-2.0	20	0.75
	40	2.75		40	1.5		40	0.60
	60	2.75		60	0.9		60	0.55
	80	4.50		80	2.25		80	1.00
	100	6.0		100	3.25		100	1.25
	150	6.3		150	3.35		150	1.45

4. Give an account of the action of the thyatron tube. Explain how it may be operated from an alternating voltage so as to control the period of conduction over a complete half-cycle of the supply (use the diagram of fig. 4.18).

## Applications of Thermionic Valves (I)

**Rectification of Alternating Voltages**

Electronic equipment requires direct voltages for valve anodes, polarised relays and for other purposes; some investigations in physical chemistry also require a direct high-voltage source—e.g. transport number determinations and electrophoresis. Although primary or secondary batteries could be used, it is generally more convenient to develop such voltages from the alternating supply mains. The thermionic diode is a ready means of converting a.c. voltages into d.c.

The circuit of Fig. 5.1(a) is suitable for providing a direct voltage up to about 500 V, at a maximum current of about 100 mA, depending upon the rating of the components. The anode voltage and anode current are shown as functions of time in Fig. 5.1(b). During the positive half-cycle (i.e. when point *A* is positive with respect to point *B*), current flows through the diode, via inductance *L* and load *R<sub>L</sub>*, returning through the secondary winding of the transformer to *A*. During the negative half-cycle, the diode anode is negative with respect to its cathode (the filament, in the directly heated diode shown), and the valve does not conduct. The capacitor *C*<sub>1</sub> charges during the positive half-cycle to a voltage almost equal to the transformer secondary peak voltage; during the negative half-cycle it discharges partially via *L* and *R<sub>L</sub>*. The time constant for discharge is much greater than for the charging process via the comparatively low impedance of the conducting diode. Hence only a part of the charge is lost, and this is made up during the next half-cycle; the voltage across *C*<sub>1</sub> is shown in Fig. 5.2, in which '+' and '-' refer to positive and negative half-cycles of the transformer voltage. Since  $E_t = E_0 \cdot \exp(-t/CR)$ , where *E<sub>t</sub>* is the voltage across the capacitor *C* after discharging for a time *t* through a resistance *R* (p. 14), we can easily show that a 16 μF capacitor discharging through a 5000 Ω load shows a fall in voltage from *E*<sub>0</sub> to 0.8*E*<sub>0</sub>,

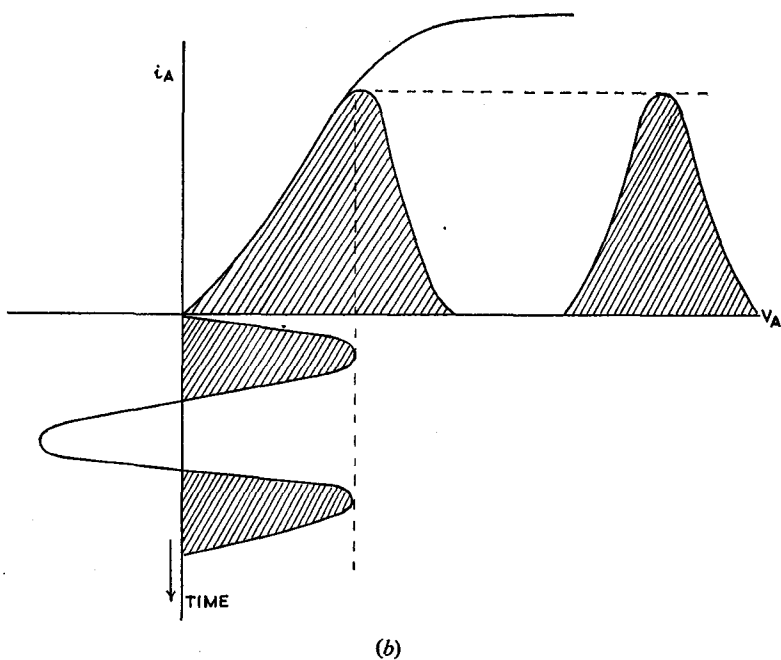
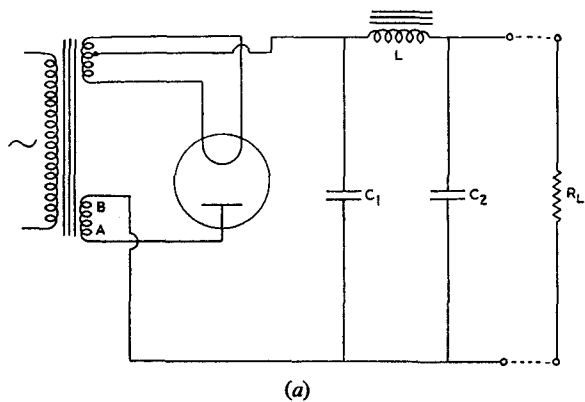


Fig. 5.1. Diode half-wave rectifier: circuit diagram and anode current ( $i_a$ )-time relationship



## APPLICATIONS OF THERMIONIC VALVES (1)

over the period of the negative half-cycle (1/100 second). The voltage across the reservoir capacitor  $C_1$  may be considered as a steady voltage  $V$ , with a superimposed ripple voltage of *twice* the supply frequency (i.e. 100 c/s). The components  $L$  and  $C_2$  form a

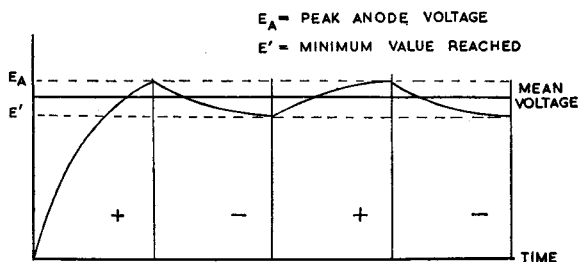


Fig. 5.2. Anode voltage ( $V_a$ )-time relationship for the diode

filter circuit which removes this ripple, providing a sensibly constant voltage  $V$  to the load. Suppose the inductance of  $L$  to be 10 H, and the capacitance of  $C_2$  to be  $32 \mu\text{F}$ ; at the ripple frequency,  $X_L = 2\pi \cdot 100L = 6.28 \text{ k}\Omega$ , whilst the reactance of the capacitor,

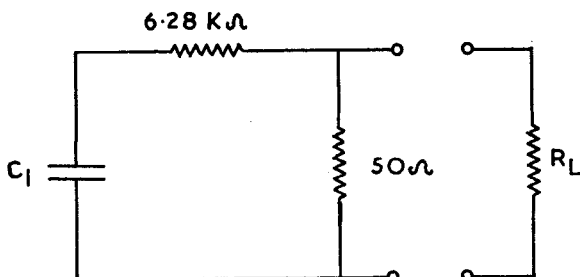


Fig. 5.3. Rectifier smoothing circuit—equivalent diagram

$X_{C_1} \approx 50 \Omega$ . The ripple voltage therefore 'sees' the circuit of Fig. 5.3, and less than 1% of it appears across  $R_L$ . From the point of view of filtering off the ripple we could replace  $L$  by a resistor of  $6.28 \text{ k}\Omega$ , with the same result; however, this would probably be much greater than the resistance of the 10 H inductor, and the output voltage would consequently be reduced. In portable equipment, where a saving in weight is important, and the load current is usually small, resistance-capacitance smoothing is often used.

## LABORATORY AND PROCESS INSTRUMENTS

A more efficient circuit is that of the full-wave rectifier, Fig. 5.4. By using a double diode, and centre-tapping the transformer secondary winding, conduction occurs on both half-cycles; the charge on  $C_1$  is maintained more nearly constant, and the ripple voltage is considerably reduced. The operating voltage for each diode must be developed by each half of the secondary; it is essential to supply the filament of the rectifier by a separate winding from that used by the other valve filaments, so that a complete specification for the transformer might be:

- primary: 200–220–240 V, 50 c/s.
- secondary: 350–0–350 V, 50 mA (H.T. for diodes).
- 6.3 V, 2 amp (for diode filament).
- 6.3 V, 1 amp (other valve filaments).

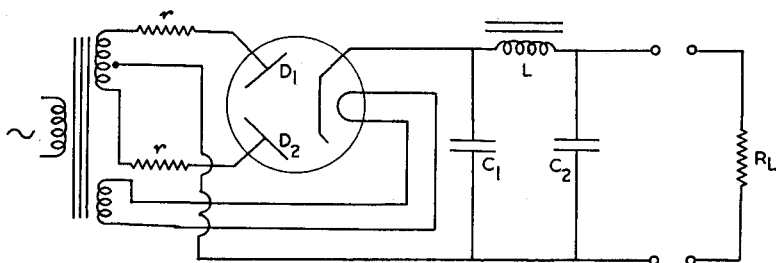


Fig. 5.4. Diode full-wave rectifier

The resistors  $r$ , in series with the diode anodes, limit the peak current through the valve before  $C_1$  has become fully charged; a minimum value of  $r$  is quoted for each valve by the manufacturer. If the primary and secondary resistances of the transformer are  $R_1$  and  $R_2$  respectively, the circuit introduces a resistance

$$\frac{R_2}{2} + T^2 R_1$$

in series with each anode,  $T$  being the turns-ratio of the transformer; if this is less than the stated minimum  $r$ , extra resistance must be included, as shown.

There may be a considerable difference of potential between the filament and cathode of an indirectly heated rectifier valve, and overloading the circuit may result in a breakdown of insulation at this point. For this reason, rectifiers supplying extra

## APPLICATIONS OF THERMIONIC VALVES (I)

high tension voltages (E.H.T.), such as required for the final anode of a cathode ray tube, are generally of the directly heated type. In this case, the rectifier filament winding must be very carefully insulated from the other windings.

The smoothing circuit,  $L$  and  $C_2$ , of Fig. 5.4 is essentially the same as that of the half-wave circuit; as the ripple voltage is smaller, however, the component values may be reduced.

### Metal Rectifiers

The valve diode or double diode may be replaced by a half-wave, or full-wave, *metal rectifier*, of which there are two main types—copper-copper oxide and selenium-steel. Surfaces of contact

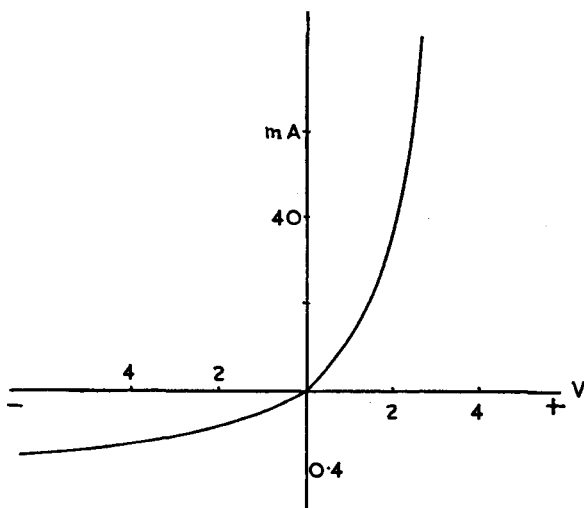


Fig. 5.5. Metal rectifier-response curve

between these pairs of substances are *polarised*, conducting very much more readily in one direction than in the other. They have similar voltage-current characteristic curves to valve diodes, as is seen from Fig. 5.5. The arrowhead of their conventional symbol points in the direction of current flow, i.e. from 'anode' to 'cathode'. Metal rectifiers may be operated at high ambient temperatures, and are available for current output as high as

## LABORATORY AND PROCESS INSTRUMENTS

10 amp. They are fitted with cooling fins to assist in the dissipation of heat. For high voltages a number of pairs of 'elements' are joined in series, so that the voltage across each section is reduced.

Full-wave metal rectifiers are often connected in the 'bridge' circuit of Fig. 5.6, in which  $R_L$  represents the load supplied by the

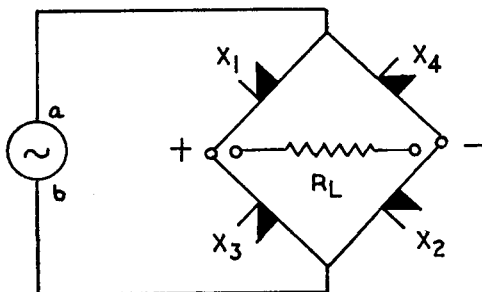


Fig. 5.6. Full-wave bridge rectifier

rectifier. If point  $a$  is positive with respect to point  $b$ , current flows via  $X_1$ ,  $R_L$  and  $X_2$ ; reversal of the polarity of  $a$  and  $b$  causes the current to flow via  $X_3$ ,  $R_L$  and  $X_4$ . In either case, however, the current flows in the same direction through  $R_L$ , so that we

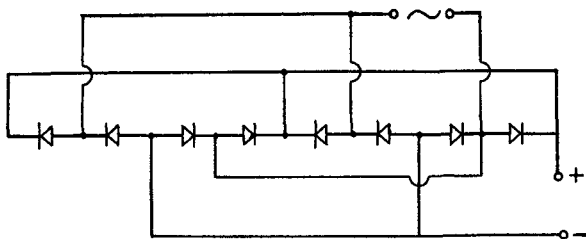


Fig. 5.7. Full-wave metal rectifier circuit for large current, e.g. battery-charger rectifier

have obtained full-wave rectification. If smoothing is required,  $R_L$  is replaced by an  $L$ - $C$  filter of the type already described (p. 103). A similar arrangement, with each 'element' duplicated in parallel, may be used to supply a large current for battery charging; the circuit is shown in Fig. 5.7.†

† In Figs. 5.6 and 5.7, alternative symbols for the half-wave metal rectifier are illustrated.

## APPLICATIONS OF THERMIONIC VALVES (I)

Metal rectifiers may also be used as *voltage doublers*, as in the circuit of Fig. 5.8.  $C_2$  charges to peak voltage during the half-cycle for which  $a$  is positive with respect to point  $b$ ; during the next half-cycle,  $C_2$  partially discharges, and  $C_1$  becomes charged. The load  $R_L$ , across  $C_1$  and  $C_2$  in series, thus experiences a voltage  $V_0$  which is almost twice the peak of the supply voltage.

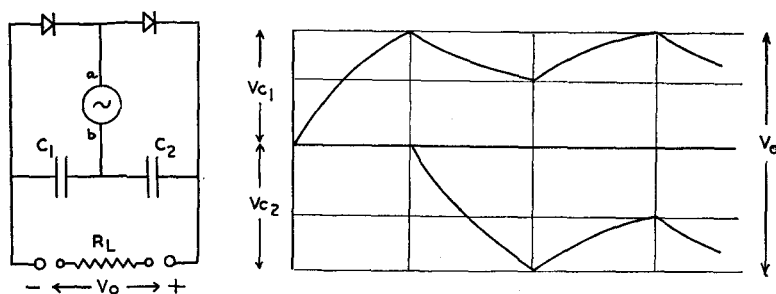


Fig. 5.8. Voltage doubler circuit and response curve

Small metal rectifiers, passing currents of a few milliamps, are used as meter rectifiers, and as 'reversed polarity' protective devices. They are also used for the 'detection' of modulated waves (p. 114).

Metal rectifiers require no filament supply, and are very robust; their reverse current is larger, however, than that of a valve diode.

### Stabilised Power Supplies

The output voltage of the rectifiers so far described is very dependent upon the input voltage, and upon load current; it will change if either of these varies. In order to maintain the output voltage constant within, say, 1% for changes of 10% or more in mains input voltage or load current, the rectifier must be *stabilised*, so that these changes are automatically compensated.

One way of doing this is to supply the rectifier transformer from the secondary of a *constant-voltage transformer*, such as that shown diagrammatically in Fig. 5.9. The primary windings are additive, so that the input voltage  $V_i = V_{1p} + V_{2p}$ ; the secondary windings are in opposition, so that the output voltage  $V_o = V_{2s} - V_{1s}$ . With the nominal  $V_i$  applied, the lower primary

## LABORATORY AND PROCESS INSTRUMENTS

winding partially saturates its core, so that increase of  $V_i$  causes  $V_{1p}$  to increase more than  $V_{2p}$ ; hence the increase in secondary voltage  $V_{1s}$  is greater than that in  $V_{2s}$ , and by suitable design it may be arranged that  $V_o = V_{2s} - V_{1s}$  remains practically constant. The constant-voltage transformer is thus a static electromagnetic voltage regulator, responding very rapidly to changes in supply voltage and maintaining  $V_o$  constant within 1% for changes in  $V_i$  of 15%. The output  $V_o$  has a considerably distorted waveform, but this may be partially corrected by a harmonic filter, which removes those components whose frequencies are multiples of the supply frequency. Constant-voltage transformers are available for normal mains voltage output (i.e. 200–250 V) and for

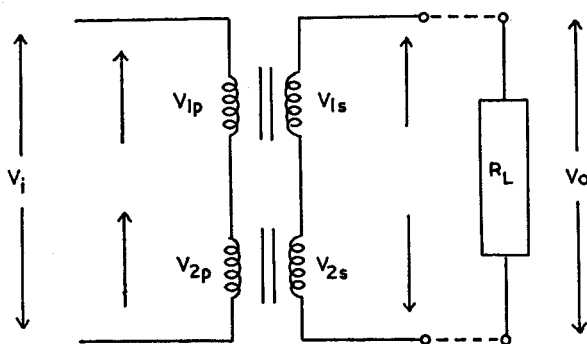
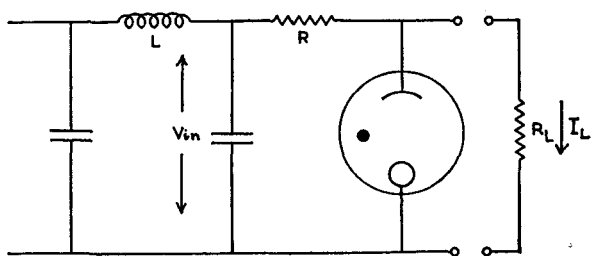


Fig. 5.9. The constant-voltage transformer—schematic diagram

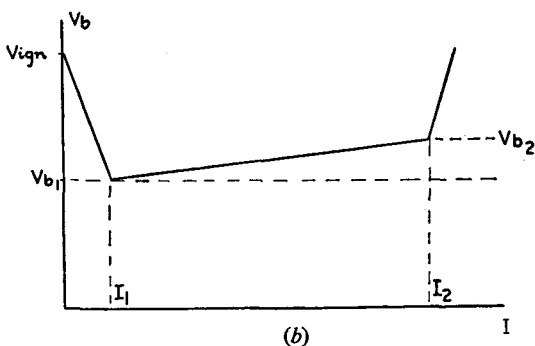
low-tension supply (6–12 V), at power ratings from 4 W to 6 kW. The ‘volstat’<sup>†</sup> is a constant-voltage transformer with variable output voltage, rated at 170 W, with a total harmonic distortion of less than 5%.

A voltage regulator tube (Chapter IV) may be included in the supply unit to maintain the output voltage practically constant for a varying load current. The circuit is shown in Fig. 5.10(a), and the characteristic curve in Fig. 5.10(b). The tube ‘strikes’ at  $V_{ign}$ , the *ignition voltage*. The voltage across the tube then falls to  $V_{b1}$ , the *burning voltage* for current  $I_1$ . As the current increases to  $I_2$ , the voltage changes only slightly to  $V_{b2}$ ; beyond

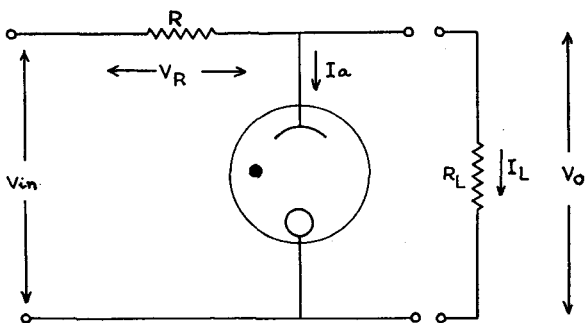
<sup>†</sup> Manufactured by Advance Components Ltd., Ilford, Essex, and by Freed Transformer Co., Brooklyn, N.Y.



(a)



(b)



(c)

Fig. 5.10. (a) Voltage regulator tube circuit. (b) Response curve of voltage regulator tube. (c) Current and voltage components

# LABORATORY AND PROCESS INSTRUMENTS

$I_2$ , current and voltage rise rapidly together. Typical values of these parameters are quoted for the Mullard 150B2 Stabiliser Tube:

$$V_{\text{ign}} 180 \text{ V}, V_{b_1} 147 \text{ V}, \text{ at } I_1 = 5 \text{ mA}$$

$$V_{b_2} 152 \text{ V}, \text{ at } I_2 = 15 \text{ mA}$$

The regulator tube is connected in series to a resistor  $R$ , which is chosen as follows. The maximum tube current  $I_{\text{max}}$  occurs when the input voltage  $V_i$  is a *maximum*, when the load current  $I_L$  is a *minimum*, and when the burning voltage has the value  $(V_b)_{\text{min}}$ , the *minimum* for a tube of this type under  $I_{\text{max}}$  conditions; this defines a *minimum* value for  $R$ , i.e.

$$R > \frac{(V_i)_{\text{max}} - (V_b)_{\text{min}}}{I_{\text{max}} + (I_L)_{\text{min}}}$$

Similarly, by considering the conditions for *minimum* tube current, we obtain a *maximum* value for  $R$ :

$$R < \frac{(V_i)_{\text{min}} - (V_b)_{\text{max}} \text{ for } I_{\text{min}}}{I_{\text{min}} + (I_L)_{\text{max}}}$$

For ignition of the tube, we also require

$$(V_i)_{\text{min}} \cdot \frac{R_L}{R_L + R} > V_{\text{ign}}$$

*Example* (Fig. 5.10(c))

If the variations of input voltage  $V_i$  extend from 255–275 V, and of the load current  $I_L$ , from 10 mA–15 mA, using the Mullard 150B2 tube, then:

$$R > \frac{275 - 152}{(15 + 10) \times 10^3}$$

$$\text{and} \quad R < \frac{255 - 147}{(5 + 15) \times 10^3}$$

$$\text{i.e.} \quad 4.92 \text{ k}\Omega < R < 5.40 \text{ k}\Omega$$

So that a suitable value of  $R$  would be 5 k $\Omega$ . Now the mean value of the load resistance  $R_L$  is  $(150/12.5) \cdot 10^3 = 12 \text{ k}\Omega$ , and

$$V_i)_{\text{min}} \cdot \frac{R_L}{R_L + R} = 255 \times \frac{12}{12 + 5} = 180 \text{ V}$$



# APPLICATIONS OF THERMIONIC VALVES (I)

which is a suitable voltage for ignition. With  $R = 5\text{ k}\Omega$ :

$V_i$ (volts)	$I_L$ (mA)	$V_R$ (volts)	$I_a$ (mA)	$V_o$ (volts)
255	10	105	11	150
275	10	123	14.6	152
255	15	108	6.6	147
275	15	125	10.0	150

The table shows that as  $V_i$  rises at constant  $I_L$ ,  $I_a$  increases, keeping  $V_o$  almost constant. As  $I_L$  increases at constant  $V_i$ ,  $I_a$  falls. An 8% rise in  $V_i$ , or a 50% rise in  $I_L$ , causes only a 2% change in  $V_o$ .

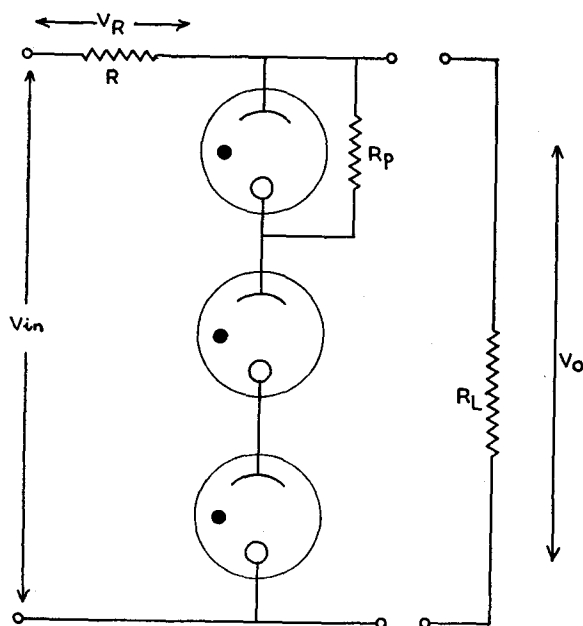


Fig. 5.11. Reduction of striking voltage for a series combination of voltage regulator tubes

Voltage stabiliser tubes are available with a range of burning voltages from about 75–150 V. To obtain regulation at higher voltages, two or more tubes may be connected in series across

# LABORATORY AND PROCESS INSTRUMENTS

the supply. A resistor  $R_p$  in parallel with one of the tubes reduces the ignition voltage of the combination. In Fig. 5.11, if the ignition voltage of the tubes is 180 V, without  $R_p$  in circuit the ignition voltage of the series combination is  $(3 \times 180 + V_R)$  V.  $R_p$  is chosen to have a low resistance (about 1 M $\Omega$ ) compared with the leakage resistance of the stabiliser tube; thus, with  $R_p$  in circuit, most of the input voltage  $V_i$  lies across the other two tubes, which ignite. For the first tube also to ignite we require  $V_i = (V_R + 180 + 2 \times 150)$ , since the burning voltage of the other two tubes is 150 V.  $R_p$  has thus reduced the ignition voltage by about 60 V.

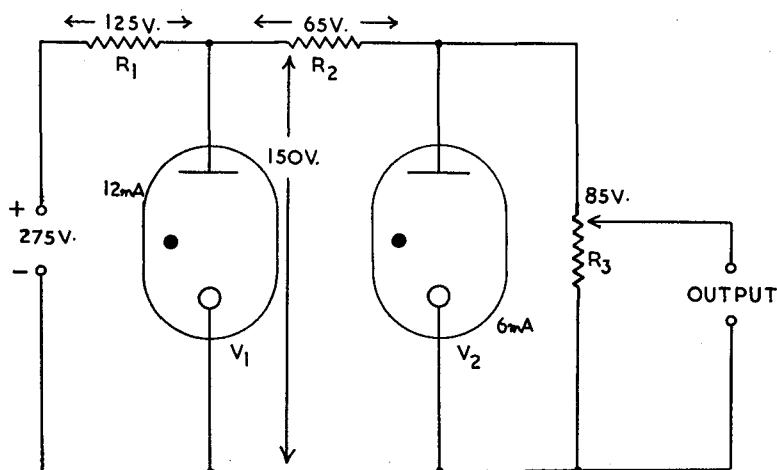


Fig. 5.12. Voltage reference tube—typical circuit.  $V_1$ , Mullard 150B2;  $V_2$ , Mullard 85A2

Voltage reference tubes are similar in construction to voltage stabiliser tubes; they are designed to provide a reference source of voltage, comparable in stability to that of a Weston Standard cell. The Mullard 85A2 tube, for example, provides a burning voltage of 83–87 V (this is the variation from tube to tube), which is constant after an initial running-in period to 0.2% or better. In Fig. 5.12 a typical circuit for supplying a reference source of voltage from an 85A2 tube is shown; voltages and currents in this figure refer to the steady burning conditions. It is essential that *negligible* current should be drawn through  $R_3$ .

### Hard Valve Stabilisation

A simple hard-valve stabilised power-supply unit is shown in Fig. 5.13. It should be noted that a current ( $I_a + I_L$ ), the sum of the anode current of the triode and the load current through  $R_L$ , flows through  $R_b$  from earth to H.T. -ve. Hence the bias on the triode grid is the sum of  $-(I_a + I_L)R_b$  and the +ve voltage determined by the position of the tapping on the potentiometer across the H.T. voltage. This will normally be adjusted for zero, or a small -ve voltage, on the triode grid.

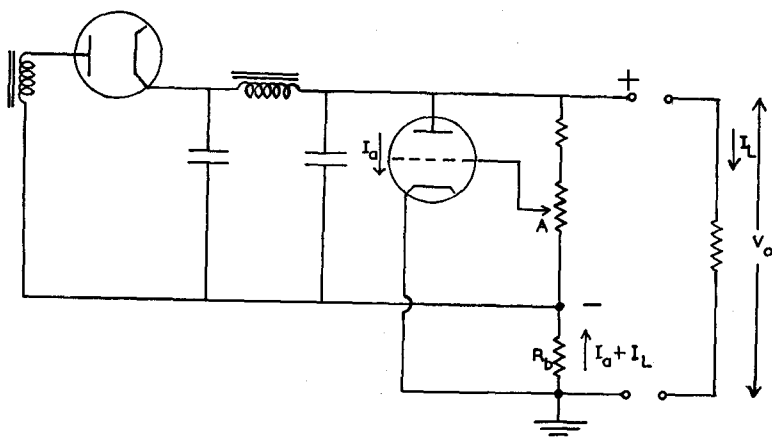


Fig. 5.13. Hard-valve stabilised power supply unit—basic circuit

If now the load current *increases*, the point *A* becomes more -ve,  $I_a$  *decreases*, and the total current (and hence the output voltage  $V_o$ ) tends to remain constant. Conversely, a *decrease* in  $I_L$  makes *A* *less* -ve, and gives rise to an increase in  $I_a$ . The change in bias, for a change  $\delta i_L$  in load current, is  $-\delta i_L \cdot R_b$ , and  $i_a$  changes by  $-g_m \cdot \delta i_L \cdot R_b$  (p. 80); the change in total current  $i_T$  is thus  $\delta i_T = \delta i_L \cdot (1 - g_m \cdot R_b)$ . For example, if  $g_m = 8 \text{ mA/V}$  and  $R_b = 100 \Omega$ ,  $\delta i_T = 0.2 \delta i_L$ .

In Fig. 5.14 is shown a stabilised power-supply circuit employing a cathode-coupled amplifier  $V_2$ ,  $V_3$ , with separate H.T. supply (shown as a battery). Suppose that the output voltage  $V_o$ , due to change of input voltage  $V_i$  or of load current  $I_L$ , tends to rise. Then the voltage drop across  $R_1$  increases and the grid of  $V_3$  becomes more -ve with respect to its anode. Hence the current

through  $V_3$  decreases, and the cathode bias across  $R_3$  is reduced, reducing also the cathode bias of  $V_2$ . Since the grid of  $V_2$  is at a fixed -ve reference voltage  $V_b$  with respect to the anode, its anode current increases, and its anode potential falls due to the increased voltage drop across  $R_4$ . The grid of  $V_1$  is thus driven

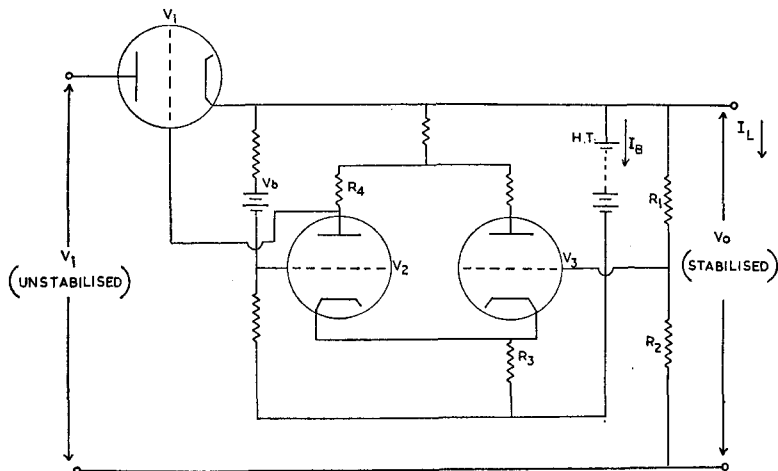


Fig. 5.14. Complete stabilised power supply unit

-ve with respect to its cathode, and the current is reduced, correcting the rise in  $V_o$ . The output voltage remains almost constant at the approximate value  $V_o = V_b \times (R_1 + R_2)/R_1$ . In practice, the H.T. battery is replaced by a separate power supply and  $V_b$  by a voltage reference tube (p. 112).

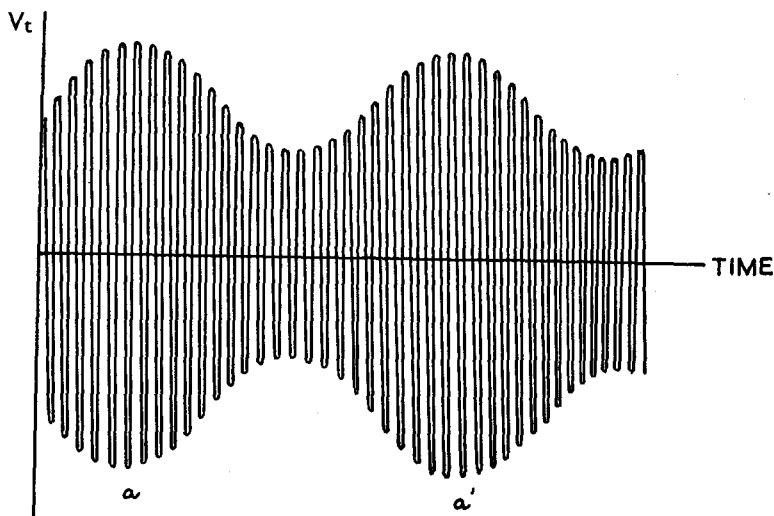
### Detection

In radio and long-distance telephone communication, information is conveyed by means of an electromagnetic wave of high frequency; this wave is called the 'carrier', and its frequency is the carrier frequency  $f_c$ . There are several ways in which the carrier may be 'modulated' so as to convey information. For example, the speech frequencies of the voice might be converted into voltages of corresponding frequencies—the modulation frequencies  $f_m$ , the amplitudes of these voltages being determined by the intensities of the original sounds. If we use the modulating voltage to vary the *frequency* of the carrier we say that this wave has been 'frequency modulated'; this type of modulation is used in the B.B.C.'s V.H.F. transmission.

## APPLICATIONS OF THERMIONIC VALVES (I)

We shall consider here a mathematically more simple type of modulation, in which the *amplitude* of the carrier is modulated. This is referred to as 'amplitude modulation'; an amplitude-modulated wave may be represented by:

$$v_t = [V_c + (V_m \sin \omega_m t)] \cdot \sin \omega_c t$$



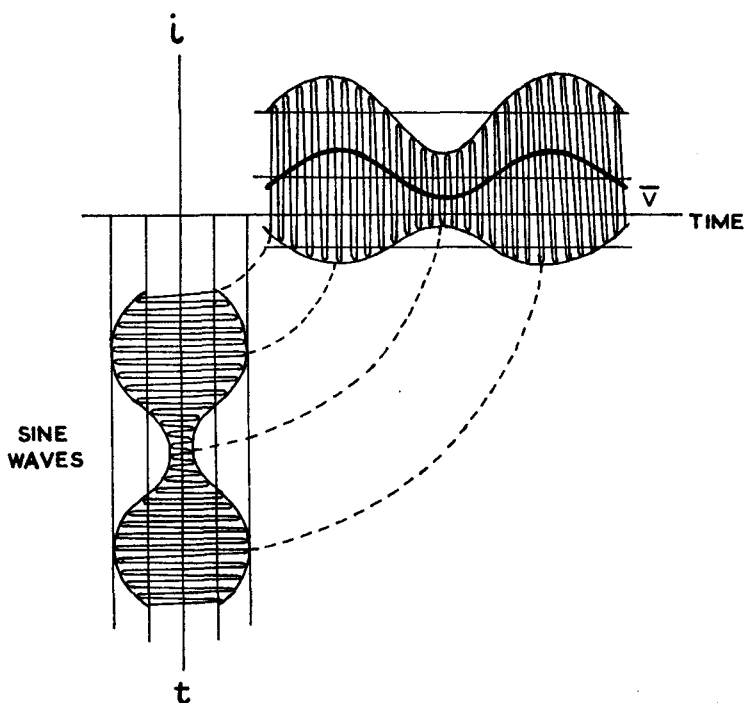
the carrier voltage being represented by  $(V_c \cdot \sin \omega_c t)$  and the modulation voltage by  $(V_m \cdot \sin \omega_m t)$ , both being sinusoidal voltages of frequency  $\omega_c/2\pi$  and  $\omega_m/2\pi$  respectively. The resultant carrier wave is shown in Fig. 5.15.

If  $f_c = 1000$  kc/s and  $f_m = 1$  kc/s, there will be 1000 complete cycles of the carrier voltage within the modulation 'envelope', i.e. within the period,  $aa'$ , of a modulation cycle. In practice, the modulation is not purely sinusoidal, but may have a very complicated waveform; for the carrier amplitude to faithfully follow the modulation,  $f_c$  must be very much greater than  $f_m$ , and  $V_c$ , the carrier amplitude, must be greater than the maximum modulation voltage.

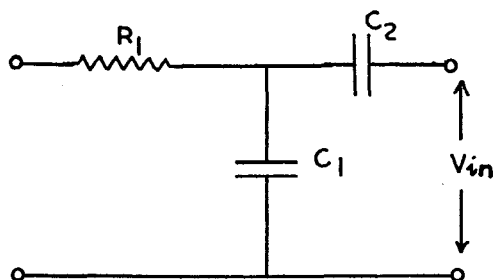
Over a period of time which is long compared with the carrier period,  $1/f_c$ , the average voltage of the modulated wave is zero. If, however, we remove about one-half of the wave, e.g. by

# LABORATORY AND PROCESS INSTRUMENTS

applying it to a diode or to a metal rectifier, the average voltage  $\bar{V}$  over such a period is no longer zero, but has a mean value between 0 and  $(V_c + V_m)$ , depending upon the amplitude of both carrier and modulation. The 'half-wave' is shown in Fig. 5.16(a); mathematically, the modulated-wave equation has been resolved



(a)



(b)

Fig. 5.16. Diode detection: waveforms and filter circuit

## APPLICATIONS OF THERMIONIC VALVES (I)

into two components of frequencies  $f_c$  and  $f_m$ , and a direct-current component. This process is called *detection*. If the half-wave (the detected signal) is applied to a filter circuit, such as that of Fig. 5.16(b), these three components may be separated. In this circuit,  $R_1 C_1$  form a potentiometer, across which the alternating components are applied; the d.c. component is 'blocked' by  $C_2$ . By suitable choice of circuit component values we may ensure that the carrier-frequency component is developed across  $R_1$ , leaving only the modulation-frequency voltage at  $V_i$ , the input voltage of the next stage.

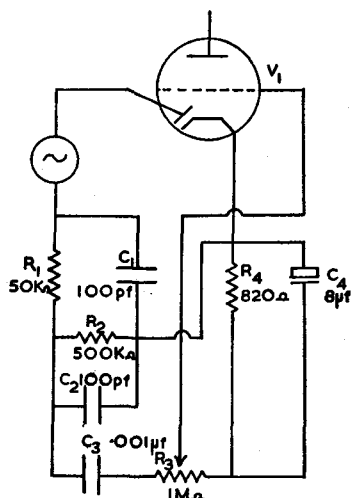


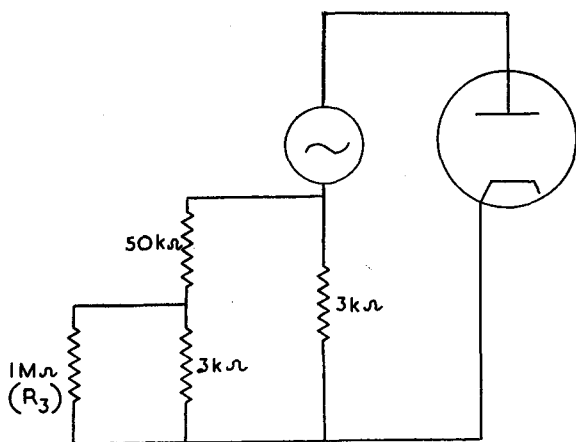
Fig. 5.17. Diode detector circuit

Suppose  $f_c = 1000$  kc/s,  $f_m = 1$  kc/s,  $R_1 = 100$  k $\Omega$  and  $C_1 = 100$  pF. At the carrier frequency, the reactance of  $C_1$ ,  $X_{C_1} = 1570$   $\Omega$ ; at the modulation frequency,  $X_{C_1} = 1.57$  M $\Omega$ . The voltages of the two components thus divide across  $R_1 C_1$ , as follows:

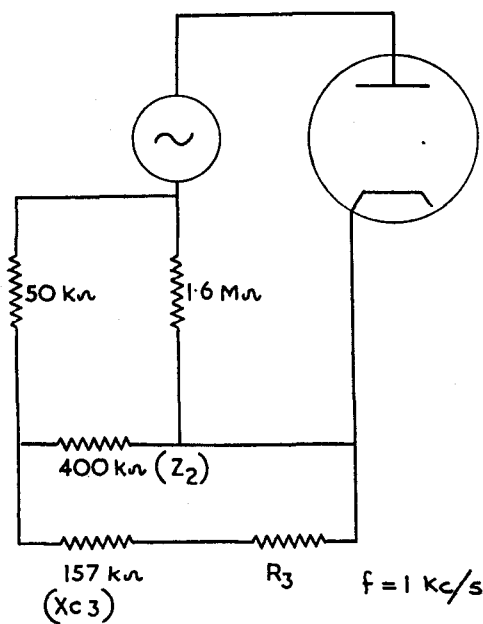
	Percentage across $R_1$		Percentage across $C_1$
$V_c$	98.5	$V_c$	1.5
$V_m$	6.4	$V_m$	93.6

A typical diode detector circuit is shown in Fig. 5.17. The 'carrier' frequency is 465 kc/s; at this frequency

$$X_{C_1}(= X_{C_2}) = 3.3 \text{ k}\Omega$$



$f = 465 \text{ kc/s}$   
(a)



(b)

Fig. 5.18. Equivalent circuits of Fig. 5.17, at carrier and modulation frequencies



## APPLICATIONS OF THERMIONIC VALVES (I)

and  $C_3$ , the d.c. blocking capacitor, has negligible reactance, so that the circuit reduces essentially to that of Fig. 5.18(a). Only a small fraction of the carrier voltage appears across the  $1\text{ M}\Omega$  resistor  $R_3$ .

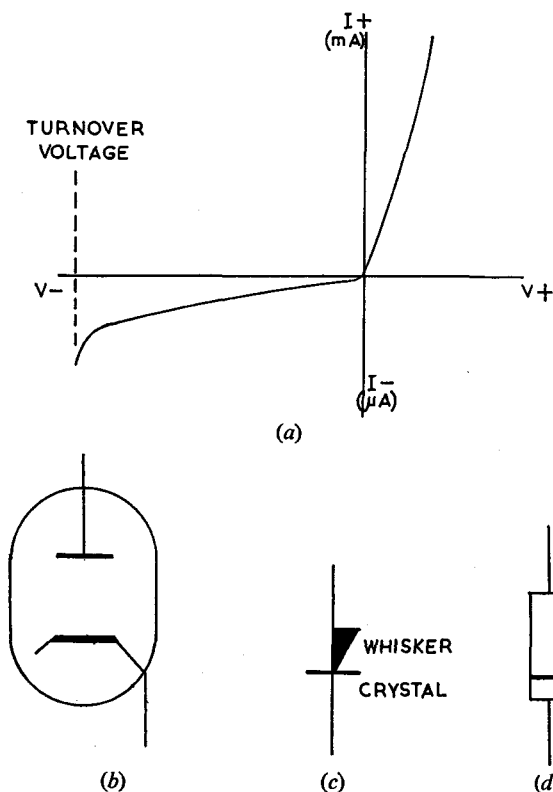
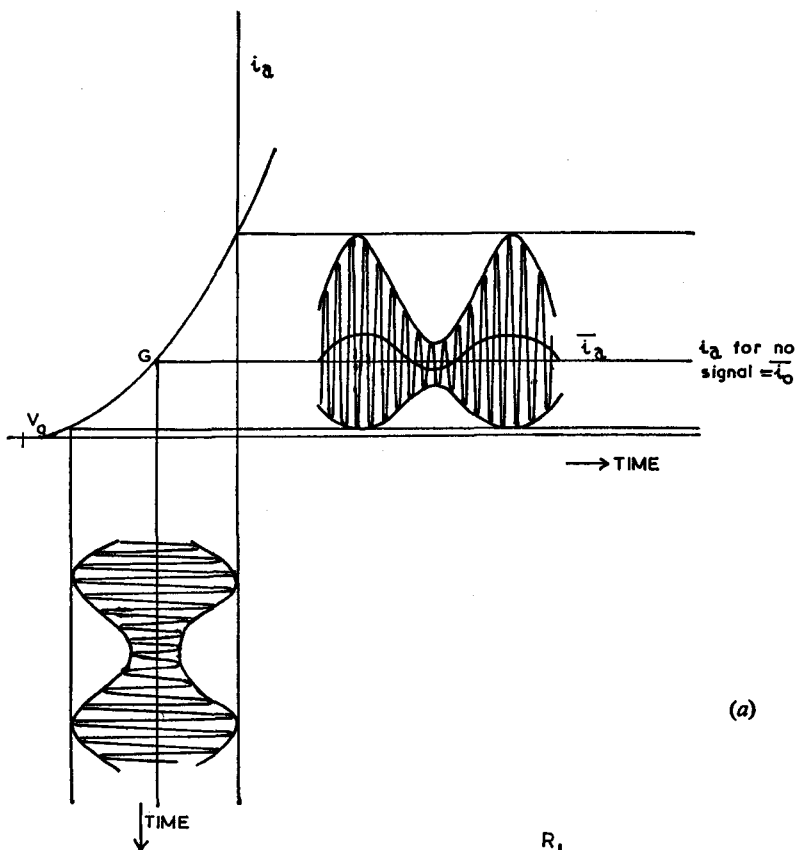
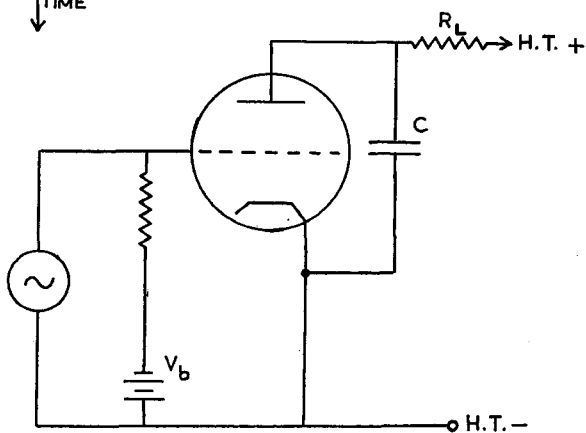


Fig. 5.19. The germanium diode: (a) characteristic curve; (b) valve diode symbol; (c) germanium diode symbol compared; (d) actual diode, with band at the cathode end

At a modulation frequency of  $1\text{ kc/s}$ , the circuit reduces to that of Fig. 5.18(b); about 90% of the modulation voltage appears across the impedance  $Z_2$  ( $Z_2$  is the impedance of  $R_2$  and  $C_2$  in parallel at  $f_m = 1\text{ kc/s}$ ) and about 80% across the load resistor  $R_3$ . The values of the circuit components are chosen so as to give almost the same output voltage for a constant input voltage, for modulation frequencies within the range  $100\text{ c/s}$  to  $12\text{ kc/s}$ .



(a)



(b)

Fig. 5.20. Bottom bend detection—circuit and waveforms

## APPLICATIONS OF THERMIONIC VALVES (I)

The modulation voltage tapped off  $R_3$  (the 'volume' or 'output' control) is fed to the grid of the diode-triode valve  $V_1$  for amplification. The cathode bias for the amplifier is derived from  $R_4$  and  $C_4$ ; it should be noted that no bias is applied between detector-diode anode and cathode, since  $R_2$  returns to the *top* of  $R_4$ . The diode valve, in these circuits, could be replaced by a small metal rectifier, or by a *crystal detector*. The original crystal detectors contained two different crystalline substances (e.g. bornite and zincite) in contact, or a single crystalline material in contact with the tip of a thin metal wire (the 'cat's whisker'). Nowadays germanium diodes (p. 202) are specially made for use at very high frequencies; such detectors are commonly used in the microwave region of the electromagnetic spectrum. The characteristic curve of a typical germanium diode is shown in Fig. 5.19(a); the symbols for the valve and germanium diodes, and the actual size of the latter, are shown in Fig. 5.19(b) to (d).

Any non-linear device will produce unequal amplification of the two half-cycles of an applied alternating signal; such a device will therefore behave as a detector. For example, consider an amplitude-modulated signal to be applied to the grid of a triode, biased to the 'bottom bend' of its mutual characteristic (Fig. 5.20(a)). The bias battery  $V_b$  (Fig. 5.20(b)) is adjusted so that the working point  $G$  falls on the bottom bend, i.e. about 1 V above cut-off. This is the 'lower anode bend' detector. The mean anode current, with no signal applied to the grid, is  $i_0$ , and this increases to  $i_a$  for a sinusoidal input—e.g. the 'carrier' wave. If the carrier is modulated,  $i_a$  follows the amplitude of the modulation voltage, varying at modulation frequency. The capacitor  $C$  removes the carrier component, and the modulation voltage appears across the load  $R_L$ .

### References

- SPREADBURY, F. G. (1956). *Electronic Measurements and Measuring Instruments*. Constable.  
STURLEY, K. R. (1949). *Radio Receiver Design*. Chapman and Hall.

### Problems

1. Explain how the diode valve may be used for (a) the half-wave rectification, (b) the full-wave rectification, of an alternating supply. What is the function of the reservoir capacitor?

## LABORATORY AND PROCESS INSTRUMENTS

2. Draw the circuit of a smoothed full-wave rectifier, which is required to supply 250 V d.c. at 100 mA, based upon a rectifier (directly-heated double diode) of the following characteristics:

heater, 6.3 V, 2.0 A;  $V_a$   $2 \times 350$  V r.m.s. max.;  $I_a$  125 mA max.  
limiting anode resistor,  $100 \Omega$  min.; reservoir capacity,  $32 \mu$  F  
max. with capacitor input to filter.

3. Modify the circuit of Question 2 so as to include voltage stabilisation at 250 V, by means of two neon tubes in series; the characteristics of the tubes are:

$V_{\text{ignition}}$  150 V;  $V_{\text{burning}}$  125 V;  $I_{\text{max}}$  40 mA;  $I_{\text{min}}$  3 mA; A.C.  
resistance  $250 \Omega$ .

4. Explain how the non-linearity of certain portions of the triode  $I_a/V_a$  characteristics enable the valve to be used as a rectifier of an amplitude-modulated sinusoidal R.F. voltage.

## CHAPTER VI

### Applications of Thermionic Valves (II)

#### Amplification—General Principles

We saw in Chapter IV that variations in grid voltage of a triode valve produce corresponding variations in anode current; a change  $\delta e_g$  at the grid produces a change  $g_m \cdot \delta e_g$  in anode current and a voltage  $g_m r_a \cdot \delta e_g = \mu \cdot \delta e_g$  across the valve, where  $g_m$  and  $\mu$  are the mutual conductance and amplification of the valve (p. 80).

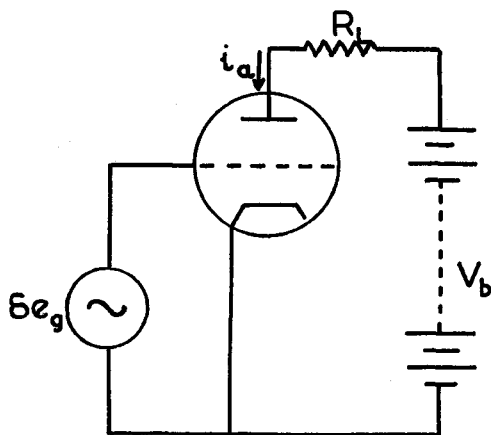


Fig. 6.1. Triode amplifier—basic circuit

In order to make use of this amplified voltage, a load-resistor,  $R_L$  must be included in the anode circuit, constituting the *anode load* (Fig. 6.1); effectively, it forms a potential divider with the anode resistance  $r_a$ . The amplified voltage across the load  $R_L$  for an applied signal  $\delta e_g$  at the grid is now  $\mu \cdot \delta e_g \cdot R_L / (R_L + r_a)$ . We may replace the conventional circuit of Fig. 6.1 by the equivalent circuit of Fig. 6.2 in which the *available* part of the amplified voltage is across  $R_L$ , and is equal to

$$(\text{input voltage at grid}) \times \mu \cdot R_L / (R_L + r_a)$$

## LABORATORY AND PROCESS INSTRUMENTS

This last term is called the *stage gain*,  $M$ , of the amplifier; evidently  $M$  is always less than  $\mu$ , but approaches  $\mu$  as  $R_L$  increases.

A signal voltage  $e_g = E_g \sin \omega t$ , applied to the grid, develops a voltage  $e_L$  across  $R_L$ , given by:

$$e_L = M \cdot e_g = M \cdot E_g \sin \omega t$$

At first sight we might imagine that  $e_L$  will be a maximum ( $= \mu \cdot e_g$ ) for  $R_L \gg r_a$ . However, the voltage applied to the anode is no longer the battery (or power supply) voltage,  $V_b$ ; if the

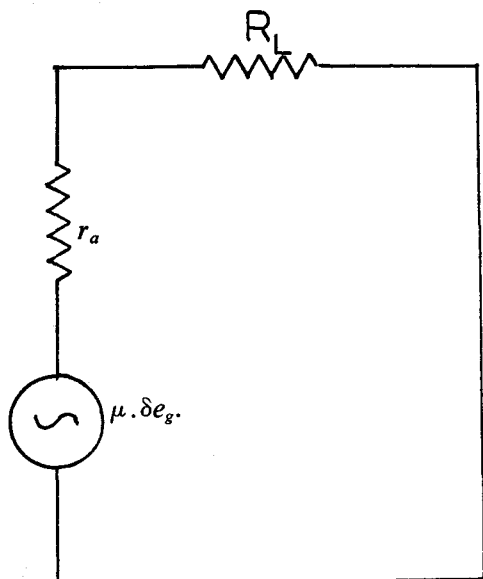


Fig. 6.2. Equivalent circuit of amplifier

steady anode current is  $I_a$ , a voltage drop ( $I_a R_L$ ) occurs across the anode load, and the anode voltage  $V_a = (V_b - I_a \cdot R_L)$ . Thus, the greater  $R_L$ , the lower  $V_a$ , and too large a load resistance may bring us on to the curved part of the  $I_a/V_a$  characteristic. In practice,  $R_L$  is often chosen to be about  $3 \times r_a$ , so that  $M \approx 0.75 \mu$ .

The valve parameters which were considered in Chapter IV applied to 'test' conditions. There was no load other than the internal resistance of the power supply in series with the anode resistance; the valve characteristics under these conditions are termed 'static'. From these may be derived a set of 'dynamic'

## APPLICATIONS OF THERMIONIC VALVES (II)

characteristics, appropriate to given values of load resistance  $R_L$  and supply voltage  $V_b$ . In Fig. 6.3 the static characteristics of a *voltage amplifying pentode* (Mullard EF86) are shown. Across these, lines are drawn representing combinations of  $R_L$  and  $V_b$ . Each line is fixed by two points; when  $I_a = 0$ ,  $V_a = V_b$ , giving one point, ( $X_1$ ); when  $I_a = V_b/R_L$ ,  $V_a = 0$ , giving the second point ( $X_2$ ). Included in the diagram is the limiting power-dissipation

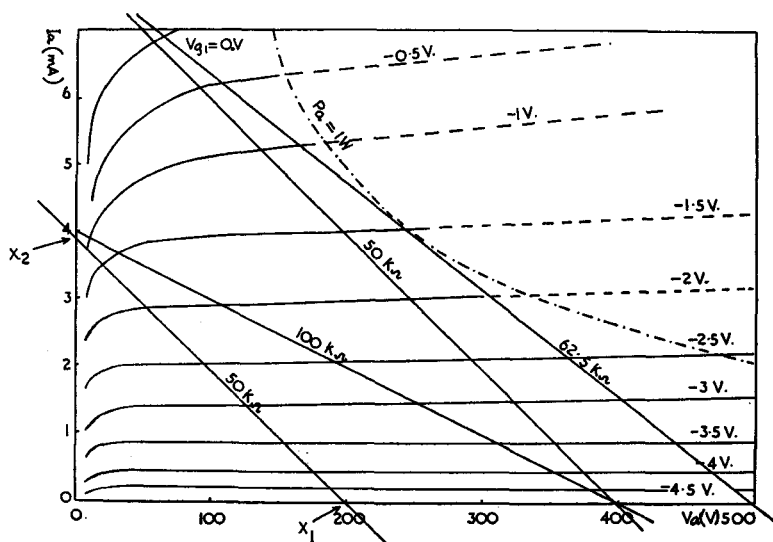


Fig. 6.3. Static characteristics of voltage amplifying pentode (Mullard EF86). Load lines and limiting power-dissipation curve

curve,  $V_a i_a = P_a$ . The limiting anode power-dissipation  $P_a$  is stated by the valve manufacturer. In the present example,  $P_a = 1$  W, so that at any anode voltage  $V_a$  the maximum permissible anode current  $(i_a)_{\max} = P_a/V_a$ , and the limiting curve is the plot of  $V_a i_a = 1$ . We are restricted to operation within the area bounded by this curve and the axes. From intersections of the load line with the static  $i_a - V_g$  characteristic curves, the dynamic parameters of the valve are obtained. After choosing a suitable grid bias voltage—the ‘working point’,  $V_g$ —the performance of the amplifier, under varying conditions of load  $R_L$  and supply

# LABORATORY AND PROCESS INSTRUMENTS

## TABLE 6.1

(EF86;  $V_{g_1} = 140$  V,  $V_{g_2} = 0$  V)

	(1)	(2)	(3)	(4)
$V_b$ (volts)	200	400	400	500
$V_g$ (volts)	-2.5	-2.0	-3.0	-2.0
$R_L$ (k $\Omega$ )	50	50	100	62.5
(a) $V_a$ (volts)	95	250	265	312
(b) $V_+$ (volts)	20	140	112	175
(c) $V_-$ (volts)	148	330	360	417
(d) Distortion (%)	17.2	15.8	23.4	13.2
(e) A.C. power (m-watts)	41.6	90.3	77.5	120
(f) Amplification	64	95	124	121

For this valve, mean  $g_m = 1.8$  mA/V,  $r_a = 2.5$  M $\Omega$ , so that  $\mu = 4500$ . Hence, with  $R_L = 100$  K $\Omega$ ,  $M = \mu R_L / (R_L + r_a) = 170$ , as compared with the practical value of 124 (column (3)).

voltage  $V_b$ , may be computed. In Table 6.1, for each value of  $V_b$ ,  $V_g$  and  $R_L$ , are listed:

- (a) the mean ('no-signal') anode voltage  $V_a$ ;
- (b) the anode voltage  $V_+$ , for an applied grid voltage

$$E_g = +1 \text{ V};$$

- (c) the anode voltage  $V_-$ , for an applied grid voltage

$$E_g = -1 \text{ V};$$

- (d) the inequality of  $V_+$  and  $V_-$ , expressed as a percentage of the total anode voltage 'swing', i.e.

$$\frac{(V_+ + V_-) \sim 2V_a^\dagger}{(V_- - V_+)} \times 100$$

(this is called the percentage distortion);

- (e) the a.c. power output, given by

$$\frac{1}{2}[(V_- - V_+)/2 \cdot (I_+ - I_-)/2] = \frac{1}{8}(V_- - V_+) \cdot (I_+ - I_-)$$

where  $I_+$ ,  $I_-$  are the anode currents at anode voltages  $V_+$ ,  $V_-$ , respectively. This is simply  $V_{r.m.s.} \times I_{r.m.s.}$ , expressed in watts.

† The symbol ' $\sim$ ' means 'subtract the smaller from the greater'. Thus, in  $A \sim B$ , the remainder is always positive, whether  $A > B$  or  $A < B$ .



## APPLICATIONS OF THERMIONIC VALVES (II)

(f) the amplification,

$$\delta V_a / \delta E_g = \frac{(V_+ - V_-)}{2}$$

in this case, where  $E_g = \pm 1$  V.

The output voltage of a valve will not be of the same waveform as the input voltage (for example, sinusoidal) if this input is applied over a curved portion of the valve characteristic. The

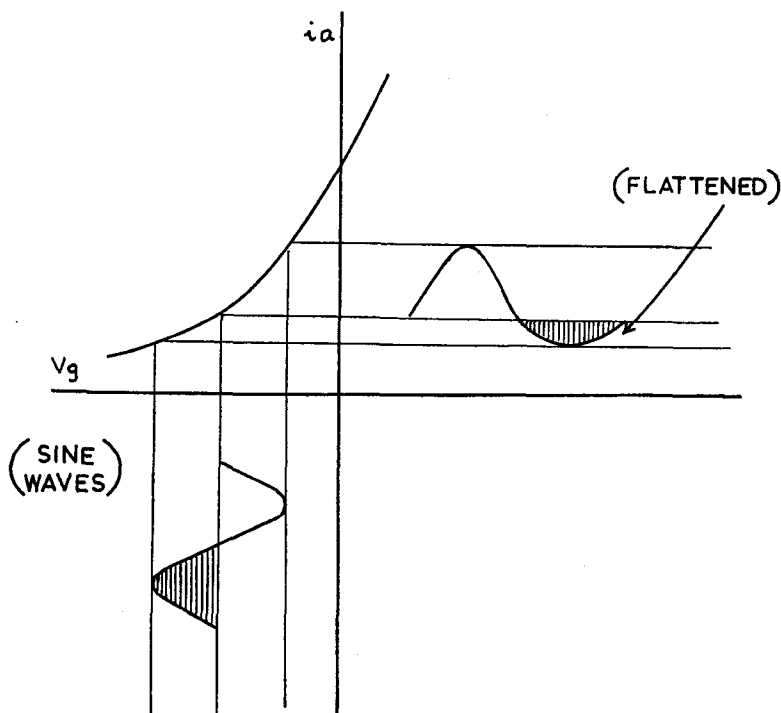


Fig. 6.4. (a) Effects of curvature of mutual characteristic curve.

bottom bend of the  $i_a/V_g$  characteristic leads to flattening of the -ve half-cycle, as shown in Fig. 6.4(a); the waveform is in fact similar to that of Fig. 6.4(b), which represents  $\Sigma(e_I + e_{II})$ , where

$$e_I = E_m \sin \omega t, \quad e_{II} = E'_m \sin (2\omega t - \pi/2),$$

i.e. the sum of a fundamental frequency voltage, and its second harmonic, displaced in phase by  $\pi/2$ . Hence, the effect of curvature of the characteristic is to introduce a second harmonic

# LABORATORY AND PROCESS INSTRUMENTS

component, and it may easily be shown that the percentage distortion computed on p. 126 is in fact the percentage of this second harmonic voltage, or  $[E'_m/(E_m + E'_m)] \times 100$ , where  $E_m$  is the amplitude of the fundamental and  $E'_m$  that of the second harmonic.

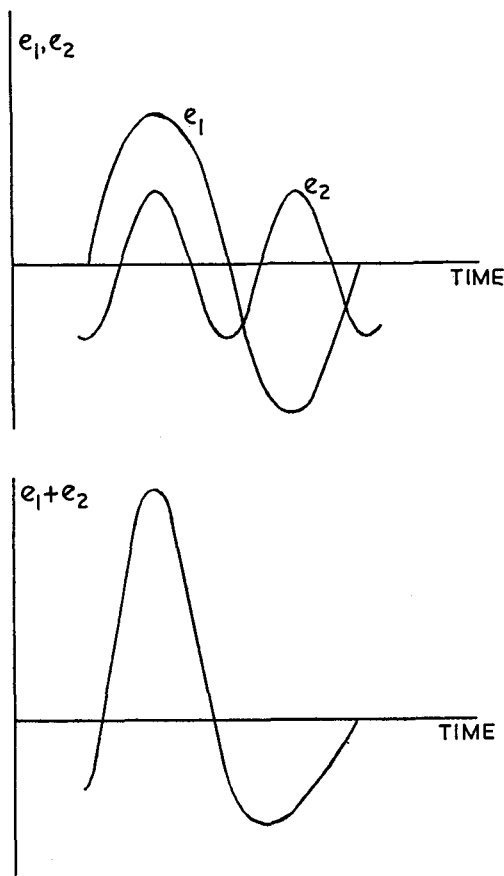


Fig. 6.4. (b) Resultant waveform—fundamental plus second harmonic

In Fig. 6.5 the dynamic mutual characteristic is drawn for  $R_L = 50 \text{ K}\Omega$  and  $V_b = 400 \text{ V}$ . It is seen to be less steep than the 'static' characteristics; from its slope the dynamic mutual conductance is  $1.3 \text{ mA/V}$ , compared with the (static)  $g_m$  of  $2.5 \text{ mA/V}$ , taken over the linear portion of the curve (*mean*

## APPLICATIONS OF THERMIONIC VALVES (II)

$g_m = 1.8 \text{ mA/V}$ ). By considering the variations in anode current resulting from a grid swing of  $E_g = \pm 1 \text{ V}$  applied to the *dynamic* mutual characteristic, the same conclusions regarding amplification and distortion may be arrived at as previously (Fig. 6.3).

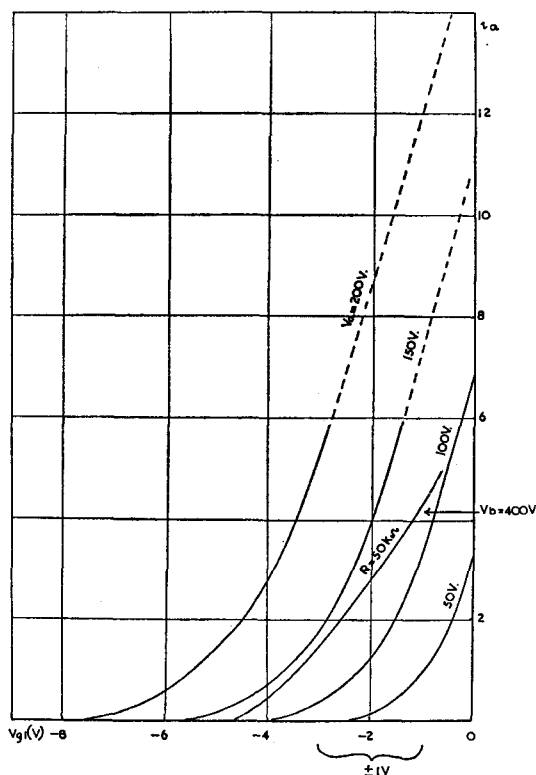


Fig. 6.5. Dynamic mutual characteristic curve (Mullard EF86)

From the data of Table 6.1 the conditions of column (2) appear to represent optimum conditions; if the extra voltage  $V_b$  is available, column (4) shows increased amplification and rather lower distortion.

### Power Amplification

The above considerations apply to a voltage amplification stage, the object of which is to amplify the voltage of an input signal. In the final stage of an amplifier, however, the large voltage swing

# LABORATORY AND PROCESS INSTRUMENTS

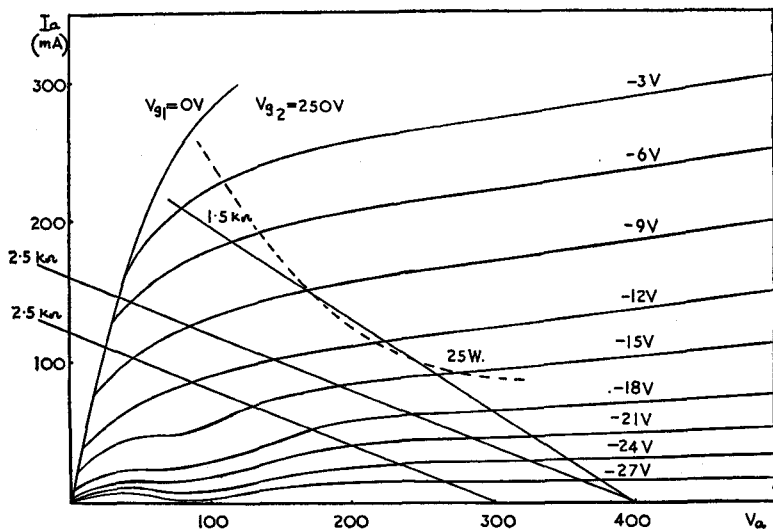


Fig. 6.6. Static characteristic curves for output pentode with resistive load (Mullard EL37). Load lines

TABLE 6.2  
(EL37;  $V_{g2} = 250$  V)

	(1)	(2)	(3)
$V_b$ (volts)	300	400	400
$V_g$ (volts)	-12	-12	-9
$R_L$ (k $\Omega$ )	2.5	2.5	1.5
$V_a$ (volts)	75	125	160
$V_+$ (volts)	37	75	110
$V_-$ (volts)	120	180	215
Distortion (%)	8.4	4.8	4.8
A. C. power (m-watts)	367	585	910
Anode dissipation (watts)	6.75	13.1	24.8
Efficiency (%)	5	4	3

The efficiency is:

$$\left( \frac{\text{A.C. power output}}{\text{Power dissipated at the anode}} \right) \times 100$$

The working conditions of column (2) would be suitable for input voltages up to about 10 V peak. The no-signal anode current is then 100 mA, so that the working point could be obtained by a cathode resistor of 120  $\Omega$ .

## APPLICATIONS OF THERMIONIC VALVES (II)

must be converted into electrical *power*, capable of operating a pen recorder, electromagnetic relay or loudspeaker. A *power output* valve is used, operating with a high anode voltage, and having an anode current considerably larger than that of the EF86. Such a valve is the Mullard EL37, typical characteristics and load lines for which are shown in Fig. 6.6. The results of a similar analysis to that described on p. 126 are listed in Table 6.2.  $V_+$  and  $V_-$  now refer to a signal voltage  $E_g = \pm 3$  V.

### Push-pull Amplification

Distortion occurs when the positive and negative half-cycles of the input voltage are unequally amplified; this can be very considerably reduced by using two output (or voltage-amplifier) valves in 'push-pull', as shown in Fig. 6.7.

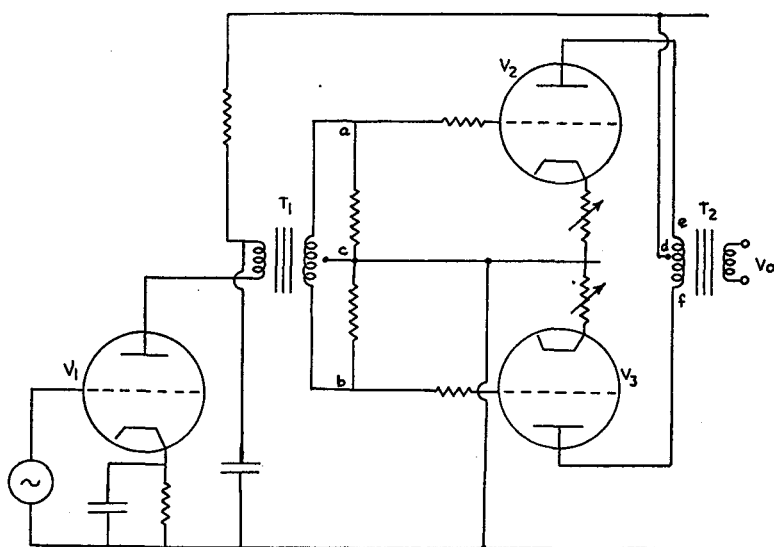


Fig. 6.7. Push-pull amplifier circuit

The ends  $a$ ,  $b$  of the transformer  $T_1$  secondary winding are in phase opposition; with respect to the centre tap  $c$ , when  $a$  is positive,  $b$  is negative, and vice versa. The grid signals applied to  $V_2$  and  $V_3$  are therefore in anti-phase, so that the outputs of these

valves are as shown in Fig. 6.8(a). The input voltages at points  $a$ ,  $b$  and  $c$  are shown at  $e_g$ .  $V_2$ ,  $V_3$  represent the anode voltages of valves  $V_2$  and  $V_3$  respectively; a curved portion of the characteristic has been chosen to show that the sinusoidal input voltage becomes distorted. The primary of the output transformer  $T_2$  is also centre tapped at  $d$ , so that the voltage across  $ef$  is the *vector sum* of  $V_2$  and  $V_3$ . This is shown as  $V_o$  in Fig. 6.8(b); it

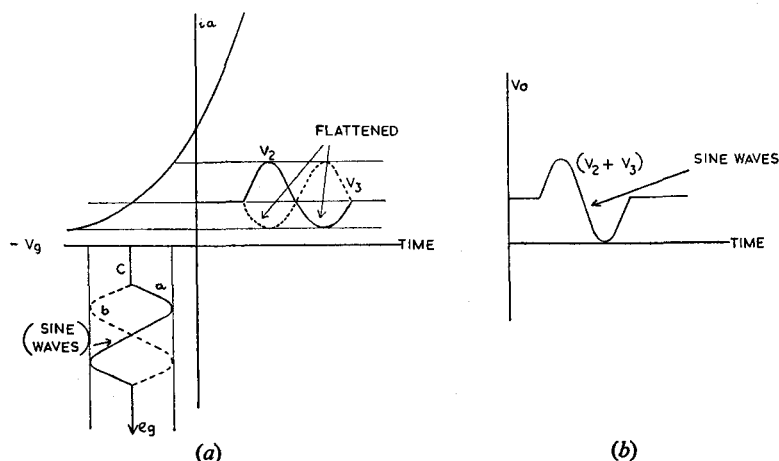


Fig. 6.8. (a) Anode current curves for push-pull amplifier. (b) Resultant output of push-pull amplifier

will be observed that the distortion has been practically eliminated. It is necessary to match  $V_2$  and  $V_3$  rather carefully, as regards both the type of valve and the working point; for this purpose, the cathode bias resistors are made independently variable.

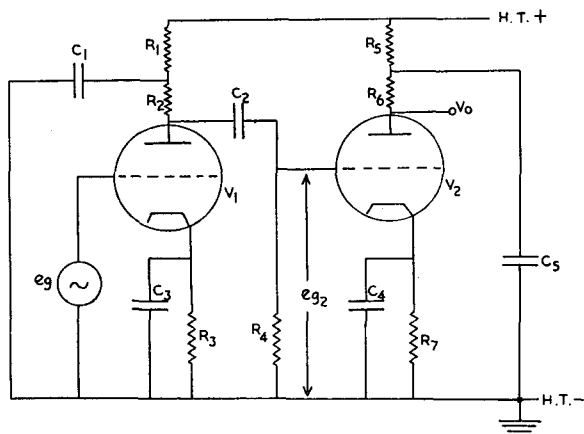
It is not necessary to feed transformer  $T_2$  in parallel from the H.T., since the d.c. components of  $V_2$  and  $V_3$  flow through the primary winding in antiphase, and do not tend to magnetically saturate the core.

### Coupled Amplifiers

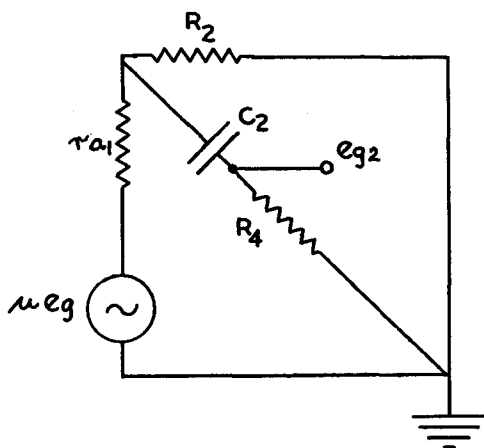
Two or more stages of voltage amplification may be connected in 'cascade' (i.e. in series). For low-frequency voltages, the valves may be triodes; for high frequencies, however, because of the

## APPLICATIONS OF THERMIONIC VALVES (II)

inter-electrode capacity coupling between the stages (mainly  $C_{g,a}$ , p. 82) it is essential to use tetrodes or pentodes in order to avoid oscillation. The connection between two stages—the *inter-*



(a)



(b)

Fig. 6.9. (a) Resistance-capacitance coupled amplifier. (b) Equivalent circuit

*stage coupling*—may be via capacitance and resistance, or via a transformer.

(i) *Resistance-capacitance (R-C) coupling*. The actual circuit, and part of the equivalent circuit, are shown in Figs. 6.9(a) and

# LABORATORY AND PROCESS INSTRUMENTS

6.9(b) respectively.  $R_2, R_6$  are the anode loads and  $R_3, R_7$  the cathode bias resistors of the two stages.  $C_2 R_4$  is the interstage coupling circuit, feeding the output of  $V_1$  to the grid of  $V_2$ . The two stages are also coupled, however, by the internal resistance of their common H.T. supply; this is *unwanted* coupling, which may lead to positive feedback and the generation of oscillations (p. 153). To prevent this, the H.T. end of the anode resistors is connected to earth, as regards alternating voltages, by the capacitors  $C_1, C_5$ ; the common H.T. resistance is increased to a few kilohms by resistors  $R_1$  and  $R_5$ , so that the a.c. component takes the low-impedance path to earth via the capacitors. The circuits  $R_1 C_1$  and  $R_5 C_5$ , are called *anode decoupling* circuits; for medium impedance triode valves operating at audio-frequencies, typical component values are:

$R_1, R_5:$	10 k $\Omega$	$C_1, C_5:$	0.5 $\mu$ F
$R_2, R_6:$	50 k $\Omega$	$C_2$	: 0.1 $\mu$ F
$R_3, R_7:$	750 $\Omega$	$C_3, C_4:$	50 $\mu$ F (electrolytic, low voltage)
$R_4$	: 250 k $\Omega$		

The equivalent circuit of the first stage of this amplifier is drawn in Fig. 6.9(b); the input voltage  $e_g$  at  $V_1$  grid appears at the anode as  $\mu e_g$ . The anode load  $R_2$  (earthed to a.c. at the top end by  $C_1$ ) is shunted by the series combination  $C_2 R_4$ ; if this reduces the resultant resistance to  $R'_2$ , the voltage at  $V_1$  anode is

$$\mu e_g \cdot R'_2 / (R'_2 + r_a)$$

where  $r_a$  is the anode impedance of  $V_1$ . This voltage is applied to the potential divider  $C_2 R_4$ ; the output across  $R_4$ , applied to  $V_2$  grid, is  $e_{g_2}$ , where:

$$e_{g_2} = \frac{\mu e_g \cdot R'_2}{(R'_2 + r_a)} \cdot \frac{R_4}{\sqrt{[R_4^2 + (1/\omega^2 C_2^2)]}}$$

The coupling capacitor  $C_2$  is made large so that practically the whole of the output voltage of  $V_1$  is applied to the grid of  $V_2$ .  $R_4$  should be large, so as not to shunt the input impedance of  $V_2$ ; it is limited only by the need to keep the time constant of  $C_2 R_4$  reasonably small, otherwise stray electrons will develop a negative bias voltage on  $V_2$  grid.

Since  $\omega$  occurs in the above equations, the grid voltage  $e_{g_2}$  is to some extent frequency dependent. If, however,  $R_4 \gg 1/\omega C_2$ ,



## APPLICATIONS OF THERMIONIC VALVES (II)

$e_{g_1} \simeq \mu R'_2 / (R'_2 + r_a) = M \cdot e_g$ .  $R'_2$  is now the resultant of  $R_2$  and  $R_4$  in parallel, neglecting the reactance of  $C_2$ . Further, if  $R_4 \gg R_2$ , as is usually the case,

$$R'_2 = R_2 R_4 / (R_2 + R_4) \simeq R_2$$

and

$$e_{g_1} = [\mu R_2 / (R_2 + r_a)] \cdot e_g$$

*Example* (refer to Fig. 6.9(a))

If  $\omega = 2000\pi$ ,  $R_2 = 50 \text{ k}\Omega$ ,  $R_4 = 250 \text{ k}\Omega$ ,  $C_2 = 0.1 \text{ }\mu\text{F}$  and  $r_a = 12 \text{ k}\Omega$ ,  $\mu(V_1) = 40$ , then  $X_{C_2} = 1.6 \text{ k}\Omega$ ,  $\ll R_4$ , and also  $R_4 \gg R_2$ . Hence,

$$e_{g_1} = \frac{40 \times 5 \times 10^4}{6.2 \times 10^4} \cdot e_g = 32e_g.$$

If the second stage is based upon a similar valve the final voltage  $V_0 = (32)^2 \cdot e_g$ , or  $1024e_g$ . Thus, a signal  $e_g = 0.03 \sin 2000\pi t$ , applied to  $V_1$  grid, produces a voltage  $e_{g_1} = 0.96 \sin(2000\pi t - \pi)$  at the grid of  $V_2$ , and an output voltage  $V_o = 30.7 \sin 2000\pi t$  at  $V_2$  anode.

The a.c. power developed at  $V_2$  anode is

$$E_{r.m.s.} I_{r.m.s.} = (30.7/\sqrt{2})(2.075/\sqrt{2}) = 11.5 \text{ mW}$$

To develop more power, we might apply the final voltage  $e_o$  to the grid of a power amplifier, such as the EL37 valve. Because of the large voltage available, however (30.7 V peak, or 21.8 V r.m.s.), we may use two EL37's in a push-pull circuit, as in Fig. 6.7. Since the anodes are supplied via the output transformer primary winding, which has a small d.c. resistance, the anode voltage for no signal applied will be practically the supply voltage  $E_b$ . If the a.c. 'resistance' (the *reactive* load) is taken as  $3 \text{ k}\Omega$ , we can draw a load line, passing through  $V_a = E_b$  at the value of  $I_a$  corresponding to zero input signal—instead of at  $I_a = 0$ , as with a resistive d.c. load. This load-line is shown in Fig. 6.10; the no-signal conditions are:

$$V_a = 400 \text{ V}; V_{g_1} = 400 \text{ V}; I_a = 50 \text{ mA}; V_g = -35 \text{ V}$$

The peak of the positive half-cycle of the input signal raises  $V_g$  to  $-4 \text{ V}$ , and  $I_a$  to  $155 \text{ mA}$ ;  $V_a$  falls to  $20 \text{ V}$ . The a.c. power is thus

$$\frac{(155 - 50)}{\sqrt{2}} \times \frac{(400 - 20)}{\sqrt{2}} \text{ mW}$$

developed by each valve in turn; i.e. output power =  $20 \text{ W}$ .

## LABORATORY AND PROCESS INSTRUMENTS

If the input impedance of this stage is 100 k $\Omega$ , the input power is  $V_1^2 \text{ (r.m.s.)} / Z_i = (21.8)^2 \cdot 10^{-5} \text{ W}$ . The stage gain is therefore

$$10 \log 20 / [(21.8)^2 \cdot 10^{-5}]$$

or 36.3 db.

(ii) *Transformer coupling.* For amplification at audio and intermediate (p. 22) frequencies, the transformer-coupled amplifier is generally used. A typical circuit is shown in outline in

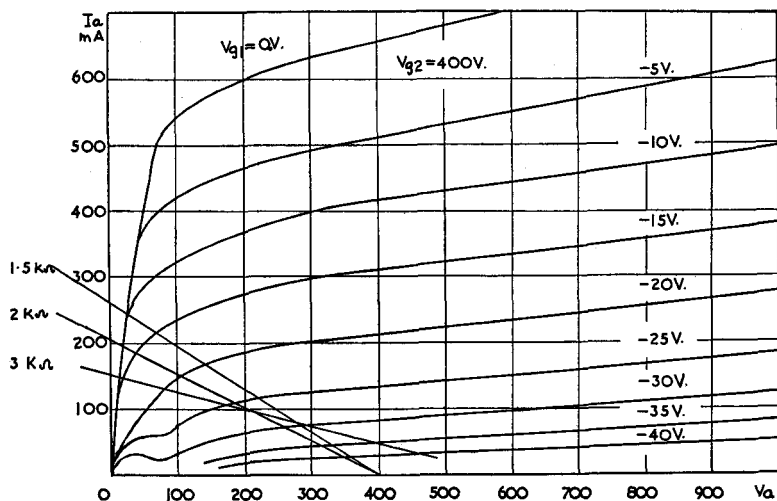


Fig. 6.10. Pentode output valve-load line for reactive load

Figs. 6.11(a) and 6.11(b). The transformer primary is parallel-fed, via  $C_1$ , so that the steady anode current of valve  $V_1$  does not flow through it; thus 'saturation' of the core is avoided. In a high-gain amplifier, anode decoupling might be necessary, but it is not shown in this diagram. If the effective resistance of the  $V_1$  anode load is  $R_L$ , and that of the  $V_2$  grid is  $R_g$ , we require a transformer of turns-ratio  $T$ , where  $T^2 = R_g / R_L$  (p. 71). For an input voltage  $e_g$ , the output voltage of  $V_1$  is given by  $(\mu \cdot R_L) / (R_L + r_a) \cdot e_g$ , and is equal to  $i_a \cdot R_L$ , where  $r_a$ ,  $i_a$  are the anode resistance and the anode current, respectively, of  $V_1$ . Hence:

$$i_a = \frac{\mu \cdot e_g}{(R_L + r_a)} = \frac{\mu \cdot e_g}{(R_g / T^2) + r_a}$$

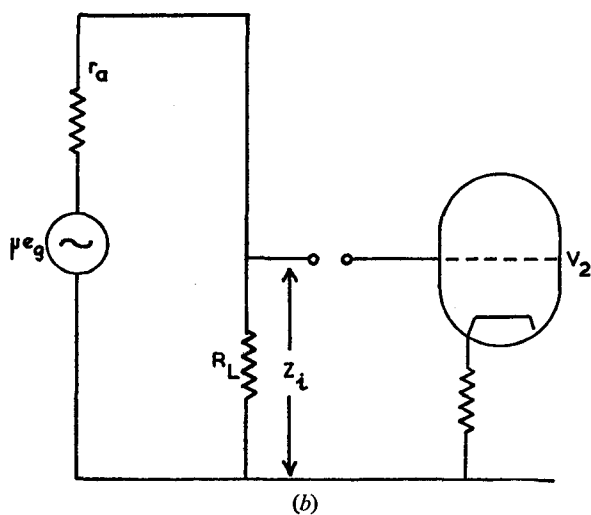
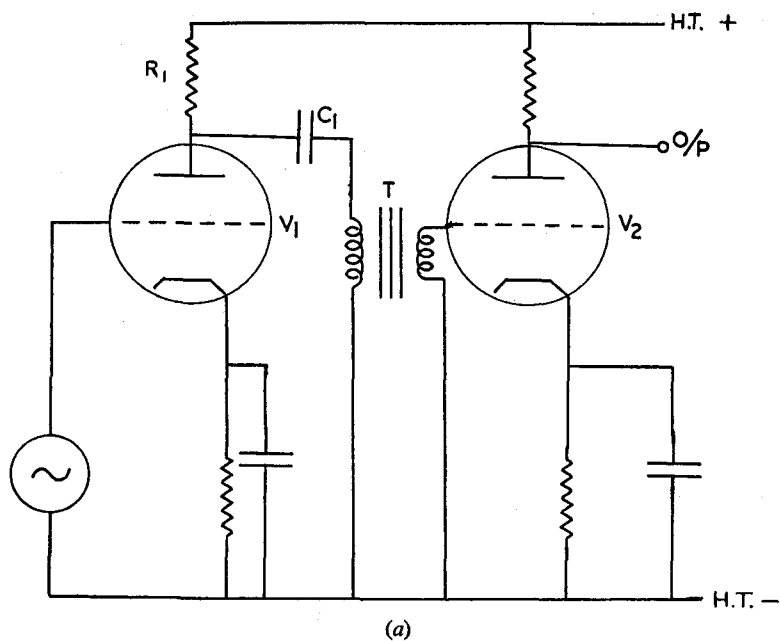


Fig. 6.11. Transformer-coupled amplifier and equivalent circuit

and  $V_p$  the primary voltage  $= i_a \cdot R_L = i_a \cdot R_g / T^2$

$$V_s \text{ the secondary voltage} = T \cdot V_p = R_g / T \cdot \frac{\mu e_g}{(R_g / T^2) + r_a}$$

and this is the input voltage to the grid of  $V_2$ .

The stage gain  $M = V_s / e_g = (\mu \cdot R_g) / (T \cdot r_a + R_g / T)$ . To find the transformer ratio for maximum gain we equate  $(dM/dT)$  to zero, obtaining  $T_{\max} = \sqrt{(R_g / r_a)}$ ;  $M_{\max} = \mu / 2 \cdot \sqrt{(R_g / r_a)} = \mu T / 2$ . For example, a triode of effective input resistance 1 M $\Omega$ , fed from a valve of  $r_a = 20$  k $\Omega$ , requires  $T = \sqrt{(10^6 / 2 \times 10^4)} = 7.1$  for maximum gain. If  $\mu$  for  $V_1$  is 20,  $M_{\max} = 20 / 2 \times 7.1 = 71$ . This is the optimum stage gain  $M$  from the input signal at the grid of  $V_1$  to the grid of  $V_2$ .

Transformers may give rise to enhanced response at certain frequencies, corresponding to resonance of the windings with stray or self-capacitance. To avoid these effects, the windings are sometimes 'damped' with parallel resistors.

At intermediate frequencies (i.e. those between audio- and radio-frequencies), usually about 500 kc/s, the transformer windings are tuned, either by small variable capacitors (trimmers), or by an iron-dust core or 'slug' within the winding. A tuned-transformer amplifier is shown in Fig. 6.12; tuning of both primary and secondary windings, since they are close-coupled, leads to the band pass characteristic shown on the right of the figure.  $R_1$   $C_1$  forms the anode decoupling circuit of valve  $V_1$ .

The amplification of higher frequencies presents considerable difficulties. Above a few megacycles per second stray capacitance, due to the proximity of components and leads, presents a comparatively low reactance; the resulting coupling between stages may lead to oscillation (p. 153). Tetrode or pentode valves must be used, because of the effects of inter-electrode capacities in the triode, and common H.T. and L.T. supplies must be decoupled. The most convenient frequency at which to carry out multi-stage amplification is about 500 kc/s; transformers and decoupling-circuit components for this frequency need not be large and tuned circuits of high 'Q' may be readily designed, whilst the effects of stray capacitance are not very serious. For this reason most of the amplification in the *superheterodyne* type of radio receiver is carried out at such a frequency—the *intermediate frequency*  $f_i$  (465 kc/s is commonly chosen)—obtained by combining

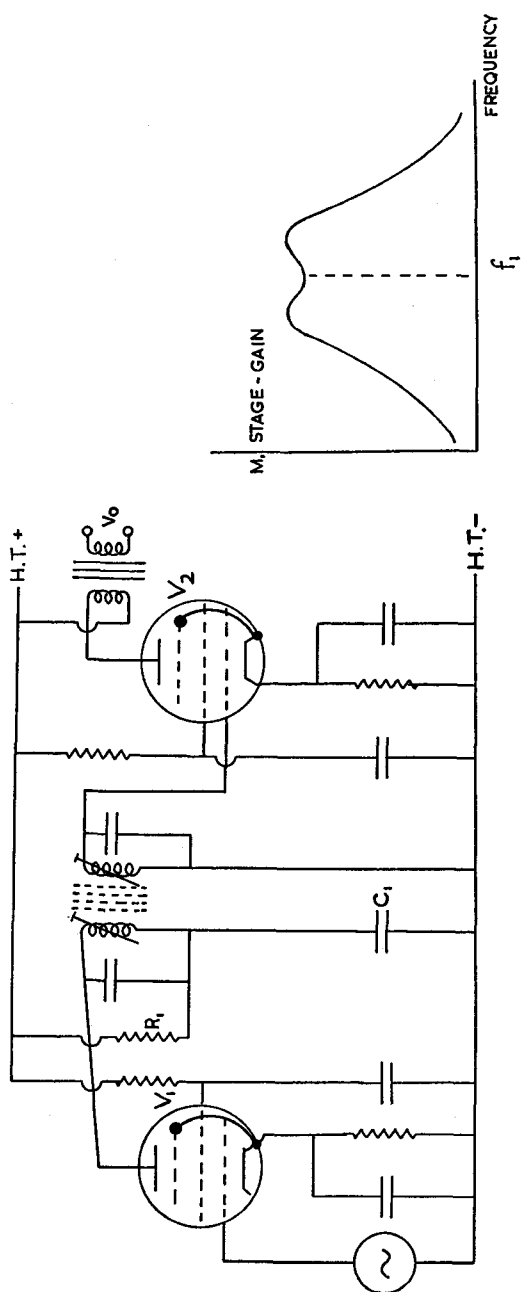


Fig. 6.12. Tuned-transformer amplifier and response curve.  $R_e$  is the effective anode load of  $V_1$ , consisting of  $R_i$  in parallel with  $C_1$  and the transformer primary winding

the signal received on the aerial with a local signal generated within the receiver. This local signal is derived from a variable-frequency oscillator—the *local oscillator*—which follows the frequency of the aerial circuit as this is 'tuned', but at a fixed distance of  $f_i$  from it. The signals are combined by a frequency-changer (or *mixer*) valve, the output of which is a tuned amplifier of the type shown in Fig. 6.12, resonant about the frequency  $f_i$ .

### Negative Feedback

We have seen (p. 131) that one way to reduce distortion due to the curved  $i_a/V_a$  characteristic of a valve is to use two similar valves in a push-pull amplification stage.

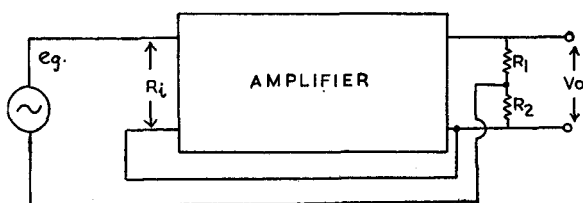


Fig. 6.13. Voltage negative feedback

An alternative method is to feed back part of the amplified signal, in opposition to the input signal; hence, if the input voltage tends to increase a large bias is developed, and the overall gain is maintained more nearly constant. This is an application of *negative feedback*.

Consider the circuit of Fig. 6.13.

$R_2$  is small compared with the input resistance  $R_i$  of the valve, so that practically the whole of the input voltage  $e_g$  appears between grid and cathode. The output voltage  $\mu e_g$  is developed across  $R_1$  and  $R_2$ , in series with the anode resistance  $r_a$ . Hence, the voltage  $V_2$  across  $R_2$  may be expressed:

$$V_2 = \frac{-\mu e_g \cdot (R_1 + R_2)}{(R_1 + R_2 + r_a)} \cdot \frac{R_2}{(R_1 + R_2)}$$

Since  $\mu R/(R + r_a) = M$ , the amplification factor:

$$V_2 = -M \cdot e_g \cdot R_2 / (R_1 + R_2) = -M \cdot e_g \cdot \beta$$

## APPLICATIONS OF THERMIONIC VALVES (II)

where  $\beta = R_2/(R_1 + R_2)$ , and represents the fraction of the output voltage which is fed back into the input; the negative sign before the expressions for  $V_2$  indicates that this voltage is in phase opposition to  $e_g$ , the input voltage. If the gain  $M$  is greater for a positive half-cycle than for a negative half-cycle, then the feedback voltage  $-\beta M \cdot e_g$  varies in the same way. By careful choice of components the output voltage, which depends upon the difference between  $e_g$  and  $\beta M \cdot e_g$  (i.e. upon the sum of  $e_g$  and  $V_2$ ), is maintained practically constant. The stage gain of an amplifier, in which a fraction  $\beta$  of the output voltage is fed back into the input in phase opposition, is reduced from  $M$  to  $M'$ , where  $M' = M/(1 + M\beta)$  (see p. 151).

### Example

For the circuit of Fig. 6.13, if  $R_1 = 30 \text{ k}\Omega$ ,  $R_2 = 3 \text{ k}\Omega$ ,  $\beta = 3/33 = 0.09$ . If the valve parameters are  $g_m = 3 \text{ mA/V}$ ,  $r_a = 10 \text{ k}\Omega$ , then  $\mu = 30$ .  $M = (30 \times 33)/(33 + 10) = 23$ . The application of negative feedback voltage:

$$e_2 = -M\beta \cdot e_g = -2.1e_g$$

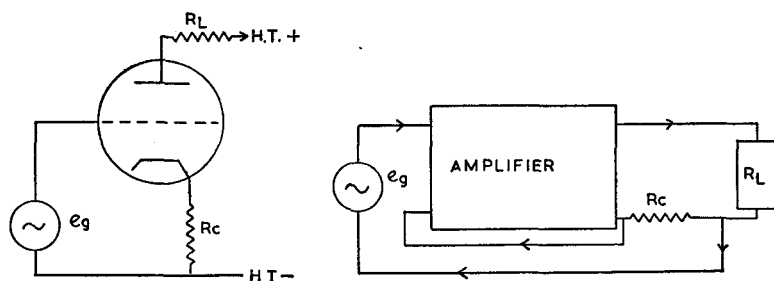


Fig. 6.14. Current negative feedback

reduces  $M$  to  $M'$ , where:

$$M' = 23/(1 + 23 \times 0.09) = 7.7$$

In the previous application of negative feedback an antiphase voltage was derived from the output, and applied to the input. An alternative method is to omit some or all of the decoupling across the cathode bias resistor of a stage; this is known as *current negative feedback*, and is illustrated in Fig. 6.14.

Since the grid and cathode voltages are in antiphase, the a.c. component across  $R_c$  tends to oppose the applied grid voltage  $e_g$ ; for example, if  $e_g$  swings more positive, the anode current  $i_a$  increases, and

the cathode becomes more positive with respect to earth—tending to reduce  $i_a$ . The fraction  $\beta$  of the output voltage which is fed back in opposition to  $e_g$  is now  $R_C/(R_C + R_L)$ . Current negative feedback tends to reduce distortion by reducing unequal amplification of the two half-cycles of the input signal, similarly to the voltage negative feedback.

The signal-to-noise ratio of an amplifier, which limits the amplification of very small input signals, may be improved by negative feedback; frequently, in small-signal amplifiers, the early stages are operated with  $\beta = 0.5$ , or greater.

The converse of negative feedback—*positive* feedback—requires that the 'returned' voltage shall be *in phase* with the input; this gives rise to oscillation (Chapter VII).

### The Cathode Follower

In the circuit of Fig. 6.15, the loading of the valve is entirely in the cathode circuit; applying the result for current negative feedback  $\beta = R_C/(R_C + R_L)$ , then, since  $R_L = 0$ ,  $\beta = 1$  and  $M = \mu R_C/(R_C + r_a)$ . Now the application of negative feedback reduces  $M$  to  $M' = M/(1 + M\beta)$ ; substituting, and putting  $\beta = 1$ , we obtain  $M' = (\mu R_C)/[r_a + (1 + \mu) \cdot R_C]$ , which is less than unity. The cathode follower, therefore, produces *current* amplification, but not voltage amplification.

For an input voltage  $e_g$ , the output voltage is  $M' \cdot e_g = i_a \cdot R_C$ . Hence

$$i_a = \frac{\mu \cdot e_g}{r_a + (1 + \mu) \cdot R_C} = \frac{[\mu/(1 + \mu)] \cdot e_g}{R_C + r_a/(1 + \mu)}$$

Thus  $\mu$  is reduced to  $\mu' = \mu/(1 + \mu)$ , and  $r_a$  is reduced to  $r_a/(1 + \mu)$ , as shown in the equivalent circuit of Fig. 6.15(b).

The output resistance of the cathode follower  $R_o$  is the resultant of  $R_C$  in parallel with  $r_a/(1 + \mu)$ , i.e.

$$R_o = \frac{R_C r_a/(1 + \mu)}{R_C + r_a/(1 + \mu)} = \frac{R_C r_a}{r_a + (1 + \mu) R_C}$$

Hence

$$R_o = \frac{R_C r_a}{(R_C + r_a + \mu R_C)} \approx \frac{R_C}{(1 + \mu R_C/r_a)} = \frac{R_C}{(1 + g_m R_C)}$$

For example, a pentode valve of  $\mu = 1000$  (e.g. the 6K7G) and  $r_a = 600 \text{ k}\Omega$ , with a cathode load  $R_C$  of  $2 \text{ k}\Omega$ , presents an output resistance  $R_o$  of  $465 \text{ }\Omega$  and  $M' = 0.76$ . This circuit may be used to match a high-impedance source to a low-impedance load.



## APPLICATIONS OF THERMIONIC VALVES (II)

The cathode follower does not introduce phase inversion of the signal as in a normal amplifier stage; a +ve pulse applied to the grid drives the top of  $R_c$  positive also. It is generally used

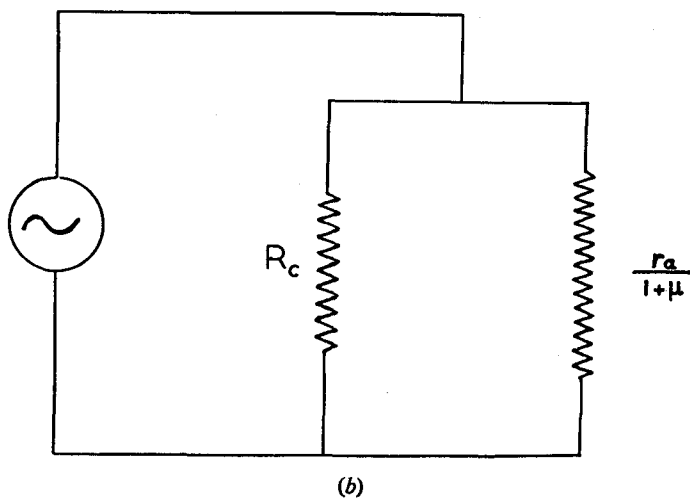
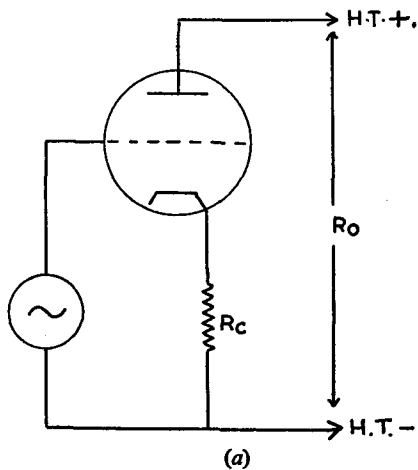


Fig. 6.15. (a) Cathode follower. (b) Equivalent circuit

where two stages of widely different impedance are to be coupled, e.g. in the connection of a Geiger-Müller tube to an amplifier (p. 190).

### The Classification of Valve Amplifiers

Amplifiers (and oscillators also) are frequently classified according to the conditions of working of the valve—i.e. the position of the 'working point' on the mutual characteristic. Although considerations of efficiency are of most importance where high power is concerned, the terms used are applied to describe quite low-power circuits operating under similar conditions; a brief description of this classification is therefore given.

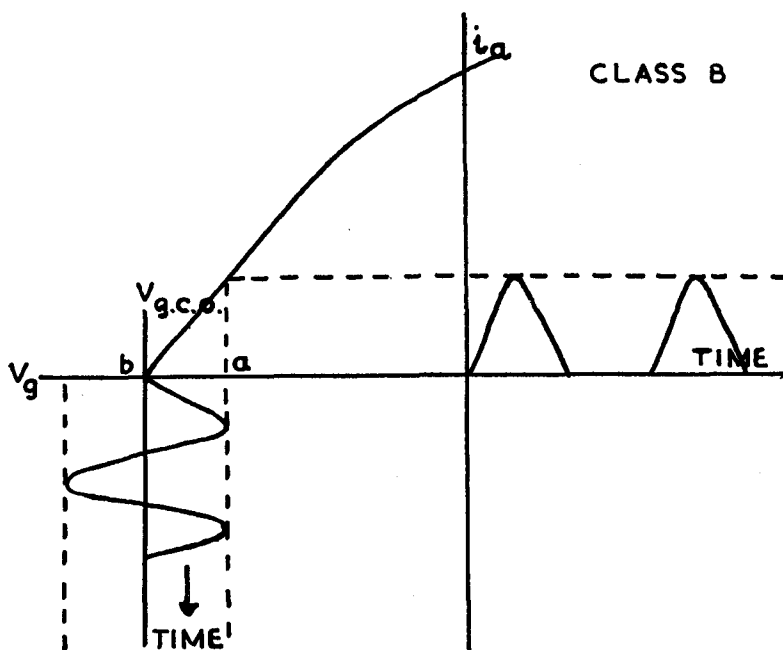


Fig. 6.16. (a) Class B operation of amplifier

If the valve is biased so that the complete input voltage swing occurs over a straight portion of the valve characteristic, it is said to be working under 'Class A' conditions. Anode current flows even when no signal is applied to the grid, and the efficiency of power conversion (from d.c. to a.c.) is less than 50%; however, the output voltage is a faithful copy of the input (in the case of an oscillator, the output is purely sinusoidal). The working is sometimes called Class AB if the negative peak of the grid swing

## APPLICATIONS OF THERMIONIC VALVES (II)

just reaches  $V_g$  c-o. This would be the case if the working-point was chosen as  $a$ , Fig. 6.16(a).

Efficiency is improved if the working point is changed to  $b$ ; anode current is now practically limited to the periods of positive grid swing with respect to  $V_b$ . There is considerable distortion, but the amplitude of the fundamental component is about the same as under Class A conditions, so that the efficiency is increased, to a maximum theoretical value of 70%. A tuned

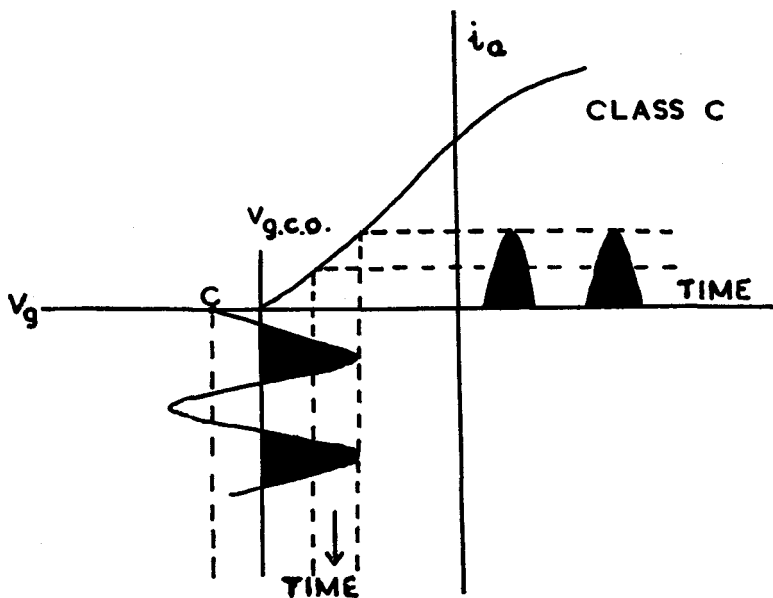


**Fig. 6.16. (b) Class C operation of amplifier**

circuit in the anode is required to select the fundamental component. Alternatively, two valves in push-pull (p. 131) may be operated under Class B conditions. This is Class B operation.

Still greater efficiency (*c.* 85% max.) results from biasing the valve beyond cut-off, as in Fig. 6.16(*b*). Only a portion of the positive grid swing causes anode current to flow; distortion of the grid input signal is greater than in Class B amplification, and this mode of operation is mainly used to amplify the high-frequency carrier voltages of radio transmitters, etc. It is called Class C operation.

**D.C. Amplifiers**

The output from a photo-cell, or from a Geiger-Müller tube, consists of unidirectional pulses; if it is required to amplify this output, a direct-coupled (d.c.) amplifier is required.

Suppose a signal of 0.5 V is applied between grid and cathode of a triode valve, for which  $g_m = 3 \text{ mA/V}$ . The change in anode current  $\delta i_a = 1.5 \text{ mA}$ , and, if the anode load is  $20 \text{ k}\Omega$ , the change in anode voltage  $\delta V_a$  will be 30 V; the d.c. input has been amplified 60 times. In practice, of course, the 'dynamic'  $g_m$  corresponding to this anode load should be used, which would reduce the

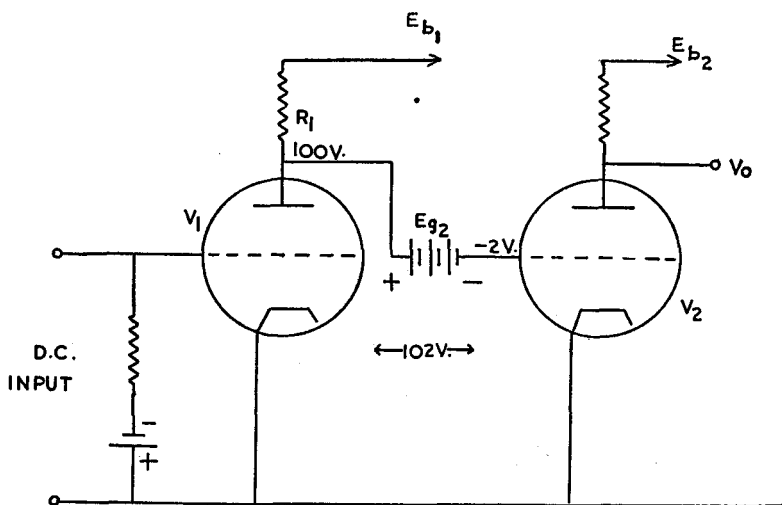


Fig. 6.17. Battery-operated d.c. amplifier

gain to about 20. Evidently, two stages of amplification would produce an overall gain of about 400.

However, there are difficulties in coupling stages for d.c. amplification, since the H.T. cannot be isolated by capacitors. To prevent the second valve from running into grid current, it would be necessary to use a high bias voltage; in the circuit of Fig. 6.17,  $E_{g2}$  must be greater than  $(E_{b1} - i_{a1} R_1)$  and  $E_{b2}$  must be greater than  $E_{b1}$ .

An 'all-mains' version of this two-stage amplifier in which the voltages are derived from a resistance chain across the H.T. supply is shown in Fig. 6.18. Suppose the anode current of valve

## APPLICATIONS OF THERMIONIC VALVES (II)

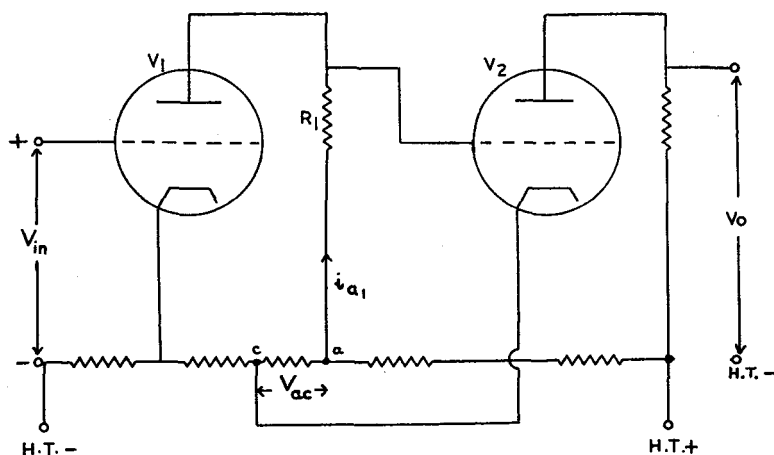


Fig. 6.18. Mains-operated d.c. amplifier

$V_1$  is  $i_{a1}$ ; then the grid of  $V_2$  is at a negative potential with respect to its cathode if  $(i_{a1} \cdot R_1) > V_{a,c}$ . If a d.c. voltage is applied to  $V_1$  grid as shown,  $i_{a1}$  increases, hence  $V_{a1}$  decreases, and the anode voltage of  $V_2$  rises. The output and input voltages are therefore in phase.

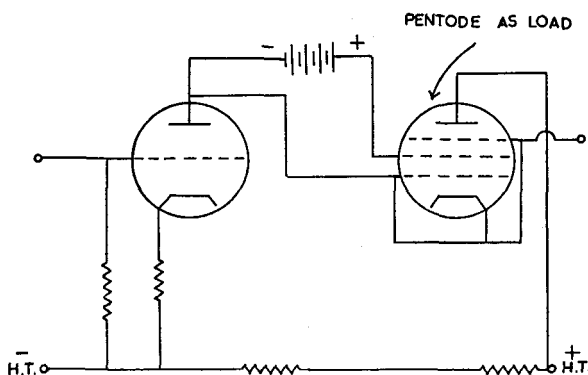


Fig. 6.19. D.C. amplifier with pentode valve load—the Horton amplifier

A variant of this circuit employs a pentode valve as the triode anode load; this is the Horton amplifier shown in Fig. 6.19. The effective anode load is the  $r_a$  of the pentode, but there is only a

small voltage drop across this load, and the gain is therefore very high.

One difficulty associated with d.c. amplification is that variations in H.T. supply voltages, or in valve characteristics, are equivalent to variations in the input, and are amplified accordingly. The useful amplification is thus sometimes limited by the stability of these factors. Such changes can be balanced out to some extent by a push-pull d.c. amplifier, as shown in Fig. 6.20. The figures without brackets show the *changes* in grid and anode

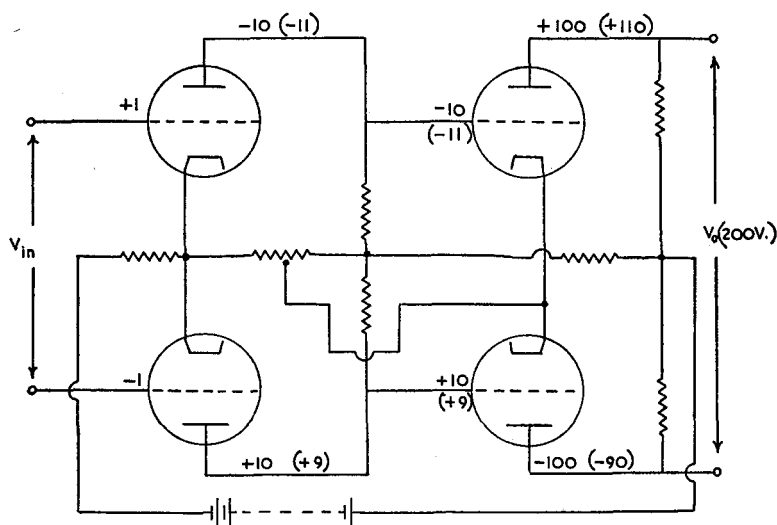


Fig. 6.20. Stabilisation of d.c. amplifier

voltages resulting from an applied voltage  $V_i$  of 2 V; the output is 200 V. Now suppose that the H.T. voltage decreases, so that the anode voltages fall; grid and anode voltages are now as given by the figures in brackets, but it will be observed that the output voltage has not changed.

An alternative method of amplifying d.c. signals makes use of the vibrating-plate capacitor. The d.c. input is converted into an a.c. voltage, and amplified by a conventional a.c. voltage amplifier; the loading on the circuit under test is reduced to about  $10^{-15}$  amp. The a.c. output is then converted back to d.c. by a suitable rectifier.

## APPLICATIONS OF THERMIONIC VALVES (II)

A commercial instrument on these lines is the Vibron electrometer†; the following is a brief account of the principle of operation. Suppose the d.c. input voltage  $V_i$  is applied to the parallel-plate capacitor  $C_1$  of Fig. 6.21; this will charge, via resistor  $R_1$ , to the input voltage. The capacity  $C_1 = A/4\pi d$ , where  $A$  is the area and  $d$  the distance apart of the condenser plates. The charge stored in the capacitor is  $Q$  coulombs, where  $Q = C_1 V_i$  (with  $C_1$  expressed in farads).

In the Vibron unit the upper plate of the capacitor is fixed, but the lower plate oscillates about a mean position, so that  $d$  is a function of time; we may write  $d_t = d_0 + d_1 \sin \omega t$ , where

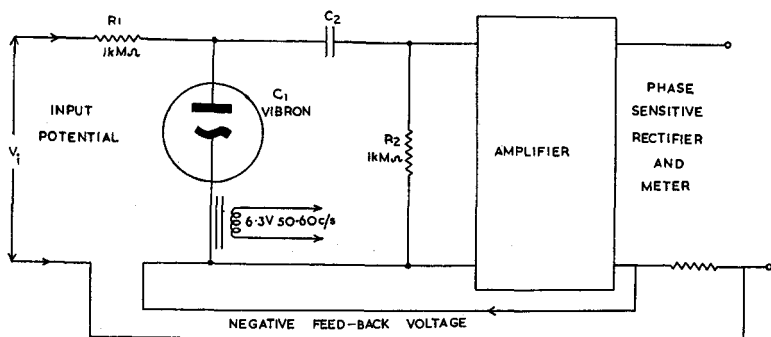


Fig. 6.21. The Vibron amplifier—basic circuit

$\omega = 2\pi \times$  frequency of oscillation. If the time-constant  $R_1 C_1$  is long, so that  $Q$  remains sensibly constant over a period of one cycle of the capacitor plate, the voltage  $V$  across the capacitor varies with  $d$ , i.e.

$$V = (4\pi Q/A) \cdot d = 4\pi Q d_0/A + \frac{4\pi Q d_1}{A} \cdot \sin \omega t$$

The first term is the d.c. voltage  $V_i$ , so that

$$V = V_i + (V_i d_1/d_0) \cdot \sin \omega t$$

Hence the a.c. component of  $V$  is proportional to  $V_i$  and to  $d_1/d_0$ ; this component is applied via  $C_2$  to the grid of an a.c. amplifier valve. The vibrating capacitor is energised by a 6.3 V 50 c/s

† Produced by Electronic Instruments Ltd., Richmond, Surrey.

## LABORATORY AND PROCESS INSTRUMENTS

solenoid, enclosed in the Vibron unit; because of the dependence of  $V$  on the ratio  $d_1/d_0$ , the plates are optically worked and polished, and are enclosed in an inert gas. The amplifier is operated with negative feedback to improve its stability; to prevent this from becoming positive feedback if the polarity of  $V_1$  is reversed, a phase-sensitive rectifier is necessary, and is incorporated in the electrometer.

## NOTES

### The Effects of Negative Feedback

In Fig. 6.22 suppose that the *applied* signal voltage is purely sinusoidal, given by  $e = E_1 \sin \omega t$ . This is not the *input* voltage to

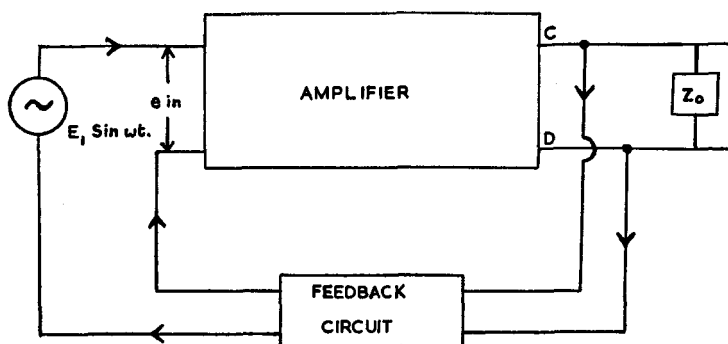


Fig. 6.22. Negative feedback network

the stage, however, because a fraction  $\beta$  of the output voltage is fed back in opposition, constituting the negative feedback. There are three voltage components in the output: the fundamental, an amplified signal-frequency component, a second harmonic component arising from the distortion of the stage, and a noise component. The output of the stage under negative feedback conditions may therefore be expressed:

$$e_o = E_0 \cos \omega t + D_f \cdot E_0 \cos 2\omega t + E_{nf} \cos \omega_n t$$

where  $E_0$  is the amplitude of the fundamental component,  $D_f$  the distortion-factor of the amplifier, and  $E_{nf}$  the amplitude of the noise component—the last two under feedback conditions. The frequency of the noise component is  $\omega_n/2\pi$ .



## APPLICATIONS OF THERMIONIC VALVES (II)

Since a fraction  $\beta$  of this output is fed back, the true input voltage  $e_i$  is given by:

$$e_i = (E_1 - \beta E_0) \cdot \cos \omega t - \beta D_f E_0 \cdot \cos 2\omega t - \beta E_{nf} \cdot \cos \omega_n t$$

If the gain of the stage *without* feedback is  $M$ ,  $e_0 = M \cdot e_i$ ,

$$\begin{aligned} \therefore e_0 &= M(E_1 - \beta E_0) \cdot \cos \omega t - M\beta D_f E_0 \cdot \cos 2\omega t - \\ &\quad - M\beta E_{nf} \cdot \cos \omega_n t + MD(E_1 - \beta E_0) \cdot \cos 2\omega t + \\ &\quad + E_n \cos \omega_n t \end{aligned}$$

the last two terms being introduced by the distortion and noise of the stage.  $D$  and  $E_n$  are respectively the distortion-factor and the noise-component amplitude under no-feedback conditions.

These two expressions for  $e_0$  must be equivalent, i.e.

$$\begin{aligned} E_0 \cos \omega t + D_f E_0 \cdot \cos 2\omega t + E_{nf} \cdot \cos \omega_n t \\ = ME_1 \cdot \cos \omega t - M\beta E_0 \cdot \cos \omega t - M\beta D_f E_0 \cdot \cos 2\omega t - \\ - M\beta E_{nf} \cdot \cos \omega_n t + MD(E_1 - \beta E_0) \cdot \cos 2\omega t + E_n \cdot \cos \omega_n t \end{aligned}$$

Equating the component terms, for the fundamental:

$$E_0 = M \cdot (E_1 - \beta E_0)$$

or  $E_0/E_1 = M/(1 + M\beta)$ . The ratio  $E_0/E_1$  defines the overall gain of the stage under feedback conditions,  $M_f$  say, so that

$$M_f = M \cdot 1/(1 + M\beta)$$

For the second harmonic component,

$$D_f(E_0 + M\beta E_0) = D \cdot (ME_1 - M\beta E_0)$$

$$\text{or} \quad D_f = D \cdot \frac{M(E_1 - \beta E_0)}{(E_0 + M\beta E_0)} = D \cdot 1/(1 + M\beta)$$

For the noise component:

$$E_{nf} = E_n - M\beta E_{nf} \quad \text{or} \quad E_{nf} = E_n \cdot 1/(1 + M\beta)$$

Thus the application of negative feedback reduces the gain by a factor  $1/(1 + M\beta)$ , and reduces the second harmonic distortion and noise in the same ratio. This 'improvement' will normally depend upon the frequency, since  $M$  depends on frequency; if, however, the term  $M\beta \gg 1$ ,  $M/(1 + M\beta) \simeq 1/\beta$ . Hence  $E_0/E_1$  becomes independent of the frequency characteristics of the

## LABORATORY AND PROCESS INSTRUMENTS

amplifier, depending only on those of the feedback circuit; a reactive feedback circuit may be used to correct the frequency response of the complete amplifier.

### References

YARWOOD, J. (1950). *Electronics*. Chapman and Hall.

STURLEY, K. R. (1949). *Radio Receiver Design*. Chapman and Hall.

### Problems

1. From the data of Fig. 6.3 plot the following load lines: (a) 50 k $\Omega$ , supply voltage 300 V; (b) 100 k $\Omega$ , supply voltage 300 V.

Compare the operation of the resultant amplifiers to alternating voltages of 4 V peak-to-peak amplitude and of audio-frequency.

2. From the 'equivalent circuit' of the triode valve, explain why it is unsatisfactory as an amplifier of high frequency alternating voltages. How may its disadvantages be overcome?

3. What is the overall gain of two such stages as those of Fig. 6.9(a), having the following component values:  $R_2 = 100$  k $\Omega$ ,  $R_4 = 250$  k $\Omega$ ,  $C_2 = 0.01$   $\mu$ F;  $r_a$  and  $\mu$  for each valve are 50 k $\Omega$  and 50, respectively. The input voltage is of fixed frequency, such that  $\omega = 1000\pi$  radians  $\text{sec}^{-1}$ .

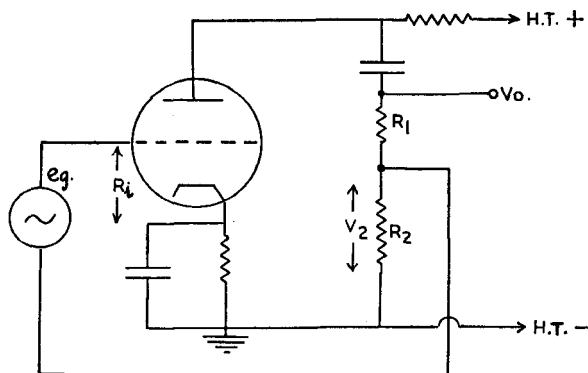
*Answer.* Overall gain = 1000.

4. What are the advantages of applying negative feedback to an amplifier?

The amplifier valve in the figure has  $r_a = 15$  k $\Omega$ ,  $g_m = 2$  mA/V. If  $R_1 = 18$  k $\Omega$  and  $R_2 = 2$  k $\Omega$  in this circuit, find the amplification,  $M$ , of the stage.

If negative feedback is now employed, calculate the reduced stage-gain,  $M'$ .

*Answer.*  $M = 17.1$ ;  $M' = 6.31$ .



## Applications of Thermionic Valves (III)

## Introduction—Valve Oscillators

We have previously considered feeding back part of the output voltage into the input, in phase opposition to the applied voltage; this constitutes negative feedback (p. 140). If the voltage fed back

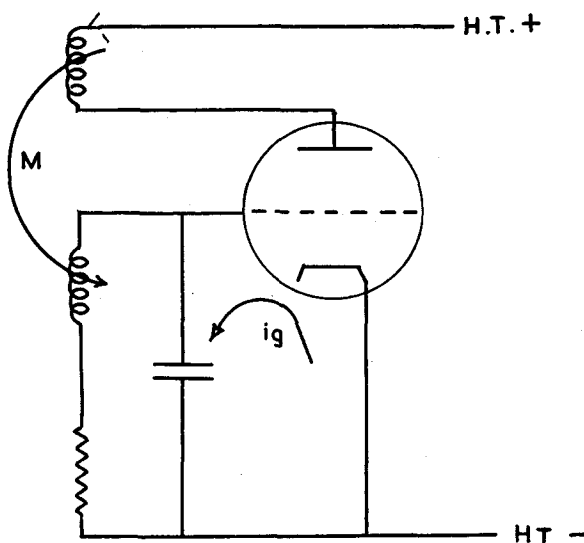


Fig. 7.1. (a) Valve oscillator—basic circuit

is *in phase* (or has a considerable component in phase) with the signal, we have *positive feedback*, and, under suitable conditions, the valve becomes a voltage generator or oscillator.

Suppose, on connecting the circuit of Fig. 7.1(a) to H.T. and L.T. supplies, a current  $i_g = I_G \sin \omega t$  flows in the grid circuit—i.e. a sinusoidal current of amplitude  $I_G$  and frequency  $\omega/2\pi$ .

# LABORATORY AND PROCESS INSTRUMENTS

If the resultant impedance of the grid circuit is capacitive, a voltage  $e_g$  is developed across it, where

$$e_g = E_G \cdot \cos \omega t = (I_G / \omega C_g) \cdot \cos \omega t$$

and  $C_g$  is the equivalent capacitance of the grid circuit.  $i_g$  leads  $e_g$  by  $\pi/2$ , and the variation in anode current is  $i_a = I_A \cdot \cos \omega t$ . This current flows in the anode coil, which is mutually coupled to the grid, and an e.m.f. is induced in the grid circuit of magnitude  $\omega M i_a$ , leading or lagging on  $i_a$  according to the sign of  $M$ , the mutual inductance. If this injected voltage has a large component in-phase with the initial voltage  $e_g$ , the current  $i_g$  is increased and

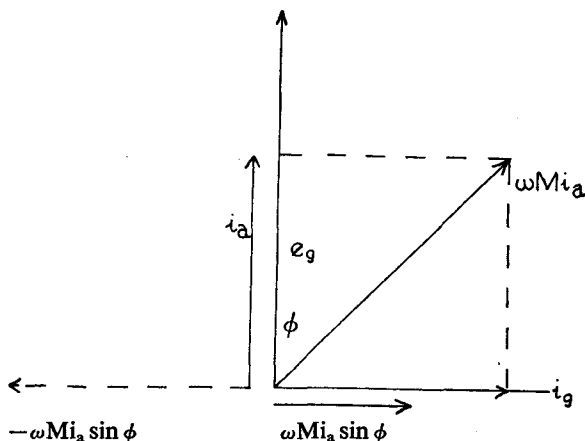


Fig. 7.1. (b) Phase diagram of oscillator

oscillations are maintained at frequency  $\omega/2\pi$ . The phase relationships are shown in Fig. 7.1(b). If  $M$  is positive, oscillations are maintained; if  $M$  is negative, they decay.

The energy fed back into the grid circuit is the product of current and voltage, i.e.

$$(\omega M i_a) \cdot i_g = (\omega M g_m \cdot e_g) \cdot i_g = (\omega M g_m / \omega C_g) \cdot i_g^2$$

The energy dissipated in the grid circuit is  $R_g i_g^2$ , where  $R_g$  is the resistive component of the circuit; hence, for oscillations to be maintained, we require:

$$R_g i_g^2 \leq M g_m \cdot i_g^2 / C_g \quad \text{or} \quad M \geq C_g R_g / g_m$$

## APPLICATIONS OF THERMIONIC VALVES (III)

A more rigorous derivation leads to the expression

$$M \geq C_g R_g / g'_m$$

where  $g'_m$  is the mutual conductance of the valve under operating conditions, i.e. the dynamic mutual conductance, as compared with the static value  $g_m$ . However, we have illustrated the importance of the mutual coupling in establishing the conditions for oscillation.

The grid circuit is similar to that considered on p. 41, having a natural frequency  $f = 1/2\pi \cdot \sqrt{1/LC - R^2/4L^2}$ . The damping of oscillations in this circuit is overcome if  $M$  satisfies the above condition, and an oscillatory voltage of constant amplitude is maintained. If  $M$  exceeds the limiting value  $C_g R_g / g'_m$ , the amplitude of the oscillatory voltage increases, but the power loss increases also; the effective value of  $g'_m$  is reduced until the equality is again established.

### Example

If  $C_g = 100$  pF,  $R_g = 10 \Omega$  and  $g'_m = 2$  mA/V, the minimum value of  $M$ , for oscillations to be maintained, is:

$$M_{\min} = \frac{10^{-10} \cdot 10}{2 \times 10^{-3}} = 0.500 \mu\text{H}$$

Where greater power output is required it is usual to include the tuned circuit in the anode, and to feed back from the grid circuit.

### Practical Valve Oscillators

In the Hartley oscillator a tapped inductor is used to provide feedback in the correct phase. The steady anode current may be in series with the oscillatory current (*series* oscillator), or in parallel with it (*parallel* oscillator); these cases are illustrated in Fig. 7.2(a) and 7.2(b). For oscillations to be maintained the voltages across  $AC$  and  $CG$  should be in phase opposition; this is ensured by the cathode tapping  $C$ , between  $A$  and  $G$ . The magnitude of the feedback voltage may be adjusted by moving the cathode tap; the usual arrangement is with  $C$  one-third along the coil from  $G$ . The frequency of the oscillator may be varied by the capacitance across the coil  $AC$ .

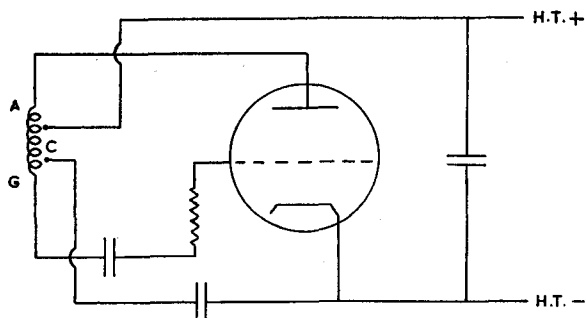


Fig. 7.2. Hartley oscillator: (a) series circuit

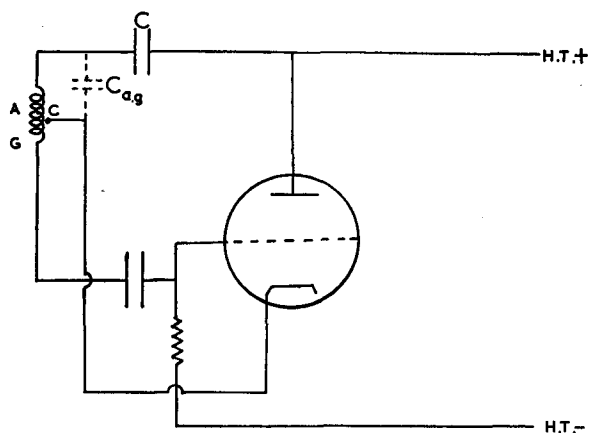


Fig. 7.2. Hartley oscillator: (b) parallel circuit

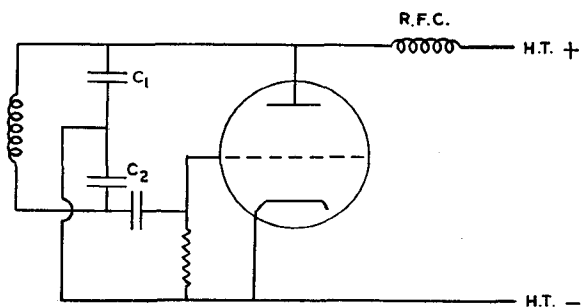


Fig. 7.3. Colpitt oscillator: (a) with external capacitors

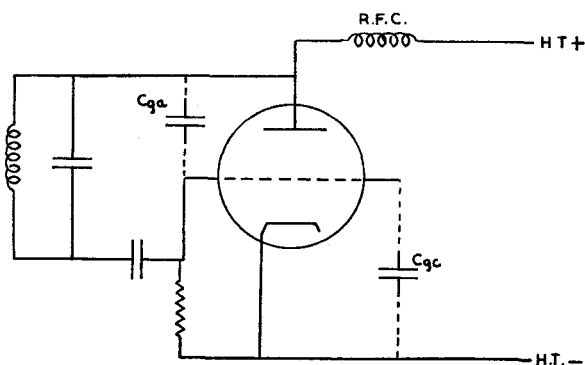


Fig. 7.3. Colpitt oscillator: (b) utilising inter-electrode capacity of valve

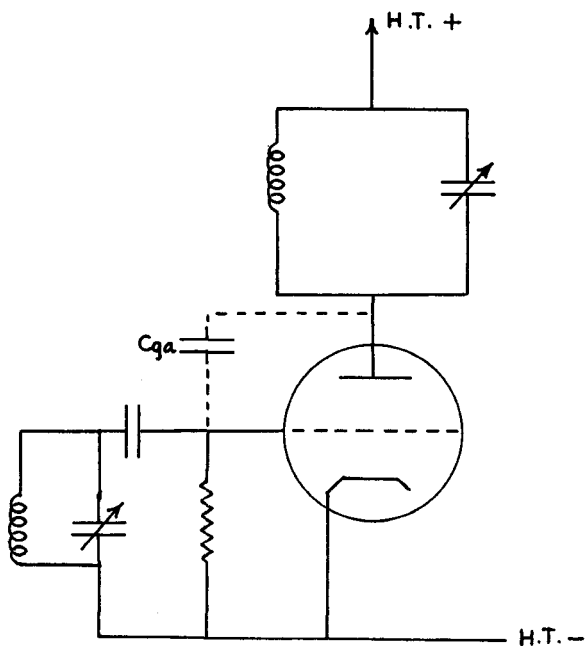


Fig. 7.4. Tuned anode-tuned grid oscillator

The Colpitt oscillator (Fig. 7.3(a)) uses a capacitance divider to provide feedback. The ratio  $C_2/C_1$  determines the feedback to the grid;  $C_1$  provides the 'tuning' of the main oscillatory circuit. At radio frequencies,  $C_1$  and  $C_2$  will be small; they may even be replaced by the inter-electrode capacitances of the valve, as shown in Fig. 7.3(b).

If the grid circuit is tuned to approximately the same frequency as the anode circuit, its impedance at the resonant frequency of the anode is high, and feedback is thus increased at this frequency; the two circuits must not be exactly 'in tune', for this conflicts with the phasing requirements. Such a circuit is illustrated in Fig. 7.4, and constitutes the tuned-anode tuned-grid oscillator. There is *no mutual coupling* between the circuits; if the valve is a triode, the grid-anode inter-electrode capacity is generally sufficient coupling, and it may be supplemented by a small external coupling capacitor.

#### Automatic Grid Bias for Oscillators

If the amplitude of oscillation is sufficiently great, the grid of the valve will be driven positive, and grid current will flow; this will introduce heavy damping into the circuit, so that the amplitude will decrease until the grid is at about zero potential. If, however,

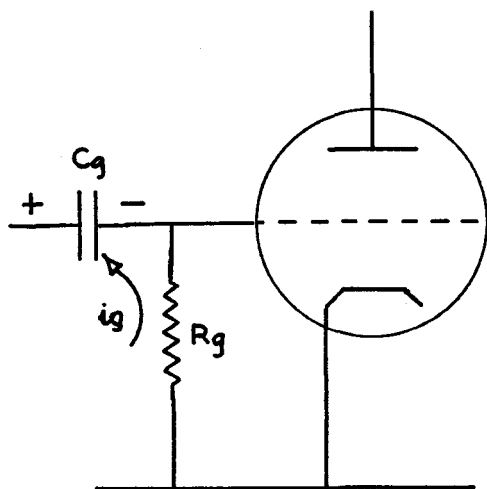


Fig. 7.5. Oscillator grid bias circuit



### APPLICATIONS OF THERMIONIC VALVES (III)

a capacitor  $C_g$  and resistor  $R_g$  are connected in the grid circuit as shown in Fig. 7.5, grid current will charge  $C_g$  as shown, and a negative bias will reduce the grid potential to zero on the peak of its voltage swing. This bias is self-adjusting; if the oscillation

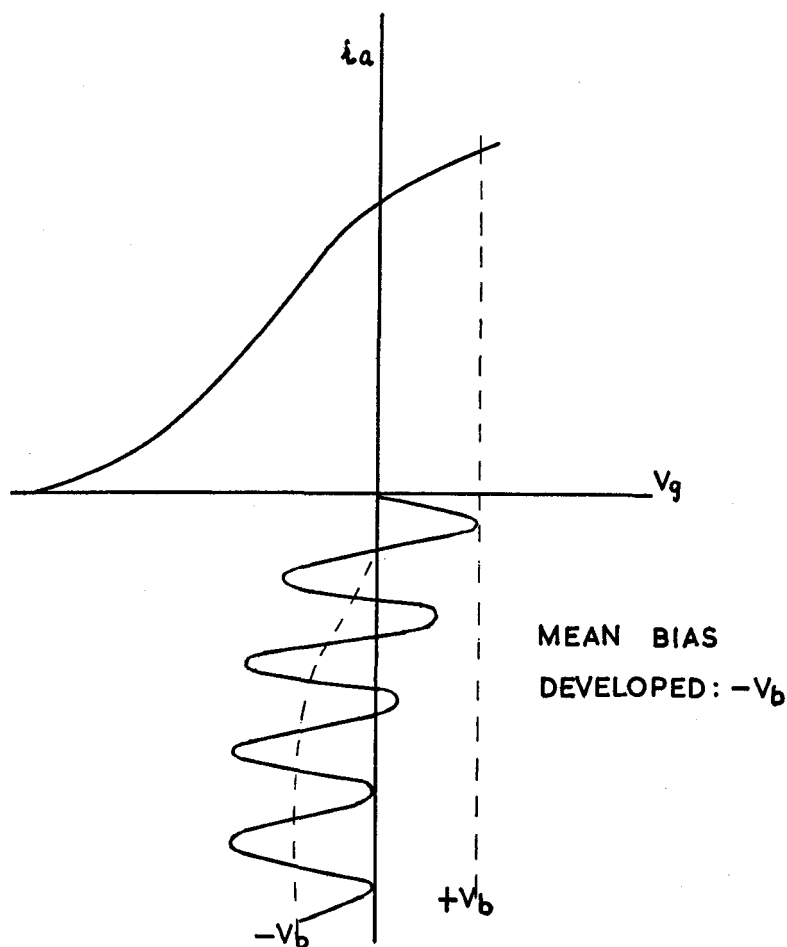


Fig. 7.6. Automatic bias adjustment

amplitude falls,  $C_g$  will discharge via  $R_g$  so as to restore  $E_g$  to zero, and vice-versa if the amplitude increases; the amplitude is thus kept practically constant. For this reason the circuit is said to develop 'automatic' grid-bias for the oscillator.

## LABORATORY AND PROCESS INSTRUMENTS

The time constant ( $CR$ ) must not be too great, or a large negative bias may reduce the anode current below the limit necessary to maintain oscillation; the valve then 'cuts-off' until this bias has leaked away, when oscillation starts again. The output thus consists of short 'bursts' of oscillation, followed by quiescent periods; this behaviour is called *squegging*.

As power is taken from the oscillator the bias automatically reduces so as to maintain the amplitude constant. In Fig. 7.6, if more power were taken from the oscillator, the bias would change to a less negative value than  $(-V_b)$ .

### Dynatron Oscillator

The anode current-anode voltage characteristic of a normal tetrode valve (i.e. without beam-forming plates) shows a region of negative  $dV_a/di_a$ , i.e. of negative resistance (p. 87). Consider

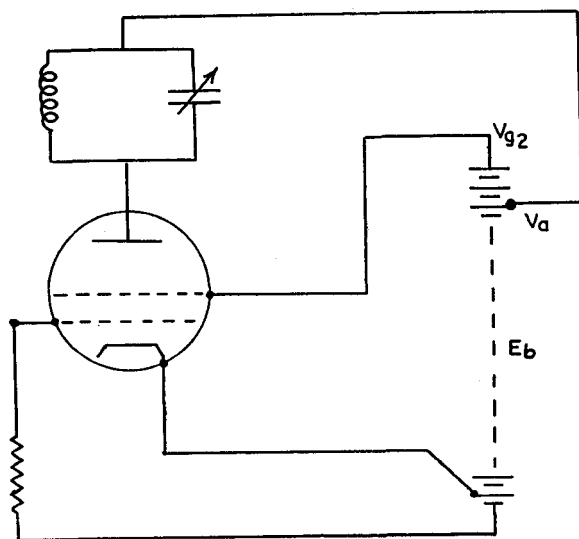


Fig. 7.7. The dynatron oscillator

the circuit of Fig. 7.7. The tuned-anode circuit oscillates at frequency  $f_0 = 1/2\pi\sqrt{(1/LC - R_D^2/L^2)}$ , where  $R_D$  is the dynamic impedance of the circuit at resonance (p. 44). Since  $R_D = L/CR$ , the condition for oscillations to be maintained is  $L/CR \leq -ve$

### APPLICATIONS OF THERMIONIC VALVES (III)

slope of  $(dV_a/di_a)$  at the working point of the valve. Thus the negative resistance of the anode circuit is used to balance its resistive loss.

The usual working condition is with  $V_a$  about 30 V below  $V_{gs}$ .

#### The R-C Oscillator

To maintain oscillations it is necessary to feed back to the grid a voltage from the anode, with a phase-change of  $\pi$  in the process. Now a series resistance-capacitance circuit produces a phase-change, between the applied voltage and that across the resistor  $V_R$  of  $\phi = \tan^{-1} . 1/\omega CR$ ,  $V_R$  leading the applied voltage. If, then, the  $V_R$  component is applied to a second, similar, circuit, a further phase-advance  $\phi$  will result, so that  $V_R$  leads  $V_i$ , the original supply voltage, by  $2\phi$ .

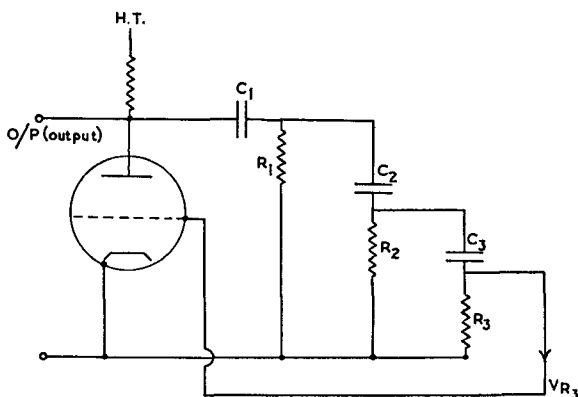


Fig. 7.8. Resistance-capacitance (phase-shift) oscillator

In Fig. 7.8 suppose each  $(CR)$  combination produces a phase-change  $\phi = 60^\circ$ . Then  $V_R$  leads  $V_a$  (the supply voltage to  $R_1 C_1$ ) by  $\pi$ , and, if this voltage is returned to the grid, we have the necessary conditions for the maintenance of oscillations. For  $\phi = 60^\circ$ ,  $1/\omega CR = \tan^{-1} . 60^\circ = \sqrt{3}$ , so that  $(CR) = 1/\sqrt{3} . \omega$ . If  $\omega$  is to be  $2\pi$  Mc/s ( $f = 1.0$  Mc/s),  $(CR) = 10^{-6}/(\sqrt{3} . 2\pi) = 10^{-7}$ . Hence a suitable combination of  $R$  and  $C$  might be  $C = 100$  pF,  $R = 1000 \Omega$ . The feedback voltage will only undergo a phase-shift of  $\pi$  at the frequency for which the circuit was designed;

the  $R$ - $C$  oscillator thus gives a sinusoidal output at a single frequency, i.e. the generated voltage is 'monochromatic'. The oscillator is sometimes constructed with a separate valve for each phase-shift, since the feedback amplitude can then be more easily adjusted (Fig. 7.9).

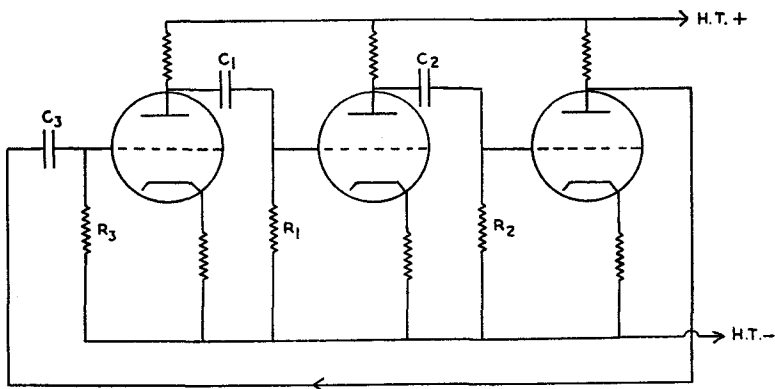


Fig. 7.9. Multi-valve resistance-capacitance oscillator

### Crystal Frequency-control

The frequency stability of an oscillator may be improved by screening it from stray magnetic and electrostatic fields, and by protecting it from mechanical vibration; the power supplies may also be stabilised. The most satisfactory method, however, makes use of the *piezo-electric* effect. This is observed in certain crystals, such as those of quartz, tourmaline and Rochelle salt.

Considering quartz, for example, the crystal axes are well defined, as shown in Fig. 7.10. Application of a force along the mechanical axis  $YY$  produces an e.m.f. between opposite faces on the electrical axis  $XX$ , and conversely. Thus a suitable electrical excitation of the crystal sets up mechanical vibrations of the same frequency, and a small in-phase impulse is given to the source of the excitation. In this way, the frequency of an electrical oscillator is maintained constant, provided that it corresponds closely to the frequency of one of the natural vibration modes of the crystal. These natural frequencies are temperature dependent; however, if two modes are chosen so that their temperature coefficients are positive and negative respectively, a 'cross-cut'

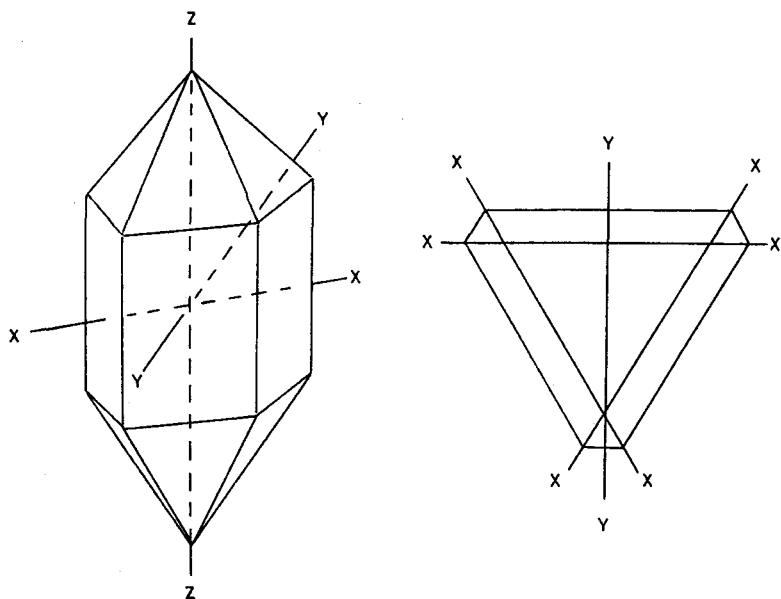


Fig. 7.10. Crystal axes of quartz. ZZ is the optic axis of the crystal

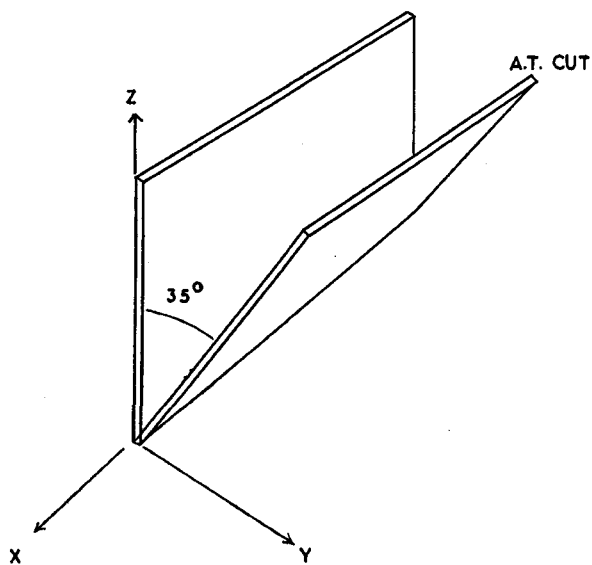


Fig. 7.11. The A.T. (temperature-independent) crystal cut

# LABORATORY AND PROCESS INSTRUMENTS

crystal involving both modes may have a resultant frequency practically independent of temperature. The 'A.T.' cut, illustrated in Fig. 7.11, is often used; it has the requisite combination of sensitivity to excitation, mechanical strength and temperature invariance of frequency.

Connection is usually made to layers of gold sputtered on to opposite faces of the crystal perpendicular to the electrical axis, and the crystal is mounted in a holder—e.g. in a small glass

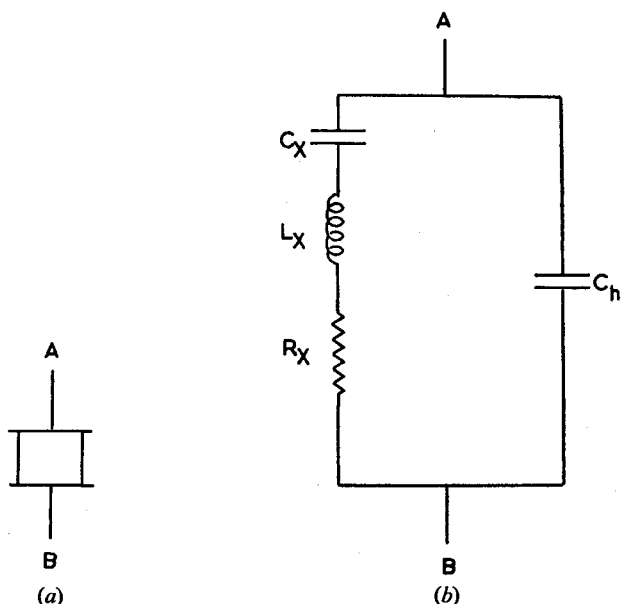


Fig. 7.12. (a) The mounted crystal. (b) Equivalent circuit of mounted crystal

envelope, like a modern thermionic valve. The equivalent circuit of the mounted crystal is shown in Fig. 7.12(b). The crystal may be considered as a series resonant circuit, shunted by the capacitance of its holder,  $C_h$ .  $C_X$  is the electrical analogue of the mechanical stiffness of the crystal,  $L_X$  represents its mass, and  $R_X$  the frictional losses of its vibration. In general,  $R_X$  is small, so that the resonant circuit has a high  $Q$ -factor (p. 54).

Typical values for the parameters of a crystal might be:

$$C_X = 0.25 \text{ pF}; L_X = 0.1 \text{ H}; R_X = 15 \Omega; C_h = 2 \text{ pF}$$

### APPLICATIONS OF THERMIONIC VALVES (III)

The combination ( $C_x L_x R_x$ ) would resonate at 1.00 Mc/s, and have a  $Q$  of  $4 \times 10^4$ ; shunted by  $C_h$ , however, the resonance frequency is changed to 1.07 Mc/s, and  $Q$  falls to about  $10^4$ . The crystal impedance-frequency characteristic curve is shown in Fig. 7.13; at 1.00 Mc/s the series resonant circuit has impedance  $R_x$ . At 1.07 Mc/s the parallel resonant circuit of crystal, plus holder, has impedance  $R_D \approx 10^{10} \Omega$ .

Since the crystal is equivalent to a tuned circuit of high  $Q$ , it may replace the grid circuit of a conventional tuned-anode/

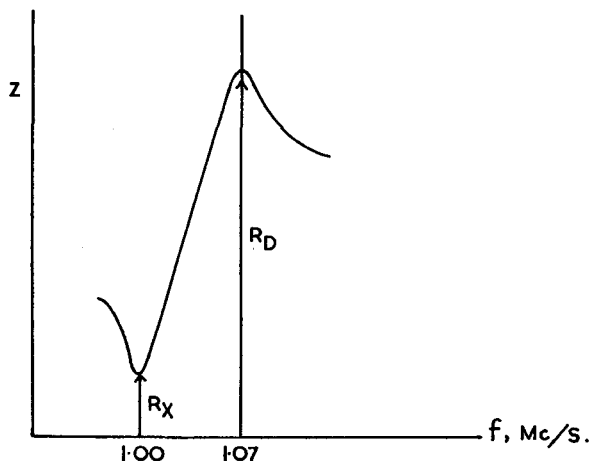


Fig. 7.13. Frequency response curve of mounted crystal

tuned-grid oscillator, as shown in Fig. 7.14(a); alternatively, it may be included in series with the grid circuit, as in Fig. 7.14(b). The R.F. choke is necessary to isolate the H.T. supply from the oscillatory circuit.

The coupling of the crystal into the circuit should be loose, which is the case if  $C_h$  is much greater than  $C_x$ , so that the reactance of the holder,  $X_{C_h} \ll X_{C_x}$ . The frequency of oscillation is then independent of the loading upon the oscillator.

Crystals may be usefully employed between the frequency limits 50 kc/s and 15 Mc/s. Below 50 kc/s, they are insensitive; above 15 Mc/s, they are too thin to be robust. Within these limits, the frequency is maintained constant to about one part in

## LABORATORY AND PROCESS INSTRUMENTS

$10^5$ , and this may be improved by enclosing the crystal in a thermostatted 'oven'; frequency constancy to within one part in  $10^7$  is then possible.

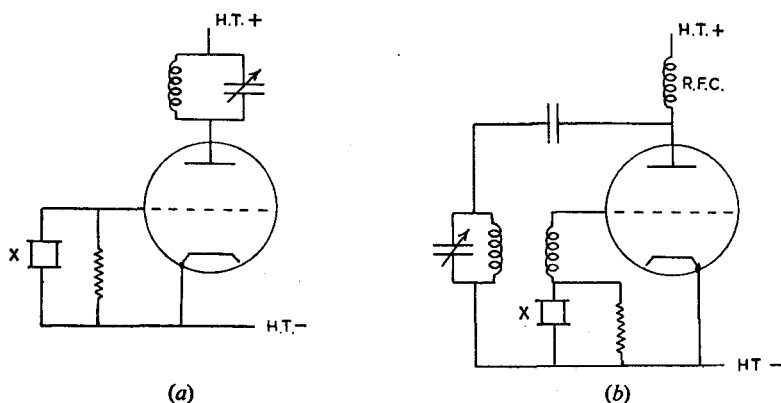


Fig. 7.14. Crystal control of oscillator frequency

### Low-frequency Oscillators

A simple audio-frequency oscillator may be constructed by using the primary and secondary windings of an A.F. transformer as

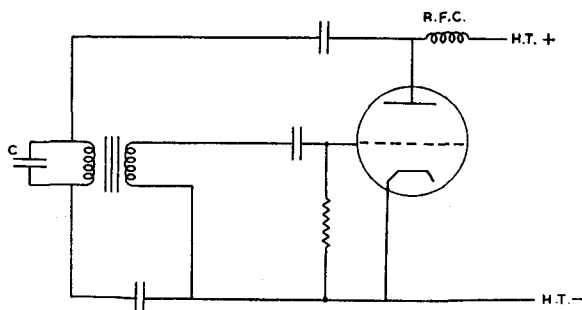


Fig. 7.15. Audio-frequency oscillator, using an A.F. transformer

anode and grid circuit. The anode circuit is tuned by a suitable capacitor  $C$  as shown in Fig. 7.15. It is necessary for connections to the windings to be in the same 'sense', so that the feedback is positive.



### APPLICATIONS OF THERMIONIC VALVES (III)

A more versatile instrument is the beat-frequency oscillator, shown schematically in Fig. 7.16. A variable-frequency oscillator and a fixed-frequency oscillator supply the grids of a mixer valve (p. 91), and the difference frequency is fed to the output terminals; the buffer amplifiers prevent the two oscillators from 'pulling' into synchronism when the difference between their frequencies is small. If  $f_2 = 1000$  kc/s, and  $f_1$  may be varied between

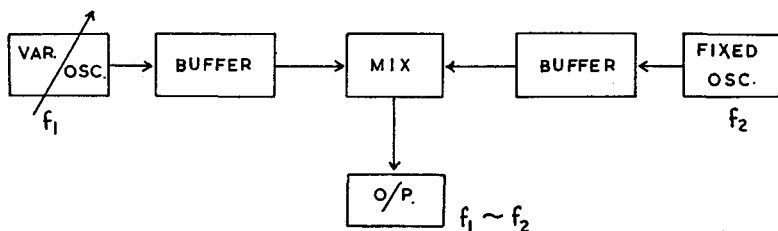


Fig. 7.16. Schematic diagram of the beat-frequency oscillator

900 and 1000 kc/s, the output may be continuously varied from zero to 100 kc/s. This is a very useful oscillator for studying the variation of conductivity of an electrolyte solution with frequency, in order to assess polarisation effects; at these frequencies, of course, the Debye-Falkenhagen ionic atmosphere effects are not apparent.

### The Multivibrator

A signal at the grid of valve  $V_1$  (Fig. 7.17) is amplified, and part of it is fed to the grid of  $V_2$ ; the amplified voltage which is returned from  $V_2$  anode to  $V_1$  grid is thus in phase with the original signal, and oscillations are maintained.

To see how oscillations originate, suppose that, on switching-on,  $V_1$  heats up more rapidly than  $V_2$ , so that at some instant,  $i_{a1} > i_{a2}$ . Due to the voltage drop across  $R_L$ , a *negative* pulse is fed to the grid of  $V_2$ , and the current  $i_{a2}$  decreases. The anode voltage of  $V_2$  therefore rises, and a *positive* pulse is fed to the grid of  $V_1$ ; the result of this cycle of operations is to increase  $i_{a1}$  still further with respect to  $i_{a2}$ . The cycle is repeated, so that very rapidly  $V_2$  is driven to cut-off, and  $V_1$  is conducting heavily. The negative charge built up on  $C_2$  now leaks away through  $R_2$ , at a rate determined by the  $CR$  time constant. Eventually,  $V_{g2}$  rises above cut-off, and  $V_2$  begins to conduct; the cycle of operations is

repeated, but in the reverse order, so that now  $V_1$  is driven to cut-off, and  $V_2$  conducts heavily. Each valve in turn conducts, and the operation is well described by an alternative name for this oscillator—the ‘flip-flop’. The output consists of a train of approximately square pulses, at a repetition frequency governed by the grid-circuit time constants.

The period of the waveform may be expressed:

$$\tau = k(R_1 C_1 + R_2 C_2)$$

where  $k$  depends upon the valve characteristics and the supply voltage. The frequency stability is, however, poor, and such oscillators are generally ‘locked’ to a stable feedback oscillator,

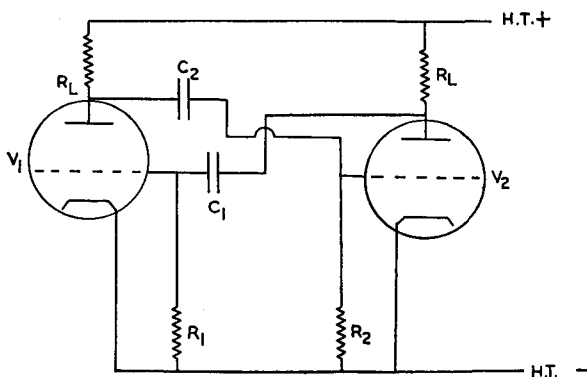


Fig. 7.17. The multivibrator

which determines the instant of cut-off with precision. The oscillator frequency must be approximately equal to that of the multivibrator.

Such a generator is useful as a source of harmonics of a known frequency. For example, a multivibrator of frequency 100 kc/s, ‘locked’ to a crystal-controlled oscillator, will provide harmonics up to about 50 Mc/s, having a good deal of the stability of the crystal; this is one form of *wavemeter*, for the determination of frequency of a signal.

### Other Relaxation Oscillators

Oscillators whose frequency is controlled by the charge or discharge of a capacitor or inductor through a resistance are called *relaxation* oscillators; the multivibrator which we have just considered is of this type.

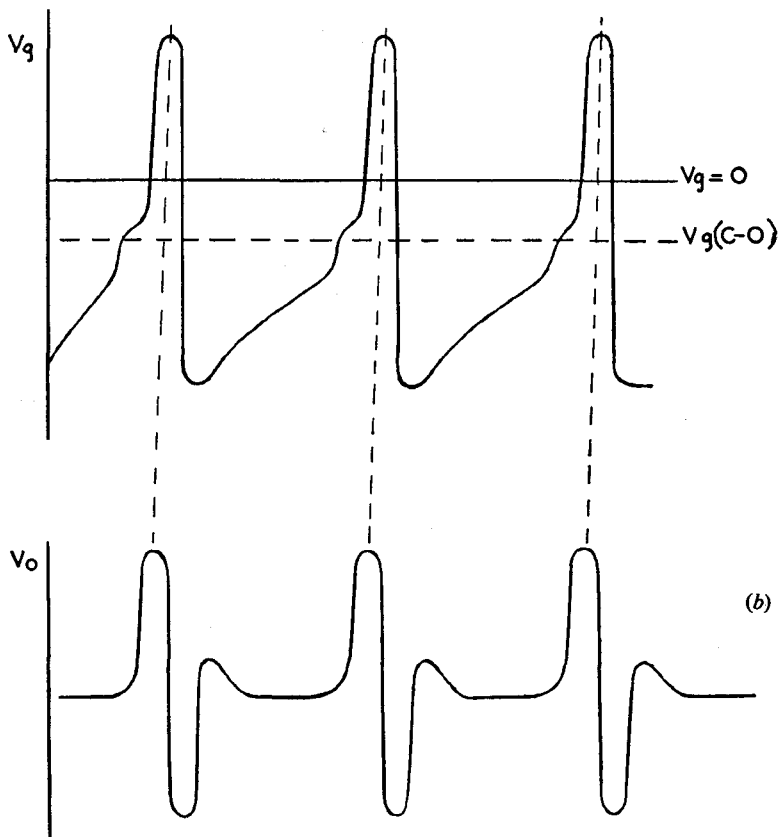
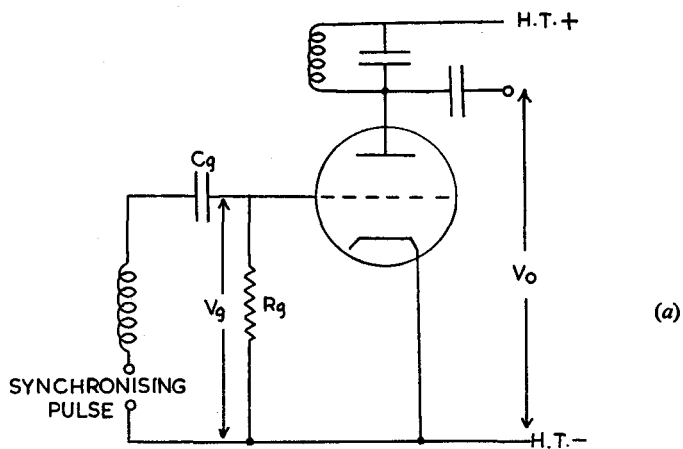


Fig. 7.18. The blocking oscillator and waveforms

# LABORATORY AND PROCESS INSTRUMENTS

A single-valve relaxation oscillator is the blocking oscillator, shown, together with its waveforms, in Fig. 7.18, where  $V_{gc.o.}$  is the cut-off value of the grid bias voltage. The anode and grid circuits are tightly coupled together, and the time constant of the grid combination  $C_g R_g$  is large. As oscillations build up, the bias

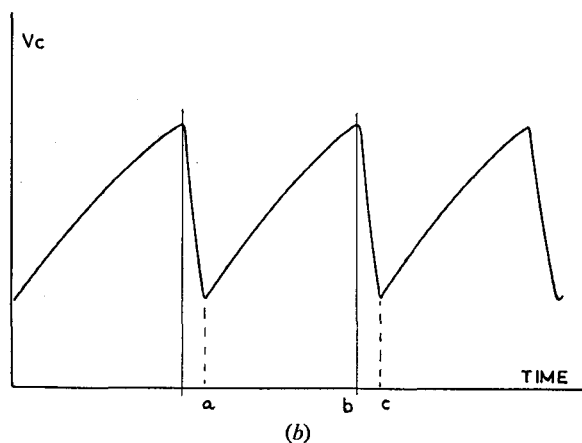
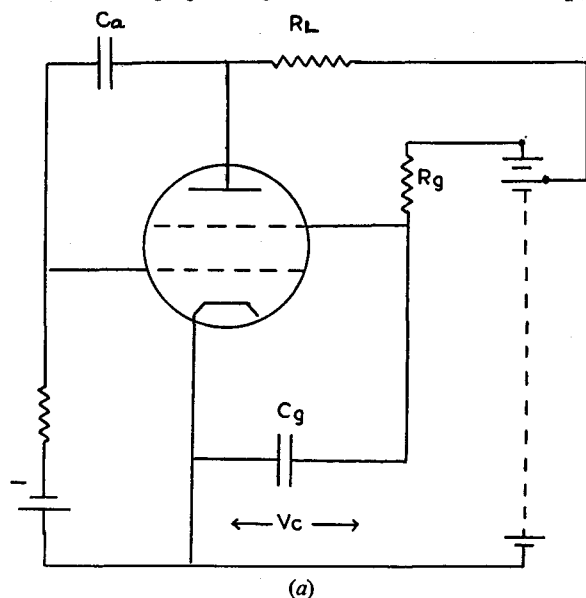


Fig. 7.19. Dynatron oscillator as a saw-tooth generator

### APPLICATIONS OF THERMIONIC VALVES (III)

rapidly falls well below cut-off, and the valve is then inoperative until this heavy bias has leaked away via  $R_g$ . The frequency at which pulses are generated can be synchronised by injecting a small voltage from a reference oscillator into the grid circuit.

The dynatron oscillator may be modified to provide a saw-tooth waveform, as shown in Fig. 7.19(a). The rise in anode voltage, which occurs over the 'negative' resistance region (p. 87) raises the control-grid voltage via capacitor  $C_a$ , and the screen current  $i_{s_1}$  increases. Capacitor  $C_g$  rapidly discharges through the valve, and  $V_{g_1}$  falls, cutting off oscillations.  $C_g$  then charges via

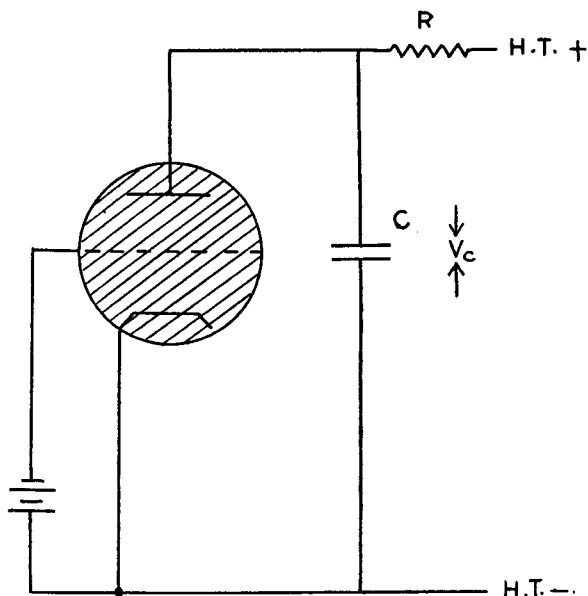


Fig. 7.20. Thyatron circuit for the generation of saw-tooth waveform

$R_g$ , and the cycle is repeated. The voltage across  $C_g$  is thus of saw-tooth pattern, with a very rapid fly-back  $bc$ , and a comparatively slow rise  $ab$  (Fig. 7.19(b)).

A similar waveform results from the gas-filled thyatron circuit of Fig. 7.20. Capacitor  $C$  charges via resistor  $R$  until the anode voltage rises to the point of striking.  $C$  now discharges rapidly through the tube, and the voltage falls below the ionisation threshold; the grid then regains control, and the tube remains cut

## LABORATORY AND PROCESS INSTRUMENTS

off until  $C$  is again charged. In order to provide linearity of the rising voltage,  $V_C$  should reach only a small fraction of the battery voltage before the tube fires. The rapidity with which the cycle may be repeated is governed by the  $CR$  time constant, but is limited by the finite de-ionisation time of the thyatron.

### References

- HEISING, R. A. (1947). *Quartz Crystals for Electrical Circuits*. D. van Nostrand.
- FAIRWEATHER, D. and RICHARDS, R. C. *Quartz Crystals as Oscillators and Resonators*. Marconi's Wireless Telegraph Co.
- THOMAS, H. A. (1939). *Theory and Design of Valve Oscillators*. Chapman and Hall.
- YARWOOD, J. (1950). *Electronics*. Chapman and Hall.

### Problems

1. The anode circuit of a tuned anode oscillator has an inductor of  $L$  H and resistance  $R$   $\Omega$  in parallel with a capacitor of  $C$   $\mu$ F. Find an expression for the mutual inductance  $M$  H between the anode and grid coils for oscillations to be maintained.
2. Explain how negative grid bias improves the efficiency of a valve oscillator; show that such bias may be automatically generated by the inclusion of a suitable grid circuit in the oscillator.
3. Discuss the mode of operation of the piezo-electric crystal, and show how it may be employed to maintain constancy of the frequency of a valve oscillator.
4. Explain what is meant by the term 'Relaxation Oscillator', and discuss the mode of operation of one such oscillator.

## CHAPTER VIII

### Miscellaneous Electronic Tubes

#### Photo-cells

The photo-electric cell converts light energy into electrical energy—the converse of the cathode ray oscilloscope (p. 191). Two main types of photo-cells are used: *photoconductive* cells, which show a marked resistance change when illuminated, and *photovoltaic cells*, which generate an e.m.f. when light falls upon a sensitive cathode.

(i) *Photoconductive cells*. These are usually of selenium, which is deposited on an iron 'base' and coated with a semitransparent silver layer: connections are made to the base and to the silver 'counter-electrode' via the metal ring *R* (Fig. 8.1). The response

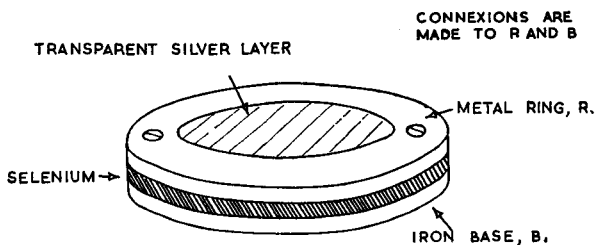


Fig. 8.1. (a) The barrier layer photo-cell

curve shows the current in  $\mu\text{amp}$  for various illumination intensities and for different loads. The spectral peak is at about  $5800 \text{ \AA}$ , but is rather broad; response is about 10% of the maximum at  $6800 \text{ \AA}$ .

Cells of a new type, in which the photo-conductive layer is of polycrystalline cadmium selenide, have a much greater sensitivity; a small voltage applied across the cell will produce a current of a few milliamps. The maximum dissipation is 10–100 mW, depending upon the area of the photosensitive surface. The spectral peak is at  $7500 \text{ \AA}$ , and the *dark current* (the current flowing when the cell is totally shielded from illumination) is

# LABORATORY AND PROCESS INSTRUMENTS

about  $10\ \mu\text{amp}$ . The following table gives some data for one cell of this type†:

## PHOTO-CELL TYPE FT422

(Cathode area,  $1\ \text{mm}^2$ ; maximum voltage, 24 V)

<i>Volts</i>	<i>Lumens</i>	<i>Light current</i> (mA)	<i>Dark current</i> ( $\mu\text{amp}$ )	<i>Sensitivity</i> (amp/lumen)‡	<i>Maximum dissipation</i> (mW)
24	$10^{-6}$	0.25	1	2.5	10
16	$10^{-5}$	0.55	0.6	0.6	12

‡ For the units of illumination intensity, see p. 176.

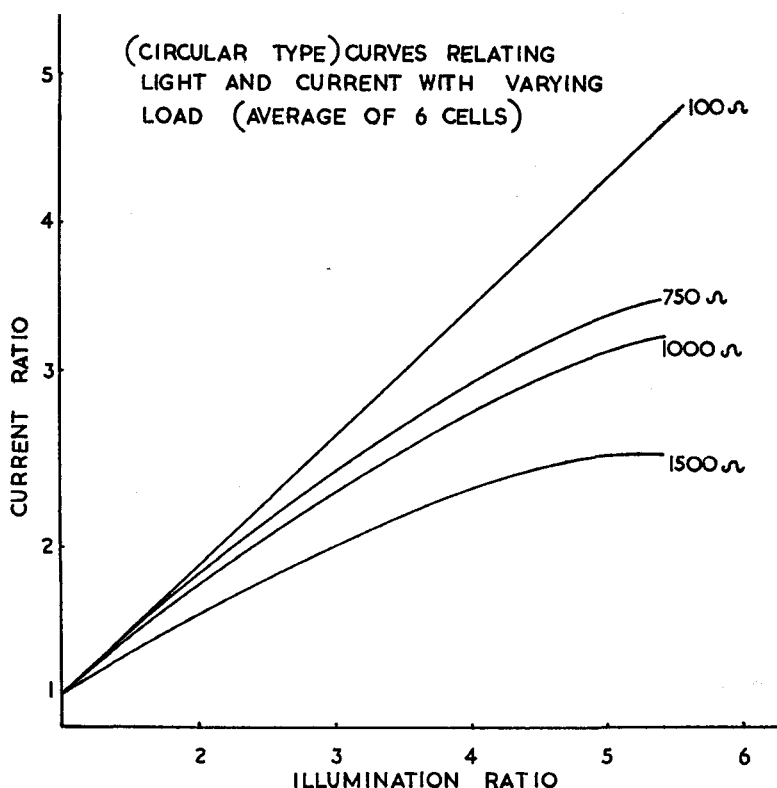


Fig. 8.1. (b) Response curves for a circular-type cell

† From a range produced by Messrs. Hilger and Watts, London, N.W.1.



## MISCELLANEOUS ELECTRONIC TUBES

(ii) *Photovoltaic (emission-type) photo-cells.* These may be either evacuated or gas-filled. The vacuum cells are of most general application, though gas photo-cells are preferred where there are rapid fluctuations in light intensity, as in sound-film equipment.

The emission-type photo-cell is a cold cathode diode, electrons being liberated from the cathode surface when light falls upon it. If the anode voltage is high enough to draw these electrons away as they are emitted, the current is proportional to the light

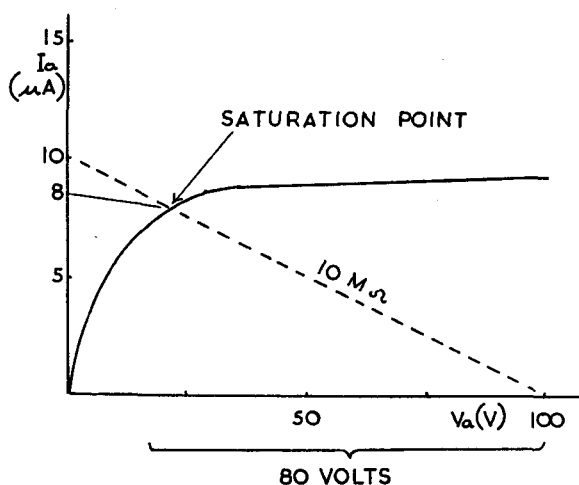


Fig. 8.2. Emission-type photo-cell. Response curve and load line

intensity. The current varies from 1–40  $\mu amp$ , depending upon the type of cell and the light intensity. The minimum anode voltage is about 20 V, derived from a battery of 100 V or so through a large resistor, so that a voltage swing of 80 V is possible; this is illustrated in Fig. 8.2 by the 10 M $\Omega$  load line (p. 125).

The spectral response of a cell depends mainly upon the photocathode material. A monatomic layer of caesium on silver oxide is sensitive to red and infra-red radiation; a layer of caesium on

# LABORATORY AND PROCESS INSTRUMENTS

antimony is sensitive to daylight and the blue end of the spectrum (Fig. 8.3).

For an electric bulb of efficiency  $\eta$  lumens per watt, the intensity at a distance  $d$  cm is given by  $I = \eta W / 4\pi d^2$ , where  $I$  is the intensity in lumens per sq. cm and  $W$  is the power of the bulb in

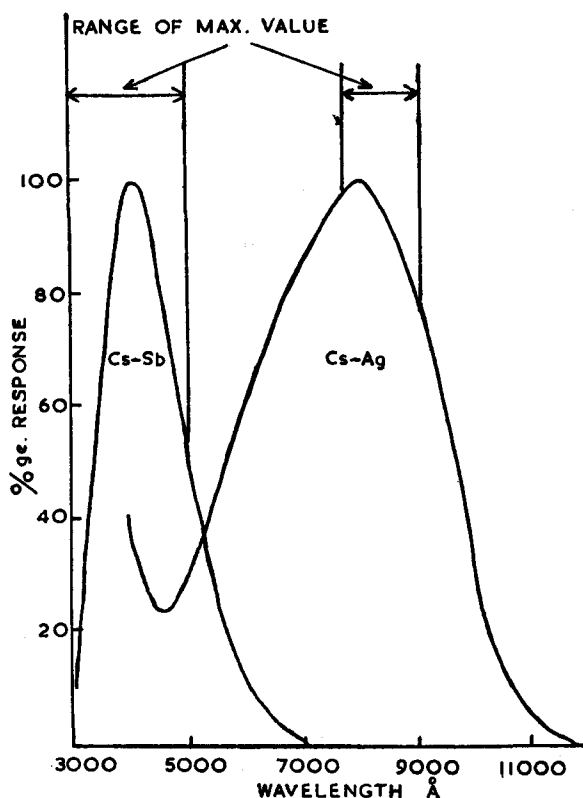


Fig. 8.3. Spectral response of photo-cathodes

watts. A 36 W tungsten filament headlamp bulb, for which  $\eta = 24$  lumens/W, produces the following intensities at various distances:

$d$ (cm)	15	30	100	200	300
$I$ (lumen/cm <sup>2</sup> )	0.305	0.076	0.0069	0.0017	0.00076

### MISCELLANEOUS ELECTRONIC TUBES

and these intensities may be considerably increased by a reflector. They refer to a 'colour-temperature' of  $2700^{\circ}\text{K}$ , and so are only approximate. The efficiency of vacuum photo-cells varies between about 20 and  $40\ \mu\text{amp/lumen}$ ; if the cell of Fig. 8.2 has a sensitivity of  $24\ \mu\text{amp/lumen}$ , the  $i_a$  maximum of  $8\ \mu\text{amp}$  is obtained from  $\frac{1}{3}$  lumen. For a cathode area of 6 sq. cm, this corresponds to  $0.06\ \text{lumen/cm}^2$ , obtainable from the above lamp at a distance of approximately 34 cm. Gas-filled tubes, in which a small degree of multiplication occurs (p. 94), are more sensitive—from 100 to  $150\ \mu\text{amp/lumen}$  is usual, and the above distance would be increased to about 83 cm. The dark current is small— $0.05$  to  $0.1\ \mu\text{amp}$ .

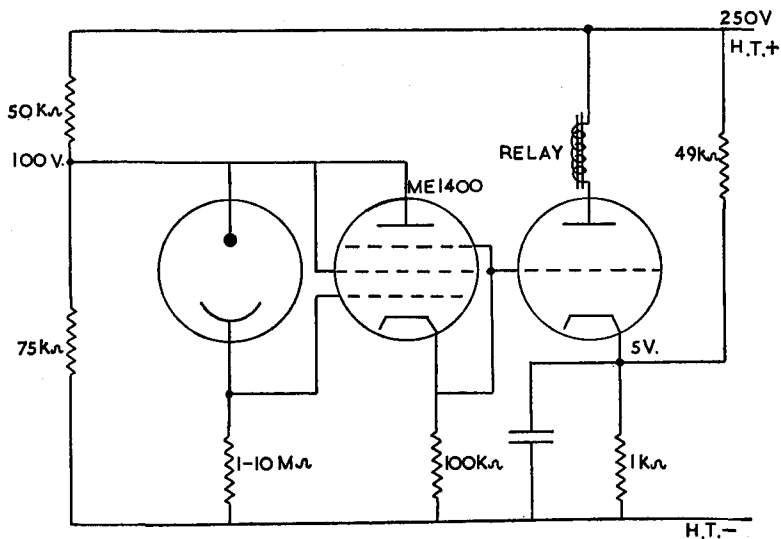


Fig. 8.4. Photo-cell amplifier, using electrometer valve

Although the anode voltage may be quite high, the power developed is negligible, so that an amplifier is needed to increase the cell output; the large grid resistor requires an electrometer valve, having an extremely low grid current. These valves are specially designed for the measurement of very small currents at very high resistance; if the output impedance of the source is about  $10^{12}\ \Omega$ , it is evident that even  $1\ \mu\text{amp}$  of grid current can seriously effect the e.m.f. Electrometer valves have low gain,

and are operated at low anode and screen voltages. Typical characteristics of this class of valve are the following:

**MULLARD ME1403: SUBMINIATURE ELECTROMETER  
PENTODE**

1.25 V heater:  $V_a = 10$  V,  $V_{g_2}$  (average) = 6.5 V

$i_a = 5$   $\mu$ A,  $V_{g_1} = -2.5$  V

$g_m = 10.5$   $\mu$ A/V

$r_a = 10.5$  M $\Omega$

$i_{g_1} = 3 \times 10^{-15}$  A (average)

$i_{g_2} = 2.2$   $\mu$ A

In the circuit of Fig. 8.4, the electrometer valve ME1400 is coupled to a triode, and a relay or other control device is operated by the triode anode current.

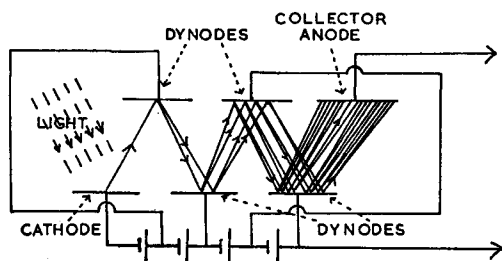
**Photomultiplier Tubes**

The photomultiplier has an emissive photo-sensitive cathode, and produces electrons as a result of illumination, as does the photo-cell; these 'primary' electrons are then accelerated through a system of anodes (the 'dynodes') of progressively increasing positive voltage. The primary electrons cause secondary emission at the first anode, and the process is continued at each successive stage; on average, about 2.5–3 electrons are produced for every one reaching the anode. There are generally either 11 or 13 stages of acceleration and amplification, so that the overall sensitivity of the tube, having a cathode sensitivity of 50  $\mu$ A/lumen, may be from 200–2000 amps/lumen. It is usual to operate with about 90–100 V per stage, so that the overall H.T. voltage is 1000–1200 V; the sensitivity is rather dependent upon the supply voltage (Fig. 8.5(b)). The dark current is about 0.05  $\mu$ A, and the maximum continuous current about 1 mA.

Photomultipliers are used to measure extremely weak light intensities. In the method of scintillation counting (p. 317), radiation falling on a suitable phosphor produces very weak flashes of light which are amplified by a photomultiplier, and the output current converted into pulses to operate a scaler unit. Again, the molecular weight of a polymer may be determined by

## MISCELLANEOUS ELECTRONIC TUBES

measuring the intensity of the light scattered from its solution in a suitable solvent. This scattered intensity is very low; in the P.C.L. Peaker Light-scattering Apparatus,† two photomultipliers are used, one monitoring continuously the main beam (via suitable neutral-density filters) and the other measuring the intensity of the light scattered through a known angle.



PRINCIPLE OF SECONDARY EMISSION PHOTOMULTIPLIER

### SEMI-TRANSPARENT CATHODE

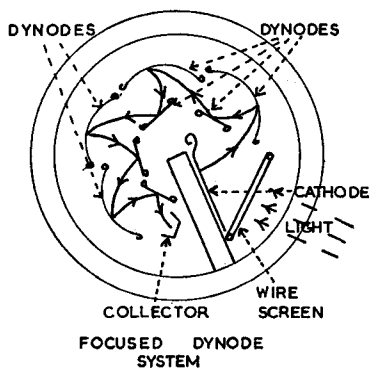
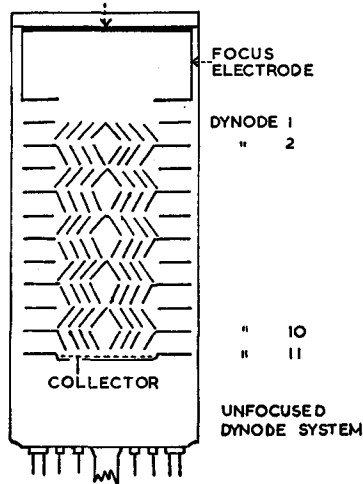


Fig. 8.5. (a) Photomultiplier

† Manufactured by Polymer Consultants Ltd., Britannia Works, Colchester.

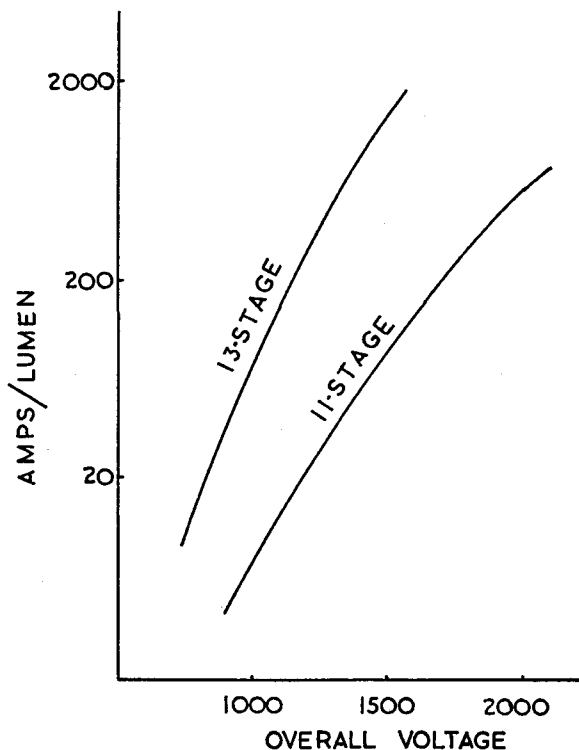


Fig. 8.5. (b) Overall sensitivity curve as a function of applied voltage

### The Dekatron Tube

The dekatron is a gas-filled tube, giving a visual indication of the number of pulses received by the cathode; it is often used in 'counter' circuits for the measurement of radioactivity (p. 334). The dekatron *counter* transfers the tenth pulse received to a second tube, or to a mechanical register; the dekatron *selector* enables an output pulse to be obtained after a given number of input pulses.

The dekatron is filled with a neon-argon mixture containing hydrogen as a quenching agent. The anode is a central disc, and the other electrodes, in the form of thin vertical wires, are arranged round it in a ring; there are thirty such electrodes in the normal dekatron, forming ten groups of three: cathode, first

## MISCELLANEOUS ELECTRONIC TUBES

guide, and second guide, in clockwise order. The first guides are connected together, and share a common pin, as do the second guides; in *counter* tubes nine of the cathodes are connected together, the tenth having a separate pin (Fig. 8.6); all the cathodes are separate in the *selector* tube. In this diagram,  $g_1g'_1 \dots$  indicate the first guides,  $g_2g'_2 \dots$  the second guides.

Suppose a glow-discharge to be established between anode  $A$  and cathode  $c_2$ , and that all the guides are at a positive potential with respect to the cathodes. Then the discharge remains at  $c_2$ , because the maximum voltage drop is across the  $A$ - $c_2$  gap; however, it has the effect of 'priming' the gaps  $A$ - $g'_1$  and  $A$ - $g_2$ ,

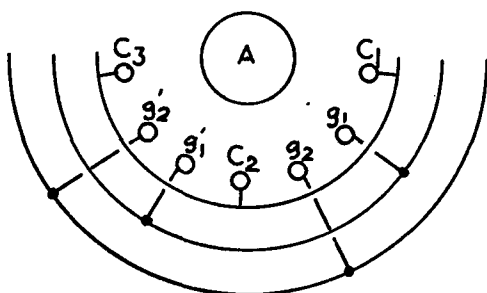


Fig. 8.6. Electron arrangement of dekatron tube

reducing their striking voltages. If the potential of the first guides  $g_1g'_1 \dots$  is now lowered, keeping that of the second guides fixed, the discharge will transfer to the  $A$ - $g'_1$  gap if this acquires a greater p.d. than  $A$ - $c_2$ ; the discharge thus moves clockwise towards the greatest potential gradient. It cannot move to  $g_2$ , since this is still at a positive potential. If now the second guides become negative, the first guides reverting to their positive potential, the discharge moves to  $A$ - $g'_2$ ; finally, restoring the positive potential to the second guides causes the discharge to move to  $A$ - $c_3$ . This cycle of operations is repeated for each pulse received, and the glow rotates clockwise round the tube. In counter tubes, the nine commoned cathodes are connected to earth; a voltage of 20–30 V is developed across a suitable load in the circuit of the tenth cathode, and is fed to the next tube whilst the discharge moves from  $c_{10}$  to  $c_1$ .

## LABORATORY AND PROCESS INSTRUMENTS

A suitable circuit for operating the dekatron from a sinusoidal input is shown in Fig. 8.7, using the 20th Century† GC10B tube. The guides are normally biased in parallel to about +9 V, and the input is fed via  $C_1$ . The value of  $C_2$  depends upon the input frequency, being so chosen that the voltage on the first guides leads that on the second guides by  $\pi/4$  ( $45^\circ$ ), as the vector diagram of Fig. 8.8 shows. The voltage drop at point  $B$  precedes that at point  $A$ . The output at the tenth cathode, load resistor  $R_c$ , is a rectangular pulse of about 20 V amplitude. Since a *negative* pulse

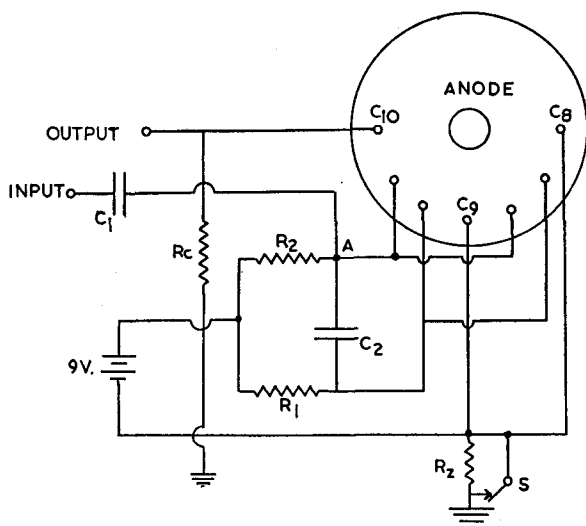


Fig. 8.7. Sinusoidal-input drive circuit for the dekatron

is required to move the discharge forwards, the output is fed to a phase-inverter (triode  $V_1$  of Fig. 8.9) via capacitor  $C_3$ ;  $V_1$  is normally biased to cut-off by  $E_g$ , so that its anode voltage is practically 300 V. The valve conducts when a positive pulse arrives on the grid, and its anode voltage falls; a negative pulse is thus transferred to the first guides via  $C_4$ . The normal positive bias on the guides is derived from the resistance chain  $R_3 R_4$ , and a similar phasing circuit to that already described provides a delayed pulse for the second guides.

† Produced by 20th Century Electronics Ltd., New Addington, Surrey.



## MISCELLANEOUS ELECTRONIC TUBES

A cold-cathode trigger tube may also be used to supply the dekatron pulses. In Fig. 8.10, a positive pulse at the priming electrode fires the trigger tube, and its anode potential falls. The

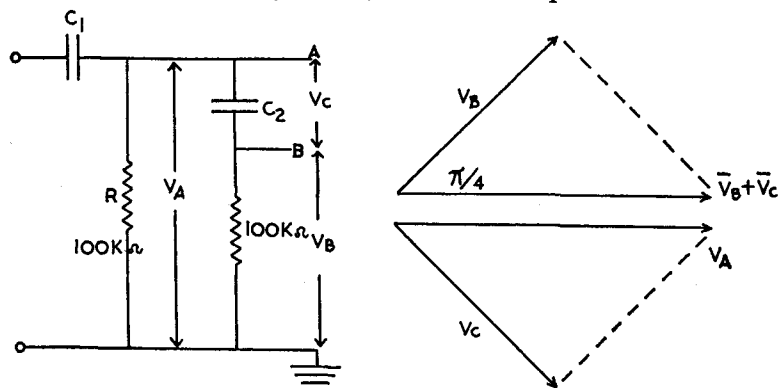
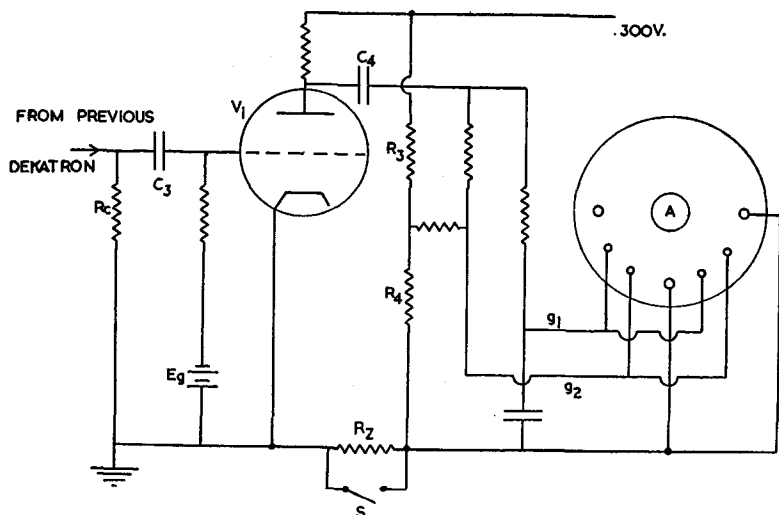


Fig. 8.8. Phasing of voltages to the dekatron guides: (a) development of voltages; (b) vector diagram



**Fig. 8.9. Interstage coupling of dekatrons**

potentials of points *A* and *B* decrease, and negative pulses are transmitted via *C*<sub>1</sub> and *C*<sub>2</sub> to the dekatron guides. This circuit may be operated from the random pulses of a Geiger-Müller tube (p. 186).

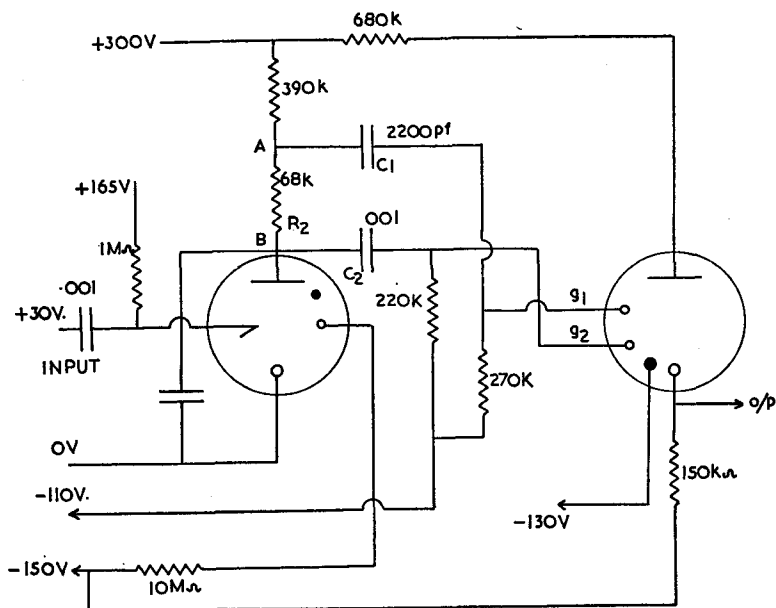


Fig. 8.10. Cold-cathode trigger tube input circuit for the dekatron

**Resetting.** It is necessary to reset the dekatrons to zero before beginning a fresh count, and this is the function of the switch *S* in Fig. 8.7.

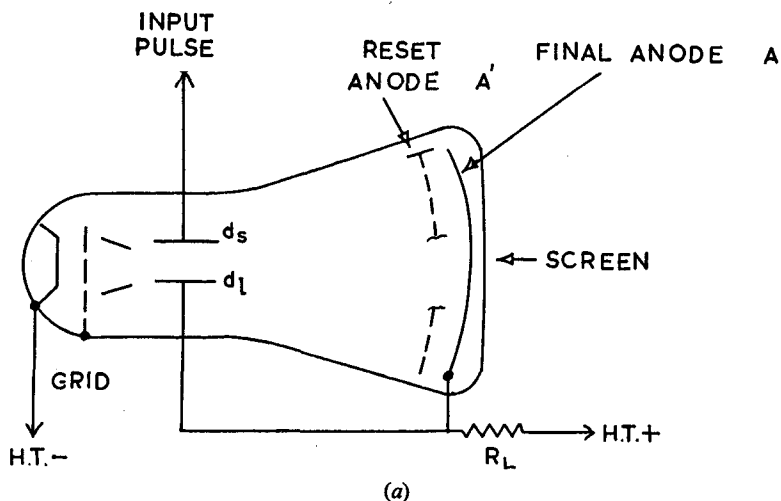
The H.T. -ve of the output cathodes and of any thermionic coupling-circuit valves is at earth potential, but the other cathodes are returned to a separate line; this is often referred to as the *zero line*. Normally, a shorting switch *S* connects the zero line directly to earth; on 'reset', however, *S* is opened, and the zero line returns to earth via a resistor *R<sub>z</sub>*, raising the potential of all the cathodes except the output cathode to about 100 V. The discharge therefore jumps to *c<sub>10</sub>*, and the next input pulse moves it to *c<sub>1</sub>*, as required.

### Ribbon Beam Tube

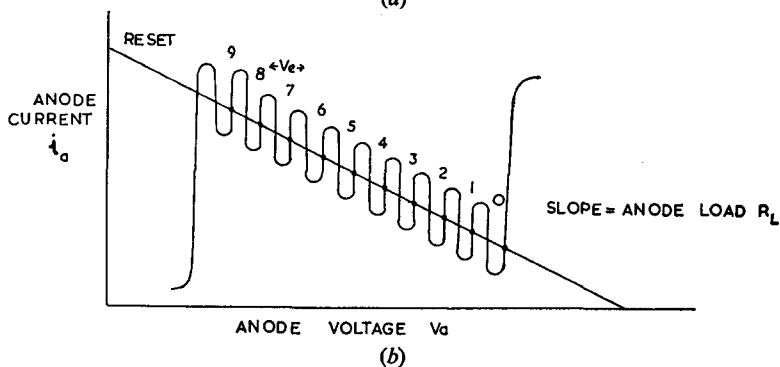
This is a more recent type of scaler tube than the dekatron. It is essentially a high-vacuum cathode ray tube, with the conventional 'gun' assembly (p. 192); a ribbon-shaped beam is produced, which passes between the deflector plates *d<sub>1</sub>d<sub>2</sub>*, through an

# MISCELLANEOUS ELECTRONIC TUBES

electrode with ten parallel slots, on to the final anode  $A$ . In order to obtain a visual indication of the position of the beam, the anode is also pierced, and part of the beam falls upon a fluorescent screen on the end of the tube (Fig. 8.11(a)).



(a)



(b)

Fig. 8.11. The ribbon beam tube: (a) electrode arrangement; (b) characteristic curve and load line

The anode current varies as the potential difference between the deflector plates is changed, being large if the beam passes through a slot, and small if it strikes the electrode between slots. The response curve is shown in Fig. 8.11(b), where the load line is drawn for a resistor  $R_L$ , connecting the anode  $A$  and one plate

(the *locking* deflector,  $d_l$ ) to H.T. + ve. Changing the potential of the second plate (the *stepping* deflector,  $d_s$ ) causes the beam to 'step' progressively along the curve, coming to rest in the stable positions 1, 2, ... 9. The input pulse to  $d_s$  must be greater than the peak-to-peak separation of the response curve,  $V_e$ .

The next step after slot 9 brings the beam on to the separate anode  $A'$  (the *reset* anode), producing a negative pulse across the reset anode load resistor; this is applied to the grid of the tube, cutting off the beam, and allowing the final anode voltage to rise. On removing the grid bias, the beam enters the 'zero' slot, i.e. it is reset to zero. The reset-anode pulse also triggers a pulse generator supplying the next scale-of-ten tube, if there is one. The resetting of the beam fixes the resolving time at about 30  $\mu$  seconds, so that it is inherently faster than the gas-filled deka-tron.

### The Geiger-Müller Tube

This is the most commonly-used monitoring tube for the estimation of radioactivity; it is comparatively simple in operation, may be incorporated in portable apparatus, and is sensitive to  $\alpha$ -,  $\beta$ - and  $\gamma$ -radiation. The 'G-M' tube consists of a cylindrical metal or graphite cathode, with a thin-wire anode mounted concentrically inside (Fig. 8.12). The tube contains a mixture of gases, including quencher molecules (p. 189), at a pressure usually rather below 1 atmosphere.

The tube is provided with a thin 'window' at one end, or in liquid-counter tubes with a thin inner glass wall. Radiation is able to penetrate these boundaries, and causes ionisation of the gas; the primary electrons formed are accelerated towards the anode, and collide with gas molecules, giving rise to secondary electrons, so that 'gas multiplication' occurs. Alternatively, the radioactive material may be passed, as a gas (e.g.  $C^{13}$  is usually counted as  $C^{13}O_2$ ) through the tube, avoiding absorption by the window or the walls.

The voltage applied across the tube varies from about 370–1500 V, depending upon its type. The potential gradient is not constant, because of the great difference in radius of the electrodes; if  $E$  is the potential gradient and  $r$  the radius,

$$E = dV/dr = k/r$$

## MISCELLANEOUS ELECTRONIC TUBES

where  $k$  is a constant of the tube. Hence, if  $r_a$  and  $r_c$  represent the radii of anode and cathode respectively,  $V = k \ln r_c/r_a$  (Fig. 8.13(a)). For example, if  $V = 10^3$  V,  $r_a = 10^{-2}$  cm,  $r_c = 1$  cm,  $k = 1000/(2.303 \times 3) = 145$ ; the potential gradient at the cathode wall  $E_c$  is therefore 145 V/cm, and that at the anode wall  $E_a$  is  $k/10^{-2} = 14.5$  kV/cm. The primary electrons are accelerated

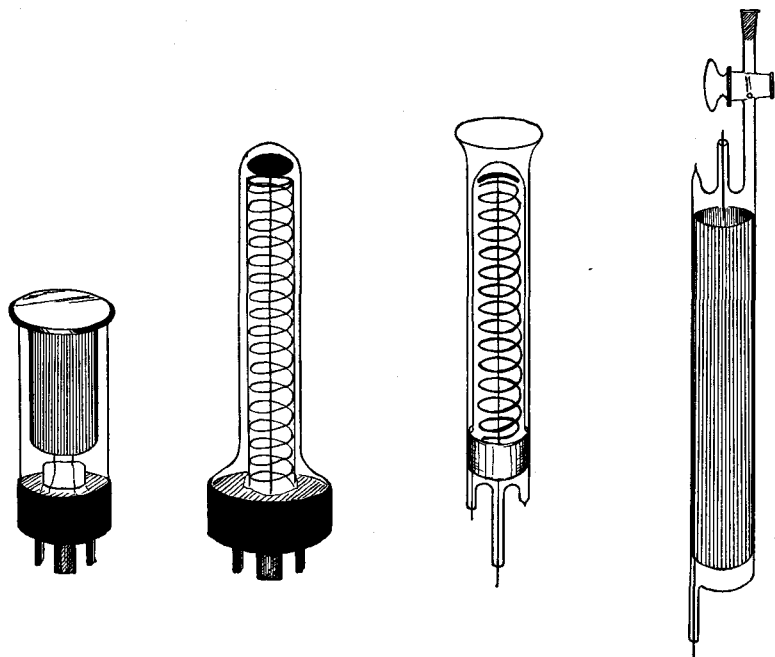


Fig. 8.12. Some Geiger-Müller tubes. Left to right: 20th Century types EW3H (end-window), B6H (probe), M6H (liquid counter), GA26 (gas counter)

towards the anode, and acquire sufficient energy to liberate secondary electrons by collision with gas molecules; if this energy is gained at distance  $d$  from the anode, and the mean free path in the gas is  $l$ , the number of such ionisations is  $d/l$ , and the gas multiplication is  $2^{d/l}$ . If  $d/l$  is 15, multiplication =  $2^{15}$ , or approximately  $3 \times 10^4$ , and is independent of the path through the tube, since  $d$  is generally less than 1 mm.

The Geiger-Müller tube is *polarised*; if the central wire is made the cathode, positive ions are insufficiently accelerated to

# LABORATORY AND PROCESS INSTRUMENTS

cause secondary emission. However, heavy-ion bombardment may *permanently damage* the tube, so that the polarity should never be reversed.

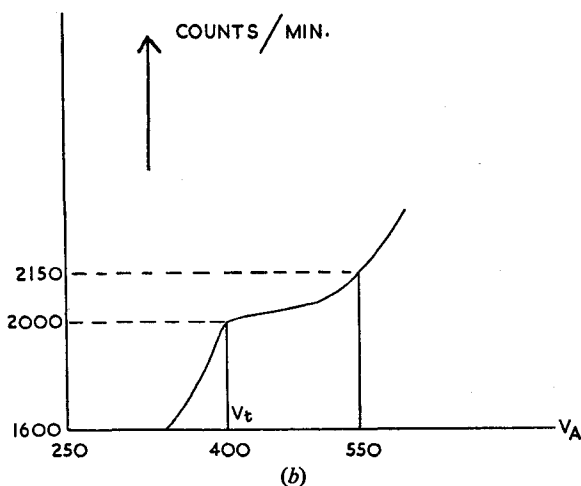
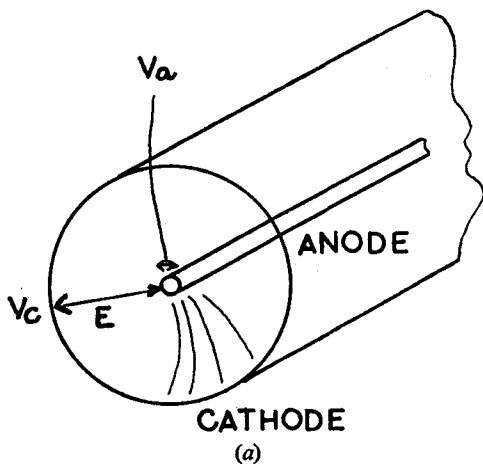


Fig. 8.13. Internal construction of Geiger-Müller tube and plateau.  
 $V_t$ : threshold voltage

The graph of count rate (counts per unit time) against anode voltage shows a characteristic 'plateau', of about 100–200 V in length (depending on the operating voltage of the tube), and

## MISCELLANEOUS ELECTRONIC TUBES

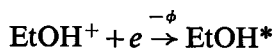
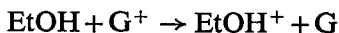
of slope less than 5% per 100 V. Typical operating voltages are  $(V_i + 100)$  V, for an organic-molecule quenched tube, and  $(V_i + 60)$  V for a halogen quenched tube (Fig. 8.13(b)).

The initial ionisation is amplified by gas multiplication, after which the discharge must be rapidly quenched, if further counts are not to be missed. The gas is itself partially self-quenching, since the sheath of positive ions between the anode and cathode lowers the potential gradient across the tube; however, this effect is not relied upon to quench the tube, and a small amount of an organic compound, such as ethyl alcohol, or of a halogen such as bromine, is added. The purpose of the quenching agent is to prevent collisions between the positive gas ions and the cathode, which would liberate electrons and maintain the discharge. The quenching agents have low ionisation potentials, so that the process:  $G^+ + Q = G + Q^+$ , where G is the gas molecule and Q the quenching molecule, occurs readily. If now the quenching ion approaches the cathode surface, it gains an electron, losing energy equal to the work function of the surface,  $\phi$ ; e.g.  $Br_2^+ + e \rightarrow Br_2^{*\phi}$ , i.e. an activated bromine molecule is formed, which dissociates:



[1 eV (one electron volt) per atom is equivalent to 23 kcal/mole]. The bromine atoms thus have insufficient energy to liberate further electrons from the surface; instead, a recombination occurs at the walls:  $Br + Br \rightarrow Br_2$ , and the quenching molecules are reformed.

With alcohol as quenching agent, the reactions are, for example,



and the quenching agent is decomposed. For this reason, organic-molecule quenched tubes have a definite life of about  $10^9$  counts.

The quench time of such tubes is about 300  $\mu$ seconds, but is not quite constant; the quiescent period is made more definite by a quenching unit, operating electronically in the tube circuit.

## LABORATORY AND PROCESS INSTRUMENTS

Most quench units have a quench time of  $400\ \mu\text{seconds}$ , called the *paralysis time*; correction should be made for this in assessing a count rate (p. 316).

Geiger-Müller tubes must operate into a high-impedance input circuit, such as a cathode follower; a suitable input circuit for a halogen quenched tube is shown in Fig. 8.14.

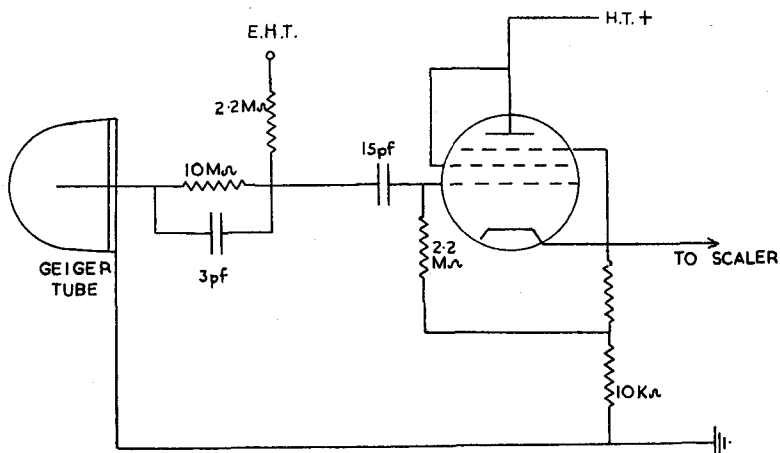


Fig. 8.14. Cathode follower circuit for G-M tubes

### The Proportional Counter Tube

The proportional counter tube is similar in construction to the Geiger-Müller tube; it is designed, however, so that the gas amplification is restricted to a small region of the anode wire, instead of spreading along its length. In Fig. 8.15 the region *B* is the operating region for proportional counting; region *A* is the ionisation chamber region and *C* the Geiger-Müller region. The proportional counter is therefore intermediate between the ionisation chamber, in which no gas amplification occurs (so that only the incident particles are registered), and the Geiger-Müller tube, in which an 'avalanche' of secondary electrons renders the output pulse independent of the incident energy.

The amplitude of the output pulse from a proportional counter is dependent upon the number and energy of the incident particles. In a normal tube, filled with methane at a pressure of



## MISCELLANEOUS ELECTRONIC TUBES

10 cm Hg, a single ion-pair may give a measurable output if the gas amplification is about  $10^3$ ; the tube feeds directly into a high-gain amplifier—the *head amplifier*.

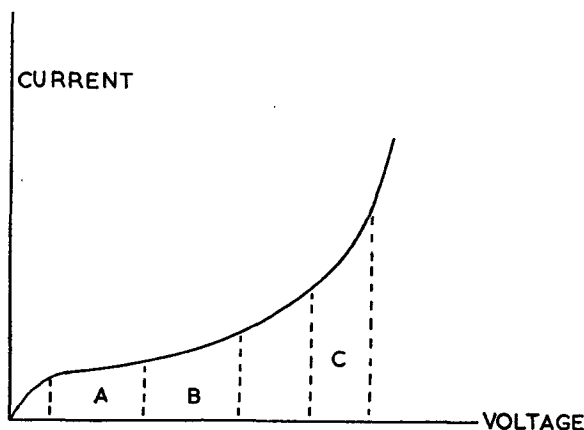


Fig. 8.15. The proportional-counter and Geiger-Müller regions

### The Cathode Ray Oscilloscope

The 'C.R.O.' is a very useful instrument for obtaining a visual indication of circuit performance; the electron beam can follow changes which are much too rapid for any mechanical system. Since the trace may be photographed to give a permanent record, transient phenomena can be studied, such as the rapid changes in concentration of free-radical intermediates of photochemical reactions.

The oscilloscope has three main components: the cathode ray tube, the power unit which supplies it, and the time-base generator. These components will be considered in turn.

(i) *The cathode ray tube.* This is usually of the high-vacuum, heated cathode type. Electrons from the cathode *C* (Fig. 8.16(a)) pass through a grid *g*, and then through an electrostatic lens system of a number of concentric anodes,  $A_1 A_2 A_3$ , at varying positive potentials. The grid is at a negative potential which may be varied (with respect to the cathode) to control the *brightness* of the trace; the grid also assists in focusing the beam on to the screen. The anode system continues this process, and the voltage

## LABORATORY AND PROCESS INSTRUMENTS

on the final anode is also made variable within limits, constituting the *focus* control. The system of cathode, grid and anodes is often called the *gun*.

The focused beam now enters the deflecting system, which is usually in the form of two pairs of plates, mutually at right angles. The incoming signal is applied to give vertical deflection of the beam, via the *Y-plates*, and a time-dependent voltage, the *time base*, is applied to the X plates to produce horizontal deflection.

The higher the voltage of the final anode, the more rapidly the electrons move, and the brighter is the trace; however, the

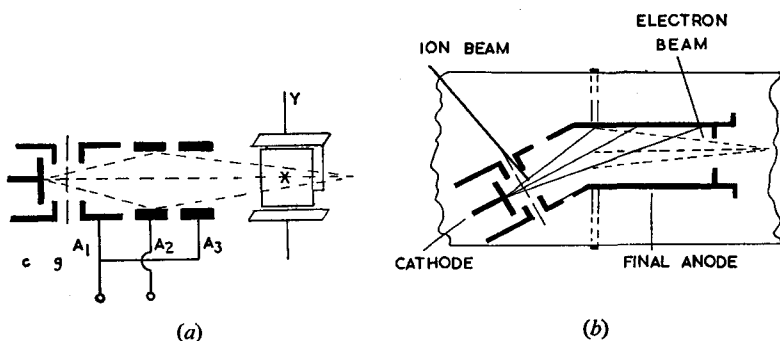


Fig. 8.16. (a) The cathode ray tube 'gun': c, cathode; g, grid; A<sub>1</sub>, first anode; A<sub>2</sub>, second anode; XY, deflector plates. (b) Ion trap

voltage required to deflect the beam also increases with the electron velocity, so that the oscilloscope is relatively less sensitive. In practice, the input signal is generally fed into a variable-gain amplifier before it is applied to the Y-plates; a compromise is still necessary, however, between brightness and sensitivity. In some modern tubes, most of the acceleration of the electrons takes place after they have been deflected by the X- and Y-plates—a process known as *post-deflection acceleration*. A graphite spiral around the inside of the tube, extending from anode to screen, is connected across a high-potential supply, so that the electrons are progressively accelerated.

The beam may also be deflected magnetically, by coils mounted outside the tube, perpendicular to the beam, and to the Y-axis; magnetic deflection is used extensively in television picture tubes.

## MISCELLANEOUS ELECTRONIC TUBES

In some double-beam tubes, such as the Cossor 89,† an earthed splitter plate divides the electron stream into equal parts; each beam responds to its own Y-plate, via separate amplifiers, but the beams share a common time base.

The screen of the tube is coated with a *phosphor*, which emits light in the visible region of the spectrum when electrons fall upon it. Secondary emission from the surface prevents the screen from becoming increasingly negatively charged, and thus repelling further electrons. The spectral peak, and the persistence of the emission (the 'afterglow') are important properties of the phosphor; some typical characteristics are:

<i>Phosphor</i>	<i>Spectral peak</i> (Å)	<i>Colour</i>	<i>Persistence</i>
ZnS+0.01 % Ag	4575	Blue	Medium
ZnS+0.01 % Cu	5280	Green	Medium
ZnSiO <sub>3</sub> +0.1 % Mn	5230	Blue-green	Long
ZnS-CdS+0.01 % Ag	5690	Yellow-green	Very short
CdSiO <sub>3</sub> +1 % Mn	6050	Orange	Long

Double-layer screens are sometimes used for greater persistence.

The X- and Y-plate deflection hardly affects the heavy negative ion beam, which may produce a 'worn' spot at the centre of the screen ('ion-burn'); this may be prevented by a magnetic ion-trap. In Fig. 8.16(b) the gun is bent, and the electron beam is magnetically deflected through the anode orifice; the heavy negative ions are not deflected, however, and collide with the anode, so that they do not reach the screen.

(ii) *The power unit.* The current required by the tube is small, but high voltages are usually required on the anodes; e.g. the DG7-36 requires 1 kV on  $A_2$  and 2.5 kV on  $A_1$  and  $A_3$ . In order for the deflector plates to be at, or near, earth potential, it is usual to connect the cathode to a high *negative* potential, when the final anode may also be near earth potential. This negative voltage may be obtained from a conventional valve rectifier circuit, but it is becoming usual to develop it from a high-frequency oscillator; smoothing chokes and capacitors are much smaller, and the use of open core step-up transformers reduces

† A. C. Cossor Ltd., Highbury, London.

insulation problems. A half-wave diode rectifies the oscillatory output.

In Fig. 8.17, valve  $V_1$  produces an oscillatory voltage of frequency 20–50 kc/s, and the step-up transformer  $T$  may develop

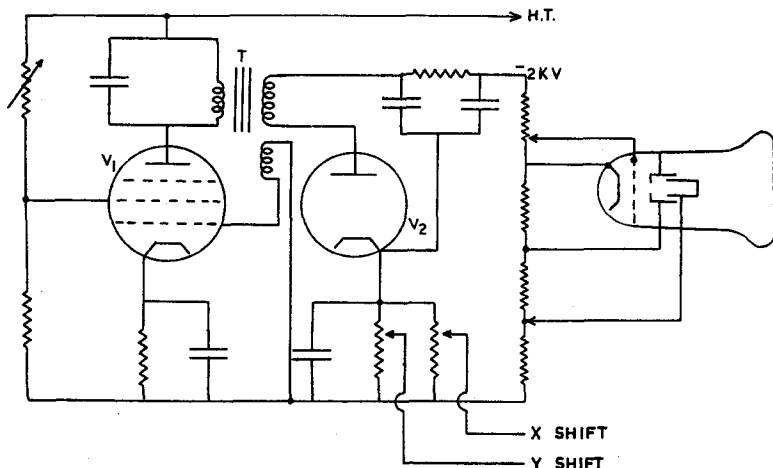


Fig. 8.17. Extra high-tension (E.H.T.) supply unit for cathode ray tube

about 3 kV across the secondary winding; rather high power is required, so that typical operating conditions would be:

$V_1$ , Mullard EL37 power pentode:  $V_a = 550$  V  
 $i_a = 50$  mA  
 Anode dissipation = 16.5 W

$V_2$ , Mullard EY51

Oscillatory voltage at primary of transformer  $T$ , 150 V

Oscillatory voltage at secondary of transformer, 3 kV at 1 mA

The 550 V H.T. supplies also the time-base and amplifier circuits, and is derived from a conventional full-wave rectifier (p. 104).

The power supply unit could be stabilised, as shown in Fig. 8.18;  $V_2$  is the E.H.T. rectifier of the previous figure. If its output voltage tends to rise, the potential of point  $A$  becomes more negative, and the grid voltage of  $V_3$  falls. Hence the anode voltage of  $V_3$ , and the grid voltage of  $V_4$ , rise, and the anode

## MISCELLANEOUS ELECTRONIC TUBES

voltage of  $V_4$  falls; this in turn reduces the screen voltage of  $V_1$ , the E.H.T. oscillator, and the rectifier output is reduced.

(iii) *Time bases.* The signal voltage is applied to the Y-plates, and causes a vertical deflection of the spot. If a voltage varying linearly with time is applied to the X-plates, the spot will trace out variations of the signal with respect to time. Usually these variations are too rapid to follow directly, so that we arrange for the spot to return very rapidly from its extreme X-deflection, and repeat the process; the complete trace then becomes visible, due to persistence of vision. The cathode ray tube is not very sensitive,

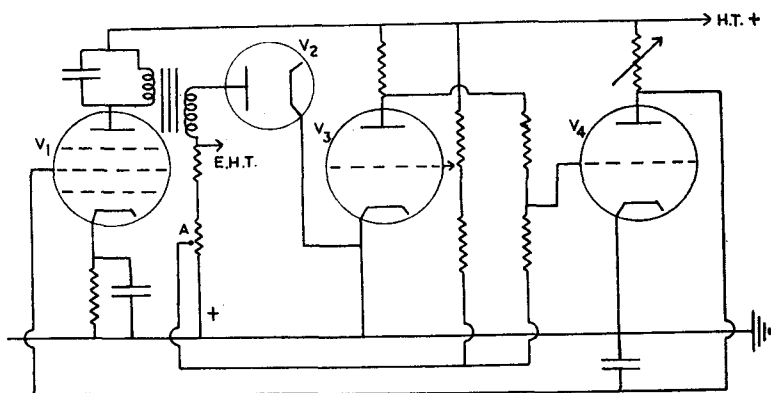


Fig. 8.18. Stabilised E.H.T. supply for cathode ray tube

and a fairly considerable voltage is required to sweep the spot horizontally.

Most time bases make use of the charge and discharge of a capacitor to provide deflection voltage and return ('fly-back'). A simple and reliable time base, illustrated in Fig. 8.19, discharges the capacitor through a thyatron. The negative grid bias voltage from  $E_g$  prevents the thyatron from conducting until  $C$  is partially charged via  $R_1$  and  $R_2$ . The voltage across  $C$  is given by (p. 14)  $V_C = E(1 - e^{-t/CR})$ , where  $R = R_1 + R_2$ . Eventually the thyatron strikes, and  $C$  is rapidly discharged via  $R_4$ , until the cut-off of the tube ( $V_{c.o.}$ ) is reached; this is about 10 V for an average tube. The rapid discharge represents the 'fly-back', after which the charge-discharge cycle is repeated.

## LABORATORY AND PROCESS INSTRUMENTS

The equation shows that the deflection is not strictly linear; the slope  $dV_C/dt = E/CR \cdot e^{-t/CR} = (E - V_C)/CR$ . If the working voltage range across  $C$  is from  $V_{c.o.}$  to  $\alpha E$ , where  $\alpha$  is some frac-

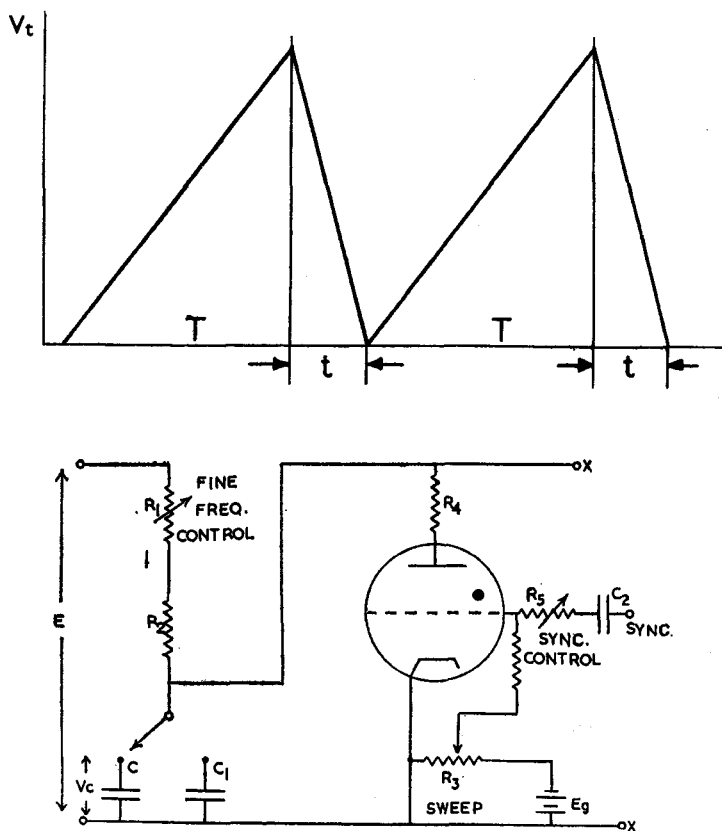


Fig. 8.19. Thyatron time-base circuit

tion of the supply voltage, the slope varies from  $S_0 (= E - V_{c.o.}/CR)$  to  $S = E(1 - \alpha)/CR$ , which decreases as  $\alpha$  increases:

$$\begin{array}{cccc} \alpha = & 0.1 & 0.2 & 0.3 & 0.5 \\ S/S_0 = & 0.9 & 0.8 & 0.7 & 0.5 \end{array}$$

For maximum variation in  $S$  of 20%,  $V_c$  must not exceed  $0.2E$ .

## MISCELLANEOUS ELECTRONIC TUBES

The sweep time  $T$  is the time required for  $V_C$  to increase from  $V_{c.o.}$  to  $\alpha E$ : by expressing  $V_C$  logarithmically:

$$\ln\left(\frac{V_C}{E} - 1\right) = t/CR$$

we obtain:

$$T = CR \ln(E - V_{c.o.})/(E - \alpha E) \approx CR \ln 1/(1 - \alpha)$$

if  $V_{c.o.}$  is small compared with  $\alpha E$ . Ignoring the fly-back time, the time-base frequency is  $1/T$ , which may be controlled by variation of  $C$  or  $R$ ; in practice, various capacitors  $C, C_1, \dots$ , are introduced by switching for coarse control, and  $R_1$  is varied (limited by the value of  $R_2$ ) as the fine control. In this way the time-base frequency may be varied without altering the sweep voltage; this last parameter may be controlled by  $R_3$ , which alters the thyatron bias, and so the period of conduction of the tube.  $R_4$  limits the current passed by the thyatron to a safe value, and should not be too large, or increase of the fly-back time will result.

A portion of the signal voltage is fed via  $C_2$  to the thyatron grid, and determines the exact point of initiation of the fly-back, thus 'locking' the time base to the signal. This is referred to as *synchronisation*;  $R_5$  is adjusted so that the synchronising voltage is just sufficient to lock the trace.

The thyatron-controlled time base is satisfactory for operation at frequencies up to  $10^4$  c/s, but above this the discharge time is a limiting factor; in practice, a fly-back ratio  $T/t$  of 1000 is the maximum obtainable.

An alternative expression for the voltage across  $C$  is

$$dV/dt = 1/C \cdot dQ/dt = 1/C \cdot I_c$$

which is linear if the charging current  $I_c$  is constant; this is approximately true if  $I_c$  is made the anode current of a pentode valve, operated beyond the 'knee' of the  $i_a/V_a$  characteristic (p. 89). The anode current of a pentode charges the capacitor in Fig. 8.20.

Various hard-valve time bases have been designed to work at higher frequencies; a very successful circuit due to O. S. Puckle will be described in outline. In Fig. 8.20,  $C$  is charged by the anode current of pentode  $V_1$ ; the grid of  $V_2$  is negative with respect to its cathode due to the voltage drop across  $R_2$ , when  $C$

# LABORATORY AND PROCESS INSTRUMENTS

is uncharged and  $V_2$  is cut off. As  $C$  charges, the cathode potential of  $V_2$  falls progressively, and eventually  $V_2$  conducts. Its anode voltage falls, and a negative pulse is delivered to the suppressor grid of  $V_3$ ; the anode current of  $V_3$  therefore falls, its anode voltage rises, and this in turn conveyed to the grid of  $V_2$ , increasing still further its anode current. There is very rapid discharge of  $C$  through  $V_2$ , after which this valve cuts off, and the cycle is repeated.

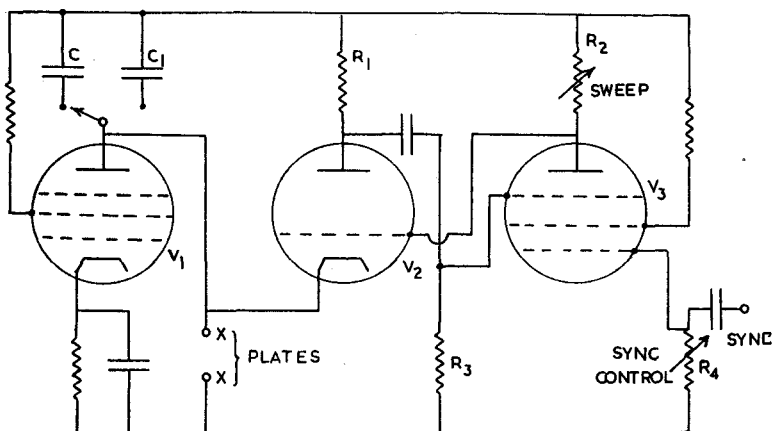


Fig. 8.20. Hard-valve time-base circuit (O. S. Puckle)

$R_2$  determines the point at which  $V_2$  conducts, discharging  $C$ , and so decides the sweep amplitude. The synchronising voltage is fed to the grid of  $V_3$ , and an amplified and phase-inverted version is fed to  $V_2$  grid, controlling the point of conduction.

In the circuit of Fig. 8.21, a constant current (e.g. from a pentode valve) is fed to the  $CR$  series circuit, so that  $V_C = 1/\omega C$ ,  $V_R = IR$ ; these voltages are in phase quadrature. If  $R = 1/\omega C$ , we can write:

$$V_C = V_m \cos \omega t, V_R = V_m \sin \omega t$$

hence  $V_C^2 + V_R^2 = V_m^2$ . This is the equation of a circle, of radius  $V_m$ , centred at the origin of co-ordinates. If the spot of light is controlled by both voltages, it will describe this circular path, with frequency  $\omega/2\pi$ . By connecting these voltages to the X- and



## MISCELLANEOUS ELECTRONIC TUBES

Y-plates of an oscilloscope, a circular time base is available, having the advantages of long length and absence of fly-back. The signal voltage is injected in series with the Y-plate voltage.

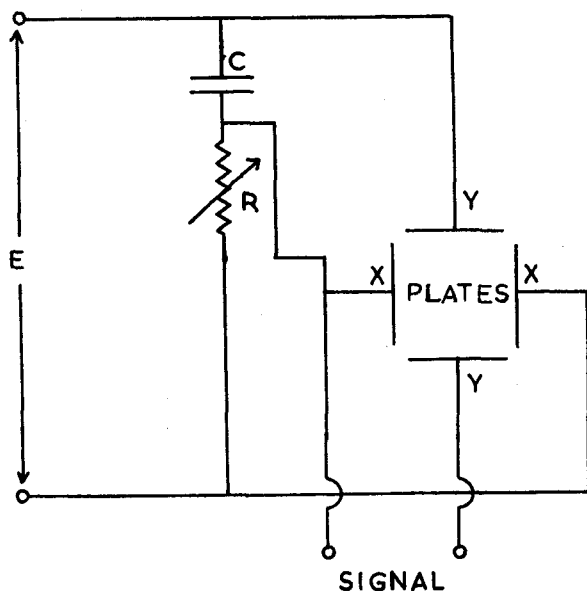


Fig. 8.21. Circular time-base circuit

### 'Tuning' Indicator ('Magic-eye' Tube)

This is a small hard-vacuum tube, having at the end a fluorescent screen like that of a cathode ray tube. The symbol is shown in Fig. 8.22(a). The grid  $g_2$  is maintained at a fixed potential with respect to the cathode, or may be joined to it. The relative currents through  $A_1$  and  $A_2$  then depend upon the voltage applied to the grid  $g_1$ ; the anode circuit of  $A_1$  contains a large load resistance (about  $1\text{ M}\Omega$ ), so that if the negative bias applied to  $g_1$  is small, the anode potential of  $A_1$  is very low. Under these conditions, a considerable current flows via  $A_2$ , and a broad patch of illumination appears on the screen, via a slotted disc limiting the sector of illumination.

The tuning of the circuit to an incoming signal applies a large -ve bias to the grid  $g_1$ . The anode potential of  $A_1$  rises, and

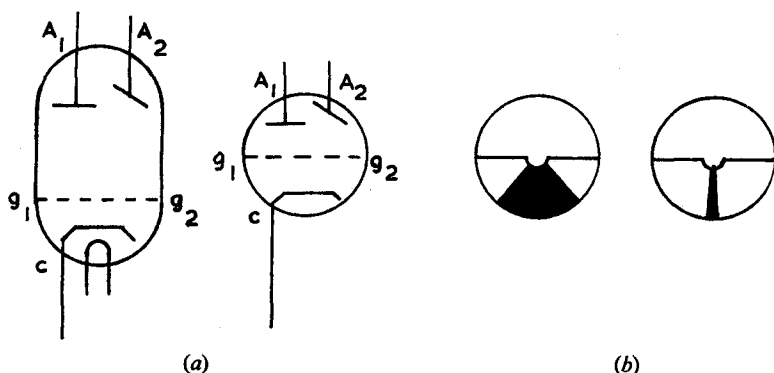


Fig. 8.22. (a) The 'magic-eye' tube. (b) Variations of the angle of illumination

a greater fraction of the (reduced) anode current flows via  $A_1$ ; the illuminated area decreases. The device thus gives a sharp indication of the correctness of tuning by a minimum angle of illumination, as in Fig. 8.22(b). The tube is shown connected as a bridge balance-detector in Fig. 8.23.

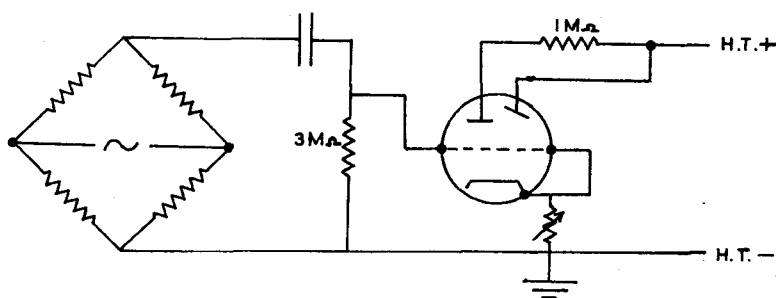


Fig. 8.23. The 'magic-eye' tube as bridge balance-indicator

### References

- Photocells*. Cinema-Television Ltd., technical publication (October 1957).
- Photocells for Industrial Applications*. Mullard technical publication MT8010 (1954).
- Photo-conductive Cells*. Hilger Division technical publication CH357/3.
- Photomultiplier Tubes*. 20th Century Electronics Ltd., technical publication (1958).

## MISCELLANEOUS ELECTRONIC TUBES

PUCKLE, O. S. (1951). *Time Bases*. Chapman and Hall.

RODDA, S. (1953). *Photoelectric Multipliers*. Macdonald.

SPREADBURY, F. G. (1956). *Electronic Measurements and Measuring Instruments*. Constable.

WALKER, R. C. (1948). *Photoelectric Cells in Industry*. Pitman.

### Problems

1. Compare the mode of operation of the barrier layer photo-cell with that of the high-vacuum photo-cell. Draw and explain one practical circuit for each type to illustrate its application (refer to Chapter XIV for their use in spectrophotometers).

2. It is required to count the number of articles passing along a conveyor belt, by recording on a series of dekatron tubes the number of interruptions of a light beam. Outline suitable circuits for the photo-cell and the dekatrons, including 're-set' facility.

3. Write an account of the cathode ray oscilloscope, under the headings: (a) Oscilloscope ('gun') Tube; (b) Power Supplies; (c) Time Bases.

4. Give an account of the operation of the Geiger-Müller tube, and explain the terms: 'threshold voltage', 'plateau length and slope', and 'paralysis time'.

## CHAPTER IX

# Semiconductors and Transistors

### Introduction

The introduction of the *transistor* has been the most important development in electronics of recent years. Although the investigation of their properties is still in a preliminary stage, it is already clear that transistors will perform many—though not all—of the functions of the thermionic valve, with advantages regarding power and stability. Further, as transistors are so much smaller than valves, and require lower supply voltages, it seems permissible to look forward to lighter, and less bulky, electronic test equipment.

The *point-contact* germanium or silicon diode has many of the properties of the crystal and 'cat's whisker' contact of early crystal radio receivers; contact between a thin metal wire and certain natural or artificial crystals produces unidirectional characteristics (p. 76), and such devices were used for the rectification of ultra-high ('radar') frequencies in World War II. Point contact transistors were described by Bardeen and Brattain, of the Bell Telephone Laboratories, in 1948; they, and to some extent the contact diodes, have been superseded by *junction* transistors and diodes, introduced in 1949. The basic materials of construction are the semiconductors germanium and silicon; the theory of conduction in these materials has been extensively investigated, notably by Shockley. They must be of far higher purity than an analytical standard or a nuclear-pile 'moderator'; special analytical techniques had to be developed for control purposes.

Germanium and silicon *diodes* have the typical applications of thermionic diodes, i.e. rectification and detection. *Junction* transistors have the applications of thermionic triodes and pentodes; amplifiers and oscillators may be constructed for

## SEMICONDUCTORS AND TRANSISTORS

a wide range of frequencies. The main advantages of transistors may be briefly listed as follows:

*efficiency*—the transistor consumes very little power, much less than a valve filament.

*small size*.

*low supply-voltage requirements*—the 'H.T.' voltage is usually 6–9 V.

*long life and reliability*—provided that the transistor is sealed from the atmosphere, its life should be infinite; having no delicate mechanical construction, it can withstand extreme shock and temperature change, such as are likely to be met with, for example, in an artificial 'satellite'.

*absence of a warming-up period*—the transistor operates immediately on switching on.

*operation at high ambient temperatures*—silicon transistors can be operated at an ambient temperature of 150°C; germanium transistors up to 75°C.

Disadvantages of transistors, which are probably only temporary, are:

*frequency limitation*—at present, transistors are not readily available for operation above 30 Mc/s.

*rather limited power*—'transmitter' transistors have yet to be developed.

Silicon diodes and transistors may be operated at higher ambient temperatures than germanium; they also have higher breakdown voltages and lower reverse currents. Germanium shows a higher efficiency in low-voltage power rectification, and has slightly better high-frequency characteristics. Further development may modify these comparisons, however.

### Symbols and Nomenclature

The three-element transistor may be roughly compared to a triode valve; the *emitter* is somewhat like the cathode, and the *base* and *collector* approximate to the grid and anode respectively. The usual symbol for the transistor is shown in Fig. 9.1. There are two types of three-element junction transistors, called PNP- and NPN-transistors; the meaning of the letters will become apparent

later. In PNP-type transistors, the (conventional) current flow is *from emitter to base*, and the arrow-head in the symbol indicates this; in NPN-type devices, *electrons* flow from emitter to base, so

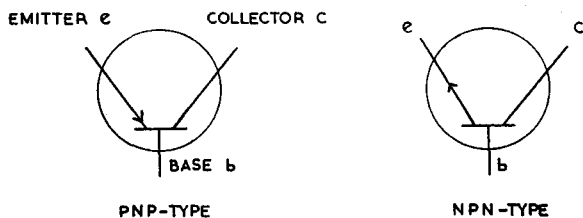


Fig. 9.1. Transistor symbols

that conventional current flow is reversed, as shown by reversing the arrow. Three wires are brought out from the envelope, for direct soldering of the transistor into its circuit; some examples of the orientation of these wires are shown in Fig. 9.2.

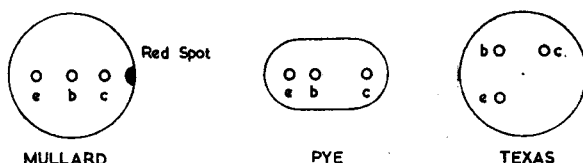


Fig. 9.2. Typical base-connection diagrams for transistors: *e*, emitter; *b*, base; *c*, collector

All junction transistors are photo-sensitive to some extent, and are protected from unwanted light by an opaque coating; this must not be scratched, or 'mains-generated' light may impose a 100 c/s modulation on the transistor output. Where considerable power is to be handled, the transistor must make good contact with a suitable heat sink; a cooling 'flag' is sometimes fitted for direct attachment to the chassis.

### Theory of Semiconductors

In a pure crystal of germanium or silicon the atoms are held in place in the crystal lattice by covalent bonds; adjacent atoms each supply an electron to form a 'shared pair', and this constitutes one covalent link between the atoms. All four electrons

## SEMICONDUCTORS AND TRANSISTORS

in the outer shells of germanium or silicon are 'shared' in this way, so that each atom is held by four covalent bonds to its neighbours. There are very few 'free' (unbonded) electrons, such as are present in the outer electron shells of a metal crystal, and so the electrical conductivity is lower than that of a metal.

The bound electrons crowd together in a region of high stability and therefore low energy—called the *valence band* of the crystal (*V*, in Fig. 9.3). Because so many electrons have almost equal energy, the energy levels of this band are said to be highly degenerate. Now at room temperature there is an additional complication. Some of the valence-band electrons acquire sufficient energy to break a bond, and these electrons leave their

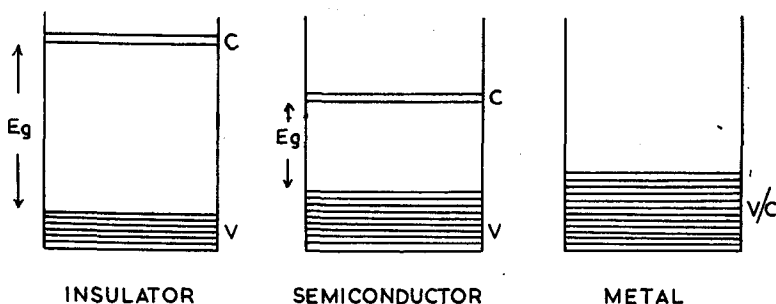


Fig. 9.3. Energy levels in crystals: carbon (diamond), silicon, and copper

fixed positions in the lattice and are the source of the small but definite electrical conductivity of these crystals at temperatures well above absolute zero. Electrons which have become 'free' in this sense are said to have left the valence band, and are now in the *conduction band* (*C*, Fig. 9.3) of the crystal. Between the two bands there is an *energy gap*; only by gaining enough energy to cross this gap may an electron become available for conduction.

The 'width' of the gap (in terms of energy) determines the resistivity of a material; thus, the difference between an *insulator* such as diamond, a *semiconductor* such as silicon, and a *metal* such as copper, is shown schematically in Fig. 9.3. The energy gap  $E_g$  is about 2–5 eV for an insulator, 0.7 eV for germanium and 1.12 eV for silicon; it is not well defined for a metal, because the valence and conduction bands overlap to some extent. The thermal energy of an electron at  $T^0$  is  $kT$ , where  $k$  is Boltzmann's

## LABORATORY AND PROCESS INSTRUMENTS

constant; at room temperature,  $kT \simeq 0.025$  eV, so that the number of electrons which can cross an energy gap  $E_g$  is given by  $n$ , where  $n \propto N \cdot \exp(-E_g/kT)$ , and  $N$  is the total number of electrons in the valence band. For  $E_g = 0.7$  eV,  $n \simeq N \times 10^{-7}$ , so that about  $4 \times 10^{15}$  electrons per c.c. are in the upper (conduction) band; for  $E_g = 2.0$  eV,  $n \simeq N \times 10^{-20}$ , so that only about 400 electrons per c.c. are present in the conduction band.† In copper, about  $2 \times 10^{21}$  electrons per c.c. are available for conduction; these varying populations of the conduction band for substances of differing  $E_g$  account for the following resistivities:

	$\rho$ ( $\Omega$ cm)
typical insulator (mica):	$9 \times 10^{15}$
pure germanium:	60
pure copper:	$1.7 \times 10^{-6}$

Conduction by electrons which have been thermally excited to the conduction band of a *pure* crystal is called intrinsic conduction; it is reduced to a minimum, in transistors, by extreme purification of the material, and by shielding from light and other ionising radiation.

In transistors the intrinsic conduction is enhanced by the addition of small and controlled amounts of 'impurity' to the lattice. Both silicon and germanium occupy places in Group IV of the periodic classification, having four outer-shell electrons, so that each atom is held in the crystal lattice by four covalent bonds, as in the diamond. If a small number of atoms of a Group III element (e.g. Indium) are introduced, having only three outer electrons, one electron from its four nearest-neighbour atoms will remain uncombined wherever the impurity takes up its position in the lattice; these uncombined electrons may 'pair' with thermally generated electrons to complete the four-covalent structure at this point leaving vacancies in the main lattice. The energy required to complete the structure is small; we may consider the electrons in the 'extra' covalent bonds to occupy an energy level about 0.01–0.02 eV above the top of the valence band. Considering the very small number of impurity atoms ( $< 1$  in  $10^7$ ), and

† One gram-atom (i.e. the atomic weight in grams) of an element contains approximately  $6 \times 10^{23}$  atoms.



## SEMICONDUCTORS AND TRANSISTORS

the low energy of promotion, the 'equilibrium' shown in Fig. 9.4 would be expected to lie entirely on the right-hand side; *all* the impurity atoms will be four-covalently bonded, at room temperature, a corresponding number of vacancies remaining in the valence band. Aluminium and indium are the usual Group III additives; since they accept electrons in order to complete four-covalent bonding into the lattice, they are called 'acceptor' impurities.

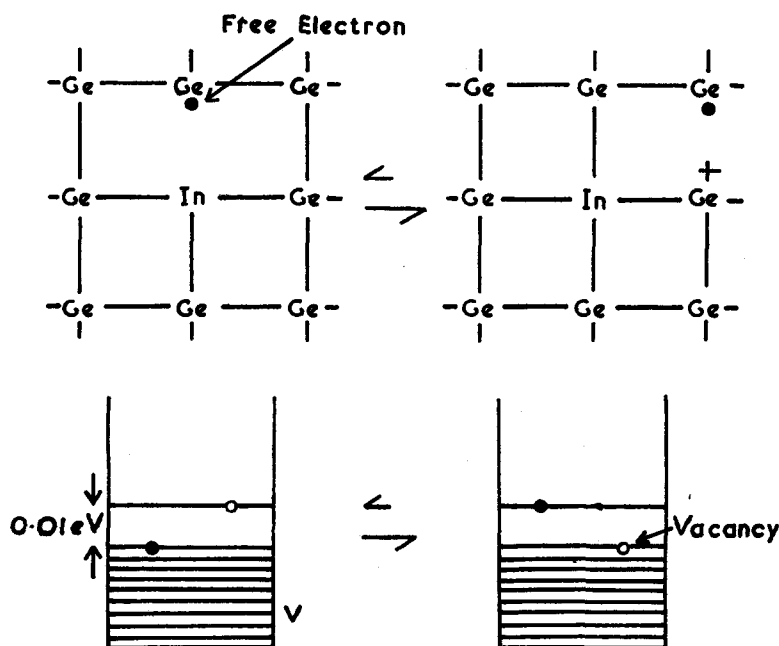


Fig. 9.4. Equilibrium in P-type germanium and energy-level diagram

Vacancies in the valence band arise through the breaking of covalent bonds in the original lattice by thermal vibration, one electron then moving away towards an impurity atom, or to another vacant site. The *absence* of an electron has been equated to the *presence* of a positive charge, so that germanium or silicon to which 'acceptor' atoms have been added is referred to as Positive, or *P-type*, material. The lattice vacancies are not static; as further covalent bonds are broken, the liberated electrons fill

old vacant sites, and create new ones, giving rise to the concept of mobile, positively charged 'holes', diffusing through the P-type lattice and accounting for most of its conductivity.

Alternatively, if traces of a Group V element, such as arsenic or antimony, are added to the lattice, one of the five outer electrons of this atom remains unpaired with an electron from its

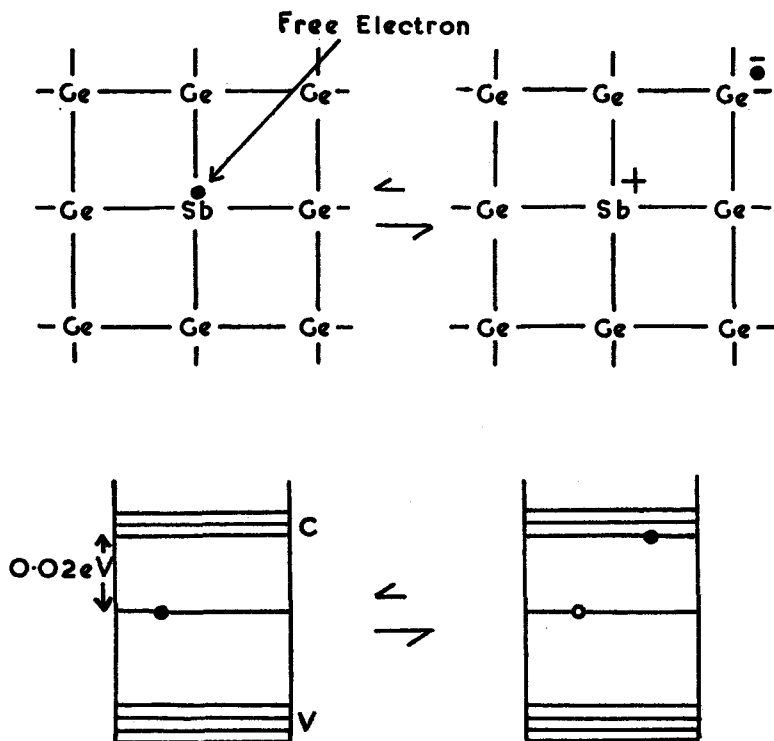


Fig. 9.5. Equilibrium in N-type germanium and energy-level diagram

nearest-neighbour atoms, and hence is at a higher energy level; the 'free' electron requires only about 0.02 eV to promote it to the conduction band. Thus at room temperature nearly all the unpaired electrons will be in the conduction band, as indicated in Fig. 9.5. Since Group V atoms increase the number of electrons in the conduction band, they are called 'donor' impurities; conduction in this type of material is mainly due to these electrons, and the lattice is referred to as Negative, or *N-type*.

## SEMICONDUCTORS AND TRANSISTORS

The effect of impurity-atom concentration on the resistivity of germanium is shown in Fig. 9.6; the concentrations, which are expressed in atoms of impurity per c.c. of germanium, are extremely small, since  $10^{12}$  atoms per c.c. corresponds to 1 part in  $4 \times 10^{10}$  parts of germanium. Donor and acceptor impurities both give similar resistivity-concentration characteristics; however, the conduction-band electrons of N-type germanium or silicon diffuse about twice as rapidly as do the valence-band electrons

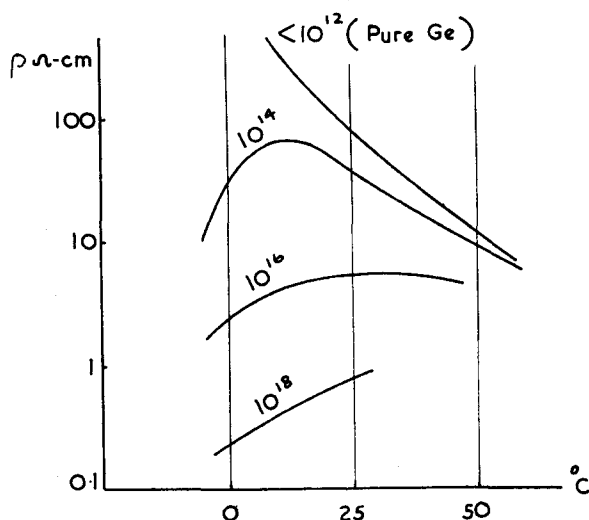


Fig. 9.6. Resistance of a semiconductor as a function of impurity concentration

which fill 'holes' in the P-type, so that a given concentration of 'donors' produces a greater increase in conductivity than an equal concentration of 'acceptors'.

If both types of impurity were added, in equivalent amounts, to germanium or silicon, the conduction-band electrons derived from donor atoms would fill the valence-band 'holes' left when the acceptor atoms become four-covalent, and the intrinsic conductivity of the material would remain unaltered. The 'majority carriers' introduced would neutralise each other; electrical neutrality would be maintained, and no potential difference would be set up within the lattice.

### The Junction Diode

Suppose now that two sections, one of P-type, the other of N-type material are brought into contact at a plane boundary; this is the open-circuited case of Fig. 9.7(a). Then electrons in the conduction band of the N-type cross the boundary, in order to fill the 'holes' in the valence band of the P-type; this leaves the N-type material with a positive charge, localised near the boundary, and also sets up a localised negative charge on the P-type. A potential

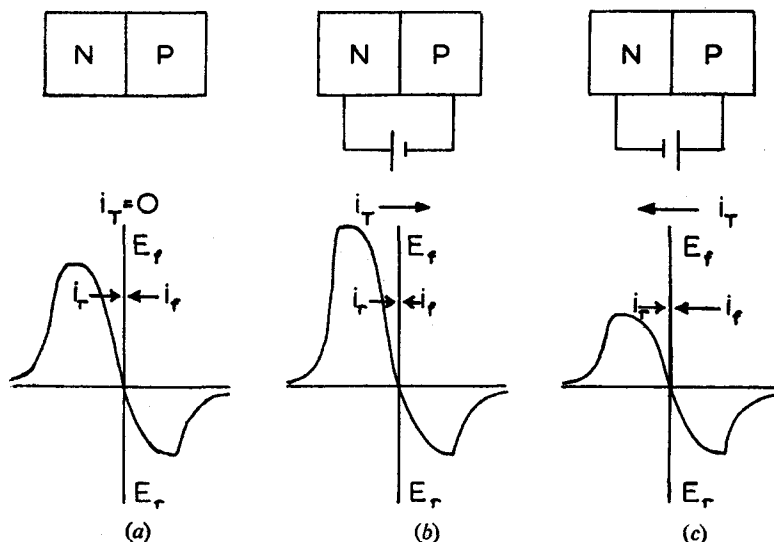


Fig. 9.7. Application of bias to junction diodes: a, zero bias; b, reverse bias; c, forward bias

difference is thus set up across the boundary, in such a direction as to reduce the flow of electrons from N- to P-, i.e. so as to reduce the *forward current*  $i_f$ . At the same time, the few thermally liberated electrons of the P-type are attracted, by the positive potential set up, towards the N-type, where they fill thermally created 'holes' in the N-type lattice; this constitutes the *reverse current*  $i_r$ . The junction p.d.  $\psi$  will increase until forward and reverse currents are equal, when we again have a condition of dynamic equilibrium;  $\psi$  will be maintained at this value, with a *net current*  $i_T$  of zero. The magnitude of  $\psi$  is indicated by the sum of the two vertical peaks.

## SEMICONDUCTORS AND TRANSISTORS

If an external e.m.f. is applied across the boundary, so as to assist the junction p.d. developed inherently—e.g. by connecting the positive pole of a battery to the N-type and the negative pole to the P-type (Fig. 9.7(b))—the forward current  $i_f$  is reduced, but

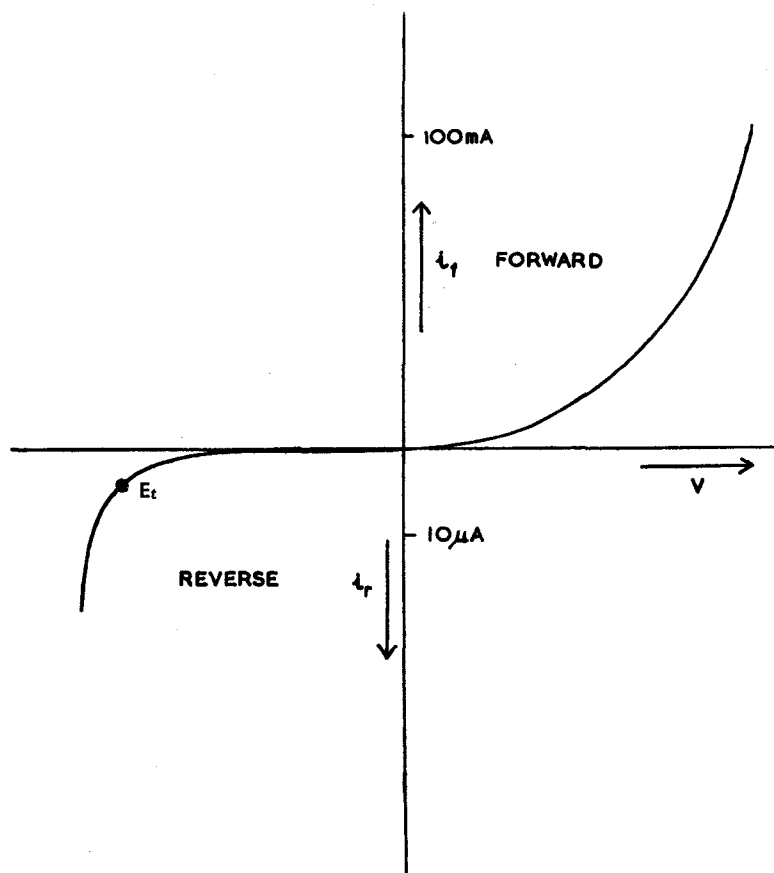


Fig. 9.7 (d).

the reverse current is practically unchanged since it is governed by the rate of thermal generation of hole-electron pairs; the junction is said to be 'reverse-biased'. Reversing the battery (Fig. 9.7(c)) increases the forward current, again without affecting the reverse current, the boundary now being 'forward biased'.

This is the principle of operation of the junction diode; it may be seen from Fig. 9.7(d) that too large a reverse bias leads to breakdown of the diode, with a large reverse current tending to overheat and destroy the device. The maximum negative value of bias voltage is shown by the 'turnover point'  $E_r$ . Increase of temperature causes both  $i_r$  and  $i_f$  to increase, and reduces  $E_r$ .

The point-contact diode behaves similarly; if a metallic contact is made to a piece of semiconducting material, electrons flow towards the metal, setting up a potential barrier similar to that across the P-N junction. The 'point-contact diode' shows, therefore, the same rectification characteristics as the junction diode; the metallic contact is usually a fine wire, or a needle-point, so as to concentrate the field at this region of the lattice.

If the bias battery is replaced by an applied alternating voltage, rectification will occur, as with a metal rectifier. For a given power dissipation, however, the junction or point-contact diode is very much smaller than a metal rectifier, and has a considerably lower resistance in the forward direction. Because of these facts, great care must be exercised in preventing accidental short-circuits leading to excessive current flow; the low value of forward resistance means that such currents will be large, and the small thermal capacity of the diode leads to very rapid overheating. Thus, overloads persisting for a few milliseconds may destroy a semiconductor diode.

### The Junction Transistor

This type has practically replaced the point-contact transistor, and so the latter will not be further described. In the junction transistor, a thin layer of one type of germanium or silicon is 'sandwiched' between layers of the opposite type, so as to form either a P-N-P system, or an N-P-N system. The three sections of the transistor are known as the *emitter*, *base* and *collector*, and are in some ways analogous to the cathode, grid and anode electrodes of a thermionic triode. Metal plates, or sputtered metallic layers, enable wires to be connected to the three regions.

If an N-P-N transistor is connected to batteries, as shown in Fig. 9.8(a), the emitter junction will be forward biased, and the collector junction reverse biased; the potential gradients set up are shown in Fig. 9.8(c). If the input terminals  $xy$  are short-circuited, 'reverse' electron flow will occur from base to collec-

## SEMICONDUCTORS AND TRANSISTORS

tor—the 'forward' electron flow across this junction being biased to zero. This is equivalent to a conventional internal (positive) current from collector to base, of magnitude  $i_c$ .† The forward flow of electrons from emitter to base will be enhanced by the forward bias; we represent this flow of electrons by  $e_f$ , and the equivalent positive current by  $i_f$ . Now if the base region is thin, many of the electrons which make up  $e_f$  cross the collector junction, attracted by the positive potential, and join  $i_c$ ; the number

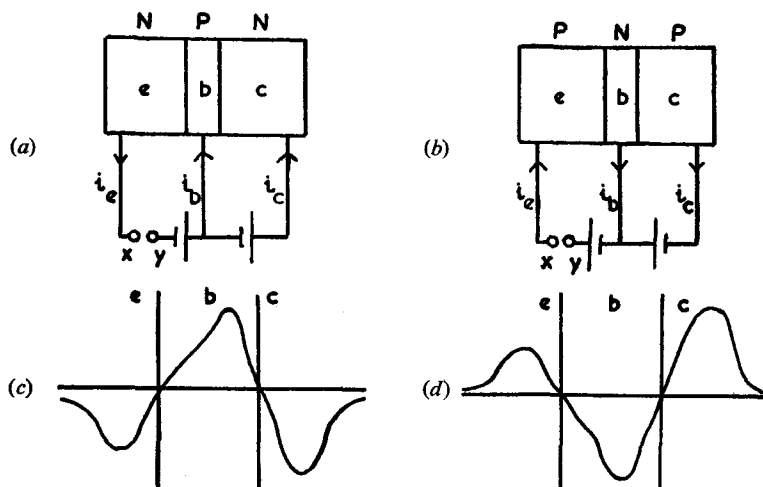


Fig. 9.8. (a) Connections to N-P-N transistor. (b) Connections to P-N-P transistor. (c) and (d) Potentials developed

which do so is controlled by the emitter-base junction potential. The fraction of  $e_f$  which cross the base region is called  $\alpha_{ce}$ ,† and in practice is about 0.90–0.95; hence the ratio  $e_f/e_b$ , where  $e_b$  represents the electron flow from the base, is about 100, designated  $\alpha_{cb}$ .§

† The more usual parameter is  $i_{co}$ , the reverse saturation current from collector to base with the emitter open-circuited.

‡  $\alpha_{ce} = (di_c/di_e)$ , the amplification factor for positive current from collector to emitter.

§  $\alpha_{cb} = (di_c/di_b)$ , the amplification factor for positive current from collector to base.

## LABORATORY AND PROCESS INSTRUMENTS

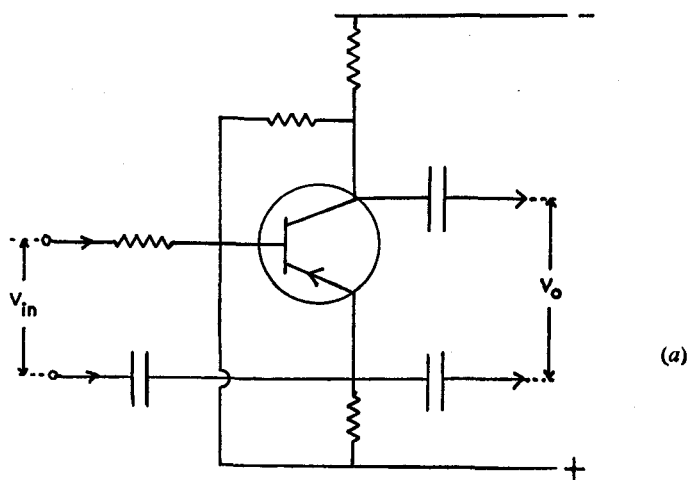
For a high efficiency of 'collection' of carriers from the emitter, we require a relatively high level of 'doping' of the emitter. Although *either* 'holes' travelling from base to emitter, or electrons from emitter to base, would give current flow in the same direction, only the latter carriers would be attracted to the collector; hence we require the base-to-emitter current to be almost entirely of electrons. High efficiency also requires that very few electron-hole recombinations should occur in the base; this necessitates a very narrow base section, which is also important in raising the limit of frequency at which the transistor will operate satisfactorily.

In terms of positive current, the total emitter current is  $i_e = i_f = -e_f$ ; this splits into  $i_b$ , the emitter-to-base current, and  $i_c$ , the emitter-to-collector current. From the definitions of  $\alpha_{ce}$  and  $\alpha_{cb}$ ,  $\delta i_c = \alpha_{ce} \cdot \delta i_e$ , and  $\delta i_c = \alpha_{cb} \cdot \delta i_b$ , where  $\delta i_c$  is the change in collector current due to changes  $\delta i_e$  in emitter current, or of  $\delta i_b$  in base current, respectively. Such changes may be the result of an applied signal. The potential across the emitter junction is modulated by an alternating signal applied to the terminals  $xy$ , and the emitter current  $i_e$  varies accordingly; the reverse-biased collector junction is not sufficiently affected to alter  $i_c$ .

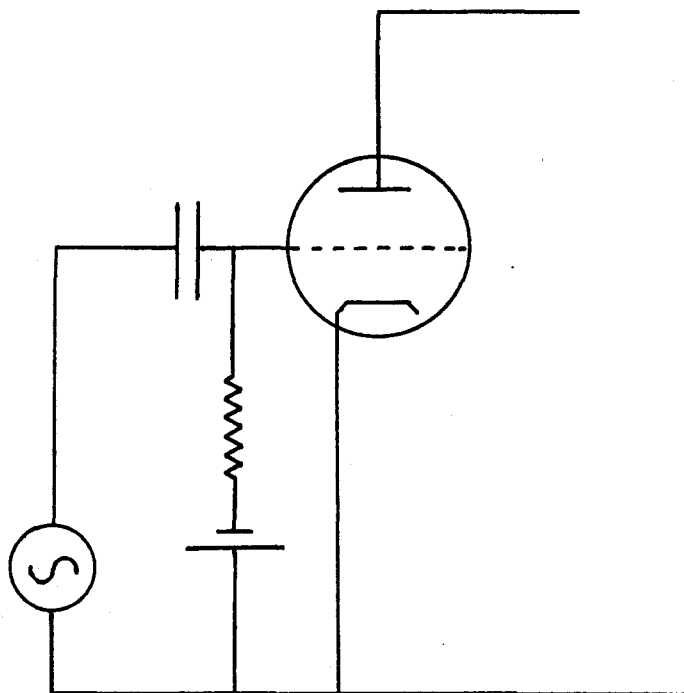
In Fig. 9.9, a 'common-base' connected transistor and a triode valve are compared. If  $\alpha_{cb}$  is 100,  $\delta i_c = 100\delta i_b$ , and an input signal of 10  $\mu\text{A}$  at the base produces an output of 1 mA at the collector. In the valve,  $\delta i_a = g_m \cdot \delta V_g$  and in the transistor  $\delta i_c = \alpha_{cb} \cdot \delta i_b$ , so that the latter is essentially a current amplifier. Both the collector and base currents are exponentially related to the applied voltage,<sup>†</sup> but are linearly connected through  $\alpha_{cb}$ . In this case, the base and collector currents are 180° out of phase, just as  $V_g$  and  $V_a$  in the valve circuit, but this is not always so. The above analysis has been applied to the N-P-N transistor of Fig. 9.8(a), but a similar explanation may be given for the P-N-P transistor. Whichever type of transistor is used, the emitter is always forward-biased, and the collector reverse-biased; reversal of polarity at the collector leads to *rapid destruction* of the tran-

<sup>†</sup> The total current across a junction is given by  $i = (e^{eV/kT} - 1) \cdot i_s$ , where  $i$  is the total current,  $i_s$  is the saturation reverse current,  $e$  is the electronic charge,  $T$  the absolute temperature,  $k$  is Boltzmann's constant, and  $V$  the bias voltage across the junction. For  $V + \text{ve}$ , the forward bias condition,  $i = i_f$ , the total forward current; for  $V - \text{ve}$ ,  $i = i_s$ .





(a)



(b)

$$Z_i = 200 \Omega; Z_o = 5 \text{ k}\Omega$$

Fig. 9.9. (a) Common emitter transistor amplifier. (b) Equivalent triode amplifier

sistor. Typical output characteristics for a silicon N-P-N transistor—the Texas Instruments 2SO01—are shown in Fig. 9.10.

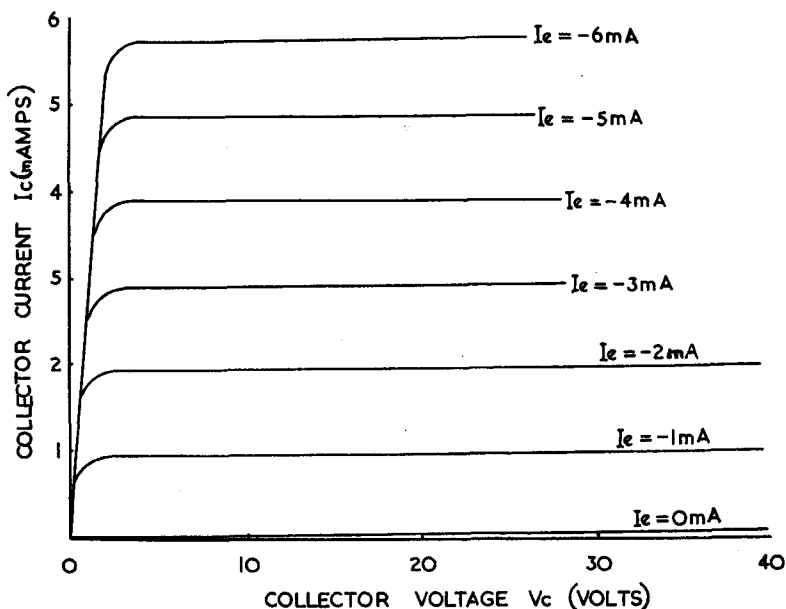


Fig. 9.10. Output characteristics of Texas Instruments 2SO01—N-P-N

### The Manufacture of Transistors

The germanium or silicon must be very highly purified before it is 'doped' by the introduction of donor or acceptor atoms; impurities are reduced to about 1 part in  $10^9$ , so that the lattice structure is practically uniform throughout the crystal. Germanium, which melts at  $940^\circ$ , is finally refined by slow passage through r.f. heating coils; the long ingot is contained in a silica boat. The molten zone is narrow, and travels slowly from end to end of the ingot; impurities tend to accumulate in the molten zone, and so are concentrated in the trailing end of the ingot. Silicon melts at  $1400^\circ$ , and cannot be 'zone-refined' in this way; a carefully purified, volatile compound of silicon is decomposed to give the pure element.

Junction transistors for use at low frequencies are made by slowly drawing a 'seed' of pure germanium or silicon from the

## SEMICONDUCTORS AND TRANSISTORS

pure melt, and then adding the requisite amount of, for example, antimony; the next section of the crystal to be drawn will thus be N-type. If now an *excess* of indium is added, the 'donor' impurity will effectively be neutralised, and this section of the crystal will be P-type. Finally, a further excess of antimony restores the crystal to N-type; if the complete drawn crystal is diced perpendicular to the junctions, a large number of N-P-N transistors are obtained. High-frequency transistors are made by alloying P-type material to either side of a *thin* section of N-type material, in order to form a P-N-P junction transistor; it is more difficult to make the N-P-N-type transistor by this method. The upper limit of frequency of the junction transistor is set by the transit time for electrons across the base region, so that this must be made as thin as possible; in alloy transistors the base thickness may be less than 0.01 mm.†

Even thinner base regions may be obtained by a diffusion technique, in which the base section is built up by diffusion under controlled vapour-pressure of suitable material on to the emitter section. The base width may be accurately controlled, and some of the prototype 300–400 Mc/s transistors are prepared in this way.

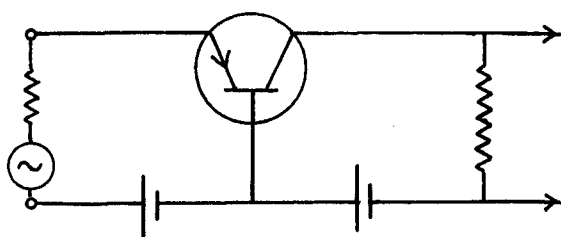
After the wire leads have been soldered to the three regions, the transistor is chemically etched to remove surface contamination before it is encapsulated, together with a dehydrating agent, in a glass envelope.

The cutting and shaping of transistors is often carried out by an ultrasonic technique, so as to preserve the surface regularity; this helps to reduce inherent 'noise'.

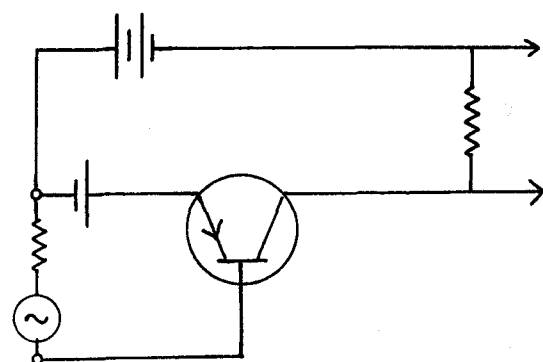
### Basic Types of Connections

Transistor circuits may be classified according to which of the three 'electrodes' is common to both the input and output circuits; these basic connections are shown in Fig. 9.11, for the

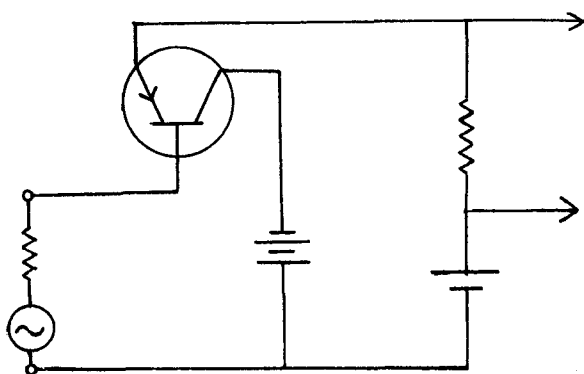
† Both  $\alpha_{ee}$  and  $\alpha_{eb}$  decrease with increase of frequency. It is usual to define a cut-off frequency,  $f_{c.o.}$ , at which  $\alpha$  is reduced to  $1/\sqrt{2}$  of its value at 1000 c/s, i.e.  $\alpha_{f_{c.o.}} = \alpha_{1000}/\sqrt{2}$ . Since power is proportional to  $\alpha^2$ ,  $W_{f_{c.o.}} = W_{1000}/2$ . The value of  $f_{c.o.}$ , as stated, is determined by the base thickness, and may be increased by making the base layer very thin; this, however, reduces its power rating. The present limit to  $f_{c.o.}$  is about 30 Mc/s for transistors generally available, although it is considerably lower for 'power' transistors.



Common base



Common emitter



Common collector

Fig. 9.11. Basic connections of transistors: common emitter, common base, common collector

## SEMICONDUCTORS AND TRANSISTORS

N-P-N-type transistor. Diagrams for the P-N-P-type would be similar, except for the directions of current flow.

The *common emitter* connection is that most commonly used for amplification. Since  $i_b = i_e - i_c$ , and  $i_c/i_e = \alpha_{ce}$ , e.g. 0.95,  $i_c/i_b = \alpha_{ce}/(1 - \alpha_{ce}) \approx 19$ , the current gain of the transistor circuit. The input circuit, under forward bias conditions, is of low impedance,  $\approx 2 \text{ k}\Omega$ ; the output circuit, under reverse bias, is of high impedance,  $\approx 200 \text{ k}\Omega$ . Thus,  $W_o/W_i = 19^2 \cdot Z_o/Z_i$ ,  $3.6 \times 10^4$ , or about 45 db gain. The voltage amplification is  $19 \times Z_o/Z_i$ , or 1900.

The *common base* circuit has a current gain of  $\alpha_{ce}$ , and the output and input impedances are approximately the same as in the common emitter connection; hence  $W_o/W_i = 0.95^2 \cdot Z_o/Z_i \approx 90$ , or 19 db gain, and the voltage gain is about 95. There is no phase-reversal in this circuit— $i_c$  is in phase with  $i_e$ .

The *common collector* circuit is equivalent to the valve cathode-follower circuit; the input impedance is high, and the output impedance low.  $i_e/i_b = i_e/(i_e - i_c) = 1/(1 - \alpha_{ce})$ . Calling this ratio  $\alpha_{be}$ , then for  $\alpha_{ce} = 0.95$ ,  $\alpha_{be} = 20$ . Typical impedance values are:  $Z_i = 100 \text{ k}\Omega$ ,  $Z_o = 1 \text{ k}\Omega$ , so that  $W_o/W_i = 20^2/100 = 4$ ; the voltage gain  $V_o/V_i = 20/100$ , or 0.2. The common collector circuit is used for impedance matching, again analogous to the cathode follower (p. 142).

### Some Transistor Circuits

The basic amplifier of Fig. 9.12 employs the Mullard OC71 P-N-P transistor in common emitter connection. Typical component values are:

$V_{coll.}$ (V)	$i_{coll.}$ (mA)	$R_1$ (k $\Omega$ )	$R_3$ (k $\Omega$ )	$i_o/i_i$	
6	1.0	39	2.2	23	For 5% distortion into a load $R_L$ of 1.5 k $\Omega$ .
9	1.0	62	3.9	28	
12	1.0	82	5.6	31	

The source impedance should be as high as possible. Notice that electrolytic capacitors are frequently used as feed and coupling components in transistor circuits.

A two-stage amplifier, using Mullard OC70 and OC71 transistors is shown in Fig. 9.13, again in common-emitter

# LABORATORY AND PROCESS INSTRUMENTS

circuits. Reverse collector-base bias is developed by the base current flowing through  $R_2$  and  $R_4$ , and the transistors are  $r$ - $c$  coupled. The load is shown as a headphone  $H$ .

A Class B (p. 145) push-pull power amplifier stage is shown in Fig. 9.14. The grounded-emitter connection is used, since this

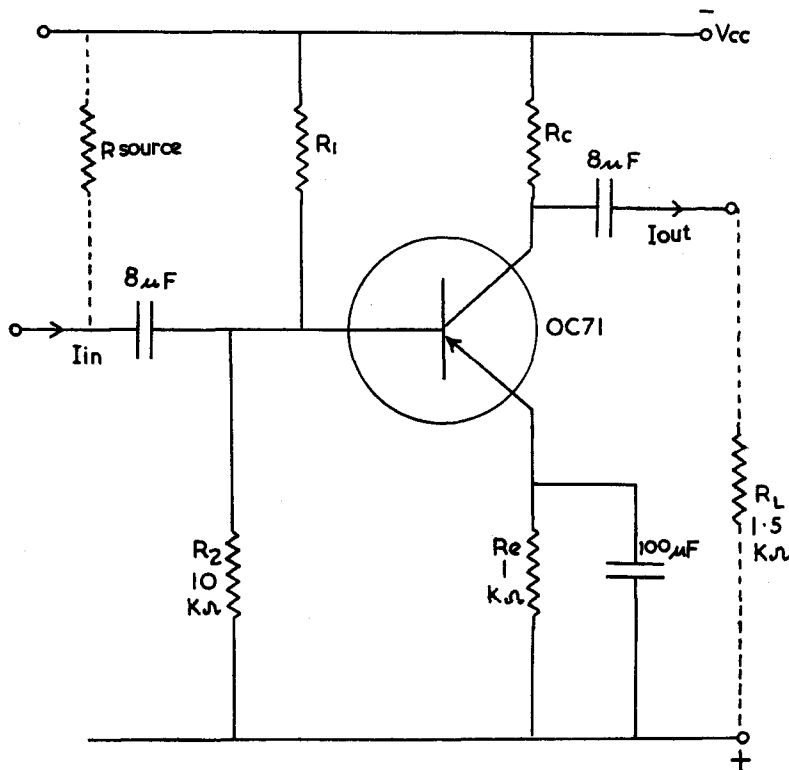


Fig. 9.12. Basic transistor amplifier (OC71)

has the greatest power gain. To avoid distortion the two transistors should be closely matched; Mullard OC72 transistors, developed for large-signal applications, are normally supplied in matched pairs for Class B operation.

The collector-to-collector load,  $R_{cc} = R_p + T^2 R_s$ , where  $R_p$  is the resistance of the output transformer primary,  $R_s$  is the secondary load and  $2T:1$  is the turns-ratio of the transformer.

## SEMICONDUCTORS AND TRANSISTORS

Thus, for  $R_{cc} = 300 \Omega$ ,  $R_s = 3 \Omega$  and  $R_p \approx 10 \Omega$ ,  $T = 10$ . A suitable ratio for the input transformer is about 3.5:1, so that the collector current of an OC71 (2 mA) will drive the output stage; with collector voltage  $-6 \text{ V}$ , a power gain of 24 db, and a maximum power of 200 mW, are obtainable.

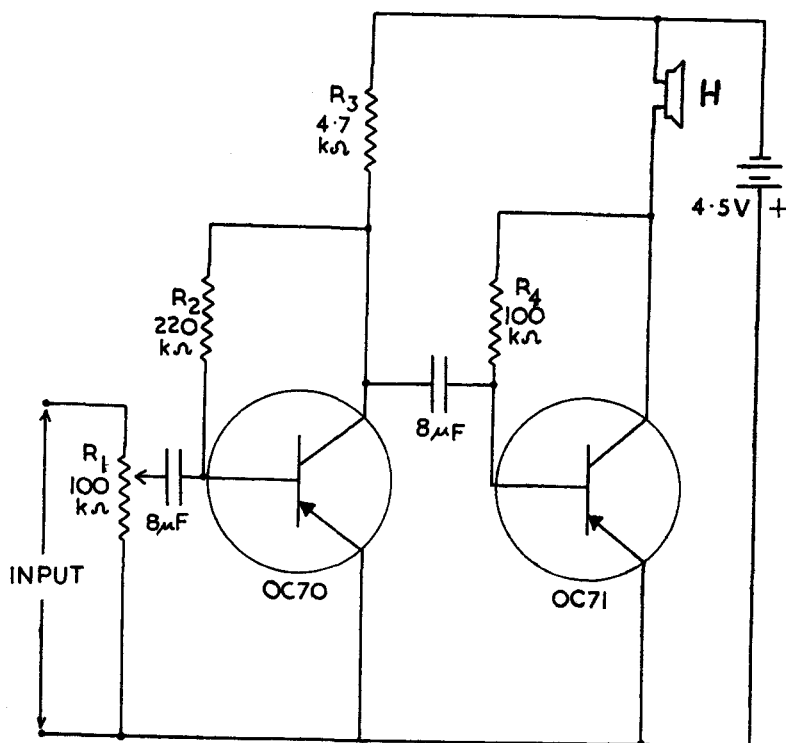


Fig. 9.13. Two-stage transistor amplifier (OC71 and OC72)

A basic circuit for a transistor low-frequency oscillator is given in Fig. 9.15(a). Current through  $R_1$  provides the reverse bias to the collector, and the positive feedback is via the transformer  $L_2$ . The oscillatory circuit may be tuned in the usual way. Fig. 9.15(b) shows a transistor version of the Colpitt's oscillator (cf. valve circuit, p. 156).

The efficient conversion of a L.T. battery supply to H.T., suitable for valve anodes, presents many problems. The rotary

## LABORATORY AND PROCESS INSTRUMENTS

converter and the electro-mechanical vibrator are unsuitable for instrument H.T. supplies, because of the noise which they introduce; they are both of low efficiency. The rapid switching action of the transistor enables it to take the place of the vibrator, and a transistor d.c. converter unit is shown schematically in Fig. 9.16.†

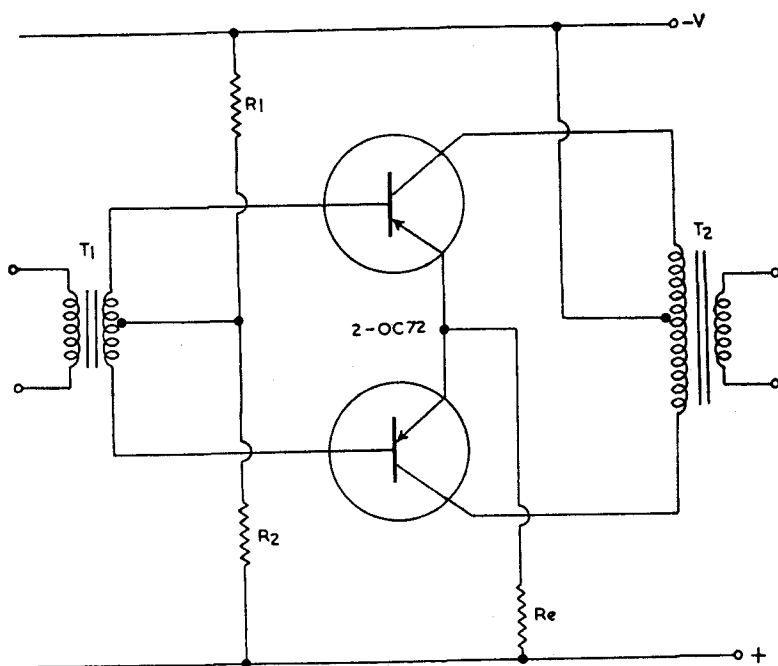


Fig. 9.14. Class B transistor output stage

The transistor operates as a switch, interrupting the battery input voltage  $V_i$ . The alternating voltage set up in the transformer secondary winding is rectified, smoothed and applied to the load. The operation is initiated by surge currents on connecting the supply voltage to the transistor. The collector current rises, passing through the primary winding  $N_p$ , and inducing a negative

† For a comparison of the transistor converter with the vibrator and other forms of H.T. supply, see *Electronic Engineering* 27, 268 (1955).



## SEMICONDUCTORS AND TRANSISTORS

bias voltage in the winding  $N_b$ , which is applied to the transistor base. The working-point moves round the 'knee' of the collector current-voltage curve, and the input resistance then rises sharply. The primary current falls and, together with the resultant decrease in the base bias, causes the transistor to move rapidly towards

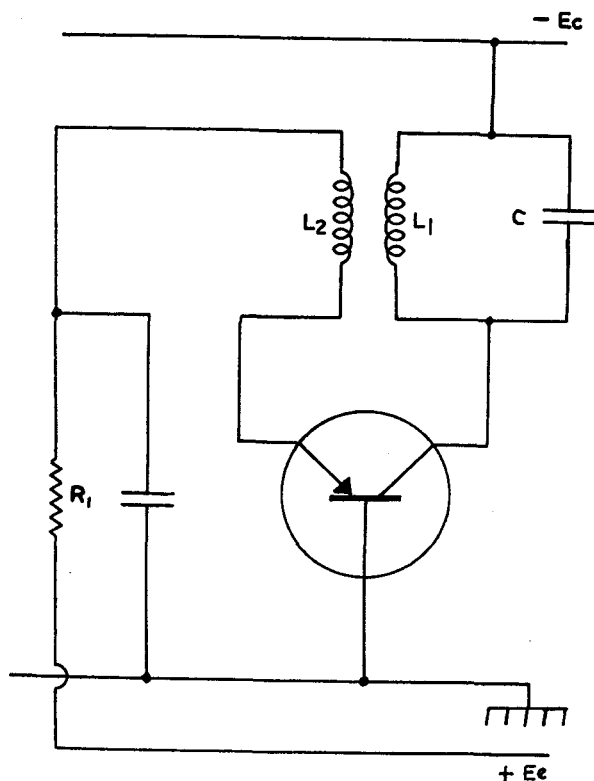


Fig. 9.15. (a) Basic transistor oscillator

cut-off. The primary flux collapses, and the voltage across the secondary winding  $N_s$  reverses; the diode  $D_1$  now conducts. When the secondary voltage falls below that across the output capacitor  $C_o$ ,  $D_1$  cuts off, and the transistor returns to its working point (in the region of the 'knee' of the appropriate curve, Fig. 9.10), ready for the next cycle of operation.

## LABORATORY AND PROCESS INSTRUMENTS

As an example of its operation with  $V_i = 6$  V,  $V_o$  may be 90 V at 12 mA, with 70% efficiency; the frequency of operation is about 1 kc/s.

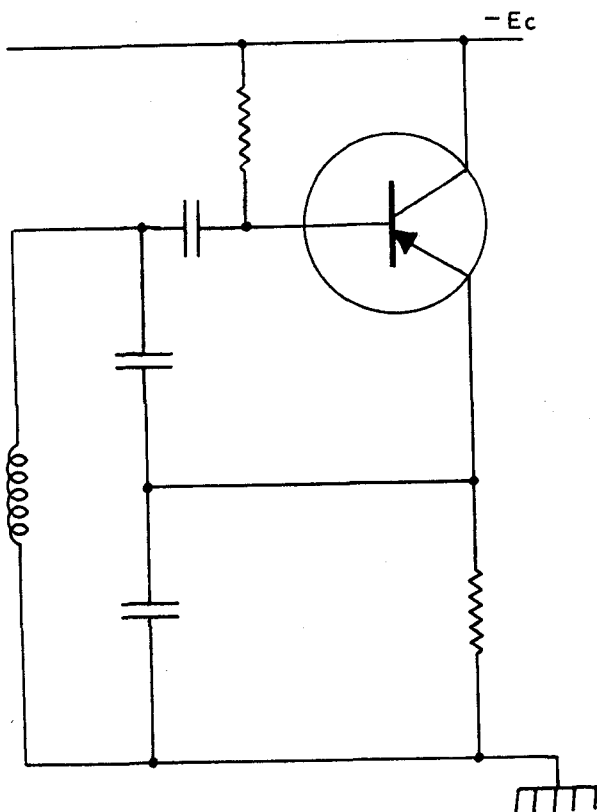


Fig. 9.15. (b) Transistor Colpitts oscillator

### Transistor Characteristics

For signal diodes, the following data is usually given: Peak inverse voltage, maximum forward current, average inverse current, average forward volts drop at  $i_{\max}$  and maximum temperature of operation.

For power diodes, details of a suitable heat sink may be included.

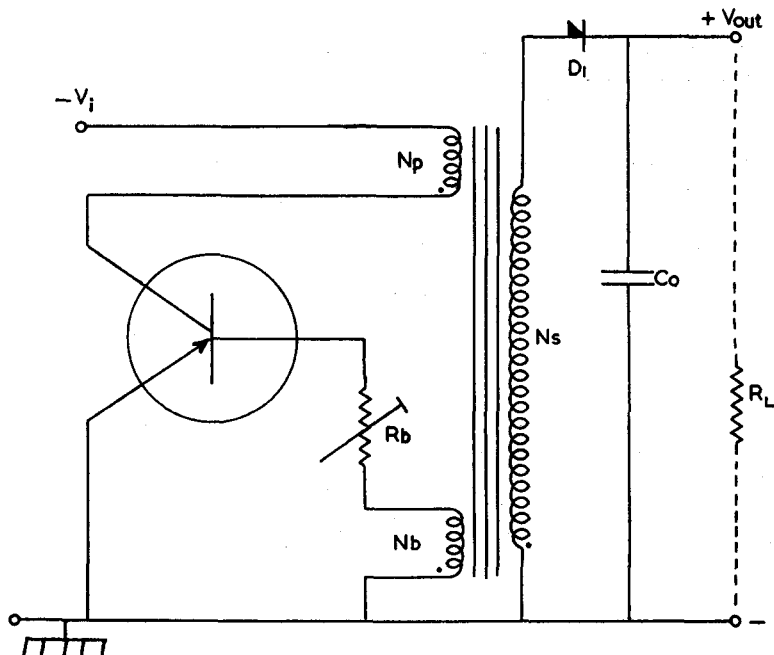


Fig. 9.16. Transistor d.c.-a.c. converter

For junction transistors, the  $\alpha$  parameter is given, together with details of: collector voltage, collector dissipation, peak collector current, maximum junction temperature and the particular applications for which the device was designed.

#### References

- GRIMSDALL, G. (1955). 'Economics of transistor d-c transformer', *Electronic Engineering* **27**, 268.
- HOULDSWORTH, J. (1955). 'A ringing choke power supply', *Electronic Engineering* **27**, 251.
- HUNTER, L. P. (1956). *Handbook of Semiconductor Electronics*. McGraw Hill.
- KIVER, M. S. (1956). *Transistors in Radio and Television*. McGraw Hill.
- KNOTT, R. D. and MISSEN, J. I. (1956). 'Transistors', *Science News* **42**, 99.
- SCOTT, T. R. (1955). *Transistors and Other Crystal Valves*. Macdonald and Evans.

## LABORATORY AND PROCESS INSTRUMENTS

*Semiconductor Application Reports*. Texas Instruments Ltd. (1958 *et seq.*).  
*The Use of Semiconductor Devices*. British Radio Valve Manufacturers' Association (1958).

### Problems

1. Illustrate the terms 'semiconductor', 'donor and acceptor impurities', and '*p*- and *n*-type conduction', with reference to the germanium or silicon diode. Draw and explain the voltage-current characteristic curve for this device.

2. Explain how the *p-n-p* junction transistor may function: (a) as an amplifier at audio-frequencies; (b) as an oscillator at audio-frequencies.

What parameters are of importance in the design of these circuits?

3. Assess the present position regarding the relative advantages and disadvantages of the transistor and the thermionic valve.

4. 'The Inverter - a device for converting d.c. power supplies into alternating supply without using moving parts - is of great interest as a replacement for machines and vibrators.' Explain this statement, and show how the transistor functions in this capacity.

## CHAPTER X

# The Measurement of Electrical Conductance of Solutions

### Introduction

The determination of the electrical conductivity of solutions is of the greatest importance in chemical technology; a number of units and terms will first be introduced. We define the resistance of a regular solid conductor by

$$R = \frac{1}{\kappa} \cdot \frac{l}{A}$$

where  $R$  is the resistance in ohms;  $\kappa$  is the specific conductance in reciprocal ohms, or mhos,  $l$  is the length of the conductor, and  $A$  its area of cross-section.

Ohm's law is obeyed by electrolyte solutions and if a 1 cm cube of solution be considered ( $l = 1$  cm,  $A = 1$  cm<sup>2</sup>)  $R = 1/\kappa$ . If  $E = 1$  V, then from Ohm's law,  $I = E/R = 1/R = \kappa$  ohms<sup>-1</sup> cm<sup>-1</sup>.

From the academic point of view it is more usual to discuss not the *specific* conductance but the *equivalent* conductance  $\Lambda$ , where  $\Lambda = 1000\kappa/C$  and  $C$  = equivalent concentration (g-equivalents per litre of solution); the dimensions of  $\kappa$  and  $\Lambda$  are ohms<sup>-1</sup> cm<sup>2</sup>, and ohms<sup>-1</sup> cm<sup>2</sup> equivalents<sup>-1</sup>, respectively.

The conductance of a solution is measured in a conductivity cell, of which there are many designs; the majority are of glass, with platinum electrodes. Some of these are illustrated in Fig. 10.1, in which the platinum electrodes are labelled *PP*.

It would appear possible to determine the specific conductance of a solution from the cell resistance if the geometry of the cell were known exactly. However, this is very difficult to determine by measurement, and the cell is calibrated using a solution of known specific conductance. It can be easily shown that

$$\Lambda = \frac{1000}{C} \cdot \frac{1}{R} \vartheta$$

## LABORATORY AND PROCESS INSTRUMENTS

where  $\vartheta$  is the *cell constant* (i.e. *effective distance apart of electrodes*  $\div$  *effective area of the column of solution between them*). In the measurement of conductivity it is necessary to control the temperature of measurement since the temperature coefficient of conductivity is about 2% per  $^{\circ}\text{C}$ , and some form of thermostat is necessary if accuracy of measurement is desired. For comparison purposes, physico-chemical measurements are usually

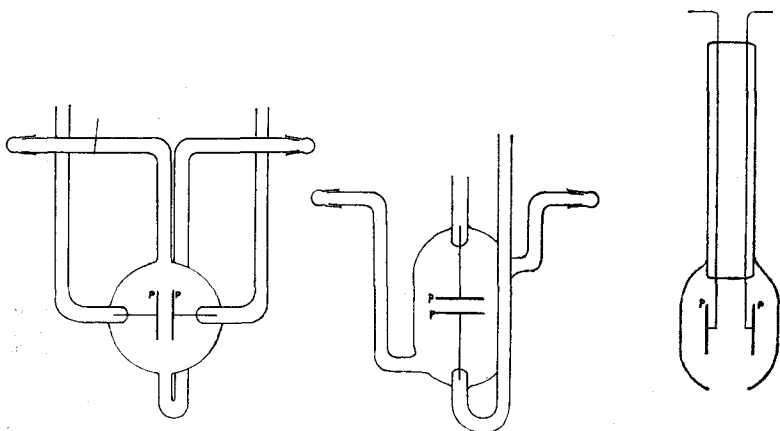


Fig. 10.1. Conductivity cells

made at  $25^{\circ}\text{C}$  where possible. Thus in practice it becomes necessary to measure the resistance of a solution, if possible at a controlled temperature, in order that the specific and equivalent conductances may be calculated. The reader is referred to the standard electrochemical textbooks for a full discussion on the significance of the various terms (for references, see the end of the chapter).

### Bridge Circuits

The majority of conductance measurements are made using an a.c. Wheatstone bridge circuit, but it will be helpful to consider first the d.c. bridge (Fig. 10.2). A battery  $B$  supplies current to a bridge network made up of resistors  $R_1$ ,  $R_2$ ,  $R_3$ , and cell  $R_4$  with a galvanometer  $G$  to detect the null point.  $R_3$  is varied until a null point is reached, when the potentials at  $d$  and  $b$  must be the same;

### ELECTRICAL CONDUCTANCE OF SOLUTIONS

then  $R_1/R_2 = R_4/R_3$ . Thus if  $R_1$  and  $R_2$  be known, the adjustment of  $R_3$  to give a null reading will enable  $R_4$ , the cell resistance, to be easily calculated.

However, it is not usually possible to determine by this means the conductivity of electrolyte solutions, since the passage of a direct current will produce polarisation within the cell. This is

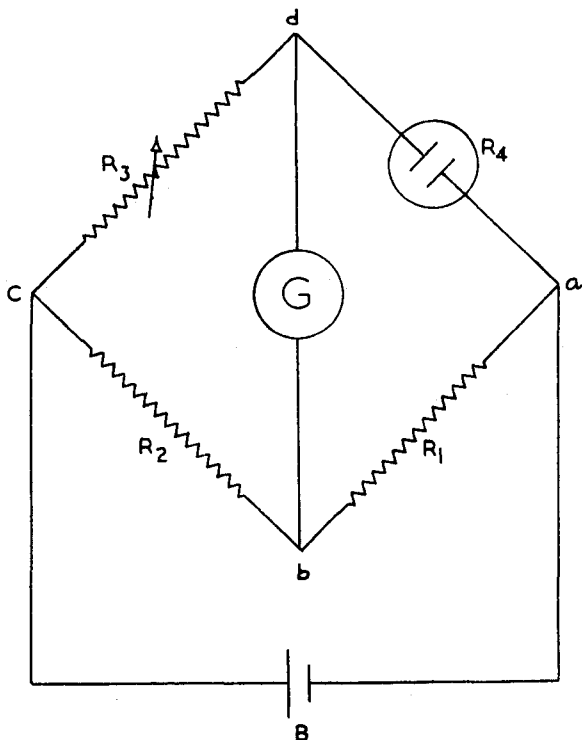


Fig. 10.2. D.C. Wheatstone bridge

made manifest by concentration changes near the electrodes, the evolution of hydrogen or oxygen from aqueous solutions, and other undesirable effects leading to erroneous results.

In practice it is possible to make d.c. measurements of conductivity using special methods which will be described later (p. 237). However for most purposes it is convenient to use an a.c. source which greatly reduces the polarisation effects. Most of the

# LABORATORY AND PROCESS INSTRUMENTS

bridges used are based upon that described by Jones and Josephs.<sup>†</sup> The bridge may be simply drawn as shown in Fig. 10.3, and there is a marked similarity to the d.c. bridge. The supply is now from an a.c. source, which may be the 50 c/s mains supply, or a supply from a valve oscillator. The most common frequency

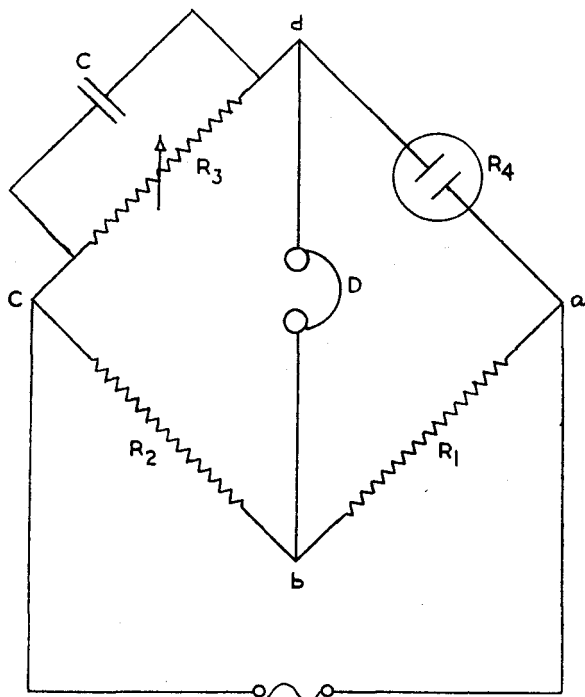


Fig. 10.3. A.C. Wheatstone bridge for conductivity measurement

used in the past has been 1000 c/s; the headphone *D* used as a detector responds to this convenient audio-frequency, and for many electrode systems this frequency is sufficiently high to minimise polarisation. If *d* and *b* are at the same potential, as shown by zero sound in the headphone, the voltages across the components are related:

$$E_2 = E_3, E_1 = E_4, \text{ and } \frac{I_2 Z_2}{I_1 Z_1} = \frac{I_3 Z_3}{I_4 Z_4}$$

<sup>†</sup> *J. Amer. Chem. Soc.* **50**, 1049 (1928).



## ELECTRICAL CONDUCTANCE OF SOLUTIONS

and if no leakage of current, either to earth or to other arms occurs,  $I_2 = I_1$  and  $I_3 = I_4$ , so that  $Z_2/Z_1 = Z_3/Z_4$ . This is possible only if  $R_2/R_1 = R_3/R_4$ , and  $X_2/X_1 = X_3/X_4$ . (For a discussion of reactance  $X$  and impedance  $Z$ , see p. 30).

In fact the cell, consisting of two parallel plates separated by a dielectric, forms a capacitor, and introduces capacitance into the  $R_4$  arm. This may only be balanced by including capacitance also in the  $R_3$  arm. Thus it is common practice to place a variable capacitor  $C$  in parallel with the variable resistance to balance out any capacity effects in the cell.

Efforts must be made to reduce the possibility of leakage currents. Jones and Josephs† moved all conducting objects away from the bridge, whilst Shedlovsky‡ used symmetrical screening on the bridge arms to produce a 'symmetrical leak'. The screens also minimise pick-up from magnetically induced external currents. Another source of current loss in a bridge of this type is due to possible differences in potential between the headphone and observer, the latter being at earth potential. Efforts are therefore made to keep the headphone at earth potential at balance without directly connecting it to earth; to this end a form of Wagner earth is used (Fig. 10.4).  $R_3$  and  $C_1$  are adjusted to give the best balance, i.e. minimum sound in the headphone. The headphone is then connected to earth by  $S_1$ , and  $R_5$ ,  $R_6$  and  $C_2$  adjusted until minimum sound is again obtained; when the headphone is reconnected to the bridge, it remains at earth potential.  $R_3$  and  $C_1$  are then readjusted to give a new balance point; if necessary the whole process is repeated. As with the screening the application of a Wagner earth does not always improve the performance of the bridge and practical experience is the best guide.

Thus from the practical point of view most conductivity bridges are based upon the simple a.c. Wheatstone bridge. Many designs exist; the salient points of a few will now be mentioned.

A simple laboratory bridge circuit is shown in Fig. 10.5(a) and (b). In this instance  $R_1$  and  $R_2$  are fixed resistors of, say, 45  $\Omega$  and  $lm$  is a slidewire of uniform resistance of approximately 10  $\Omega$ . It is possible to completely 'short-out' either  $R_1$  or  $R_2$  using a

† For references to the work of Grinnell Jones and his collaborators, see p. 253.

‡ *J. Amer. Chem. Soc.* **52**, 1793 (1930).

thick copper connecting link, giving a very wide range of ratios. A schematic diagram of such a ratio-arm is given in Fig. 10.5(a).

The headphone may be replaced by some other detector of

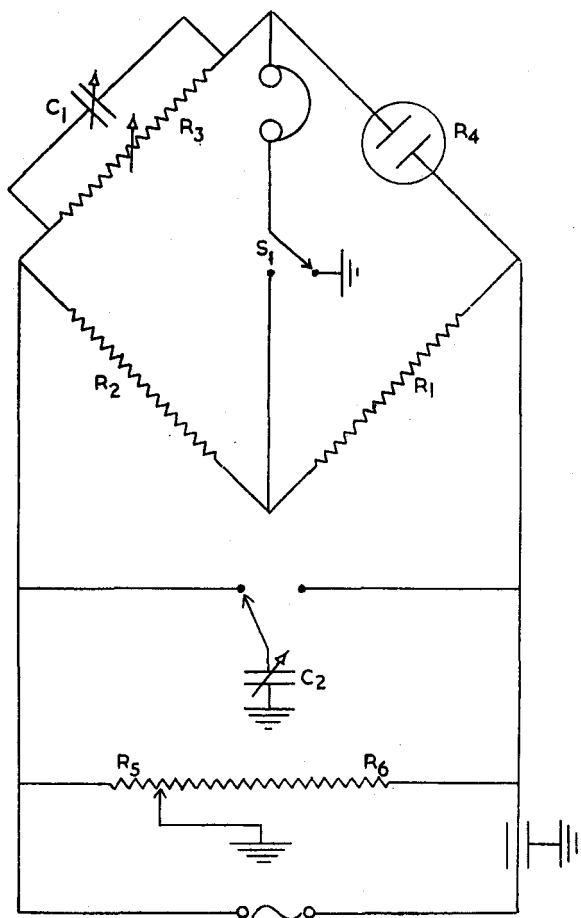
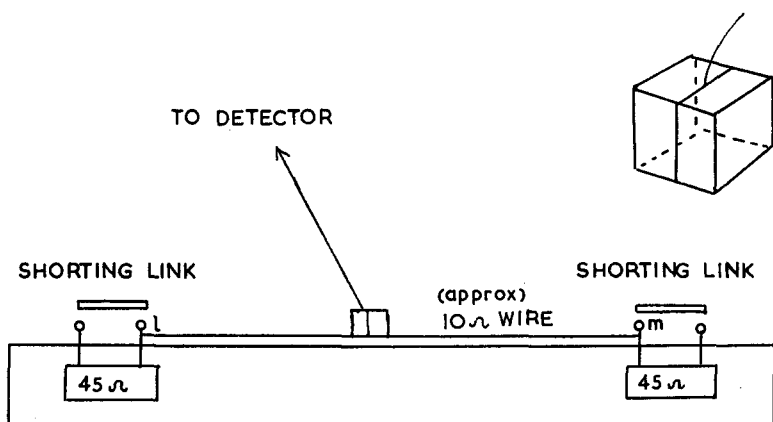
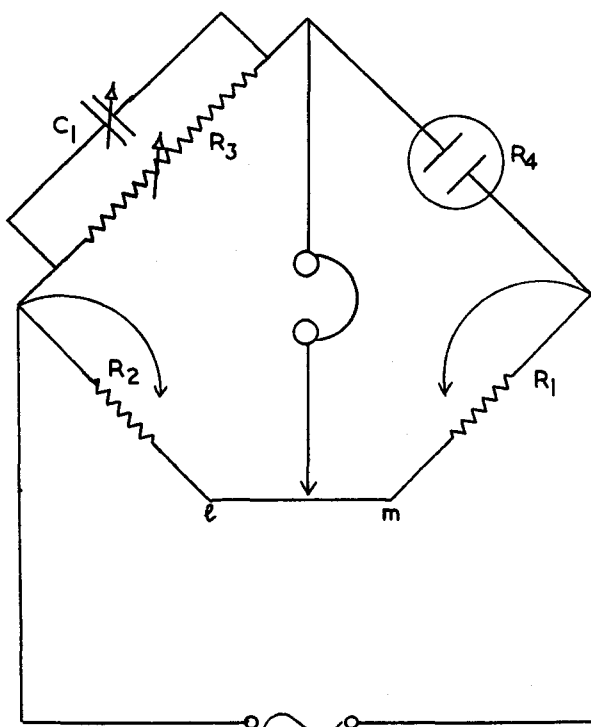


Fig. 10.4. A.C. Wheatstone bridge with Wagner earth

a.c.; e.g. the a.c. may be rectified, amplified and applied to a meter. In some commercial instruments the 'magic eye' (described earlier) is used as detector, whilst in others use is made of a cathode ray oscilloscope (Fig. 10.6). This gives a circular or elliptical trace, degenerating to a line when the bridge is balanced.



(a)



(b)

Fig. 10.5. Practical bridge: (a) slide-wire; (b) circuit diagram of bridge

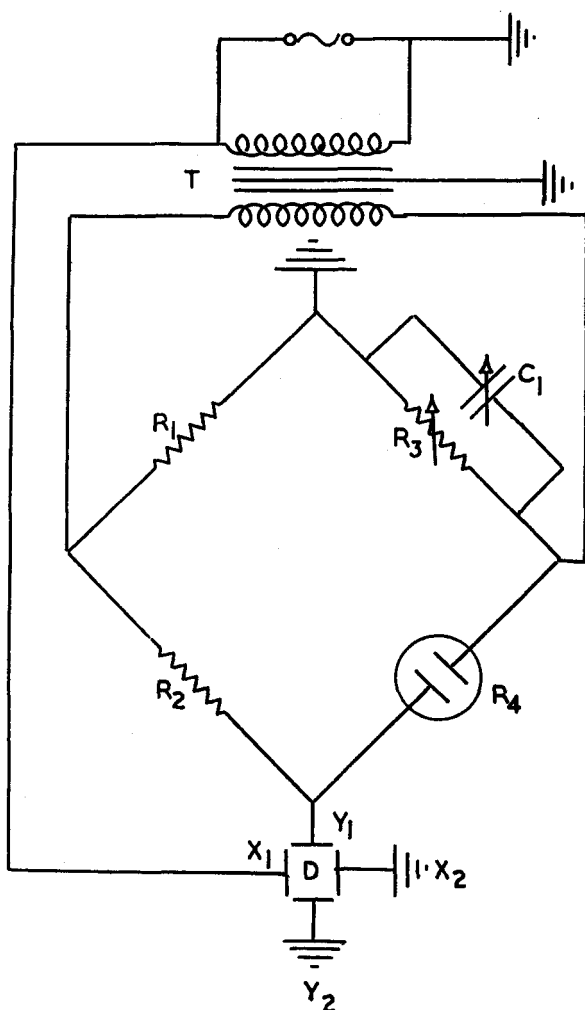


Fig. 10.6. Cathode ray oscilloscope as bridge balance detector:  $T$ , audio transformer matching oscillator to bridge;  $R_1$ ,  $R_2$ ,  $R_3$ , decade resistance boxes;  $R_4$ , conductivity cell;  $C_1$ , decade capacitor, with variable air-dielectric capacitor in parallel;  $D$ , detector. Cathode ray oscilloscope with plates connected as shown

## ELECTRICAL CONDUCTANCE OF SOLUTIONS

$R_1$  and  $R_2$ , the ratio-arm resistances, are often included together in a variable ratio box. Industrially it is often impractical to thermostat the cell and some method of temperature compensation of conductivity must be used. One method involves the substitution of one of the ratio arms by a cell containing an electrolyte whose temperature coefficient is the same as the test solution, and indeed in many cases a further sample of this solution is used. The sealed compensation cell is then enclosed in the same vessel as the measuring electrodes, and consequently it will be subject to the same temperature variations as the *measured solution*.

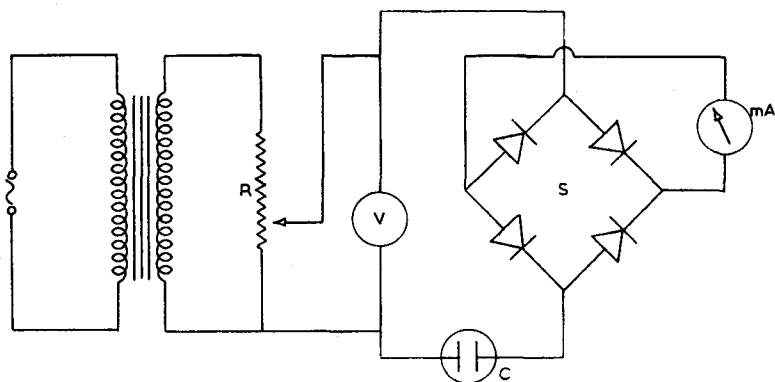


Fig. 10.7. A simple conductivity meter

The very simple, though not very accurate, conductivity meter is used to measure changes of conductivity, as in conductivity titrations. The conductivity is measured by the current flowing in the cell  $C$  when a constant a.c. voltage is applied across it. A circuit is shown in Fig. 10.7. The transformer serves to reduce the input voltage to about 4 V and by means of the potential divider  $R$  the voltage, as read by the a.c. voltmeter  $V$ , is maintained constant. The current which passes is rectified, e.g. by the selenium bridge rectifier  $S$  and measured on a milliammeter.

### The Fixed-resistance Potential Drop Method (Fig. 10.8)

A fixed resistance  $R_1$  is connected in parallel with the conductivity cell  $C$  and the secondary winding  $T_1$  of a transformer which is energised by the a.c. supply  $O$ . If  $R_1$  is small compared with

# LABORATORY AND PROCESS INSTRUMENTS

the electrolyte resistance the potential drop across  $R_1$  is proportional to the conductivity of the solution. Thus it is only necessary to measure this potential using an a.c. potentiometer. As both potentiometer cell and resistance are supplied from the same transformer, variation of mains supply is of little importance. The balance point detector  $D$  which is used depends upon the

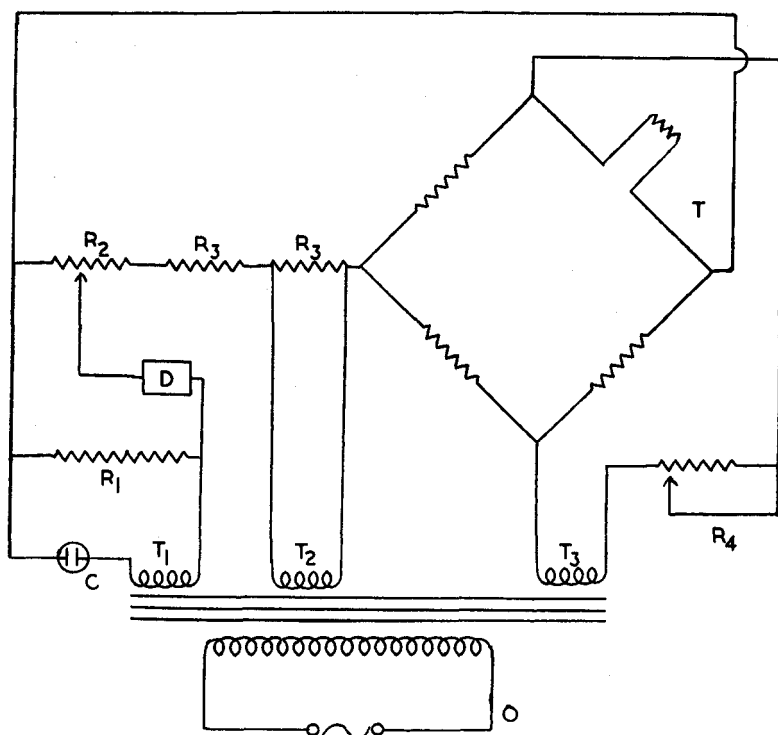


Fig. 10.8. Fixed-resistance potential drop conductance measurement

supply frequency; it may be a valve amplifier-detector and d.c. meter. Industrially 50 c/s mains supply are often used and an a.c. dynamometer galvanometer can be used. In this the exciting magnetic field is produced by an electromagnet supplied from the same transformer. The magnetic field thus varies in step with the alternating electric field produced in the deflecting coil by the measuring circuit, and a deflection is obtained when the bridge is out of balance.

## ELECTRICAL CONDUCTANCE OF SOLUTIONS

To compensate for temperature variation of the electrolyte conductivity a resistance thermometer  $T$  is immersed in the solution under test, this resistance being one arm of a Wheatstone bridge which is powered by current from the secondary winding  $T_3$  of the mains transformer. Should the temperature of the solution change the resistance of  $T$  will change; the bridge will become unbalanced and an additional e.m.f. (positive or negative) will be fed into the potentiometer circuit. This additional e.m.f. can be varied by  $R_4$ , which is so adjusted that it just compensates for changes of cell resistance due to temperature variation.

### A Direct-current Instrument

Industrially, direct-current methods find a great deal of application where high accuracy of measurement is not required. The majority of instruments are designed for solutions having very low conductivities, such as the determination of purity of a water

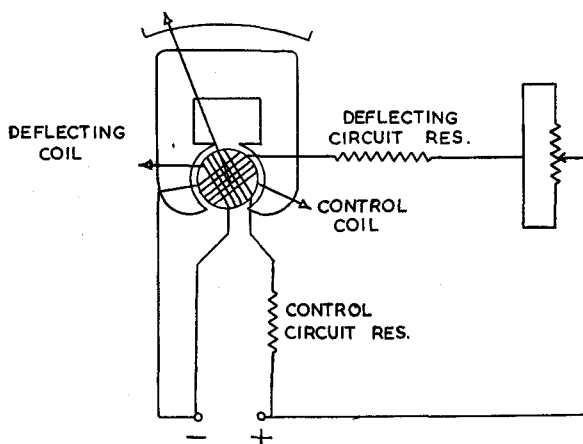


Fig. 10.9. (a) D.C. conductance meter

sample that is almost 'pure'; the current flowing is very small and the polarisation error is also small. Indeed often a constant polarisation error can be assumed and allowance made in calibration of the instrument. These instruments are usually powered by batteries or rectified a.c. mains; the circuit of a typical instrument is shown in Fig. 10.9(a).

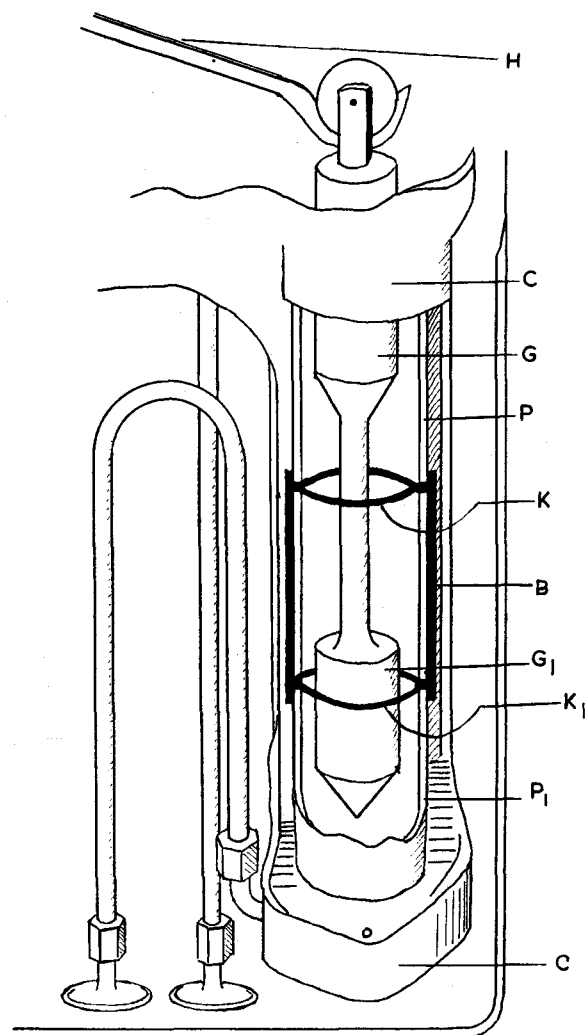


Fig. 10.9. (b) Cell for temperature-compensation of conductivity: *H*, bimetallic strip; *C*, cell casing—negative electrode; *PP*<sub>1</sub>, insulating tubes, separated by conducting cylinder *B*, to which are attached the positive electrodes *KK*<sub>1</sub>; *GG*<sub>1</sub>, float



## ELECTRICAL CONDUCTANCE OF SOLUTIONS

The indicating meter is a specially designed ohmmeter, the moving element consisting of two coils, a deflecting coil and a control coil, which are connected in parallel across the d.c. supply but arranged in such a way as to oppose one another. The deflecting coil is in series with an unknown resistance and the control coil in series with a fixed control resistance. The deflection of the moving coil is thus determined by the ratio of the currents flowing in the two coils, a ratio which is determined by the unknown resistance. Using this technique any effect due to mains-voltage variation is eliminated, whilst control springs in the meter are not necessary. The cell which is used is of ingenious design so as to compensate for temperature variations; it is illustrated in Fig. 10.9(b).

The bimetallic strip  $H$  is temperature-controlled, and moves the 'float'  $GG_1$  so as to compensate for temperature change, by variation of the volume of solution enclosed between electrodes  $PP_1$ .

### The Transformer Bridge

The transformer ratio-arm bridge, recently introduced, overcomes a number of disadvantages of the resistance-ratio Wheatstone bridge, in particular the stray-impedance effects, and the

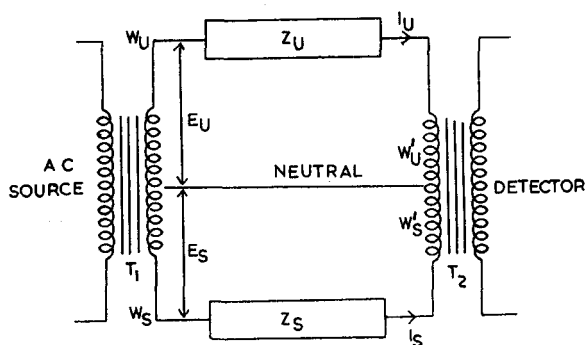


Fig. 10.10. Basic circuit of the transformer bridge

need for a Wagner earth. Screening of the more compact transformer bridge is also simpler. An outline of the transformer bridge is given in Fig. 10.10.

## LABORATORY AND PROCESS INSTRUMENTS

The value of an impedance  $Z$  is defined by the ratio  $E/I$ , where  $E$  is the voltage across the impedance when a current  $I$  is flowing in it, but since it is very difficult to measure  $E$  or  $I$  absolutely with great accuracy this ratio is seldom measured directly—the practice is to make a comparison measurement with a known impedance using a bridge. Adopting the subscripts  $u$  and  $s$  for unknown and standard respectively, since:

$$Z_u = \frac{E_u}{I_u}, \text{ and } Z_s = \frac{E_s}{I_s}, \therefore Z_u = \left( \frac{E_u}{E_s} \cdot \frac{I_s}{I_u} \right) \cdot Z_s$$

This is a fundamental equation for the comparison of impedances, and if  $Z_s$  be a standard fixed impedance, the product of two ratios is involved. In the bridge shown  $T_1$  and  $T_2$  are transformers which for convenience may be called the *voltage* and *current* transformer respectively.  $T_1$  is energised by an a.c. source and the secondary winding is tapped to give  $W_u$  and  $W_s$  turns.

$T_2$  is also tapped to give  $W'_u$  and  $W'_s$  turns, and the secondary winding of this transformer is connected to a tuned detector. In a simple theoretical treatment of the bridge circuit we may assume that the transformers  $T_1$  and  $T_2$  are ideal transformers. Consider the case where  $Z_s$  has been adjusted to a null position; under these conditions zero flux is produced in the current transformer  $T_2$  and there is no voltage drop across its windings. The voltage across the two impedances are  $E_u$  and  $E_s$ , so that the currents may be written as

$$I_u = \frac{E_u}{Z_u}, \quad I_s = \frac{E_s}{Z_s}$$

But since zero core flux condition exists in the current transformer, the algebraic sum of the ampere turns is zero,

$$I_u W'_u = I_s W'_s$$

Substituting for  $I_u$  and  $I_s$  gives:

$$E_u/Z_u \cdot W'_u = E_s/Z_s \cdot W'_s \quad \text{or} \quad Z_u = Z_s \cdot E_u/E_s \cdot W'_u/W'_s$$

Since the transformers are assumed ideal, the voltage ratio is equivalent to the turns ratio on the voltage transformer  $T_1$ , i.e.

$$E_u/E_s = W_u/W_s \quad \text{or} \quad Z_u = Z_s \cdot W_u/W_s \cdot W'_u/W'_s$$

## ELECTRICAL CONDUCTANCE OF SOLUTIONS

Thus it can be seen that two turns ratios are involved, both of which may be of the order of 1000:1 giving an effective ratio of  $10^6:1$  without loss of sensitivity. The practical arrangement of such a bridge is shown where the impedances  $Z_u$  and  $Z_s$  have been divided into reactive and resistive components (Fig. 10.11). Since at balance the in-phase (resistive) and quadrature (reactive) ampere-turns separately sum to zero, the conductance standard

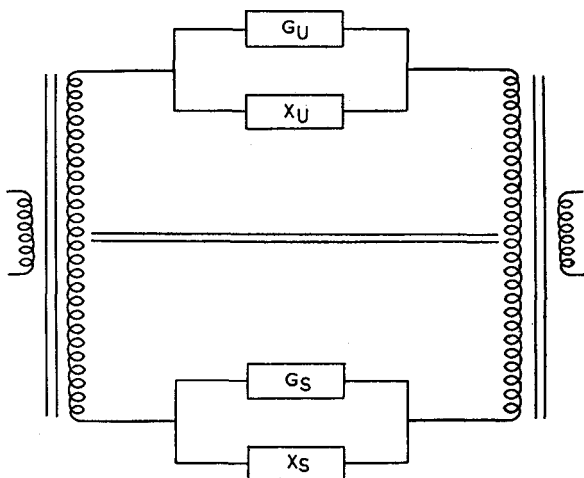


Fig. 10.11. Transformer bridge circuit—resistive and reactive components of bridge impedances

$G_s$  and reactance standard  $X_s$  can be connected to different tapings on the transformers to balance out the currents produced by the unknown impedance.

If the conductance term be considered it can be shown that

$$G_u = G_s \cdot \frac{W_s \cdot W'_s}{W_u \cdot W'_u} = (G_s W_s) \cdot \frac{W'_s}{W_u W'_u}$$

( $G_s$ , the standard conductance,  $= 1/R_s$ ).

It is convenient to consider the term  $(G_s W_s)$  as the standard term, and it is immaterial whether  $G_s$  is maintained constant and  $W_s$  varied, or  $W_s$  kept constant and  $G_s$  varied; both  $W_s$  and  $G_s$  may be varied, and in the industrial bridge the last of these techniques is used, giving rise to the use of relatively few fixed standard conductances. Ideal transformers cannot easily be

produced; in practice, however, the transmission loss between the primary and secondary windings of the voltage transformer only reduces the *sensitivity* of the bridge, which can be compensated by increasing the detector gain. The important factor is the actual voltage ratio between the unknown and standard, both tapped across the secondary windings of the voltage transformer. This ratio is dependent upon (i) the turns-ratio, (ii) the flux linkage, (iii) the effective series impedance of the windings compared with that of the load. The voltage induced in a coil is proportional to the product of the number of turns and the rate of change of flux. Therefore, if all the windings embrace the same flux the ratio of induced voltages is equal to the turns-ratio. Commercially the windings are precision-wound upon a common core of high permeability. The (core flux):(air flux) ratio is of the order of 1000:1 and it is arranged that the air flux is common to both windings. It can be shown that if the windings are so badly arranged that none of the air flux is common the error is only 0.01 %; the series impedance of the windings can be shown to be of negligible importance.

The conventional Wheatstone bridge may be regarded as a two-terminal arrangement; the transformer ratio-arm bridge however, with its 'neutral' connection, may be regarded as a three-terminal arrangement. Diagrammatically the network can be represented as in Fig. 10.12(a) and in bridge form in Fig. 10.12(b).

$Z_{EN}$  shunts the voltage transformer  $T_1$  and  $Z_{IN}$  shunts the current transformer  $T_2$ . At balance no voltage exists across  $T_2$  and the only effect of  $Z_{IN}$  is to reduce the input impedance to the detector, reducing the sensitivity; this can be compensated by increasing the detector gain.  $Z_{EN}$  shunts the windings of the voltage transformer and at balance has the full voltage across it. It thus loads the source, and by drawing current through the source impedance reduces the applied voltage  $E_u$ . The measurement does not depend on the absolute voltage but on the ratio  $E_u/E_s$ . In an ideal transformer this is a constant equal to the turns-ratio, and a shunt on one winding reduces the voltages on all windings in the same proportion. In practice, whilst the transformers cannot be regarded as ideal and shunt impedances will produce small errors, careful construction can reduce the errors to negligible proportions.

# ELECTRICAL CONDUCTANCE OF SOLUTIONS

The transformer bridge may be used with conventional dip-type electrodes, or with an 'electrode-less' cell; the latter is in the form of a loop, coupling the voltage and current transformers. If, in the previous argument, we make  $W_u$  and  $W'_u$  single turns (i.e.  $W_u = W'_u = 1$ ), we have  $G_u = G_s$ .  $W_s W'_s$ . This single-turn coil

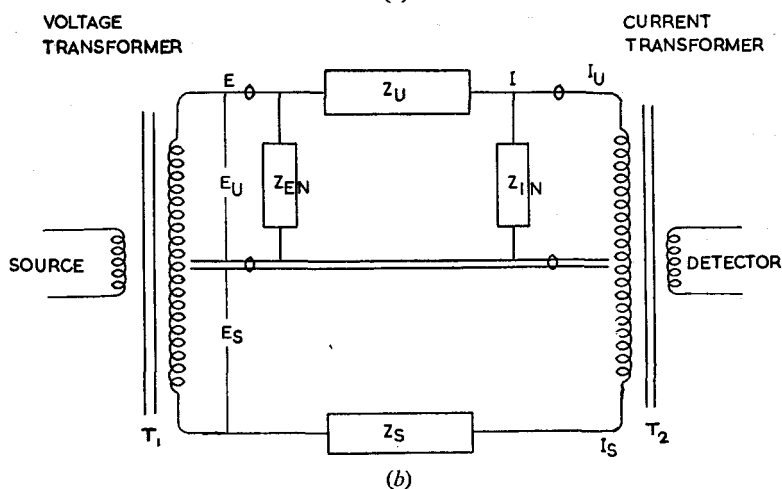
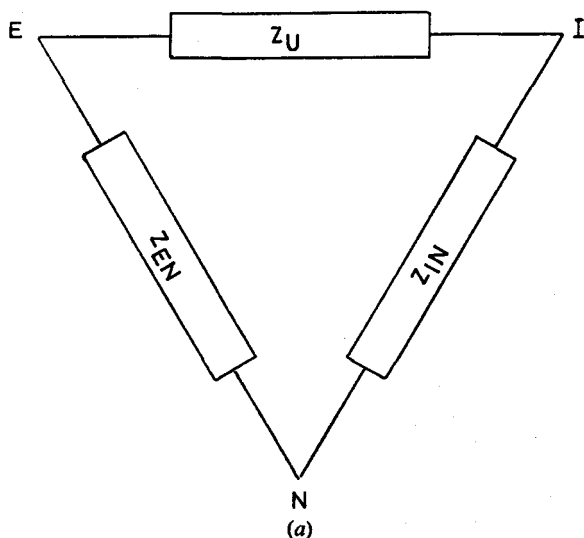


Fig. 10.12. Three-terminal arrangement of the transformer ratio-arm bridge

linking the transformer cores may consist of a closed loop of the conducting solution under test, contained in a glass tube; such a cell is shown in Fig. 10.13.

In this discussion emphasis has so far been placed upon the measurement of conductance; however, the measurement of capacitance, whether alone or with the conductance term, can just as easily be made with the transformer bridge (p. 239).

It is of interest to consider a somewhat controversial point, with regard to the experimental determination of conductivity. It is apparent that the capacitance effect of a conductivity cell is usually balanced by a *parallel* capacitor across the variable bridge resistor. Now the equivalent electrical circuit of a conductivity cell is quite complex; some authors suggest that the simplest approximation is a capacitance and resistance in *series*. Thus a parallel arrangement on the bridge is used to measure a series arrangement in the cell. If the measured parallel capacitance and conductance be  $C_p$  and  $G_p$ , respectively, then

$$C_s = C_p + G_p^2/\omega^2 C_p \quad \text{and} \quad G_s = G_p(1 + \omega^2 C_p R_p) \quad (\text{cf. p. 49})$$

$\omega/2\pi$  is the frequency of the current and  $C_s$  and  $G_s$  are the equivalent series values of capacity and conductance respectively. The use of these formulae often makes a considerable difference to the true values of conductance determined by cell measurements.

### High-frequency Conductivity

It is about ten years since the first papers appeared on the measurement and interpretation of conductance at radio frequencies in cells with external electrodes, and it seems convenient to consider the advantages and limitations of this potentially powerful technique. It differs from the low-frequency conductance measurements already described in two main respects.

1. The frequency is raised from the audio to the radio range; frequencies of 1–50 Mc/s are generally employed, and much higher frequencies have been used for particular purposes.
2. The normal dip-type electrodes are replaced; either the 'cell'—which may be an ordinary beaker or boiling tube—has two metal bands wound round the *outside*, or it may be inserted directly into the oscillator coil.

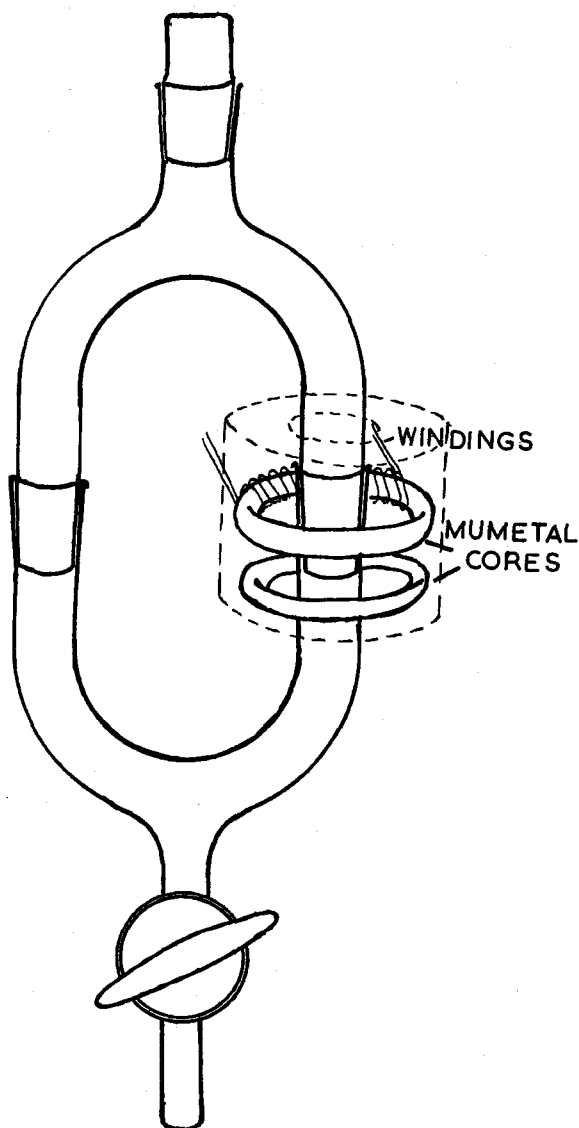


Fig. 10.13. Cell for transformer bridge

External electrodes cannot of course become polarised by the cell contents, or contaminated by a precipitate; their use necessitates raising the frequency. The technique is most suitable for

## LABORATORY AND PROCESS INSTRUMENTS

comparative measurements, e.g. the indication of the equivalence point in a volumetric titration; it is much more difficult to obtain absolute measurements of conductance. The apparatus and methods may in fact be sub-divided according to the object in view.

In absolute-conductance measurements, and in theoretical investigations, the test apparatus of an electronics laboratory has generally been used. As an example, we may consider the arrangement used by Monaghan *et al.*,<sup>†</sup> shown schematically in Fig. 10.14.

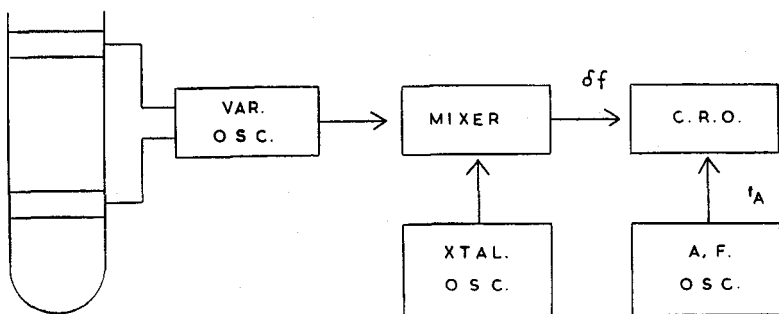


Fig. 10.14. Block diagram of apparatus for the measurement of conductivity at radio frequencies

The variable and crystal oscillators supply the mixer stage, and the difference frequency  $\delta f$  is fed to the X-plates of a cathode ray oscilloscope. The Y-plates are connected to an audio-frequency oscillator, of frequency  $f_A$ . If the variable oscillator is adjusted so that  $\delta f = f_A$ , the oscilloscope trace is circular. Changes in the cell contents, e.g. during the course of titration, alter the frequency of the variable oscillator; the A.F. oscillator is adjusted to restore the circular trace, and the changes in frequency  $f_A$  enable the titration to be followed. With this circuit, the equivalent electrical circuit of the cell may be investigated by the methods indicated later (p. 247), since the changes in  $f_A$  may be related to those caused by resistance-capacitance combinations replacing the cell.

Use has also been made of the simultaneous measurement of capacitance and conductance of the cell and its contents at

<sup>†</sup> Monaghan, Moseley, Burkhalter and Nance (1952). *Analytical Chemistry* 24, 193.



## ELECTRICAL CONDUCTANCE OF SOLUTIONS

radio frequency; for this purpose the 'Twin-T' test bridge, or, for example, the Wayne-Kerr R.F. bridge, with separate oscillator and a radio-receiver as detector, is very suitable.†

Routine analysis has generally employed simpler pieces of apparatus, specifically designed for comparative measurements. Commercial instruments are available in America‡ and in Germany,§ and a similar instrument will shortly appear in this country.|| A brief description of this last follows.

A Clapp oscillator, of high frequency-stability, is driven from a stabilised power supply. The anode current of the oscillator valve is almost 10 mA, but this is 'backed-off' by the reverse voltage developed from a separate stabilised supply, so that *changes* in anode current are registered on a sensitive micro-ammeter. The variations in oscillator current reflect changes in the cell contents, affecting the loading on the oscillator. The backing-off voltage, and the sensitivity of the meter, are both made variable.

In relating changes in the parameter followed to changes within the cell, use is made of the equivalent circuit of Fig. 10.15(a).  $C_2$  is the resultant capacity of the glass-dielectric capacitors, made up of electrode/glass/cell contents.¶  $C_1$  and  $R_1$  are the capacitance and resistance, respectively, of the path between the electrodes *through* the cell contents. A change in conductance within the cell affects mainly  $R_1$ ; change of solvent (i.e. change in dielectric constant) affects mainly  $C_1$ .  $C_2$  remains constant for a given cell and electrode disposition. This circuit reduces to the  $R_p C_p$  parallel combination of Fig. 10.15(b) at frequency  $\omega/2\pi$  if:

$$R_p = \frac{\kappa^2 + \omega^2(C_1 + C_2)^2}{\kappa\omega^2 C_2^2}$$

$$C_p = \frac{\kappa^2 C_2 + \omega^2 C_1 C_2(C_1 + C_2)}{\kappa^2 + \omega^2(C_1 + C_2)^2}$$

where  $\kappa (= 1/R_1)$  is the conductance of the cell contents.

† The Wayne-Kerr Laboratories Ltd., Chessington, Surrey, and Wayne-Kerr Corpn., Philadelphia, U.S.A.

‡ The 'Oscillometer' of E. H. Sargent Inc., Chicago, U.S.A.

§ Wissenschaftlich-Technische Werkstätten, Weilheim, Germany.

|| Messrs. Polymer Consultants Ltd., Britannia Works, Colchester.

¶ The corresponding resistance  $R_2$  in parallel with  $C_2$  is so large as to be negligible, i.e. we consider  $C_2$  as an ideal capacitor.

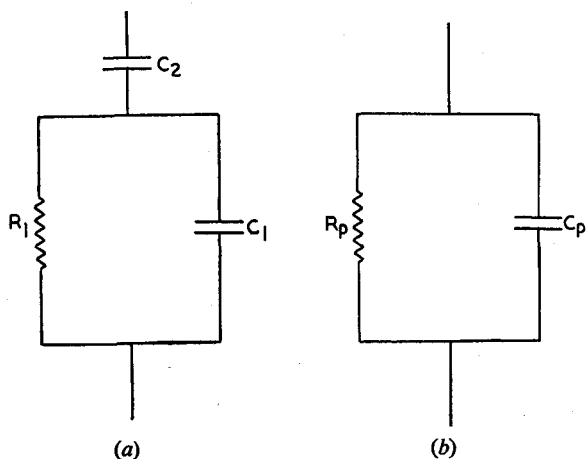


Fig. 10.15. Equivalent circuit of the high-frequency conductivity cell, and the corresponding parallel  $CR$ -combination

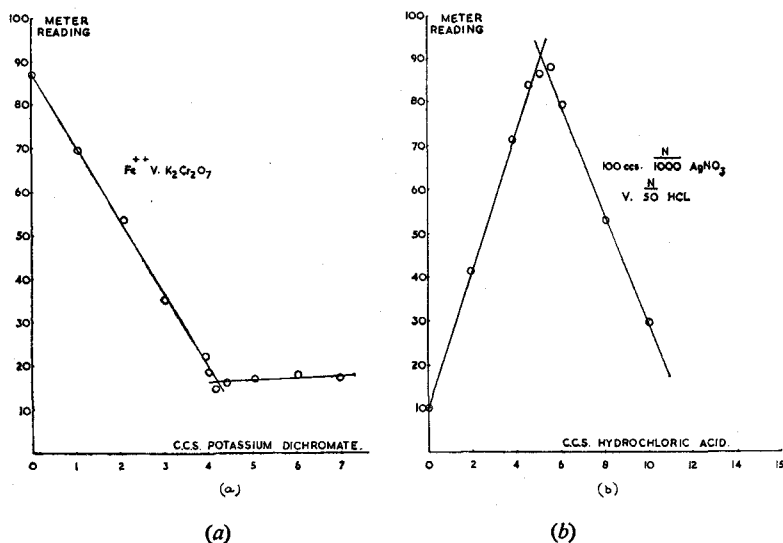


Fig. 10.16. Titration of: (a) Ferrous ethylene diamine sulphate by potassium dichromate; (b) 10 ml N/1000 silver nitrate by N/50 hydrochloric acid

## ELECTRICAL CONDUCTANCE OF SOLUTIONS

By calibration against a standard variable capacitor in place of the cell,  $C_p$  may be found; to interpret this in terms of  $\kappa$ , at a given

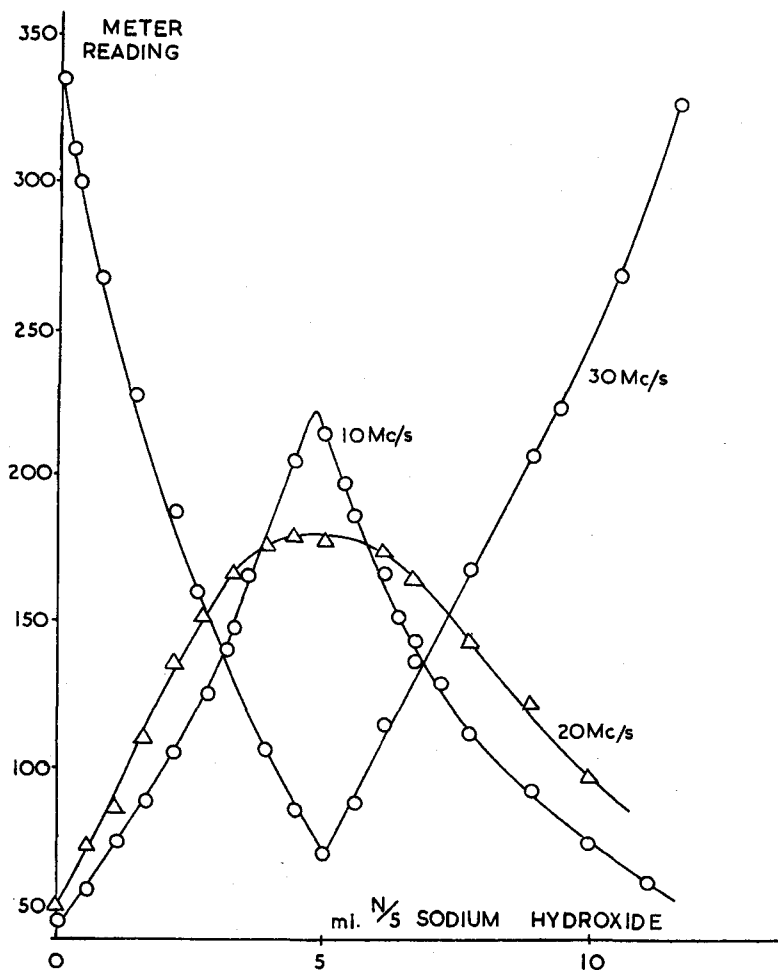


Fig. 10.17. (a) Titration of N/100 hydrochloric acid by sodium hydroxide at frequencies: 10 Mc/s, 20 Mc/s, 30 Mc/s

frequency,  $C_1$  and  $C_2$  are required. Now if the cell is filled with mercury,  $C_p$  reduces to  $C_2$  (since  $\kappa$  is much greater than  $\omega C_2$ , and

# LABORATORY AND PROCESS INSTRUMENTS

$C_1$  is short-circuited); if it is filled with conductivity water  $\kappa \approx 0$ , and

$$C_p = \frac{C_1 C_2}{C_1 + C_2}$$

and, knowing now  $C_2$ ,  $C_1$  may be found. Typical values are:

$$C_p(\text{Hg}) = 28 \text{ pF}; C_p(\text{H}_2\text{O}) = 22.3 \text{ pF}$$

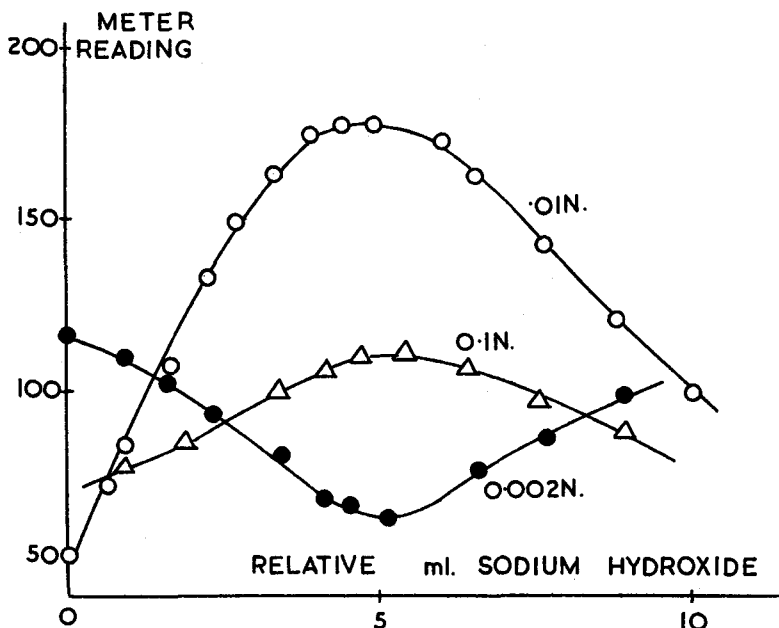


Fig. 10.17. (b) Titration of three electrolyte concentrations. Hydrochloric acid v. sodium hydroxide, at 20 Mc/s

As already explained, in titrations only *changes* in anode current (or some similar variable) are required; typical curves for a number of volumetric estimations, which have been carried out with a practical instrument, are shown in Figs. 10.16(a) and (b). It will be observed that the shape of the titration curve differs in different titrations, as of course it does in low-frequency conductimetric titrations.

One important characteristic of high-frequency titrations is the variation in shape of the titration curve with change of frequency and/or concentration.

## ELECTRICAL CONDUCTANCE OF SOLUTIONS

In Fig. 10.17(a), meter readings are recorded for the titration of 0.01N HCl, at three frequencies; in Fig. 10.17(b), the middle frequency is employed in the titration of three concentrations of HCl. Evidently, the frequency should be chosen for optimum sensitivity near the equivalence point.

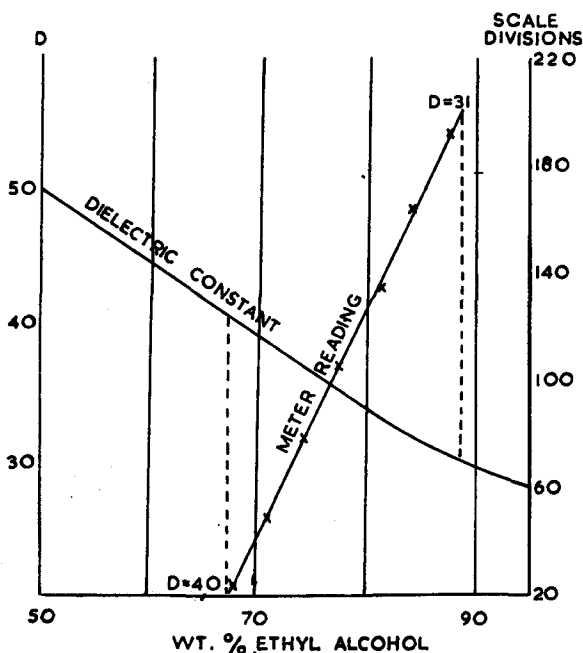


Fig. 10.18. Dielectric constant of ethanol-water mixtures and corresponding meter reading

As an example of change in dielectric constant, at constant conductance, the effect of adding water to ethanol is shown in Fig. 10.18; sensitivity falls off outside the range within the vertical dotted lines.

In order to retain sensitivity at higher concentrations, much higher frequencies have been used. Lane† suggests that a frequency of 250 Mc/s may be used for concentrations up to 0.7 normal.

† E. S. Lane (1957). *Analyst* 82, 406.

## LABORATORY AND PROCESS INSTRUMENTS

Instead of backing-off the anode current, a direct reading microammeter may be connected in the grid circuit, and its indication used to determine the titration end-point. Anode and grid meter readings are compared, for the titration of N/100 hydrochloric acid by sodium hydroxide, in Fig. 10.19.

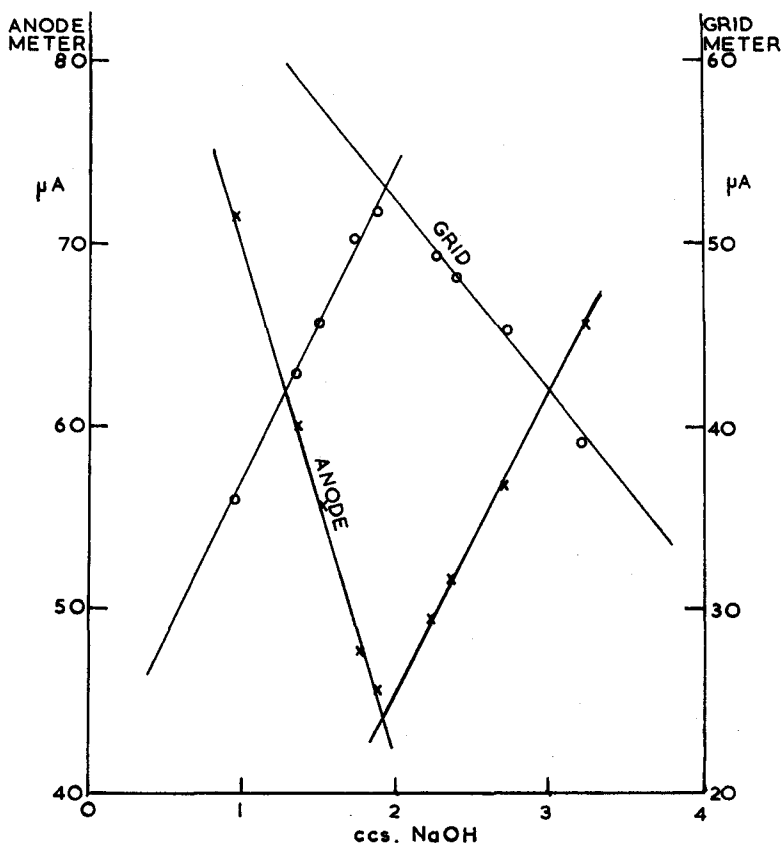


Fig. 10.19. Comparison of anode and grid meters in the titration of 100 ml N/100 hydrochloric acid by N/2 sodium hydroxide

The high-frequency titration technique has been employed for a large and varied series of estimations—some of which are listed in the bibliography at the end of this chapter. We may summarise by saying that this method is a rapid and direct method for

## ELECTRICAL CONDUCTANCE OF SOLUTIONS

following changes in conductance and/or dielectric constant, such as arise in the course of various chemical reactions; it is, however, very difficult to convert the results to an absolute scale of measurement.

### References

- DAVIES, C. W. (1933). *Conductivity of Solutions*. Chapman and Hall.  
GRIFFITHS, V. S. *et al.* (1958). *J. Phys. Chem.* **62**, 47.  
JONES, G. and BOLLINGER, G. M. (1931). *J. Amer. Chem. Soc.* **53**, 411;  
(1935) **57**, 280.  
JONES, G. and BRADSHAW, B. C. (1933). *J. Amer. Chem. Soc.* **55**, 1780.  
JONES, G. and CHRISTIAN, S. M. (1935). *J. Amer. Chem. Soc.* **57**, 272.  
JONES, G. and JOSEPHS, R. C. (1928). *J. Amer. Chem. Soc.* **50**, 1049.  
LADD, M. F. C. and LEE, W. H. (1960). *Laboratory Practice* **9**, 98.  
LADD, M. F. C. and LEE, W. H. (1960). *Talanta* **4**, 274.  
ROBINSON, R. A. and STOKES, R. H. (1959). *Electrolyte Solutions*, 2nd edition. Butterworth.

### Problems

1. The electrical conductivity of solutions may be measured using a.c. and d.c. techniques. Describe apparatus suitable for making both types of measurements emphasising the limitations of the methods.

2. A conductivity cell is filled with a solution of potassium chloride containing 0.150 g of salt per litre. The resistance of the cell is 17.55  $\Omega$ . Given that the specific resistance of the solution at the temperature of the experiment is  $2.70 \times 10^{-3} \text{ ohm}^{-1} \text{ cm}^{-1}$ , calculate the cell constant of the cell. Show how this constant may be used in the evaluation of the equivalent conductivity of any other solution which would give sensible experimental results if used in this cell.

*Answer.* 0.0474.

3. 'The transformer ratio-arm bridge offers great advantages in the measurement of the conductivity of electrolyte solutions.' Discuss this statement critically.

4. What are the advantages and disadvantages of 'electrodeless' (radio-frequency) conductivity measurement, as compared with the low-frequency internal electrode technique?

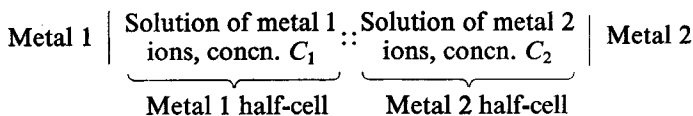
## CHAPTER XI

### Section I: The Measurement of Electromotive Force and Electrode Potential

The measurement of electromotive force and the determination of electrode potential is of importance in many electrochemical studies, and in 'pH' measurement; some theoretical principles involved will first be discussed.

#### Electrode Potentials

When a metal rod is immersed in a solution of one of its salts a redistribution of charge occurs; the metal tends to dissolve to form positive ions leaving the metal electrode itself negatively charged: at the same time the metal ions in solution tend to deposit on the electrode, charging it positively. Equilibrium is soon established, when these two processes occur at equal rates; the position of equilibrium depends upon the concentration of metal ions in the solution, the nature of the electrode system and the temperature. In a normal solution of its ion zinc acquires a negative potential, since the tendency to dissolve predominates; copper, on the other hand, gains a positive potential by deposition from a normal solution of cupric ions. These two electrode systems, often in a modified form, are combined in the familiar Daniell cell, so that the cell e.m.f. is the algebraic sum of the electrode potentials set up; we may ignore at this stage any e.m.f. set up at the solution interface (the 'liquid junction' potential). The generalised form of such cells is written:



The symbol '::' denotes that the solutions are not free to mix with one another and also that the liquid junction potential has been minimised (p. 260).



## THE MEASUREMENT OF ELECTROMOTIVE FORCE

If we chose the metal 1 half-cell as reference standard we could compare the electrode potentials of a series of other metals by combining them with metal 1 in cells of the type shown. This in

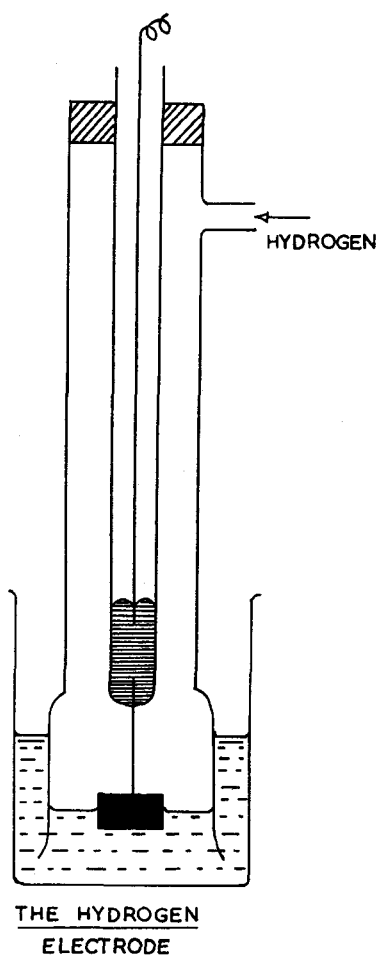
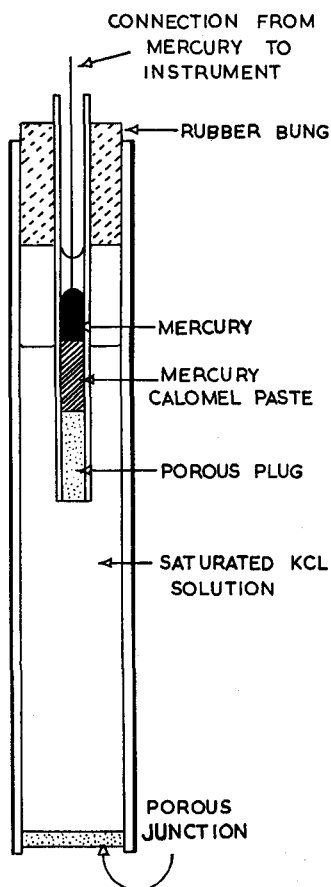


Fig. 11.1. Hydrogen electrode

fact is done; the reference half-cell however is the Normal Hydrogen Electrode, as suggested by W. Nernst (Fig. 11.1). Hydrogen gas at a partial pressure above the solution of 1 atmosphere bubbles through a solution containing hydrogen ions, and

## LABORATORY AND PROCESS INSTRUMENTS

over the surface of the platinum foil electrode. The electrode surface is coated with finely-divided platinum ('platinum black'), and the solution contains hydrogen ions at unit activity.† The



THE REFERENCE  
CALOMEL ELECTRODE

Fig. 11.2. Standard calomel electrode

† For our purpose we may define the activity of an ion in solution as its *effective* concentration; because of interionic attractions the activity is lower than the actual concentration except in very concentrated solutions. Thus in 1.228 normal hydrochloric acid solution, the hydrogen ion activity at 25°C is 1.000.

## THE MEASUREMENT OF ELECTROMOTIVE FORCE

platinum black speeds-up the attainment of equilibrium in the process:  $2\text{H}^+ + 2e \rightleftharpoons \text{H}_2$ .

Thus, if a cell is constructed with the normal hydrogen electrode (N.H.E.) as one half-cell, the potential of the other electrode  $E_X$  may be expressed  $E_X = E_{\text{cell}} - E_{\text{N.H.E.}}$ . Now by convention we take the electrode potential of the normal hydrogen electrode as zero, i.e.  $E_{\text{N.H.E.}} = 0$ , and the unknown potential  $E_X = E_{\text{cell}}$ .

It is not necessary to make the partial pressure of hydrogen exactly one atmosphere, or the activity of hydrogen ions exactly unity; corrections may be made for departure from these standard states. Nevertheless the hydrogen electrode is rather inconvenient, necessitating a cylinder of hydrogen gas, an accurate manometer, and a freshly platinised (i.e. coated with platinum black) electrode. More convenient electrode systems, whose potentials have been accurately determined with respect to the normal hydrogen electrode, are used as secondary standards. The standard calomel electrode, which is a very convenient reference electrode, is shown in Fig. 11.2. It will be noticed that the mercury-calomel paste electrode eliminates the strain potential sometimes present in metals and that the electrode potential varies according to the concentration of chloride ion in the adjacent solution, as follows:

0.1N KCl, $E = 0.3338\text{ V}$ at $25^\circ\text{C}$	
1.0N KCl, $E = 0.2880\text{ V}$	„
Saturated KCl, $E = 0.2415\text{ V}$	„

## Hydrogen Ion Concentration and the pH Scale

In conjunction with a suitable reference electrode, the hydrogen electrode could be used to determine the concentration (or, more exactly, the *activity*) of hydrogen ions in a given solution. For a normal solution of a strong† acid this concentration is 1.0; in a normal solution of sodium hydroxide the hydrogen ion concentration is  $10^{-14}$ . In 1909 Sørensen introduced the very convenient pH scale of hydrogen ion concentration: if the concentration is  $C$  g-ions per litre of solution,  $\text{pH} = -\log_{10} C$ ; thus for

† A 'strong' acid or alkali is one which is fully dissociated into its ions at concentrations below approx. 2 normal.

the two solutions mentioned the pH of the acid is 0, and of the alkali, pH = 14. The potential of a hydrogen electrode in an aqueous solution is given by:

$$E = -1.983 \times 10^{-4} T \cdot \text{pH} - 0.9915 \times 10^{-4} T \log_{10} p_{\text{H}_2}$$

where  $T$  is the absolute temperature and  $p_{\text{H}_2}$  is the partial pressure of hydrogen gas above the solution. At a fixed  $p_{\text{H}_2}$ , the potential is evidently proportional to the pH of the solution.

For convenience, the hydrogen electrode is usually replaced by a secondary electrode which does not require the use of hydrogen gas (e.g. the glass electrode, p. 260). In order to determine the pH of a solution, the secondary electrode is combined with a reference electrode (e.g. the calomel electrode) and the e.m.f. of the resulting cell measured. In principle, the e.m.f. could be measured by a voltmeter, but in practice this results in too large a current being drawn from the cell, so that a potentiometer or valve voltmeter is used. (For further discussion on electrode reactions and potentials, and on the significance of pH in various solutions, reference may be made to the texts quoted at the end of this chapter.)

### Potentiometric Measurement

In Fig. 11.3,  $AA$  is a thin wire of uniform resistance on which the sliding contact  $B$  moves;  $W$  is a Weston cadmium cell, and  $C$  a 2 V accumulator. With switch  $S$  in the 'calibrate' position ( $S_1$ ) contact  $B$  is moved until the galvanometer  $G$  registers no deflection; the length  $AB$  is noted,  $AB_s$ , say. With the switch in position  $S_2$  the unknown cell  $U$  replaces the Weston cell, and a new balance point is found,  $AB_u$ ; then  $E_u = E_s \cdot AB_u / AB_s$ , where  $E_u$  and  $E_s$  are the e.m.f.s of the unknown and the standard cell, respectively.

To achieve adequate sensitivity an extremely long slide wire  $AA$  would be needed, and it is general practice to replace the wire by a number of series combinations of resistance coils and a short slide wire. The dials are standardised to indicate the e.m.f. directly; when the switch is set to position  $S_1$  ('standardise'), an internal connection sets the contact to position  $AB_s$  corresponding to the voltage of the standard cell,† and resistance  $R$  is

† For the Weston cell the e.m.f. at  $t^\circ\text{C}$  is given by:

$$1.018300 - 4.6 \times 10^{-5} (t - 20) - 9.5 \times 10^{-7} (t - 20)^2 \text{ volts}$$

### THE MEASUREMENT OF ELECTROMOTIVE FORCE

varied to produce the balance. The potentiometer is now standardised to read directly in volts, and its resistance coils and slide-wire may be calibrated.

This method of determining the e.m.f. of a cell, known as the Poggendorf compensation method, can be used where the internal resistance of the unknown cell is relatively small—a few thousand ohms; such is the case with low-resistance electrode systems, e.g. the hydrogen, quinhydrone or antimony electrodes

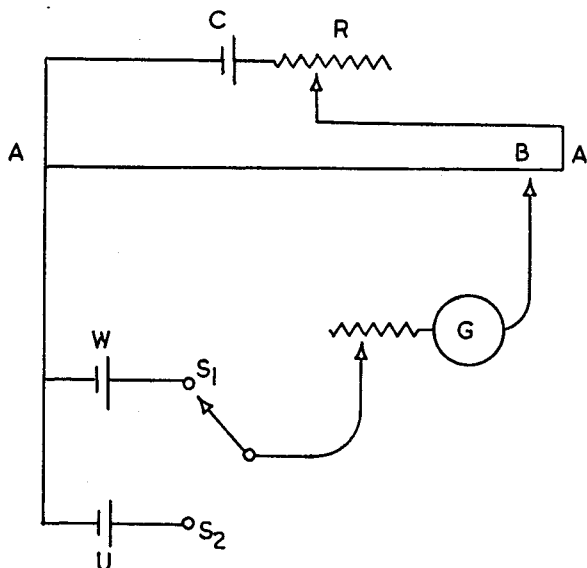


Fig. 11.3. Simple potentiometer circuit

combined with a calomel electrode (p. 257). This type of potentiometer is also used to measure the e.m.f. generated in a thermocouple circuit. Thermocouple potentiometers in which the potentiometer, galvanometer, standard cell and driving cell are placed in one case, may be calibrated in temperature units; the e.m.f.s to be measured are comparatively small.

However, as the internal resistance of the cell increases the current which can be drawn without invalidating the measurement rapidly decreases and the conventional galvanometer must be replaced by a more sensitive device such as a quadrant

electrometer, or the more convenient electrometer-valve voltmeter (p. 177). The important practical combination of the glass and calomel electrodes is a high-impedance system of many megohms which requires this form of potentiometer.

### The Glass Electrode

It has already been shown that the hydrogen electrode can be used to measure the pH of a solution and it is the most precise electrode for this purpose. However, it is inconvenient to set up and other more convenient hydrogen-ion electrode systems, e.g. the quinhydrone and antimony electrodes, have been used. The former of these may be used below a pH value of 8, whilst the latter, although robust, requires some time to reach equilibrium and cannot be used in the presence of oxidising or reducing agents, or in the presence of certain metals which deposit on the antimony. Thus whilst being of some importance, such electrodes can hardly be described as versatile. The *glass electrode*, however, is unaffected by most chemical substances, and when specially constructed may effectively cover the whole pH range; as such it is the most versatile secondary pH electrode. Some of its limitations will be mentioned later.

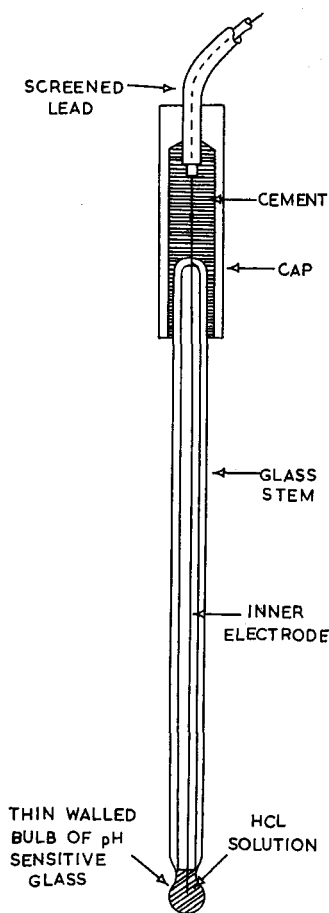
The electrode (Fig. 11.4) consists of a thin glass bulb, made of relatively conducting glass, attached to a stem of stouter non-conducting glass. If now the bulb is filled with a dilute solution of an acid, and the whole immersed in a solution also containing hydrogen ions, a potential is developed across the glass membrane which is proportional to the difference in hydrogen ion concentration between the liquids in contact with the two sides of the membrane. Since the bulb is filled with a solution of fixed hydrogen ion concentration, the potential developed is a measure of the hydrogen ion concentration or pH of the solution outside the bulb. In order to measure the potential developed, a cell must be set up as illustrated:

Reference electrode	Glass membrane	Solution of unknown pH	Salt bridge	Reference electrode
------------------------	-------------------	---------------------------------	----------------	------------------------

The 'salt bridge' is a device for minimising the liquid junction potential; it can be shown that this is achieved if the liquids are

## THE MEASUREMENT OF ELECTROMOTIVE FORCE

joined by a concentrated electrolyte solution in which the cation and anion have practically equal ionic conductances. Thus, the salt bridge is in practice a concentrated aqueous solution of



A GLASS ELECTRODE

Fig. 11.4. Glass electrode

potassium chloride or ammonium nitrate; free diffusion is prevented by a sintered glass disc between this and the adjacent solutions, or by adding agar agar to the hot solution so that it sets, on cooling, to a conducting 'jelly'.

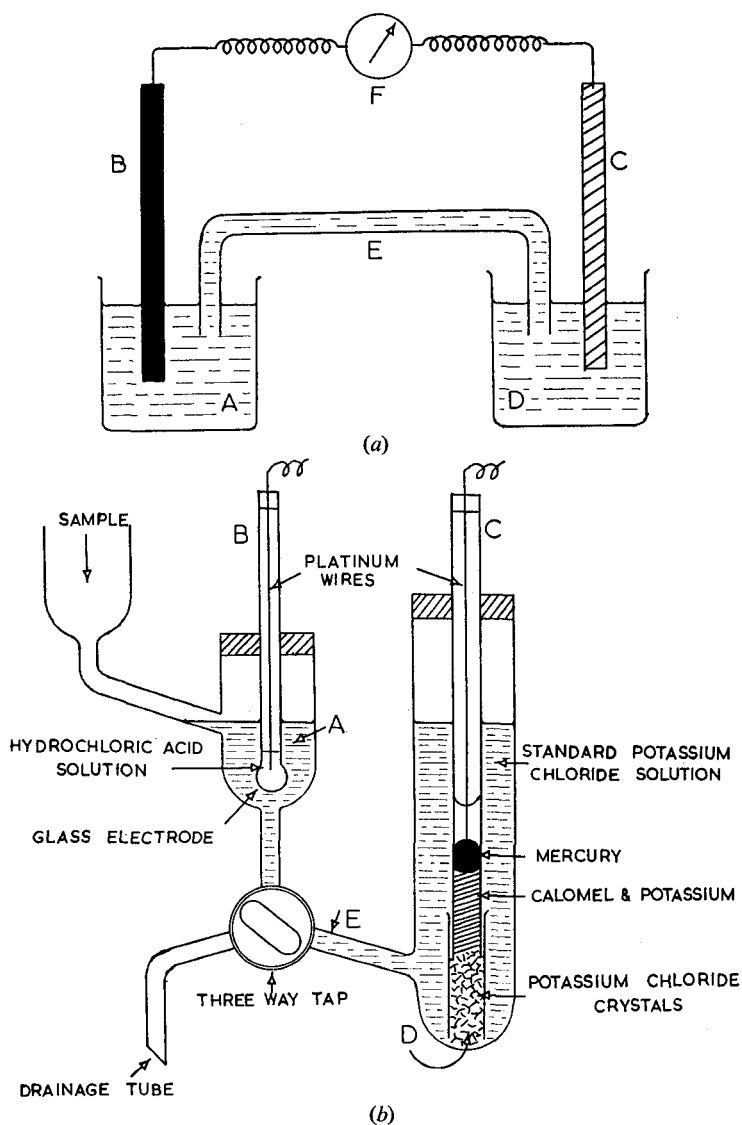
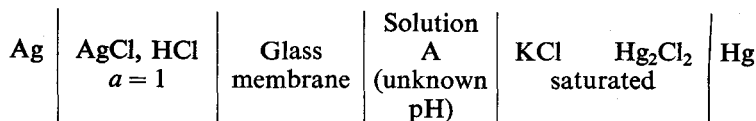


Fig. 11.5. A typical electrode assembly: (a) Diagrammatic. *A*, sample solution; *B*, suitable electrode (e.g. glass); *C*, reference electrode (e.g. calomel); *D*, standard solution; *E*, liquid junction, or salt bridge; *F*, potentiometer or indicator. (b) A practical glass electrode assembly (Morton pattern)



## THE MEASUREMENT OF ELECTROMOTIVE FORCE

In Fig. 11.5, the glass electrode is combined with a saturated-KCl calomel electrode to form a complete cell; the potassium chloride solution forms the salt bridge. The complete cell may be written:



Some of the limitations of the glass electrode will be mentioned briefly. Firstly, the glass membrane has a very high resistance (10–100 MΩ), necessitating the use of a valve voltmeter of high-input impedance. This also requires that the insulation resistance of the leads, supports, etc., must be extremely high (100,000 MΩ), and consequently these must be kept short and made of highly-insulating materials with good moisture-resisting properties. Modern insulators such as polythene, P.T.F.E. and silicone rubber have suitable insulating properties and it has been found helpful to coat the upper part of the electrode with water-repelling silicone oil.

Secondly, using a normal glass, i.e. sodium glass as the electrode, errors may arise in alkaline solutions (above pH 9), known variously as the cation error, the sodium ion error and the alkali error; these become considerable at pH values above 11. The error arises from the mechanism by which the glass electrode operates and which is still not completely elucidated. Basically, however, the glass acts as a conductor due to the sodium ions contained in it, and to the fact that water and its ions are able to pass through the membrane; when the membrane separates two solutions of different hydrogen ion concentration it may be assumed that the potential develops by virtue of transfer of hydrogen ions from the higher to the lower activity. Even when the solutions on the two sides of the membrane have the same hydrogen ion activity a potential difference often exists. This is the *asymmetry potential*, which varies from day to day, and is probably produced by strain in the glass because of the different treatment of the two sides of the membrane. Such potentials are often produced when the electrode surface is allowed to dry out, or if it has been immersed in strong acid or alkali; the asymmetry potential may be very considerably reduced by immersing the

electrode in N/10 hydrochloric acid for about 24 hours. By virtue of its structure the glass electrode is sensitive to the transfer of other cations; in alkaline solutions, particularly at elevated temperature, some cations readily penetrate the glass electrode leading to a low indicated pH value. The effects of various cations have been listed; the largest error is produced by the sodium ion, with lithium ion producing about half the sodium value, and the majority of cations producing errors of about one-tenth that due to sodium. The alkali error is reasonably reproducible and

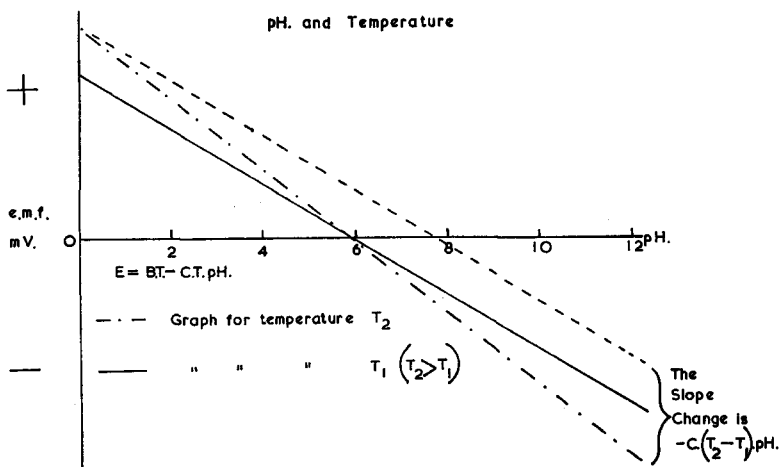


Fig. 11.6. E.M.F./pH graph at temperatures  $T_1$  and  $T_2$

may be allowed for; alternatively, by use of 'high alkalinity electrodes' the error is made very much smaller. These electrodes are made of special glass containing lithium, potassium, caesium or mixtures of these elements for use in strongly alkaline solutions.

In addition, a temperature error may also exist. Firstly, the pH of a solution may vary with temperature, the extent of the variation depending upon the nature of the solution. Further, the e.m.f. developed by the type of cell shown is given by:

$$E = A + BT - CT.pH$$

where  $A$  and  $B$  depend upon the nature of the electrodes,  $C$  is the Nernst equation temperature coefficient ( $1.983 \times 10^{-4}$  per  $^{\circ}\text{C}$ ) and  $T$  the absolute temperature.

## THE MEASUREMENT OF ELECTROMOTIVE FORCE

Now in practice the cell is calibrated using solutions of known pH (*buffer solutions*); since  $A$  is independent of both pH and temperature, by modifying the bias of the measuring circuit the equation can be reduced to  $E = BT - CT \cdot \text{pH}$ , and a graph illustrating this effect is shown in Fig. 11.6.

Consideration of the graph shows how the relationship between e.m.f. and pH will vary with temperature and the zero shift. It is possible to compensate for these errors in *pH meters*.

### Measurement of E.M.F.s Produced in High Resistance Electrode Systems

A typical glass electrode has a resistance of  $100 \text{ M}\Omega$ , and if an accuracy of  $0.02 \text{ pH}$  units is required it is necessary to measure the electrode potential to at least  $1 \text{ mV}$ . Thus the detector must

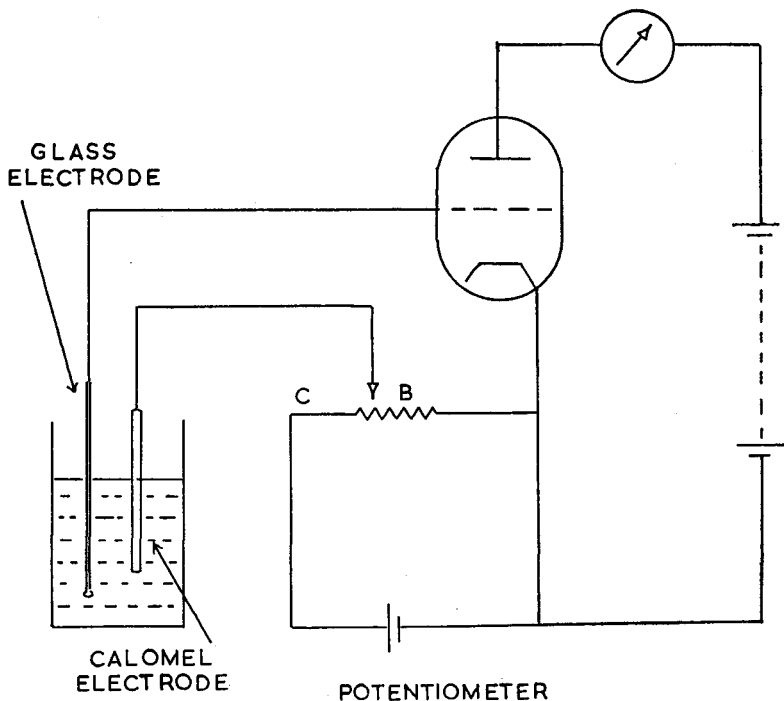


Fig. 11.7. Electrometer triode and milliammeter as indicator in a potentiometric circuit

## LABORATORY AND PROCESS INSTRUMENTS

be sensitive to at least  $10^{-11}$  amp; nowadays valve voltmeters are frequently used for this purpose. These incorporate an electrometer valve (p. 177), the main characteristics required being: very low grid current, stable anode current for a fixed electrode potential and the maximum mutual conductance, consistent with the other requirements, for adequate sensitivity.

The electrometer valve may be used in a null-deflection instrument using a potentiometer (Fig. 11.7). The voltage generated by the cell is opposed by a known voltage from an ordinary

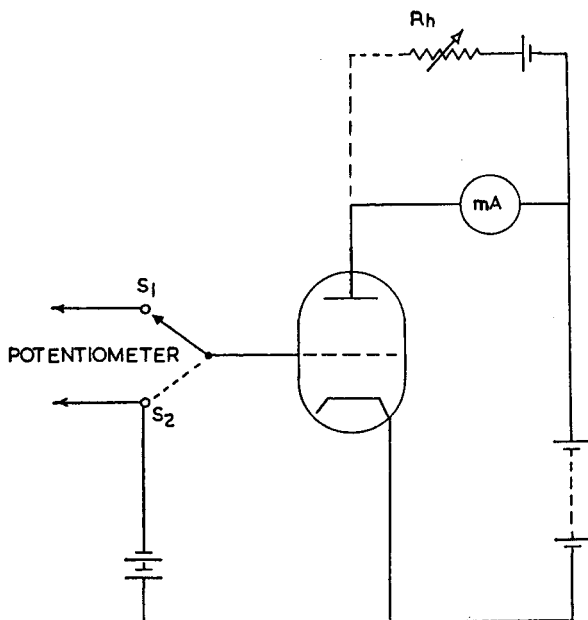


Fig. 11.8. Null-indicating potentiometer. Anode current meter with backing-off circuit

potentiometer. Under these circumstances there will be zero voltage on the grid of the valve, which is indicated by a meter in the anode circuit. This is simply an extension of the simple potentiometer circuit in which the galvanometer is replaced by an electrometer-valve voltmeter.

In previous chapters it has been shown that for a triode valve a relatively large anode current can be controlled by small changes in grid voltage, whilst drawing very little grid current. In the

## THE MEASUREMENT OF ELECTROMOTIVE FORCE

case of an electrometer valve the grid current may be as low as  $10^{-15}$  amp; for a valve with a mutual conductance of  $5 \times 10^{-5}$  amp/V, a change of 1 mV in the grid voltage produces a *change in anode current* of  $5 \times 10^{-8}$  amp. Such a valve passes an anode current of 40  $\mu$ amp, and it is necessary to 'back-off' the standing current so that the sensitive detecting meter responds only to the *change* in anode current.

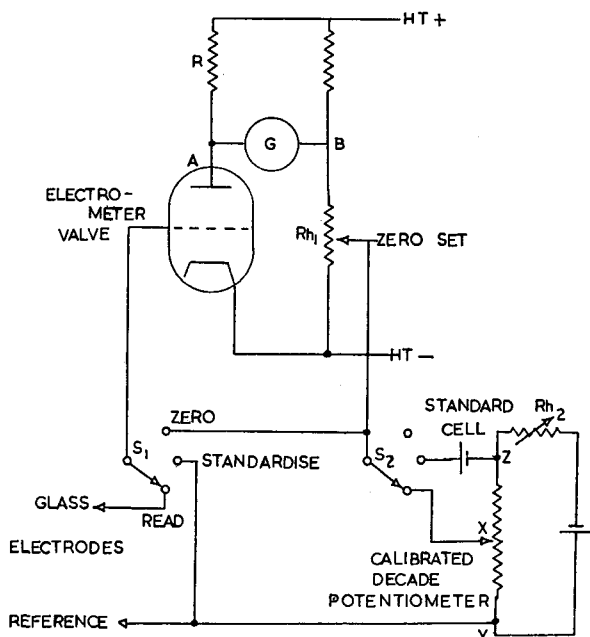


Fig. 11.9. Basic circuit of pH meter ( $S_1$  and  $S_2$  are ganged)

With the switch in position  $S_2$  (Fig. 11.8) the backing-off rheostat  $Rh$  is adjusted until no deflection is shown by the meter.

The switch is now moved to  $S_1$ , and the potentiometer readjusted for zero. The points  $S_1$  and  $S_2$  are now at the same potential, and the unknown e.m.f. may be read from the potentiometer—the valve circuit again simply replacing the potentiometer galvanometer. This combination of valve voltmeter and laboratory type potentiometer is quite satisfactory, and they may be combined in one instrument to give a pH meter; the basic circuit is shown in Fig. 11.9.

## LABORATORY AND PROCESS INSTRUMENTS

With the ganged selector switch  $S_1 S_2$  in the 'zero' position, the 'set zero' rheostat  $Rh_1$  is adjusted so that no current flows in the galvanometer. With the selector switch in the 'standardise' position, the e.m.f. of the standard cell will act in opposition to the potential difference across the potentiometer wire  $YZ$ .  $Rh_2$  is adjusted to give null deflection, when the potential difference across  $YZ$  equals the e.m.f. of the standard cell, and the wire is calibrated. In the 'read' position the cell potential acts in opposition to the potential difference across the wire  $XY$ , and by moving  $X$  until zero deflection is obtained, the potential represented by  $XY$  is the cell potential. In practice, the slide-wire is calibrated both in volts and in pH units.

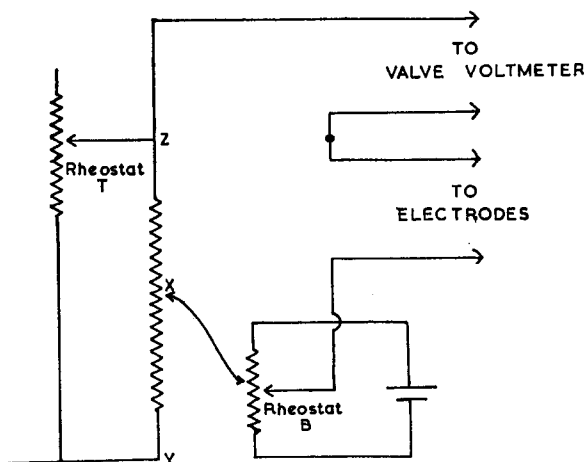


Fig. 11.10. Temperature-compensation circuit

We have seen that temperature compensation must be applied if the potentiometer wire is to be directly calibrated in pH units, and this may be achieved by the following circuit (Fig. 11.10). The temperature adjustment is made by adjusting rheostat  $T$  which is in parallel with the potentiometer wire  $YZ$ . The potential difference decreases as  $T$ , which is calibrated in  $^{\circ}\text{C}$ , decreases. Consequently  $T$  is adjusted to the temperature of the solution and  $X$  set to the known pH of the buffer solution at the standard temperature. With the switch in the 'read' position, rheostat  $Rh_B$  is then adjusted for balance; the potentiometer circuit of

## THE MEASUREMENT OF ELECTROMOTIVE FORCE

which  $Rh_B$  is part compensates for the  $A$  term (which varies from cell to cell) in the equation:

$$E = A + BT - CT.pH$$

The instrument now records directly the pH of the solution under investigation, at the temperature of measurement.

The potentiometer-type instrument requires a steady d.c. voltage to be applied to the potentiometer, so that many of these instruments are battery-operated.

### Direct Reading Instrument

In principle this type of instrument could be represented by the circuit of Fig. 11.7, with slider  $B$  moved to  $C$ , so that the voltage from the cell is applied between the grid and cathode of the valve;

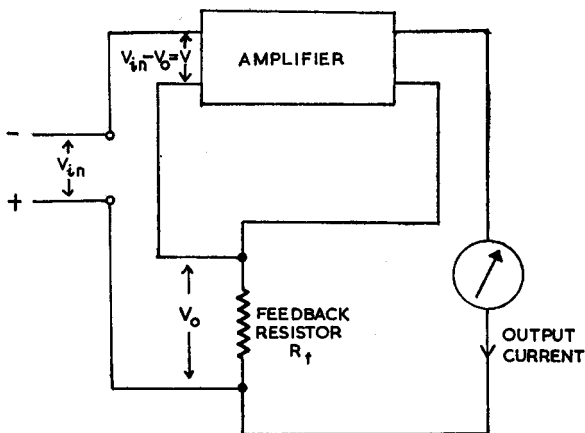


Fig. 11.11. Feedback d.c. amplifier

as the grid voltage varies so also does the anode current, the variation being shown on a meter directly calibrated in pH units. In order to increase the sensitivity the anode current of the electrometer valve may be amplified. The requirements of a suitable d.c. amplifier are: it must draw negligible current from the cell; it must be independent of supply voltage variations; and the input potential and output current must be linearly related. These are achieved by the use of heavy negative feedback (p. 308). The input voltage  $V_i$  and the output voltage  $V_o$  are linearly

## LABORATORY AND PROCESS INSTRUMENTS

related by  $V_o = 1/\beta \cdot V_i$  (where  $\beta$  is the fraction of the output which is fed back in phase opposition to the input), so long as the feedback resistor  $R_f$  (Fig. 11.11) remains constant. The effect of voltage variations is reduced by the factor  $1/\beta$ .

In balanced amplifiers two valves are used, connected so that variations in supply voltage affect both valves of the pair. In Fig. 11.12, the points *A* and *B* remain at the potentials determined by the grids, practically irrespective of H.T. variations.

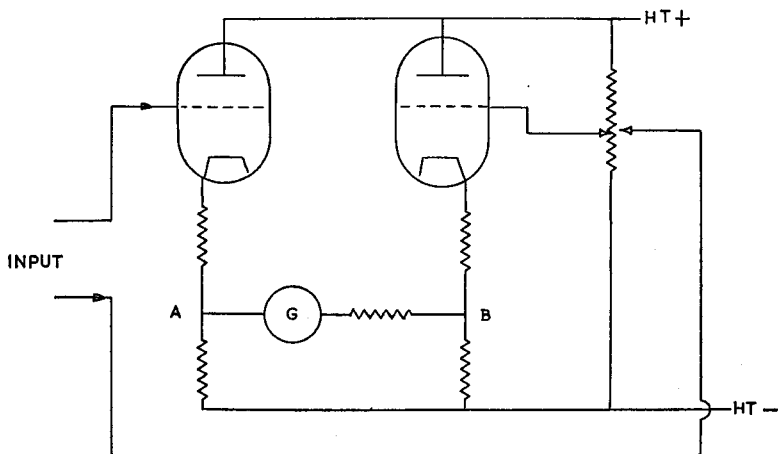


Fig. 11.12. Balanced amplifier with variable feedback

A combination of balanced amplifiers and negative feedback enables the required zero stability, sensitivity and linearity to be obtained.

Another type of d.c. amplifier which has been used very successfully in accurate pH measurement, is the Vibron electrometer of Messrs. E.I.L., Richmond, Surrey, which we have already considered (p. 148).

Throughout this chapter the measurement of an e.m.f. has largely been associated with the determination of pH, but it must be emphasised that the methods described may be used to measure any e.m.f., the choice of a particular instrument depending upon the circumstances.



## Section II: Dielectric Constant and Capacitance Measurement

### Procedure

The determination of dielectric constants of gases, liquids and solutions is generally made by chemists in order to calculate electrical dipole moments of molecules. Further, the value of the dielectric constant of a material may be a most useful control quantity, e.g. in the determination of the moisture content of an organic liquid such as acetone. The method is only easily applicable if the solution is relatively non-conducting; because of this, it is largely limited to dilute solutions of polar compounds in non-polar solvents. (In non-polar molecules there is a coincidence of positive and negative charge centres, whilst in polar molecules there is a lack of coincidence. Compare the polar HCl molecule with the non-polar  $N_2$  molecule, Fig. 11.13). The measurement of dielectric constant is fundamentally the measurement of capacitance, in as much as the dielectric constant ( $D$ ) of a material  $M$  may be defined:

$$D = \frac{\text{Capacitance of a capacitor with dielectric } M \text{ between the plates}}{\text{Capacitance of the same capacitor with a vacuum between the plates}}$$

the dielectric constant of a vacuum being taken to be unity. Practically this is difficult to measure and generally the capacitor or dielectric constant cell is calibrated with a substance of known dielectric constant, e.g. benzene ( $D = 2.2925$  at  $25^\circ\text{C}$ ) or air ( $D = 1.0006$  at N.T.P.).

The capacitor bears little resemblance to those described in the earlier chapters of this book; it is usually a glass dielectric-constant cell, such as that shown in Fig. 11.14. The electrodes are normally of silver, chemically deposited on to the walls of the inner glass compartment; contact is made via platinum wires sealed through the walls of the vessel. It is necessary to immerse

## LABORATORY AND PROCESS INSTRUMENTS

the cell in a thermostat bath of a non-conducting liquid such as transformer oil, and care must be taken to standardise the depth of immersion. Whilst a glass cell is shown, any insulating material may be used for its construction; many designs of cells have been produced.

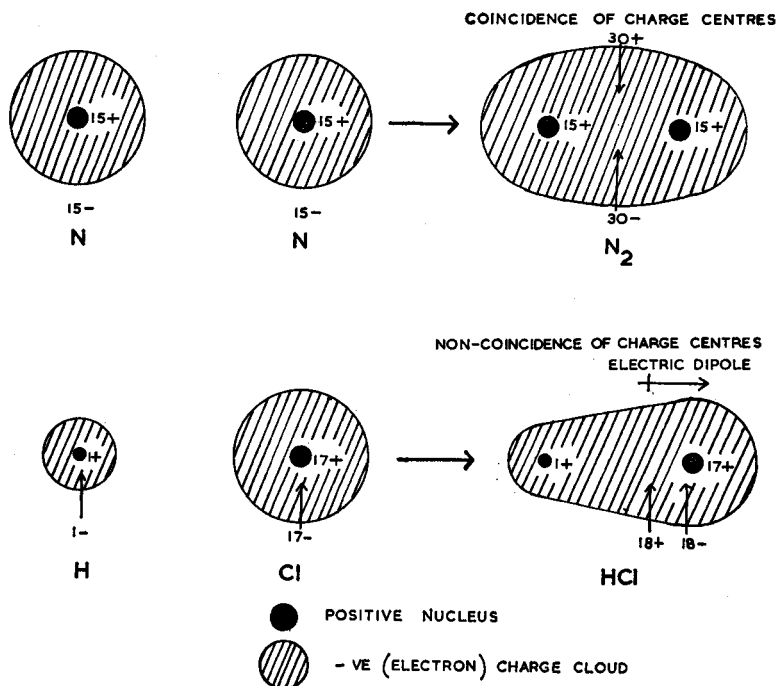


Fig. 11.13. Comparison of polar molecule (HCl) and non-polar molecule ( $N_2$ )

We may now consider the experimental methods used to measure the dielectric constant of substances. In this context only the conventional methods will be discussed, employing frequencies around  $10^6$  c/s, the techniques involving molecular beams and microwaves being outside the scope of this text. The exact method used depends upon the physical state of the substance; gases present relatively greater difficulties than liquids in that their dielectric constants are usually very close to unity. However, the general principles of measurement are the same: in both cases capacitance changes are measured with reference to a

# THE MEASUREMENT OF ELECTROMOTIVE FORCE

high-precision standard capacitor. Two ways of doing this are described. The first is the 'parallel method' in which the total capacity of the system is maintained constant, by varying the

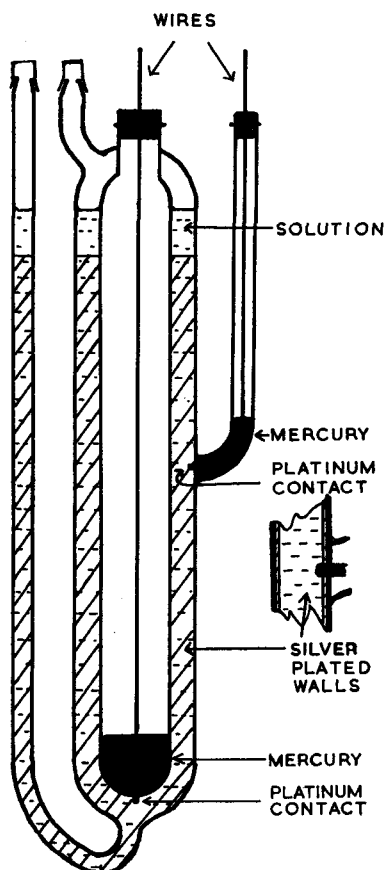


Fig. 11.14. Dielectric constant cell for liquids

capacity of the standard capacitor in opposition to changes in the cell capacitance (Fig. 11.15(a)).

The second and more satisfactory method is the substitution method in which the cell is replaced by the standard capacitor, and this is adjusted to maintain the total capacitance of the circuit constant. The wiring, and a suitable ballast capacitor  $C_b$ , remain common to both circuits (Fig. 11.15(b)).

## LABORATORY AND PROCESS INSTRUMENTS

The methods are dependent upon the constancy of the source frequency; it is necessary to make corrections for stray capacity in the connections, etc., if these are not eliminated by the technique adopted. Having dealt in outline with the procedure, we now consider some of the methods of comparison in more detail.

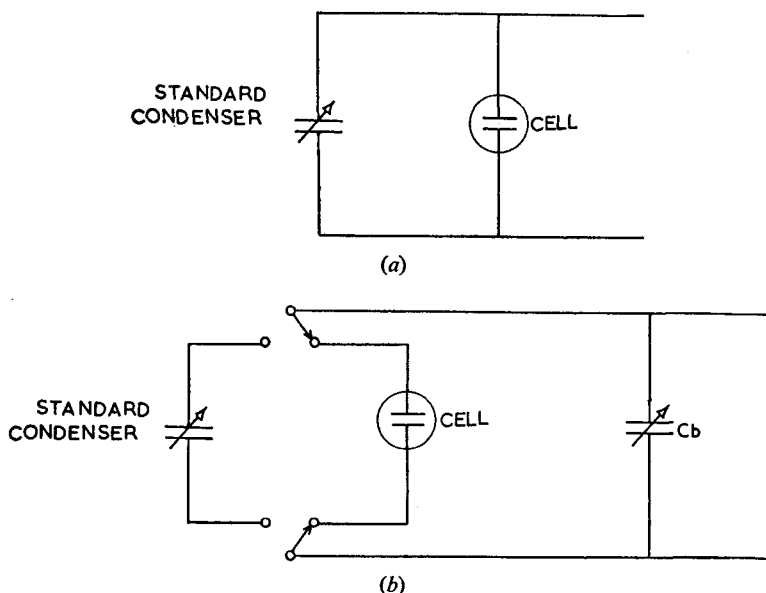


Fig. 11.15. (a) Parallel method of capacitance measurement. (b) Substitution method

### Experimental Methods of Measurement

(i) *Capacity bridge method.* The bridge shown in Fig. 11.16(a) has many similarities to the modified Wheatstone bridge described under conductivity measurement; in this case it is assumed that the bridge is constructed from ideal capacitors,  $C_1$  representing the cell,  $C_4$  the variable and  $C_2, C_3$  the fixed capacitors. At balance it can be shown that

$$C_1 = \frac{C_2}{C_3} \cdot C_4$$

## THE MEASUREMENT OF ELECTROMOTIVE FORCE

However, if the liquid in the cell has an electrical conductivity the circuit must be modified, and the bridge is now represented by Fig. 11.16(b), where it has become necessary to place a variable resistor  $R_v$  in parallel with the variable capacitor  $C_4$ . If, however, the conductivity is very small, the bridge method is satisfactory,

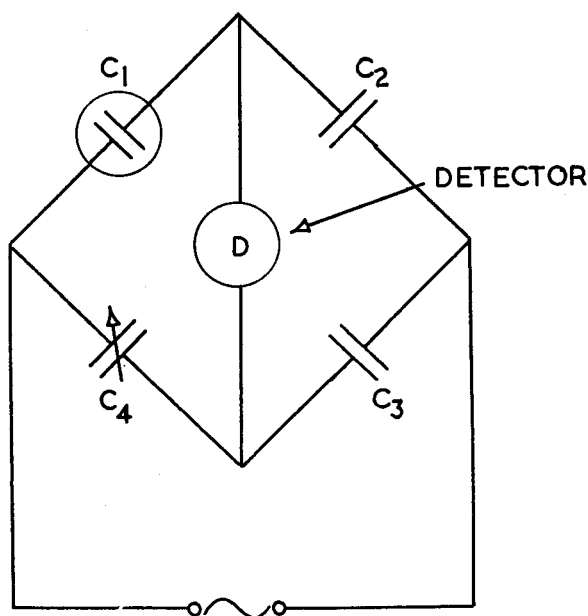


Fig. 11.16. (a) Capacitance bridge—perfect capacitor  $C_1$

and the measurements are sensibly frequency independent. In practice,  $C_4$  is often a non-standard variable capacitor, the actual cell being replaced by the standard capacitor in the substitution technique already described.

(ii) *Transformer ratio-arm bridge method.* This method has been described under conductivity measurements as the bridge measures both conductivity and capacity simultaneously. In this technique it is possible to use a variation of the cell already described. Such a dielectric cell is shown schematically in Fig. 11.17.

# LABORATORY AND PROCESS INSTRUMENTS

The 'measured' series readings which are obtained must be corrected for the capacity of the glass dielectric using the simple formulae:

$$\frac{1}{C_{c.s.}} = \frac{1}{C_{m.s.}} - \frac{1}{C_g}$$

where  $C_{c.s.}$  = corrected series capacity,

$C_{m.s.}$  = measured series capacity,

$C_g$  = glass capacity.

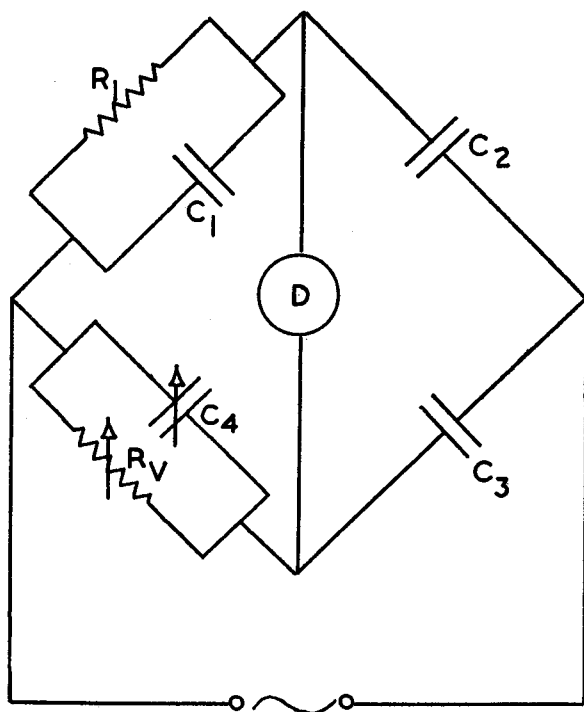
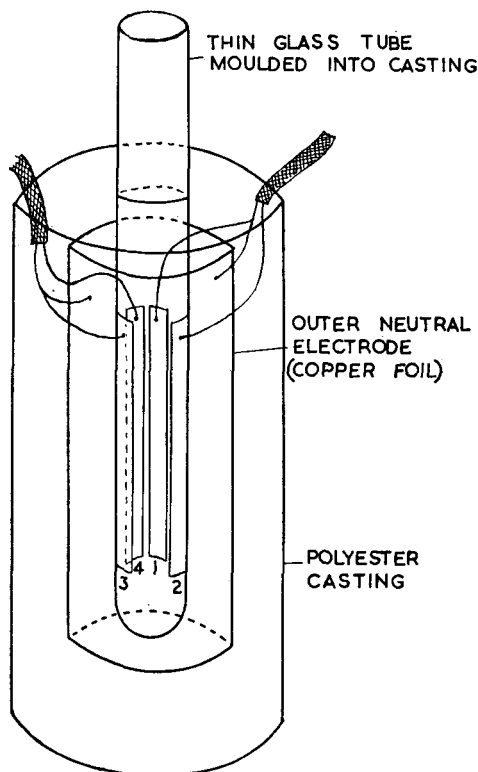


Fig. 11.16. (b) Resistance  $R_1$  of  $C_1$  included

The value of  $C_g$  is easily obtained by completely filling the central glass tube with mercury and measuring the residual capacity of the cell. Again, it is possible to make the reading directly or to use the substitution method.

## THE MEASUREMENT OF ELECTROMOTIVE FORCE

(iii) *The heterodyne beat method.* This method is generally used for measurements on liquids and solutions, but there is no reason why a well-designed apparatus should not be used for gases. The principle involved is that of the beat-frequency oscillator (p. 167), as illustrated in Fig. 11.18.



1 and 3=INNER NEUTRAL ELECTRODES  
2=VOLTAGE ELECTRODE 4=CURRENT ELECTRODE

Fig. 11.17. Alternative form of dielectric constant cell

The frequency of oscillator I is fixed but the frequency of oscillator II may be varied by altering capacitor  $C_2$ , the beat frequency of circuit III changing as  $C_2$  changes. Practically, it is common to maintain the beat frequency constant and make  $C_2$  a substitution circuit as shown in Fig. 11.15(b).

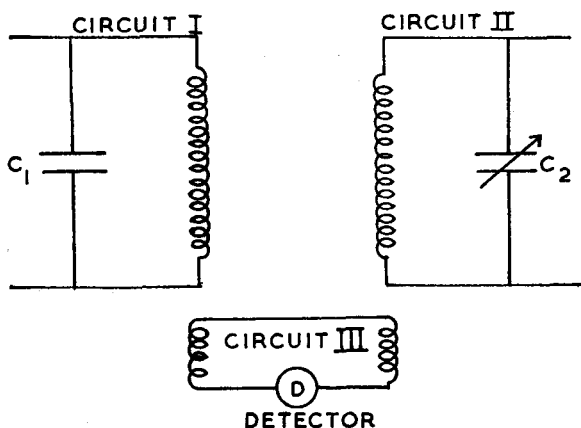


Fig. 11.18. Beat-frequency method of capacitance measurement

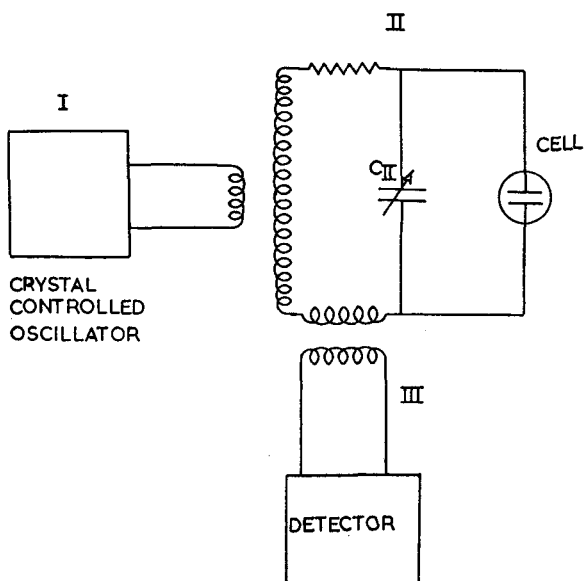


Fig. 11.19. Resonance method of capacitance measurement



## THE MEASUREMENT OF ELECTROMOTIVE FORCE

(iv) *The resonance method.* It has been shown that the impedance of an  $L$ - $C$ - $R$  series circuit can be found from the formula:

$$Z = \sqrt{\left[ R^2 + \left( 2\pi fL - \frac{1}{2\pi fC} \right)^2 \right]}$$

where  $f$  is the frequency. The current is a maximum at resonance, consequently if both  $f$  and  $L$  be fixed, resonance will occur for a unique value of  $C$  and this obviously suggests a means of measuring the value of a capacitor. The principle is illustrated in Fig. 11.19. Oscillations of a fixed frequency are induced in circuit II by means of a crystal-controlled oscillator and  $C_{II}$  is adjusted until resonance occurs. This may be detected by means of a loosely-coupled detecting circuit III as shown, or by means of a valve voltmeter connected across a resistor in circuit II. A typical detecting circuit consists of a rectifier in series with a galvanometer, which shows maximum deflection at resonance. Once again in practice the capacitor system is usually of the type described under the 'substitution method' (Fig. 11.15(b)).

### Solid Dielectrics

So far the discussion of dielectric constant measurements has been restricted to gases, liquids and solutions. The dielectric properties of solids, too, are of great technical interest; in outline

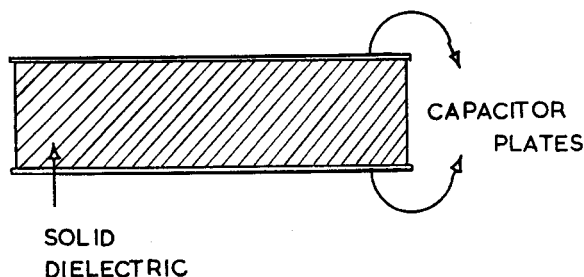


Fig. 11.20. (a) Solid dielectric capacitor

the methods are similar to those used for the liquids and gases, the only major difference being in the design of the cell. At first sight it would appear that the solid could easily be machined to make the dielectric between the plates of a capacitor (Fig. 11.20(a)); but there are certain practical difficulties, due to the

imperfect and inconsistent contact of the dielectric with the plates, the compression of powdered materials to a reproducible 'cake', etc. Despite these difficulties useful results can be obtained from such a simple system, e.g. in the determination of the water

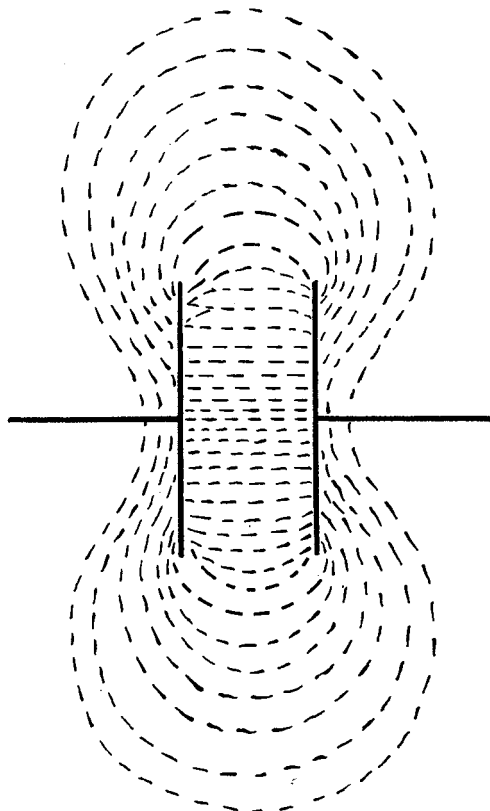


Fig. 11.20. (b) Fringing of field— $d$  comparable with  $l$

content of wood, flour, etc., but of necessity these are empirical in nature. A three-terminal bridge method for the determination of the dielectric constant of a slab of solid dielectric has been described by Lynch.<sup>†</sup> The specimen is placed between the plates of a capacitor fitted with a guard ring (see below) and so

<sup>†</sup> *Proceedings of the Institute of Electrical Engineers* **104B**, 359 (1957).

# THE MEASUREMENT OF ELECTROMOTIVE FORCE

arranged that one plate may be moved on a micrometer drive (Fig. 11.20(c)), and an electrical balance is obtained on a capacity bridge. The specimen is then removed from the plates when the capacity of the system is altered, and the bridge goes out of

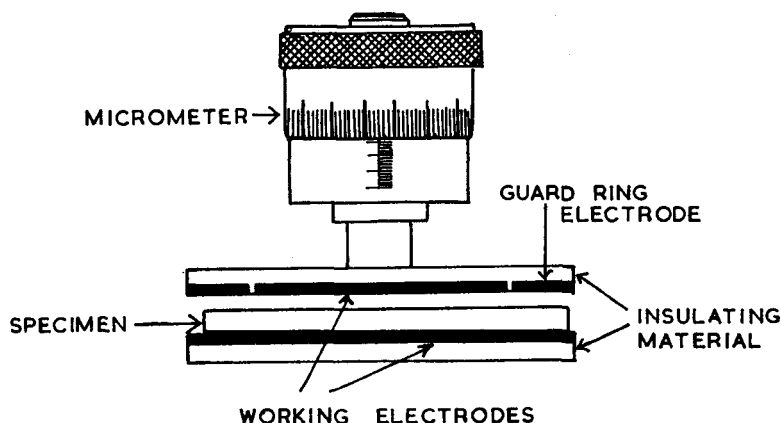


Fig. 11.20. (c) Micrometer cell

balance. The balance is restored by adjusting the gap between the capacitor plates.

- Let  $C_1$  = capacity of capacitor with specimen,  
 $C_2$  = capacity of capacitor without specimen,  
 $A$  = area of electrode,  
 $t_s$  = thickness of specimen,  
 $t_0$  = gap between electrodes and specimen,  
 $\Delta t$  = reduction in separation of electrode,  
 $D$  = dielectric constant of the specimen.

It can be shown that

$$\frac{1}{C_1} = \frac{4\pi}{A} \left( \frac{t_s}{D} + t_0 \right) \quad \text{and} \quad \frac{1}{C_2} = \frac{4\pi}{A} (t_s - \Delta t + t_0)$$

But the measurement is such that  $C_1 = C_2$  and thus

$$D = \frac{t_s}{t_s - \Delta t}$$

Thus, the measurement is such that the electrodes do not have to make intimate contact with the specimen, and from the final equation the dielectric constant is obtained without the use of either areas or capacitances.

Capacitance measurements may also be used to determine mechanical displacements. The capacitance  $C_p$  of a pair of parallel plates is given by:  $C_p = K.(A/d)$  where  $K$  is a constant,  $A$  the area of the plates and  $d$  their separation. Using a two terminal bridge, if the plates are small this equation is meaningless

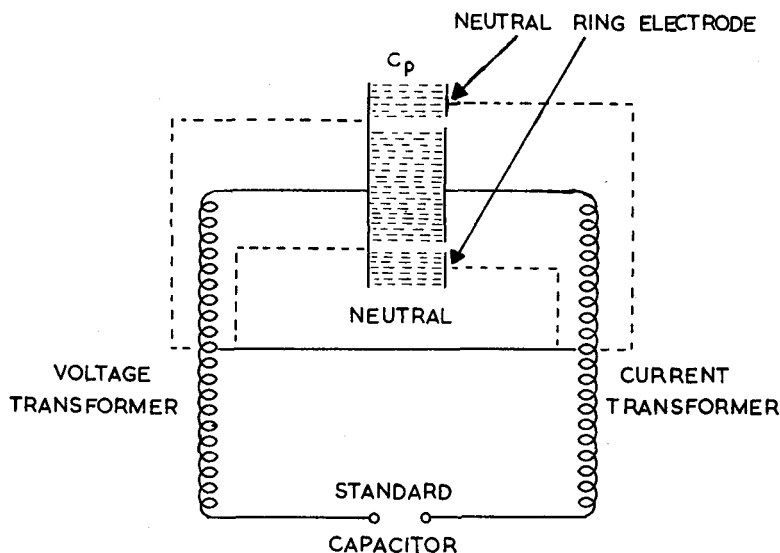


Fig. 11.21. Transformer ratio-arm bridge for capacitance measurement

because the fringe flux is the major component of the electrostatic field (see Fig. 11.20(b)). To measure  $d$  using a capacitance probe of fixed plate area the curved flux lines must be eliminated; this can be done using a three-terminal transformer ratio arm bridge and a 'neutral' guard-ring (Fig. 11.21).

The only current entering the current transformer is collected by the central electrode of the probe capacitance  $C_p$ , the current resulting from the 'fringing flux' being returned to the neutral line. Thus if the area of the probe electrode is known, measure-

## THE MEASUREMENT OF ELECTROMOTIVE FORCE

ment of the capacitance  $C_p$  allows the distance  $d$  to be determined.

In the 'standard' arm of the bridge, an enlarged model of the capacitance probe takes the place of a standard capacitor, and the spacing between the electrodes of this model is controlled by a micrometer. If the plate areas of the probe and the enlarged model are  $A_p$  and  $A_m$ , and the respective separations are  $d_p$  and  $d_m$ :  $C_p = K \cdot A_p/d_p$  and  $C_m = K \cdot A_m/d_m$ . At balance, with a bridge ratio of 1:1,  $C_p = C_m$  and  $d_p = d_m \cdot A_p/A_m$ . Thus if the probe has an electrode diameter of 0.1 in. and the model a diameter of 1.0 in. the area ratio is 1:100, and the spacing at the probe is 1/100 that of the model. Movement of the plate of the model through 0.001 in. compensates for a probe electrode movement of only  $10^{-5}$  in.; variation of the area and bridge ratios allows a wide range of mechanical displacements to be measured very accurately.

## NOTES

### Reversible Hydrogen Electrodes

For an electrode to be reversible to hydrogen ions, the basic equilibrium set up at the electrode-solution interface must involve the concentration of hydrogen ions in the solution. Thus, at the platinised platinum electrode, in the presence of hydrogen gas, we have the equilibrium  $2H^+ + 2e \rightleftharpoons H_2$ . The position of this equilibrium determines the e.m.f. established between the electrode and the solution.

The quinhydrone electrode consists of a bright-platinum wire, dipping into the solution containing hydrogen ions, into which is added the sparingly-soluble organic compound quinhydrone. This is a loose compound of the oxidation-reduction pair, quinone-hydroquinone, which we may designate Q and HQ, respectively. The equilibrium set up is  $Q + H^+ + e \rightleftharpoons QH$ .

The e.m.f. developed depends upon the Q:QH ratio, which in turn is fixed by the hydrogen ion concentration in the solution; the sparing solubility of quinhydrone ensures that the solution is always saturated with respect to this compound.

The antimony electrode consists of a rod of antimony metal, dipping into the solution. A film of the oxide  $Sb_2O_3$  on the surface leads to the equilibrium:  $Sb_2O_3 + 6H^+ + 6e \rightleftharpoons 2Sb + 3H_2O$ . Again, the e.m.f. is a function of the hydrogen ion concentration.

### References

- BRITTON, H. T. S. (1955). *Hydrogen Ions*, Vol. I, 4th edition. Chapman and Hall.
- MCDougALL, F. H. (1955). *Physical Chemistry*, 3rd edition. Macmillan.
- SMITH, J. W. (1955). *Dipole Moments*. Butterworth.
- WEBBER, R. B. (1957). *The Book of pH*. Newnes.

### Problems

1. Outline experimental methods available for the potentiometric determination of pH, including both low and high impedance systems.
2. The fundamental theory of most electrochemical measurements is based upon concepts of behaviour in very dilute solutions, whereas most practical industrial measurements are made upon relatively concentrated solutions. In the light of this, discuss critically the significance of both pH and conductivity measurements made in these concentrated solutions.
3. Describe suitable apparatus, including circuit details, for the measurement of electrode potentials. Discuss the difficulties in determining the absolute values and how these difficulties can be overcome, in the practical sense, by the choice of a suitable reference electrode.
4. Describe experimental techniques suitable for measuring the dielectric constants of materials: (a) in the gaseous form; (b) in the liquid form; (c) solid materials in slab form.
5. From measurements made on the dielectric constants, densities and refractive indices of dilute solutions of polar compounds in non-polar solvents, information regarding molecular structure may be obtained. Outline, with specific cases, the methods used and the assumptions made in obtaining this information.
6. Dielectric constant measurements have been used in quality control, e.g. in the determination of moisture in grain, wood, etc. Describe suitable equipment for making these measurements.

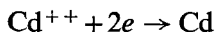
## CHAPTER XII

# Polarography

### Principles

The technique of d.c. polarography is based upon the interpretation of current-voltage curves obtained during the electrolysis of a solution under special conditions. In the polarographic cell the cathode consists of mercury falling in a regular series of small drops (about one every three seconds) from a glass capillary, into a pool of mercury which serves as an anode; the reason for this electrode system will be explained later. The basic arrangement is that of Fig. 12.1(a), and an idealised current-voltage curve is seen in Fig. 12.1(b); the step-height of this curve is proportional to the concentration of the species which is being reduced at the dropping mercury electrode (abbreviated to 'd.m.e.'), and the half-wave potential  $V_{1/2}$  is characteristic of this same species.

As we increase the -ve potential of the cathode, by moving the slider in the direction  $AB$ , a small steady current flows until a certain potential  $V_0$  is reached, when there is a sharp increase in the current; this continues until ultimately the limiting current  $i_d$ , of the order of a few micro-amperes, is reached. The processes occurring at the cathode are complicated, but a simplified account may be given as follows. At a certain potential, applied e.m.f., or voltage, the ion being considered (e.g. cadmium  $\text{Cd}^{++}$ ) will commence to be discharged at the d.m.e., the resulting metal forming an amalgam with the mercury; for this and other reasons the potential at which deposition occurs in polarography is very different from the reversible metal-electrode/ion potential. When the drop falls it is carried down to the pool anode, and a fresh mercury surface appears. The reaction involving discharge of the ion which is one of reduction may be written:



As a result, the concentration of cadmium ions in a thin layer close to the drop (the *depletion layer*) falls, and in order to minimise the concentration gradient set up  $\text{Cd}^{++}$  ions will *diffuse*

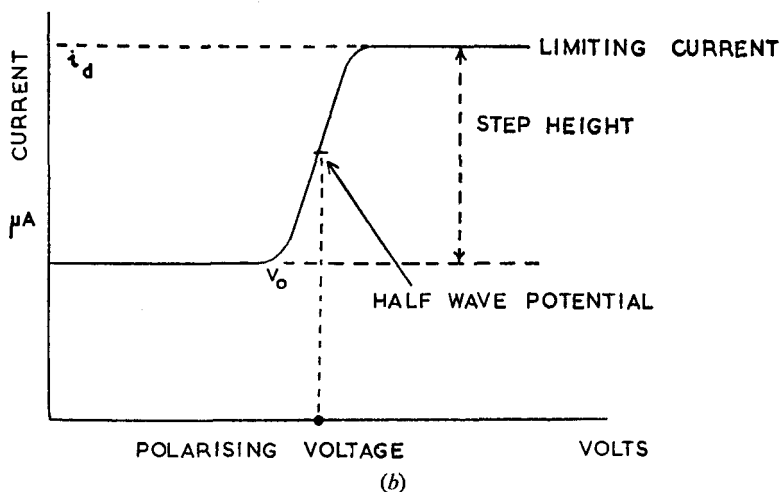
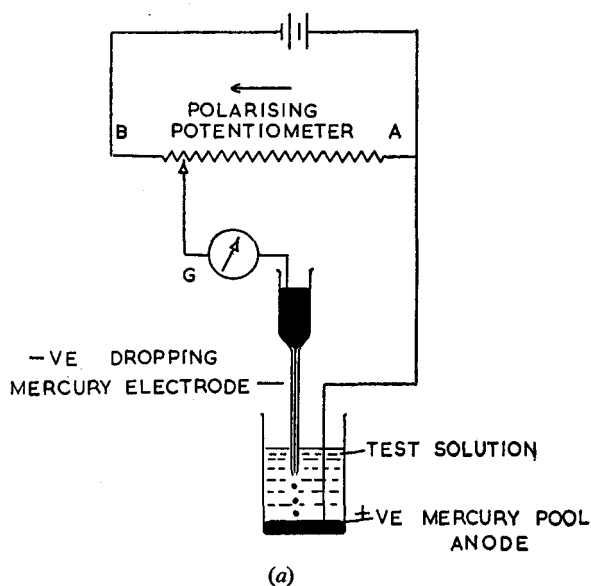


Fig. 12.1. (a) Basic arrangement of polarograph: *G*, long-period galvanometer. (b) Idealised current-voltage curve for a single reducible species



## POLAROGRAPHY

into this layer (see Fig. 12.2); this movement of the charged ions is equivalent to a current flowing in the external circuit. The rate of diffusion of an ion, and the potential at which it is reduced at the d.m.e., under given conditions, are both unique properties of that species of ion; it is for this reason that an ion may be identified from its half-wave potential. By utilising the large overpotential at a mercury surface we are able to study the deposition of ions, such as those of the alkali metals, which would not normally be reduced in an aqueous solution. The dropping

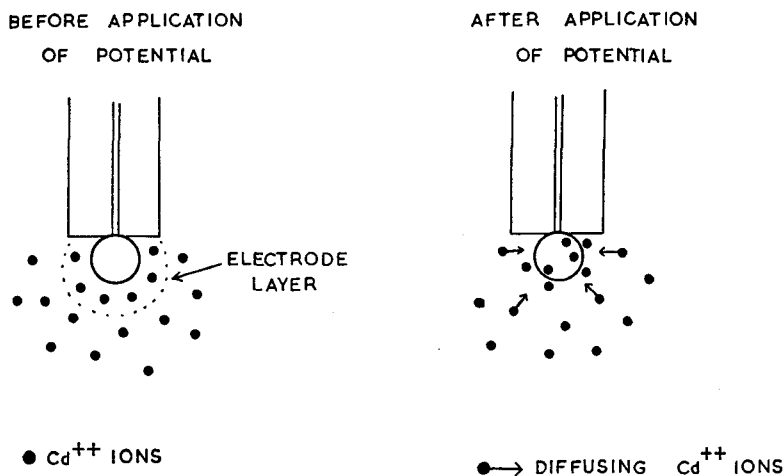


Fig. 12.2. Diffusion of ions under the concentration-gradient at the mercury drop

mercury cathode presents a fresh surface to the ions so that diffusion and deposition take place under constant conditions. The limiting currents are so small that only minute amounts of the reducible species are deposited during electrolysis, so that sections of the curve may be repeated on the same solution.

The rate of diffusion of the ions is a function of the concentration difference between the depletion layer and the bulk of the solution, and it will be a maximum when the ions are reduced as fast as they arrive at the d.m.e.; the concentration of ions at the surface of the drop is then zero, and this is the condition for limiting (i.e. maximum) current. The magnitude of this limiting current will thus depend upon the bulk concentration of the

## LABORATORY AND PROCESS INSTRUMENTS

ions; it depends also upon the viscosity and the temperature of the solution. From a practical point of view the concentration of the reducible ions may be obtained from a measurement of the step-height, but this is affected by other factors, such as size and rate of flow of the mercury drops. An equation has been derived by Ilkovic† relating the limiting current to the concentration of the reducible species in terms of all the parameters; usually, however, a calibration curve of step-height against concentration is prepared for quantitative analysis.

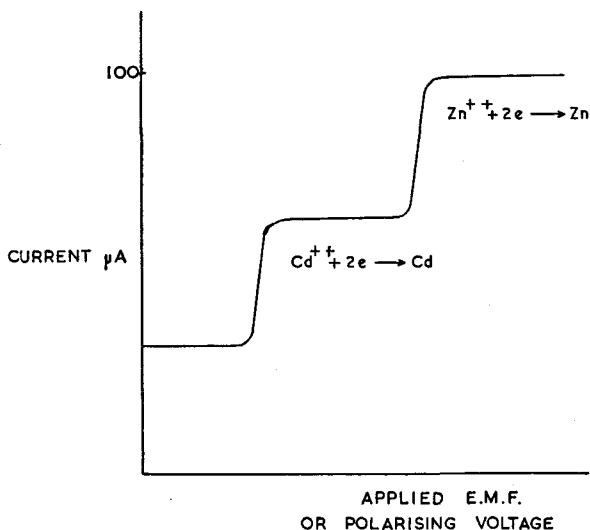


Fig. 12.3. (a) Idealised current-voltage curve for two reducible species

We have so far assumed that the ions move only under the influence of the concentration gradient, but of course migration under the effect of the applied field (that is, normal 'transport' of ions) will also occur. To minimise this effect, a base solution or base electrolyte is used, which provides a large excess (at least twenty-fold) of some 'neutral' ion, i.e. an ion which does not react with the test ion, and which is not reduced in the same e.m.f. range. The 'neutral' ions will carry the bulk of the current but since they are not reduced, there will be no concentration

† Ilkovic (1938). *J. Chim. Phys.* **35**, 129.

## POLAROGRAPHY

gradient of this species at the electrode, and hence no diffusion current. The choice of a suitable base electrolyte—which may have other roles than the prevention of migration currents (e.g.

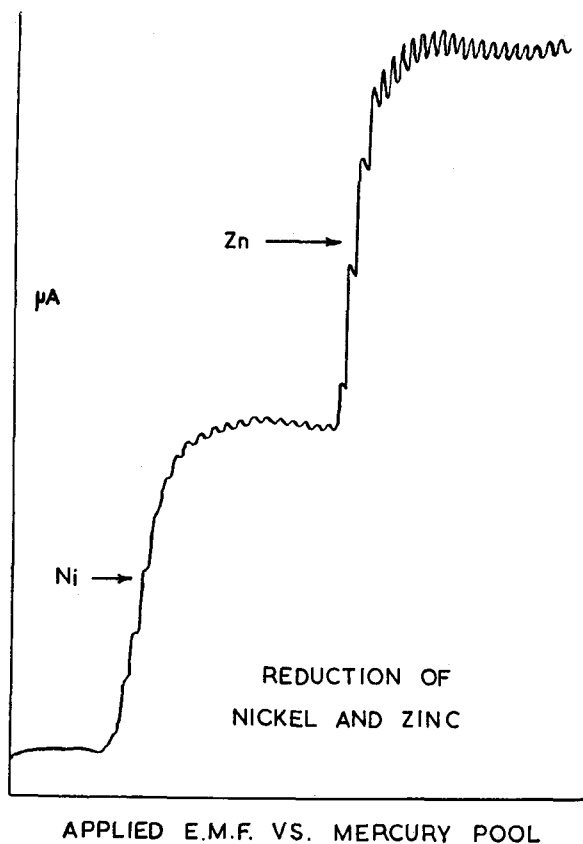


Fig. 12.3. (b) Actual curve for  $\text{Ni}^{++}$  and  $\text{Zn}^{++}$

the complexing of undesirable reducible species)—is a matter of considerable chemical knowledge and familiarity with polarography and reference should be made to the standard textbooks.†

The method may be applied to solutions containing more than

† See, for example, Kolthoff and Lingane (1952). *Polarography*, 2nd edition, 2 vols. Interscience.

## LABORATORY AND PROCESS INSTRUMENTS

one reducible species, provided their half-wave potentials can be resolved by the instrument in use. An idealised curve for two cations is shown in Fig. 12.3(a). The practical curves obtained on a recording d.c. polarograph are similar in shape to the idealised curves but the line is not smooth; this is illustrated in Figs. 12.3(b) and 12.4. The oscillations are inherent in the nature of the dropping mercury cathode; the area varies from zero, to a

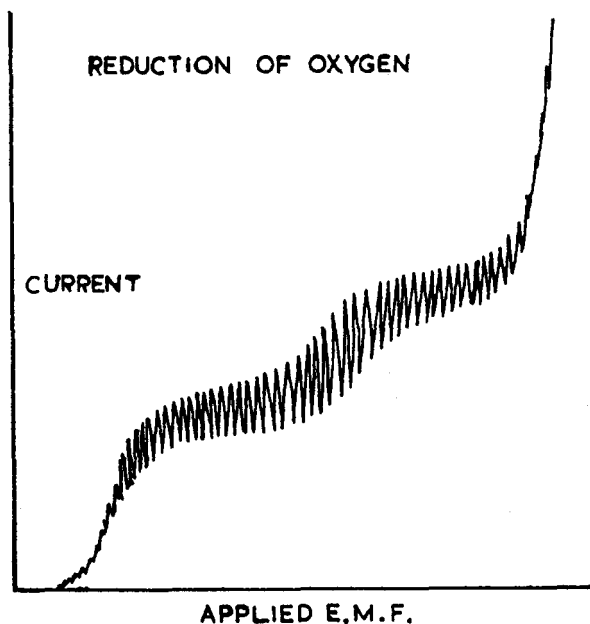


Fig. 12.4. Practical d.c. polarogram—undamped

maximum value immediately before fall-off, and the current at any particular e.m.f. will also vary from zero to a maximum; the galvanometer will attempt to follow the excursions, and because of its long period it will produce the type of record shown. This causes certain difficulties in determining step-height, and a standardised procedure must be adopted. It is possible to modify the curve by use of a variable capacitor in parallel with the galvanometer, which damps its movement; the result is shown in Fig. 12.5. Whilst curve (b) shows smaller oscillations, a certain degree of resolution has been lost.

## POLAROGRAPHY

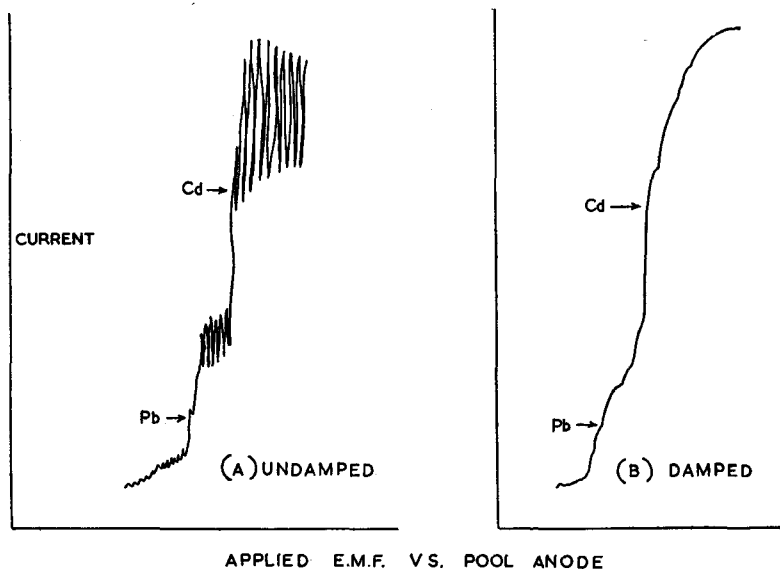


Fig. 12.5. (a) Undamped curve:  $\text{Pb}^{++}$  and  $\text{Cd}^{++}$ . (b) Effect of damping

In addition to the diffusion and migration currents, other parasitic currents and effects exist, which may lead to incorrect results being obtained. It cannot be emphasised too strongly that the interpretation of a polarographic curve requires a good knowledge of the physical chemistry involved in the reaction processes.

### Instruments

A number of d.c. polarographs are available commercially. The simplest instruments are based entirely on the circuit of Fig. 12.1, where the polarising potential is applied by a calibrated potentiometer and the current read off directly from the galvanometer; the polarographic curve is plotted manually. The natural development of the simple instrument was to record the curve automatically, and indeed the name *polarograph* was coined by Heyrovsky for the first photographically recording instrument using a dropping mercury electrode system. This instrument is shown schematically in Fig. 12.6†

† The Model XII Sargent Polarograph (E. H. Sargent, Inc., Chicago, Ill.) is based upon the original Heyrovsky instrument.

## LABORATORY AND PROCESS INSTRUMENTS

The applied e.m.f. to the cell is varied by means of the precision rotating potentiometer and the current flowing detected by a moving-coil reflecting galvanometer. The reflected light spot falls upon the slit in the external recorder drum, which is fixed; the internal drum, around which photographic paper is wrapped, is driven from the potentiometer directly or via a gear train. The next development was to eliminate photographic development by

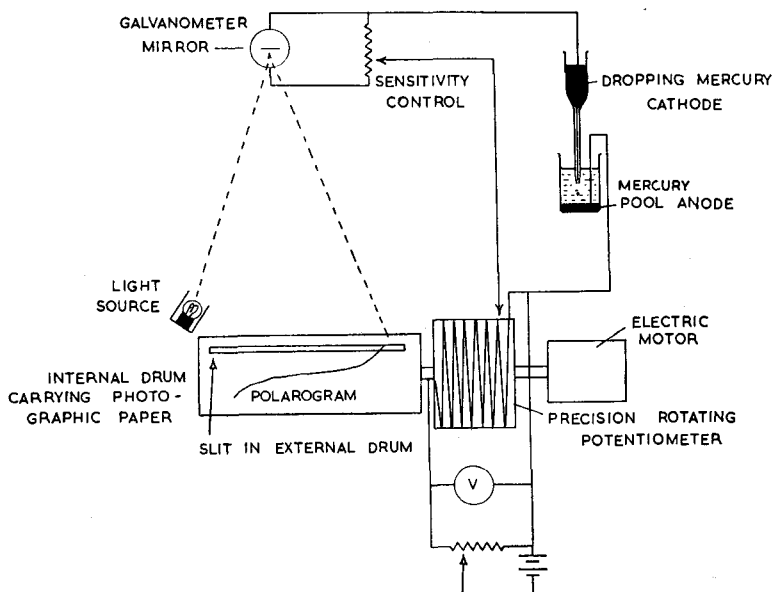


Fig. 12.6. Heyrovsky photographic-recording polarograph

the use of a pen recorder, by no means a simple extension. It must be remembered that the d.c. currents produced are only a few tens of microamperes and that such currents would not directly operate available recorders. Consequently, once again the question of d.c. amplification arises, and the manufacturers of commercial instruments have developed a number of different stable d.c. amplifiers based upon conventional principles. In the section dealing with infra-red spectrometers various photo-electric devices are described (p. 356), and one British polaro-

## POLAROGRAPHY

graph† makes use of a photo-electric amplifier. Fig. 12.7 shows the basic circuit of the instrument.

The photo-cell is of the caesium cathode (red-sensitive) photo-emissive type (p. 175); light from a low-power light source, which is run well below its rated voltage to prolong its life, falls on the

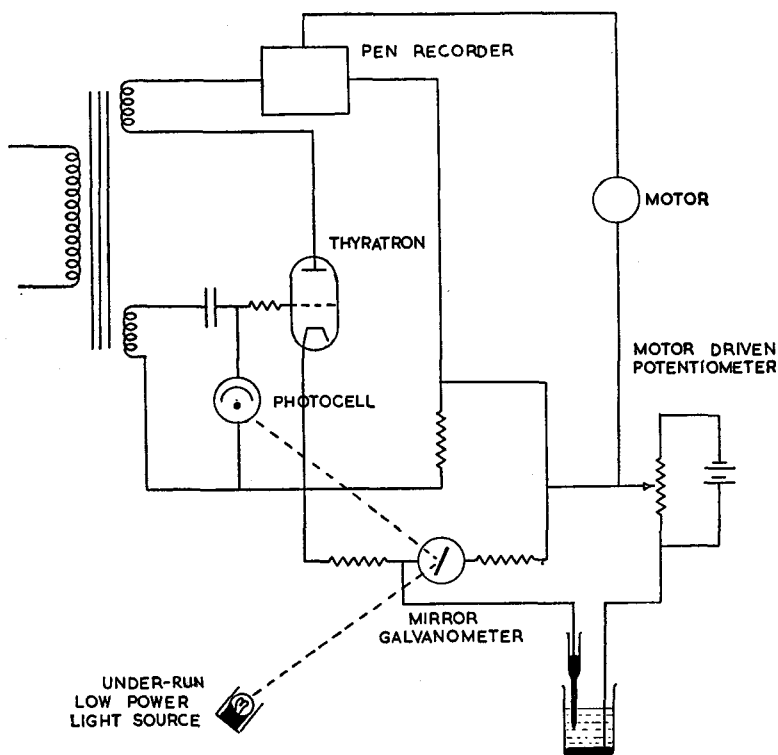


Fig. 12.7. Tinsley polarograph—basic circuit

mirror of the galvanometer and thence to the cathode of the photo-cell. The polarising voltage is applied by a motor-driven potentiometer which is coupled to the chart drive of a pen recorder. The resulting polarographic current produces a deflection of the mirror, and alters the position of the light spot; hence the

† The Tinsley Polarograph of Evershed and Vignoles Ltd., Chiswick, London, W.4.

intensity of illumination of the photo-cell cathode changes, and the cell resistance alters. The photo-cell forms part of resistance-capacitance circuit in the grid of a thyatron (p. 95), fed with an alternating voltage  $V_B$  at both grid and anode; their relative phases depend upon the component values (Fig. 12.8). If  $R_E$  is the equivalent resistance of the photo-cell, the current  $I_a$  is given by:

$$I_a = \frac{V_B}{\sqrt{[R_E^2 + (1/\omega C)^2]}}$$

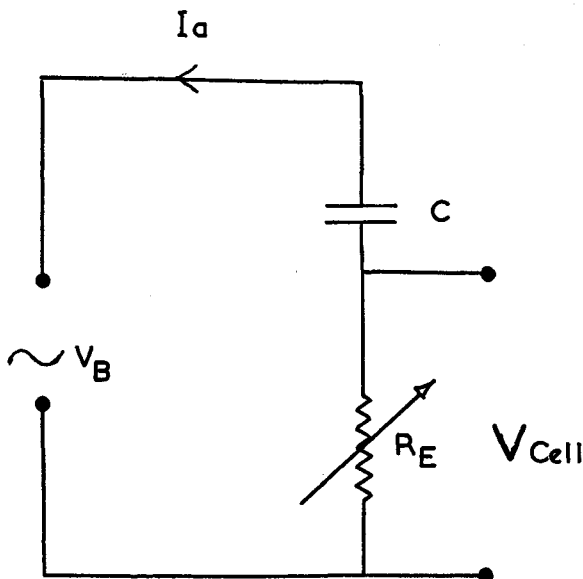


Fig. 12.8. Grid-circuit of thyatron

and leads  $V_B$  by the phase-angle  $\phi$ , defined by  $\tan \phi = 1/\omega CR_E$ . At high illumination intensity,  $R_E$  is comparatively small;  $I_a$  is large, but  $\phi$  is also large. At low illumination,  $R_E$  is large,  $I_a$  is small, and  $\phi$  is small. The voltage across the cell is  $I_a R_E$ ; hence the illumination on the cell controls the amplitude and phase of the voltage applied to the thyatron grid. From our previous consideration of the thyatron it is evident that only when the grid exceeds the striking potential *during a positive anode half-cycle* will the tube strike; the thyatron output is thus pulsating, varying in amplitude with the illumination on the photo-cell.



## POLAROGRAPHY

The output is amplified, using heavy current-negative feedback, to stabilise the gain and reduce the input resistance. The input resistance of the measuring device must be kept as low as possible, to prevent part of the voltage applied to the electrodes from being lost; voltage negative feedback would result in *increased* input impedance. A quantitative example illustrating the effect is given in the appendix (p. 308).

Thus this circuit employs photo-electric amplification followed by thyatron rectification and amplification with current negative feedback, which produces sufficient power to operate a chart recorder without reducing the polarising voltage at the electrode system to any appreciable extent.

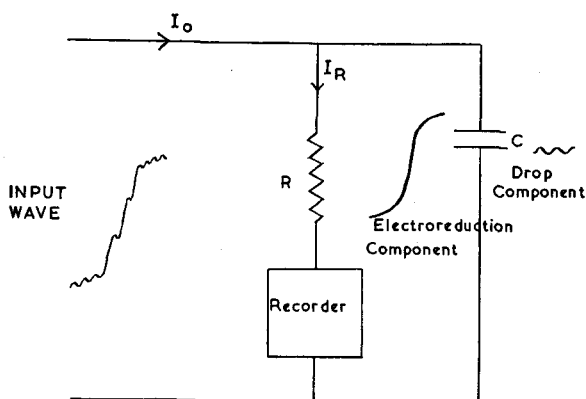


Fig. 12.9. Waveforms produced by shunting the recorder by a large capacitor  $C$

It has already been mentioned that the trace which is obtained is a fluctuating one due to variation in the area of the drop. Inflections in the polarogram may be masked by these 'noise' variations, and a means of discriminating against this must be sought. One way of doing this is to place a large capacitor  $C$  in parallel with the moving coil recorder  $R$  (see Fig. 12.9). When the cell current, which consists of slowly-varying and rapidly-varying components (the electro-reduction component and the drop component, respectively), is applied to the capacitor-shunted recorder, the drop component is effectively short-circuited, leaving the electro-reduction component across the recorder, so that it responds to this component alone.

## LABORATORY AND PROCESS INSTRUMENTS

The polarographs so far mentioned have had a dropping mercury cathode as the polarisable electrode, and a mercury-pool anode as the non-polarisable electrode; in practice, many variations of this electrode system exist. For instance, the mercury pool anode is unsatisfactory for accurate work, and is often replaced by a calomel electrode. Since the total resistance of the polarographic cell is of importance in virtue of the 'IR' drop across it, the calomel electrode used should have a reasonably low resistance—which is not true of all commercial calomel electrodes. An H-type cell of low internal resistance is shown in Fig. 12.10(a).

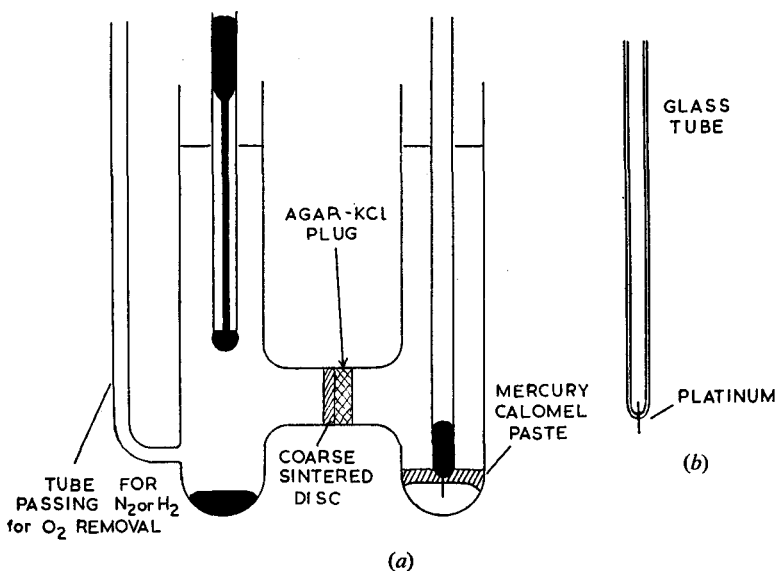


Fig. 12.10. (a) H-type calomel reference electrode. (b) Solid micro-electrode

The curves obtained are similar to those with the pool anode but the half-wave potentials will have different numerical values; care should be taken to ensure that the values obtained from tables are those relevant to the non-polarised electrode used. For certain purposes small solid micro-electrodes have been used (Fig. 12.10(b)) as polarisable electrodes. These are generally made of the noble metals gold or platinum and are often rotated by an electric motor at speeds of about 1000 r.p.m. According to

## POLAROGRAPHY

Heyrovsky this is not true polarography, but textbooks on this subject generally devote a section to the rotating micro-electrode.

The process occurring at the polarisable *cathode* is one of reduction, but it is possible to study oxidation processes by reversal of the electrodes, so that the polarisable electrode is now

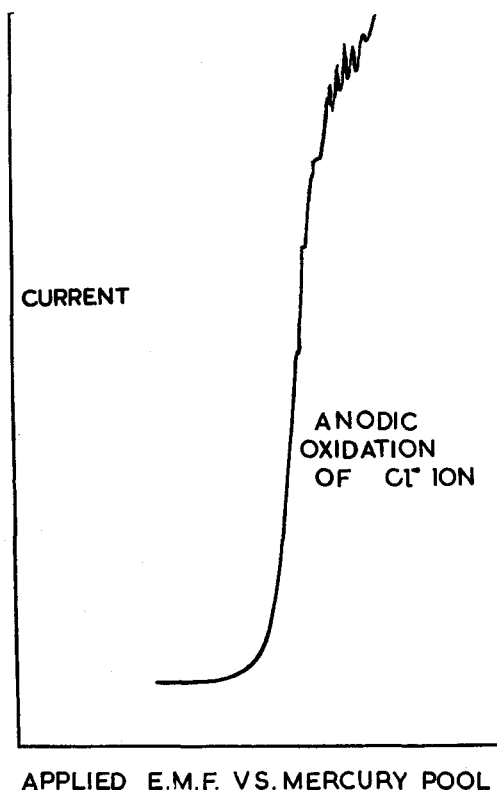


Fig. 12.11. Anodic oxidation of  $\text{Cl}^-$  ion

the *anode*. For example, in Fig. 12.11 the anodic oxidation of  $\text{Cl}^-$  is shown, M/10 potassium nitrate being the base electrolyte. The working range however is limited by the anodic dissolution of mercury, which takes place at +0.5 V. The platinum micro-electrode enables this range to be extended.

**Residual or Charging Currents**

Mention of interfering non-polarographic currents has already been made, and the residual current of a pure solution of supporting electrolyte is made up mainly of the *condenser* or *charging* current. This is due to the effect of the double layer at the electrode, i.e. the layer consisting of the negative charges on the drop and the positive ions in the solution close to the drop. This is equivalent to the setting up of a capacitor which must be charged with the formation of each drop, thus leading to the term 'charging' or 'capacitor' current. The magnitude of this current places a limiting value on the sensitivity of the normal polarographic technique, because it interferes with waves due to small concentrations of reducible species. When working with small concentrations it is necessary to use the galvanometer at maximum sensitivity, and under these conditions the residual-current slope is large and masks the waves. A number of circuits to minimise this interference have been devised and fitted to commercial instruments; that to be described is due to Ilkovic and Semerano.<sup>†</sup> A current of equal magnitude but opposite in direction to the residual current is sent through the galvanometer (see Fig. 12.12).

It is necessary that the residual current, which varies in an approximately linear manner with applied e.m.f., should be balanced out at all values of the e.m.f. That portion of the potential drop across the galvanometer due to the residual current must be zero, which is the case if the potential drop across  $R_3$  is equal to that across  $R_2$ . If  $i_r$  is the residual current, this p.d. is  $i_r R_3$ ; if  $E_a$  is the applied e.m.f., the drop across  $R_2$  is

$$E_a \cdot \left( \frac{R_2}{R_1 + R_2} \right)$$

so that

$$i_r R_3 = E_a \cdot \left( \frac{R_2}{R_1 + R_2} \right)$$

Now  $R_1$  must be relatively large in order that the e.m.f. applied to the cell should not be affected to any great extent by its introduction, and  $R_3$  is larger than the relatively small  $R_2$ . The actual

<sup>†</sup> Collection Czechoslovak Chem. Comm., 1932.

## POLAROGRAPHY

resistance values have to be chosen by trial and error; the designers of the circuit found that with  $R_1 = 1000\ \Omega$ ,  $R_2 = 10\ \Omega$  and  $R_3 = 75\ \Omega$ , good compensation was obtained.

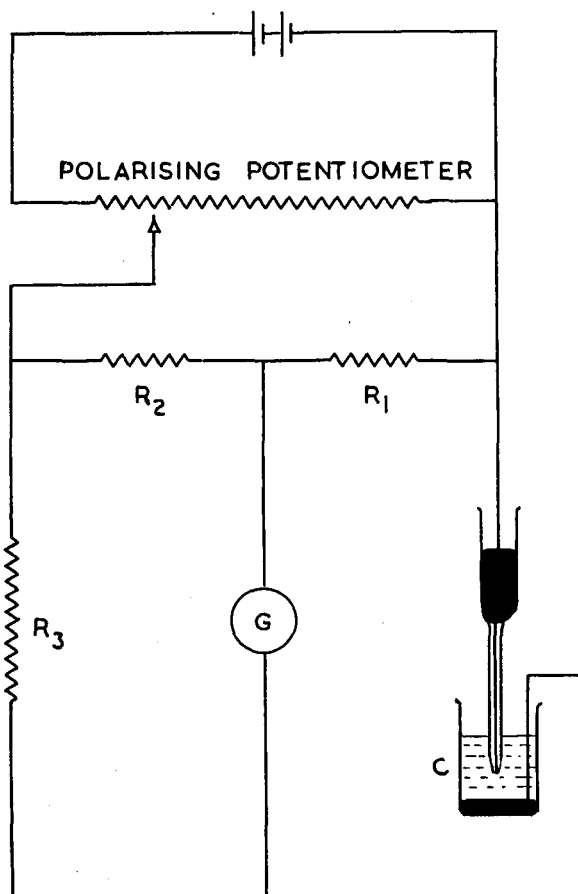


Fig. 12.12. Circuit to reduce the effect of residual currents:  $G$ , galvanometer;  $C$ , polarographic cell

### Differential and Derivative Polarography

The determination of small concentrations of one reducible species in the presence of large concentrations of a more easily-reduced species presents difficulty; the very large wave produced

by the latter species tends to mask the small wave due to reduction of the former species. The polarogram for the reduction of Cu and Cd, as shown in Fig. 12.13, illustrates this point. Experimental methods have been developed to overcome this difficulty, namely *differential* and *derivative* d.c. methods; a.c. techniques have also proved useful in this connection.

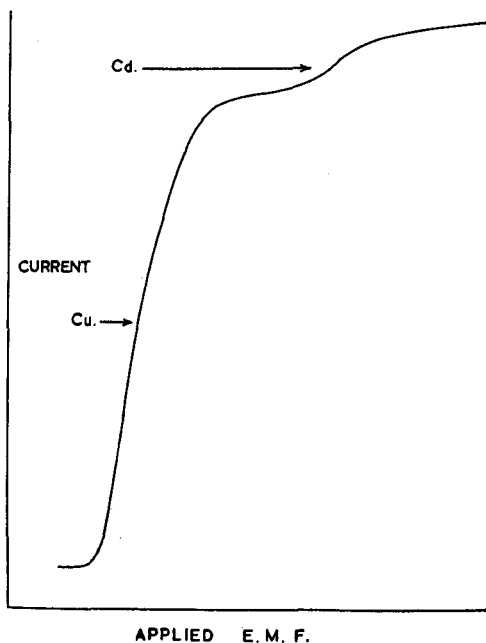


Fig. 12.13. Polarogram of  $\text{Cu}^{++}$  -  $\text{Cd}^{++}$  reduction

(i) *Differential polarography*. This was originally devised by Semerano and Ricoboni† and an outline of the circuit is given in Fig. 12.14.  $C_1$ ,  $C_2$  are two polarographic cells with identical dropping electrodes.  $C_1$  contains the sample under investigation, and  $C_2$  the base electrolyte only. The galvanometer  $G$  records any difference in the potential drops across  $R_3$  and  $R_4$ , and thus the currents flowing in the cells  $C_1$  and  $C_2$ . The two dropping electrodes should be identical even to the extent of having synchronised drops, but this is very difficult to achieve practically;

† *Gazzetta Chem. ital.* 72, 297 (1942).

## POLAROGRAPHY

the resistors  $R_1$  and  $R_2$  may be used to 'trim out' the effects due to small departures from the ideal. The polarising e.m.f. is adjusted until a large diffusion current is obtained from the most easily-reduced species, i.e. the interfering ion present in excess. A solution of this interfering species is then added to  $C_2$  until the galvanometer reads zero. The galvanometer sensitivity

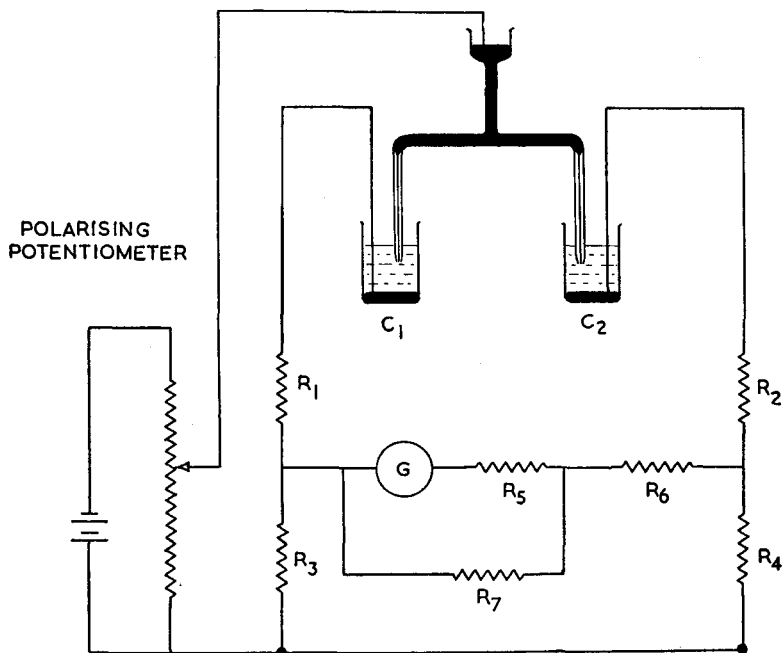


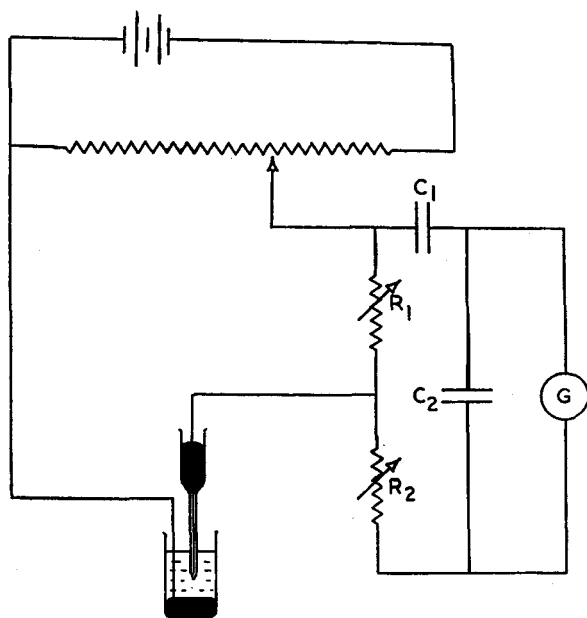
Fig. 12.14. Differential polarograph—basic circuit

may now be increased, and the whole polarogram recorded; only the wave due to the minor component will appear.

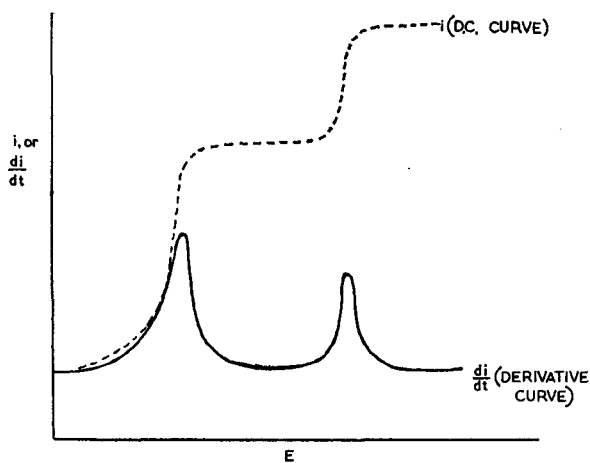
(ii) *Derivative polarography*. Many circuits have been devised for derivative polarography, and the single-electrode circuit of Leveque and Roth† will be described in outline; a diagram representing the circuit is given in Fig. 12.15(a).

Essentially a high-value capacitor  $C_1$  (2000  $\mu\text{F}$ ) is in series with the galvanometer, so that the latter records only the rate of change of potential drop across  $R_1$ . Thus the rate of change of current

† *J. chim. phys.* **46**, 480 (1949).



(a)



(b)

Fig. 12.15. (a) Derivative polarograph. (b) Typical derivative curve



## POLAROGRAPHY

flowing in the cell is obtained;  $C_1$  prevents the flow of a constant current, forming with the galvanometer resistance  $R_g$  a differentiating circuit (p. 320). The galvanometer remains undeflected before and after the ordinary d.c. 'step', but gives a maximum deflection at the half-wave potential. In Fig. 12.15(b), an idealised derivative curve is shown, in which the peak heights are proportional to the concentrations of the various reducible species.

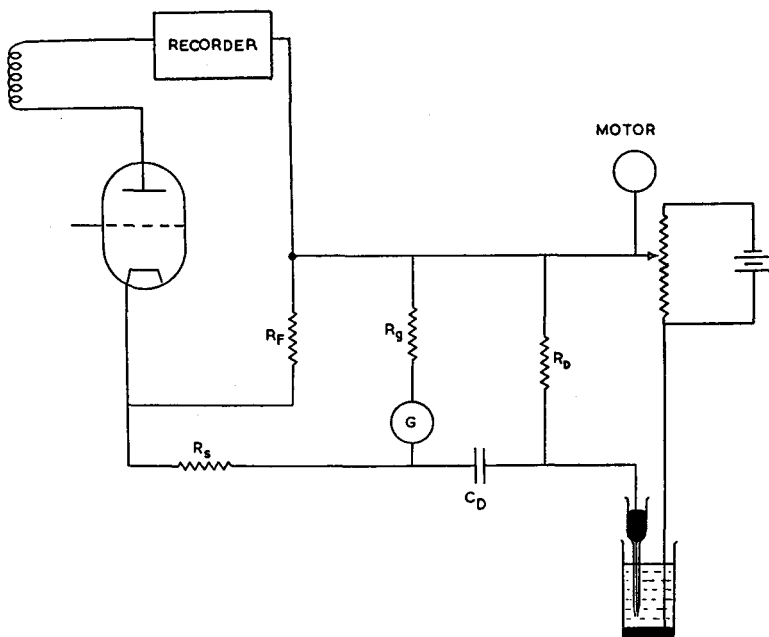


Fig. 12.16. Tinsley d.c. polarograph: circuit for derivative polarography

In the circuit of Leveque and Roth† the resistors  $R_1$  and  $R_2$  control the galvanometer sensitivity, and capacitor  $C_2$  is the usual damping capacitor for the galvanometer. It can be shown that if  $i_2$  is the current through the galvanometer, and  $i_1$  the cell current;  $i_2 = C_1 R_1 \cdot di_1/dt \cdot (1 - \exp[-t/RC_1])$ , where

$$R = R_1 + R_2 + R_g$$

If the time constant  $RC_1$  is small this approximates to

$$i_2 = C_1 R_1 \cdot di_1/dt$$

† *J. chim. phys.* **46**, 480 (1949).

The values of  $R$  and  $C_1$  are carefully chosen so that the peak of the derivative curve approximates to the half-wave potential. It can also be shown that the maximum value of  $i_2$  is dependent upon  $dE/dt$  and the sensitivity can be varied by altering the rate of application of the polarising potential. For this reason if reproducibility is sought, it is necessary to apply the polarising potential via a motor-driven potentiometer of constant speed.

The Tinsley d.c. polarograph already described (p. 293) has facilities for producing derivative polarograms; the basic derivative circuit is shown in Fig. 12.16, where  $C_D$  and  $R_D$  are the derivative capacitor and resistor.

### A.C. Polarography

The development of alternating-current polarography has been fairly rapid since its introduction some 15 years ago by Breyer.<sup>†</sup> A small low-frequency alternating voltage of about 50–60 c/s and 5–30 mV r.m.s. is superimposed on to the direct polarising potential applied to the dropping mercury electrode; the basic circuit is shown in Fig. 12.17(a). The section within the dotted lines is similar to the normal d.c. circuit except that the small a.c. component is injected as shown, and the conventional galvanometer is replaced by a dropping resistor. The magnitude of the voltage drop across this resistor is directly proportional to the current flowing in the polarographic cell. The d.c. component is filtered out by the blocking capacitor, and the a.c. component amplified and measured. Fig. 12.17(b) shows the type of curve obtained where the direct polarising voltage  $E$  applied to the dropping electrode is plotted against the alternating current  $i$  flowing in the cell circuit.

The summit potential  $E_s$  corresponds to the usual half-wave potential of the reducible species and the peak height is proportional to its concentration. It is found that only reversible electrode processes give this well-defined wave. The Cambridge polarograph with Univector unit<sup>‡</sup> is an instrument working on

<sup>†</sup> Breyer, B. and Gutmann, F., *Austr. J. Sci.* **8**, 21 (1945); **8**, 163 (1946); *Trans. Farad. Soc.* **42**, 645, 650 (1946); **43**, 685 (1947); *Farad. Soc. Discussions* **1**, 19 (1947). See also *Malayan Pharm. J.* **5**, 116 (1956) (Royal Institute of Chemistry, Malaya Section, monograph).

<sup>‡</sup> Manufactured by Cambridge Instrument Co. Ltd., Grosvenor Place, London, S.W.1.

## POLAROGRAPHY

these principles. An alternating voltage, applied to the polarographic cell, results in two current-components: one an in-phase resistive current, representing the discharge of the reducible ion, the other a capacitive current representing the charging of the

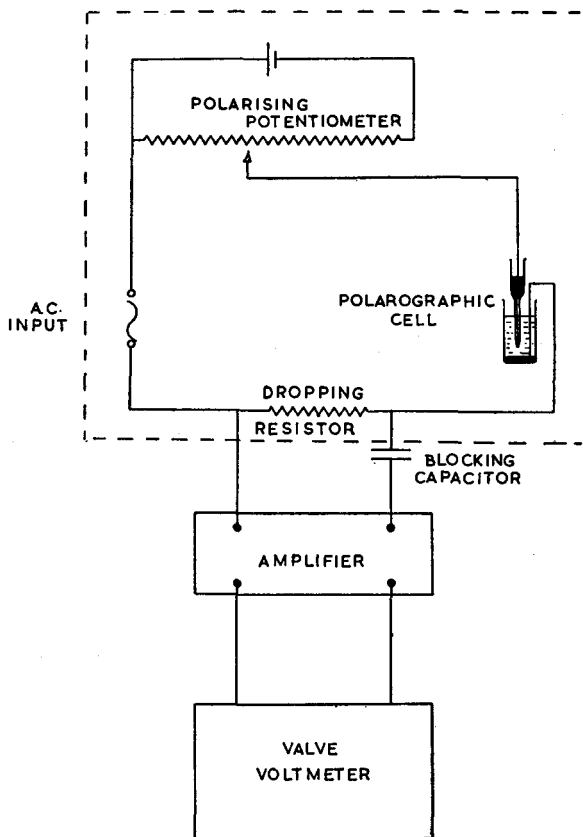


Fig. 12.17. (a) A.C. polarograph—basic circuit

double layer at the drop surface. This current, which is considerably larger than the resistive current, is in phase quadrature with it, so that a phase-sensitive detector may be designed to separate the two. The 'stray' series resistance in the circuit, e.g. solution resistance, instrument resistance, etc., which also produces an

in-phase component, is compensated for by feeding-back a portion of the current output.

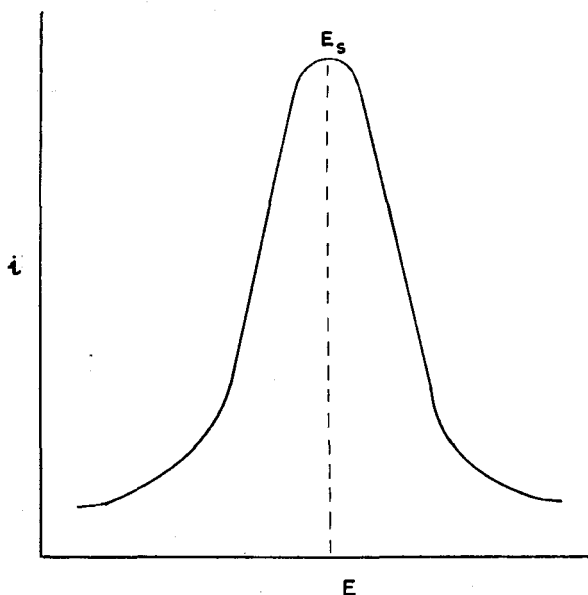


Fig. 12.17. (b) Typical current-voltage curve

### Cathode Ray Polarographs

A number of polarographs are available commercially which make use of the properties of the cathode ray oscilloscope; this section of the subject is usually called *oscillographic polarography*. In addition the so-called square-wave polarograph is now firmly established as an extremely sensitive instrument.

A review of the principles underlying oscillographic polarography was made by Randles<sup>†</sup> and a circuit was described by Airey.<sup>‡</sup> Use is made of the ability of a cathode ray oscilloscope to follow rapidly changing currents. Consider a micro-electrode to which a potential sufficient to produce reduction is applied, so that reducible ions are removed from the layer in contact with the electrode. A current will be produced due to ions flowing in

<sup>†</sup> *Analyst* **73**, 1263 (1947).

<sup>‡</sup> *Analyst* **72**, 301 (1947).

## POLAROGRAPHY

under the resultant concentration gradient, and proportional to this gradient; the diffusion current varies also with time. In practice a series of sweeps are applied at a late (and constant) stage in the drop life, so that the rate of change of electrode area is small. The sweep is provided by the charging capacitor  $C$  (Fig. 12.18).

The starting potential of the sweep is controlled by the potentiometer  $Q$ , and the rate of charge by the variable resistor  $R_2$ . The sweep is terminated by the relay contact  $K$  short-circuiting  $C$ ; the relay coil is operated by a trigger circuit of the multivibrator

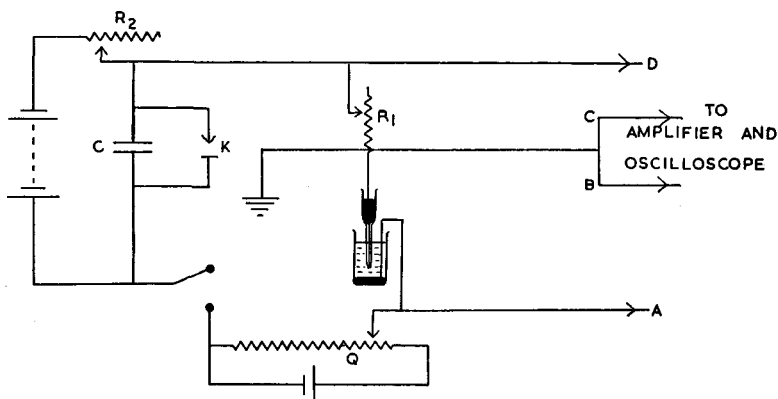


**Fig. 12.18. Cathode ray polarograph—basic circuit**

type. The trigger is impulsed from an amplifier the input of which is the p.d. across  $R_1$ ; the impulse arises because of the sudden change in cell current when the drop falls from the capillary. After a chosen delay time which is controlled by a resistor in the trigger circuit, another sweep starts; this ensures that the sweep is applied at the same stage in the drop life. The resulting outputs from  $AB$  and  $CD$  are amplified and applied to the cathode ray tube. The horizontal axis is the cell polarising potential, and the vertical axis the current flowing. Whilst this gives an outline of the type of circuit used it should be realised that much more complicated circuits are required in practice.

The square-wave polarograph, developed by Barker and Jenkins at Harwell, is a complicated instrument but one which gives great sensitivity. In outline it resembles the a.c. instrument

## LABORATORY AND PROCESS INSTRUMENTS

in that a modulating voltage is applied to the cell in addition to the polarising voltage, but in this case square-wave rather than sine-wave modulation is used. The current flowing is measured only at the 'step' in the modulating voltage, at which time the charging component for the double layer capacity is negligibly small. The square-wave modulation is applied only during a late stage in the drop life, so that the area variation is small; the type of curve obtained may be seen from Fig. 12.19.



Fig. 12.19. Square-wave polarograph—typical current-voltage curve

## NOTES

### The Application of Negative Feedback to the Polarographic Current

Consider the block diagram of Fig. 12.20(a).

Suppose the amplifier has an input resistance  $R_i$  of  $3 \times 10^3 \Omega$ , and requires an input current  $I_i$  of  $1 \times 10^{-7}$  amp for the full output current  $I_o$  of 20 mA into a load  $R_o$  of  $1000 \Omega$ .

## POLAROGRAPHY

The current gain,

$$\frac{I_o}{I_i} = \frac{20 \times 10^{-3}}{1 \times 10^{-7}} = 20 \times 10^4$$

Now apply negative feedback across the feedback resistor  $R_f$ , via the series resistor  $R_s$  (Fig. 12.20(b)).

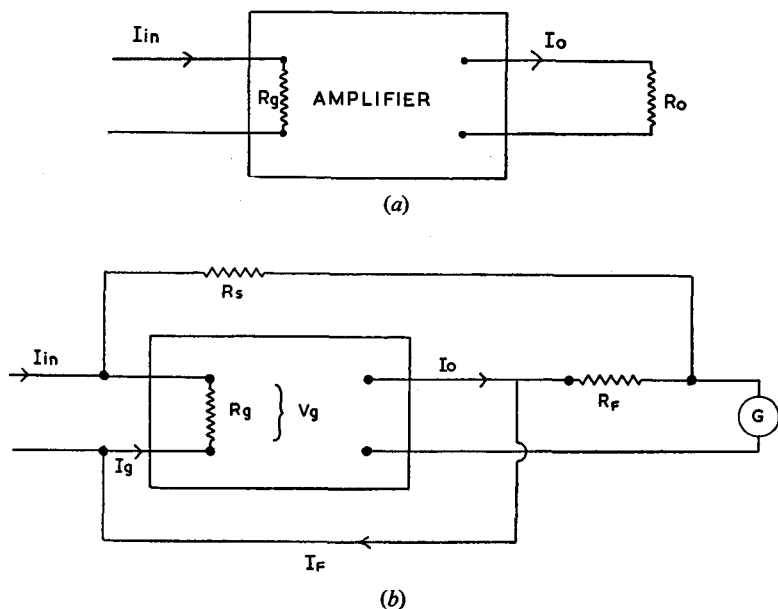


Fig. 12.20. (a) and (b) Feedback circuits

For  $I_o$ , the full output current to be produced, the effective input current of the amplifier, which is now  $I_g$  and equal to  $I_i - I_f$  (where  $I_f$  is the feedback current), must remain at  $10^{-7}$  amp.

Let  $R_f = 1 \Omega$  and  $R_s$  the series resistance be equal to the galvanometer resistance  $R_g$ , i.e.

$$R_g = R_s = 3000 \Omega, \text{ say}$$

Now

$$I_f = \frac{I_o R_f}{R_s + R_g}$$

Since

$$I_g = I_i - I_f \quad (\text{and } R_g = R_s)$$

$$I_g = I_i - \frac{I_o R_f}{2R_g}$$

$$\therefore I_i = I_g + \frac{I_o R_f}{2R_g}$$

Numerically,

$$I_i = 1 \times 10^{-7} + \frac{20 \times 10^{-3} \times 1}{6 \times 10^3} = 1 \times 10^{-7} + 3.33 \times 10^{-6} \\ = 3.43 \times 10^{-6} \text{ amp}$$

$$\text{New current gain} = \frac{20 \times 10^{-3}}{3.43 \times 10^{-6}} = 5.83 \times 10^3$$

The voltage drop across the amplifier terminals

$$= V_g = I_g R_g = 1 \times 10^{-7} \times 3 \times 10^3 = 3 \times 10^{-4} \text{ V}$$

Since

$$I_i = 3.43 \times 10^{-6} \text{ amp}$$

$$\text{The effective input resistance} = \frac{3 \times 10^{-4}}{3.43 \times 10^{-6}}$$

i.e. approximately 87  $\Omega$ .

Thus, the feedback reduces the current gain from  $20 \times 10^4$  to  $5.83 \times 10^3$ , but with stabilisation as in the case of voltage feedback, and reduces the input resistance from  $3 \times 10^3 \Omega$  to 87  $\Omega$ .

### References

- KOLTHOFF, I. and LINGANE, J. J. (1955). *Polarography* (2 vols.). Interscience.  
 MEITES, L. (1955). *Polarographic Techniques*. Interscience.  
 MILNER, G. W. C. (1957). *Principles and Applications of Polarography*. Longmans.  
 YOE, J. H. and KOCH, H. J. (Ed.) (1955). *Trace Analysis*. Wiley.

### Problems

1. Review the application of direct current and simple alternating current polarography to inorganic analysis.
2. Describe and discuss the role of the base electrolyte and maximum suppressors in polarography.



### POLAROGRAPHY

3. The theory underlying 'oscillographic polarography' differs from that of the more familiar direct current polarography. Discuss this theory and describe apparatus, including circuit details, suitable for making measurements using this technique.

4. Write an account of the use of solid microelectrodes in polarography.

5. Describe apparatus, including circuit details, for carrying out differential and derivative polarography.

## CHAPTER XIII

# Radioactivity Measurement

### Introduction

In quantitative radioactivity studies, we are concerned with measuring the number of disintegrations of radioactive atoms in a known time interval. The nuclear disintegration is a true *first-order* process; if the number of atoms present at the commencement of observation, i.e. at time  $t = 0$ , is  $n_0$ , the number remaining after a period of time  $T$  (i.e. at  $t = T$ ) is  $n_T$ , where  $n_T = n_0 \cdot \exp(-\lambda T)$ .  $\lambda$  is the *decay constant*, characteristic of a given radioactive species;  $\lambda$  covers a very wide range of values. If  $T$  is chosen so that  $n_T$  is one half of  $n_0$ ,  $t = T_{1/2}$ , the half-life of the species; hence

$$n_T = n_0/2 = n_0 \cdot \exp(-\lambda T_{1/2})$$

or  $\log n_0 - \log 2 = \log n_0 - \lambda T_{1/2}/2.303$

The decay constant  $\lambda$  and the half-life are evidently related by

$$T_{1/2} = 2.303 \log 2 / \lambda = 0.6932 / \lambda$$

$\lambda$  and  $T_{1/2}$  values for a number of isotopes are listed in Table 13.1.

TABLE 13.1

Isotope	Disintegration process	$\lambda$ ( $\text{sec}^{-1}$ )	$T_{1/2}$
$^3\text{H}$	$\beta$	$1.76 \times 10^{-9}$	12.46 years
$^8\text{Be}$	$2\alpha$	$6.93 \times 10^{16}$	$10^{-16}$ seconds
$^{14}\text{C}$	$\beta$	$3.96 \times 10^{-12}$	5568 years
$^{32}\text{P}$	$\beta$	$5.7 \times 10^{-7}$	14.3 days
$^{35}\text{S}$	$\beta$	$9.27 \times 10^{-8}$	87.1 days
$^{40}\text{K}$	$\beta$	$1.68 \times 10^{-17}$	$1.3 \times 10^9$ years
$^{60}\text{Co}$	$\beta, \gamma$	$4.25 \times 10^{-8}$	5.2 years
$^{131}\text{I}$	$\beta, \gamma$	$1.00 \times 10^{-6}$	0.8 days
$^{217}\text{At}$	$\alpha$	3.85	$1.8 \times 10^{-2}$ seconds
$^{221}\text{Fr}$	$\alpha$	$2.4 \times 10^{-3}$	4.8 minutes
$^{226}\text{Ra}$	$\alpha, \gamma$	$1.38 \times 10^{-11}$	$1.6 \times 10^3$ years
$^{238}\text{U}$	$\alpha$	$4.9 \times 10^{-18}$	$4.5 \times 10^9$ years

## RADIOACTIVITY MEASUREMENT

From the equation

$$n_T = n_0 \cdot \exp(-\lambda T), \log n_T = \log n_0 - \lambda T/2.303$$

and the graph of  $\log n_T$  (i.e number of disintegrations per unit time at  $t = T$ ) against time  $T$  should be linear, of slope  $-\lambda/2.303$ . This is a good test of the homogeneity of the source; for a *mixed* source containing two species of differing  $\lambda$ , the decay curve is shown in Fig. 13.1.

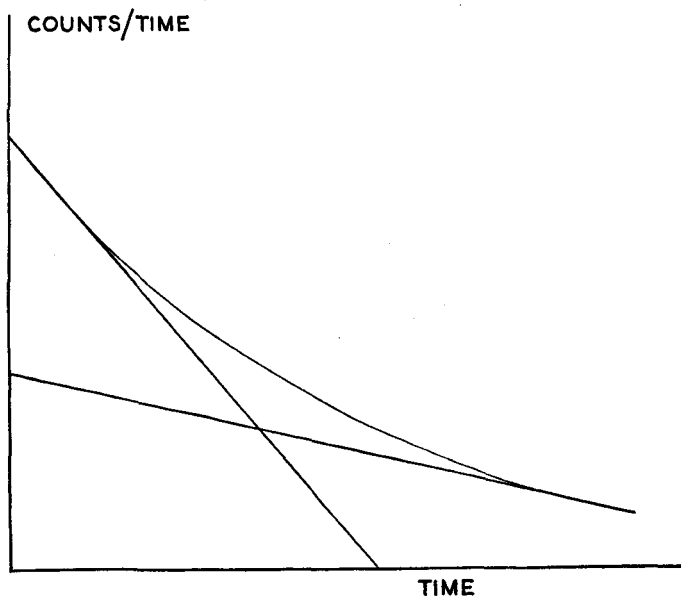


Fig. 13.1. Decay curves of a mixed radioactive source

Assuming a homogeneous source, if  $\lambda$  or  $T_{1/2}$  is known,  $n_0$  may be calculated from  $n_T$ . Hence the determination of concentration of a particular species in a sample is resolved into counting the number of disintegrations within it, per unit time. This is quite analogous to the treatment of 'first-order' reactions in chemical kinetics.

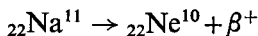
The primary disintegration products are:  $\alpha$ -particles, or helium nuclei;  $\beta^-$ -particles or fast-moving electrons;  $\beta^+$  particles, or positrons, of electronic charge and mass, but positive in sign;

## LABORATORY AND PROCESS INSTRUMENTS

and  $\gamma$ -rays, or short-wavelength X-rays. Examples of typical decay processes producing these are:



the symbol \* indicating that this is a nuclear-excited state of nickel, decaying to the nuclear ground state by  $\gamma$ -emission.



The process of K-shell capture (the nucleus absorbing an electron from the inner shell of the atom) leads to longer wavelength X-rays (K-photons):



The interaction of these primary products with matter is the basis of their detection and estimation. Charged particles are detected by the ionisation produced by their passage through a gas. Both charged particles and  $\gamma$ -rays may be detected by their photo-electric effect on a suitable medium, or *phosphor*. We shall deal with these two means of detection separately.

### **Ionisation Instruments**

(i) *The proportional counter.* A mixture of gases is ionised by the incidence of primary charged particles, and a partial short-circuit is established between two electrodes in the gas. The resultant current flow develops a more or less sharp voltage pulse across the load resistor  $R$  (Fig. 13.2), and the number of such pulses in a given time is measured.

The proportional counter (p. 190) is used for weak sources of radiation such as  ${}_{14}\text{C}$  and  ${}_3\text{H}$  (tritium). The radioactive atoms may be introduced into the chamber as a gas ( ${}_{14}\text{CO}_2$ ,  ${}_3\text{H}_2$ ), together with a diluent 'flow' gas, often a mixture of argon and methane. The essential feature of the proportional counter is the limited degree of gas amplification which takes place, so that the output pulse is proportional to the energy of the incident particle. However, this pulse is still comparatively small, and requires a high-gain amplifier, and a power supply unit of very high stability. It is probably true to say that, at present the usefulness of proportional counters is limited by the availability of suitable

## RADIOACTIVITY MEASUREMENT

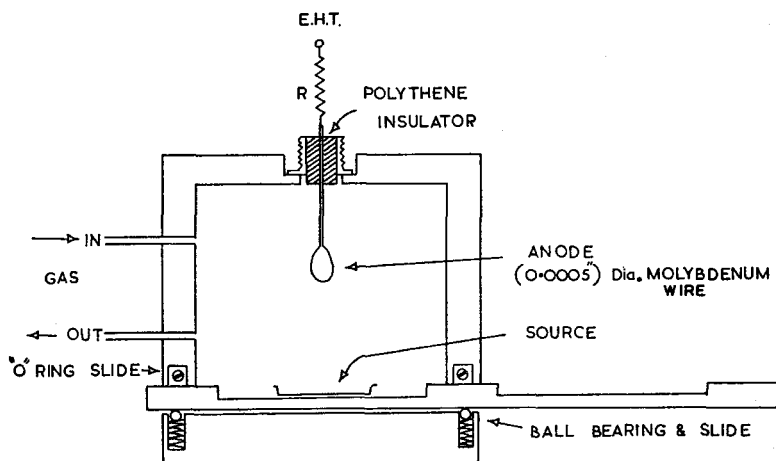


Fig. 13.2. Proportional counter and load resistor

ancillary equipment. A block diagram of the complete apparatus is shown in Fig. 13.3; typical plateau curves were shown in Fig. 8.14. The 'head' amplifier is maintained close to the proportional counter chamber, so as to minimise cable capacity.

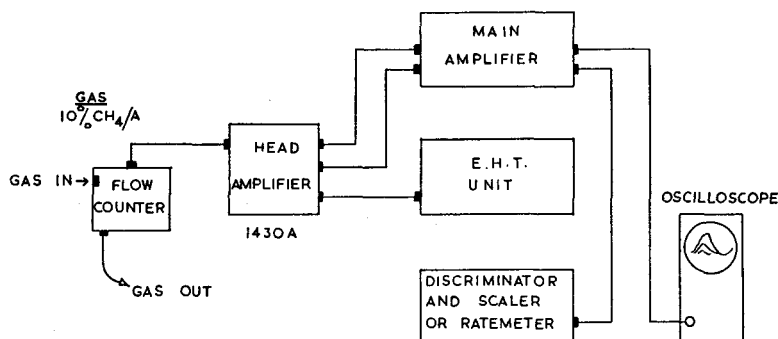


Fig. 13.3. Block diagram of proportional counter circuit

The gain and bandwidth of the main amplifier are both variable; circuit details are discussed on p. 327. The output feeds a counter unit, or scaler, in which the number of pulses is registered by dekatrons (p. 180) or other scaling circuits.

## LABORATORY AND PROCESS INSTRUMENTS

(ii) *The Geiger counter.* The Geiger-Müller tube (p. 186) is the most generally used detector of radioactivity. The tube delivers a voltage pulse for each incident particle, of considerably greater amplitude than the pulse from the proportional counter; moreover, this pulse is of constant amplitude, irrespective of the incident-particle energy. This arises because each particle causes an ionisation 'avalanche' throughout the tube. Since, however, it takes a certain time for the ion pairs to re-combine, a Geiger tube is inoperative for a certain period after it has fired, and it will not record pulses arriving during this quiescent period. The process of 'recovery' of a Geiger tube is indicated in Fig. 13.4. If the

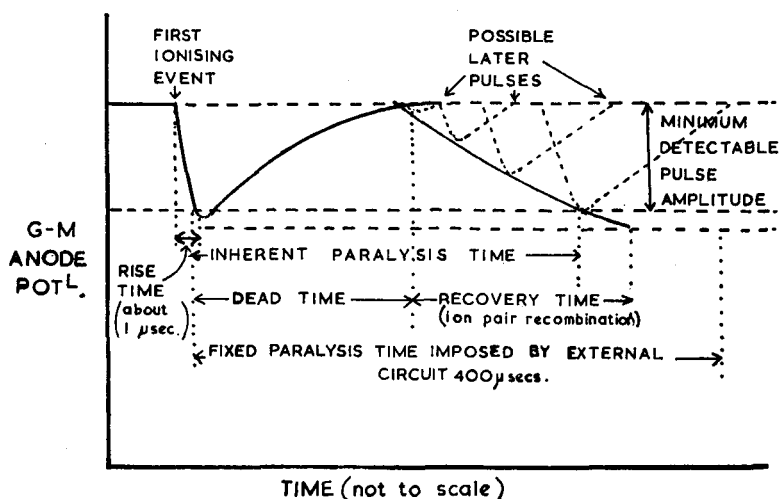


Fig. 13.4. Recovery time of the Geiger-Müller tube

time for which the tube is quiescent is  $T_p$  seconds ('the paralysis time' of the tube) and the observed number of counts per *minute* is  $N_0$ , the *corrected* number of counts  $N$  is given by:

$$N = \frac{N_0}{1 - N_0 T_p / 60} \text{ min}^{-1}$$

$T_p$  is usually about 200  $\mu$ seconds, but varies with the age of the tube and the E.H.T. supply voltage; it is not a very definite quantity when determined solely by the Geiger tube. Usually

## RADIOACTIVITY MEASUREMENT

therefore, the tube is 'quenched' by the output pulse of a quench unit (p. 323), for a constant time  $T_q$  ('quench time'), which is usually made 400  $\mu$ seconds.

We then have:

$$N = \frac{N_0}{1 - (4 \times 10^{-4} N_0)/60} = \frac{N_0}{1 - 6.67 \times 10^{-6} N_0} \text{ min}^{-1}$$

The importance of this correction may be seen from the following table:

TABLE 13.2

( $T_q = 400 \mu$ seconds)

$N_0$ ( $\text{min}^{-1}$ )	$N$ ( $\text{min}^{-1}$ )	$N_0$ ( $\text{min}^{-1}$ )	$N$ ( $\text{min}^{-1}$ )
300	301	10,000	10,720
1000	1007	20,000	23,000
3000	3061	30,000	37,500

The action of quenching agents, such as organic compounds or halogen molecules, within the tube, has already been discussed (p. 189). Halogen-quenched tubes generally operate at a much lower anode voltage than organically-quenched tubes, and as the halogen molecules are regenerated, their 'life' is not limited to about  $10^9$  counts. However, organically-quenched tubes have a longer, and rather flatter, plateau; compare the typical characteristics:

*halogen tube*—370 V threshold; 100 V plateau; average slope 0.1 % per volt.

*organically-quenched tube*—1500 V threshold; 300 V plateau; average slope 0.03 % per volt.

(iii) *The scintillation counter.* This type of detector was used in the earliest investigations of radioactivity; the flashes of light produced when radiation impinged upon screens coated with a thin layer of zinc sulphide were counted. A great deal of research into phosphors has produced a variety of materials of varying decay time and efficiency of conversion of the incident energy into light; some of these are listed in Table 13.3. We may define

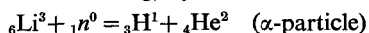
# LABORATORY AND PROCESS INSTRUMENTS

a *phosphor* as a material converting the energy of incident radiation into light of suitable wavelength for the operation of a photo-cell.

TABLE 13.3

<i>Phosphor</i>	<i>Emission peak</i> (Å)	<i>Decay time</i> (μsecond)	<i>Efficiency</i>
NaI (thallium-activated)	4100	0.25	~0.045, α ~0.09, β
LiI (europium-activated)†	4400	1.2	~0.03, α ~0.03, β
ZnS (silver-activated)	4500	10	0.28, β
Anthracene	4470	0.03	1.0‡
Stilbene	4100	0.006	0.45
Tetraphenylbutadiene (in polystyrene plastic)	3900/4300	0.005	0.35
α-Naphthylamine (soln. in xylene, 2 g/l.)	3900/5600	0.003	0.17
Li-alkaline earth silicate glass, cerium activated.	3950	0.05–0.1	~0.008, α ~0.004, β
p-Terphenyl in toluene soln.	3400/3700	0.003	0.43

† Suitable for neutron counting, by means of the reaction:



‡ For *organic* phosphors, the conversion efficiency is usually quoted relative to anthracene, which has about half the efficiency of NaI; these phosphors have approximately the same α-β ratio.

The solid phosphor is encapsulated; in the case of hygroscopic materials such as sodium iodide, the crystal is coated with magnesium oxide and sealed with a transparent plastic coating in an aluminium capsule. The face of the capsule is coated with a silicone oil, and firmly attached to the 'window' of a photomultiplier tube (p. 178) (see Fig. 13.5). Radiation causes the emission of flashes of light within the phosphor, which expel electrons from the photo-cathode; electron multiplication then occurs between successive dynodes. Each incident particle gives rise to a comparatively large output pulse; the rise time is very short, so that high counting rates (up to  $10^7$  per second) are possible. In conjunction with a typical pulse amplifier of about 40 db gain,



## RADIOACTIVITY MEASUREMENT

the photomultiplier may be operated at quite a low overall voltage—e.g. 750 V. The power-supply unit should be very stable, since the scintillation-photomultiplier assembly has a shorter plateau than a Geiger-Müller tube.

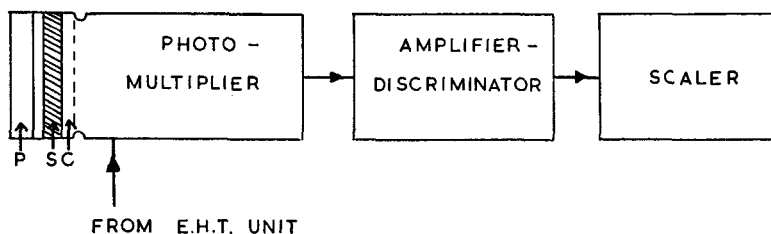


Fig. 13.5. Scintillation counter-block diagram. P, phosphor; S, optical coupling of silicone oil; C, photo-cathode

### Other Methods of Measurement

Very early detectors of radiation made use of the blackening of a photographic plate or film on exposure to the source; this is essentially a method of integrating the amount (or 'dose') of radiation received over an interval of time. The method is now used in the auto-radiography of metal castings, and in assessing the dose received by a person exposed to radiation.

For monitoring the dose of radiation received, film badges are generally worn in the lapel of the laboratory overall, or on the wrist; part of the film is covered with lead foil, so that the  $\gamma$ -radiation component of the total dose may be measured. A service is maintained for the processing and evaluation of film badges.†

Another portable radiation monitor is the pocket electroscope, or *dosimeter*. This is a small quartz-fibre electroscope, about the size of a fountain pen, which may be charged from a battery or other source; the fibre (or its image on a screen) is then observed to rest at the zero of a scale. Radiation causes ionisation of the gas in the electroscope, and the charge leaks away; the fibre thus moves towards the uncharged position. The leakage is a measure of the number of ion-pairs produced in the gas, so the scale may be directly calibrated in energy-dosage, or *Röntgens*; this unit is the amount of energy which must be absorbed by 1 c.c. of air at N.T.P. to produce  $2 \times 10^9$  ion-pairs in this volume of the gas.

† The Radiological Protection Service, Sutton, Surrey.

# Electronic Equipment

Both the proportional counter and the Geiger-Müller tube are high-impedance devices; for adequate power transfer, this impedance must be matched to the input impedance of the amplifier (p. 71) and this is achieved by a cathode-follower circuit (p. 142) in the *probe unit*.

The amplifiers for use in connection with radioactive measurement are designed rather differently from those of Chapter VI, since they deal with discrete pulses rather than more or less continuous waves. Now the passage of a voltage through a circuit

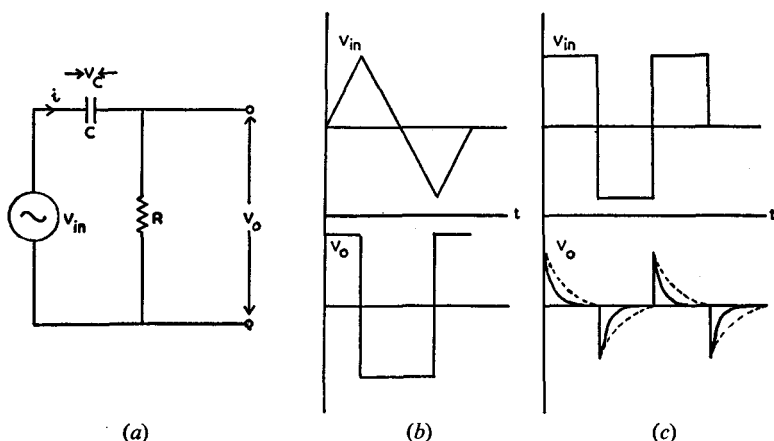


Fig. 13.6. (a) Differentiating circuit. (b) Differentiation of a triangular waveform. (c) Differentiation of a square waveform

which contains both resistance and capacitance (i.e. through *any* practical circuit) introduces differentiation of the pulse with respect to time; hence, only a pure sine wave will pass through the circuit undistorted, since its differential, a cosine wave, is merely the original altered in phase. A 'pulse' consists of a rather large number of frequency components, of varying amplitude and phase, and hence suffers distortion, to an extent dependent upon the repetition frequency of the pulse, the sharpness of its rise and fall, and the time constant of the circuit to which it is applied. Consider the circuit of Fig. 13.6(a). Since

$$i = Cdv_c/dt, V_o = iR = CR \cdot dv_c/dt$$

## RADIOACTIVITY MEASUREMENT

Now  $V_i = V_c + V_o$ , but if  $(RC)$  is *small*, compared with the period of the input voltage

$$V_i \simeq V_c \quad \text{and} \quad V_o = CR \cdot dV_c/dt$$

Thus, the output voltage is approximately equal to  $CR$  times the differential of the input voltage, and this is called a *differiating circuit*. Its effect upon some input waveforms is shown at (b) and (c). Note that if the time constant  $CR$  is increased, the 'spikes' in Fig. 13.6(c) become broader, as shown by the dotted lines, revealing the exponential discharge of the capacitor  $C$ .

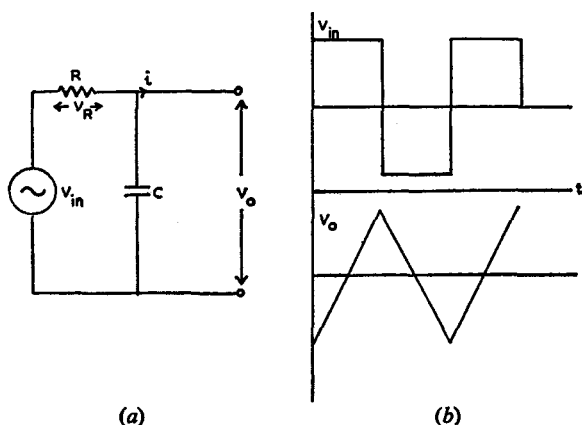


Fig. 13.7. (a) Integrating circuit. (b) Integration of square waveform

Interchange of  $C$  and  $R$  in the above circuit produces the *integrating circuit* of Fig. 13.7(a). If  $(CR)$  is *large* compared with the period of the input voltage,

$$V_i \simeq V_R \quad \text{and} \quad V_o = \frac{1}{C} \cdot \int i dt = \frac{1}{CR} \cdot \int V_R \cdot dt$$

$$V_i = V_R + V_o, \text{ i.e. } V_o \simeq \frac{1}{CR} \cdot \int V_i dt$$

So that the output voltage is the time integral of the input voltage, as shown at Fig. 13.7(b).

## LABORATORY AND PROCESS INSTRUMENTS

*Applications of these circuits.* The voltage pulses obtained in nuclear measurements vary according to the detecting element used; typical pulses from a Geiger-Müller tube, and from a scintillation counter, are shown in Fig. 13.8. The random nature

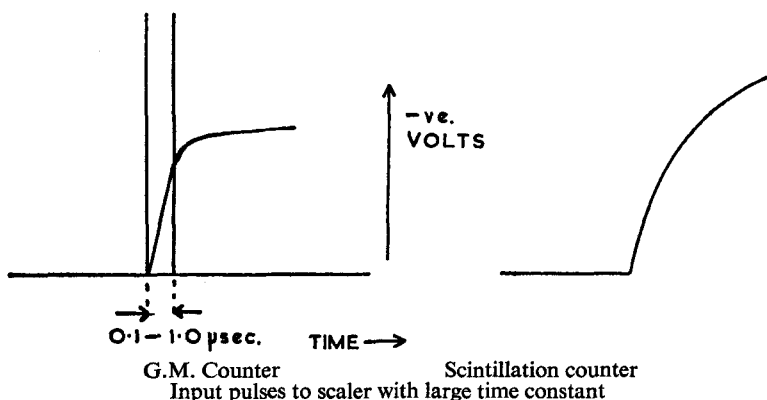


Fig. 13.8. Output pulses of Geiger-Müller tube and scintillation counter

of the disintegration process produces a train of pulses such as that of Fig. 13.9(a), which is reduced to the orderly single-amplitude system of Fig. 13.9(b) by passage through a differentiating

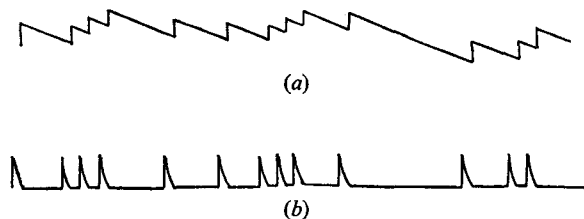


Fig. 13.9. The differentiation of a random pulse train

circuit. A very short time constant  $CR$  gives high resolution, but pulse amplitude is lost, and the signal-to-noise ratio reduced. The amplifiers used in nucleonic measurement include a differentiating circuit, usually with a variable time constant; this circuit also reduces low-frequency 'noise', and in fact fixes the *lower* limit of the amplifier frequency bandwidth.

## RADIOACTIVITY MEASUREMENT

In principle, each  $R$ - $C$  coupled stage of the amplifier acts as an integrating circuit; however fast the leading edge of an applied pulse, it will rise exponentially according to a time constant  $R(C_i + C_s)$ , where  $C_i$  is the input capacitance to the next stage, and  $C_s$  is the associated stray capacitance. This evidently sets an *upper* limit to the amplifier bandwidth, and this may also be made variable by alternative  $RC$  circuits.

Some of the more important items of electronic measuring equipment used in radioactivity measurement will now be dealt with briefly.

### Quenching Probe

The probe usually consists of a cathode-follower circuit, mounted close to the Geiger-Müller tube, reducing the loading of the cable connections to the amplifier. To fix the quiescent period of the tube, and to eliminate spurious pulses, the Geiger pulse may

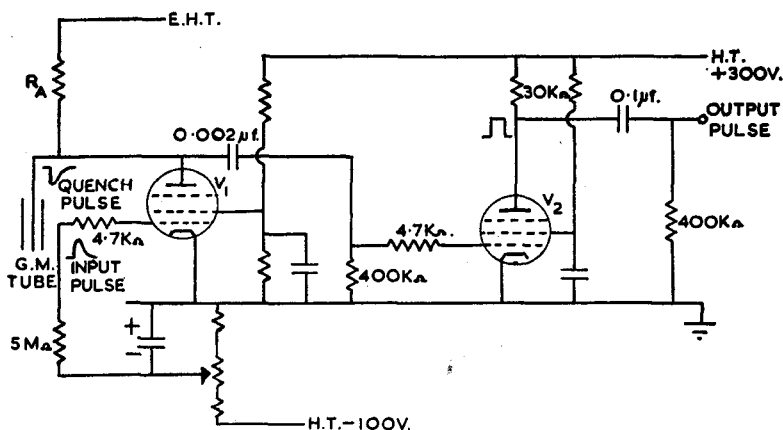


Fig. 13.10. Geiger-Müller quench circuit

be arranged to trigger a pulse generator in the probe unit, producing a *quenching* pulse. In Fig. 13.10 the grid bias of  $V_1$  is normally set just beyond cut-off. A positive pulse causes  $V_1$  to conduct, and the fall in voltage across  $R_A$  ( $5\text{ M}\Omega$ ) quenches the Geiger tube. The sudden fall in anode potential produces a positive square-wave pulse at the anode of  $V_2$ . The time constant for decay of the quenching pulse is generally fixed at  $400\text{ }\mu\text{s}$ .

### Ratemeter

The *scaler* records the total number of disintegrations in a given interval of time, whilst the *ratemeter* records the rate at which disintegrations are occurring at any instant. The ratemeter responds rather slowly; it attains its final reading (within 1%) only after about 4 time constants. It is used to integrate the pulse output of a 'kicksorter' (p. 331), and its output may be applied to a pen recorder; otherwise, its main use is in monitoring apparatus and equipment for radioactive contamination. The block diagram of a typical ratemeter is shown in Fig. 13.11.

The input pulses from the Geiger-Müller tube are amplified and shaped, before being used to trigger a Kipp relay circuit, of the type shown in Fig. 13.12(a). In the quiescent state  $V_2$  is cut off by the heavy negative grid bias voltage; the grid of  $V_1$  is at earth potential and the capacitor  $C_1$  is charged to H.T.<sup>+</sup>. A

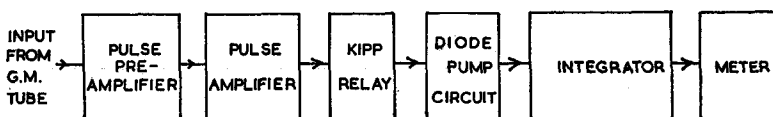


Fig. 13.11. Block diagram of ratemeter

negative input pulse cuts-off  $V_1$  and switches on  $V_2$ , by a mechanism similar to that of the multivibrator (p. 167), and the circuit is insensitive to further pulses in this state. The circuit returns to its original condition by the recharging of  $C_1$  in a time determined by the  $R_1C_1$  time constant; the circuit thus provides a series of uniform output pulses for all input pulses of sufficient amplitude to trigger it. Some of the waveforms are shown in Fig. 13.12(b).

The standardised output pulses are applied to a *diode pump* circuit, shown in outline in Fig. 13.13. The capacitor  $C_p$  is small so that it charges completely from each pulse. This charge is drawn from the H.T. supply and is 'pumped' through diode  $d_2$  to the reservoir capacitor  $C_r$ , which is made sufficiently large for the potential at the anode of  $d_2$  to remain practically constant throughout the pulse. The charge on  $C_r$  leaks away through an integrating circuit of variable resistance  $R$ ; the potential across the capacitor decreases until the decay rate just balances the charging rate, and this potential is recorded on a voltmeter cali-

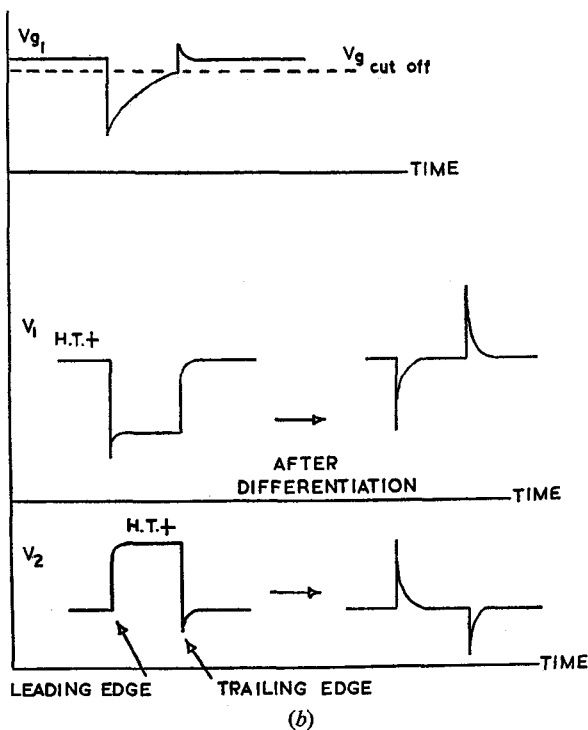
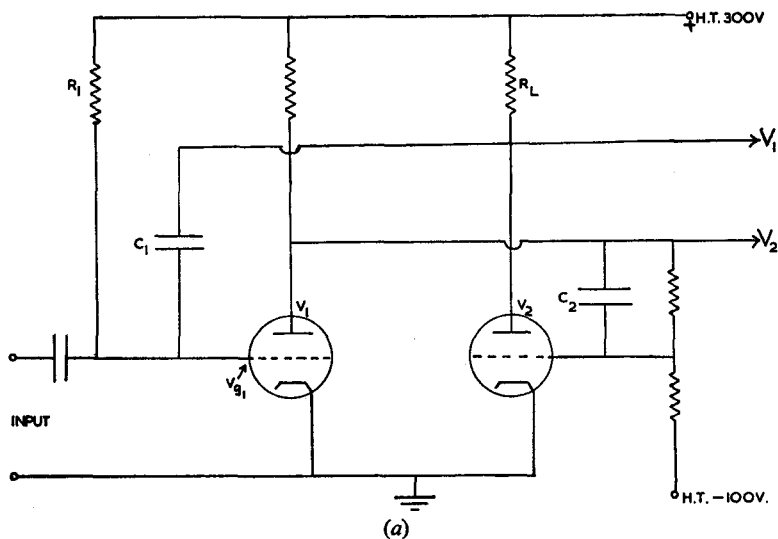


Fig. 13.12. Kipp relay and waveforms

brated in pulses per second. If the pulse amplitude is  $V$  volts, and the potential difference across the reservoir  $C$  is  $v$ , the charge transferred per pulse  $= C_p \cdot (V - v)$ . Hence the current through  $R = v/R = n_p C_p (V - v)$ , where  $n_p$  pulses arrive per second at  $C_r$ . Hence

$$v = \frac{R \cdot n_p \cdot C_p \cdot V}{1 + n_p \cdot C_p \cdot R}$$

so that  $v$  is linearly related to  $n_p$  for  $V \gg v$ . The diode pump capacitor  $C_p$  is pre-set according to the count-rate corresponding to full-scale deflection, i.e. according to the sensitivity required.

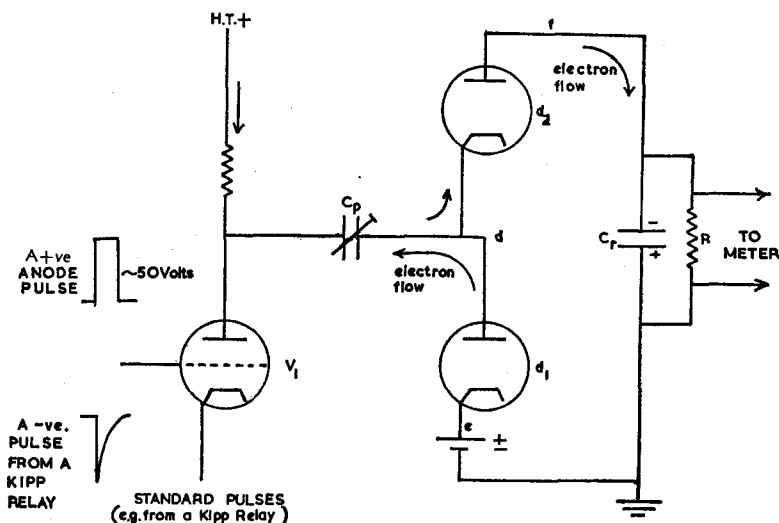


Fig. 13.13. Diode pump circuit

With the effective value of  $C_r = 25 \mu\text{F}$ , the integrating resistor may have values of 40 K $\Omega$ , 200 k $\Omega$  and 1 M $\Omega$ , to give time constants of 1, 5 and 25 seconds respectively, and the meter reading is the average rate over these periods. The output current of the integrator may be used to operate a pen recorder, and an aural indication is often provided by feeding part of the generated pulse to a loudspeaker.

The ratemeter smooths out statistical variations of counting rate over a period of about four times the time constant  $\tau$ , so that  $\tau$  should be chosen as large as is convenient.



# Pulse Amplifiers

The pulses from the various nuclear detectors differ considerably in amplitude, width and rise time; a general-purpose pulse amplifier thus requires the following characteristics:

*High gain*—up to  $10^6$  for the smallest pulses.

*Wide bandwidth*—a series of pulses, 1  $\mu$ second wide, corresponds to a signal frequency of 1 Mc/s.

*Low input capacity, and low level of 'noise' in the first stage*—always of great importance in a high-gain amplifier.

*Output voltage* in the range 5–50 V, according to the input-pulse amplitude; this output is suitable for the operation of the pulse analyser.

*Variable time constants* for the differentiating and integrating circuits.

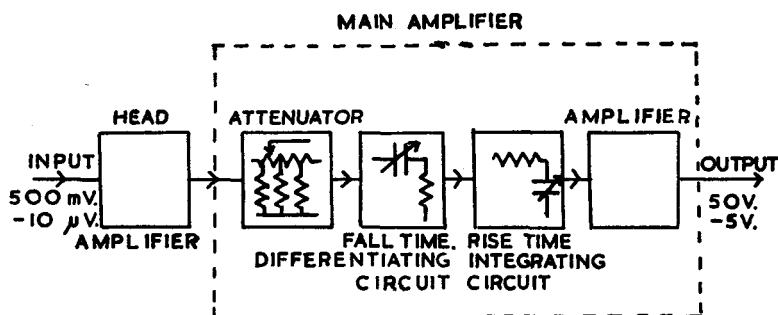


Fig. 13.14. Block diagram of typical pulse amplifier

A block diagram of a typical pulse amplifier is shown in Fig. 13.14. The head amplifier is essential for use with a proportional counter, but is replaced by a cathode-follower impedance-matching circuit for the amplification of pulses from a Geiger-Müller tube or scintillation counter. The shaping of pulses by differentiating and integrating circuits has already been described (p. 320).

As in the majority of instrument amplifiers, stability and linearity of response are obtained by the extensive use of negative feedback. Consider an amplifier of basic gain  $A$ , to which negative feedback is applied, so that the gain is reduced to  $B$  by returning a fraction  $\beta$  of the output in phase opposition. If  $A$  is large,  $B \approx 1/\beta$ ; changes in power-supply voltages, or in the

characteristics of components, which would produce a change of  $\delta A$  in  $A$  are reduced by the application of negative feedback, so that a smaller change  $\delta B$  occurs in the final gain  $B$ , where

$$\delta B = (B/A) \cdot \delta A = \delta A / A\beta$$

This reduction-factor  $1/A\beta$  is called the *feedback factor*.

If there are several stages of amplification, feedback may be applied in a number of ways. Consider an amplifier of  $n$  stages, each of inherent gain  $A$ ; without feedback, the overall gain would be (ideally)  $A^n$ . If feedback is applied to each stage, reducing its gain to  $B$ , the overall gain is now  $B^n$ ; alternatively, the feedback might be applied as a single loop from output to input, again reducing the overall gain from  $A^n$  to  $B^n$ . A change of  $\delta A$  per stage produces an overall change, in the former case, of  $\delta B = (B/A) \cdot n\delta A$ ; in the latter case, of  $(B/A)^n \cdot n\delta A$ . Since  $B/A$  is  $< 1$ , the latter case is evidently preferable; for example, with individual feedback, if  $n = 2$ ,  $A = 50$ , and  $B^n$  (the overall gain) = 100, then  $B = 10$ , and an  $x\%$  change in  $A$  results in  $2 \times 10/50 \cdot x = 0.4x\%$  change in  $B$ ; with a single feedback loop, the change in  $B$  is  $2 \times (10/50)^2 \cdot x$ , or  $0.08x\%$ . From this analysis, it is evidently better to include several stages within the feedback loop; the variation of gain and phase with frequency, however, modify this conclusion to some extent. The ratio of (high frequency gain):(low-frequency gain), and the phase shift of output voltage with respect to input, are shown as functions of frequency in Fig. 13.15, for a 2-stage amplifier.

If the phase-angle  $\phi$  exceeds  $90^\circ$ , the feedback has an in-phase component, and a damped oscillation, or 'ring', appears on the output pulse. A very useful circuit, in which these effects are minimised, is the 'ring-of-three' amplifier, illustrated in Fig. 13.16. A cathode follower stage  $V_3$  couples the feedback from  $V_2$  to  $V_1$ , producing very small capacity loading at  $V_2$  anode. The d.c. loading is also small; if this were achieved by increased values of  $R_x$  and  $R_y$ , considerable individual feedback would be generated by  $V_1$  (due to  $i_{a1} R_y$ ), and the overall stability would be reduced. The capacitor  $C_x$  improves the high-frequency stability by limiting the phase shift to  $90^\circ$ , and also maintains the feedback factor practically constant up to the limit of bandwidth. With optimum adjustment of  $C_x$ , a gain of about 100, at a bandwidth of a few Mc/s, is obtainable.

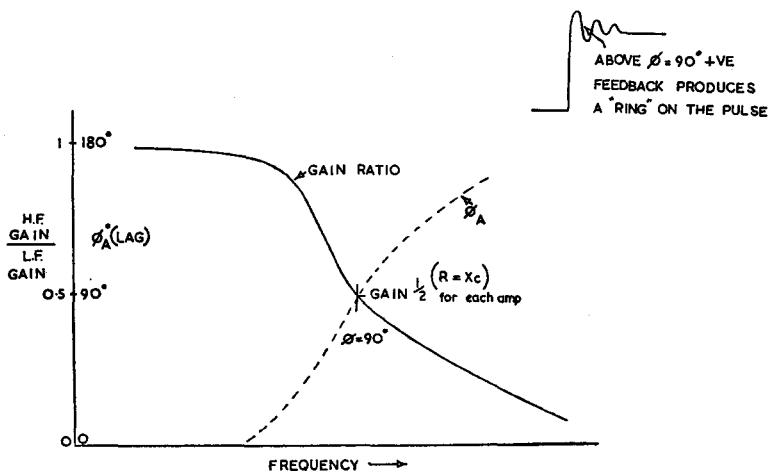


Fig. 13.15. Variations of gain and phase with frequency for a 2-stage amplifier with negative feedback

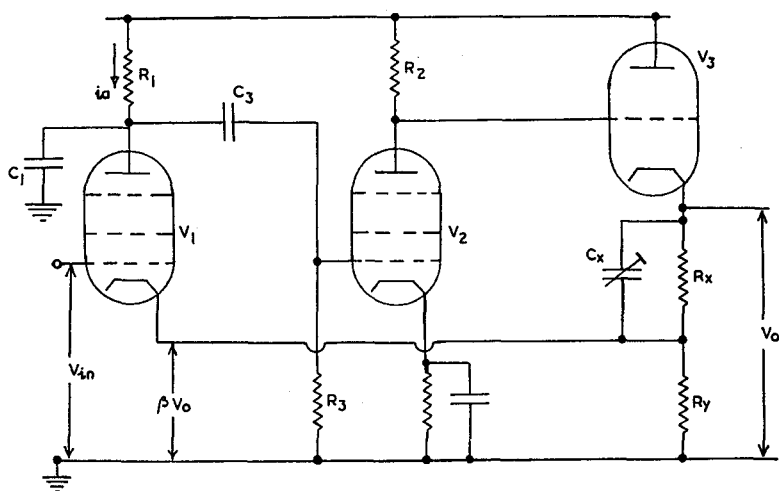


Fig. 13.16. The ring-of-three amplifier

# LABORATORY AND PROCESS INSTRUMENTS

The H.T. supply to the ring-of-three amplifier is normally derived from a stabilised source (p. 107), but stabilisation of the low-tension (heater) supplies is also desirable for the maximum linearity. Connection of the circuit as in Fig. 13.17 may avoid this necessity; a rise in heater voltage lowers the anode voltage of  $V_2$ , and this is fed back to the cathode of  $V_1$ , resulting in an

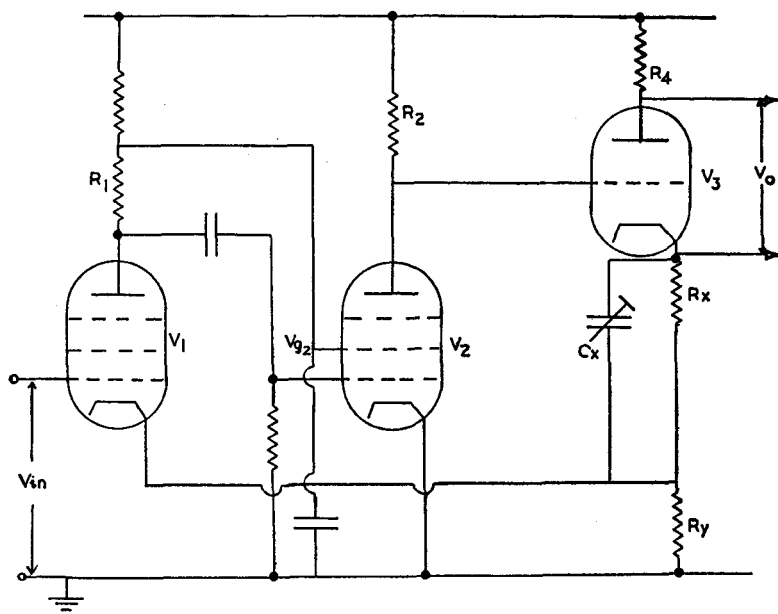


Fig. 13.17. Alternative circuit for eliminating the effects of heater-voltage variation

amplified decrease in anode voltage of  $V_1$ . Since  $V_2$  screen is connected to this point, its potential  $V_{g2}$  falls, and opposes the original rise of heater voltage. The small anode load  $R_4$  enables a positive output pulse to be obtained. This method of stabilisation is used in the I.D.L. amplifier.† This amplifier contains two ring-of-three circuits, with an overall maximum gain of

† Produced by Messrs. Isotope Developments Ltd., Aldermaston, Berks. Similar equipment is manufactured by Packard Instrument Co., Lagrange, Ill., and by Nuclear Measurements Corpn., Indianapolis, Ind.

## RADIOACTIVITY MEASUREMENT

10,000; 40 db of variable attenuation is provided. The bandwidth is 5 Mc/s, and a 5–50 V discriminator circuit is included (p. 332). The rise and fall time constants may both be varied.

Very careful choice of the input valve, and design of the input stage, is necessary in order to keep the noise as low as possible; 'grid-noise', arising from the statistical fluctuation in the number of electrons 'caught' by the grids, is reduced by using

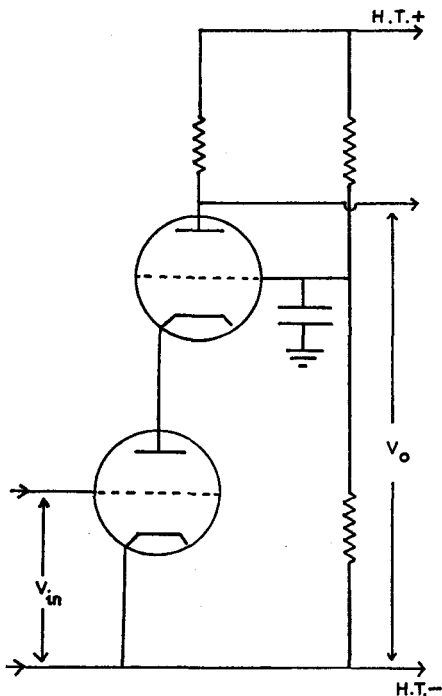


Fig. 13.18. 'Cascode' triode input circuit

a triode valve. This advantage may be maintained together with the low input capacity of a pentode valve, by the circuit of Fig. 13.18, sometimes called the 'cascode' circuit. The  $C_{g,a}$  capacities of the triode do not shunt the input circuit.

### Pulse Analyser or 'Kicksorter'

Positive incoming pulses of amplitude from 5–50 V are accepted. By means of a variable bias voltage the amplifier is arranged to cut-off all pulses below a given threshold voltage. Thus,

considering the pulse train of Fig. 13.19, with the bias set to  $V_1$ , pulses  $B$ ,  $C$  and  $D$  will register; if the bias is increased to  $V_2$  only  $C$  will be recorded. Alternatively, the analyser may be set to accept only pulses within a narrow band about a mean bias voltage, both the bandwidth and the mean voltage being variable between limits. Thus, if the mean voltage is  $V_3$  and the bandwidth  $\delta V$ , only pulses  $B$  and  $D$  will be recorded.

The fundamental circuit of the analyser is the Schmitt discriminator, shown in Fig. 13.20. If  $R_1$  is small and the bias is set to cut off  $V_1$ ,  $V_2$  conducts; a positive pulse causes  $V_1$  to conduct, and a positive pulse appears at the anode of  $V_2$ .

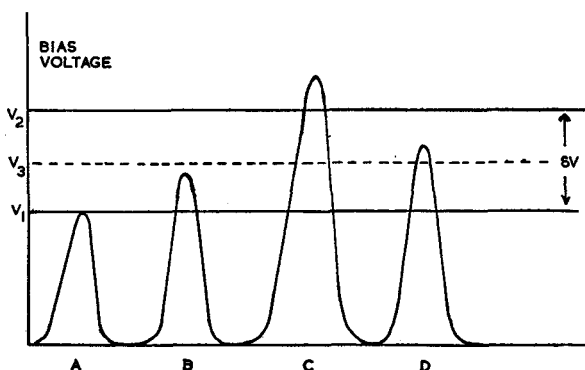


Fig. 13.19. Effects of bias on a train of pulses of varying amplitude

If  $R_1$  is increased, eventually the circuit 'triggers', and conduction of  $V_1$  causes  $V_2$  to cut off. With further increase of  $R_1$ , the circuit acquires electrical backlash, i.e. the transition from  $V_1$ -conducting to  $V_2$ -conducting occurs at a grid voltage  $E_a$  (bias + pulse), whilst the reverse change occurs at a grid voltage  $E_b$ ;  $E_a > E_b$ . In this way, an input pulse with superimposed 'noise' gives only one output pulse (Fig. 13.21). For short-duration pulses, the input capacitance  $C_1$  of  $V_2$  causes its switching-off to be relatively slow, and a capacitor  $C$  is included to speed up the response:  $CR_3 = C_1R_2$ .

The lower limit to the threshold voltage with a normal Schmitt discriminator is 5 V. The pulses within the given channel may be integrated by a *ratemeter* (q.v.) and the output applied to a pen recorder. The chart drive may be arranged to scan the mean

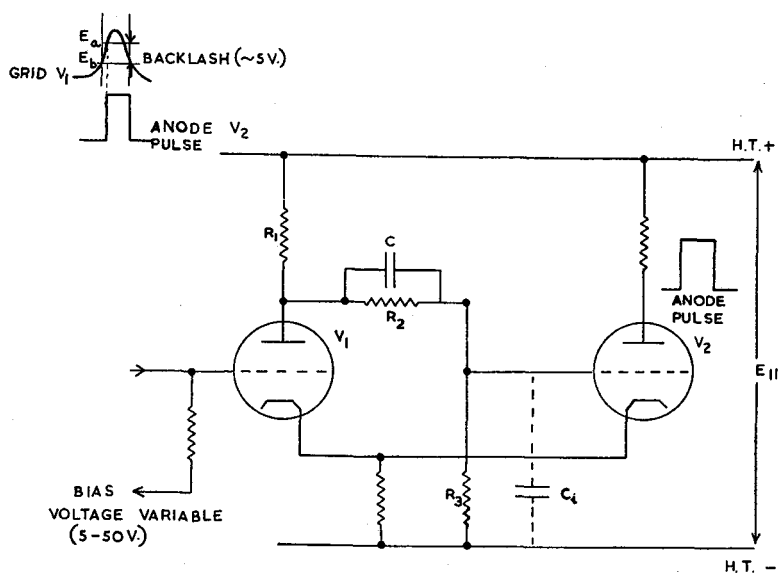


Fig. 13.20. Schmitt discriminator

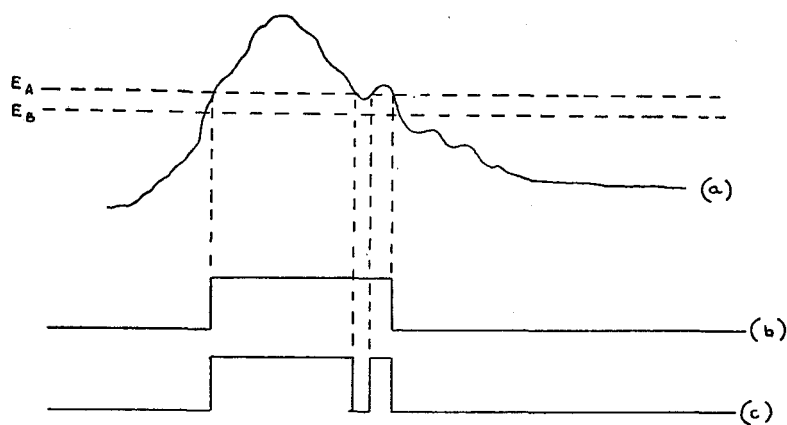


Fig. 13.21. Removal of 'Noise' component from a pulse: (a) Signal pulse with superimposed noise pulse; (b) Output pulse using backlash; (c) Output pulse with no backlash

bias voltage, so that an energy spectrum is obtained (Fig. 13.22).

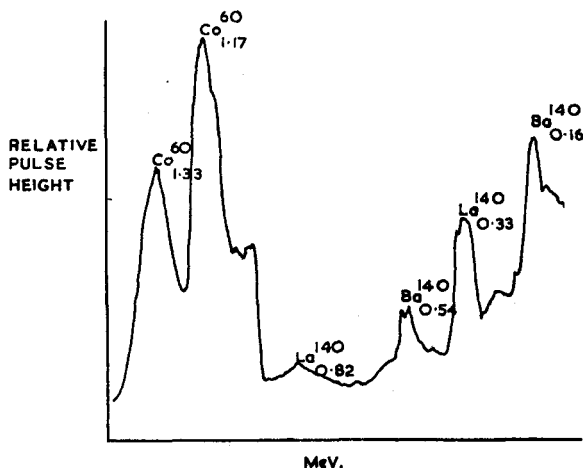


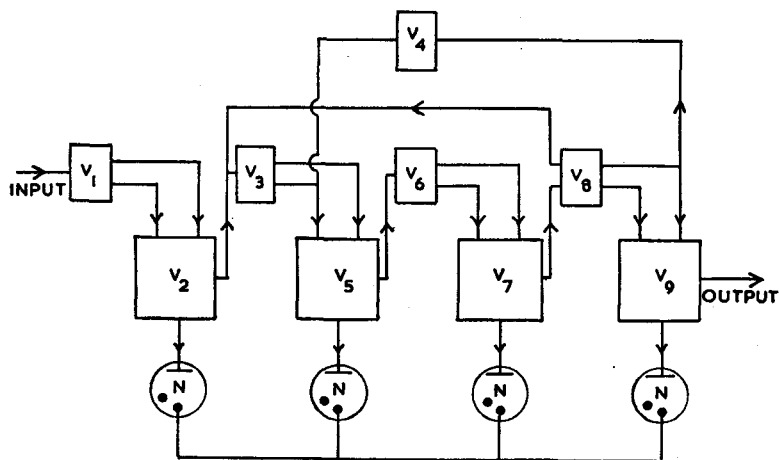
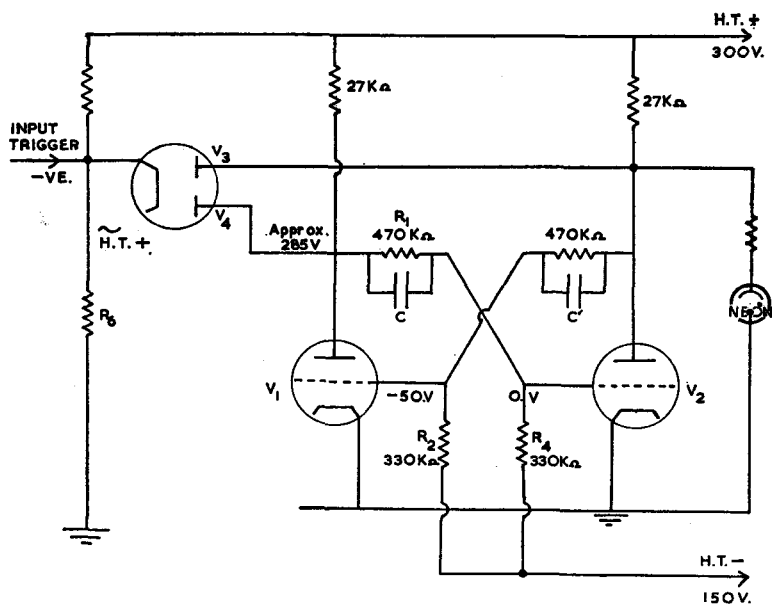
Fig. 13.22. Pulse Analyser spectrum

### Scalers

The scaler records the total number of pulses which have been received, either from the Geiger-Müller tube or from the pulse analyser, since the commencement of counting. The operation of dekatron and ribbon-beam tubes in scaling circuits has already been described (p. 180). *Hard-valve* scalers, which preceded these, may have a resolving time as low as 2–5  $\mu$ seconds. The basic scale-of-two circuit (often called the *Eccles-Jordan* circuit) is shown in Fig. 13.23.

Normally  $V_1$  is conducting, with a low anode potential and grid potential close to that of the cathode.  $V_2$  is cut off by heavy negative grid bias. A negative input pulse via diode  $V_4$  to the grid of  $V_1$  rapidly drives  $V_2$  into conduction, and  $V_1$  to cut off. The next pulse reverses these conditions. The capacitors  $CC'$  offset the integration of the pulse by  $R_1$  and the grid-to-earth capacities; they also operate as 'memory' capacitors, ensuring that the valves operate in strict succession. Thus the change-over from  $V_1$  conducting to  $V_2$  conducting marks the first pulse, and this is indicated by the glowing of a neon tube connected to  $V_2$  anode.





# LABORATORY AND PROCESS INSTRUMENTS

Any number of binary circuits may be connected in 'cascade' so as to form a counting scale of  $2^n$ . In order to obtain a decimal scale, ten stable states are required, and this scale is provided by four binary circuits, connected as shown in outline in Fig. 13.24(a). The first three binary circuits operate normally, count-

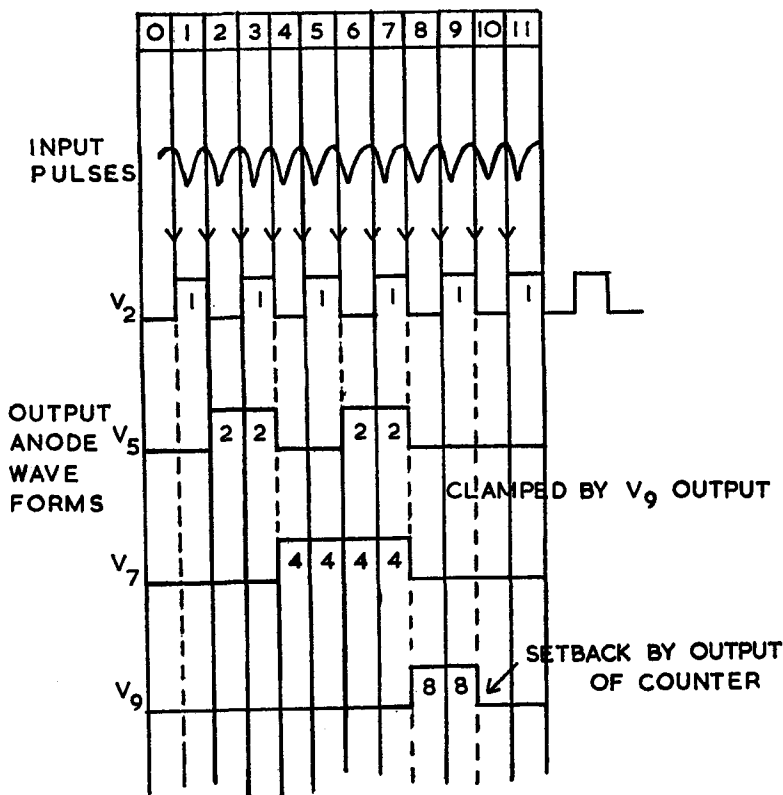


Fig. 13.24. (b) Waveforms

ing up to seven, including zero. The eighth pulse registers at the fourth binary, and applies a gating pulse to the second binary; thus the next pulse to this binary (i.e. the tenth input pulse) returns the fourth binary to the zero state, removes the grating from the second binary, and also applies an output pulse to the next scale of ten. The time disposition of these pulses is shown in Fig. 13.24(b).

## RADIOACTIVITY MEASUREMENT

### References

- BELL, C. G. and HAYES, F. N. (Ed.) (1958). *Liquid Scintillation Counters*. Pergamon.
- CURRAN, S. C. and CRAGGS, J. D. (1949). *Counting Tubes*. Butterworth.
- HANDLOSER, J. S. (1959). *Health Physics Instrumentation*. Pergamon.
- WILKINSON, D. H. (1950). *Ionisation Chambers and Counters*. Cambridge.

### Problems

1. Discuss the effects of (a) a differentiating circuit, and (b) an integrating circuit, on an input voltage of square waveform. What is the significance of these results?
2. Compare the measurement of radioactivity by the Geiger-Müller tube and by the scintillation counter, and show that pulse height analysis is feasible with the latter technique.
3. Draw a block diagram (circuit details not required) of a rate-meter, and give an account of the operation of this instrument.
4. Give a general account of the amplification and shaping of the train of pulses from a scintillation counter, with regard to stability and low 'noise'.

## Photometers and Spectrophotometers

### Introduction

The application of colorimetric and photometric methods to chemical analysis has increased to a marked extent over the past few years. The phenomenon of the absorption of light is well known inasmuch as coloured solutions exist; all materials absorb light to some extent but the amount varies markedly with the wavelength. If 'white light' is incident upon the material and some wavelengths are selectively absorbed, the transmitted light will possess different characteristics from the incident light, i.e. it will be coloured; the colours of solutions are due to this effect. It is necessary to measure the ratio of the intensities of the incident ( $I_0$ ) and transmitted light ( $I$ ) at a known wavelength. The logarithm of this ratio is called the *optical density* or *extinction*,  $E$ , i.e.  $E = \log I_0/I$ . Photometric measurements of solutions are based upon the validity of the *Beer-Lambert law*, which for monochromatic light may be expressed  $\epsilon = T \cdot E/(c \times l)$ . Hence, the intensity  $I_l$  transmitted by a thickness  $l$  of solution is  $I_l = I_0 e^{-\epsilon cl}$ , where  $\epsilon$  = molar extinction coefficient,  $c$  = concentration in g mol/l.,  $l$  = path length through the solution, in cm.

For a particular substance at a given wavelength  $\epsilon$  is a constant, and thus the degree of absorption is proportional to the concentration of the solution; this latter expression is one way in which *Beer's law* is sometimes rather loosely stated. The testing of the validity of the Beer-Lambert law has attracted much attention, and it may be said to hold for 'normal' solutions. The law does not hold for 'weak-electrolyte' solutions in which the degree of dissociation changes with dilution and where the undissociated and dissociated forms have dissimilar absorptions, nor for solutions which scatter the incident light, e.g. colloidal solutions, turbid solutions, etc. It should be noted that the solvent may absorb at the same wavelengths as the solute; correction for this effect can be made. Practically, it is convenient to use two similar cells,

# PHOTOMETERS AND SPECTROPHOTOMETERS

one containing pure solvent and the other solution, and to allow the same radiation to fall on both cells. The light transmitted by the solvent is taken as the incident light-intensity  $I_0$  which falls

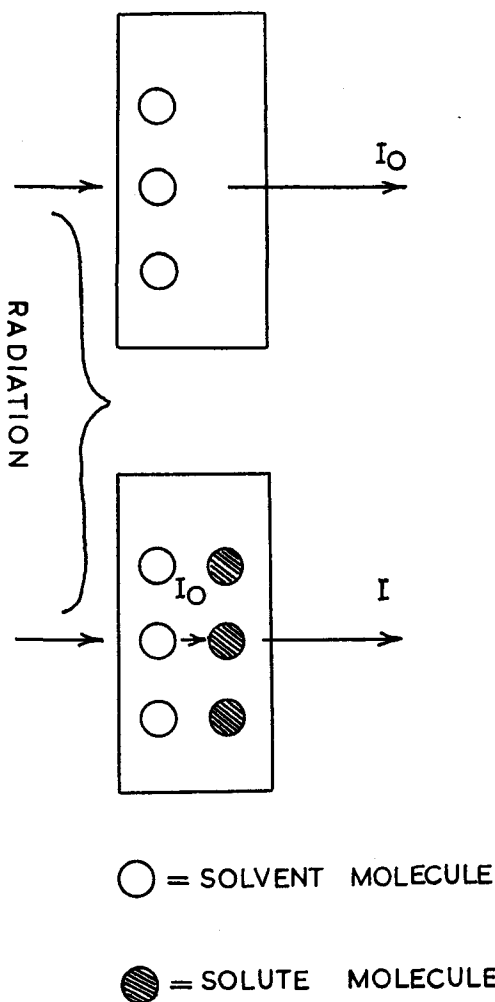


Fig. 14.1. Incident and transmitted intensities of radiation

on the solute molecules in the solution, and the light transmitted by the solution is the transmitted light intensity  $I$  (Fig. 14.1). There are basically two methods which may be used to measure

## LABORATORY AND PROCESS INSTRUMENTS

the intensity of the transmitted light. In the first method, the radiation after passing through the cells is dispersed using an optical system and the resulting spectrum analysed, e.g. using photographic techniques. The second method, and the one described here, produces a beam of more or less *monochromatic* radiation which is allowed to fall upon the cells, and the decrease in intensity of the radiation measured.

In the visible region of the spectrum such radiation may be produced in one of three ways.

(i) Continuous radiation, i.e. 'white light', is produced from a tungsten filament lamp and an absorbing filter is used which will transmit a relatively narrow range of wavelengths. Examples are the usual gelatine or glass photographic filters, or the newer type of dielectric filters which transmit a much narrower band.

(ii) A series of discontinuous bands of radiation is produced by certain discharge lamps, e.g. mercury or sodium lamps, and if such a source is used in conjunction with well-chosen filters nearly monochromatic light may be obtained.

(iii) A monochromator, using either gratings or prisms and slits, may be used to obtain a very narrow band of wavelengths. This produces a relatively complicated instrument which is called a *spectrophotometer*; such instruments will be described later.

### Photoelectric Colorimeters or Absorptimeters

Instruments of this type are commonly used in chemical and metallurgical analysis. They are frequently called 'abridged spectrophotometers', and generally consist of a light source of

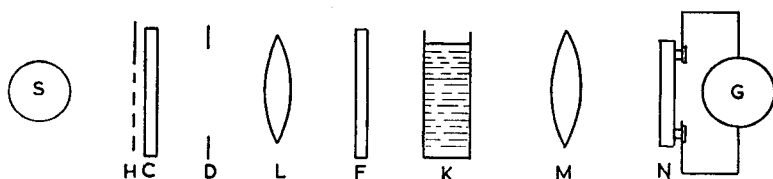


Fig. 14.2. Single-photo-cell absorptimeter

type (i) or (ii), with a colour filter, barrier layer photo-cell and galvanometer. The various types of instruments may be divided into two groups, the single-photo-cell type and the two-photo-cell type. An example of the former is shown diagrammatically in Fig. 14.2.

*S* is the light source, e.g. an 18 W gas-filled lamp run from accumulators or from a constant-voltage transformer. *H* is a spring-loaded shutter which returns to the 'closed' position when readings are not being taken, thus preventing fatigue of the photo-cell. It is also used to check the galvanometer zero. Radiations from the source pass through a heat-absorbing Calorex glass filter *C*, an adjustable diaphragm *D*, and a lens *L* which causes a parallel beam of light to pass through the colour filter *F* and specimen cell *K*. The transmitted light then passes on through a lens *M*, which forms an image of the lamp filament on the photo-cell *N*.

The current produced by the photo-cell is indicated by the galvanometer *G*. In such an instrument two absorption cells are required, one for the solvent and one for the solution, which are placed alternately in the beam. The readings are made in terms of galvanometer deflections, which may be marked directly in optical density and/or percentage transmission.

Perhaps the most frequently used absorptiometer in this country is the Spekker absorptiometer.† This is a two-photo-cell instrument, the outputs of the cells being fed in opposition to a galvanometer via a shunt to prevent overloading. This method has the advantage of reducing errors which may be produced by variation of the supply to the lamp. Fig. 14.3 is a diagrammatic representation of this instrument.

In many ways the construction of the two-photo-cell model is similar to the single-photo-cell instrument already described. The *compensating* photo-cell receives light which has passed through a suitable colour filter (i.e. one having maximum transmission near the absorption peak of the solution) and an uncalibrated iris diaphragm with coarse and fine aperture controls; the *indicating* photo-cell receives light which has passed through a similar colour filter, a *calibrated* diaphragm and the solvent or solution in the absorption cell. When the photo-cell currents are equal, the galvanometer shows no deflection. The calibrated diaphragm is operated by a large drum marked in optical density; since the lens system produces an image of the filament on the photo-cell, there is no change in the area illuminated when the aperture is changed.

In one method of operation, the calibrated aperture is set fully

† Manufactured by Messrs. Hilger and Watts Ltd., London.

## LABORATORY AND PROCESS INSTRUMENTS

open, i.e. to 'density = 0'; the absorption cell containing the solution is moved into the beam and with the shutter held open the uncalibrated iris diaphragm is adjusted until the photo-cell currents balance each other, i.e. there is no zero deflection on the galvanometer. The absorption cell containing solvent is then moved into the beam, where more light falls upon the indicating photo-cell and a galvanometer deflection is produced. This is reduced to zero by decreasing the calibrated aperture and the optical density is read from the drum. This density is in general an *arbitrary quantity*, since in most cases a wide waveband is

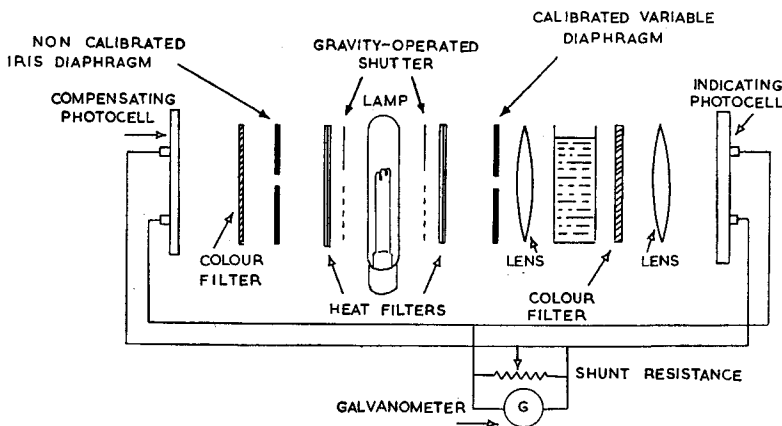


Fig. 14.3. Spekker double-photo-cell absorptiometer

transmitted by the colour filter and Beer's law is not strictly applicable. If, however, the tungsten lamp is replaced by a mercury lamp with suitable filters, monochromatic radiation can be obtained and Beer's law is applicable. An alternative procedure is to put the *solvent* cell into the beam with the aperture at an arbitrary setting, e.g. density = 1.0, and equalise the photo-cell currents. The solution cell is then put into the beam and the calibrated aperture *increased* to once again equalise the currents. A plot of drum reading against concentration, for the arbitrary solvent optical density, can be constructed for analytical use; this technique is somewhat more rapid where large numbers of samples have to be handled. The accuracy of measurement with



## PHOTOMETERS AND SPECTROPHOTOMETERS

these instruments is largely determined by the stability of the photo-cells. In the authors' experience errors are more frequently introduced by the lack of cleanliness of cells, filters, etc., than by instrumental variations.

### Spectrophotometers

The spectrophotometer may be described as an instrument which measures the amount of light a substance transmits or reflects at a chosen wavelength. Since simple filters cannot give monochromatic light of variable wavelength it is necessary to use some form of monochromator. However, the available energy is often reduced by a factor of 1000 in passing through the monochromator, and consequently it is common practice to use the more sensitive photo-emissive cells as detectors. Even so the currents produced are very small and demand amplification; methods of doing this will be described later. It should also be noted that no photo-emissive cells are available at the moment which are sensitive to all wavelengths, and it is necessary to use two photo-cells, one of which is sensitive to the red end of the spectrum (6000–10,000 Å) and the other to shorter wavelengths (the blue end of the spectrum). Photo-emissive cells normally show a very small current in the dark, due to thermionic emission at room temperature. This is called the 'dark current' and is of the order of  $10^{-8}$ – $10^{-9}$  amp; provision is made in the spectrophotometer for backing-off this current. If the range of such instruments is to be extended into the ultra-violet region of the spectrum the envelope of the photo-cell and the optics must be of quartz, since glass is opaque at these wavelengths.

Several spectrophotometers are available commercially and in this account it is not possible to describe more than one or two in detail. The emphasis will be on non-recording visible and ultra-violet spectrophotometers since these are the instruments most commonly found in laboratories at present. There is a current interest in recording instruments for the visible and ultra-violet regions of the spectrum; these operate on the double-beam principle which will be described later (p. 359).

It is convenient to classify these instruments according to the operational wavelength range, i.e. Class I, approximately 4000–10,000 Å, Class II, 1800–10,000 Å; Class III, infra-red spectrophotometers.

## LABORATORY AND PROCESS INSTRUMENTS

*Class I.* The Unicam† SP350 uses a diffraction grating and slit as monochromator, giving a bandwidth of approximately 350 Å, or 35 millimicrons; there is sufficient energy available to operate barrier layer photo-electric cells. The working range is 4000–7000 Å.

The Unicam† SP600 has a spectral range of 3600–10,000 Å using a glass optical system and two vacuum-type photo-cells: a

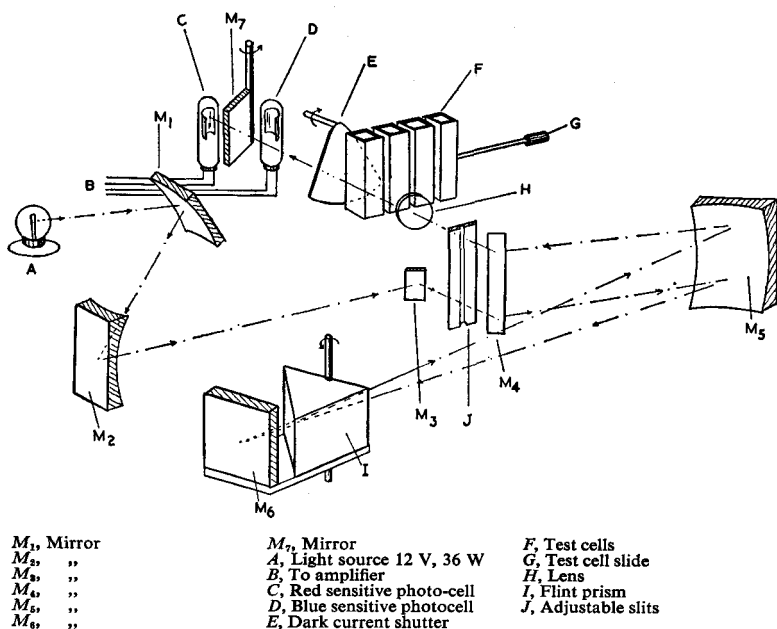


Fig. 14.4. Optical system—Unicam SP600

‘red’ cell for the range 6200–10,000 Å and a ‘blue’ cell for the shorter wavelengths. The bandwidth of the instrument is about 30 Å, with maximum values of 100 Å at the extreme of the range. A schematic diagram of the optical system is given in Fig. 14.4, where the path of the light beam can be clearly seen. A control altering the position of mirror  $M_7$  allows the light to fall on either the red or the blue photo-cell.

† Manufactured by Unicam Instruments Ltd., Cambridge, England.

## PHOTOMETERS AND SPECTROPHOTOMETERS

The output of the photo-cells is developed across a  $1000\text{ M}\Omega$  load resistor, and since the change of p.d. across the resistor is the product of the current in amperes and the resistance in ohms, a very small current ( $10^{-9}$  amp) will produce a change in p.d. of 1V. The p.d. is applied to a single cathode follower d.c. amplifier and the amplifier output balanced by a potentiometer supplied by dry batteries, using a sensitive meter as detector. The

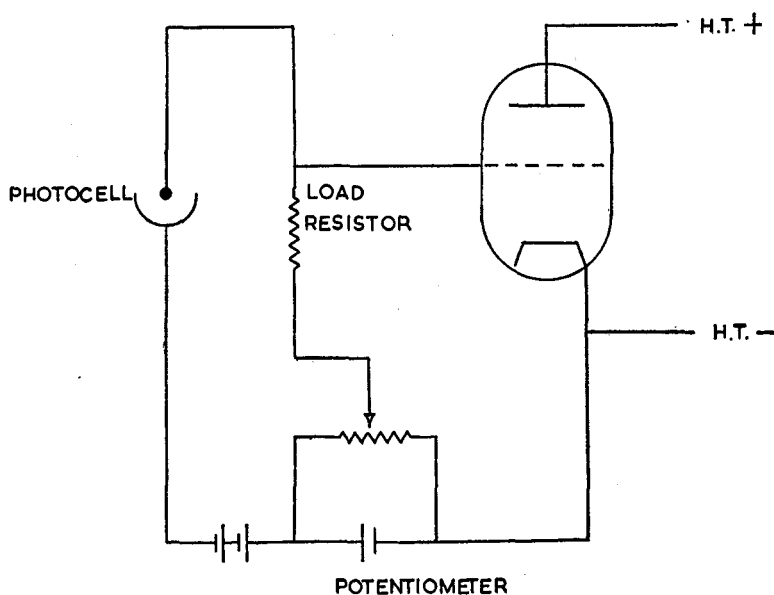


Fig. 14.5. Photo-cell circuit—SP600

potentiometer is calibrated in both percentage transmission and optical density; in outline the circuit can be regarded as that of Fig. 14.5.

The tungsten source lamp and the valve heaters are supplied from the mains supply through a constant-voltage transformer or an accumulator. The system used, i.e. the null method, minimises changes in supply voltage. In use, the required wavelength and photo-cell are selected and the dark current of the photo-cell is backed off. The 'solvent' cell is put into the light beam, the potentiometer adjusted to 100% transmission, and the adjustable slit varied to give zero reading on the meter. (In

## LABORATORY AND PROCESS INSTRUMENTS

practice, the 'check' position of the instrument switch automatically selects the 100% transmission position on the potentiometer.) The 'solution' cell is now introduced into the light beam; if absorption at the chosen wavelength occurs the intensity of the

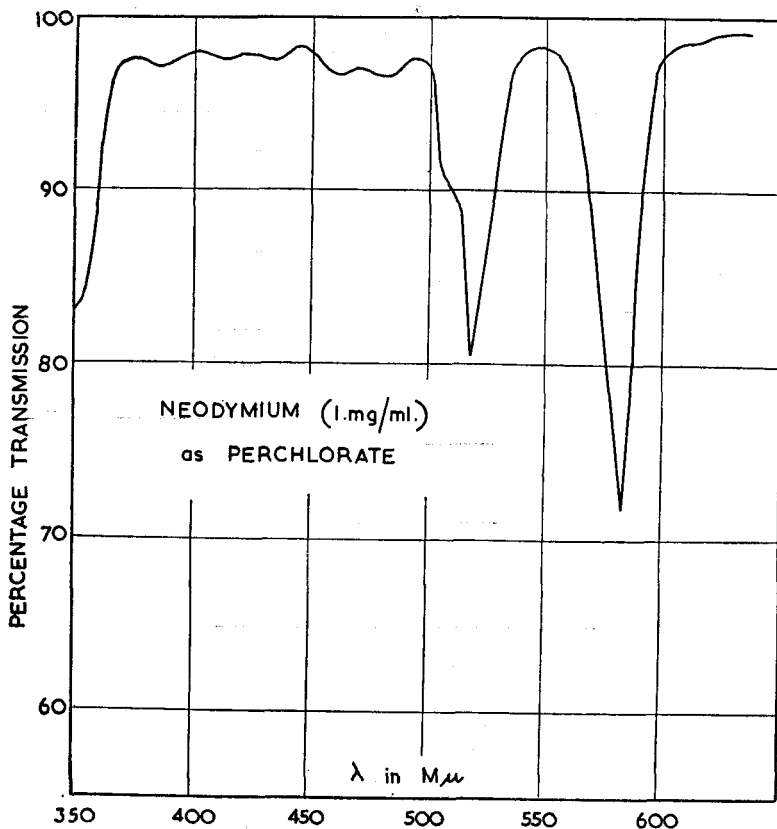


Fig. 14.6. Typical absorption curve

light falling on the photo-cell will fall, and the transmission-density control potentiometer must be adjusted for zero deflection of the meter. A typical absorption curve is shown in Fig. 14.6.

*Class II. (i) Visible and ultra-violet spectrophotometers.* These instruments use optics which are transparent in the visible and ultra-violet regions. In practice, quartz or fused silica optics in

## PHOTOMETERS AND SPECTROPHOTOMETERS

combination with mirrors or gratings in combination with mirrors are used; a diagram of the optical layout of the Beckmann spectrophotometer† is shown in Fig. 14.7.

The light source  $S$ , which is either a tungsten-filament lamp (for the visible region) or a hot-cathode hydrogen tube (for the ultra-violet region), is focused on a double slit  $L$  by means of a condensing mirror  $M_1$  and a plane mirror  $M_2$ ; the light passes through the lower part of slit  $L$  (entrance slit), is made parallel by the collimating mirror  $M_3$ , and falls upon the quartz prism  $P$ . The

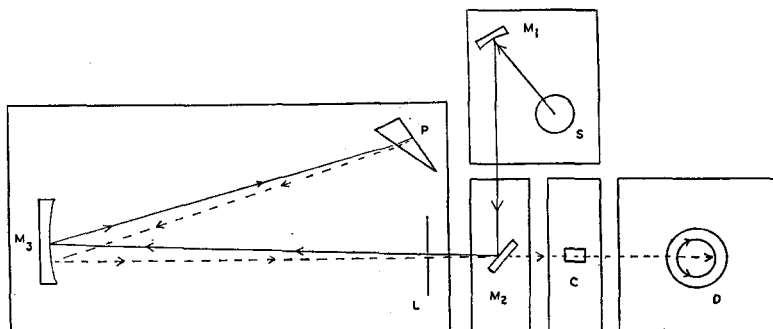


Fig. 14.7. Optical system—Beckmann spectrophotometer

back surface of this prism is aluminised and the light is reflected back on to the collimating mirror and thence to the upper part of the slit  $L$  (the exit slit). By varying the position of the prism about a vertical axis by means of a cam, light of a selected wavelength leaves the slit and passes through the absorption cell  $C$  on to a red- or blue-sensitive photo-cell  $D$ .

In Fig. 14.8 (the Hilger 'Uvispek'), light from the source  $H$  is focused on the entrance slit  $S_1$ , is collimated by the mirror  $M_3$  and passes to the  $30^\circ$  prism  $P$  which is metallised on the back surface. After reflection the light is focused on to the exit slit  $S_2$ , and passes to the photo-cell  $D$  via the absorption cell  $C$ . In this particular instrument provision is made for changing to a glass prism for use in the visible region, which gives greater dispersion in this range. Fig. 14.9 is a diagram of the Unicam SP500; taken in conjunction with descriptions of the other instruments, this diagram is self-explanatory.

† Beckmann Instrument Corp., Pasadena, California.

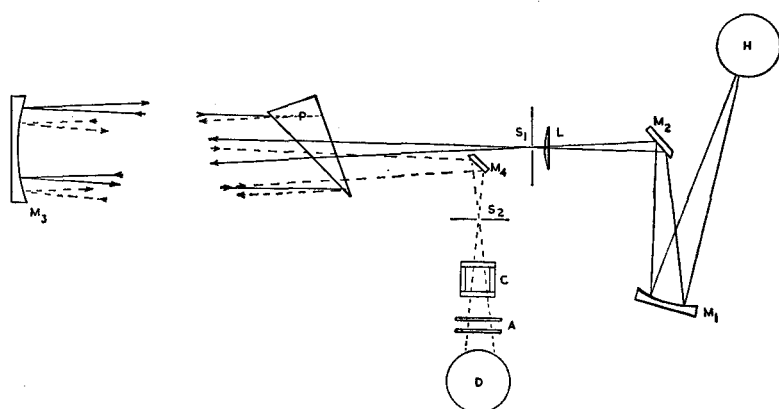
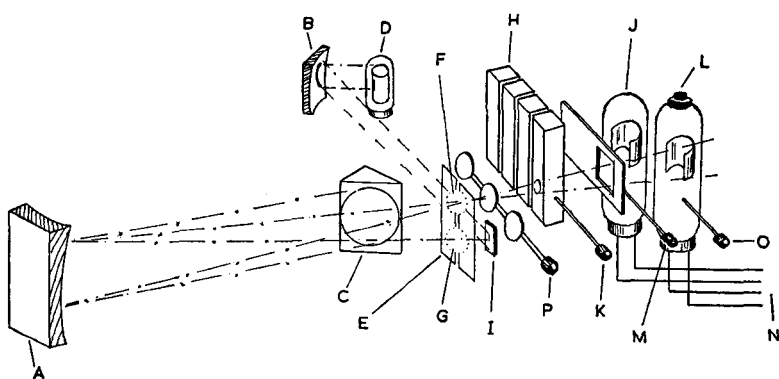


Fig. 14.8. Optical system—Hilger Uvispek



SP 500.

A, Collimating mirror  
B, Condensing mirror  
C, Quartz prism  
D, Light source  
E, Bilateral curved slits  
F, Quartz lens

G, Quartz disc  
H, Quartz test cells  
I, Plane mirror  
J, Blue sensitive photo tube  
K, Test cell slide

L, Red sensitive photo tube  
M, Dark current slide  
N, To amplifier  
O, P.E. test slide  
P, Filter slide

Fig. 14.9. Optical system—Unicam SP500

## PHOTOMETERS AND SPECTROPHOTOMETERS

All the instruments described use a single photo-cell and rely on the constancy of the light source. The ultra-violet source (a hydrogen lamp) is usually supplied from a stabilised power pack, whilst the visible source (a tungsten lamp), is supplied from a

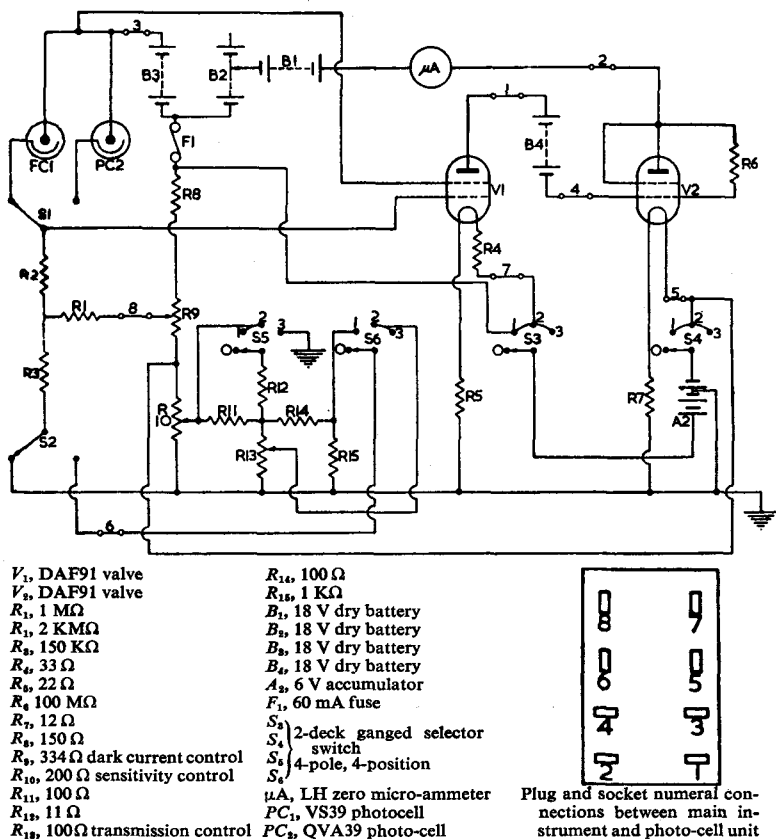


Fig. 14.10. (a) Measuring circuit, SP500

large-capacity accumulator or stabilised mains supply. As in the instruments for visible-region operation described earlier, two photo-emissive cells are used as balance detectors, and amplification of the output signal is necessary. One again potentiometer principles are used. As an example the Unicam SP500 system is shown in Fig. 14.10; (a) is a diagram of the measuring circuit,

# LABORATORY AND PROCESS INSTRUMENTS

and (b) is a simplified diagram of the amplifier. The photo-tube current is measured by balancing the voltage drop across the 2000 M $\Omega$  resistor, ( $R_2$ ), after amplification by the two DAF91

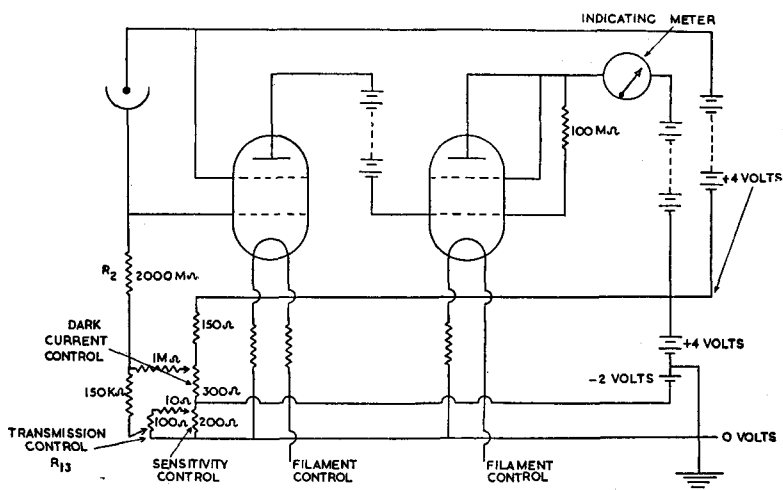


Fig. 14.10. (b) Simplified diagram of amplifier, SP500

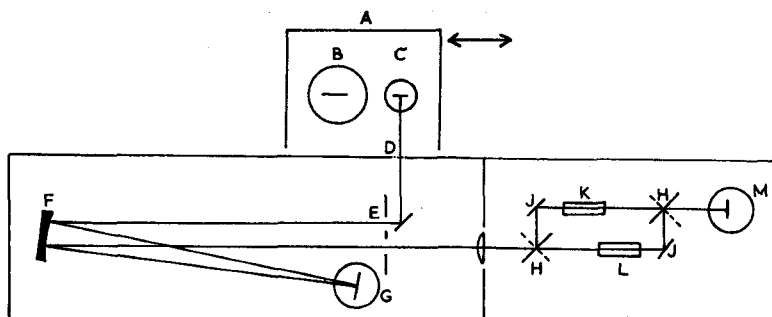


Fig. 14.10. (c) Optica double-beam spectrophotometer

valves, by means of a slide-wire potentiometer ( $R_{13}$ ), calibrated in percentage transmission and in optical density. A sensitivity control allows variation of the transmission scale sensitivity, which permits the use of a wide range of predetermined spectral bandwidths.



## PHOTOMETERS AND SPECTROPHOTOMETERS

As mentioned earlier there is considerable interest in an instrument which automatically plots the absorption curve on a chart recorder. Several such instruments are available in America† and British instruments are now coming into the market.‡ The one described below, the Optica CF4,§ differs from most others in that a plane diffraction grating is used as the dispersion element thus providing almost linear dispersion. A schematic diagram is shown in Fig. 14.10(c).

A sliding lamphouse *A* allows the choice of a hydrogen lamp *B*, or a tungsten lamp *C*, as source unit. The light passes via a filter *D* through the slits *E* on to a collimating mirror *F*, and to the grating *G*, which is slowly rotated. After dispersion the light beam is reflected into the 'double-beam portion' of the instrument. The double beam is achieved by use of rotating mirrors *HH* and fixed mirrors *JJ*, the light passing alternately through reference cell *K* and test cell *L*, and finally into a photomultiplier *M* which is used as detector.

(ii) *Infra-red spectrophotometers*. The general principles involved in the construction of infra-red spectrophotometers are similar to those of visible and ultra-violet instruments; a source emitting in the infra-red region sends a beam through a monochromator, which selects the desired wavelength, and the transmitted intensity is measured by a detector sensitive to this wavelength.||

The source consists of an incandescent solid, usually operated without an envelope (since the common envelope materials absorb in this region); the usual sources are the Nernst filament and the 'Globar'.

The Nernst filament is a semiconductor of rare earth oxides, e.g. zirconia, thoria, etc., manufactured in the form of a short rod. The rod is non-conducting when cold and must be heated by an external source until it becomes conducting, when the passage of the current (about 0.3 amp at 50 V) maintains the

† E.g. Applied Physics Corpn., Pasadena, Cal., U.S.A.; Beckmann Instrument Corpn., Pasadena, Cal., U.S.A.

‡ Hilger and Watts Ltd., London; Unicam Ltd., Cambridge.

§ Optica United Kingdom Ltd., Gateshead-on-Tyne, England.

|| Typical instruments are manufactured by: Messrs. Hilger and Watts, London, Unicam, Ltd., Cambridge, England. Sir Howard Grubb Parsons and Co. Ltd., Newcastle, England.

incandescence. As a semiconductor, it has a negative coefficient of resistance, and is operated in series with a ballast resistor in a constant-voltage circuit. The external source which heats the filament initially may be either a Bunsen flame, or radiation from a series of small adjacent electric heaters. The emissivity of the Nernst filament is high in the visible, low in the region  $1-6\ \mu$ , and rises again beyond this wavelength; it has been used up to a wavelength of  $25\ \mu$ .

The 'Globar' is a carborundum rod which is conducting at room temperature, and so does not need the starting devices of the Nernst filament.† In the longer wavelengths beyond  $15\ \mu$  it has a greater energy output than the Nernst filament, and for a great part of its range the energy spectrum approximates to that of a black body at the same temperature. Its disadvantages are its relatively large size, its heat dissipation (which necessitates water cooling), its relatively short life, particularly if its temperature rises above  $1200^{\circ}\text{C}$ , and the increase in resistance with length of time in operation, necessitating some means of progressively increasing the voltage across it.

It has already been stated that the so-called visible and ultra-violet spectrophotometers extend their range into the near infra-red. This is because the ordinary tungsten-filament lamp is a reasonably good source of infra-red radiation up to about  $2\ \mu$  (beyond which point the glass of the envelope becomes opaque), whilst the red photo-cell detectors are also operative over a part of the infra-red spectrum.

### Monochromators

In a previous section (p. 344) selection of a narrow band of wavelengths has already been described and in broad outline the methods used for the infra-red region of the spectrum are very similar. The optical materials must be transparent to the radiation used, and must also have reasonable dispersion in that region. Table 14.1 gives the transmission ranges of some optical materials suitable for the infra-red region.

At first sight it would seem advantageous to use potassium bromide as this material has a wide transmission range, but in practice greater dispersion is obtained for a particular material near the limits of its range. Consequently, if prisms are to be used

† The Globar consumes about 200 W at 40–50 V.

## PHOTOMETERS AND SPECTROPHOTOMETERS

it is preferable to use interchangeable prisms to cover the complete range to 25  $\mu$ . For example, we could use quartz below 3  $\mu$ , fluorite from 6–9  $\mu$ , rock salt from 8–15  $\mu$ , and potassium bromide to 25  $\mu$ . The most commonly used material at present is rock salt, largely because of price, but a choice of optical materials is now offered by the manufacturers of commercial instruments.

In general, diffraction gratings give greater resolution than prism systems and with the development of the Merton–N.P.L. gratings a number of grating instruments are now available. However the intensity of spectrum obtainable with a grating is generally less than that obtainable with a prism, and the overlapping of different-order spectra creates a problem in grating

TABLE 14.1

<i>Material</i>	<i>Transmission range</i> ( $\mu$ )
Crystalline quartz	0.19–3.5
Lithium fluoride	0.12–6.5
Fluorite	0.20–9
Rock salt	0.20–16
Potassium bromide	0.21–28

instruments. The low intensity has to some extent been overcome by careful design and by the improved sensitivity of detectors, whilst the overlapping of orders can be eliminated either by the use of suitable filters, or by preliminary dispersion with a prism. It is not conventional to regard the absorption cell as part of the monochromator, although the windows of such cells must be transparent in the region under study.

In an earlier section of this chapter abridged spectrophotometers for the visible region were described; such instruments also exist for the infra-red region, and will be described in the section on non-dispersive spectrophotometers, or as they are better known, *infra-red gas analysers* (p. 361).

### Detectors

Photographic and photo-electric methods can be used to detect infra-red radiation up to wavelengths of about 2  $\mu$ , but beyond this other methods must be used. A number of instruments have been made which use *photoconductive cells* as detectors. These

cells change their resistance when light falls upon them; World War II saw the development of lead sulphide cells, which are very sensitive to radiations in the near infra-red (to about  $3\ \mu$ ). More recently, lead selenide (max.  $5.5\ \mu$ ), lead telluride (max.  $5.8\ \mu$ ), cadmium sulphide and indium antimonide have attracted attention, in efforts to extend the range. These photo-cells become more sensitive and more stable if maintained at a low temperature, and arrangements may be made for cooling them with liquid air or solid carbon dioxide. Despite advances in photo-conductive cells, it is at present more satisfactory to use a thermal detector, e.g. a bolometer or thermopile, in the infra-red region of the spectrum. The bolometer consists of two similar metal strips which form two arms of a balanced Wheatstone bridge. The strips are usually blackened to increase absorption of incident energy. One of the strips is placed in the beam; radiant energy serves to increase the temperature of the strip, and its resistance changes, throwing the bridge out of balance. The strips were formerly made of nickel, which has a large temperature coefficient of resistance, but the use of thermistors (p. 5) as bolometers is a recent development; in particular; niobium nitride shows great promise in that its temperature coefficient is many hundreds of times greater than that of most semiconductors. The conventional bolometer is not as sensitive as the multi-junction thermopile, although its speed of response is greater.

A thermopile is an assembly of junctions of different metals which gives a small e.m.f. when radiant energy falls upon it; again, the end of the pile is generally blackened to increase absorption of energy. The design of thermopiles is very complicated, and the two main requirements of speed of response and sensitivity often conflict. Enclosing the thermopile in a vacuum renders it more sensitive, but at the expense of the speed of response.

The Unicam SP100 infra-red spectrometer uses as detector the Golay pneumatic infra-red detector†; illustrated in Fig. 14.11 it is claimed that the sensitivity of this detector is comparable with that of the best thermopile. In principle it consists of a small chamber containing a gas of low thermal conductivity, e.g. xenon, sealed at one end with a potassium bromide disc *A* through which

† *Rev. Sci. Instr.* **20**, 816 (1949).

## PHOTOMETERS AND SPECTROPHOTOMETERS

the radiation reaches a thin absorbing aluminium film *B*, of low thermal capacity. This absorbs the radiation, becoming heated, and so warms the gas in the chamber; the resultant increase in pressure distorts the mirror membrane *C*. A slow leak *D* connects the chamber to a ballast gas supply to minimise changes in ambient temperature.

Light from a stabilised low-wattage lamp *E* passes through the condenser lens *L* and the grid *G* via a lens *M* to the membrane mirror *C*. In the absence of deformation of the membrane mirror the image of one part of the grid is superimposed on another part, i.e. gap coincides with gap and line with line. Under these circumstances light passes to the photo-cell *F* via the mirror *N*.

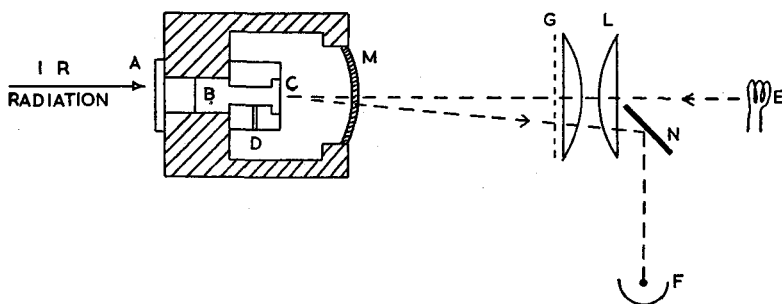


Fig. 14.11. Golay infra-red detector

If deformation occurs coincidence at the grid will not be obtained and the lines and gaps will coincide, resulting in reduction of light intensity at the photo-cell *F*. Thus photo-electric amplification is produced, the output from which can be still further amplified.

In practice, as well as high speed and sensitivity, the 'noise level' of the detector is of importance, and indeed it often seems that high sensitivity is allied with high noise level. Cells which are infra-red sensitive often have a thermionic emission which fluctuates in an irregular fashion, whilst Brownian fluctuations set a limiting value on the sensitivity which can be achieved. Additionally 'practical noise' from valves, etc., also sets a limit on useful sensitivity.

**Amplifiers**

The e.m.f. produced by the thermopile is only a few microvolts, and must be amplified. A number of amplifiers have been specially developed for spectroscopic instruments, and some of these are now considered.

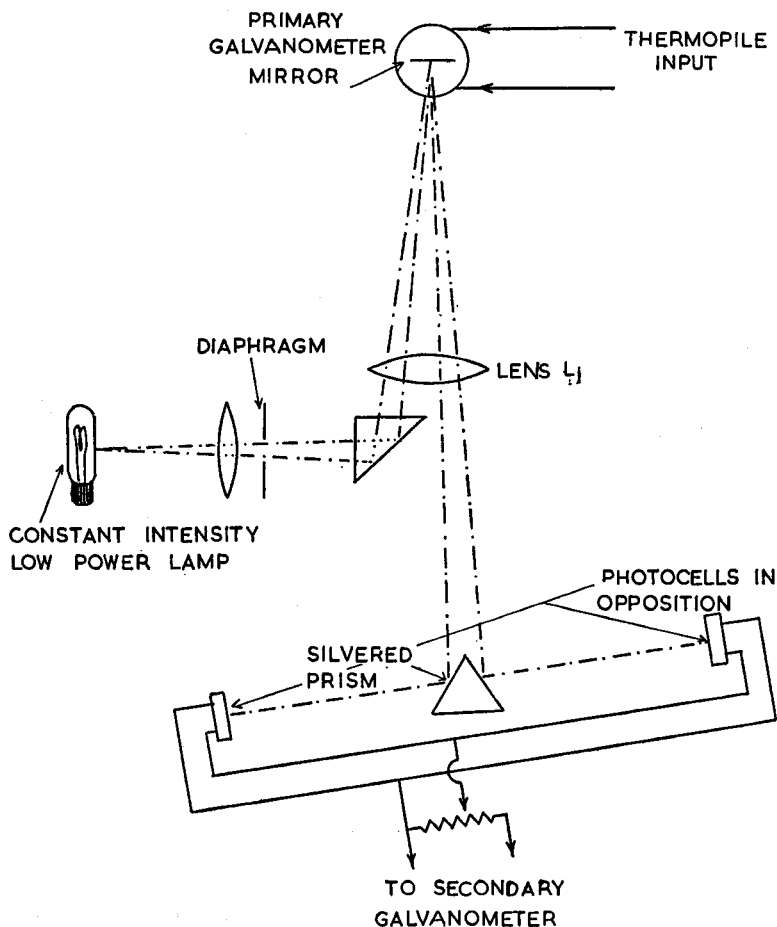


Fig. 14.12. Photo-electric galvanometer relay

*Hilger galvanometer amplifier or photo-electric galvanometer relay.* The principle is illustrated by Fig. 14.12. When the primary galvanometer mirror is in its rest position, i.e. with zero thermopile input, the light from the low-power lamp is reflected from

## PHOTOMETERS AND SPECTROPHOTOMETERS

this mirror via lens  $L_1$  and the faces of the prism so that equal amounts of light fall on both photo-cells. These are connected in opposition, and assuming equality, they will produce no current in the secondary galvanometer. If a small e.m.f. is now produced by the thermopile the primary galvanometer mirror is deflected and more light will fall on one photo-cell than on the other; the photo-electric currents will not balance, leading to deflection of the secondary galvanometer. The speed of response

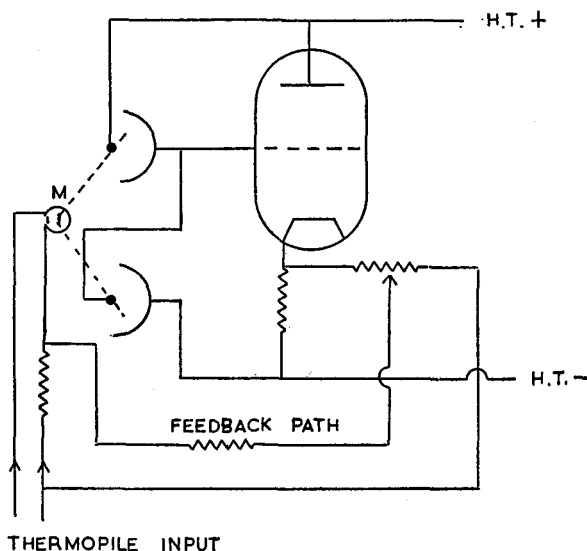


Fig. 14.13. Thermopile amplifier

of such a circuit is largely limited by the period of the galvanometer; at the expense of some sensitivity the speed of response may be increased by using negative feedback (see Fig. 14.13).

Light from the galvanometer mirror  $M$  is allowed to fall on the cathodes of two photo-emissive photo-cells. In the undeflected position the grid of the valve will take up a certain potential with respect to the cathode. When the thermopile generates a small e.m.f. the mirror is rotated and one photo-cell will be illuminated to a greater extent than the other, leading to a change in grid voltage, and hence of anode current; part of this is fed back into the galvanometer circuit to oppose the thermopile current.

It has been shown (p. 150) that if  $\beta$  is the fraction of the current fed back then the amplification is approximately  $1/\beta$ , which is independent of the circuit parameters. If  $A$  is the amplification in the absence of feedback then the restoring moment of the galvanometer is multiplied by a factor  $(1 + A\beta)$ ; this effectively increases the stiffness of the suspension, giving a higher speed of response.

Many designs of d.c. amplifiers have been used in the past, but no matter how sensitive or fast none of them has eliminated zero drift due to the effect of ambient-temperature variation on the thermopile; most modern instruments use a.c. methods of amplification. The radiant energy beam is 'chopped' by some mechanical means at a low frequency (e.g. 10 c/s) and the pulsating output of the thermopile is amplified using somewhat specialised a.c. circuits based upon the principles set out in Chapter VI. The output is then rectified and fed to a recording millivoltmeter. A thermopile having a rapid response is necessary; as this is inherently less sensitive than the 'slow' thermopile, the gain of the amplifier must be high (up to  $10^6$ ). The chopping frequency is about 10 c/s, and decoupling circuits become very bulky in this region, so that push-pull amplification (p. 131) is generally adopted. The chopping frequency must be maintained accurately constant, since the amplifier is usually rather sharply tuned in order to pass a narrow transmission band.

### The Complete Instrument

As an example of a typical modern infra-red spectrophotometer the Hilger H800 recording single- and double-beam spectrometer will be briefly described. The optical system is shown in plan in Fig. 14.14. The spectrometer uses a  $60^\circ$  prism of material transparent to the spectral range being studied, e.g. quartz, rocksalt, potassium bromide, etc., with the mirror  $M_6$  acting as the collimator. The source is a Nernst filament  $N$ , which is heated for starting purposes by a series of electrical heaters, and the detector  $R$  is a Schwarz thermopile. Two beams, the test beam and the reference beam, are obtained from the source by means of a mirror system  $M_1, M_2, M'_2, M_2$  being mounted vertically above  $M'_2$ . The two beams follow the same path but in different planes, through the cells  $C$  and  $C'$ , which contain the test and reference samples respectively, to the mirrors  $M_3, M'_3$ .



## PHOTOMETERS AND SPECTROPHOTOMETERS

A motor-driven shutter  $A$  is placed in the reference (i.e. the lower) beam, in front of  $M'_3$ . The two beams from  $M_3, M'_3$  converge on to the mirror  $M_4$ , which vibrates between two extreme positions at a frequency of 12.5 c/s, so that this optical switch presents light alternately from  $M_3$  and from  $M'_3$  (i.e. the test and reference beams) to the entrance slit  $S_1$ .

From this point there is only one path through the spectrometer to the detector  $R$ . Mirror  $M_5$  reflects the beam on to the

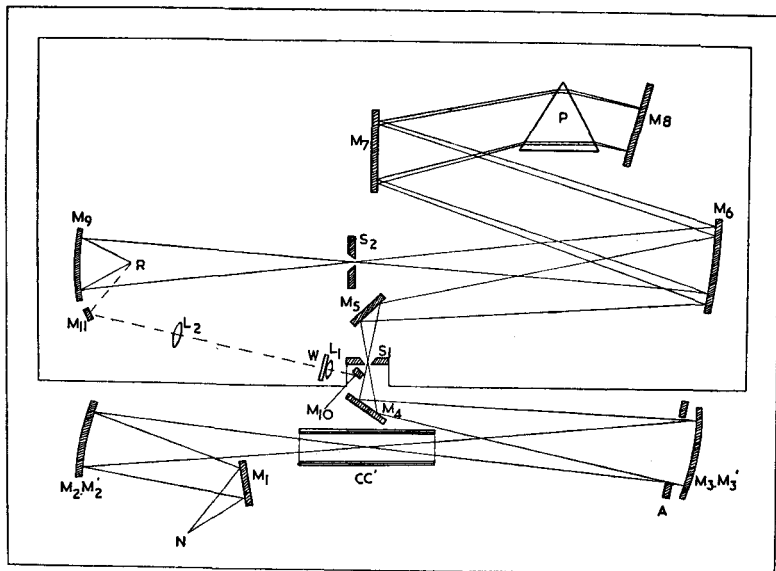


Fig. 14.14. Arrangement of components—Hilger H800 double-beam spectrometer

off-axis paraboloid mirror  $M_6$ , and thence to the prism  $P$  via mirror  $M_7$ . After passing through the prism the beam passes to the mirror  $M_8$ . The spectrum is scanned by rotating  $M_8$ , and the dispersed light is reflected via  $M_7$  on to  $M_6$  which focuses it on to the exit slit  $S_2$ . The elliptical mirror  $M_9$  then focuses the light on to the detector  $R$ .

Hence in its operation as a double-beam instrument, a chosen wavelength from the test and reference beams falls alternately upon the detector. If the absorption in the two beams is the same, the energy falling on the detector will be the same for both; if greater absorption occurs in the test beam, the difference in

# LABORATORY AND PROCESS INSTRUMENTS

energy between the two beams causes a fluctuating intensity of radiation at the detector which will produce an a.c. signal. This signal is amplified and fed to a phase-sensitive servo-motor (12.5 c/s) which drives the rectangular-aperture shutter *A* in such a way as to reduce the energy difference. Thus the energies in the two beams are maintained at balance. The area of the aperture

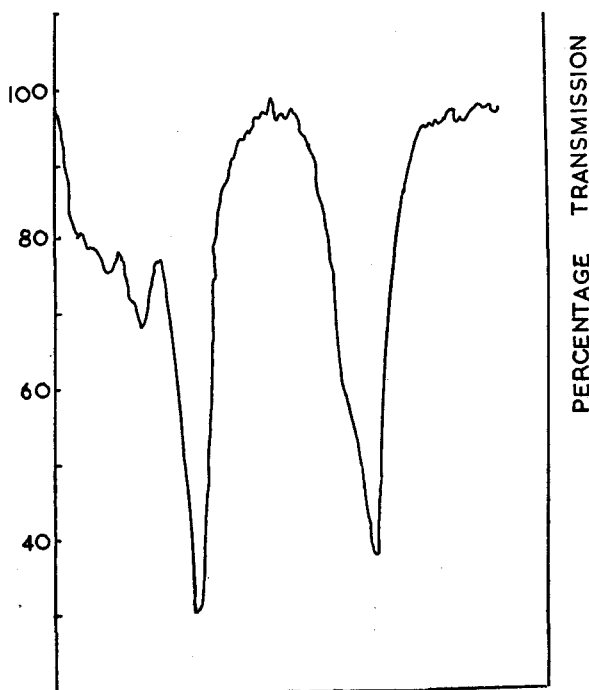


Fig. 14.15. Absorption curve of anisole

is a measure of the energy in the test beam relative to the full energy in the reference beam at the chosen band of wavelengths, i.e. it measures percentage transmission of the test sample. The size of the aperture is continuously recorded on the pen-recorder chart by means of a d.c. signal voltage derived from a potentiometer coupled to the drive of the aperture and provides the ordinate value on the chart. The movement of the chart is indirectly coupled to the movement of the mirror  $M_8$ , i.e. to the wavelength presented to the exit and thus wavelength is the abscissa. A typical trace is shown in Fig. 14.15.

## PHOTOMETERS AND SPECTROPHOTOMETERS

For single-beam working the condenser mirror  $M'_3$  in the reference beam is tilted from the double-beam position, and the reference beam after passing the servo-controlled aperture and vibrating mirror, misses the entrance slit and enters an optical by-pass system (the mirrors  $M_{10}$  and  $M_{11}$ , and lens  $L_1$ ) which leads it through an adjustable attenuator (the optical wedge  $W$ ) directly to the detector. The servo-controlled aperture maintains the balance as before; the reference beam energy does not now vary during the scan but remains at a constant value determined by the position of the attenuator. The area of the aperture is now a measure of the energy in the test beam relative to the constant reference energy, and a single-beam record is obtained. If a solution were being studied, it would be necessary to subtract the solvent spectrum to obtain the solute spectrum.

The energy from the source within equal wavelength intervals throughout the infra-red spectrum is not constant; in order to maintain a reference energy level the slit-width is arranged to vary throughout the scan.

### Non-dispersive Infra-red Gas Analyser

In Great Britain two non-dispersive gas analysers are available, one of which may be described as deflectional (Grubb-Parsons Ltd.†) and the other as a null-balance instrument (Infra-Red Development Co. Ltd.‡). The latter instrument will be described in outline; a schematic diagram is given in Fig. 14.16.

The unit consists of the analysis tube  $A$ , and the comparison tube  $B$  which is filled with dry air, both tubes being fitted with infra-red transparent windows. The energy source is a Nichrome wire which heats a small quartz tube to about  $600^\circ\text{C}$ ; this then emits radiations in the range  $2\text{--}15\ \mu$ . The beam is split into two by the reflectors, one beam passing through the analysis tube and the other through the reference tube. The radiation then falls upon the two sections of the detector unit ( $C$ ,  $D$ ), each section consisting of an absorbing chamber fitted with infra-red transparent windows connected to a central chamber. Both chambers of the detector unit are filled with the test gas, and the sections are separated by a thin metal diaphragm. From the optical point of view, if no test gas but only dry air is present in the analysis

† Sir Howard Grubb Parsons and Co. Ltd., Newcastle, England.

‡ Infra-Red Development Co. Ltd., Welwyn Garden City, England.

## LABORATORY AND PROCESS INSTRUMENTS

tube, then the energy falling upon the two sections of the detector will be equal and the pressures in the chambers will also be equal. If now the test gas is introduced into the analysis tube, absorption of some of the infra-red energy within its own particular infra-red absorption range will occur. The two sections of the detector unit, which are filled with the test gas, will absorb different amounts of the incident energy over this waveband, and the energy difference will manifest itself as heat; the gases in the two sections

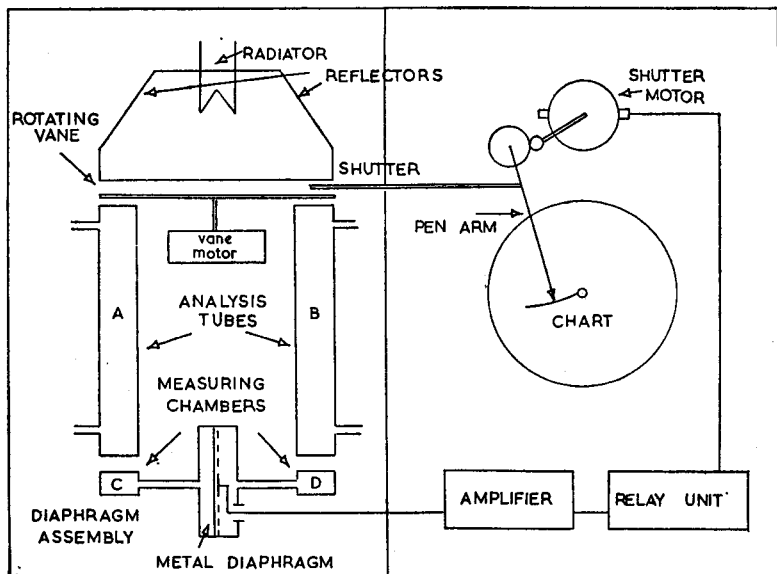


Fig. 14.16. Non-dispersive infra-red gas analyser

will not expand equally, setting up a pressure difference. The metallic diaphragm will thus move in the direction *D* to *C* by an amount proportional to the concentration of test gas in the analysis tube.

The aluminium diaphragm forms one electrode of a small electrical capacitor, the other electrode being a fixed insulated metal plate within the detector, and thus movement of the diaphragm is detected as a change in electrical capacitance. The fixed plate is connected to a constant polarising voltage through a high-value resistor. A rotating vane interrupts the radiation

## PHOTOMETERS AND SPECTROPHOTOMETERS

from the filament, allowing it to fall simultaneously on the two tubes, and then cutting it off from both tubes simultaneously, at a frequency of a few cycles per second. The periodic changes in capacitance give rise to charging and discharging currents of the capacitor which appear as an alternating voltage across the load resistor. The alternating voltage is amplified and made the input of a mechanical rectifier which is driven by the shaft of the rotating-vane drive motor, and it will thus respond only to the signal frequency. The rectified voltage is used to drive a servo-operated shutter into the reference beam until the energy incident on the reference section *D* equals that on the test section *C*, and the diaphragm returns to its undisturbed position. Thus at equilibrium the shutter position is an indication of the concentration of gas in the sample cell, and by a suitable linkage to the pen of a recorder a continuous record may be obtained.

### References

- GILLAM, A. E. and STERN, E. S. (1958). *An Introduction to Electronic Absorption Spectroscopy*. Arnold.  
LOTHIAN, G. F. (1949). *Absorption Spectrophotometry*. Hilger.

### Problems

1. The basic units of a spectrophotometer may be considered as being a radiation source, an optical cell unit, a dispersing system, a detector and a recorder. Discuss the requirements needed for these units, and describe errors which may arise in a complete instrument. (Reference can be made to the sources listed in the text and to *Chemical Applications of Spectroscopy* – see Question 8.)
2. Describe what you understand by 'stray light' in spectrophotometers, how it can be detected and its effects reduced or eliminated.
3. 'Quantitative absorption spectroscopy is based upon the Beer-Lambert law.' Discuss this statement critically, and show how apparent deviations from Beer's law may occur.
4. Describe in detail the construction of suitable double-beam spectrophotometers for use in (a) the ultra-violet region, (b) the infra-red region, of the electromagnetic spectrum.
5. Review the application of infra-red analysis to hydrocarbons. (Reference may be made to Sheppard and Simpson, *Quart. Rev. Chem. Soc.* 6, 1 (1952), and 7, 19 (1953).)
6. Write a general account of the application of visible and ultra-violet spectroscopy to inorganic chemistry. The field is wide and your account should contain only the general principles (see Question 7).

## LABORATORY AND PROCESS INSTRUMENTS

7. Describe in detail the application of the method of continuous variation to a reaction involving the formation of a single complex. Describe how the method has been extended for systems of greater complexity. (Reference may be made to Vosburgh and Cooper, *J. Amer. Chem. Soc.* **63**, 437 (1941); Gould and Vosburgh, *ibid.* **64**, 1630 (1942); and to Bjerrum, *Metal Ammine Formation in Aqueous Solution*. Haase and Son, Copenhagen (1941).)

8. A recording spectrophotometer may be considered as being made up of five units, namely a radiation source, an optical cell unit, a dispersing system, a detector and a recorder. Discuss suitable units which could be used in the construction of single-beam spectrophotometers suitable for use in the range 1850 Å to 30 microns. (Reference may be made to *Chemical Applications of Spectroscopy* (Editor, W. West). Interscience Publishers, New York (1956), and Lothian, G. F., *Absorption Spectrophotometry*, 2nd edition. Hilger.)

## Index

### A

Absorptiometers, 340  
Acceptor circuit, 58  
Admittance, 55  
Alternating current and voltage,  
  measurement of, 23  
Amplification factor, 81  
Amplifiers, classification of, 144  
  power, 129  
  pulse, 327  
  push-pull, 131  
  ring-of-three, 328  
  thermopile, 357  
  voltage, 125  
Anode resistance, 80  
Apparent power, 47  
Asymmetry potential, 263  
Automatic bias in oscillators, 158  
Autotransformer, 69

### B

Bandwidth of tuned circuit, 55  
Barretter, 3  
Base electrolyte, 288  
Beam tetrode, 87  
Beat frequency oscillator, 167  
Beer-Lambert Law, 338  
Bridge rectifier, 106  
Buffer solutions, 265

### C

Calomel electrode, 257, 296  
Capacitance, 10  
  in a.c. circuit, 32  
  in d.c. circuit, 14  
Capacitor, charge and discharge, 15  
Capacitors, 11  
  colour code for, 13  
  electrolytic, 12

Cathode follower, 142  
  ray oscilloscope, 191  
  E.H.T. circuit, 193  
  time bases, 195  
  polarograph, 306  
  tube, 192  
Charging current in polarography,  
  298  
Chokes, 9  
Coaxial cable, 16  
Cold-cathode tubes, 96  
Colour code for resistors, 2  
Conductivity meter, 235, 237  
Constant voltage transformer, 107  
Conversion conductance, 93  
Coupled amplifiers, 132  
  circuits, 60  
Coupling factor, 60  
Critical coupling, 63  
  damping of oscillatory circuit, 17  
Crystal detector, 121  
  equivalent circuit of, 164  
  frequency control, 162

### D

Decay constant, radioactive, 312  
Decibel scale, 50  
Dekatron, 180  
  circuits, 182, 183  
Derivative polarography, 301  
Detection, 114  
Dielectric constant, measurement,  
  274  
  of solid dielectrics, 279  
Dielectrics for capacitors, 11  
Differential polarography, 300  
Differentiating circuit, 320  
Differentiation of pulse train, 322  
Diode, 76  
  detector, 117  
  saturation current, 76

## INDEX

- Direct-current amplification, 146, 358
  - amplifiers, stabilisation of, 148
- Dosimeter, radiation, 319
- Dynamic characteristics, 125
  - impedance, 44
- Dynatron oscillator, 160
  
- E
- Electrode potential, 254
- Electromagnetic spectrum, 21
- Equivalent conductance, 227
  
- F
- Form factor, 26
- Frequency, classification of, 22
- Full-wave rectification, 23, 104
  
- G
- Galvanometer amplifier, 356
- Gas-filled tubes, 93
- Geiger-Müller tube, 186, 316
  - quenching in, 189, 317
  - recovery time, 316
- Germanium diode, 119
- Glass electrode, 260
- Global I.R. source, 352
- Golay I.R. detector, 354
  
- H
- Half-wave rectification, 24, 101
- Hard-valve stabilisation, 113
- Head amplifier, 191, 315
- High-frequency conductance, 244
  - equivalent circuit of cell, 247
  - titrations, 250
- Hydrogen electrode, 255, 283
  - ion concentration, 257
  
- I
- Impedance, 32
  - matching, 71
- Inductance, 7
  - in a.c. circuit, 29
  
- Inductors, 8
  - calculation of inductance, 8
  - in series and parallel, 10
- Infra-red gas analyser, 361
  - spectrophotometers, 351
- Integrating circuit, 321
  
- J
- Junction diode, 210
  - characteristic curve, 211
  - transistor, 212
  
- K
- Kipp relay, 324
  
- L
- Line cord, 4
- Liquid junction potential, 254
- Load line, 125
  
- M
- Metal rectifiers, 105
- Micrometer cell, 280
- Monochromators, 352
- Multivibrator, 167
- Mutual conductance, 80
  - inductance, 10, 60
  
- N
- Negative feedback, 140, 150, 308
  - resistance, 4, 160
- Nernst filament, 351
- Neutralisation of interelectrode capacitance, 82
- Noise, 6
- Non-dispersive I.R. gas analyser, 362
  
- O
- Optical density, 338
- Oscillation, maintenance of, 153
- Oscillatory charge and discharge, 15
- Oscilloscope, cathode ray, 191



# INDEX

## P

- Parallel  $L-C-R$  circuit, 38
  - combination of resistance and inductance, 18
- Pentode, 88
- pH scale, 257
  - meter, 269
- Phosphor, 318
- Photo-cell amplifier, 177
- Photo-conductive cells, 173, 340, 353
  - emissive cells, 175, 343
- Photomultiplier tubes, 178, 318
- Polarogram, 290
  - smoothing of, 295
- Polarograph, basic circuit, 285
  - cathode-ray, 306
- Polarography, 285
  - differential, 300
  - derivative, 301
- Positive feedback, 153
- Potentiometer, 258
- Potentiometric titration, 262
- Power amplifiers, 129
  - maximum transfer of, 70
  - factor, 46
  - of capacitors, 49
- Power in a.c. circuits, 45
- Proportional counter, 190, 314
- Pulse analyser, 331
- Push-pull amplifier, 131

## Q

- $Q$ -factor, 54
- Quenching probe, 323

## R

- Ratemeter, 324
- Reactance of capacitor, 33
  - inductor, 30
- Rejector circuit, 58
- Relaxation oscillator, 167, 168
- Resistance, 1, 27
  - capacitance coupling, 133
  - oscillator, 161
  - negative, 4, 85
- Resistors, 2

## Resistors—cont.

- colour code, 2
- metal film, 7
- variable, 6
- wire-wound, 3
- Resonant frequency, 37
- Ribbon beam tube, 185

## S

- Scaler, 334
  - decimal, 336
- Schmitt discriminator, 332
- Scintillation counter, 317
- Secondary emission, 85
- Selectivity of tuned circuit, 53
- Semiconductor diode, 202
  - nomenclature, 203
  - theory, 204
- Series combination of capacitors, 18
  - a.c. circuit, 35
  - d.c. circuit, 15
- Skin effect, 28
- Smoothing of rectified a.c., 103
- Specific conductance, 227
- Spectrophotometers, 343
  - visible and U.V., 346
  - I.R., 351
- Square wave, 26
  - polarograph, 307
- Stabilisation of power supply, 107
- Stage gain of amplifier, 124
- Synchronisation of time base, 197

## T

- Tetrode, 84
  - beam, 87
- Thermionic emission, 74
- Thermistors, 5, 354
- Three-terminal bridge, 242
  - measurement of small displacements, 282
- Thyratrons, 94, 171, 196, 294
- Time constant, capacitive circuit, 14
  - inductive circuit, 8
- Transformer, 65
  - coupling, 136
  - ratio-arm bridge, 239, 275

## INDEX

Transformer—*cont.*  
  with complex load, 68  
  with resistive load, 67  
Transistor, 212  
  amplifier, 219  
  d.c./a.c. convertor, 221  
  oscillator, 221  
  parameters, 213  
Transistors, manufacture of, 216  
Trigger tube, 183  
Triode, 78  
Tuning indicator, 199

## V

Valve bases, 96

Valve oscillator circuit, 155  
  principles, 153  
Variable- $\mu$  valves, 90  
Vibron amplifier, 149, 270  
Voltage doubler, 107  
  reference tube, 112  
  regulator tube, 94, 107

## W

Wagner earth, 231  
Wattless current, 30  
Wattmeter, 47  
Wheatstone bridge, a.c., 230  
  d.c., 229

# Other Technical Books from CHATTO & WINDUS

## Audio Frequency Engineering

E. HAYDN JONES  
B.Sc., A.M.I.E.E., A.M.Brit.I.R.E.  
*35s net*

## Automatic Data Processing Systems

ROBERT H. GREGORY and RICHARD L. VAN HORN  
*55s net*

## Concrete Practice

CHARLES H. HOCKLEY  
M.I.Struct.E.  
*12s 6d net*

## The Elements of Heat Flow

D. A. WRANGHAM  
M.Sc.Lond., D.I.C., A.C.G.I., M.I.Mech.E.  
*70s net*

## Manufacturing Processes

### *An Introduction to Basic Workshop Technology*

J. V. HARDING  
A.M.I.Mech.E., A.M.I.Prod.E.  
*25s net*

## Mechanical Engineering Craft Practice

H. C. TOWN  
M.I.Mech.E., M.I.P.E., F.R.S.A.  
*16s net*

## Elementary Design and Construction in Prestressed Concrete

J. D. HARRIS and I. C. SMITH  
B.Sc., M.I.C.E. M.E., D.I.C.  
*Probably 25s net*

## Involute Gear Geometry

W. A. TUPLIN  
D.Sc., M.I.Mech.E.  
*40s net*

## Ultimate Load Analysis of Reinforced and Prestressed Concrete Structures

L. L. JONES  
M.A., A.M.I.C.E.  
*45s net*

## THE ELECTRONICS OF LABORATORY AND PROCESS INSTRUMENTS

V. S. GRIFFITHS  
and  
W. H. LEE

42 WILLIAM IV STREET LONDON WC2

CHATTO  
and  
WINDUS